GEOLOGICAL SURVEY OF CANADA
COMMISSION GÉOLOGIQUE DU CANADA

PAPER 81-1B
ETUDE

CURRENT RESEARCH
PART B

RECHERCHES EN COURS
PARTIE B

Canada

85-1200/

Notice to Librarians and Indexers

The Geological Survey's thrice-yearly *Current Research* series contains many reports comparable in scope and subject matter to those appearing in scientific journals and other serials. All contributions to the Scientific and Technical Report section of *Current Research* include an abstract and bibliographic citation. It is hoped that these will assist you in cataloguing and indexing these reports and that this will result in a still wider dissemination of the results of the Geological Survey's research activities.

Avis aux bibliothécaires et préparateurs d'index

La série Recherches en cours *de la Commission géologique paraît trois fois par année; elle contient plusieurs rapports dont la portée et la nature sont comparable à ceux qui paraissent dans les revues scientifiques et autres périodiques. Tous les articles publiés dans la section des rapports scientifiques et techniques de la publication* Recherches en cours *sont accompagnés d'un résumé et d'une bibliographie, ce qui vous permettra, nous l'espérons, de cataloguer et d'indexer ces rapports, d'où une meilleure diffusion des résultats de recherche de la Commission géologique.*

Technical editing and compilation
Rédaction et compilation techniques
R.G. Blackadar
P.J. Griffin
H. Dumych
E.R.W. Neale
L. Machan

Produc[illegible]diting and layout
Prépar[illegible] mise en page
Leona [illegible]y
Lorna [illegible]
Michael J. [illegible]

Typed and checked by
Dactylographie et vérification
Debby Busby
Judy Côté
Janet Gilliland
Shirley Kostiew
Janet Legere
Madeleine Marier
Sharon Parnham

GEOLOGICAL SURVEY
PAPER 81-1B

COMMISSION GÉOLOGIQUE
ÉTUDE 81-1B

CURRENT RESEARCH
PART B

RECHERCHES EN COURS
PARTIE B

1981

© Minister of Supply and Services Canada 1981

Available in Canada through

authorized bookstore agents
and other bookstores

or by mail from

Canadian Government Publishing Centre
Supply and Services Canada
Hull, Québec, Canada K1A 0S9

and from

Geological Survey of Canada
601 Booth Street
Ottawa, Canada K1A 0E8

A deposit copy of this publication is also available
for reference in public libraries across Canada

Cat. No. M44-81-1BE — Canada: $8.00
ISBN 0-660-10893-3 — Other countries: $9.60

Price subject to change without notice

Geological Survey of Canada – *Commission géologique du Canada*

W.W. HUTCHISON
Director General
Directeur général

J.G. FYLES
Chief Geologist
Géologue en chef

E. HALL
Scientific Executive Officer
Agent exécutif scientifique

M.J. KEEN
Director, Atlantic Geoscience Centre, Dartmouth, Nova Scotia
Directeur du Centre géoscientifique de l'Atlantique, Dartmouth (Nouvelle-Ecosse)

J.A. MAXWELL
Director, Central Laboratories and Technical Services Division
Directeur de la Division des laboratoires centraux et des services techniques

R.G. BLACKADAR
Director, Geological Information Division
Directeur de la Division de l'information géologique

W.W. NASSICHUK
Director, Institute of Sedimentary and Petroleum Geology, Calgary, Alberta
Directeur de l'Institut de géologie sédimentaire et pétrolière, Calgary (Alberta)

J.C. McGLYNN
Director, Precambrian Geology Division
Directeur/par int. de la Division de la géologie du Précambrien

A.G. DARNLEY
Director, Resource Geophysics and Geochemistry Division
Directeur de la Division de la géophysique et de la géochimie appliquées

J.S. SCOTT
Director, Terrain Sciences Division
Directeur de la Division de la science des terrains

G.B. LEECH
Director, Economic Geology Division
Directeur de la Division de la géologie économique

R.B. CAMPBELL
Director, Cordilleran Geology Division, Vancouver, British Columbia
Directeur de la Division de la géologie de la Cordillère, Vancouver (Colombie-Britannique)

Separates

A limited number of separates of the papers that appear in this volume are available by direct request to the individual authors. The addresses of the Geological Survey of Canada offices follow:

601 Booth Street,
OTTAWA, Ontario
K1A 0E8

Institute of Sedimentary and Petroleum Geology,
3303-33rd Street N.W.,
CALGARY, Alberta
T2L 2A7

Cordilleran Geology Division
100 West Pender Street,
VANCOUVER, B.C.
V6B 1R8

Atlantic Geoscience Centre,
Bedford Institute of Oceanography,
P.O. Box 1006,
DARTMOUTH, N.S.
B2Y 4A2

When no location accompanies an author's name in the title of a paper, the Ottawa address should be used.

Tirés à part

On peut obtenir un nombre limité de "tirés à part" des articles qui paraissent dans cette publication en s'adressant directement à chaque auteur. Les adresses des différents bureaux de la Commission géologique du Canada sont les suivantes:

601, rue Booth
OTTAWA, Ontario
K1A 0E8

Institut de géologie sédimentaire et pétrolière
3303-33rd, St. N.W.,
CALGARY, Alberta
T2L 2A7

Division de la géologie de la Cordillère
100 West Pender Street
VANCOUVER, Colombie-Britannique
V6B 1R8

Centre géoscientifique de l'Atlantique
Institut océanographique de Bedford
B.P. 1006
DARTMOUTH, Nouvelle-Ecosse
B2Y 4A2

Lorsque l'adresse de l'auteur ne figure pas sous le titre d'un document, on doit alors utiliser l'adresse d'Ottawa.

SCIENTIFIC AND TECHNICAL REPORTS
RAPPORTS SCIENTIFIQUES ET TECHNIQUES

D.F. STOTT: Bickford and Gorman Creek, two new formations of the Jurassic-Cretaceous Minnes Group, Alberta and British Columbia 1

G.R. DUNNING: The Annieopsquotch ophiolite belt, southwest Newfoundland 11

F.C. THOMAS and F.M. GRADSTEIN: Tertiary subsurface correlations using pyritized diatoms, offshore Eastern Canada. 17

J. RIMSAITE: Isotope, scanning electron microscope, and energy dispersive spectrometer studies of heterogeneous zircons in radioactive granites from the Grenville Structural Province, Quebec and Ontario 25

I.R. JONASSON and W.D. GOODFELLOW: Modified spot test for Pb and Zn sulphides in ore samples 37

E.H. OWENS, R.B. TAYLOR, M. MILES, and D.L. FORBES: Coastal geology mapping: An example from the Sverdrup Lowland, District of Franklin. 39

K. ATTOH: Pre- and post-Doré sequences in the Wawa volcanic belt, Ontario 49

GUSTAVS VILKS and YING WANG: Surface texture of quartz grains and sedimentary processes on the southeastern Labrador Shelf 55

T.P. POULTON: Stratigraphic distribution and taxonomic notes on bivalves of the Bathonian and Callovian (Middle Jurassic) Upper Yakoun Formation, Queen Charlotte Islands, British Columbia. 63

H.H. BOSTOCK: A granitic diapir of batholitic dimensions at the west margin of the Churchill Province 73

R.M. EASTON: Geology of Grant Lake and Four Corners Lake map areas, Wopmay Orogen, District of Mackenzie 83

A.L. LITTLEJOHN: Alteration products of accessory allanite in radioactive granites from the Canadian Shield. 95

R.H. FILLON, I.A. HARDY, F.J.E. WAGNER, J.T. ANDREWS, and H.W. JOSENHANS: Labrador Shelf: Shell and total organic matter – ^{14}C date discrepancies 105

A.N. LECHEMINANT, T.R. IANNELLI, B. ZAITLIN, and A.R. MILLER: Geology of Tebesjuak Lake map area, District of Keewatin: A progress report 113

J.R. MACKAY: Dating the Horton River breakthrough, District of Mackenzie 129

R.J. MOTT and E.A. CHRISTIANSEN: Palynological study of slough sediments from central Saskatchewan. 133

R.D. LORRAIN, R.A. SOUCHEZ, and J.L. TISON: Characteristics of basal ice from two outlet glaciers in the Canadian Arctic – Implications for glacier erosion 137

N.C. OLLERENSHAW: Parcel 82, Dominion Coal Block, southeastern British Columbia 145

P. McLAREN, W.B. BARRIE, and J.M. SEMPELS: The coastal morphology and sedimentology of Cape Hatt: Implications for the Baffin Island Oil Spill Project (BIOS) 153

SCIENTIFIC AND TECHNICAL NOTES
NOTES SCIENTIFIQUES ET TECHNIQUES

T.J. LEWIS and G.J. WOODSWORTH: Heat generation in the northern Hogem Batholith and nearby plutons of McConnell Creek map area, British Columbia 163

R.M. GAGNÉ: Bedrock topography of the Tilbury area, Ontario 165

W.M. SCHWERDTNER, C.K. MAWER and A.F. HUBBS: Geology of the Gravenhurst region, Grenville Structural Province, Ontario: Preliminary mapping results 167

S.G. EVANS and D.M. CRUDEN: Landslides in the Kamloops Group in south-central British Columbia: A progress report 170

SCIENTIFIC AND TECHNICAL REPORTS
RAPPORTS SCIENTIFIQUES ET TECHNIQUES

1.

BICKFORD AND GORMAN CREEK, TWO NEW FORMATIONS OF THE JURASSIC-CRETACEOUS MINNES GROUP, ALBERTA AND BRITISH COLUMBIA

Project 780039

D.F. Stott
Institute of Sedimentary and Petroleum Geology, Calgary

Stott, D.F., Bickford and Gorman Creek, two new formations of the Jurassic-Cretaceous Minnes Group, Alberta and British Columbia; in *Current Research, Part B, Geological Survey of Canada, Paper 81-1B, p. 1-9, 1981.*

Abstract

A thick succession of marine to continental clastic rocks of latest Jurassic (Tithonian) to early Cretaceous (Berriasian to Valanginian) age, are included in the Minnes Group. In Carbon Creek basin, the group can be subdivided into four formations, which are, in ascending order, Monteith, Beattie Peaks, Monach, and Bickford (new). In the Kakwa region, only two formations are recognized, Monteith and the overlying Gorman Creek (new). Both the Bickford and Gorman Creek formations are truncated in an easterly to northeasterly direction by the pre-Bullhead unconformity and probably are not represented in the Plains.

The Bickford Formation, about 350 m thick in the type region, comprises carbonaceous mudstone, siltstone, and sandstone with thin coal seams. It is of mid- to late Valanginian age. The Gorman Creek Formation, about 1100 m thick in the type region, also contains carbonaceous sediments with coal seams. It is equivalent of the Beattie Peaks, Monach, and Bickford formations and is of early to late Valanginian age.

Introduction

As part of regional studies of Cretaceous rocks in the northern Foothills of Alberta and British Columbia (Fig. 1.1), the writer, over a period of many years, has accumulated much data on the Jurassic-Cretaceous succession lying between the Jurassic Fernie Formation and the Lower Cretaceous Cadomin Formation. In the meantime, coal exploration in northeastern British Columbia has proceeded rapidly and created a need for the definition of stratigraphic units currently in use. Thus, two formations not previously defined are briefly described and named, pending completion of a comprehensive report on the Jurassic-Cretaceous Minnes Group, in which the complex facies and various formations will be described in detail.

The early history of geological investigations in this region was summarized by Stott (1967, 1968, 1974). McLearn (1918, 1923, 1940) outlined the Cretaceous stratigraphy in the vicinity of Peace River, but lowermost Cretaceous marine rocks were first recognized by Mathews (1947) in the Carbon Creek basin between Pine and Peace rivers. McLearn and Kindle (1950) summarized the regional geology as known at that time. Springer et al. (1964) included the succession now assigned to the Minnes Group in their description of the Jurassic stratigraphy of the Western Canada Sedimentary Basin. Much new information has become available in recent years. The Halfway map area was mapped by Irish (1970); Pine Pass map area, by Muller (1961); Dawson Creek map-area, by Stott (1961); and the Pine River valley, by Hughes (1967). The lowermost Cretaceous succession in the vicinity of Pine River was described by Hughes (1964), and the Minnes succession north of Peace River was outlined by Stott (1967, 1969). South of Pine River, Geological Survey open file maps are available for Monkman Pass, Dawson

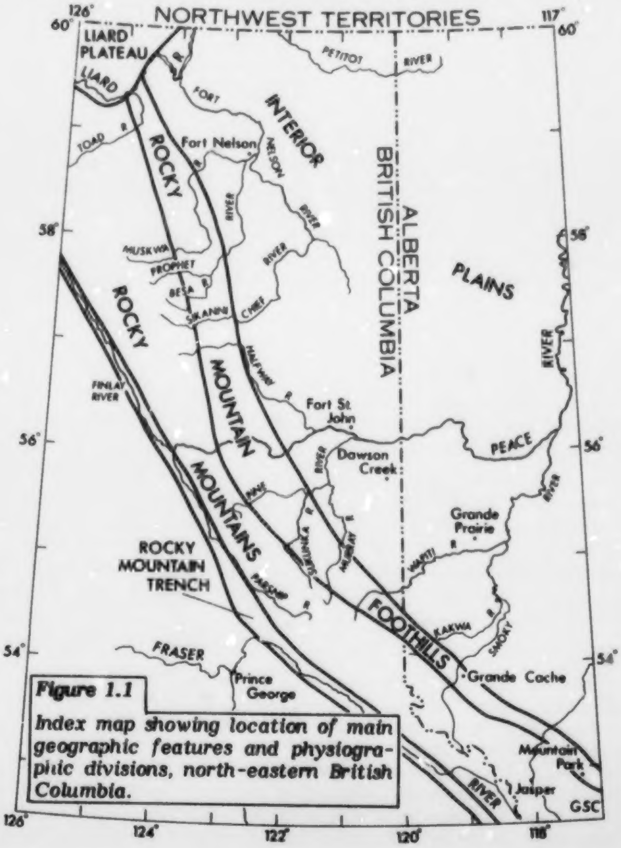
126°
60°
NORTHWEST TERRITORIES
117°
60°
LIARD PLATEAU
LIARD
R.
PETITOT RIVER
FORT
TOAD R.
INTERIOR
ROCKY
Fort Nelson
NELSON
RIVER
RIVER
ALBERTA
BRITISH COLUMBIA
58°
58°
MUSKWA
PROPHET
RIVER
BESA R.
SIKANNI CHIEF
PLAINS
ROCKY
MOUNTAIN
HALFWAY R.
RIVER
FINLAY RIVER
Fort St. John
56°
56°
PEACE
MOUNTAINS
Dawson Creek
RIVER
PINE
RIVER
Grande Prairie
ROCKY MOUNTAIN TRENCH
PARSNIP R.
WAPITI R.
KAKWA R.
SMOKY
FOOTHILLS
54°
54°
FRASER
Prince George
Grande Cache
RIVER
Mountain Park
Jasper
GSC
126°
124°
122°
120°
118°

Figure 1.1

Index map showing location of main geographic features and physiographic divisions, north-eastern British Columbia.

Creek, Pine Pass and part of Wapiti map areas (Stott, 1975; Taylor and Stott, 1979). Ziegler and Pocock (1960) reported on the extremely thick succession of Jurassic-Cretaceous clastic sediments in the region of Smoky and Kakwa rivers. To the south, in the vicinity of Athabasca River, the Jurassic-lowermost Cretaceous rocks were described originally by McKay (1929, 1930) and subsequently documented between Athabasca and Smoky rivers by Irish (1965) and also Mountjoy (1960, 1962). The writer (Stott, 1975a) briefly summarized the geology of the Minnes Group between Athabasca and Prophet rivers.

In a previous report, the writer (Stott, 1967) reviewed the nomenclatural problems related to the mainly lowermost Cretaceous beds lying between the Jurassic Fernie Formation and the Lower Cretaceous Cadomin Formation. At that time, the Minnes Formation, originally defined by Ziegler and Pocock (1960), was raised to group rank, specifically to comprise the Monteith, Beattie Peaks and Monach formations, as defined by Mathews (1947), and overlying unnamed shaly beds of the Carbon Creek basin. It is the unnamed beds to which part of this discussion will be directed.

Reconnaissance mapping and stratigraphic studies of the Foothills region between Carbon Creek basin and Athabasca River have revealed major facies changes in which marine shale, siltstone, and sandstone, assigned to the Beattie Peaks and Monach formations in the Carbon Creek basin, grade laterally southward into a continental sequence. The basal sandstones are a southward extension of the Monteith Formation and appropriately can be included in it. The overlying continental beds, although equivalent of the sequence overlying the Monteith in the Carbon Creek basin, cannot be subdivided into meaningful, mappable units, and a second new formation, therefore, is required within the Minnes succession. The relationships were illustrated by the writer (Stott, 1975a, Fig. 2) and are further shown in Figure 1.2.

Minnes Group

The Minnes Group, consisting of uppermost Jurassic and lowermost Cretaceous rocks, attains a maximum thickness of 2100 m between Smoky and Peace rivers. It lies transitionally on the Jurassic Fernie Formation and is overlain unconformably by the Lower Cretaceous Bullhead Group (Stott, 1974). The Minnes Group is bevelled eastward and northeasterly by an erosional unconformity and lowermost Cretaceous beds do not extend far into the Plains.

The distribution of strata now included in the Minnes Group is shown by the maps listed previously. A map at scale of 1:500 000 (Stott, in press) summarizes the distribution of Cretaceous rocks, including the Minnes Group, in northeastern British Columbia.

Four formations are included in the Minnes succession near Peace River; in ascending order, Monteith, Beattie Peaks, and Monach, defined by Mathews (1947), and the new Bickford Formation. Between Sukunka and Berland rivers south of Grande Cache, only two formations are recognized, the Monteith and the new Gorman Creek Formation.

Monteith Formation

The Monteith Formation (Mathews, 1947) consists predominantly of fine grained argillaceous sandstone, and in the northern area near Peace River, also contains fine- to coarse-grained quartzose sandstone. The formation attains a maximum thickness of almost 600 m along the western Foothills but decreases to less than 150 m in the easternmost exposures. The Monteith ranges in age from Tithonian (latest Jurassic) to earliest Valanginian (see Stott, 1975a).

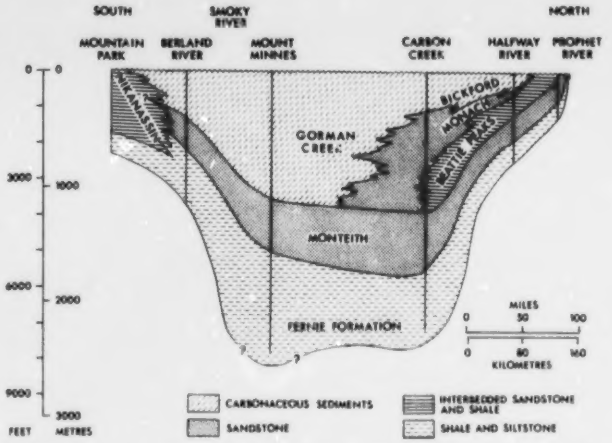

Figure 1.2 *Fernie-Minnes sequence along the Foothills between Mountain Park and Prophet River.*

Beattie Peaks Formation

The Beattie Peaks Formation (Mathews, 1947), comprising marine mudstone and siltstone, ranges from about 270 to 390 m. It is best developed between Pine and Peace rivers and northward to its erosional edge near Sikanni Chief River. The formation contains a fauna dated by Jeletzky as mid- to late Valanginian age.

Monach Formation

The Monach Formation (Mathews, 1947), 45 to 300 m thick, consists of quartzose to argillaceous sandstone, quite similar to that of the Monteith Formation. The Monach is recognized as far south as the big bend of the Sukunka River and north to Sikanni Chief River. In an earlier report (Stott, 1967), equivalent beds north of Peace River were assigned to Unit 2 of the "Beattie Peaks and ?Younger Beds", but are now included in the Monach Formation. The formation is dated as mid- to late Valanginian (see Stott, 1975a).

Bickford Formation

In previous reports (Stott, 1962, 1967, 1975a), the writer pointed out that the Monach Formation was separated from Cadomin conglomerate by a succession of interbedded fine grained, brown, laminated sandstone and silty shale. The unit was left unnamed until more data were obtained. Now, the succession of carbonaceous mudstone, siltstone, and sandstones with thin coal seams lying above the Monach sandstone and beneath conglomerate of the Cadomin Formation is defined as the Bickford Formation. The name is derived from Mount Bickford north of Pine River where the beds occur in several sections.

Hughes (1964, p. 21), from his studies in Carbon Creek basin and of the subsurface of the region to the east, defined beds lying below the conglomerate herein included in the Cadomin Formation as the Brenot Formation in the French Petroleum-Richfield Brenot Creek No. 1 Well near Hudson Hope in the eastern Foothills. Hughes extrapolated that unit westward into the Carbon Creek basin believing that the subsurface strata were equivalent of the sediments lying above the Monach sandstone. The depositional concept, implicit in Hughes' proposal, is that the Beattie Peaks, Monach and overlying shaly beds decrease dramatically in thickness eastward from the Foothills into the Plains and that no hiatus occurs at the base of the massive conglomerate.

The writer (Stott, 1967) has demonstrated that the upper units of the Minnes thin gradually basinward and has shown further (Stott, 1967, 1968, 1975) that, regionally, the Minnes, older Mesozoic and Paleozoic beds are truncated drastically below the Cadomin Formation. Hughes misidentified, in the Brenot well, as much reduced Beattie Peaks and Monach formations, a major cycle of mudstone and quartzose sandstone that forms the top of the Monteith Formation. Part of the Beattie Peaks, the Monach sandstone and overlying shaly beds are missing, owing to pre-Cadomin erosion. The type Brenot beds are part of the Beattie Peaks Formation and are not equivalent in any way to beds above the Monach Formation. The name Brenot cannot be applied with validity to the exposed beds occurring above the Monach in the Carbon Creek basin. Similarly, the application of Brenot by Gilchrist (1979) to beds between the Monach and Cadomin in the vicinity of Mount Jilg near Sukunka River is incorrect.

The type section is defined as those exposures that occur on the ridge extending westward from the main peak of Mount Bickford (latitude 53°37'N, longitude 122°26'W; U.T.M. co-ordinate 363634, Topographic Map 93 0/9 West, Mount Hulcross, British Columbia). A description of the section is given in the Appendix. The formation is best exposed on the south-facing slopes where contacts with the underlying Monach and overlying Cadomin Formation are present. Another section was examined on the long northwest-trending ridge off the next peak north of Mount Bickford, and a third section, poorly exposed, was measured on the ridge north of Bickford Lake that extends eastward to Fisher Creek.

The lower contact of the Bickford with the underlying Monach is drawn at a distinct change from thick bedded, quartzose sandstone to thin, cyclic units of alternating mudstone, siltstone, and sandstone. The contact is drawn above different sandstone units from one locality to another and forms no persistent stratigraphic horizon. This relationship is evident between The Monach, Mount Wrigley, and Mount Rochfort, where the Monach sandstone grades northward into a cyclic succession characteristic of the Bickford.

The upper contact is distinct with an abrupt change from the recessive cyclic units of the Bickford to the resistant conglomerate of the Cadomin Formation. Channel-structures are evident at the base of the Cadomin in many localities. Regionally, the contact can be shown to be an erosional unconformity, with truncation eastward of beds ranging from Cretaceous, through Jurassic and Triassic, to Mississippian and Devonian. It is possible that in the Carbon Creek basin and western Foothills, there is little or no hiatus between the Bickford and Cadomin but diagnostic faunal or floral evidence is lacking.

The Bickford Formation is best developed in the Carbon Creek basin where its moderately recessive character contrasts with the prominent, resistant Monach sandstone and Cadomin conglomerate. The formation is 348 m thick at Mount Bickford and 395 m near Bickford Lake, northeast of the type section. It is in the order of 350 m at Mount McAllister and at least that thick at Mount Rochfort where the upper contact is missing. Owing to the development of additional sandstone units included in the Monach Formation at The Monach, the Bickford is reduced to 255 m.

Recently, Stott and Gibson (1980) equated upper Minnes beds at Mount Rochfort with a thick succession of coal-bearing beds at the Utah Mines property within Carbon Creek basin. The Bickford Formation is exposed on the west flank of the Carbon Creek syncline and dips gently eastward below the surface of the mining property. It is represented in many of the bore holes and is in the order of 400 m thick.

North of Peace River, the Bickford Formation appears to be present above quartzose sandstone now assigned to the Monach Formation. Previously (Stott, 1967), the Bickford beds were assigned to Unit 3 of "Beattie Peaks and ?Younger Beds". They range in thickness between 97 and 185 m. Eastward thinning and northward disappearance of these beds is attributed to pre-Bullhead erosion.

The Bickford Formation is not well exposed in the region south of Pine River and it is not recognized as a mappable unit south of the big bend of Sukunka River. Gilchrist (1979) reported that strata between the Monach and Cadomin formations north of Mount Merrick have a thickness of about 150 m. To the south, equivalent beds are included in the newly defined Gorman Creek Formation.

In the Carbon Creek basin, the Bickford sandstones are fine grained, brown, finely laminated, crossbedded and thin bedded to flaggy. Some of the sandstones are similar to typical Nikanassin sandstone farther south, being extremely finely laminated, black, carbonaceous, limonitic, and weathering orange-brown. The interbedded shales are rubbly to platy, dark olive brown to black, and commonly carbonaceous.

Coal occurs throughout the Bickford Formation. Although Mathews (1947, p. 13) did not give seam thickness, he did indicate that coal occurred about 90 m above the Monach Formation in Carbon Creek basin. Hughes (1967, p. 870) also recognized the presence of coal above the Monach. In a recent paper, Stott and Gibson (1980), correlated the coal-bearing succession drilled within Carbon Creek with the surface exposures of the Minnes Group. Gibson (pers. comm.) in his studies encountered 20 to 25 seams in the section equivalent of the Bickford, ranging from less than 0.3 m to a maximum of 3.6 m, and a medium to high volatile rank. In the outcrop section in the vicinity of Mount Rochfort and also Mount Bickford, the coals within the Bickford appear to be relatively thin. Gilchrist (1979) noted several seams, of less than 1 m to a maximum of 3.2 m, between the Monach and Cadomin formation near Sukunka River.

The Bickford Formation lies on the Monach Formation which contains a fauna assigned by Jeletzky to the mid- to late Valanginian zone of **Buchia** n. sp. aff. **B. inflata.** No fauna has been recovered from typical Bickford rocks in the Carbon Creek basin although several collections were obtained from equivalent beds at the headwaters of Carbon Creek. Fauna obtained from those upper beds of the Minnes Group include **Buchia** n. sp. aff. **B. inflata** (Toula), **B.** aff. **B. crassicollis** var. **solida** (Lahusen) and **B.** cf. **B. bulloides** (Lahusen) of the mid- to late Valanginian zone of **B.** n. sp. aff. **B. inflata.**

Palynological and microfaunal studies have not been successful in providing additional dates for age determinations or correlation.

The Bickford Formation is considered to be equivalent of the upper Gorman Creek Formation (newly defined) of the Kakwa River region. Equivalent beds are not present in the subsurface of the Plains where the pre-Bullhead unconformity truncates Beattie Peaks and older strata.

Gorman Creek Formation

South of Pine River, the upper Minnes Group undergoes a lateral facies change which results in the disappearance of typical Beattie Peaks and Monach sediments, and their replacement by a cyclical succession of carbonaceous mudstone, siltstone, argillaceous sandstone and thin coal seams. That succession is assigned to the Gorman Creek Formation. The name is derived from Gorman Creek, a north to northeasterly flowing tributary of Torrens River, lying between Mount Minnes and Mount Gorman on the west side of the British Columbia-Alberta border. The headwaters of Gorman Creek lie within the original section of the Minnes described by Ziegler and Pocock (1960). The Gorman Creek Formation is defined as a cyclical succession of carbonaceous sediments with thin coal seams, lying between the thick bedded sandstone of the Monteith Formation and the coarse grained sandstone and conglomerate of the Cadomin Formation.

Ziegler and Pocock (1960) included the basal predominantly marine sandstone in the Nikanassin **facies** and the continental sequence in the Kootenay **facies**. Use of those names is misleading as both are applied differently in their type region where they are valid, useful stratigraphic terms. The Kootenay strata, lying between the Fernie and Cadomin formations of southwestern Alberta and southeastern British Columbia, were reviewed recently by Gibson (1979) who elevated the former Kootenay Formation to group rank, and subdivided the strata into three formations. Although the Kootenay Group does include important coal-bearing strata, it also includes marine sandstone at the base (Jansa, 1972; Gibson, 1979; Hamblin and Walker, 1979). Similarly, interbedded sandstone and shale between the Fernie and Cadomin formations in the Athabasca River region are included in the Nikanassin Formation (McKay, 1929, 1930; see also Mountjoy, 1960, 1962) which, although apparently dominantly marine, includes some carbonaceous, nonmarine strata. Owing to significant differences in lithology, Kootenay, Nikanassin, and Minnes are useful lithostratigraphic terms within specific geographic areas of the Rocky Mountain Foothills.

The type section of the Gorman Creek Formation occurs within the original section of the Minnes (Ziegler and Pocock, 1960), located on Mount Minnes (latitude 54°10'N, longitude 120°04'W; U.T.M. co-ordinates 916054 to 954053, NTS map 93 I/1 East, Jarvis Lakes, British Columbia). The section is reasonably well exposed along the east ridge off the main peak of Mount Minnes, southeasterly over a small hill at the headwaters of Gorman Creek, across the creek and up onto the slope of a ridge which extends northward to the main peak of Mount Gorman. The upper part of the ridge is capped by massive beds of Cadomin conglomerate.

Ziegler and Pocock (1960) included about 1200 m of nonmarine beds at Mount Minnes in their Kootenay facies which is essentially the Gorman Creek Formation as defined herein. The writer's measurement was about 100 m less, the difference may result from a variation in compensation for minor folds within the section.

The writer's description is not appended to this report, partly owing to space limitations, but also as the original description by Ziegler and Pocock is adequate for the purposes of this report.

The Gorman Creek Formation lies on the Monteith sandstone with apparent conformity. No major break or regional discontinuity is evident. The contact is drawn at the change from thick bedded sandstone units of the Monteith to the cyclical succession consisting of thin units of mudstone, siltstone and sandstone. It is possible, owing to local facies variations, that the contact may be drawn above different sandstone from place to place, but, in general, the stratigraphic position appears to be consistent.

The upper contact of the Gorman Creek with the Cadomin conglomerate, like that of the Bickford and Cadomin, is abrupt with evidence of channelling and a widespread regional erosional unconformity.

The Gorman Creek Formation is recognized within the Foothills from Berland River in the south, northward across Smoky River as far as Sukunka River. Because of intense deformation, the lack of weathering contrast between it and the underlying Monteith, and the heavy vegetation cover, the Gorman Creek is not easily mapped on a reconnaissance basis. Nevertheless, in all the sections examined, a marked lithologic contrast exists between the Monteith and Gorman Creek and the two are readily differentiated.

The Gorman Creek Formation is characterized by a cyclical coal-bearing succession of mudstone, siltstone, and sandstone. Cycles of several different magnitudes appear to be present, with the smallest being in the order of only 1 to 2 m, some being several tens of metres, and major cycles of hundreds of metres comprised of the smaller subcycles. The smallest cycle (subcycle) comprises a sequence of sandstone, siltstone, mudstone, and may or may not end in a thin layer of coal or coaly mudstone. The base of channel sandstone may be marked by thin conglomerate, woody debris, and small-scale erosional features. The largest cycles contain extremely thick sand units, and commonly have a basal conglomerate and channel structure. No internal correlation or markers were obvious, although sections measured by the writer are not closely spaced. Ziegler and Pocock (1960, p. 59) remarked on the variation found in two sections on Mount May where they found no similarity over a distance of only a few thousand metres.

The sediments of the Gorman Creek Formation tend to be carbonaceous, and are similar to those of the Bickford Formation. The sandstones are quartzitic, commonly fine grained but some of the channel-fill is coarse grained to conglomeratic. Beds of conglomerate are not abundant although conglomeratic sandstones are present in the upper part of the formation. Conglomerates with the largest pebbles or cobbles occur in the westernmost exposures, and a general decrease in grain size is found in the west to east direction. Ripple marks, graded bedding, laminated, and trough crossbedding occur throughout the section. The sandstones grade into siltstone which is argillaceous and commonly carbonaceous. The mudstone is olive brown to dark brown and brownish grey, and like the coarser sediments, contains large quantities of carbonaceous debris. Thin coal seams and carbonaceous mudstone occur throughout the succession but he coal generally does not exceed 1 m and is usually less. Some leaf fragments and wood occur but are not abundant. Good fossil material is rare. Dinosaur tracks are present on bedding plane surfaces along Narraway River.

Thin coal seams are present throughout the Gorman Creek Formation. As noted by Ziegler and Pocock (1960), the coals may be 1 m or more in thickness but thick seams do not appear to be present. The coal from Mount Gorman is bituminous and of high volatile rank (W.D. Kalkreuth, pers. comm.).

The age of the Gorman Creek Formation is determined mainly from its stratigraphic position because its contained flora and fauna are not completely diagnostic.

The Gorman Creek Formation lies on the Monteith Formation which, in Carbon Creek basin, ranges in age from Tithonian (latest Jurassic) to earliest Valanginian (Stott, 1975a, p. 448). In the vicinity of Mount Minnes, the upper beds of the Monteith are not dated by macrofossils, but the basal beds are known to be latest Jurassic and there seems little reason to suspect that the Monteith differs greatly in age from that of the type region. The upper Minnes succession (Beattie Peaks, Monach, and Bickford formations) of Carbon Creek basin range in age from the late (latest?) Berriasian zone of **B. uncitoides** or early Valanginian Zone of **Tollia tolli** to the mid- to late Valanginian zone of **B.** n. sp. aff. **B. inflata** (see Stott, 1975a). It seems likely that the Gorman Creek Formation, which appears to be equivalent of the upper Minnes of Carbon Creek, is also of early to late Valanginian age. The overlying Bullhead Group is not well dated but lies below beds within the Early Albian **Arcthoplites** Zone. There is some indication that beds within the Gething Formation may be Aptian in age and that the underlying Cadomin conglomerate may be as old as Barremian.

Ziegler and Pocock (1960) suggested, on the basis of palynological data, that the upper 1158.2 m of the Minnes at the type section was possibly correlative with the Quartz Sand Member of the Alberta Plains, which they stated to be of Barremian age. They also indicated, by similar correlation with the Deville Member, that the lower part of the section (herein assigned to the Monteith) was possibly Berriasian to Valanginian in age. However, Singh (1965), also using palynological evidence, dated the Deville and Ellerslie (Quartz Sand Member) as Barremian-Aptian and correlated them with Gething and Cadomin formations, which overlie the Minnes Group. Thus the palynological evidence from the Minnes remains questionable.

If the Minnes Group is no younger than Valanginian, and if the Bullhead Group is indeed as old as Barremian, then the erosional unconformity separating these two groups represent an interval of time that ranges from latest Valanginian through Hauterivian to earliest Barremian.

The Gorman Creek Formation is equivalent of the Beattie Peaks, Monach and Bickford formations of the Carbon Creek basin to the north. Farther south, the basal Nikanassin beds in the Foothills of the Athabasca area lie within the Jurassic Kimmeridgian to Portlandian Zone of **Buchia mosquensis** and most or all of the Nikanassin may be older than the type Gorman Creek. In the central and southern Foothills of Alberta and particularly in the Fernie basin of southwestern British Columbia, some of the upper Kootenay Group (see Gibson, 1979) may be of Cretaceous age and could be equivalent to some part of the Gorman Creek. In the subsurface of the Plains to the east, beds between the Fernie and Cadomin formations are generally assigned to the Nikanassin Formation. The pre-Bullhead unconformity truncates those beds and only the lower, if any, part of the Gorman Creek and the older Monteith Formation may be represented.

Acknowledgments

The author is indebted to a great many people who, over a period of more than 20 years, have assisted him and contributed to the study of Lower Cretaceous rocks. Many of these individuals have been acknowledged in previous publications. Once again, the major contribution made by J.A. Jeletzky in identifying, dating and correlating Late Jurassic and Early Cretaceous fossils is deeply appreciated. The generosity in 1980 of Utah Mines Limited and Denison Mines Limited allowed the writer to review several localities critical to this report. Discussions concerning stratigraphy, palynology, and coal rank with D.W. Gibson, W.D. Kalreuth, A.R. Sweet, and N.S. Ioannides have been most helpful.

References

Gibson, D.W.
1979: The Morrissey and Mist Mountain Formations – newly defined lithostratigraphic units of the Jura-Cretaceous Kootenay Group, Alberta and British Columbia; Bulletin, Canadian Petroleum Geology, v. 27, no. 2, p. 183-208.

Gilchrist, R.D.
1979: Burnt River area (93O/4,5); Geological Fieldwork, 1978; British Columbia, Ministry of Energy, Mines and Petroleum Resources, Paper 1979-1, p. 79-83.

Hamblin, A.P. and Walker, R.G.
1979: Storm-dominated shallow marine deposits: the Fernie-Kootenay (Jurassic) transition, southern Rocky Mountains; Canadian Journal of Earth Sciences, v. 16, no. 9, p. 1673-1690.

Hughes, J.E.
1964: Jurassic and Cretaceous strata of the Bullhead succession in the Peace and Pine River Foothills; British Columbia Department of Mines and Petroleum Resources, Bulletin 51, 73 p.
1967: Geology of the Pine Valley, Mount Wabi to Solitude Mountain, northeastern British Columbia; British Columbia Department of Mines and Petroleum Resources, Bulletin 52, 137 p.

Irish, E.J.W.
1965: Geology of the Rocky Mountain Foothills, Alberta (between latitudes 53°15' and 54°15'); Geological Survey of Canada, Memoir 33[illegible], 228 p.
1970: Halfway River, British Columbia; Geological Survey of Canada, Paper 69-11, 154 p.

Jansa, L.
1972: Depositional history of the coal bearing Upper Jurassic – Lower Cretaceous Kootenay Formation, southern Rocky Mountains, Canada; Geological Society of America, Bulletin, v. 83, no. 11, p. 3199-3222.

MacKay, B.R.
1929: Brûlé mines coal area, Alberta; Geological Survey of Canada, Summary Report 1928, pt. B, p. 1-29.
1930: Stratigraphy and structure of bituminous coalfields in the vicinity of Jasper Park, Alberta; Canadian Institute of Mining and metallurgy, Transactions, v. 33, p. 473-509.

Mathews, W.H.
1947: Geology and coal resources of the Carbon Creek – Mount Bickford map-area, 1946: British Columbia Department of Mines, Bulletin 24, 27 p.

McLearn, F.H.
1918: Peace River section, Alberta; Geological Survey of Canada, Summary Report 1917, pt. C, p. 14-21.
1923: Peace River Canyon coal area, B.C.; Geological Survey of Canada, Summary Report 1922, pt. B, p. 1-46.
1940: Notes on the geography and geology of the Peace River Foothills; Royal Society of Canada, Transactions, 3rd series, v. 26, sec. 4, p. 157-175.

McLearn, F.H. and Kindle, E.D.
1950: Geology of northeastern British Columbia; Geological Survey of Canada, Memoir 259, 236 p.

Mountjoy, E.W.
1960: Miette, Alberta; Geological Survey of Canada, Map 40-1959.
1962: Mount Robson (southeast) map-area, Rocky Mountains of Alberta and British Columbia (83 E/SE); Geological Survey of Canada, Paper 61-31, 114 p.

Muller, E.
1961: Pine Pass, British Columbia; Geological Survey of Canada, Map 11-1961.

Singh, Chaitanya
1964: Microflora of the Lower Cretaceous Mannville Group, East-Central Alberta; Research Council of Alberta, Bulletin 15, 239 p.

Springer, G.D., MacDonald, W.D. and Crockford, M.B.B.
1964: Jurassic; Chapter 10 in Geological History of Western Canada, McCrossan, R.G. and Glaister, R.P. (eds.), Alberta Society of Petroleum Geologists, Calgary, p. 137-155.

Stott, D.F.
1961: Dawson Creek map-area, British Columbia; Geological Survey of Canada, Paper 61-10, 32 p.

1962: Cretaceous rocks of the Peace River Foothills, British Columbia, Edmonton Geological Society, Fourth Annual Guidebook, p. 22-45.

1967: The Fernie and Minnes strata north of Peace River, Foothills of northeastern British Columbia; Geological Survey of Canada, Paper 67-19, pt. A, 58 p.

1968: Lower Cretaceous Bullhead and Fort St. John Groups, between Smoky and Peace Rivers, Rocky Mountain Foothills, Alberta and British Columbia; Geological Survey of Canada, Bulletin 152, 279 p.

1969: Fernie and Minnes strata north of Peace River, Foothills of northeastern British Columbia; Geological Survey of Canada, Paper 67-19, pt. B, 132 p.

1974: Lower Cretaceous Bullhead Group between Bullmoose Mountain and Tetsa River, Rocky Mountain Foothills, northeastern British Columbia; Geological Survey of Canada, Bulletin 219, 228 p.

Stott, D.F. (cont.)
1975a: The Cretaceous System in northeastern British Columbia; in The Cretaceous System in the Western Interior of North America, W.G.E. Caldwell (ed.); The Geological Association of Canada, Special Paper 13, p. 441-467.

1975b: Dawson Creek map-area, Monkman Pass map-area, Pine Pass map-area, British Columbia; Wapiti map-area, Alberta; Geological Survey of Canada, Open File Report 286.

Lower Cretaceous Fort St. John Group and Upper Cretaceous Dunvegan Formation, Foothills and Plains, Alberta, British Columbia, District of Mackenzie and Yukon Territory; Geological Survey of Canada, Bulletin 328. (in press)

Stott, D.F. and Gibson, D.W.
1980: Minnes Coal, northeastern British Columbia; in Current Research Part C, Geological Survey of Canada, Paper 80-1C, p. 135-137.

Taylor, G.C. and Stott, D.F.
1979: Monkman Pass (93I) map-area, northeastern British Columbia; Geological Survey of Canada, Open File Report 630.

Ziegler, W.H. and Pocock, S.A.J.
1960: The Minnes Formation; Edmonton Geological Society, Second Annual Field Conference Guidebook, p. 43-71.

APPENDIX

Section 80-1 Bickford Formation, Mount Bickford, Pine Pass map-area, British Columbia, 55°37'N, 122°26'W. Along ridge west of main peak. Measured in metres and converted to feet

Unit	Description	Thickness		Height above base	
		feet	metres	feet	metres
	Measurement begins at base of Cadomin Formation on south side of ridge.				
	Cadomin Formation				
	Sandstone, medium- to coarse-grained, grey, massive; beds, pods and lenses of conglomerate, cross-bedded laminated; pebbles 1/8-3/4"				
	MINNES GROUP				
	Bickford Formation				
44	Covered	122	40	1060.4	347.9
43	Sandstone, fine grained, brownish grey, laminated, brownish grey weathering; platy to flaggy, crossbedded	79	24	938.5	307.9
42	Covered	49	15	865.3	283.9
41	Sandstone, fine grained, laminated, brownish grey, brownish grey weathering; platy to flaggy, crossbedded	8	2.5	819.6	268.9
40	Covered	9.1	3	812.0	266.4
39	Sandstone, fine grained, grey to brownish grey, laminated, brownish grey weathering; platy to flaggy, crossbedded	7.3	2.4	802.8	263.4
38	Covered	15.2	5	795.5	261.0
37	Sandstone, as above, grey weathering	3.0	1	780.3	256.0
38	Covered	18.3	6	777.2	255.0
35	Sandstone, very fine grained, brown weathering, laminated, crosslaminated; platy	3.4	1.1	759.0	249.0
34	Mostly covered. Two small intervals of sandstone, as above	115.8	38	755.6	247.9
33	Sandstone, fine grained, brownish grey calcareous, laminated, crosslaminated; brownish grey weathering; platy to flaggy, massive appearance; strong crossbedding	24.4	8	639.8	209.9
32	Covered	15.2	5	615.4	201.9
31	Sandstone, as above	3.0	1	600.1	196.9
30	Covered. Some platy sandstone, as above	27.4	9	597.1	195.9

		Thickness		Height above base	
Unit	Description	feet	metres	feet	metres
29	Sandstone, very fine grained, brown laminated, crosslaminated; platy to flaggy; partly covered at base	21.3	7	569.7	186.9
28	Sandstone, fine grained, brownish grey, grey to brownish grey weathering; medium bedded, massive appearance	31.7	10.4	548.3	179.9
27	Sandstone, fine grained, brown, laminated crosslaminated, orange-brown to brown weathering; platy, crossbedded	7.6	2.5	516.6	169.5
26	Mostly covered. Appears to be brown mudstone with few thin carbonaceous intervals; some sandstone	25.9	8.5	509.0	167.0
25	Sandstone, fine grained, brown, calcareous, laminated, brownish grey weathering; platy to flaggy	29.0	9.5	483.1	158.5
24	Mudstone, brown, carbonaceous; interbedded sandstone, very fine grained, laminated, orange weathering, crosslaminated; thin coaly beds.	12.2	4	454.1	149.0
23	Sandstone, fine grained, brown, brown weathering, laminated, crosslaminated; flaggy	3.0	1	442.0	145.0
22	Mudstone, brownish grey, silty, hard; grading into overlying sandstone	6.1	2	438.9	144.0
21	Sandstone, very fine grained, laminated, crosslaminated, brown to orange-brown weathering; crossbedded; worm markings	9.1	3	432.8	142.0
20	Mudstone, platy, hard; interbedded sandstone (40%), very fine grained, laminated, brown weathering	27.4	9	423.7	139.0
19	Mudstone, brown, silty, carbonaceous; some thin sandstone, very fine grained, laminated; thin coal beds, partly covered	50.3	16.5	396.2	130.0
18	Covered	15.2	5	345.9	113.5
17	Sandstone, very fine grained, laminated, brown weathering; platy, crosslaminated	13.7	4.5	330.7	108.5
16	Mudstone, grading upward into sandstone, partly covered	13.7	4.5	317.0	104.0
15	Sandstone, very fine grained, laminated, crosslaminated, brown weathering, platy; dolomitic siltstone in middle, orange weathering; large plant fragments; worm burrows	13.7	4.5	303.3	99.5
14	Mudstone, with coaly intervals, partly covered	13.7	4.5	289.6	95.0
13	Sandstone, very fine grained, brownish grey, laminated, crosslaminated; platy to flaggy; orange-brown weathering; interbedded mudstone, 30%	27.4	9	275.8	90.5

Unit	Description	Thickness feet	Thickness metres	Height above base feet	Height above base metres
12	Mudstone; interbedded sandstone; coaly intervals, partly covered, recessive	38.1	12.5	248.4	81.5
11	Sandstone, brownish grey, laminated, brownish grey, flaggy; topped by grey weathering sandstone with ripple marks	35.0	11.5	210.3	69.0
10	Mostly covered, recessive; brown mudstone at top	15.3	5	175.3	57.5
9	Sandstone, fine grained, brownish grey, laminated, grey weathering; flaggy to thin bedded, worm burrows; not well exposed and recessive at base	35.0	11.5	160.0	52.5
8	Partly covered, recessive at base; sandstone in upper part with recessive intervals	21.3	7	125.0	41.0
7	Sandstone, very fine grained, laminated, crosslaminated, brown weathering; platy; thin silty intervals; some silty mudstone at base	12.2	4	103.6	34.0
6	Sandstone, fine grained, brownish grey, laminated, crosslaminated, brown weathering, calcareous; crossbedded, platy to flaggy	10.7	3.5	91.4	30.0
5	Mudstone, black, silty, hard; interbedded, laminated sandstone	18.3	6	80.8	26.5
4	Sandstone, fine grained, grey weathering; thin bedded	4.6	1.5	62.5	20.5
3	Mudstone, black to brown; some hard siltstone	13.7	4.5	57.9	19.0
2	Sandstone, very fine grained, laminated, orange-brown weathering	3.0	1	44.2	14.5
1	Mudstone, silty, dark grey to black, and brownish grey; some interbedded siltstone and sandstone	41.1	13.5	41.1	13.5
	MONACH FORMATION				
	large dip slope of sandstone				

2.

THE ANNIEOPSQUOTCH OPHIOLITE BELT, SOUTHWEST NEWFOUNDLAND

Project 770026

G.R. Dunning[1]
Precambrian Geology Division

Dunning, G.R., The Annieopsquotch ophiolite belt, Southwest Newfoundland; in *Current Research, Part B, Geological Survey of Canada, Paper 81-1B, p. 11-15, 1981.*

Abstract

The Annieopsquotch ophiolite belt is composed of five massifs forming a line trending northeast from King George IV Lake to a point north of Shanadithit Brook. They are composed of various portions of oceanic crust and face southeast. In the south the ophiolites occur at the boundary between granitic and gneissic rocks to the northwest, and volcanic rocks of the Ordovician Victoria Lake group, to the southeast, and may mark the edge of the ancient North American continent. The northern massifs are surrounded by younger rocks.

Mafic volcanics of the Annieopsquotch ophiolite are in fault contact with bedded cherts which in turn are in fault contact with pyroclastics of the Victoria Lake group. This sequence is interpreted to be a structurally modified stratigraphic succession. Faults and penetrative cleavage affect the ophiolitic volcanics and the Victoria Lake group.

Several gabbro and diorite bodies with distinctive magnetic expressions were emplaced into the Annieopsquotch ophiolite and Victoria Lake group after deformation.

Introduction

Mapping in 1977 and 1978 in the Puddle Pond area (NTS 12A/5) revealed the presence of a previously undescribed ophiolite complex in the Annieopsquotch Mountains of southwest Newfoundland (Herd and Dunning, 1979). In 1979 the Annieopsquotch ophiolite was mapped in detail and ophiolitic fragments were identified at Star Lake, Padille Pond, Puddle Pond and south of Little Grand Lake (Dunning and Herd, 1980). Mapping in 1979 by company geologists revealed the presence of another massif of ophiolitic affinity south of King George IV Lake (Sterenberg, personal communication, 1979). These ophiolites define a belt trending northeast through west central Newfoundland parallel to the Lloyds River and Red Indian Lake, northwest of the Victoria Lake group metavolcanic belt (Fig. 2.1, 2.2).

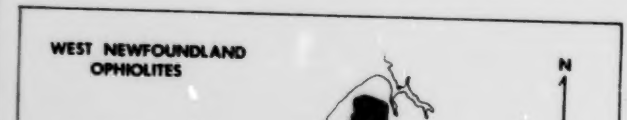
WEST NEWFOUNDLAND
OPHIOLITES
N
0
25
50
Km
BAY OF ISLANDS
Grand Lake
GLOVER I. COMPLEX
Victoria Lake
ANNIEOPSQUOTCH OPHIOLITE BELT
Area of figure 22
LONG RANGE COMPLEX

Figure 2.1. *The Annieopsquotch ophiolite belt and other ophiolite complexes of western Newfoundland.*

During the 1980 field season, mapping of the Annieopsquotch ophiolite and sampling for geochemistry was continued and the Victoria Lake group was examined in greater detail. The Star Lake ophiolite (in NTS map area 12A/11) was mapped in detail and the sheeted dyke zone of the King George IV Lake ophiolite was examined. Reconnaissance mapping of two hills north of Shanadithit Brook determined that they are ophiolitic fragments

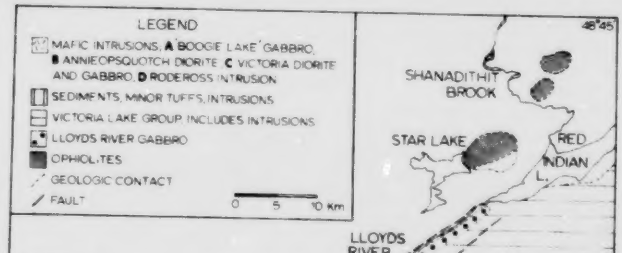
LEGEND
MAFIC INTRUSIONS, A 'BOOGIE LAKE' GABBRO, B ANNIEOPSQUOTCH DIORITE, C VICTORIA DIORITE AND GABBRO, D RODEROSS INTRUSION
SEDIMENTS, MINOR TUFFS, INTRUSIONS
VICTORIA LAKE GROUP, INCLUDES INTRUSIONS
LLOYDS RIVER GABBRO
OPHIOLITES
GEOLOGIC CONTACT
FAULT
0
5
10 Km
48°45'
SHANADITHIT BROOK
STAR LAKE
RED INDIAN L.
LLOYDS RIVER
ROUTE 480
LLOYDS LAKE
VICTORIA LAKE
HOWLEY WATERS
48°15'
KING GEORGE IV LAKE
48°15'
GRANITE LAKE
58°00'
57°00'

Figure 2.2. *The Annieopsquotch ophiolite belt, southwestern Newfoundland. General geology after Kean (1977), Dunning and Herd (1980) and Kean and Jayasinghe (1981).*

---

[1] Department of Geology, Memorial University of Newfoundland, St. John's, Newfoundland A1B 3X5

(Fig. 2.2). Several gabbro and diorite bodies in the region were examined to determine whether or not they are of ophiolitic affinity.

Petrological, geochemical and geochronological studies of the Annieopsquotch ophiolite and volcanics of the adjacent Victoria Lake group are in progress as part of the author's Ph.D. thesis program at Memorial University.

Access

Some mapping was done from the Burgeo Road (Route 480), which passes between the Annieopsquotch and King George IV Lake ophiolites, but most was done from flycamps and supported by helicopter or floatplane service from Pasadena.

Annieopsquotch Ophiolite Complex

Further work on the Annieopsquotch ophiolite concentrated on the gabbro at the stratigraphic base in the southwest corner and on contact relationships with the Victoria Lake group.

Gabbro

Coarse grained gabbro is present up to the eroded basal edge of the ophiolite in the southwest corner, in contrast to the central area where layered ultramafic rocks thought to represent MOHO lithologies occur (Dunning and Herd, 1980). The basal gabbros are locally well layered as they are throughout the basal part of the complex. The layering is due to changes in the plagioclase:clinopyroxene ratio. Minor olivine is often present and, in thin section, coronas of colourless amphibole, green spinel + (rarely) orthopyroxene commonly separate olivine from plagioclase. Alteration of clinopyroxene to fine fibrous actinolite is moderate to complete. Brown hornblende, in minor amounts, occurs rimming clinopyroxene in some gabbros. This is interpreted to be a late primary crystallization product.

A large sill, 0.3 km wide by 1.3 km long, intrudes the northwest edge of the mountains. It is fresher than the host gabbro and varies from cumulate mafic troctolite at its base to subophitic olivine gabbro at the top. Serpentinization and formation of secondary magnetite in the sill along with interstitial oxide in the host gabbro probably accounts for the magnetic high over this portion of the ophiolite (GSC Map 250G). The extension of this magnetic high to the southwest suggests that the sill may extend in that direction in the subsurface.

Ophiolite-Victoria Lake Group Contact Relationships

The contact between the Annieopsquotch ophiolite and Victoria Lake group is nowhere exposed. It occurs in low bog or heavily wooded ground northwest of Victoria Lake. At locality 1, west of the south end of Victoria Lake (Fig. 2.2), mafic flows are separated from steeply dipping, thinly bedded pale and dark grey cherts by a minor fault scarp which borders an elongate bog. These cherts, interpreted to mark the top of the ophiolitic volcanic sequence are structurally overlain to the southeast by sheared intermediate to felsic tuffs of the Victoria Lake group. While the stratigraphic sequence is not preserved intact as first suggested (Herd and Dunning, 1979), the lithologies present are interpreted to be in their original relative positions, though now faulted and sheared. The degree of deformation is greater in the tuffs and sediments of the Victoria Lake group than in the Annieopsquotch ophiolite. This probably reflects: (1) the closer proximity of the former to the major fault parallel to the south shore of Victoria Lake, and (2) the greater competence of the basaltic flows of the ophiolite. In general the ophiolite behaved as a rigid block during the deformation which affected the Victoria Lake group. However, pillow lava at the top of the ophiolitic sequence is cut by major and minor fault zones (most of which have topographic expression) and has a penetrative cleavage especially near the faults. Locally, along minor faults, chlorite schist has formed, the only evidence for its protolith being rafts of undeformed interpillow red chert floating in the schist.

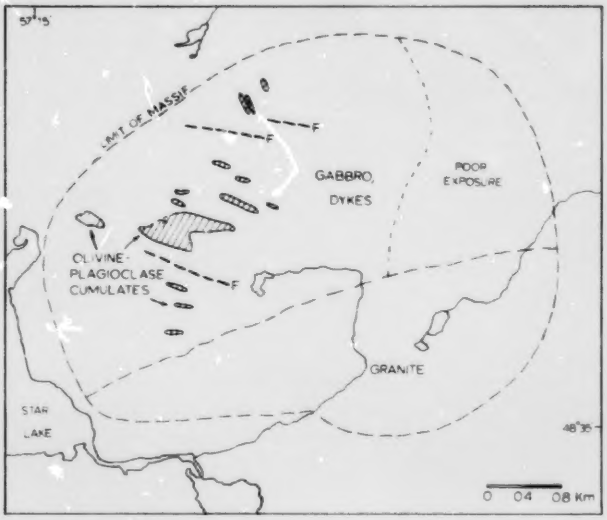

Figure 2.3. Preliminary geological map of the Star Lake ophiolite.

In Wigwam Brook (informal name), locality 2 (Fig. 2.2) at the west edge of the Victoria Lake area (NTS 12A/6), the same general sequence is seen as at locality 1. Mafic volcanics occur approximately 1.5 km north of Victoria Lake. To the southeast, a zone with no exposure separates these lavas from mafic and intermediate tuffs which contain a sequence of bedded grey cherts identical in hand specimen and outcrop to those at locality 1. Cherts in Wigwam Brook are folded and overturned to the northwest towards the ophiolite.

Victoria Lake Group

To the south of the bedded chert unit, which is 3 to 5 m thick, andesite, quartz- and feldspar-rich dacite, and rhyolite tuffs occur. Tuffaceous crystal-rich sandstones, some showing graded beds, as well as pyrite-bearing graphitic shale occur interbedded with the tuffs. In Wigwam Brook these tuffaceous sediments are strongly deformed, some display ptygmatic folds and are cut by many minor faults between which the beds strike in divergent directions. Thin lenses and beds of rusty-weathering carbonate up to 7 m long occur in the tuffaceous sediments in Wigwam Brook.

On a regional scale, deciphering the geology of the Victoria Lake group is made difficult by limited outcrop, rapid facies changes and isoclinal folding and faulting. For the latter reasons it is likely that the map pattern (Kean, 1977) showing several parallel black shale horizons, for example, is due to repetition of one or two units. Basaltic flows, gabbro sills, intermediate agglomerate + sills + rhyolite flows of the Victoria Lake group have been sampled for geochemical analysis to test the hypothesis that they are related to dykes and lavas of the Annieopsquotch ophiolite.

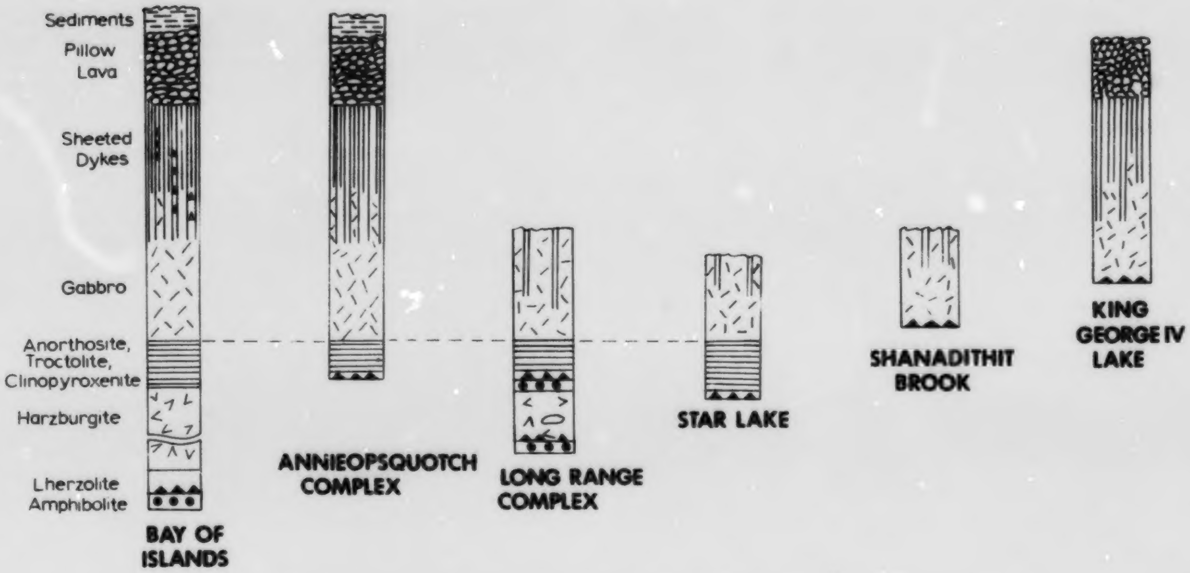

Figure 2.4. *Schematic cross sections of west Newfoundland ophiolites. Thicknesses uncertain as some lithological units are separated by faults. Bay of Islands complex modified from Malpas and Strong (1975); Annieopsquotch complex after Dunning and Herd (1980); Long Range complex after Brown (1976); King George IV Lake ophiolite after Kean and Jayasinghe (1981).*

Star Lake Ophiolite

According to the Geological Society of America's Penrose conference definition (Anonymous, 1972) the massifs described below are 'ophiolitic fragments' rather than ophiolites because they do not preserve the entire stratigraphic section from mantle peridotites to lavas + sediments.

Layered Series

A massif northeast of Star Lake with 230 m of relief (Fig. 2.2), composed of mafic plutonic rocks, was identified as being the basal portion of an ophiolite complex (Dunning and Herd, 1980). Mapping during 1980 revealed that its northwest side is composed of coarse grained gabbro similar to that of the Annieopsquotch ophiolite but containing several large bodies of olivine-rich rocks, some with cumulate textures, ranging from felsic dunite through troctolite and olivine gabbro to anorthosite. These rocks display igneous layering, trough structures, slump folds and graded beds similar to those seen in the layered series of the Annieopsquotch ophiolite. However, at Star Lake these bodies are relatively narrow and elongate like sills but are oriented in a northwest-southeast direction and appear to pinch out to the southeast (stratigraphic top). The igneous layers in these bodies strike the same direction and are steeply dipping. Some patches of fine grained mafic granulite are present near the layered rocks, as they are in the Annieopsquotch ophiolite.

Gabbro

The rest of the massif is composed of coarse grained gabbro, which is fairly homogeneous and contains small pods of coarse grained white-weathering trondhjemite. These are cut by diabase dykes and irregular anastomosing masses of diabase which increase in number towards the east. Rocks on the east side appear to be the same as those of the transition zone of the Annieopsquotch ophiolite. They represent the highest stratigraphic level present in the Star Lake ophiolite as the east side is cut off by a Devonian(?) granitic intrusion (Kean, 1978).

Shanadithit Ophiolite

Two massifs previously mapped as gabbro and diorite with minor diabasic phases (Kean, 1978) are present north of Shanadithit Brook (Fig. 2.2). They are each slightly smaller in area than the Star Lake body, but like the latter are significant topographic highs with eroded peneplain tops and considerable outcrop, in marked contrast to the surrounding low, lake- and bog-filled ground. During the 1980 field season only a reconnaissance examination was made of these bodies; they consist of coarse grained gabbro intruded by diabase dykes and cut by amphibolite shear zones. The easternmost part of these bodies was not examined so a higher stratigraphic level may be preserved if they are oriented the same way as the other ophiolites. So far, only rocks typical of the gabbro zone have been identified.

A considerable area around the Shanadithit ophiolite is shown on previous geological maps (Riley, 1957; Kean, 1978) to be the same unit as the ophiolite. The larger area is of low relief and much less well exposed. Further work will be required to determine whether or not it is of ophiolitic affinity.

King George IV Lake Ophiolite

This body forms a relatively flat-topped massif 100 m high on the south shore of King George IV Lake. It occupies essentially the area described by Riley (1957) as massive to pillowed andesite and basalt, basic tuff and agglomerate. The outline of the ophiolite shown in Figure 2.2 is taken from Kean and Jayasinghe (1981) who identified several fault-bounded blocks consisting predominantly of gabbro, sheeted dykes or pillow lava. A narrow zone of mafic lava + tuff, tentatively correlated with the Victoria Lake group by Kean and Jayasinghe (1981) occurs wedged between blocks of sheeted dykes and pillow lava. The author has examined only the zones of sheeted dykes and mafic lava + tuff. Both zones have about 10 to 15 per cent outcrop exposure.

Sheeted Dykes

Within the sheeted dyke zone, dykes trend roughly north-south to northwest-southeast as they do in the nearby Annieopsquotch ophiolite. They vary from 0.3 m to several metres in width and have well developed chilled margins which often weather in relief. In the eastern fault-bounded block of sheeted dykes dips are shallow; in the other block dykes are steeply dipping. Three types of dykes have been recognized and these also occur in the Annieopsquotch ophiolite: (1) red-weathering picritic(?) dykes which strike at a high angle to the diabase dykes and contain plagioclase and chrome-diopside phenocrysts; (2) plagioclase porphyritic diabase dykes; and (3) aphyric diabase dykes. No intermediate or felsic dykes were observed.

Faults breaking up the zone are marked by cliffs, hematized shear zones and alteration veinlets. Albite-epidote veinlets are common, crosscutting the dykes and occasionally concentrated along dyke margins.

Lava-Tuff Zone

This narrow unit is exposed in small whaleback outcrops and in a series of ledges along the southern fault zone. It is composed of mafic flows, which pass into mafic tuffs to the south, then into basalt flows, locally sheared and hematized along the fault zone itself. Some of the basalts contain abundant nearby spherical calcite-filled amygdules.

Lloyds River Gabbro

This elongate body, exposed in hills on the south side of Lloyds River between Lloyds Lake and Red Indian Lake, is strongly sheared and altered, presumably by deformation along the Lloyds River fault zone. In some outcrops coarse grained gabbro is preserved and several diabase dykes that cut the gabbro were seen. Epidote alteration veinlets are common and most of the gabbro appears bleached, probably due to albitization of feldspars.

This body may be ophiolitic but gabbro sills are present in the Victoria Lake group and this could be a larger sill related to the adjacent volcanics.

Intrusive Mafic Rocks in the Region

'Boogie Lake' Gabbro

The 'Boogie Lake' gabbro occurs between the King George IV Lake and Annieopsquotch ophiolites forming a series of hills west of route 480 and lakeshore outcrops south of the Annieopsquotch ophiolite (Fig. 2.2). It occupies essentially the same area as the diorite body identified by Riley (1957). The main lithologies are gabbro, diorite, diabase and granite, the latter occurring as irregular small bodies and dykes in the mafic lithologies. Diabase dykes of the suite also cut the granitic phase and locally it appears that mafic and felsic liquids coexisted. A large portion of the mafic rocks have a well developed, coarse grained subophitic texture and the suite bears a strong resemblance to that described by Carew (1979) from the northeast corner of the Main Gut area (NTS 12B/8).

The 'Boogie Lake' gabbro appears on the regional scale to be intrusive but no definite intrusive contacts have been observed. It is little deformed, being affected primarily by late faulting. Both it and the Main Gut area intrusion are located near major faults, the Lloyds River (Cape Ray) and Long Range (Cabot) faults respectively.

Annieopsquotch Diorite

A hornblende diorite intrusion, roughly circular in outline and several kilometres in diameter, intrudes sheeted dykes and pillow lava at the east end of the ophiolite. It is marked on GSC aeromagnetic map 250G by a series of approximately circular magnetic high anomalies. The diorite is significantly fresher than rocks of the ophiolite complex and has a discontinuous zone of hypersthene and augite-bearing hornfels surrounding it. Brown hornblende poikilo blasts also occur overgrowing the granular pyroxenes.

Granodiorite, apparently a felsic differentiate of the intrusion, contains variable amounts of hornblende and biotite. It occurs in an irregular pattern and is cut by quite fresh undeformed, though faulted, diabase dykes. These late dykes are the youngest igneous rocks so far recognized in the Annieopsquotch Mountains proper. They may be related to diabase dykes cutting the Victoria Lake group on the north shore of Victoria Lake.

Other Mafic Intrusions

Several other mafic intrusions in the Victoria Lake area (Kean, 1977) were examined to compare them to those described above and to ophiolitic gabbros.

Two intrusions on the south shore of Victoria Lake at the entrance to Howley Waters (Fig. 2.2), one gabbroic, the other primarily composed of diorite, intrude sediments overlying the Victoria Lake group. They are entirely undeformed but their age is not known. The diorite locally contains large hornblende crystals and appears similar to the Annieopsquotch diorite.

The Rodeross Lake intrusion was examined because of its reported similarity to olivine-rich rocks of the layered series of the ophiolite. However, troctolite and olivine gabbro of this body are perfectly fresh and undeformed. No definite intrusive relationships were seen with the surrounding sediments, probably due to very limited outcrop. The Rodeross intrusion is undeformed and might be as young as Jurassic as suggested by Kean (1977). All three intrusions just described have strong circular magnetic anomalies on GSC Map 249G.

Discussion and Conclusions

The Annieopsquotch ophiolite belt consists of five massifs along a line from King George IV Lake to a point 20 km southwest of Buchans. The southern King George IV Lake and Annieopsquotch ophiolites occur in contact with the western margin of the Victoria Lake group but, to the north, the Star Lake and Shanadithit ophiolites have been isolated by later granitic intrusions.

The Annieopsquotch ophiolite is complete from layered olivine-plagioclase cumulates, thought to represent MOHO lithologies, to mafic pillow lava and bedded chert. The other massifs are ophiolitic fragments (Fig. 2.4). The King George IV Lake ophiolite comprises mainly the upper volcanic portion of oceanic crust and the northern bodies the basal plutonic section. No mantle ultramafics have been identified from any of the five massifs suggesting that oceanic crust was systematically separated from the mantle during emplacement. All five massifs appear to face southeast and have their lowermost units exposed in cliffs facing northwest; these are MOHO lithologies, gabbro or sheeted dykes. No basal mélange or metamorphic aureole lithologies have been identified but the base of each massif is obscured by talus slopes, bog or lake.

Edge of the Ordovician North American Continent

As a first approximation, all ophiolites in the belt appear to be transported about the same distance as they all occur in a line parallel to the regional Appalachian trend. The Annieopsquotch ophiolite separates gneissic and granitic rocks to the northwest from volcanic rocks to the southeast. The line between the ophiolite and the gneissic terrane may mark the surface trace of the eastern margin of the North American continent in Ordovician time. The presence of a granite intruding the stratigraphic top of the ophiolite (Dunning and Herd, 1980) indicates that continental crust probably underlies all of the Annieopsquotch ophiolite. Indeed, it is likely that the entire southern portion of the central volcanic belt is underlain by continental crust.

Ophiolitic and other volcanic rocks are found on Glover Island (Knapp et al., 1979; Fig. 1) well to the west of the Star Lake ophiolite and the stratigraphy there is comparable to that along the Baie Verte lineament. It may be that the surface trace of the continental margin takes a major jog to the east, south of Grand Lake as suggested by our mapping and shown by Colman-Sadd (1980).

Acknowledgments

I am grateful to M. Best for providing cheerful assistance in the field despite experiencing one of the coldest and rainiest Newfoundland 'summers' on record. Thanks to R.K. Herd for administrative, logistical and moral support and to B.F. Kean, T. Krogh, J. Malpas, R. Smyth, D.F. Strong, and H. Williams for discussions in the field.

Viking Helicopters Nfld. Ltd. and Newfoundland Air Transport provided efficient air support and Environment Canada provided base camp facilities at the Newfoundland Forest Research Centre in Pasadena. The assistance and hospitality of P. Lassila and others of Hudson's Bay Oil and Gas Company is gratefully acknowledged.

R.M. Easton, R.K. Herd and K.L. Currie read drafts of the manuscript and suggested improvements.

References

Anonymous
1972: Penrose field conference on ophiolites. Geotimes, v. 17, p. 24-25.

Brown, P.A.
1976: Ophiolites in south-western Newfoundland; Nature (London), v. 264, p. 712-715.

Carew, W.
1979: A layered appinitic intrusion in southwest Newfoundland: A field, petrographical and geochemical investigation; unpublished B.Sc. thesis, Memorial University of Newfoundland, 53 p.

Colman-Sadd, S.P.
1980: Geology of south-central Newfoundland and evolution of the eastern margin of Iapetus; American Journal of Science, v. 280, p. 991-1017.

Dunning, G.R. and Herd, R.K.
1980: The Annieopsquotch ophiolite complex, southwest Newfoundland, and its regional relationships; in Current Research, Part A, Geological Survey of Canada, Paper 80-1A, p. 227-234.

Herd, R.K. and Dunning, G.R.
1979: Geology of Puddle Pond map area, southwestern Newfoundland; in Current Research, Part A, Geological Survey of Canada, Paper 79-1A, p. 305-310.

Kean, B.F.
1977: Geology of the Victoria Lake map area (12A/6), Newfoundland; Mineral Development Division, Newfoundland Department of Mines and Energy, Report 77-4.

1978: Geology of the Star Lake east half sheet (12A/11E), Newfoundland; in Report of Activities for 1977, Mineral Development Division, Newfoundland Department of Mines and Energy, Report 78-1, p. 129-134.

Kean, B.F. and Jayasinghe, N.R.
1981: Geology of the King George IV (sic) map area (12A/4), Newfoundland; in Current Research, Mineral Development Division, Newfoundland, Department of Mines and Energy, Report 81-1, p. 32-39.

Knapp, D., Kennedy, D., and Martineau, Y.
1979: Stratigraphy, structure and regional correlation of rocks at Grand Lake, western Newfoundland; in Current Research, Part A, Geological Survey of Canada, Paper 79-1A, p. 317-325.

Malpas, J. and Strong, D.F.
1975: A comparison of chrome-spinels in ophiolites and mantle diapirs of Newfoundland; Geochimica et Cosmochimica Acta, v. 39, p. 1045-1060.

Riley, G.C.
1957: Red Indian Lake (west half), Newfoundland; Geological Survey of Canada, Map 8-1957.

3.

TERTIARY SUBSURFACE CORRELATIONS USING PYRITIZED DIATOMS, OFFSHORE EASTERN CANADA

Project 740004

F.C. Thomas and F.M. Gradstein
Atlantic Geoscience Centre, Dartmouth

Thomas, F.C. and Gradstein, F.M., Tertiary subsurface correlations using pyritized diatoms, offshore Eastern Canada; in Current Research, Part B, Geological Survey of Canada, Paper 81-1B, p. 17-23, 1981.

Abstract

Ditch cutting samples from 16 offshore wells in Eastern Canada have been analyzed for the presence of pyritized diatoms. Four different species, all informally assigned to the genus ***Coscinodiscus*** *and designated* ***C.*** *spp. 1, 2, 3 and 4 are described and illustrated, with comparison to descriptions in European literature.*

Numerical peaks of diatoms occur in Labrador Shelf and Grand Banks well at various stratigraphic levels, and are composed largely of ***C.*** *spp. 1, 3 and 4. No abundance peaks are present in wells on the Scotian Shelf.*

Some conclusions regarding these peaks are as follows: On the Labrador Shelf ***Coscinodiscus*** *spp. 3 and 4 occur abundantly below the Middle Eocene while above this* ***C.*** *sp. 1 is generally the most common form. In the northern Grand Banks area two distinct frequency peaks occur at different stratigraphic levels. In the southern Grand Banks and Scotian Shelf areas, diatoms are much less common in Tertiary strata. The Late Paleocene-Early Eocene abundance peak of* ***C.*** *spp. 3 and 4 noted in Labrador Shelf and Grand Banks wells is also present in strata of similar age in various northern European localities. Peaks of diatom abundance occur in sediments from both bathyal and neritic environments.*

Introduction

Discoid diatoms are a common constituent of the Tertiary microfossil assemblages of many wells of offshore Eastern Canada, particularly on the Labrador Shelf and Grand Banks. These diatoms are, with few exceptions, completely pyritized and appear to represent the internal mold of the space between the two silicious frustules comprising the test of a whole specimen. This contrasts with the remains of discoid diatoms found in recent sediments which usually occur as single, disjointed frustules.

This paper describes these occurrences and defines their areal and temporal extent by comparing the diatom assemblages found in 16 wells located on the Labrador Shelf, the Grand Banks, and the Scotian Shelf. These wells are; Karlsefni H-13, Gudrid H-55, Indian Harbour M-52, Bonavista C-99, Cumberland B-55, Dominion O-23, Egrit N-46, Egret K-36, Heron H-73, Petrel A-62, Kittiwake P-11, Puffin B-90, Hermine E-94, Sable Island C-67, Sable Island E-48 and Triumph P-50 (Fig. 3.1).

The samples examined were taken from ditch cuttings; each sample representing a 10 m composite interval, and sample spacing being approximately 30 m.

The combined 10 m samples were disintegrated and washed through a standard 75 µ sieve; four picking trays of each sample residue were examined and all the shelly microfossils found were mounted in 60 hole slides. The slides represent to a reasonable extent the microfossil assemblages encountered in the composite samples.

Counts were made of the number of diatoms present in each slide and the geographic/stratigraphical distribution of the different types observed were compiled from these.

Correlation of the relative numerical peaks in each well conforms to a large extent to broad chronostratigraphical correlation based on foraminifera. Tentative interpretations are offered for the relative frequency fluctuations observed.

Regional Stratigraphy and Depositional Environments

The Canadian Atlantic margin, commonly divided into the Scotian Shelf, Grand Banks and Labrador Shelf, spans the mid to high latitudinal realm (north of 42°). Cenozoic sediments in excess of 3000 m thickness were encountered in exploratory wells; foraminifera abound in the majority of Cenozoic drilling samples. These microfossils provide a 7 to 12 fold stratigraphic subdivision based on a latitudinally differentiated zonation which employs stratigraphic exits (tops) (Gradstein and Agterberg, in press).

Planktonic foraminifera are most useful in the southern Grand Banks and Scotian Shelf were 12 zones have been recognized based on species of standard zonations (Stainforth et al., 1975) which are common enough to be of practical value in correlation. Similarly, on the northern Grand Banks and Labrador Shelf a sevenfold subdivision of the Cenozoic sediments based on planktonics is possible. In this northern area the regional application of the planktonics zonation is limited due to the patchy distribution of taxa and their relatively rare occurrence, but the zonation improves chronostratigraphic calibration for the benthonic foraminifera zones.

The benthonic foraminiferal zonation is based on optimum sequences and optimum groupings methods discussed by Gradstein and Agterberg (in press). It provides a relatively conservative zonation based on all of the exits of benthonic (and planktonic) taxa that are potentially useful in correlation (including **Coscinodiscus** spp.). A total of 206 taxa were used.

Figure 3.2 summarizes the zonation for the Labrador Shelf and northern Grand Banks, and is a comparison of probabilistic and conventional zonations for the region. Chronostratigraphic nomenclature is at the series level and is followed in Figure 3.3.

Plate 3.1

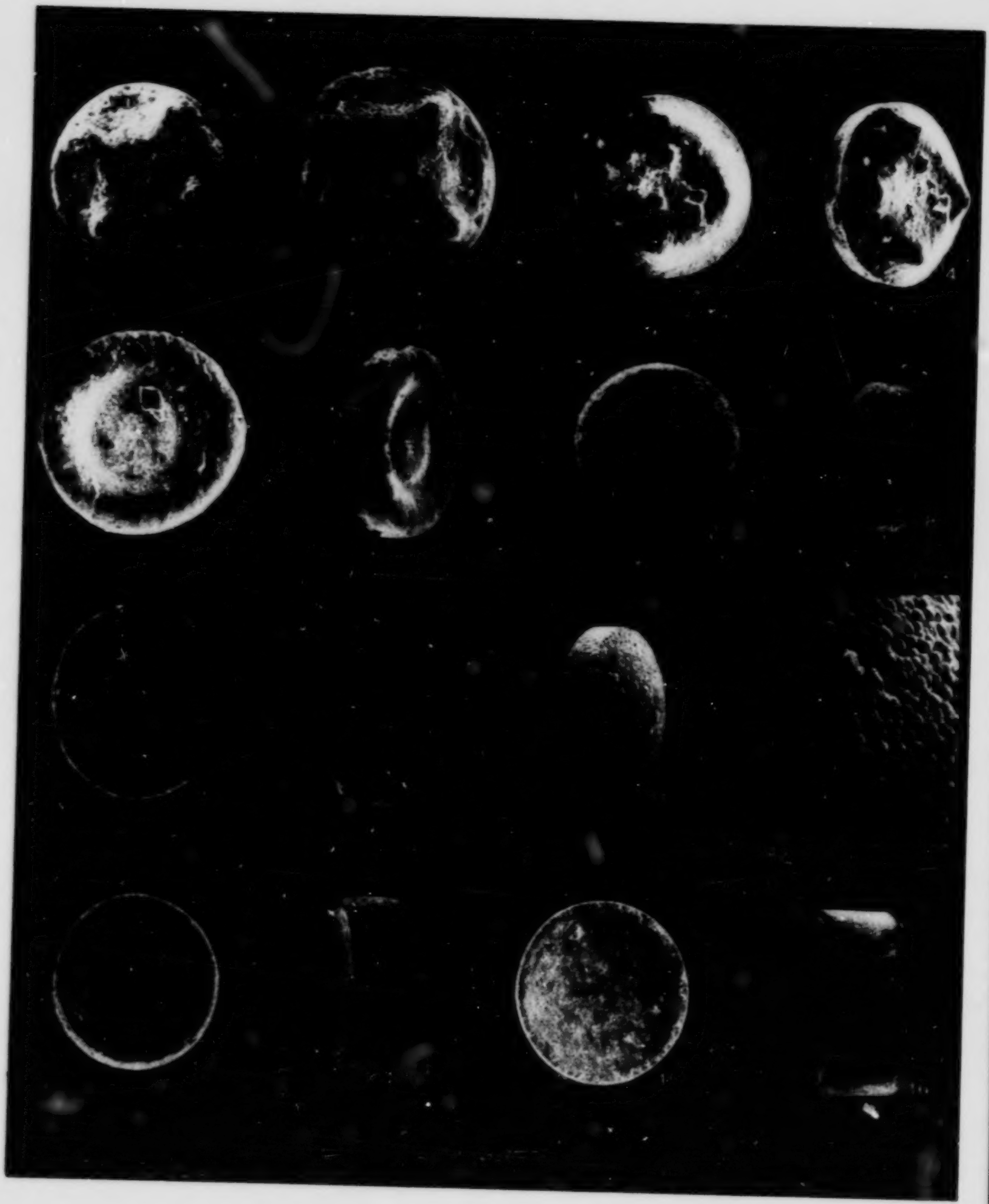

Depositional environment interpretations as used in Figure 3.3 are grouped into three basic categories, according to water depth and distance from shore. They are:

1. Shallow neritic; which comprises marginal marine to inner shelf sediments laid down in water less than approximately 100 m deep.
2. Deep neritic; which comprises sediments laid down in water depth between approximately 100 and 200 m.
3. Bathyal (middle to upper slope); which comprises sediments laid down between 200 and 1000 m water depth.

The micropaleontological criteria (including foraminifera and palynomorphs) for these interpretations have been discussed by Jenkins et al. (1974), Gradstein and Williams (1976) and Gradstein and Srivastava (1980).

Taxonomic Information

Four species of diatoms can be readily distinguished in the well assemblages studied. Unfortunately, the high degree of pyritization of these forms precludes the possibility of exact identification; for the purposes of this study the generic name **Coscinodiscus** has been adopted to apply to these forms. Two of them appear to be conspecific with two species originally described by Staesche and Hiltermann (1940) and assigned to this genus.

The species described in this study are simply designated **Coscinodiscus** spp. 1, 2, 3 and 4.

Coscinodiscus sp. 1

Plate 3.1, fig. 1-4

Valve discoid, averaging 0.2 mm in diameter, flat to slightly convex on both sides. Four raised knobs are present on each side, located near the perimeter of the valve, one in each quadrant and equidistant from each other. A slightly raised ridge connects each knob to the next one, forming a square pattern with a depression in the central part of the valve. In some specimens, however, the ridge connects opposite knobs, creating a cruciform pattern.

This species ranges all through the Tertiary, but is more common in sediments of Late Eocene to Pliocene age. **Coscinodiscus** sp. 1 is a major constituent of diatom abundance peaks in the Miocene in some wells (e.g. Indian Harbour M-52).

Coscinodiscus sp. 2

Plate 3.1, fig. 5, 6

Valve discoid, rectangular in girdle view, and averaging 0.2 mm in diameter. A well defined, broad, raised rim is present along the perimeter of each valve and extends inward approximately half the length of the radius, creating a depressed area in the centre of the valve.

This is the least common of the four species encountered in this study, and occurs in very small numbers or as scattered individuals in most wells, in sediments of Early Eocene to Miocene age.

Coscinodiscus sp. 3

Plate 3.1, fig. 7-12

Valve discoid, slightly to strongly convex. In well preserved specimens the girdle is flat and well defined, but in more poorly preserved ones it is less distinct and somewhat rounded. In general this species corresponds very well with the descriptions and figures given by Staesche and Hiltermann, 1940 (who term it **? Coscinodiscus**, 1940, p. 14-15, pl. 6), Bettenstaedt et al. (1962, p. 357-358, pl. 52, fig. 18-19) and Jacqué and Thouvenin (1975, p. 461, pl. II fig. A-E) for the form they designate **Coscinodiscus** sp. 1.

This is the most common of the diatom species encountered. It occurs in relatively large numbers throughout the Tertiary interval in most wells, and is often the principal component species of the Early Eocene diatom abundance peak (e.g. Karlsefni H-13).

Coscinodiscus sp. 4

Plate 3.1, fig. 13-16

Valve discoid, flat to slightly concave on both sides. It averages 0.2 mm in diameter and often exhibits a thin raised rim around the perimeter. As in **C.** sp. 3, the girdle is flat and well defined in well preserved specimens, less so in others. This species appears to be very similar or identical to the form designated **? Coscinodiscus** by Staesche and Hiltermann (1940, p. 14-15, pl. 6) and that termed **Coscinodiscus** sp. 2 by Bettenstaedt et al. (1962, p. 358, pl. 52, fig. 20 a-b) and Jacqué and Thouvenin (1975, p. 461, pl. II fig. F).

After **C.** sp. 3 this is the second most common form, ranging throughout the Tertiary, though it is most common in the Early Eocene.

Diatom Stratigraphy

Labrador Sea

In Karlsefni H-13, (Fig. 3.3) the most northerly of the wells studied, **Coscinodiscus** sp. 3 appears first in Paleocene sediments, and only in small numbers. At the Paleocene Eocene boundary a diatom abundance peak is encountered with many **C.** sp. 3 and smaller numbers of **C.** sp. 4 and **C.** sp. 1 and very few **C.** sp. 2. The peak extends up into the Middle Eocene where the number of **C.** sp. 4 diminishes to zero. From late Eocene through Plio-Pleistocene only small numbers of diatoms are found, the majority of which are **C.** sp. 1 with very few **C.** sp. 3 and **C.** sp. 4 types present.

The Paleocene strata of Gudrid H-55 contain small numbers of all species of diatoms with **C.** sp. 3 predominat-

---

Plate 3.1

Figures 1-16.

1. **Coscinodiscus** sp. 1 x 170 (from Dominion O-23, 1362-1399 m)
2. **Coscinodiscus** sp. 1 x 163 (from Dominion O-23, 1362-1399 m)

3,4. **Coscinodiscus** sp. 1 x 180 (from Bonavista C-99, 3356-3487 m, 2 views of the same specimen)

5,6. **Coscinodiscus** sp. 2 x 180 (from Dominion O-23, 1362-1399 m, 2 views of the same specimen)

7,8. **Coscinodiscus** sp. 3 x 140 (from Bonavista C-99, 3356-3487 m, 2 views of the same specimen showing characteristic biconvex form)

9,10. **Coscinodiscus** sp. 3 x 143 (from Dominion O-23, 1362-1399 m, 2 views of the same specimen, as in 7, 8)

11. **Coscinodiscus** sp. 3 x 184 (from Dominion O-23, 1362-1399 m)
12. **Coscinodiscus** sp. 3 x 644 (same specimen as no. 11, with higher magnification illustrating the pyritized nature of the test)

13,14. **Coscinodiscus** sp. 4 x 179 (from Dominion O-23, 1362-1399 m, 2 views of the same specimen revealing characteristic biconcave form)

15,16. **Coscinodiscus** sp. 4 x 123 (from Dominion O-23, 1362-1399 m, 2 views of the same specimen)

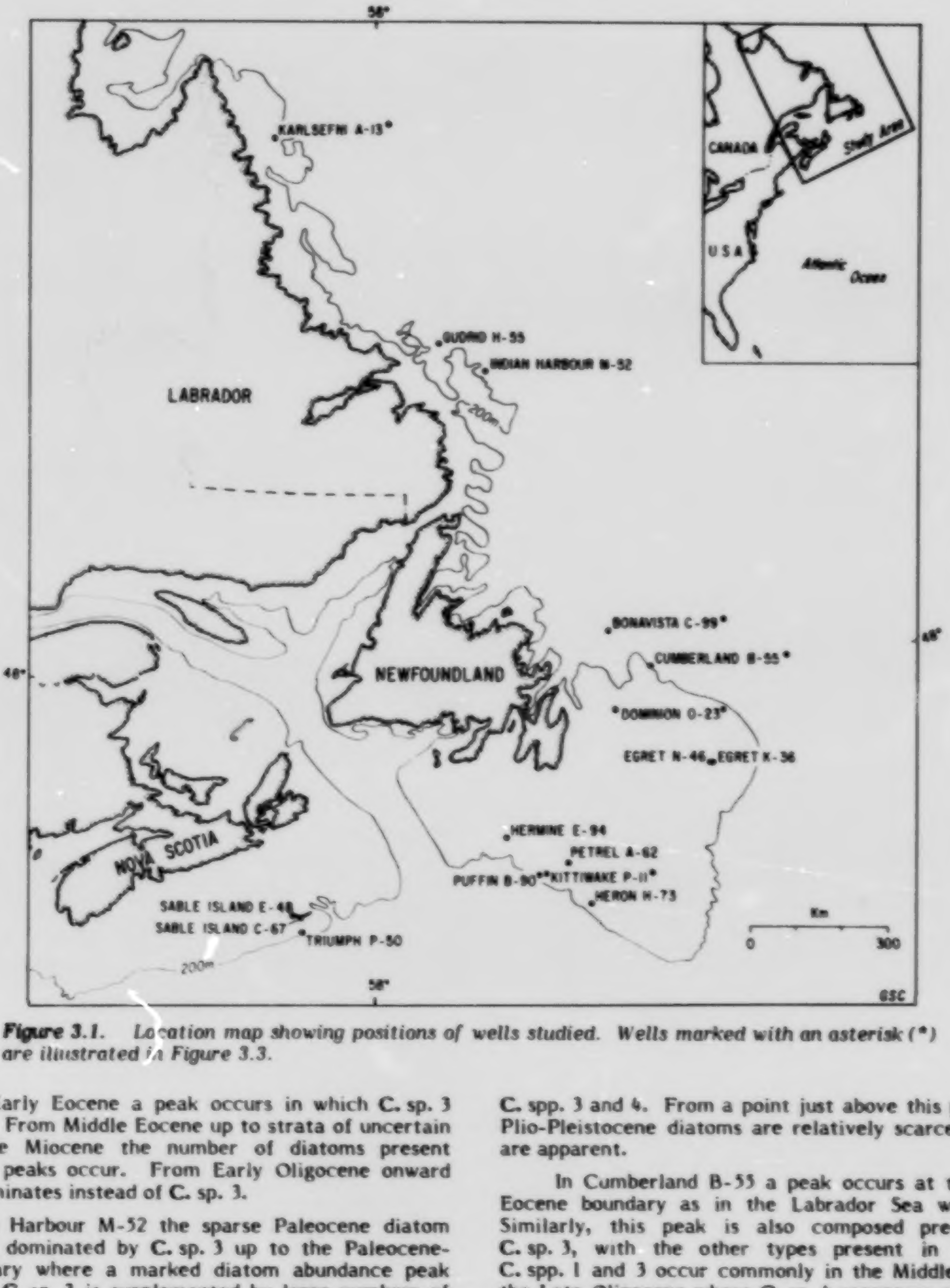
58°
KARLSEFNI A-13*
GUDRID H-55
INDIAN HARBOUR M-52
LABRADOR
200m
BONAVISTA C-99*
CUMBERLAND B-55*
48°
48°
NEWFOUNDLAND
DOMINION O-23*
EGRET N-46
EGRET K-36
HERMINE E-94
PETREL A-62
PUFFIN B-90*
KITTIWAKE P-11*
HERON H-73
NOVA SCOTIA
SABLE ISLAND E-48
SABLE ISLAND C-67
TRIUMPH P-50
200m
Km
0
300
58°
GSC
CANADA
Study Area
U.S.A.
Atlantic Ocean

Figure 3.1. *Location map showing positions of wells studied. Wells marked with an asterisk (*) are illustrated in Figure 3.3.*

ing. In the Early Eocene a peak occurs in which C. sp. 3 predominates. From Middle Eocene up to strata of uncertain age above the Miocene the number of diatoms present fluctuates; no peaks occur. From Early Oligocene onward C. sp. 1 predominates instead of C. sp. 3.

In Indian Harbour M-52 the sparse Paleocene diatom flora is again dominated by C. sp. 3 up to the Paleocene-Eocene boundary where a marked diatom abundance peak occurs. Here C. sp. 3 is supplemented by large numbers of C. sp. 2 and smaller numbers of C. sp. 1 and C. sp. 4. Diatoms (predominately C. sp. 1) are relatively common in the sediments of this well from the Middle Eocene through Middle Pliocene with a second peak occurring from the Upper Oligocene to the Middle Miocene. This peak, in contrast to the Late Paleocene-Early Eocene one, is composed almost exclusively of C. sp. 1. Above this peak, small numbers of C. sp. 4 dominate the diatom assemblages.

Northern Grand Banks

Only the upper portion of the Paleocene is present in Bonavista C-99 (Fig. 3.3) but this, and the Early Eocene section shows a very large diatom peak composed mostly of C. spp. 3 and 4. From a point just above this peak up to the Plio-Pleistocene diatoms are relatively scarce and no peaks are apparent.

In Cumberland B-55 a peak occurs at the Paleocene-Eocene boundary as in the Labrador Sea wells (Fig. 3.3). Similarly, this peak is also composed predominately of C. sp. 3, with the other types present in low numbers. C. spp. 1 and 3 occur commonly in the Middle Eocene up to the Late Oligocene where C. sp. 4 reappears and contributes to a minor peak in the Middle to Late Miocene section, which rapidly diminishes in Plio-Pleistocene sediments.

The lower boundary of the Tertiary in Dominion O-23 is at an unconformity which separates Lower Cretaceous from Lower Eocene strata (Fig. 3.3). Just above this unconformity, and possibly truncated by it, is a large abundance peak of almost exclusively C. sp. 3. The peak diminishes rapidly stratigraphically upward, leaving a small, mixed diatom fauna which continues up to the Late Eocene where a second large peak composed of C. spp. 3, 4 and 1 begins. This second peak extends up through the condensed Oligocene section and ends abruptly in Late Oligocene time. Diatoms occur commonly through the Miocene footage with C. sp. 3 remaining predominant.

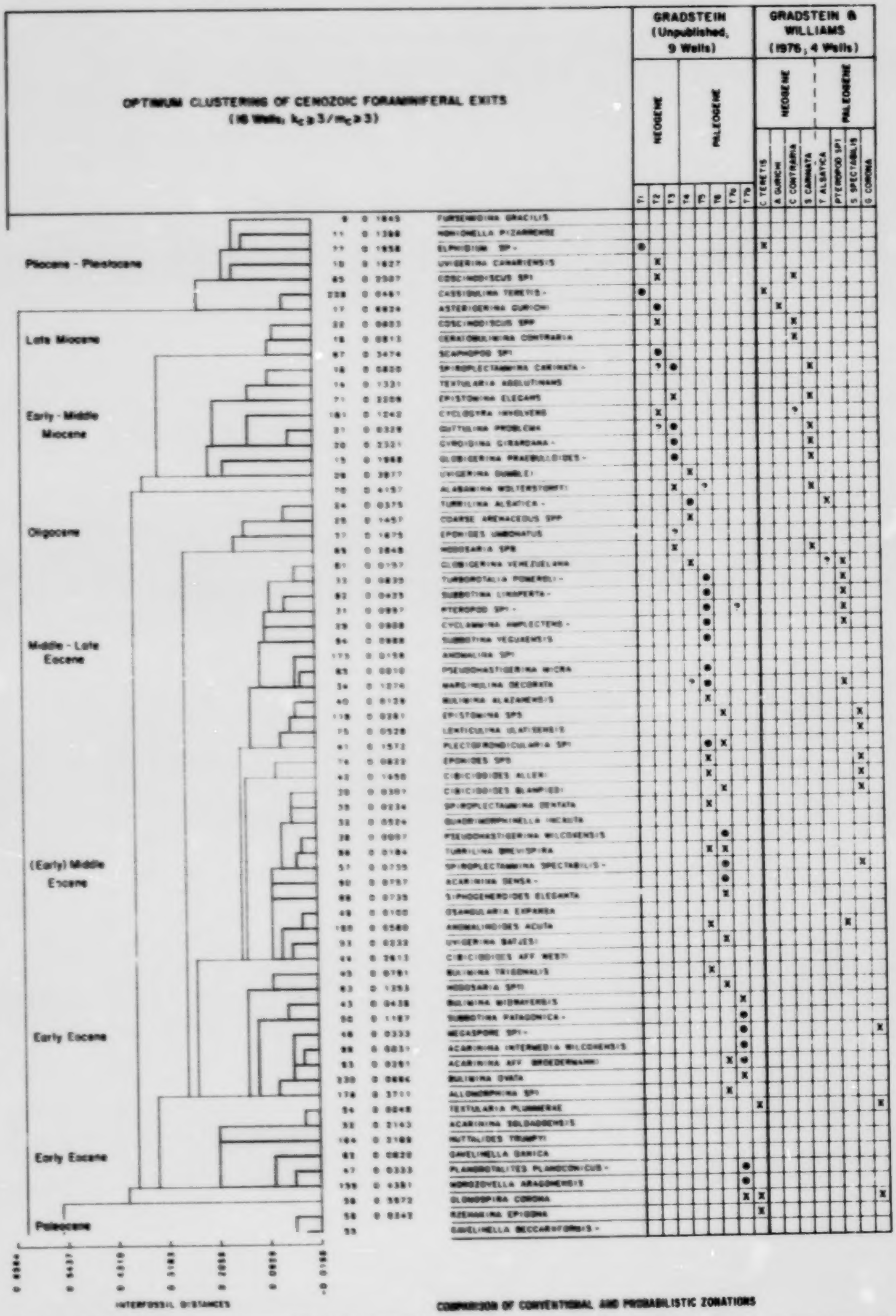

Figure 3.2. *Summary of zonation for Labrador Shelf to Grand Banks based on a comparison of probabilistic and conventional zonations for the region, based on optimum clustering of microfossil exits (from Gradstein and Agterberg, in press).*

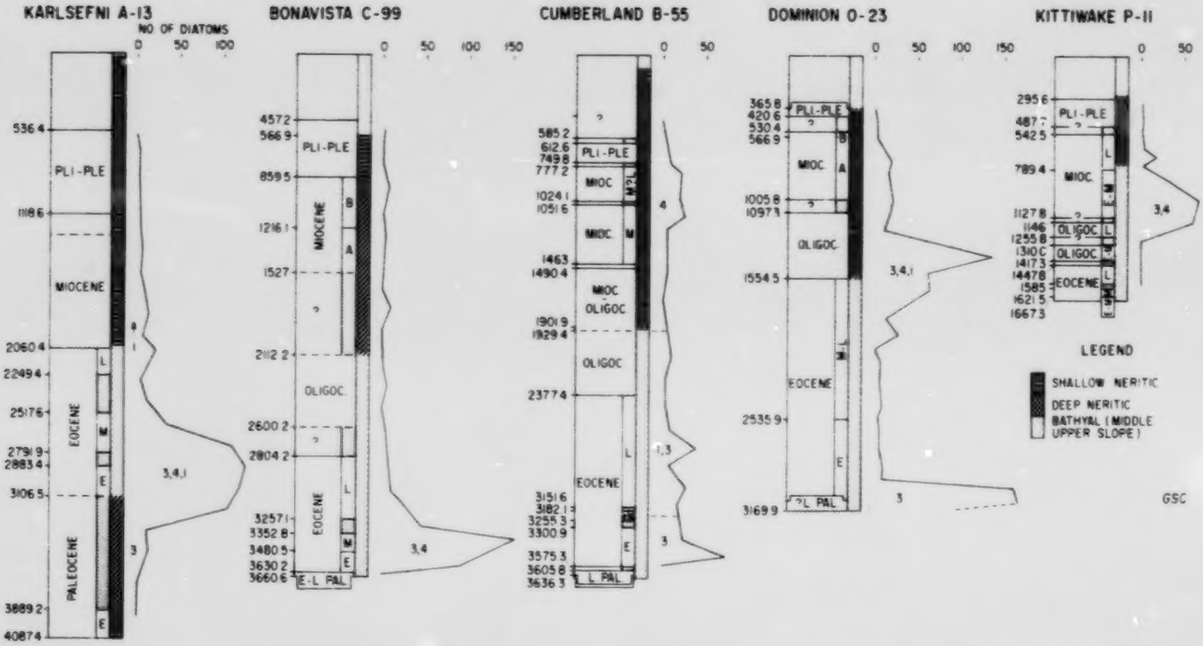

Figure 3.3. *Comparison of five wells from Labrador Shelf and Grand Banks showing stratigraphic locations of diatom abundance peaks. Paleoenvironmental information is also shown. Numbers (1, 2, 3 and 4) indicate dominant diatom species.*

In the very condensed Tertiary interval of Egret N-46 the number of diatoms present decreases sharply from a large peak in the Early Eocene down to a very low value in Early-Middle Miocene strata. Throughout this well **C.** sp. 3 out numbers **C.** sp. 1 by a factor of 3:1, with the other species all but absent.

Egret K-36, situated very close to N-46, exhibits a similarly condensed Tertiary interval. In this well however, diatoms are quite scarce throughout the sampled interval, indicating that the diatom-rich sediments were not penetrated, due to the presence of an unconformity separating Middle Eocene and Maastrichtian sediments.

Southern Grand Banks

In Heron H-73 a small number of diatoms of **C.** spp. 3 and 4 are present at the unconformity separating the Cretaceous from the Lower Eocene. Above this are only a few specimens of **C.** sp. 1, which continue up through the Tertiary.

The condensed Tertiary interval of Petrel A-62 contains only small numbers of pyritized diatoms, mostly **C.** sp. 1.

In Kittiwake P-11 (Fig. 3.3), few diatoms are present up to the Upper Oligocene level where a peak composed mostly of **C.** spp. 3 and 4 appears and continues up through strata of Early Miocene age. The peak disappears in the Middle Miocene where **C.** sp. 1 becomes more common. Above that, few diatoms exist in the well samples.

Puffin B-90, situated within 20 km of Kittiwake P-11 contains a somewhat thicker Tertiary interval but all species of diatoms remain scarce throughout the well and no peaks appear.

In the very condensed Tertiary interval of Hermine E-94 (520 m) diatoms are practically absent except for a small number of **C.** sp. 1 in the few samples believed to be of Early Oligocene age.

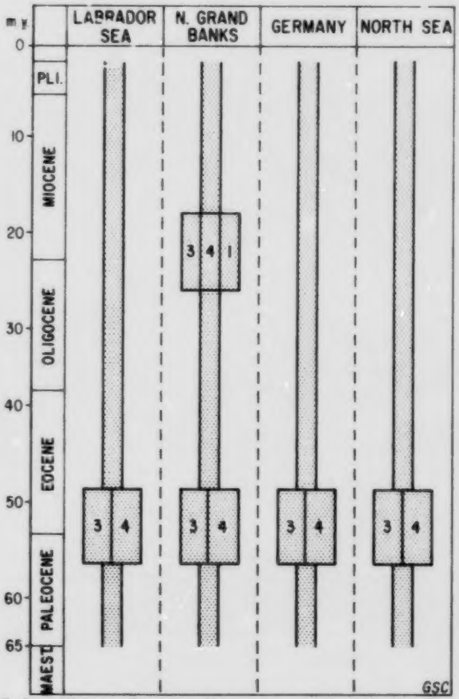

Figure 3.4. *Generalized diagram comparing the stratigraphic location and composition of diatom abundance peaks in offshore eastern Canada and European locations. The normal background count of diatoms is indicated by the narrow stippled bars. Peaks are shown as boxes containing numbers which indicate dominant diatom species present.*

The Late Paleocene-Early Eocene peak is present in regions, while the Late Oligocene-Early Miocene peak in Dominion O-23 (Northern Grand Banks) is restricted to that locality.

Scotian Shelf

The Tertiary intervals of the three Scotian Shelf wells studies are all condensed, ranging from 600 to 1500 m in thickness, and diatoms are rare in all three wells.

In Sable Island C-67 some specimens of **C.** sp. 1 are present in Lower Miocene strata and they constitute the entire diatom assemblage in the well.

Sable Island E-48 also contains very few diatoms, represented only by occasional specimens of **C.** spp. 1 and 3 in sediments of Paleocene to Oligocene age.

In Triumph P-50, the most southerly of the wells studied, a few specimens of **C.** sp. 3 occur in sediments of Early to Middle Eocene age. Above that, scattered individuals of **C.** sp. 1 are present up to the Middle Miocene, where all diatoms disappear.

Comparison With Diatom Distribution in Northwestern Germany and the North Sea

In a summary of occurrences of various microfossil groups in Germany, Bettenstaedt et al. (1962) citing Staesche and Hiltermann (1940) report our **Coscinodiscus** sp. 3 (which they designate **Coscinodiscus** sp. 1) as being frequently found in the lowermost Eocene of Germany, Denmark and Holland and occasionally found in Middle Eocene and Lower-Middle Miocene, though it is very rare in the Upper Eocene. This stratigraphic distribution is rather similar to that described in this report for the Labrador Sea wells (Fig. 3.4).

Coscinodiscus sp. 4, (which Bettenstaedt et al. designate as **C.** sp. 2) is found in northwestern Germany quite frequently in Middle and Lower Eocene but is rarer in lowermost Eocene, Paleocene and Middle Miocene. On the Canadian continental shelf this species is also most common in the Middle and Lower Eocene and occurs in small numbers throughout the Tertiary interval.

In a study of Lower Tertiary volcanic activity in the North Sea Jacqué et al. (1975) found **Coscinodiscus** spp. 3 and 4 to be abundant in tuffaceous sediments of Ypresian (Early Eocene) age. They attribute this frequency peak to the enrichment of seawater in silica and/or CaO caused by explosive volcanic eruptions. This interpretation does not, however, explain the presence of diatom peaks on the Canadian continental shelf where no evidence of volcanic activity is found in sediments of that age.

Environmental Parameters

Paleoenvironmental evidence from the wells studied for this report (Fig. 3.3), indicate that while no diatom peaks appear in sediments originating in very shallow water, they are found in strata deposited under neritic and bathyal conditions.

If as we reasonably expect, the peaks reflect diatom blooms, higher nutrient levels in the upper water mass level may be responsible. The Early Eocene and Miocene peaks broadly correspond to periods of maximum northward excursion of lower latitude surface waters (Gradstein and Srivastava, 1980) which may have led to improved surface water mixing and (slope) upwelling due to convergence. The pyritized nature of the molds of the original silicious diatom frustules indicates a weakly reducing or reducing diagenetic regime.

Conclusions

1. On the Labrador Shelf **Coscinodiscus** spp. 3 and 4 occur abundantly in Upper Paleocene - Lower Eocene sediments. Above this, **Coscinodiscus** sp. 1 becomes the most common form but no distinct frequency peaks occur, with the exception of one in the Late Oligocene - M. Miocene time in Indian Harbour M-52.
2. In the northern Grand Banks area this Late Paleocene - Early Eocene frequency peak of **Coscinodiscus** spp. 3 and 4 is also present; a second peak occurs in Miocene - Oligocene sediments in Cumberland B-55 and Dominion O-23, two of the wells most distant from the present landmass.
3. In the southern Grand Banks and Scotian Shelf areas, diatoms are much less common in Tertiary strata and only one abundance peak occurs (in the Oligocene-Miocene of Kittiwake P-11).
4. Broadly defined, the temporal distributions of **Coscinodiscus** spp. 3 and 4 generally concur with those given by Staesche and Hiltermann (1940), Bettenstaedt et al. (1962) and Jacqué et al. (1975) for northwest Europe and the North Sea. In these areas the two species are abundant in Lower Eocene sediments and occur less frequently in some strata of both older and younger age.
5. Diatom peaks occur in sediments from both bathyal and neritic environments.

References

Bettenstaedt, F., Fahrion, H., Hiltermann, H., and Wick, W.
1962: Tertiar Norddeutschlands in Leitfossilien der Micropalaontologie, Gebrüder Borntraeger, Berlin, 2 vol., 431 p.

Jacqué, M. and Thouvenin, J.
1975: Lower Tertiary Tuffs and Volcanic Activity in the North Sea. In Petroleum and the Continental Shelf of North-west Europe, ed. A.W. Woodland; J. Wiley and Sons, New York, I, p. 455-465.

Jenkins, W.A.M., Ascoli, P., Gradstein, F.M., Jansa, L.F., and Williams, G.L.
1974: Stratigraphy of the Amoco IOE A-1 Puffin B-90 well, Grand Banks of Newfoundland; Geological Survey of Canada, Paper 74-61; p. 1-9.

Gradstein, F.M. and Agterberg, F.
Models of Cenozoic Foraminiferal Stratigraphy - Northwest Atlantic Margin. Proceedings of the 26th International Geological Congress Paris, July 7-17, 1980. (in press)

Gradstein, F.M. and Williams, G.L.
1976: Biostratigraphy of the Labrador Shelf, Part 1. Geological Survey of Canada Open File Report 349, p. 1-39.

Gradstein, F.M. and Srivastava, S.P.
1980: Aspects of Cenozoic stratigraphy and paleoceanography of the Labrador Sea and Baffin Bay; Paleogeography, Paleoclimatology, Paleoecology, v. 30 (1980), p. 261-295.

Staesche, K. and Hiltermann, H.
1940: Mikrofaunen aus dem Tertiar Nordwestdeutschlands; Abhandlungen der Reichsstelle fur Bodenforschung Neue Folge, Heft 201; 26 p., 53 pl.

Stainforth, R.M., Lamb, J.L., Luterbacher, H., Beard, J.H., and Jeffords, R.H.
1975: Cenozoic planktonic foraminiferal zonation and characteristics of index forms; University of Kansas Paleontology Contributions Article 62, 425 p.

4.

ISOTOPE, SCANNING ELECTRON MICROSCOPE, AND ENERGY DISPERSIVE SPECTROMETER STUDIES OF HETEROGENEOUS ZIRCONS FROM RADIOACTIVE GRANITES IN THE GRENVILLE STRUCTURAL PROVINCE, QUEBEC AND ONTARIO

Project 770061

J. Rimsaite
Economic Geology Division

Rimsaite, J., Isotope, scanning electron microscope, and energy dispersive spectrometer studies of heterogeneous zircons from radioactive granites in the Grenville Structural Province, Quebec and Ontario; in Current Research, Part B, Geological Survey of Canada, Paper 81-1B, p. 25-35, 1981.

Abstract

Heterogeneous zircons yielded discordant Pb-U, Pb-Th and ^{207}Pb-^{206}Pb isotopic ages. Most data points fall below the concordia curve, implying losses of daughter elements, but they define a discordia line that intersects the concordia at approximately 90 Ma and 1020 Ma.

To obtain evidence for mobilization of U and radiogenic Pb, zircon grains were studied using a scanning electron microscope coupled with an energy dispersive spectrometer. High magnification backscattered and secondary electron images of the zircon (cyrtolite) revealed narrow fractures (<1 μm in width), zoning and diverse mineral inclusions.

Three groups of mineral inclusions observed were:

1. *those predating zoned zircon and apparently serving as a nucleus: quartz, shattered uranothorite, and groups of small shattered zircons;*
2. *uraninite, feldspar, and apatite associated with the growth and zoning of the host zircon; and*
3. *fracture-fillings that postdate crystallization of the host zircon: grains bearing rare-earth elements, a FeAs phase, unidentified U-rich material, and galena.*

The U- and Pb-rich inclusions, incorporated into the zircon grains during and after its crystallization markedly affect isotopic ages of the host zircon.

Electron scanning images of heterogeneous zircons show their highly fractured nature and episodic growth zones. Migration of Pb and U have occurred along fractures in zircon. Zircon, uraninite, and other associated minerals have decomposed and complex reactions have taken place between the liberated Zr, U, Th and other elements to produce overgrowths on mineral grains and unidentified Zr-bearing material in fractures.

Introduction

Petrological and mineralogical studies of radioactive occurrences in the Grenville Structural Province revealed the hybrid nature of granitic rocks and heterogeneity of radioactive and accessory minerals. The hybrid rocks are made up of paleosome remnants and xenoliths in neosome hosts consisting of late microcline, albite, and quartz. The heterogeneous minerals are characterized by interrupted zonal growths, variations in chemical composition, particularly in U/Th and U/Pb ratios within a single radioactive grain, by different degrees of alteration and by the abundance and nature of inclusions. This study of heterogeneous zircons is an extension of the author's mineralogical and isotopic studies of radioactive occurrences. By use of a scanning electron microscope (SEM) and an energy dispersive spectrometer (EDS), the study documents chemical variations of zircon grains due to alteration and the nature of mineral inclusions and impurities and of subsequently formed U-, Th-, Pb-, and Zr-bearing compounds in overgrowths and fractures. The hybrid character of the radioactive granite is considered to have resulted in the observed complex zircon grains and heterogeneous mineral overgrowths, and thus the application of zircon morphology as suggested by Poldervaart (1956) and Pupin (1980) is extremely difficult and would require a special study. The morphological classification proposed by Pupin (1980) is based on the presence and preferential growth of prismatic and pyramidal crystal faces, aspects which are dependent on environmental conditions. Thus, the relationship between size and number of the prismatic and pyramidal faces of zircon grains can indicate the temperature and chemical environment during crystallization, and different zircon morphologies are considered by this author to be indicative of differentiation trends of granitic and other magmas. Such morphological studies are planned for Grenville zircons in the future. In the present author's opinion, the external morphology of large "barrel-shaped" zircon crystals in high grade uranium ore is in part a function of the nucleus on which they grew and in part a function of the space available between the tightly intergrown clusters of zircon and other accessory and radioactive minerals (Rimsaite, 1970a, Fig. 38.5).

Most of the isotope analyses presented in this and previous studies for radioactive minerals (including zircons) from radioactive occurrences in Grenville Province, indicate discordant Pb-Th, Pb-U and ^{207}Pb-^{206}Pb isotopic ages, correlative with their Pb/U ratio. Secondary minerals containing high Pb/U ratios (kasolite, masuyite, galena, anglesite, and wulfenite) formed from various proportions of remobilized uranium, radiogenic lead and other ions, yielded points above the concordia curve (Rimsaite, 1978b, 1980a; Cumming and Rimsaite, 1979). Concentrates of selected minerals that are associated with zircons yielded the following ^{207}Pb-^{206}Pb ages: kasolite from fractures with Pb/U = 1/4.5, 1088 Ma (point above the concordia curve); thorianite, 1072 Ma (point slightly above the concordia curve); uraninite enclosed in fluorite, Pb/U = 1/6, 1051.7 Ma (point on the concordia curve); uraninite leached from monazite, Pb/U = 1/5.5, 991.7 Ma (point above the concordia curve); uraninite leached from zircon (4UZ), Pb/U = 1/6.7, 991.9 Ma (this paper); heterogeneous allanite, Pb/U = 1/10, 900 Ma (point below the concordia curve); heterogeneous metamict pyrochlore, U/Pb = 1/59, 230 Ma (Rimsaite, 1980a, Fig. 38.7). Some of these primary and secondary minerals are

Table 4.1

Properties of selected zircons and of their contained radioactive inclusions

Mineral & Occurrence	Description Illustration (This paper)	Shape/size (type)*	(in µm) length	breadth	Optical Properties	No.	Si	Partial chemical analysis** (element weight per cent) Zr	Hf	Ca	Fe	U	Th	Pb	Pb/U	Other Elements
I. Zoned zircon	Rimsaite, 1980a Fig. 38.5	barrel (S_1,S_6)	420	300	anisotropic	1	13.7	40.3	ND†	1.8	1.3	ND	ND	ND	ND	ND
					isotropic	2	13.8	45.8	ND	1.2	(-)††	ND	ND	ND	ND	ND
II. Zoned zircon	(Fig. 4.2B)	overgrown	250	200	SEI low relief	3	13.5	43.	1.0	2.6	0.8	1.2	(-)	(-)	(-)	Al,K,Y
					high relief	4	14.5	44.	2.2	0.8	0.8	(-)	(-)	(-)	(-)	Mn
III. Group of zircons	(Fig. 4.4A)	prism $(S_2, G\text{-}1)$	240	80	anisotropic	5	15.	47.	ND	(-)	(-)	ND	ND	ND	ND	ND
IV. Zircon in gummite	(Fig. 4.4B)	rounded	100	83	BEI grey core	6	12.6	38.	2.6	0.4	5.8	4.4	3.8	(-)	(-)	Cr,Mn,Y
					white periphery	7	11.8	20.	1.0	0.4	10.2	17.6	10.8	(-)	(-)	Al,Cr,P,Y
V. Zircons in zircons	(Fig. 4.3E)	(S_2,S_3)	27	13	isotropic	8	15.	47.4	1.8	0.1	0.4	(-)	(-)	(-)	(-)	(-)
		zoned	200	100	isotropic	9	13.	35.	1.8	0.6	3.2	6.8	7.8	(-)	(-)	Al,P,Y
		prism	30	27	BEI white prism	10	11.	24.	1.2	0.2	2.4	27.8	1.6	(-)	(-)	Al,P,REE,Y
Inclusions in core of zircon II	(Fig. 4.2C)	uraninite	3	2	BEI white chip	11	0.6	(-)	(-)	0.2	0.4	58.2	5.2	6.4	1/9	Y
		U-thorite	8	3	BEI pale chip	12	8.6	2.8	(-)	1.4	0.6	17.4	25.8	0.8	1/21	Ce
		crusts	10	1	BEI grey rim	13	7.6	7.0	(-)	1.2	0.4	19.6	18.4	1.2	1/16	(-)
Inclusions in zircon I	Rimsaite, 1980a Fig. 38.5	U-thorite	60	40	BEI grey grain	14	3.6	(-)	(-)	1.8	(-)	16.4	41.4	1.8	1/9	(-)
		uraninite	10	10	BEI white grain	15	(-)	(-)	(-)	0.7	(-)	62.9	5.5	9.1	1/7	(-)
Overgrowths crusts, and specks in zircon	Like in (Fig. 4.3E)	Th-rich	30	5	BEI grey crust	16	5.8	1.4	(-)	2.2	3.4	9.2	17.4	3.4	1/2.7	Al,P,REE,Y
		U-rich	10	1	BEI pale crust	17	7.8	1.8	(-)	0.6	7.0	15.6	3.0	6.8	1/2.3	Al,Ce
		galena	15	1	BEI white rim	18	(-)	(-)	(-)	(-)	(-)	(-)	(-)	86.6	(-)	S=14.7

* Examples of characteristic zircon types using classification symbols of Pupin (1980).

** Semiquantitative energy dispersive spectrum analysis by G.J. Pringle of Central Laboratories and Technical Services Division, Geological Survey of Canada (Method described by Pringle and Thorpe, 1980).

†ND = not determined.

††(-) = not detected in energy dispersive spectrum.

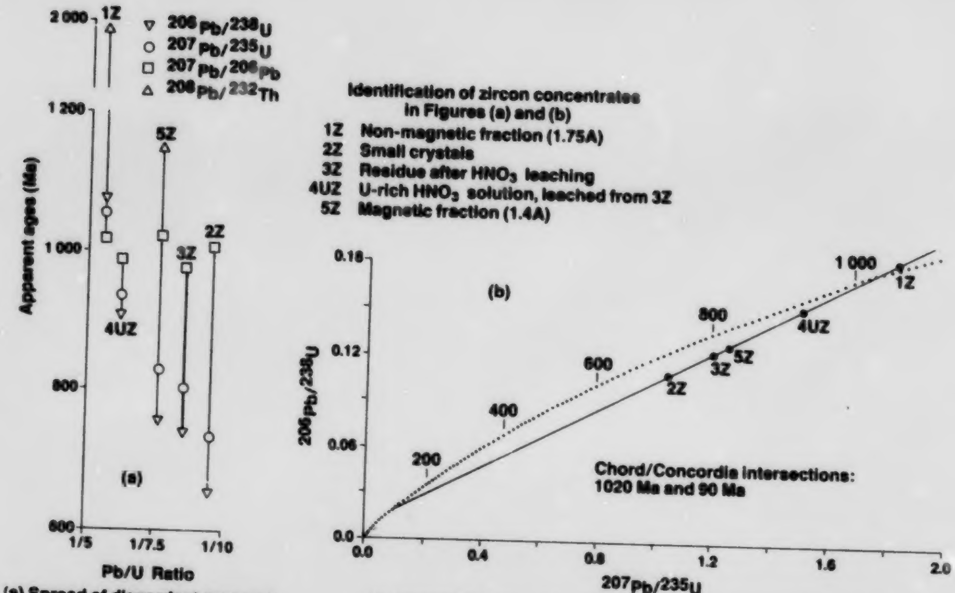

(a) Spread of discordant apparent ages in relation to Pb/U ratio

(b) Concordia diagram for Pb/U data on zircon concentrates from sample RF-1. Isotope data from G.L. Cumming

Figure 4.1. Diagrammatic representation of isotopic data for zircons from high grade uranium ore RF-1 at the Madawaska uranium mine, Bancroft area, Ontario.

present in zircons as inclusions and/or overgrowths and affect the isotopic "ages" obtained for the host zircon when the composite material is analyzed.

The heterogeneous zircons from the radioactive granites in Grenville Structural Province are zoned contain numerous inclusions and resemble zircons from Hercynian granites described by Veniale et al. (1968) and Köhler (1970) who identified three generations of zircon within a single grain. Köhler (1970) has shown that discordant isotopic ages of such heterogeneous zircons cannot be explained by a continuous loss of radiogenic lead because these zircons have formed during, and represent the following different geological events: the core is pre-Hercynian (sedimentary), this is overgrown by a zone formed during the Hercynian orogeny and this, in turn, by an anhedral zone that apparently grew during the Alpine orogeny. Several other authors have also attempted to explain discordant isotopic ages as due to either the presence of temporally different zircon populations in the rock, or a heterogeneous distribution of radioactive and radiogenic elements in the zircon crystals (Koeppel and Sommerlauer, 1974; Gulson and Krogh, 1975; Gulson and Rutishauser, 1976). Zircon crystals, however, are difficult to study by conventional optical, X-ray diffraction, and chemical methods because of their high indices of refraction, the presence of poorly crystallized (metamict) domains, and their very low concentrations of radioactive and radiogenic elements. Therefore various special and very sensitive techniques have been used, such as electron and proton microprobe methods (Clark et al., 1979), fission track analyses (Graubert et al., 1974), and electron microscopy coupled with energy dispersive spectrometry (Rimsaite, 1980a, 1981). Fission track images are produced by tracks of heavy fission particles (Fleischer et al., 1975) and permit detection and mapping of domains containing high and low concentrations of radioactive elements without showing the actual image of the emitter. Nonetheless, fission track mapping is very useful for detecting low concentrations of radioactive emitters and this method is widely used. On the other hand, back-scattered electron images are useful in studies of higher (and contrasting) concentrations of radioactive materials and show actual outlines of radioactive particles and domains on the basis of their mass differences. Heavy mineral particles appear light or white in colour, whereas lower density minerals appear dark, thus permitting one to see domains of relatively high and low density as small as 1 μm in size, provided that the mass contrasts are of sufficient magnitude to produce different shades of grey.

This paper presents the results of extended studies of U-Th-Pb systems in uranium deposits in granitic rocks (Rimsaite, 1978a, 1980a, 1981) with a special emphasis on heterogeneity of zircon crystals. The purposes of this presentation are to elucidate discordant isotopic ages and to discuss causes for the heterogeneous nature of zircon grains on the basis of the following features:

1. mode of occurrence of zircon and associated minerals;
2. size, shape and evolution of zoned crystals;
3. fractures in zircon grains and their contained mineral impurities; and
4. evidence of alteration, mobilization of zirconium and reactions between liberated Zr, U, Th, and other elements.

This study is an extension of a paper presented at the 12th General Meeting of the International Mineralogical Association (Rimsaite, 1980c).

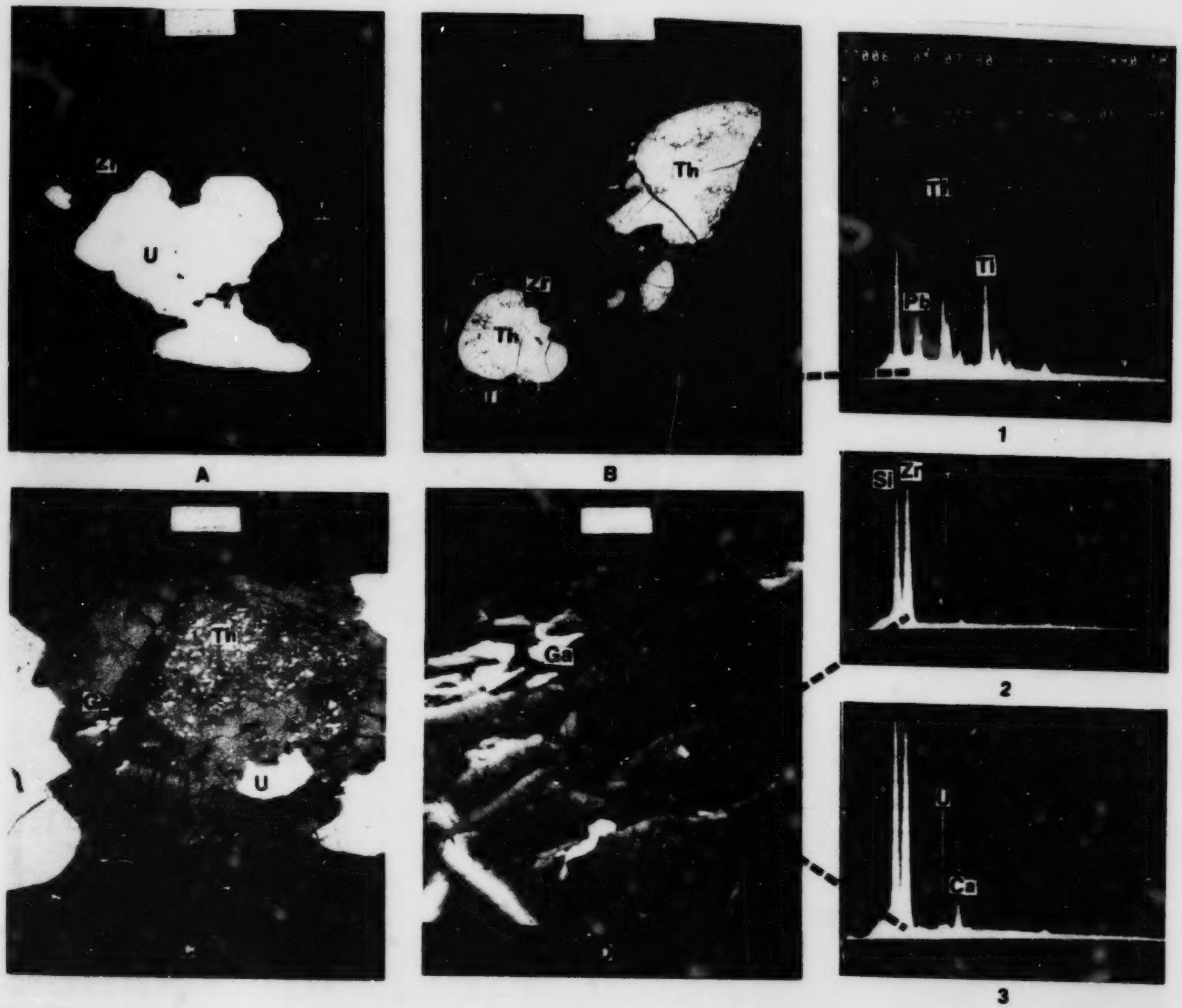
Zr
U
Th
Zr
Th
Th
Pb
Ti
1
A
B
Si
Zr
2
Th
U
Ga
U
Ca
3

Geological Setting of Radioactive Granites and Sampling Localities

In Grenville Structural Province, radioactive granites and pegmatites are associated with metasedimentary and metamorphosed mafic rocks. Bands of metasedimentary rocks and xenoliths of mafic rocks are common in the radioactive granites. The three areas studied were: (1) Bancroft area, Ontario, mapped by Hewitt (1957); (2) Mont-Laurier area, Quebec, studied by Allen (1971), Tremblay (1974), and Kish (1977); and (3) Johan Beetz area, Quebec, mapped by Cooper (1957) and described by Baldwin (1970) and Rimsaite (1981).

One characteristic of radioactive rocks in these areas is their heterogeneity, namely marked variations in grain size, nature and abundance of xenoliths, and erratic distribution of uranium and thorium minerals (Rimsaite, 1980b).

In the deposits studied, primary uranium and thorium minerals are partly altered and have lost from 10 to 80 per cent of their uranium, thorium and radiogenic lead. Part of the mobilized uranium and lead crystallized in secondary, hydrous Pb-rich and Pb-poor mineral aggregates that in part replace primary minerals and form overgrowths on mineral grains, commonly of apatite, titanite and zircon, and also crusts along fractures. The Pb-rich secondary minerals are of special interest because they contain only less than 0.2 per cent common lead and yield isotopic Pb/U ratios that fall above the concordia curve. Such "above concordia" ratios were obtained independently in two laboratories, the Oak Ridge National Laboratory, U.S.A., and at the Department of Physics, University of Alberta (Rimsaite, 1978b; Cumming and Rimsaite, 1979).

Radioactive rocks were collected for geochemical, isotope, and mineralogical studies by the author and sampling localities are shown on a geological sketch map published previously (Rimsaite, 1978a).

Specimens and Laboratory Procedures

Mineral associations and petrology of the radioactive granites were studied in polished thin sections and suitable minerals were selected for more detailed studies. The latter included scanning electron microscope studies of heterogeneous minerals; chemical analyses of selected mineral phases on spots less than 1 μm in diameter, using an energy dispersive spectrometer; and Pb-U-Th isotopic analyses of mineral concentrates. Zircon grains and associated allanite, pyrochlore, titanite, uraninite, and thorianite concentrates were prepared for isotopic analyses and preliminary results were summarized by Rimsaite (1980a, Fig. 38.7).

Figure 4.2. *Intimately associated zircon, uraninite, uranothorite and magnetite from the Madawaska uranium mine. (GSC 203577-S)*

A. *BEI[1] of zircon "Zr" adjacent to uraninite ("U", white) and magnetite ("M", dark grey).*

B. *BEI of zoned zircon "Zr" between two uranothorite grains "Th".*

C. *Enlarged portion of zircon in Figure 4.2B showing shattered core with disseminated specks of uranothorite "Th" and inclusions of uraninite "U" and galena "Ga".*

D. *Further enlargement of the zircon in Figure 4.2B showing galena specks (white) and shattered (hard) and darker smooth (soft, uraniferous) portions of zircon band in Figures 4.2B and C.*

1. *ED spectrum of Ti-bearing inclusion in uraninite.*

2. *ED spectrum of shattered (hard) relatively clean zircon.*

3. *ED spectrum of uraniferous, impure (soft) portions of zircon.*

Note: dashed lines connect mineral spots analyzed with the corresponding spectrum.

High grade ore material containing 3.61% U, 1.02% Th, 2% Zr and more than 50 per cent heavy minerals (mainly allanite) was selected for concentration of zircon and associated ore and accessory minerals for chemical and isotopic studies. Zircons of the cyrtolite variety occur as inclusions in allanite, tourmaline, biotite, apatite, uraninite, uranothorite, pyroxene, feldspar, quartz, and REE-bearing mineral aggregates, and in turn contain numerous impurities and mineral inclusions described in more detail in the following section on fractures and mineral impurities in zircon. As already observed by Pupin (1980), the morphology of a zircon crystal appears to be related to the host mineral or environment in which it crystallized. Thus G-1 type (according to the classification of Pupin, 1980) seems to be related to the matrix of secondary REE-bearing mineral aggregates, whereas type S-2 is included within larger zircon grains and in allanite. Zircons of the G-1 type consist of (101) and (110) faces, whereas those of type S-2 consist of two faces of a pyramid, the (101) face being better developed than (211), and two faces of a prism, (110) face being broader than (100) face (Pupin, 1980, Fig. 1).

The "barrel shaped" subhedral to anhedral cyrtolite grains intergrown with uraninite and uranothorite constitute more than 90 per cent of the zircon population in the high grade ore studied. The zircons are zoned, partly overgrown by anhedral rims and are unusually large in size, up to 1 cm in diameter. These large crystals were hand-picked from a heavy mineral concentrate prepared from a 160 μm size fraction. The crushed material was purified again in heavy liquids and separated into magnetic and nonmagnetic fractions using a Frantz separator. The U- and Pb-rich inclusions within grains of cyrtolite were removed by HNO_3 acid treatment and the acid solution (4UZ) and zircon residue after acid treatment (3Z) were analyzed separately for their contents of REE, Th, U, and Pb. The average zircon concentrate contains 4 weight per cent water. The acid solution (4UZ) contains more U, Th, and Pb than the zircon residue and most of the REE, with the exception of Y, Yb, Tm, and Er which are concentrated in the acid-purified zircon (cyrtolite) residue (3Z), as reported by Rimsaite (1980a, Tables 38.1, 38.2). The elongate transparent zircon crystals, separated also by hand-picking, are much smaller than the "barrel-shaped" grains and constitute less than one per cent of the total zircon population in the high grade ore. Some of the chemical and physical properties of zircon (cyrtolite) grains and their mineral impurities discussed in this paper are summarized in Table 4.1, and reference is made where possible to the morphological types of Pupin (1980). Figure 4.1 and Table 4.2 summarize isotopic data obtained on the following fractions of ground zircon:

1Z = nonmagnetic fraction (1.75 Å);
2Z = elongate transparent crystals;
3Z = zoned barrel-shaped crystals, residue after leaching with HNO_3;
4UZ = HNO_3 solution from 3Z concentrate;
5Z = magnetic fraction (1.4 Å), nonmagnetic (1.0 Å).

Copies of illustrations exhibited at the Poster Session during the 12th General Meeting of the International Mineralogical Association (IMA'80), Orléans, France, and more detailed information on the procedures are available from the author upon request.

---

[1] BEI = backscattered electron images

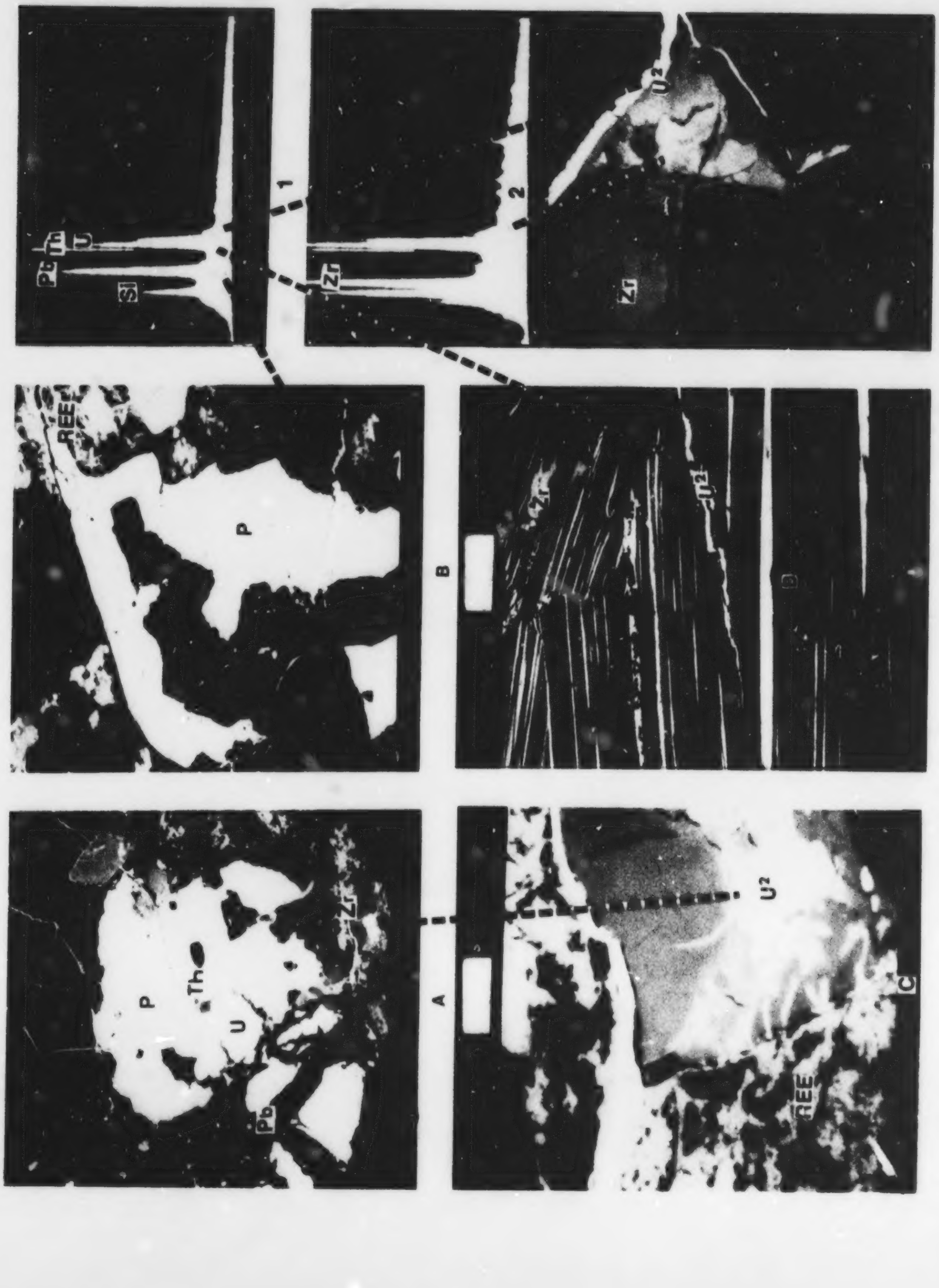
A
B
C
P
Th
U
Pb
Zr
U²
REE
P
REE
Zr
U²
Pb
Th
U
Si
Zr
1
2
U²
Zr

Results and Discussion

Mode of Occurrence of Zircon and Associated Minerals

In the radioactive rocks studied, zircon grains commonly occur in clusters associated with uraninite, uranothorite, allanite, apatite, xenotime, pyrochlore, magnetite and Ti minerals (Fig. 4.2A and 4.2B; Rimsaite, 1978a, Fig. 9.5). These clusters of accessory and radioactive minerals surround, or occur within, ferromagnesian silicate minerals or paleosome domains. However, zircon also commonly occurs as single grains in biotite, feldspar and quartz (Fig. 4.3D). In unaltered rocks, zircon crystals are fresh, but under oxidizing conditions, magnetite-uraninite-uranothorite intergrowths have been partially altered to iron-rich, gummite-like aggregates, and associated zircon grains (cyrtolite "C") have partially decomposed and reacted with liberated U, Th and other elements (Fig. 4.4B). As a result of alteration, zircon grains in thorogummite have irregular or rounded edges.

The heterogeneous nature of zircons and their episodic growth are discussed in the next section.

Size, Shape and Evolution of Zoned Crystals

Although zircons are commonly intergrown with other minerals, their characteristic features and zonal growths are visible under petrographic and binocular microscopes, and more clearly in scanning electron micrographs (Fig. 4.2B,C,D; also Rimsaite, 1978a, Fig. 9.6, 1980, Fig. 38.5, 38.6). Two types of zircon grains are present. Some zircon grains are clear, elongate and prismatic, whereas others are barrel-shaped, dull grey with interbanded dark brown to black zones (Table 4.1; Rimsaite, 1980a, Fig. 38.5). The zoned crystals consist of a core and alternating anisotropic and isotopic (metamict) growth zones. The cores consist of a group of small euhedral zircon crystals, fragments of apparently shattered zircon, uraninite and uranothorite grains, or irregular quartz grains (Fig. 4.2C, 4.4A,B; Rimsaite, 1980a, Fig. 38.5). Zircon grains have grown in a number of episodes as shown by the fragments of minerals, including zircon, that form their cores and by the disposition of growth zones. Specks and fragments of uraninite, uranothorite, apatite, galena and feldspar are interpreted as coeval with hosting zircon zones or to have formed at the end of a cycle of episodic zircon growth and thus to be close in age to both adjacent growth zones. However, after some interruption, new overgrowth zones form, and many crystals provide evidence of several interrupted episodes of growth. The wide zones alternate with densely packed narrow zones, thus resembling growth rings of a tree. A new zone may form in the same crystallographic orientation as the preceding zone, or it may be oriented at 45° or 90° to the inner zone, that is, the diamond-shaped cross section of a pre-existing crystal can be overgrown by terminal pyramids or a prism (Fig. 4.2C, 4.3E). Köhler (1970) illustrated similar relationships between the outer and inner zones. Furthermore, individual zones are commonly made up of two phases, one fractured with high relief and a very clean ED spectrum[1] of zircon; the other apparently softer because it has low relief, and with traces of U, Ca and Fe visible in ED spectra (Table 4.1, Fig. 4.2D, spectra 2 and 3). Terminal faces of zircon crystals are commonly fractured and overgrown by anhedral tails or patches.

Results of the microscope and energy dispersive spectrometer studies indicate the presence of several generations of zircon represented by zoned crystals. In addition to mineral inclusions associated with growth zones, zircon grains are fractured and contain postcrystallizational inclusions in fractures. Chemical analysis of radioactive inclusions in cores, in a zoned portion and in overgrowths of zircon crystals are given in Table 4.1.

Fractures in Zircon Grains and their Contained Mineral Impurities

Secondary electron images reveal the presence of an intricate network of narrow (<1 μm in width) fractures in zircon (cyrtolite). These fractures are either void or filled with various materials, namely, secondary uranyl-bearing aggregates, iron oxides, iron arsenide phases, galena, and REE-bearing compounds (Fig. 4.3C, ED spectrum 1; Rimsaite, 1980a, Fig. 38.6, ED spectrum C). Fractures in some cases are restricted to, or much more abundant in, anisotopic growth zones of pure composition. Thus fractures and their contained minerals may be either younger or older than overgrown zones. Fracture fillings consisting of Pb-, U-, and Th-bearing material may be derived from zircon by processes of continuous diffusion and migration during episodic alterations. On the other hand, this study suggests that in rocks containing abundant altered uraninite crystals, uranyl-bearing fracture fillings in zircon and Pb-rich crusts along (001) cleavage fractures of biotite and on zircon grains originate from the altered more radioactive grains. Strong evidence for this process is provided by the specimen from the Johan Beetz area that contains decomposed uraninite and phosphates (Fig. 4.3). Consequently, the postcrystallizational radioactive and radiogenic inclusions can be introduced into fractures in zircon from an external source and thus alter the original Pb-U, Pb-Th and Pb-Pb isotopic relationships. Furthermore, a network of open fractures would increase permeability to percolating aqueous solutions and would enhance alteration of zircon (cyrtolite) grains.

Evidence of Alteration, Mobilization of Zirconium and Reactions Between Liberated Zr, U, Th, and Other Elements

Fragmented and partly decomposed cyrtolite crystals occur in an amorphous Fe-rich grain of thorogummite (Fig. 4.4B). The elements in this thorogummite probably originated from some or all of the minerals of a magnetite-uranothorite-uraninite-zircon assemblage, similar to that illustrated in Figure 4.2A, under hydrous oxidizing conditions.

A. *BEI of zircon grains ("Zr", grey euhedral) associated with phosphates ("P", monazite and xenotime), uranothorite "Th", and uraninite "U".*

B. *BEI of altered remnants of monazite "P" and acicular secondary REE-bearing aggregates that partially replace monazite. Veinlets of Pb-rich uraniferous aggregates transect the phosphate grain.*

C. *Enlarged portion of zircon in Figure 4.3A (dashed line) with fractures and cavities containing secondary Pb-rich uraniferous aggregates.*

D. *BEI of biotite with zircon inclusion ("Zr") and white (in this photograph) uraniferous aggregates along (001) cleavages.*

E. *BEI of a portion of a zoned zircon showing euhedral grains in the core ("Zr") followed by banded overgrowths and by a pale grey uraniferous termination. Secondary Pb-rich uraniferous aggregates ("U^{2}") coat the grain and occupy adjacent fractures.*

1. *ED spectrum of Pb-rich uraniferous aggregates.*

2. *ED spectrum of uraniferous domain (termination) in zircon.*

Figure 4.3. *Intergrowths of zircon with phosphates, uraninite and biotite; and mineral inclusions in zircon bands. Samples from Johan Beetz area, Quebec. (GSC 203577-R)*

---

[1] Spectrum obtained using an energy dispersive spectrometer.

Table 4.2.

Isotopic data for zircon concentrates[1]. Sample identification is given in Figure 4.1.

	Specimen Numbers				
	1Z	2Z	3Z	4UZ	5Z
Specimen weight (mg)	127.13	65.4	59.7	66.8	144.23
U (%)	6.572	0.613	0.567	44.0	1.007
Th (%)	0.7439	ND*	ND	ND	0.3540
Pb (%)	1.173	0.0658	0.0667	6.92	0.1346
Pb/U	1/5.6	1/9.2	1/8.5	1/6.3	1/7.7
Common Pb (%)	0.21	0.37	0.27	0.34	0.60
$^{207}Pb/^{206}Pb$	0.07367	0.07373	0.07222	0.07299	0.07477
$^{208}Pb/^{206}Pb$	0.06516	0.10139	0.05206	0.13332	0.17547
$^{204}Pb/^{206}Pb$	0.00003	0.00006	0.00004	0.00005	0.00057
$^{207}Pb/^{235}U$	1.838	1.066	1.202	1.508	1.252
$^{206}Pb/^{238}U$	0.1822	0.1106	0.1217	0.1515	0.1240
$^{208}Pb/^{232}Th$	0.09964	ND	ND	ND	0.05864
Apparent ages (Ma)					
$^{207}Pb/^{206}Pb$	1019	1011	976	992	1021
$^{207}Pb/^{235}U$	1059	737	801	734	824
$^{206}Pb/^{238}U$	1079	650	740	909	753
$^{208}Pb/^{232}Th$	1920	ND	ND	ND	1152

[1] Data supplied by Department of Physics, University of Alberta.

*ND - not determined.

As a result of susceptibility to hydration and oxidation, magnetite, uraninite, and uranothorite were altered to hydrated oxides, "gummite" and uranyl-bearing phases along fractures. On the other hand, the relatively resistant zircon grains were altered to a lesser degree. They lost some zirconium and mobilized U, Th and Fe reacted with them to form U-rich domains along the periphery and terminal pyramids, although they retained their general grain outlines (Fig. 4.3E, ED spectrum 2, and 4.4B, ED spectrum D). In addition, the mobilized Zr, U, Th, Si, and Fe reacted with one another to form complex secondary compounds which precipitated in fractures in the Fe-rich thorogummite away from the altered zircon grains (Fig. 4.4B, ED spectra E and F). Finally, it is important to point out that the Th/U ratio in the thorogummite is the highest, and uranium is relatively enriched in fracture fillings in the thorogummite. The fracture fillings outside of thorogummite contain only a small proportion of Th compared to U, thus confirming the mobile nature of the liberated uranium. Although fragments of uranothorite are closely associated with shattered zircon in the core of zoned cyrtolite crystals, reflecting a close "mineralogical affinity" of Zr and Th, secondary zirconium-bearing compounds contain more uranium than thorium indicating at least an elemental association between Zr and U.

Reactions between the zircon host and uranium, thorium, and lead occurred also in narrow rims surrounding uraninite and uranothorite inclusions within the core of a zircon grain (Fig. 4.2C, analysis 13 in Table 4.1) and in overgrowths (Fig. 4.3E, and analysis 10 in Table 4.1). These reactions produced uraniferous zirconian compounds containing as much as 27% U and 18% Th. The Pb-rich crusts and rims in fractures and overgrowths on zircon grains contain 9 to 16% U, 3 to 17% Th, and 3 to 6% Pb. Crusts of pure galena are also common (Table 4.1, analyses 16, 17 and 18). It is obvious that the presence of reaction products containing both U and Zr, of Pb-rich rims and fracture fillings, or of zircon overgrowths of various ages, could markedly affect the Pb-Pb and parent-daughter ages determined for a zircon.

Isotopic Data

Five zircon concentrates yielded discordant isotopic data and the differences between Pb-U, Pb-Th and $^{207}Pb/^{206}Pb$ isotopic ages are illustrated in Figure 4.1A. Only one concentrate, the nonmagnetic fraction "1Z" having the highest Pb/U ratio of 1/5.6, yielded a lead isotopic composition that falls above the concordia curve and the highest apparent Pb-Th age of 1920 Ma, thus confirming similar results obtained on Pb-rich concentrates of associated minerals from the same high grade ore. Namely, Pb-rich radioactive crusts on associated biotite have a high Pb/U ratio of 1/4.5 and yielded an apparent Pb-Pb age of 1088 Ma and Pb/U isotopic ratios that fall above the concordia curve (recent results by G.L. Cumming). The excess radiogenic lead in such samples is present in secondary hydrous Pb-rich kasolite-like aggregates that form crusts in fractures and coatings on minerals (analyses 16 and 17 in Table 4.1). The remaining four concentrates yielded points below the concordia curve and the chord connecting the five points intersects the concordia at 1020 Ma and 90 Ma (Fig. 1b). The acid-leached fraction (4UZ), having a Pb/U ratio of 1/6.3, similar to that in associated separate grains of uraninite, yielded Pb/U isotopic ratios that fall just below the concordia curve. The zircon residue after leaching (3Z, Pb/U ratio = 1/8.4) falls between the magnetic fraction (5Z) and a

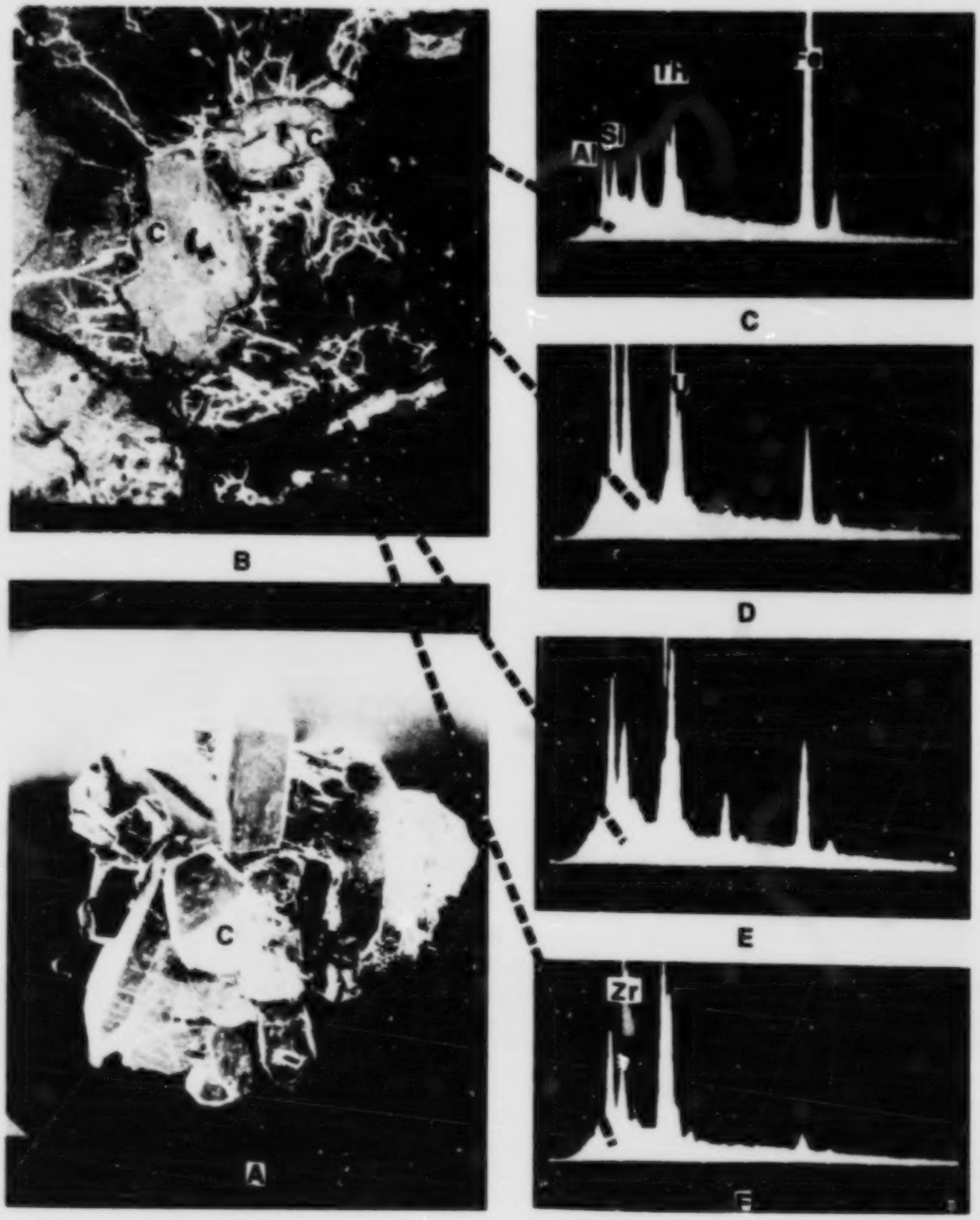

A. *SEI* of a group of cyrtolite crystals "C", hand-picked for isotopic analysis.*

B. *BEI of highly decomposed cyrtolite grains "C" in Fe-rich altered radioactive grain.*

C. *ED spectrum of radioactive U, Th, Fe-bearing host.*

D. *ED spectrum of uraniferous Th-bearing rim of the highly decomposed cyrtolite.*

E. *ED spectrum of complex Zr, U and Th-bearing material filling a fracture in the altered Fe-rich grain.*

F. *ED spectrum of chemically complex U and Zr-bearing interstices surrounding Fe-rich grain.*

Figure 4.4. *Alteration and decomposition of cyrtolite in radioactive oxidized Fe-rich grains and evidence for remobilization of zirconium in altered samples from the Madawaska mine. (GSC 203577-J)*

concentrate of small zircon prisms (2Z, type S-2) that yielded the lowest point on the discordia line, the lowest Pb/U ratio of 1/9.2 and the greatest discordancy of apparent isotopic ages (Fig. 4.1, Table 4.2).

---

* SEI = secondary electron images

The 1020 Ma age for heterogeneous zircons indicated by the upper intersection of the discordia line is lower than almost concordant ages obtained on thorite (1072 Ma) and uraninite (1050 Ma) that occur as inclusions in fluorite in the same deposit. The lower intersection at approximately 90 Ma is similar to the lower intersection of a chord connecting other radioactive minerals from the same deposit and of another chord for metamict pyrochlore (Rimsaite, 1980a). The latter mineral has the lowest Pb/U ratio, 1/59, and a very heterogeneous distribution of U, Ta, Nb, and Y within a single crystal. The metamict minerals in the high grade uranium ore have suffered radiation damage to their structures and mechanical and chemical damages, namely fracturing, hydration and oxidation. The episodic differential losses, redeposition and redistribution of radiogenic and radioactive elements by percolating aqueous solutions occurred along fractures in the metamict minerals several times during the geological history of the deposit. The earliest of these times was related to crystallization of vein quartz, which was followed by recurring fracturing and crystallization of hydrous minerals in fractures, such as muscovite, sericite and chlorite. The latest fractures are filled with serpentine and H_2O-rich montmorillonite-like mineral aggregates. The hydration apparently increased during the last 100 Ma (the lower intersection).

Ion probe studies of radioactive inclusions and crusts and of uraniferous areas within the zircon grains, such as materials characterized by analyses 6, 7, 10 and 13 would provide information on the age of incorporated mineral inclusions and on episodic reactions between U, Th, Zr and other elements.

Conclusions

This study of heterogeneous zircon crystals provides additional information on their history of crystallization and on modes of alteration of their Pb-U-Th systems in radioactive rocks that can be summarized as follows:

1. Backscattered electron images show distributions of heavy (white and light grey) and less dense (black and dark grey) inclusions in zircon (grey). Cores of quartz, shattered uranothorite and groups of small zircons form nuclei for the zoned host.
2. Fragments of uraninite, feldspar, apatite and quartz enclosed in inner and outer bands of zircon crystals are probably coeval with the associated growth zones, whereas some Pb-, REE-, U-, and As-bearing phases are younger because they fill fractures in, and coat zircon grains.
3. Although zircon (cyrtolite) is one of the most stable minerals, it becomes altered as do associated uraninite, uranothorite, magnetite and phosphates, in oxidation zones. Zircon crystals enclosed in goethite and "gummite" aggregates decompose and the liberated Zr reacts with other ions to form complex unidentified Zr, U, Th, P, Si compounds in fractures. Chemical compositions of the Zr-bearing compounds, uraniferous zircon overgrowths and reaction rims containing as much as 27.8% U are illustrated in energy dispersive spectra and listed in Table 4.1.
4. Discordant isotopic ages for zircon from the Madawaska mine are interpreted to result from the presence of both zircon formed in a number of stages and inclusions of Pb- and U-bearing phases introduced after crystallization of the host. Zircon concentrates having an excess of radiogenic Pb, which is introduced apparently in the form of Pb-rich kasolite-like crusts and/or galena, yield points above the concordia curve whereas those with additional U, or differential loss of Pb, yield points below the concordia curve (Fig. 4.1, 4.2, 4.3).
5. A portion of a zoned zircon grain (Fig. 4.3E, ED spectrum 1) provides evidence of episodic growth and of subsequent additions of radioactive elements, namely: (a) crystallization of small zoned crystals (Zr); (b) zoned overgrowths around this core; (c) apparent reaction of outer zones of the zircon with uranium to form a uraniferous zircon phase; and finally (d) narrow rims of secondary Pb-Th-U aggregates, resembling in chemical composition Pb-rich kasolite, around the entire grain and filling adjacent fractures. Such complex zircon grains contain at least four generations of radiogenic and radioactive elements and consequently can provide only an approximation of the minimum age of crystallization of the host rock.

Acknowledgments

Grateful acknowledgments are due to G.J. Pringle and D.A. Walker of the Central Laboratories and Technical Services Division, Geological Survey of Canada for providing scanning electron microscope and energy dispersive spectrometric analyses; to G.L. Cumming and D. Krstic of the Department of Physics, University of Alberta, for isotopic data (research contracts OSU77-00353 and OSU79-00273); to R.L. Alexander and D.R. Wilson of Madawaska Mines Limited for specimens and guidance in the mine; and to R.I. Thorpe, Geological Survey of Canada, for constructive criticism of the manuscript and valuable suggestions.

References

Allen, J.M.
1971: The genesis of Precambrian uranium deposits in Eastern Canada, and the uraniferous pegmatites at Mont-Laurier, Quebec; unpublished M.Sc. thesis, Queen's University, Kingston, Ontario, 83 p.

Baldwin, A.B.
1970: U and Th occurrences on the north shore of the Gulf of St. Lawrence; Canadian Mining and Metallurgical Bulletin, v. 63, p. 699-707.

Clark, G.J., Gulson, B.L., and Cookson, J.A.
1979: Pb, U, Tl, Hf and Zr distribution in zircons determined by proton microprobe and fission track techniques; Geochimica et Cosmochimica Acta, v. 43, no. 6, p. 905-918.

Cooper, G.E.
1957: Johan Beetz area, Electoral district of Saguenay; Department of Mines, Quebec, Geological Report 74, 54 p.

Cumming, G.L. and Rimsaite, J.
1979: Isotope studies of lead-depleted pitchblende, secondary radioactive minerals and sulphides from the Rabbit Lake deposit, Saskatchewan; Canadian Journal of Earth Sciences, v. 16, no. 9, p. 1702-1715.

Fleischer, R.L., Price, P.B., and Walker, R.M.
1975: Nuclear Tracks in Solids; University of California Press, 605 p.

Graubert, B., Steitz, M.G., and Soptrajanova, G.
1974: U and Pb gain of detrital zircon studied by isotopic analyses and fission track mapping; Earth and Planetary Science Letters, v. 21, p. 389-399.

Gulson, B.L. and Krogh, T.E.
1975: Evidence of multiple intrusion, possible resetting of U-Pb ages, and new crystallization of zircons in the post tectonic intrusions (Rapakivi "granites") and gneisses from S. Greenland; Geochimica et Cosmochimica Acta, v. 39, p. 65-82.

Gulson, B.L. and Rutishauser, H.
1976: Granitization and U-Pb studies of zircon in the Lauterbrunnen crystalline complex; Geochemical Journal, v. 10, p. 10-23.

Hewitt, D.F.
1957: General Geology in Satterly, J. – Radioactive mineral occurrences in the Bancroft area, Ontario; Ontario Department of Mines 65th Annual report, v. 65, pt. 6, p. 5-26.

Kish, L.
1977: Patibre (Axe) Lake area; Preliminary Report, Ministère des Richesses Naturelles, Service des Gites Mineraux, DPV-487, 13 p. and geological map 1:20 000 of DPV-487.

Koeppel, V. and Sommerlauer, J.
1974: Trace elements and behaviour of U-Pb systems in inherited and newly formed zircons; Contributions to Mineralogy and Petrology, v. 43, p. 71-82.

Köhler, H.
1970: Die Anderung der Zirkonmorphologie mit dem Differentiations-grad eines Granits; Neues Jahrbuch Mineralogie, Monatshefte, v. 9, p. 405-420.

Poldervaart, A.
1956: Zircon in rocks. 2. – Igneous rocks; American Journal of Science, v. 254, p. 521-554.

Pringle, G.J. and Thorpe, R.I.
1980: Bohdanowiczite, junoite and laitakarite from the Kidd Creek mine, Timmins, Ontario; Canadian Mineralogist, v. 18, p. 353-360.

Pupin, J.P.
1980: Zircon and granite petrology; Contributions to Mineralogy and Petrology, v. 73, p. 207-220.

Rimsaite, J.
1978a: Mineralogy of radioactive occurrences in the Grenville structural Province, Ontario and Quebec: a preliminary report; in Current Research, Part B, Geological Survey of Canada, Paper 78-1B, p. 49-58.

1978b: Application of mineralogy to the study of multistage uranium mineralization in remobilized uranium deposits, Saskatchewan; Mineralogical Association of Canada, Short Course in Uranium Deposits, Toronto, Ontario, p. 403-430.

1980a: Mineralogy of radioactive occurrences in the Grenville Structural Province, Bancroft area, Ontario: a progress report; in Current Research, Part A, Geological Survey of Canada, Paper 80-1A, p. 253-264.

1980b: Selected mineral suites and evolution of radioactive pegmatites in the Grenville Structural Province, Canada; 26 Congrès Géologique International (Paris), Résumés III, p. 999.

1980c: Isotope, scanning electron microscope and energy dispersive spectrometer studies of heterogeneous zircons in radioactive granites in the Grenville Structural Province, Canada; 12th General Meeting of International Mineralogical Association'80, Orléans (France), Collected Abstracts, p. 112.

1981: Petrochemical and mineralogical evolution of radioactive rocks in the Baie-Johan-Beetz area, Québec: a preliminary report; in Current Research, Part A, Geological Survey of Canada, Paper 81-1A, p. 115-131.

Tremblay, P.
1974: Mineralogy and geochemistry of the Mont-Laurier area, Quebec; unpublished M.Sc. thesis, Queen's University, Kingston, Ontario, 133 p.

Veniale, F., Pigorini, B., and Sogetti, F.
1968: Petrological significance of the accessory zircon in the granites from Baveno, M. Orfano and Alzo, North Italy; 23rd International Geological Congress (Prague), v. 13, p. 243-268.

5.

MODIFIED SPOT TEST FOR Pb AND Zn SULPHIDES IN ORE SAMPLES

Project 740081

I.R. Jonasson and W.D. Goodfellow
Resource Geophysics and Geochemistry Division

Jonasson, I.R. and Goodfellow, W.D., Modified spot test for Pb and Zn sulphides in ore samples; in Current Research, Part B, Geological Survey of Canada, Paper 81-1B, p. 37-38, 1981.

Abstract

The well-known spot test for Zn in acid soluble secondary minerals utilizing formation of a red zinc ferricyanide complex species has been modified to permit detection of zinc, present as finely dispersed sulphide, at levels greater than 5000 ppm in whole rock. The test has been applied conventionally to readily resolubilized Zn species such as hemimorphite, smithsonite or hydrozincite and adsorbed forms in iron oxides and organic residues. By treating rock surfaces with strong nitric or hydrochloric acid for at least one minute and then neutralizing with sodium bicarbonate solution, zinc can be rendered reactive to "zinc zap" reagent. Similarly, galena surfaces can be decomposed by strong acids to produce a coating of relatively soluble lead sulphate or chloride which will react with dilute potassium iodide solution to give a bright yellow precipitate of lead iodide. The limit of sensitivity of this test for finely dispersed galena in whole rock is around 10 000 ppm (1%). The techniques are rapid and can be undertaken on site.

An example of the application to lead-zinc sulphide bearing black shales and cherts is given. Comparisons between average values for lead and zinc determined analytically on a suite of drill-core samples and estimates of intensity of colour development for the spot tests are made. Results indicate that the zinc profiles are similar over the entire test section but that the lead test fails to detect dispersed galena when the carbonate content of samples increases markedly.

Introduction

Formation of zinc ferricyanide complex species provides the basis for the well-known "zinc-zap" spot test on geological materials. Conventionally, the test is applied to samples where a secondary accumulation of zinc, commonly as carbonate or silicate, or as an adsorbed species on say hydrous iron oxides is suspected. It has proved useful as a field test particularly where the secondary zinc carbonates, smithsonite and hydrozincite or the silicate hemimorphite are present as coatings but are not readily visible. Reaction is immediate to yield a brownish red stain which is diagnostic for zinc (Raffinot, 1953).

The formation of bright yellow lead iodide crystals is no less diagnostic for lead which can be solubilized by dilute acid when it is present as the carbonate, cerussite or as the sulphate, anglesite.

To date, the tests have found little application in the search for unoxidized finely disseminated zinc and lead sulphides which are not directly reactive to the reagents. The prime objective of this work was to investigate the applicability of zinc and lead spot tests to low grade disseminations in graphitic or carbonaceous shales and cherts where grey-black sphalerite, especially, is often inconspicuous at concentrations of five per cent or less. Fine grained galena may be similarly obscured.

The Methods

The zinc test reagent comprises the following solutions:
Reagent A - 3% potassium ferricyanide and
Buffer B - 3% oxalic acid; 0.5% diethylaniline

These are mixed in equal proportions before use and stored away from sunlight to minimize photolytic oxidation of the reagents. Drill core or other siliceous rocks bearing sulphides, are treated with a drop or two of strong nitric acid. This is allowed to react for a few minutes; likely it will dry up or soak in. A few drops of a solution saturated in sodium bicarbonate are placed carefully on the acid-leached area to neutralize excess acid. It is important to retain drop form and to avoid run-off of the solutions which now contain dissolved zinc and lead. In the absence of iron sulphides a red stain is immediately visible upon addition of a drop of zinc reagent. When iron sulphides are present bright Prussian blue stains of ferrous ferricyanide may camouflage the zinc colour; however by dabbing with a tissue or filter paper, the red colour will become visible. Similarly in rusty rocks, or when zinc content is minimal, use of a paper absorbent improves recognition sensitivity considerably.

To test for lead, the same procedure of acid oxidation and neutralization is followed, then a drop or two of 1% potassium iodide is added. This reagent must also be stored away from sunlight. Some experimentation may be necessary to ensure complete neutralization of nitric acid since acid residues will oxidize iodide ions to yellow iodine solution and thereby re-dissolve or otherwise mask the lead iodide precipitate. This last problem can be circumvented by using concentrated hydrochloric acid rather than nitric acid but galena dissolution will be much slower. It is also necessary to work with minimum volumes and to avoid run-off. The process mechanism involves oxidation of lead sulphide to lead sulphate and subsequent precipitation of lead iodide at galena surfaces. Fine grained galena is therefore stained yellow and with care, textures may be highlighted for inspection or for photography.

Field Observations

The methods were tested on several hundred feet of drill core comprising dissemination of fine grained sphalerite and galena with lesser amounts of pyrite in highly carbonaceous (up to 8% C) cherts and shales. Some bands of carbonate enriched rocks (up to 20% CO_2) often galena bearing, were also tested. Results are presented for the section as averaged profiles using arbitrary scales based on intensity of colour or precipitate development. These are plotted in Figures 5.1a and 5.1b as zero, weak, moderate, and strong responses. Analytical results for zinc and lead are plotted on the same profiles where values in ppm and percentage represent abundance ranges for a sequence of samples rather than individual datum points. Detection thresholds for the field tests, 0.5% for Zn and 1% for Pb, are also indicated in Figure 5.1.

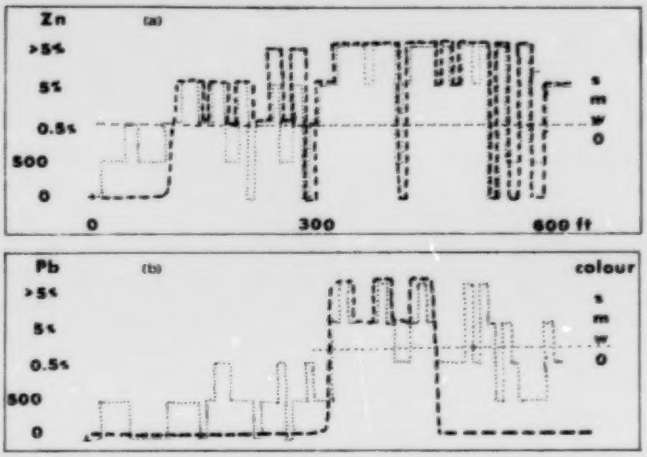

Analytical profile
Colour profile

o = zero
w = weak
m = moderate
s = strong

Detection thresholds

Figure 5.1. *Analytical and colour profiles for Pb and Zn (lower values in ppm).*

Both elements were determined analytically in the Geological Survey of Canada laboratories by repeated aqua regia dissolution followed by an atomic absorption spectrometric finish. High lead values were confirmed on selected samples by check analyses using concentrated hydrochloric acid solutions.

Discussion

Results presented indicate a generally good correspondence in concentration profiles between the colour tests and the chemical analyses. It is therefore fair to conclude that the methods are accurate under most conditions and useful in gauging relative lead and zinc contents, particularly at low levels.

Preliminary investigations of thin sections of ore samples indicate that the sulphides are present as fine grained disseminations or as finely banded layers; sphalerite is commonly more abundant and more homogeneously dispersed than galena, which tends to form small grains or aggregates or is remobilized into tiny fractures. Although lead occurrence appears confined to the mineral galena, zinc is somewhat more ubiquitous being present at moderate levels (about 1%) in samples where sphalerite is not discernible even in thin sections. In these cases zinc is finely dispersed, perhaps as a sulphide, in highly carbonaceous particles and in hydrocarbon impregnated cleavage planes common in the upper levels of the ore section studied. Further investigation of the nature of these concentrations is underway.

Profiles from the zinc tests closely parallel analytical data over the entire section, however the lead tests failed to detect galena at levels up to 5 per cent in the lower 45 m of core, between depths 137-183 m (450-600 ft), where carbonate content increases markedly (up to 20% CO_2). This is interpreted as indicating greater rates of dissolution of sphalerite over galena under the conditions of these tests. In the presence of significant amounts of lime, concentrated nitric acid is effectively neutralized before extensive alteration of exposed galena grains can take place. By persisting with acid etching for some time, exposed carbonate can eventually be dissolved permitting oxidation of galena to occur. Under these conditions the test for lead is usually positive. However, since an objective of this work was to devise rapid and convenient spot tests for lead and zinc in sulphides, such a prolonged procedure is unacceptable.

Alternatively, ore bearing samples can be painted with strong hydrochloric acid and left to react and dry overnight. Application of a 1% potassium iodide solution produces yellow coatings at galena surfaces. This is the best procedure if the aim is to highlight ore texture for photography. However, the presence of carbonate minerals restricts Pb detection as noted above. All ore samples should be well flushed with water on completion of any of these tests.

Acknowledgments

We appreciate the co-operation of our colleagues in Geochemistry Subdivision who made the check analyses recorded here. These studies were carried out as part of the Nahanni Integrated Multidisciplinary Pilot Project.

Reference

Raffinot, P.
1953: Identification of mineral grains by surface colouration; Revue de l'Industrie Minérale, Pt. C No. 602, p. 31-36.

6.

COASTAL GEOLOGY MAPPING: AN EXAMPLE FROM THE SVERDRUP LOWLAND, DISTRICT OF FRANKLIN

Project 780043

E.H. Owens[1], R.B. Taylor, M. Miles[2], and D.L. Forbes[3]
Atlantic Geoscience Centre, Dartmouth

Owens, E.H., Taylor, R.B., Miles, M., and Forbes, D.L., Coastal geology mapping: an example from the Sverdrup Lowland, District of Franklin; in *Current Research, Part B, Geological Survey of Canada, Paper 81-1B, p. 39-48, 1981.*

Abstract

A system for coastal geology mapping is discussed which has been tested at scales ranging from 1:4800 to 1:125 000, in a variety of Canadian coastal environments including the Sverdrup Lowland. The system is compatible with the surficial geology mapping schemes used by the Geological Survey of Canada. Initially, the coast is progressively subdivided into shore units, zones and components which are the building blocks used to define the physical coastal characteristics and a limited number of replicate shore types. Use of standardized codes allows a direct comparison between coasts of different geographic areas. All available coastal information is systematically listed on coding sheets and a summary of the primary coastal elements is shown on the maps using coded descriptors. Also displayed on the maps is the distribution of replicate shore types.

Introduction

The growth of interest in coastal geological studies over the past decade has focussed in part on mapping of physical shoreline features. At present, coastal geology maps are available for only selected parts of the Canadian coastline. Several methods have evolved to compile and display coastal information. For example, some mapping schemes used in eastern Canada include those of Dubois (1973), Scarlett et al. (1976), Barry et al. (1977) and McLaren (1980). Important now is the need to develop a mapping system so that a uniform series of coastal maps can be produced for the country. The system should be applicable at a variety of scales and to the variety of coastal settings found in Canada. The system should be multi-user oriented and suitable for storage of information on computer files for quick retrieval and analysis. In an attempt to develop such a system, it was thought desirable that it also be compatible with the existing surficial geological mapping schemes used by the Geological Survey of Canada (GSC). Consequently, a system was designed based on systems developed for surficial geology by the Survey (e.g. Fulton et al., 1974, 1975; Barnett et al., 1975, 1976; Boydell et al. 1975a, b) and refined by the Environment and Land Use Committee (E.L.U.C.) (1978). The system was developed initially as a joint study with the Resource Analysis Branch of the British Columbia Ministry of the Environment and was also partially funded by Lands Directorate of Environment Canada. The mapping was tested at scales of 1:4800 (Capital Regional District, 1979) and 1:20 000 (Owens, 1980). Additional mapping using the system has also been carried out in British Columbia by D. Howes (personal communication, 1980) and by J.R. Harper (personal communication, 1980) at scales of 1:25 000 and 1:10 000 respectively. Low altitude, oblique colour video tapes were used as the primary data base for these studies.

The objective of this paper is to describe and illustrate how physical coastal information is organized, coded and displayed in the proposed mapping system by using an example of a mapping program recently completed in central Sverdrup Lowland, District of Franklin (Woodward-Clyde Consultants, 1980). Shores in the Sverdrup Lowland (Fig. 6.1) represent a very simple model with which to introduce the mapping system because of the limited coastal information base and the scale of mapping (1:125 000). Although some oblique, low-altitude, colour photography and field observations were available (Taylor, 1980, Fig. 6.2), the majority of the program was conducted using vertical aerial photography (1:60 000). Mapping was completed on King Christian, Lougheed, and Cornwall islands, south Amund and Ellef Ringnes islands, and Sabine Peninsula, Melville Island (Fig. 6.1).

Coastal Geology Mapping System – Conceptual Framework

The mapping system involves three key elements:

a. use of a progressive subdivision or hierarchy of scales to examine the coast;
b. development of a flexible information format using coding sheets, and standardized codes to describe the physical coastal characteristics; and
c. preparation of maps which summarize the basic shore-zone characteristics and the distribution of replicate shore types.

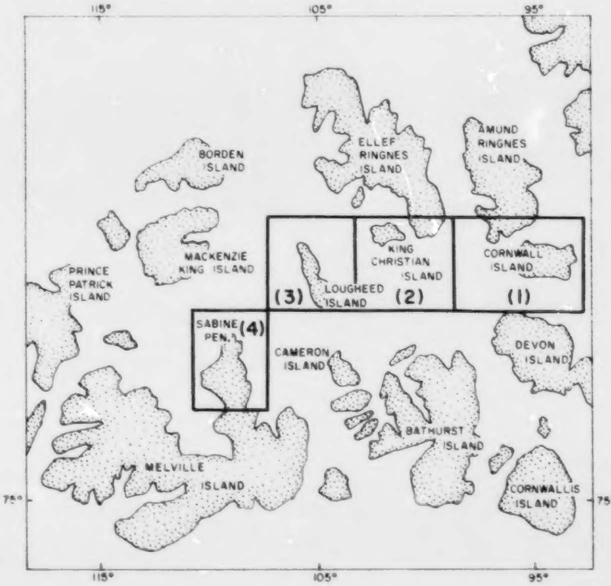

Figure 6.1. *Location of the coastal mapping project in the central Sverdrup Lowland. For each of the four geographic areas outlined, a set of maps (scale 1:125 000) was completed that summarize the physical coastal characteristics.*

---

[1] Woodward-Clyde Consultants, Victoria, B.C.

[2] Miles and Associates, Victoria, B.C.

[3] University of British Columbia, Vancouver, B.C.

Table 6.1

Detailed physical characteristics of each shore unit, e.g. KC 4 are documented on coding sheets. In this case, only two across-shore zones are described for each shore unit. They are the terrain zone and the shore zone. Information on the surficial materials, trafficability and sensitivity of the terrain is derived from reports by Hodgson (1977, 1978). A summary of the primary shore zone characteristics is provided in columns 3 and 4 and displayed on the map (Fig. 6.3).

LOCATIONS King Christian Island KC MAP SHEET 69C (469D)
Elief Ringnes Island ER CODING SHEET 1 of 8

King Christian Island KC MAP SHEET 69C (469D)
Ellef Ringnes Island ER CODING SHEET 1 of 8

UNIT					SUMMARY		TERRAIN CHARACTERISTICS									SHORE ZONE CHARACTERISTICS: PROCESSES									
IDENTIFICATION	COMPOSITION: HOMOGENEOUS	PRIMARY	SECONDARY	VARIANT	COASTAL CLASS	COASTAL UNIT DESCRIPTOR	PHYSIOGRAPHY	GEOLOGICAL FORMATION	SURFICIAL MATERIALS	SLOPE CLASS	SLOPE MODIFIERS	POOR DRAINAGE	DRAINAGE DENSITY	GULLYING/NIVATION	INSTABILITY FEATURES	TEXTURE	EOLIAN	FLUV. PRESENCE	FLUV. SEDIMENT SUPPLY	COLLUVIAL	THERMOKARST	WAVES MAX. OBS. FETCH	LEAD WIDTH	ICE THRUSTING	ICE PILING
1	2				3	4	5	6	7	8	9	10	11	12	13	14	15	16	17	18	19	20	21	22	23
KC1	4				4	sIWm-SBw	Lp	Ki	sW(b)	1	r	-	L	Y	-	s	-	Y	M	-	-	4	1	2	Ps
KC2	4				7	sFl-T	Lp	Ki	sFd^{A}	1	-	NA	NA	Y	-	s	-	Y	M	-	-	4	1	2	-
KC3	4				4	sIWl-SBw	Lp	Ki	sW(b)+Fj	1	r	-	M	Y		s	Y	Y	M	-	-	4	0	2	Ps
KC4		3			4	sIWl-SBRw	Rel	Ki	sWb + Ff	1	r	-	M	Y	Pl	s	Y	Y	M	-	-	4	3	3	Ps
			2		7	sFl-T	Rel	Ki	sFd^{A}	1	-	NA	NA	Y	-	s	-	Y	M	-	-	4	1	3	Ps
				v^{1}			Rel	Ki	sWb + Ff	1	-	-	NA	-	-	s	Y	-	-	-	-	4	3	3	Ps
KC5		3			4	fIWl-SBRw	Rel	Ki	$\frac{dW}{R}$	2	-	-	M	Y	Pl	f	Y	Y	M	-	-	4	0	2	Ps
			2		7	sFl-T	Rel	Ki	sFd^{A}	2	-	NA	NA	Y	-	s	Y	Y	M	-	-	4	0	2	Ps
KC6		4			8	fIm-SRi	Lp	Ki	fW + Fd^{1}	1	-	Y	L	-	Rl	f	-	Y	M	S	-	4	1	3	Po
			1		7	sFl-T	Lp	Ki	sf Fd^{A}	1	-	NA	NA	-	-	s	Y	Y	M	-	-	4	1	3	Po
KC7		4			8	fIKm-FRib	Lp	Kcl	fW + Fd^{1}	2	-	Y	M	Y	RIS	f	-	Y	M	S	-	4	1	3	Po
			1		7	$\frac{s}{f}$Fl-T	Lp	Kcl	$\frac{s}{f}$Fd^{1}	2	-	NA	NA	Y		$\frac{s}{f}$	Y	Y	M	-	-	4	1	3	Po

UNIT	SHORE ZONE CHARACTERISTICS: FORM									LAND USE INTERPRETATIONS					RELIABILITY						
IDENTIFICATION	NEAR SHORE SLOPE	FORESHORE SLOPE	CLIFF	BEACH	DELTA	BARRIER	SPITS	SHORELINE CHANGE	NET. SED TRANSPORT	ICE RICH	AGGREGATES	WATER SUPPLY	TRAFFICABILITY	TERRAIN SENSITIVITY	A/P SCALE	OBLIQUE A/P	GROUND PHOTOS	BEDROCK GEOLOGY	SURFICIAL GEOLOGY	OTHER DATA	AIR PHOTOGRAPH NUMBERS
1	24	25	26	27	28	29	30	31	32	33	34	35	36	37	38	39	40	41	42	43	44
KC1	mb	L	-	Bt	T	-	-	0	-	-	2	1	A2/1	L	6	A	-	A	A		A17217 (29 - 30)
KC2	mb	L	-	Bt	T	-		+	-	-	2	1	A2/1	L	6	A	-	A	A		same
KC3	lb	L	-	Bt	T	-	-	0	-	-	2	1	A2/1	L	6	A	-	A	A		same
KC4	mp	L	-	Bb	T	D	-	0	R?	-	2	1	A2/1	L	6	A	A	A	A	1	A17217 (29 - 31)
	mp	L		Bt	T	D	-	+	-	-	2	1	B2/2	Mbc	6	A	-	A	A		same
	mp	L	-	Bb	-	-	-	0	R?	-	2	1	A2/1	L	6	A	A	A	A	1	same
KC5	sb	L	lb	Bb	T	D	-	0	-	-	2	1	B3/2	Mabc	6	A	-	A	A		A17217 (31 - 32)
	sb	L	-	Bt	T	D	-	+	-	-	2	1	B3/2	Mabc	6	A	-	A	A		same
KC6	sb	M	-	Bt	-	-	-	+	-	Y	1	0	B2/2	Mbc	6	A	-	A	A	1	same
	sb	L	-	Bt	T	D	-	+	-	-	1	1	B2/2	Mbc	6	A	-	A	A		same
KC7	sb	M	(lb)	Bt	T	D	-	0	R?	Y	0	0	A3/2	Mabc	6	A		A	A		A16751 (197 - 199)
	sb	L		Bt	T	D	-	+	R?	-	1	1	A3/2	Mabc	6	A	-	A	A		same

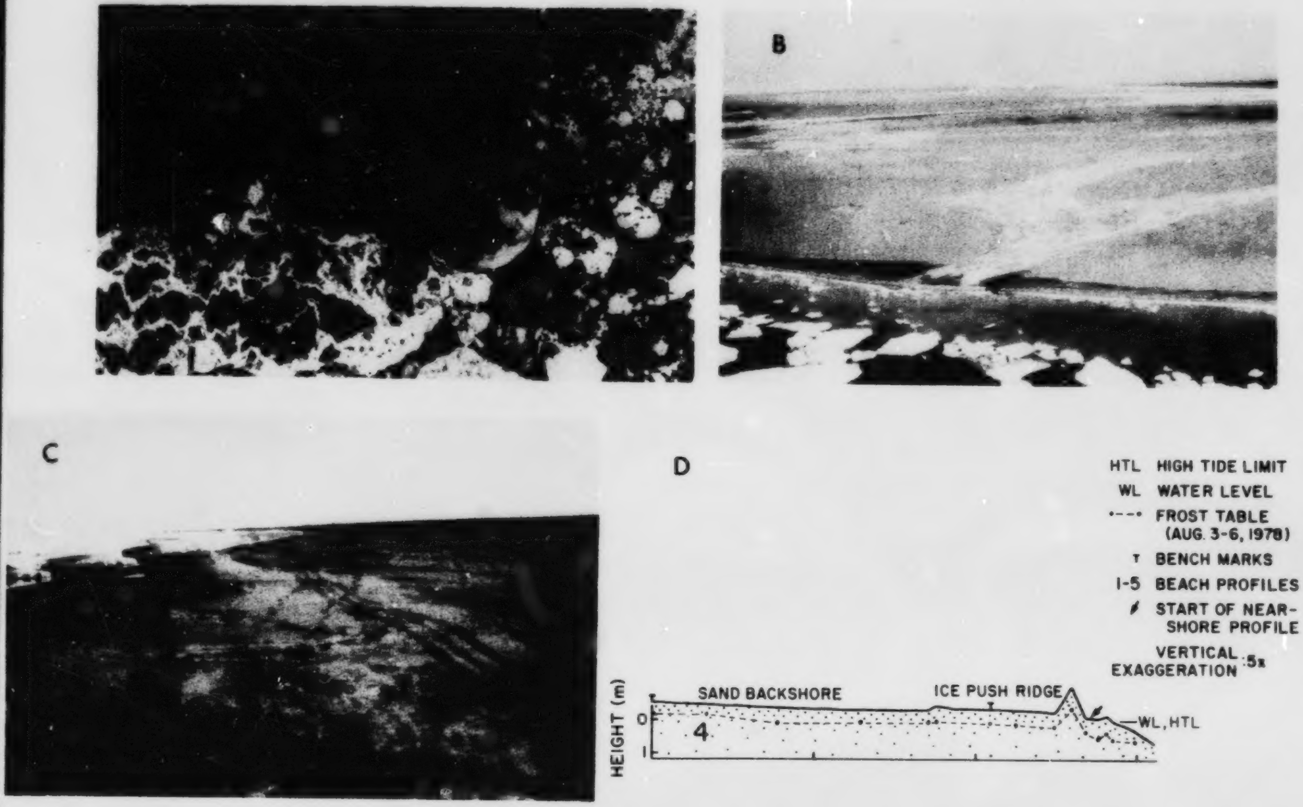

Figure 6.2. *An example of the information base used to interpret the coastal characteristics in the Sverdrup Lowland. Often only vertical aerial photography (1:60 000) was available (A), however for King Christian, S. Ellef Ringnes and Cornwall islands there was also oblique coastal photography (B) flown at 125 m altitude in 1976 or 1978 and some field observations (C, D). This figure illustrates the shore zone at and just north of Cape Abernethy, King Christian Island (KC 4 – Fig. 6.3).*

Subdivision of Coastal Zone

A flexible and practical method for coastal-zone analysis is to subdivide the coast into smaller sections until the desired or most appropriate scale is achieved. A systematic examination of a coastline reveals segments of coast which are very similar and others which are different. Thus, the coast is initially divided into a series of shore units each of which is homogeneous alongshore e.g. a continuous sand beach. The units are described in terms of across-shore zones which are usually divided on the basis of tidal zones (supratidal, intertidal, subtidal). The alongshore boundaries of a unit (indicated by a double slash – Fig. 6.3) are defined by a change in character of one or more across-shore zones. For instance, a new shore unit is defined where the slope or texture change in one of the tidal zones. A shore unit usually extends from the seaward limit of nearshore processes to the landward limit of marine processes or the top of a coastal cliff

The across-shore zones can be further divided into components which define specific geomorphological features (e.g. storm ridge) which implicitly provide information on the process(es) that controls or developed each feature.

The extent to which a coast is subdivided is a function of the availability of information and of the proposed scale of mapping for each mapping program. For instance, in the British Columbia coastal mapping programs cited above, shore components were the primary building blocks used to describe the shore zone. In the present study, the extremely limited coastal information base restricted the extent to which the shore unit could be divided. Moreover, there was a requirement for information about the adjoining hinterland for the planning of support facilities for marine terminals. As a result, the shore units were divided into only two across-shore zones – the terrain zone and the shore zone. The terrain zone included land adjoining the beach extending to the 30 m contour, and the shore zone included the beach and, where information was available, the nearshore.

Often a section of coast is characterized by a close repetitive series of two or more homogeneous units, e.g. KC 4 (Fig. 6.3) – sequence of sand beaches and river deltas. Since mapping of each individual homogeneous unit would involve considerable repetition, it is more practical to use composite units. Each composite unit is subdivided into primary and secondary parts. The primary subdivision is the predominant repetitive sequence and it accounts for 50 per cent or more of the unit length. The secondary subdivision (indicated on maps by single slashes encompassing the symbol $S^{1,2,3}$...n) is the minor repetitive association and may account for up to 50 per cent of the unit length. It is possible that two or more secondary subdivisions may be identified. If the physical characteristics are similar the secondary subdivisions are identified by the same superscript, e.g. S^1; if their characteristics change, the superscript also is changed, e.g. S^2.

Table 6.2

Eight generalized shore types are defined for the central Sverdrup Lowland. The distinguishing physical characteristics of each shore type and the pattern used on the maps (Fig. 6.3) to identify each are as follows:

1. Cliffed Coast

▥

consolidated or unconsolidated material, with or without talus

greater than 3 m in height

may be fronted by a beach

2. Banked Coast

▤

erosional coast characterized by scarps less than or equal to 3 m in height

may be fronted by a beach

banks may be discontinuous

3. Gravel Beaches

▩

generally associated with well-preserved raised beaches having a distinguishable surface relief

characterized by a moderate foreshore slope

4. Sand Beaches (Fig. 6.2)

░

characterized by a low to moderate foreshore slope; may include a low erosional bank in the backshore

frequently exhibit a dense network of consequent rills or streams

preferentially associated with sands and sandstones, most notably Isachsen and Eureka Sound Formations

5. Fine Textured Beaches (Fig. 6.4B)

▒

preferentially developed on shales, particularly on Christopher Formation

see text for additional information

6. Wide Intertidal Coasts

▦

shores with a wide shallow subtidal/intertidal area

contiguous terrain is generally lowlying but may have local areas of moderate angle slopes; the coastal area may be complex with many small embayments, discontinuous low banks, and localized deposits of marine reworked sediments (Lougheed Island)

7. Deltaic Coasts

coasts dominated by active deltaic sedimentation

▩

active deltas are invariably fan shaped with an arcuate front; channels are wide, shallow, and braided; deltas may project as much as 2 km beyond the adjacent coastline; channels frequently incised in older deltaic sediments; coastal areas at the active channel mouth may have discontinuous barriers which are initiated by ice thrusting, but may be reworked by waves and breached by river action

8. Ridged Coast (Fig. 6.4A)

>>>

generally associated with fine textured sediment derived from other fine textured materials (e.g., siltstone or shale) or with gravel deposits; may include low banks and beaches with a berm, but both are frequently and extremely modified by ice thrust

see text for additional information

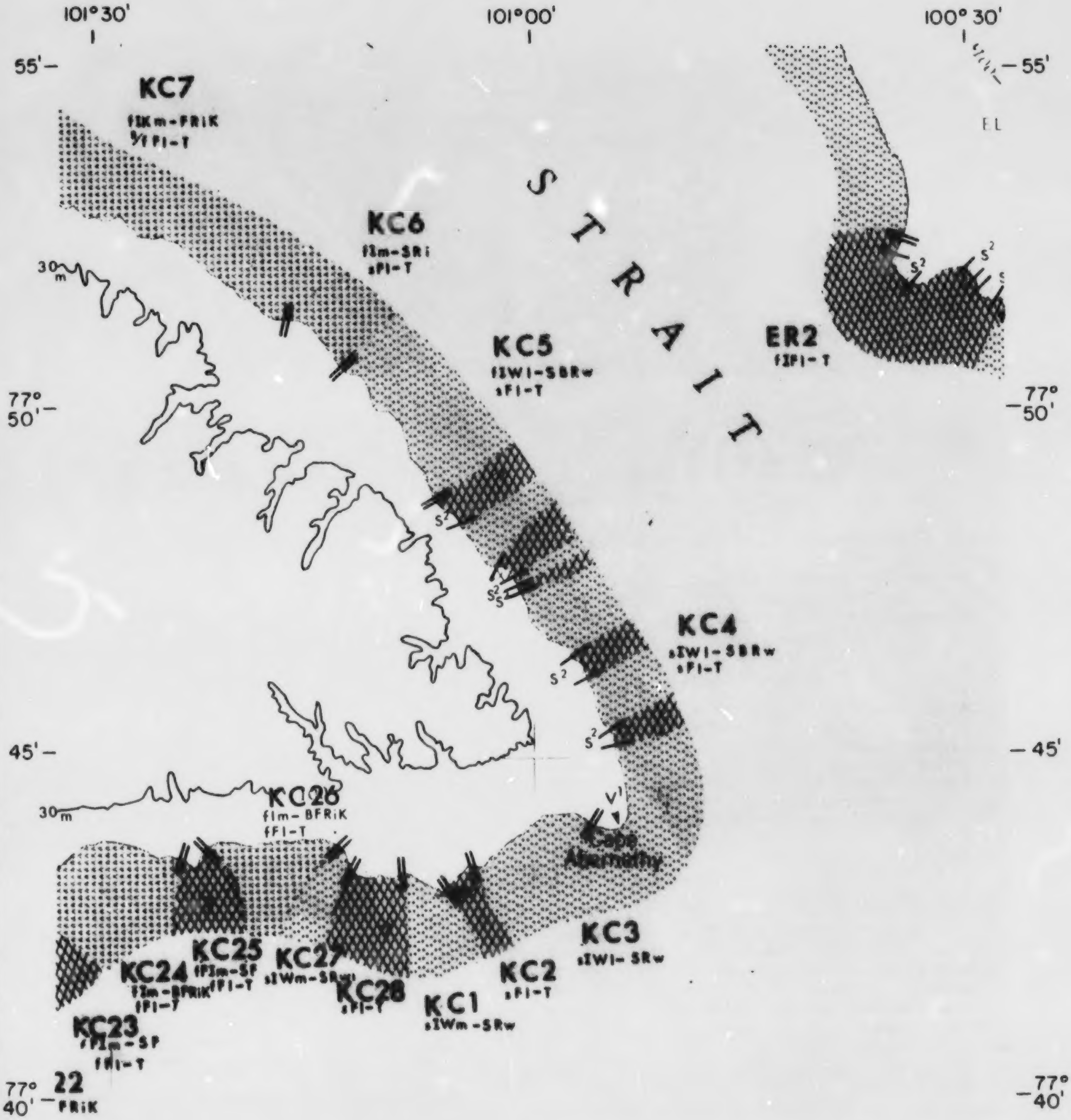
101°30'
101°00'
100° 30'
55'
55'
77° 50'
77° 50'
45'
45'
77° 40'
77° 40'
KC7
fIKm-FRIK
s/f FI-T
KC6
fIm-SRi
sFI-T
S T R A I T
KC5
fIWI-SBRw
sFI-T
ER2
fIFI-T
EL
S2
KC4
sIWI-SBRw
sFI-T
V1
Cape Abernethy
KC3
sIWI-SRw
KC2
sFI-T
KC1
sIWm-SRw
KC28
sFI-T
KC27
sIWm-SRwi
KC26
fIm-BFRiK
fFI-T
KC25
fFIm-SF
fFI-T
KC24
fIm-BFRiK
fFI-T
KC23
fFIm-SF
fFI-T
22
FRiK
30m
30m

Figure 6.3. *The coastal geology map of southeastern King Christian Island illustrates how the primary coastal characteristics are summarized and displayed. Initially shore units (outlined by double slashes) are defined e.g. KC 4, and each is described using a coded descriptor (Table 6.3). The distribution of generalized shore types (Patterns – Table 6.2) are shown alongshore and where applicable, secondary shore units (S^2) and variants (V^1) also are located.*

Table 6.3

Shore unit descriptor – a simple descriptive code provides a summary of the physical character of each shore unit. The descriptor is defined in terms of four parameters. These are examples of some of the codes used to describe each parameter.

1. Texture of material

s	sand	(0.063 < D < 2 mm)
f	fines	(D < 0.25 mm)
ꞩ	silt	(0.004 < D < 0.063 mm)
¢	clay	(D < 0.004 mm)

2. Dominant process or processes operating on the shore zone

F	fluvial
I	marine (ice)
W	marine (wave)
K	thermokarst

3. Slope of foreshore

l	low slope
m	moderate slope
s	steep slope (angle of repose or steeper)

4. Shore zone morphology

B or Bb	beach with berm
F	bank, height <3 m
S	simple inclined surface
T	delta, braided channel, fan
Ridged morphology –	
Ri	due to sea ice thrusting
Rk	due to thermokarst
Rw	due to presence of raised beaches

Example of Descriptors

Descriptor	sWm – SBF ↑↑↑ ↑ ↑	This unit exhibits a moderate sloping sandy shore zone dominated by marine wave processes. The foreshore has a simple incline topped with a berm. A low bank less than 3 m in height divides the backshore from the adjoining terrain.
Parameters	123 4	
	$\frac{\text{fIKm – SFRik}}{\text{sFl – T}}$	This unit exhibits a moderate-slope fine-textured shore zone dominated by ice thrusting and thermokarst activity. The shore has a simple incline backed by a bank less than 3 m high and by a series of ridges formed from a combination of ice thrusting and thermokarst activity. A secondary coastal type which occurs within this unit is a low angle, sandy shore which primarily reflects the presence of fluvial processes and associated sediment deposition in a deltaic environment.

Often the continuity of a shore unit is interrupted by minor shore-zone features such as a spit or a small stream. A variant (indicated by the symbol $V^{1,2,3}$...n – Fig. 6.3) is used to delineate these minor features. Variants may in some cases be repetitive, but account for less than 10 per cent of the unit length. More than one variant may be identified in each shore unit.

In the Sverdrup Lowland study, primary subdivisions, because of the scale of mapping, were restricted to lengths greater than 2 km. Features or areas less than 2 km but more than 0.5 km in length were identified as secondary subdivisions or variants. To avoid unnecessary clutter, secondary subdivisions less than 0.5 km in length were generally not plotted on the maps; however, they were identified in the unit descriptor and described on the coding sheets, e.g. KC 5 (Fig. 6.3, Table 6.1). The relative percentage of the total shore unit length occupied by primary or secondary subdivisions or variants is coded on the coding sheets (Table 6.1: 1 ≡ 0-20%,... 4 ≡ 80-100%).

Detailed Information Base – Organization and Coding

The detailed physical characteristics of each coastal unit are compiled on coding sheets (Table 6.1) by making use of standardized codes. The codes, which are a simple translation of descriptive terminology into alphabetic notation, are standardized for use in any coastal region of Canada. Although the total array of codes is already large, the system is flexible so that new codes can be added if necessary. For instance, additional codes were required in the Sverdrup Lowland project to reflect arctic conditions and the presence of sea ice and permafrost. In this paper, it is not possible to define all of the codes used; the reader is referred to the code books which accompany each mapping project (e.g. Owens, 1980; Woodward-Clyde Consultants, 1980).

The objective of the coding sheets is to display, in a systematic fashion the detailed physical characteristics of the shore units, across-shore zones, and shore components.

A

Figure 6.4A. *The dominant characteristic of the 'Ridged coast' is its very irregular hummocky topography. The desiccated ridges shown here on south King Christian Island (KC 26, Fig. 6.3) were formed by ice push.*

B

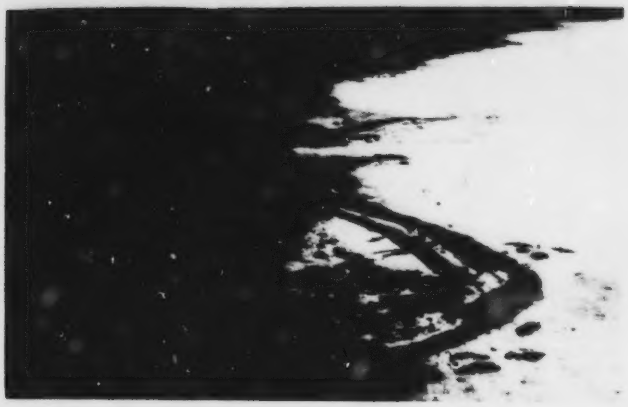

Figure 6.4B. *An absence of normal beach form and the presence of one year old all-terrain cycle tracks (faint ones) across the intertidal zone, suggest little or no reworking by littoral processes along the shores of northern King Christian Island.*

The coding sheets allow a user to pull out relevant information for a specific purpose and the codes facilitate the storage and analysis of the data by computer.

Information on the coding sheets focuses on sediment texture, primary geomorphological features, and primary processes affecting each shore unit. However, flexibility in the coding sheet format allows it to be adapted to individual mapping projects. In the present study, the shore units were divided into only two zones but additional information on geology, land use interpretations and specific hazards to development were included because of their usefulness in the preliminary selection and assessment of sites for marine terminal facilities.

Each shore unit is identified on the maps and the coding sheets by an alphabetic code and a number. The alphabetic code refers to a specific island and the units on each island are numbered consecutively e.g. KC 3 is King Christian Island unit 3 (Fig. 6.3). Once the physical characteristics of each unit are listed on the coding sheets, the primary elements of each shore unit are summarized and displayed as a coded unit descriptor (Tables 6.1, 6.3). The shore unit descriptor summarizes the following information: (1) sediment texture, (2) dominant process or processes operating on the unit, (3) foreshore slope, and (4) shore zone morphology. Two examples of shore unit descriptors and their interpretation are provided in Table 6.3. In the case of a composite shore unit, the descriptor of the primary subdivision is displayed above the descriptor of the secondary subdivision.

The detailed physical coastal information is also used to define a limited number of generalized replicate shore types or coastal classes for the study area. In the central Sverdrup Lowland eight replicate shore types are defined (Table 6.2). The most common shore type is the sand shore or 'Sandflat' coast (McLaren, 1977; Taylor, 1980) which is characterized by continuous sand beaches with a very gradual slope (Fig. 6.2). Two other shore types strongly reflect the arctic environment. (1) The 'Ridged' coast is characterized by very irregular hummocky ridges, generally formed by sea ice thrust, but due in some cases to retrogressive thaw flow slides (KC 26, 7 – Fig. 6.3, 6.4A). The 'Ridged' coast is often associated with shores composed of fine grained sediments. (2) The 'fine-textured' beaches are composed of sediment finer than medium sand. Although the size of sediment is primarily a function of the underlying bedrock or source rock, the absence of a normal wave-built beach profile reflects the limited wave energy conditions due to fetch restricted by sea ice (Fig. 6.4B).

Coastal Geology Maps – A Summary

A synthesis of the detailed physical coastal information listed in the coding sheets is displayed on maps so that a user can obtain a quick overview or summary of the primary shore characteristics. A set of two maps is prepared for each island. The first map (Fig. 6.3) focuses attention on the location of shore units, the shore zone characteristics and the distribution of replicate shore types. Adjacent to each shore unit is a coded descriptor which summarizes the physical characteristics of the unit. The distribution of replicate shore types is shown using distinctive patterns (Fig. 6.3) and their distinguishing characteristics are listed in the map legend (Table 6.2). The only terrain information provided is the map contours. The 100 foot (30 m) contour is accented in the present study because it is used to compute a representative slope between it and the shoreline. Additional information pertaining to the coastal hinterland e.g. terrain sensitivity, is displayed only in the coding sheets.

On the second map, emphasis is on plotting process elements, e.g. winds, tides, currents, waves, and factors which affect littoral processes, e.g. nearshore bathymetry. However in the central Sverdrup Lowland, process information is extremely limited. In this study symbols were used to indicate shores affected by sea ice-thrusting and ridging, the direction of longshore sediment transport, nearshore bathymetry, and the extent of raised beaches (Fig. 6.5). As more process information becomes available, it can be added to the maps. Boundaries of shore units are plotted on the second map to facilitate a comparison with information on the first map.

Other relevant coastal information such as field observations of beach profile or sediment sample data are included on one or both of the maps as inset diagrams or tables.

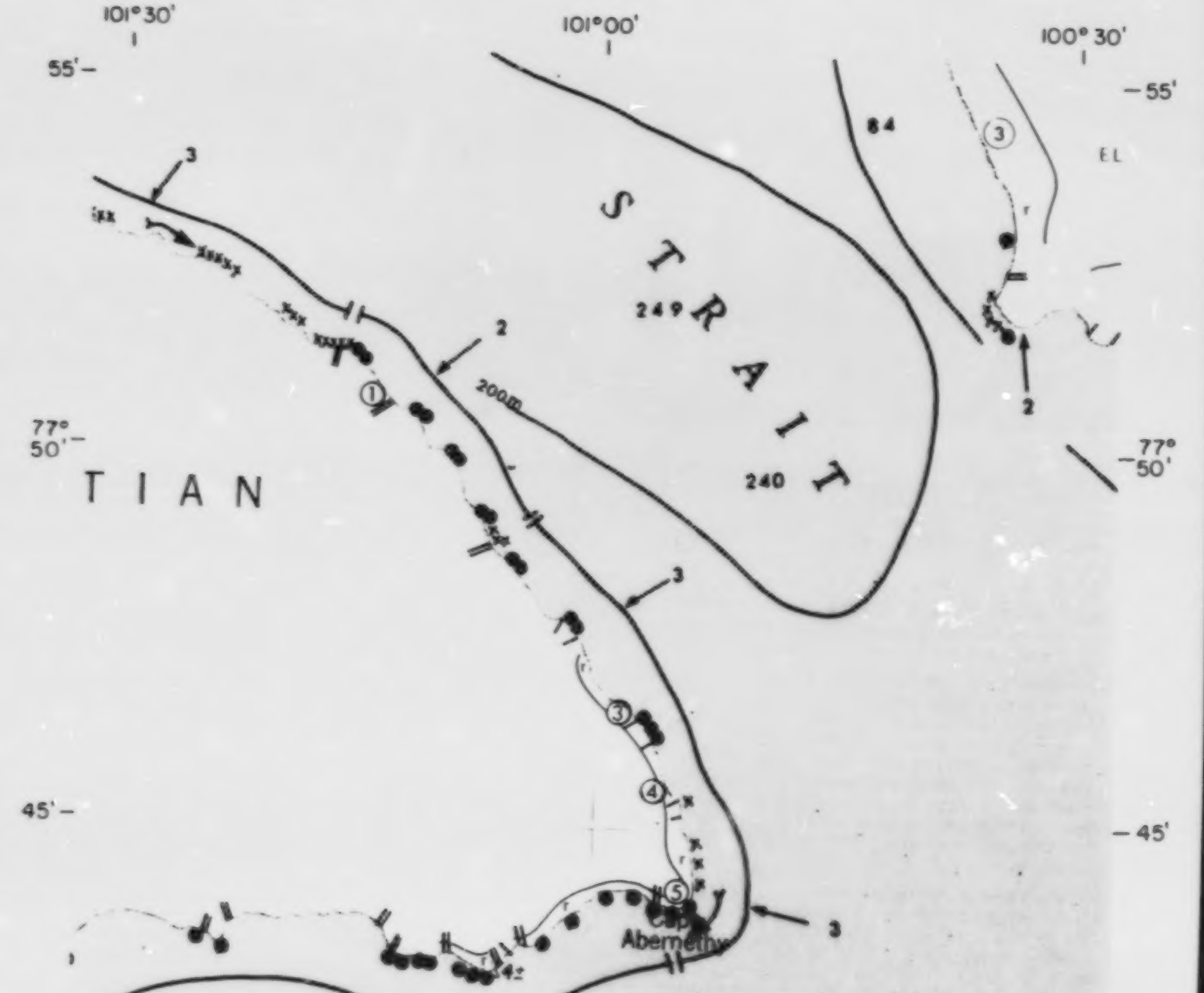
101°30'
101°00'
100°30'
55'
55'
77° 50'
77° 50'
45'
45'
77° 40'
77° 40'
STRAIT
TIAN
249
240
200m
84
EL
3
2
①
③
④
⑤
Cape Abernethy
106
101°30'
101°00'
100°30'

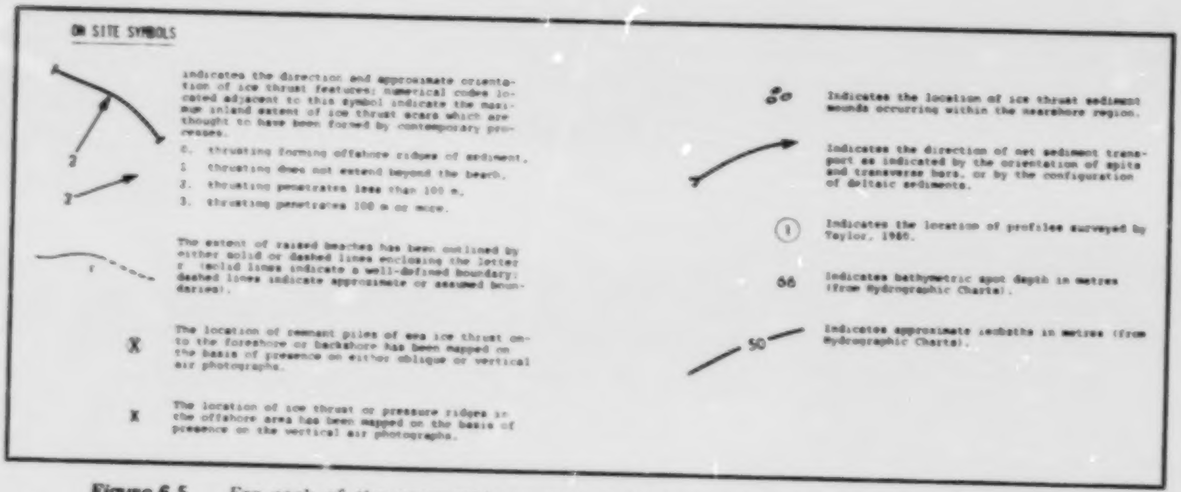

ON SITE SYMBOLS

indicates the direction and approximate orientation of ice thrust features; numerical codes located adjacent to this symbol indicate the maximum inland extent of ice thrust scars which are thought to have been formed by contemporary processes.

0. thrusting forming offshore ridges of sediment.
1. thrusting does not extend beyond the beach.
2. thrusting penetrates less than 100 m.
3. thrusting penetrates 100 m or more.

The extent of raised beaches has been outlined by either solid or dashed lines enclosing the letter r (solid lines indicate a well-defined boundary; dashed lines indicate approximate or assumed boundaries).

The location of remnant piles of sea ice thrust onto the foreshore or backshore has been mapped on the basis of presence on either oblique or vertical air photographs.

The location of ice thrust or pressure ridges in the offshore area has been mapped on the basis of presence on the vertical air photographs.

Indicates the location of ice thrust sediment mounds occurring within the nearshore region.

Indicates the direction of net sediment transport as indicated by the orientation of spits and transverse bars, or by the configuration of deltaic sediments.

Indicates the location of profiles surveyed by Taylor, 1980.

Indicates bathymetric spot depth in metres (from Hydrographic Charts).

Indicates approximate isobaths in metres (from Hydrographic Charts).

Figure 6.5. *For each of the geographic areas mapped, a second coastal geology map was used to depict process parameters (when information was available) and coastal characteristics which result from or affect the processes which dominate a particular shoreline. This map is of southeastern King Christian Island.*

Summary

A coastal geology mapping system is proposed which can be used at a variety of scales, in a variety of coastal environments in Canada. Thus far, the system has been used at scales ranging from 1:4800 to 1:125 000 for coastlines in both temperate and arctic regions. The system is compatible with the surficial geology maps published by the Geological Survey; thus a uniformity of mapping is achieved and terrain information now can be directly incorporated into the coding sheets of the coastal geology maps. Following a systematic approach, all available physical coastal data can be included. The system is designed to present detailed information on the coding sheets and a summary of the primary coastal elements on the maps. With the coding sheets, a user can pull out relevant data for specific purposes such as oil spill countermeasures, coastal zone planning, etc. Also, since all available data are included, costly remapping of an area for specific users is eliminated. New information, when it becomes available, can be added to the data base because of the flexibility of the system. An index of reliability of the mapped data and other information is built into the scheme by listing all sources of information and by identifying field study areas and the location of reconnaissance aerial surveys.

Acknowledgments

The authors wish to thank C.F.M. Lewis and S.B. McCann for their constructive comments on an earlier version of this manuscript.

References

Barnett, D.M., Edlund, S.A., Dredge, L.A., Thomas, D.C., and Prevett, L.S.
1975: Terrain classification and evaluation, Eastern Melville Island, N.W.T.; Geological Survey of Canada, Open File 252, 11 maps, 3 legends and 1318 p.

Barnett, D.M., Edlund, S.A., and Dredge, L.A.
1976: Terrain characterization and evaluation: an example from Eastern Melville Island; Geological Survey of Canada, Paper 76-23.

Barry, R.G., Crane, R.G., Locke, C.W., Locke, W.W., and Miller, G.H.
1977: The coastal environment of southern Baffin Island and Northern Labrador-Ungava; Institute of Arctic and Alpine Research, University of Colorado, Boulder, Report to Arctic Petroleum Operators Association, Project 138, 166 p.

Boydell, A.N., Drabinsky, K.A., and Netterville, J.A.
1975a: Terrain inventory and land classification, Boothia Peninsula and Northern Keewatin; in Report of Activities, Part A, Geological Survey of Canada, Paper 75-1A, p. 393-395.

1975b: Surficial geology and geomorphology maps of Boothia Peninsula, N.W.T.; Geological Survey of Canada, Open File 285.

Capital Regional District
1979: District of North Saanich Shoreland Protection Program; unpublished report prepared jointly by Willis, Cunliffe & Tait and by Woodward-Clyde Consultants, 59 p., plus map.

Dubois, J-M. M.
1973: Essai de classification de la zone côtière et d'identification d'unités physiographiques sur la côte du Saint-Laurent, Pointe-des-Monts – Blanc Sablon; Étude des Rivers du St-Laurent, Ministère de Travaux Publics du Canada, Montreal, 71 p.

Environment and Land Use Committee
1978: Terrain classification system; report to the E.L.U.C. Secretariat, prepared by the Resource Analysis Branch, British Columbia Ministry of the Environment, 56 p.

Fulton, R.J., Boydell, A.N., Barnett, D.M., Grant, D.R., Hodgson, D.A., and Rampton, V.N.
1974: Terrain mapping in northern environments; in Canada's Northlands, Proceedings of Technical Workshop to develop an integrated approach to base data inventories for Canada's Northlands, Environment Canada Land Directorate, April 17-19, 1974, Toronto, Canada, p. 14-60.

Fulton, R.J., Hodgson, D.A., and Minning, G.V.
1975: Inventory of Quaternary geology southern Labrador: an example of Quaternary geology-terrain studies in undeveloped areas; Geological Survey of Canada, Paper 74-46, 14 p.

Hodgson, D.A.
1977: A preliminary account of surficial materials, geomorphological processes, terrain sensitivity and Quaternary history of King Christian and southern Ellef Ringnes Islands, District of Franklin; in Report of Activities, Part A, Geological Survey of Canada, Paper 77-1A, p. 458-493.

1978: Surficial materials, southern Ellef Ringnes and King Christian Islands, Northwest Territories; Geological Survey of Canada, Open File 538.

McLaren, P.
1977: The coasts of eastern Melville and western Byam Martin Islands; coastal processes and related geology of a high arctic environment; unpublished Ph.D. thesis, University of South Carolina, Columbia, South Carolina, 304 p.

McLaren, P. (cont.)
1980: The coastal morphology and sedimentology of Labrador: A study of shoreline sensitivity to a potential oil spill; Geological Survey of Canada, Ottawa, Paper 79-28, 41 p. and maps.

Owens, E.H.
1980: Physical shore-zone analysis, Saltspring Island, B.C.; unpublished report to Lands Directorate, Pacific and Yukon Region, Environment Canada, Vancouver, 155 p.

Scarlett, M.S., Adams, D., Hoffman, L., Kirby, G., O'Brien, D., Pinsent, J., and Williams, W.
1976: Shoreline of Atlantic Canada; Memorial University, St. John's unpublished report, 60 p.

Taylor, R.B.
1980: Coastal reconnaissance for marine terminal planning in the Sverdrup Basin, Northwest Territories; Geological Survey of Canada, Open File 693, 150 p.

Woodward-Clyde Consultants
1980: Coastal geology maps, central Sverdrup Basin, Northwest Territories; Geological Survey of Canada, Open File 549.

7.

PRE- AND POST-DORÉ SEQUENCES IN THE WAWA VOLCANIC BELT, ONTARIO

Project 770070

K. Attoh
Precambrian Geology Division

Attoh, K., Pre- and post-Doré sequences in the Wawa volcanic belt, Ontario; in *Current Research, Part B, Geological Survey of Canada, Paper 81-1B, p. 49-54, 1981.*

Abstract

An unconformity at the base of Doré Formation and equivalent sedimentary rocks marks a significant stratigraphic break with which the volcanic-sedimentary succession in the Wawa area can be subdivided into pre- and post-Doré sequences. The pre-Doré sequence includes at least two cycles of mafic to felsic volcanic rocks, each containing an iron formation unit; only the lower mafic-felsic volcanic cycle, which is terminated by an extensive siderite deposit, is completely preserved. The post-Doré sequence comprises a mafic flow unit which conformably overlies the sedimentary rocks (Doré), and a younger succession, structurally discordant with the underlying mafic flow and the pre-Doré sequence, which is characterized by a distinct breccia unit and possibly includes the felsic volcanic rocks near Catfish Lake. Post-Doré sequences do not contain iron formation units.

Introduction

A sedimentary unit, which in the type locality near Lake Superior is referred to as the Doré Formation, comprises conglomerate and laterally equivalent shales and siltstones that can be traced as a single stratigraphic unit which defines major east-west folds in the Wawa volcanic belt (Fig. 7.1). Lithologic units stratigraphically above and below the Doré can be correlated over broad areas (e.g. Attoh, 1980). Previous studies in the Wawa area, including the work by Collins et al. (1926) and Cooke (1937) have been summarized in Goodwin (1962). The compilation map of the Wawa-Manitouwadge area (Ontario Department of Mines, 1972) incorporates some of the data from recent mapping and provides the basis for selecting areas for detailed study.

The area west of Mildred Lake fault south of Magpie River was mapped during the summer of 1980 to determine the stratigraphic relations among various volcanic rock units and the sedimentary rocks considered to be equivalent to the Doré. The Mildred-Magpie River area is suitable for testing the correlation which was previously proposed (Attoh, 1980) on the basis of mapping in the "fume-burnt" area east of the Mildred Lake fault. Moreover, the stratigraphic information from this area can be extended to the northwestern part of the Wawa belt because a distinct breccia unit, which is exposed along Highway 17, can be traced southeastward into the Mildred Lake area. The areas described in this report are:

a. Michipicoten Harbour area

b. Magpie River-Helen Mine area

c. Highway 17 between McCormick Lake and Catfish Lake

Michipicoten Harbour Area

The Michipicoten area is situated about 15 km southwest of Wawa and lies between Mission Falls, Michipicoten Harbour and the shore of Lake Superior (Fig. 7.2). Fieldwork in the area was done in July 1979 and this report incorporates chemical data on the rock types.

Characteristics of pre-Doré Volcanic Rocks

The volcanic rocks are mainly mafic but some felsic flows and pyroclastic rocks occur. The mafic rocks are composed of pillowed lavas, massive flows and dyke rocks. The massive rocks are generally coarser grained than the pillowed flows and some may represent sills. Pillow structures 1-2 km west of Sandy Beach are very large, up to 3 m long, and may represent lava tubes although internal concentric structures and budding were not observed. The long dimensions of the pillows are aligned parallel to the tectonic fabric defined by cleavage in massive flows and hyalotuffs. Thinly laminated, cherty sediments are interbedded with the pillowed flows.

Figure 7.2 shows the distribution of the main chemical types in the mafic flows based on over 50 chemical analyses of samples mostly from the shore and inland outcrops. Calc-alkaline (high alumina) basalts and andesites are the most abundant volcanic rocks whereas tholeiites, which are almost exclusively basalts, constitute less than 30 per cent of the mafic rocks analyzed. Because it was not possible to distinguish between tholeiitic and calc-alkaline mafic rocks (andesites and basalts) in the field, the boundaries shown in Figure 7.2 are based only on chemical analyses and therefore are poorly defined where outcrops are limited. The boundaries between the chemically-defined types were drawn subparallel to local pillow stratification.

Felsic rocks in the Michipicoten Harbour area are calc-alkaline and are mostly rhyolitic in composition. The felsic rocks, which are subordinate to the mafic rocks in volume, include rhyolite flows and fragmental rocks. The unit trending from Mission Falls to Lake Superior is composed of lapilli and ash flow tuffs, whereas northeast of Sandy Beach the felsic rocks are aphyric rhyolite flows and flow breccias. The quartz monzonite stock at Sandy Beach is clearly intrusive into the mafic volcanic rocks to the west and must be younger than the older felsic volcanics to the east.

Unconformity at the top of the Volcanic Succession

The stratigraphy in the volcanic rocks as determined from the facing of pillow structures in the mafic flows indicates a west to southwest younging monoclinal structure. This westerly facing structure is clearly truncated by the northeast trend of the Doré sediments (Fig. 7.2). The contact between the volcanic succession and the sediments is exposed at two places (marked C in Fig. 7.2) and is constrained by outcrops along most of the boundary shown. At the contact there is no discordance between the planar structures in the Doré Formation and the mafic volcanics; rather, the boundary dips at 50-60° southeast such that the mafic volcanics structurally overlie the Doré sediments. Cooke (1937) was the first to recognize the significance of this boundary and interpreted it as an unconformity or a fault, thereby demonstrating that the Doré sediments stratigraphically overlie the volcanic succession. Other lines of evidence supporting the unconformable relationship include the nature of the matrix of the Doré conglomerate, now a mafic schist, which can readily be interpreted as mafic volcanic debris and the occurrence of mafic volcanic rock fragments in the Doré conglomerate.

The unconformity at the base of Doré Formation is an erosional surface which can be traced from the Michipicoten Harbour area where the Doré overlies mafic volcanics to Parks Lake where the equivalent sedimentary unit overlies iron formation (Fig. 7.3). The uplift and attendant erosion represented by the unconformity marks a major break in volcanism which is at least as important as those marked by iron formation units.

Doré Sediments

The Doré sediment at Michipicoten Harbour is a polymictic conglomerate in which cobble and rare boulder size clasts include dacitic quartz porphyry, rhyolite and quartz-feldspar vein rock. Fragments of iron formation and more rarely mafic volcanics occur. The matrix is a mafic chloritic schist derived from the underlying mafic volcanic rocks. At the contact the mafic schist containing a few granule-size clasts appears to grade into more massive mafic volcanics over a zone 2 m thick. Small isoclinal folds in this zone indicate that the contact is at least in part tectonic. The conglomerate in this locality is similar to conglomerate along Highway 17 south of Black Trout Lake and west of Mildred Lake fault (Fig. 7.3). At Michipicoten Harbour and along Highway 17, the Doré conglomerate contains no sedi-mentary structures except for crude zoning of clast size; therefore no information about the facing of the unit is directly available from the Doré itself.

Helen Mine-Magpie River Area

Pre-Doré Sequence

The area shown in Figure 7.3 is located in south-central part of the Wawa belt (Fig. 7.1), about 12 km northeast of the Michipicoten Harbour area described above. From Figure 7.3 the stratigraphic succession below the sediment unit east of Mildred Lake fault can readily be correlated with the succession below the iron formation unit southeast of Helen Mine. However, the succession of lithic units west of Mildred Lake fault between Mildred Lake fault, Magpie River and Helen Mine cannot be so readily correlated with the succession east of the fault (Fig. 7.3). The description which follows relates the succession west of Mildred Lake fault to the stratigraphic succession in the Michipicoten Harbour area and to the east of the Mildred Lake fault.

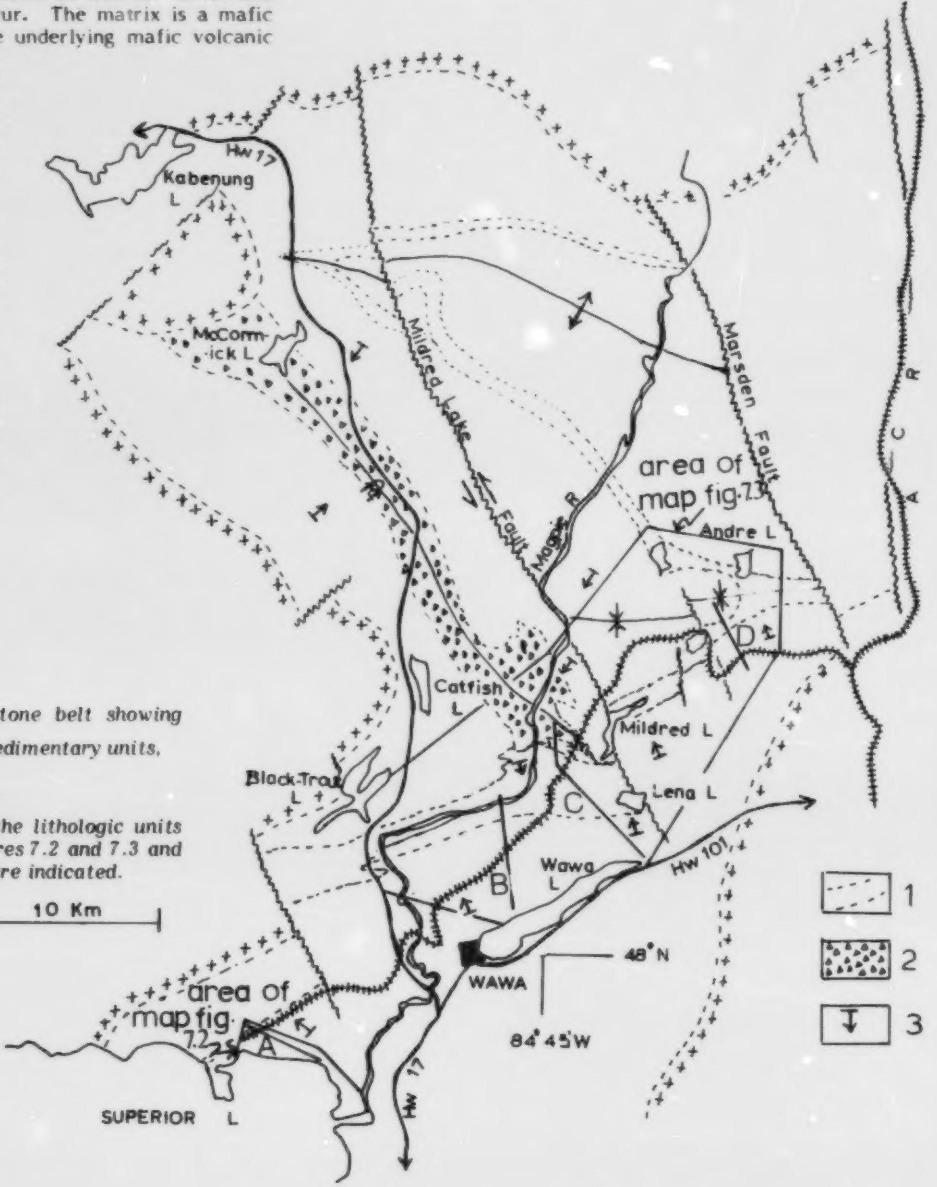

Figure 7.1.

Index map of the Wawa greenstone belt showing

1. *limits of Doré and equivalent sedimentary units,*
2. *the breccia unit, and*
3. *major facing directions.*

Structural trends as defined by the lithologic units are also shown and areas of Figures 7.2 and 7.3 and the lines of section in Figure 7.4 are indicated.

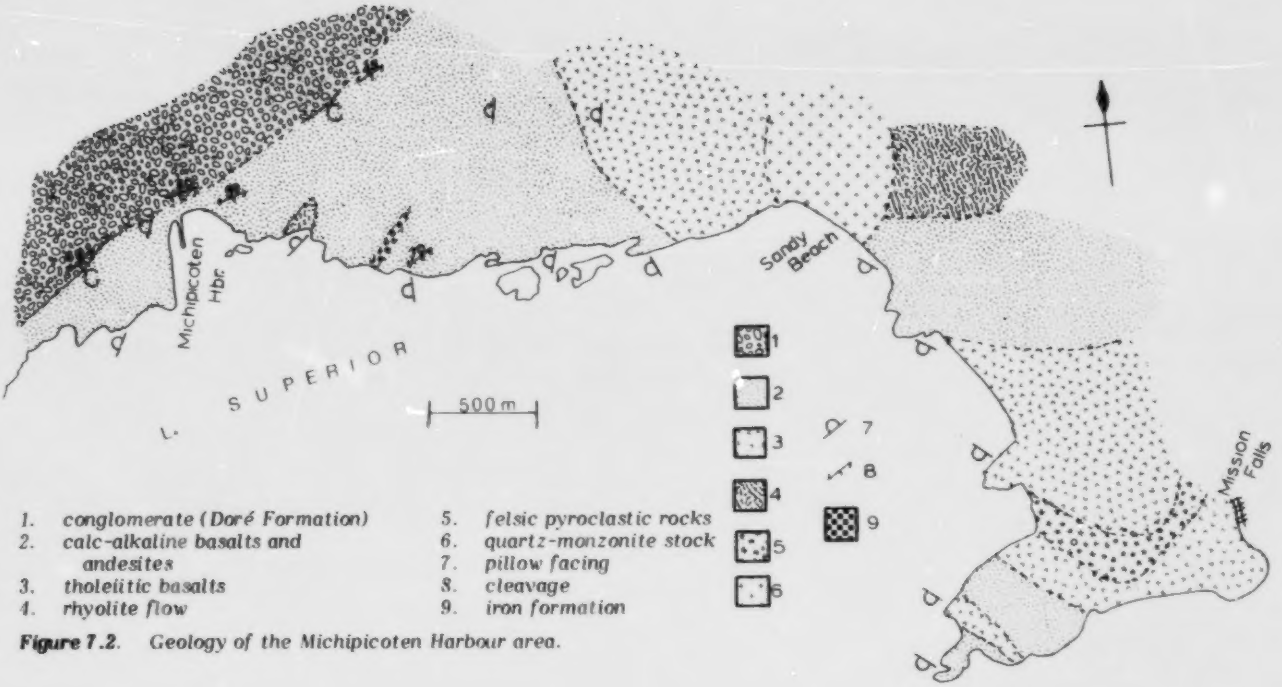

Figure 7.2. *Geology of the Michipicoten Harbour area.*

Felsic Pyroclastic Rocks

Extensive deposits of pyroclastic rocks are well preserved south and north of the iron formation unit at Helen Mine. The pyroclastic rocks are white to grey-weathering rocks composed of lapilli and ash flow tuffs and some agglomerate which is composed of block-size ejecta, some of which have fusiform (bomb) shapes. South of Helen Mine a zone of accretionary lapilli about 50 m thick can be traced from Highway 101 east of Wawa Lake to southwest of Helen Mine. Above the lapilli tuff zone, southwest of Helen Mine, the pyroclastic rocks have well preserved sedimentary structures which may indicate deposition at the distal ends of a pyroclastic flow. The felsic volcanic rocks east of Wawa Lake include quartz-phyric dacite and rhyolite flows and dacitic tuffs. Chemically, the unit is calc-alkaline and the composition ranges from rhyolite to rhyodacite. The pyroclastic unit overlies calc-alkaline basalt unit along Highway 101.

Felsic pyroclastic rocks overlying iron formation and mafic volcanic rock units north of Helen Mine can be traced westwards to where they merge with underlying felsic pyroclastic rocks (Fig. 7.3). Near Lagarde Lake the pyroclastic rocks are mostly ash and lapilli tuffs and are similar to those south of Helen Mine except for the presence of quartz-porphyry dyke rocks and reworked volcanic conglomerate zones. West and southwest of Artliss Lake, the felsic rocks include distinct quartz-porphyry dyke rocks (Fig. 7.3) which may be feeders to poorly sorted lapilli and block tuffs that occur nearby.

Iron Formation

Two iron formation units of variable thickness and lateral extent occur in the map area (Fig. 7.3). The lower iron formation unit is essentially a siderite rock which is up to 700 m thick in the Helen Mine and can be correlated with the iron carbonate unit in the Parks Lake area, where it is less than 100 m thick. The base of the iron formation is marked by a breccia composed of felsic volcanic fragments in a siderite matrix which is partly replaced by sulphide minerals. Sulphide-rich zone near the top of the iron formation unit consists of lenses of massive and disseminated pyrite and arsenopyrite.

The upper iron formation unit north of Lagarde Lake is thinner than the lower unit and is sandwiched between thin mafic flow and pyroclastic units (Fig. 7.3). These strata are truncated by the base of the overlying sedimentary unit and are not preserved in the succession east of Mildred Lake fault. This observation, together with the fact that the clastic sedimentary unit directly overlies the lower iron formation unit to the east of Goetz Lake, is interpreted as a stratigraphic break which is correlated with the unconformity in the Michipicoten Harbour area. In addition, the cycle of volcanism and iron formation represented by these strata may record the youngest pre-Doré volcanic activity in the area.

Mafic Volcanic Units

The mafic volcanic rocks overlying the lower iron formation are mostly pillowed flows and show considerable variation in thickness. For example, the unit thins to zero northwest of Helen Mine, whereas in a fault-bounded block north of Walbank Lake it is up to 1500 m thick. The overlying felsic pyroclastic unit, which is thin over the mafic volcanic unit north of Walbank Lake, thickens west of Artliss Lake and eventually disappears southwest of Artliss Lake.

This suggests that an irregular topographic surface produced by subvolcanic faulting may have controlled the deposition of the pyroclastic unit.

Sedimentary Rocks

The sedimentary unit referred to as the Eleanor Slate Formation by Collins et al. (1926) comprises black shales, greywackes, siltstones and conglomerate and associated volcanic breccias. Black shale is volumetrically the most abundant rock type in the unit west of Mildred Lake fault and is best preserved north of Artliss Lake where the thinly laminated rocks are strongly folded. Siltstone beds up to a few metres thick, are interbedded with the black shales and define the main stratification in the unit. Greywacke and siltstone are preserved north of Magpie River and southeast of Steephill Falls. Flame structures, graded and ripple bedding are well developed, but crosslamination is rare.

The conglomerate can be distinguished from the coarse pyroclastic rocks by the presence of rounded lithic clasts in an arenaceous matrix. Conglomerate can be examined along the railway cuttings from Lena Lake to Siderite Junction (SJ) on the A.C.R. tracks (Fig. 7.3) and is composed of quartz porphyry and mafic dyke rocks in a mafic matrix. The conglomerate zones are discontinuous and some show evidence of erosion (channels) at the base.

Volcanic Breccia – This white-weathering unit is a monomict breccia in which the essential fragments are poorly rounded rhyolite fragments, which may be up to 3 m across. The unit, which is exposed north of Magpie River, is interbedded with greywacke, siltstone and thin conglomerate beds. The greywacke-siltstone beds show sedimentary structures such as grading and load casts but only rare crossbedding. Westward the breccia unit appears to grade into felsic pyroclasts and flow rocks. The breccia is considered part of the sedimentary unit and may represent reworked volcanic rocks.

Correlation of Pre-Doré and Doré Successions

The sedimentary rocks in Lena Lake-Artliss Lake area (Fig. 7.3) which were formerly referred to as the Eleanor Slate Formation (Collins et al., 1926) are considered to be

Figure 7.3. *Geology of Magpie River-André Lake-Wawa Lake area. Symbols are:*

1. *conglomerate*
2. *breccia*
3. *shale siltstone and greywacke*
4. *mafic flow*
5. *felsic pyroclastic rocks*
6. *rhyolite flow*
7. *zone of quartz porphyry (feeder?) dykes*
8. *coarse rhyolite breccia associated with Doré sediments*
9. *iron formation*
10. *mafic and ultramafic dyke rocks*

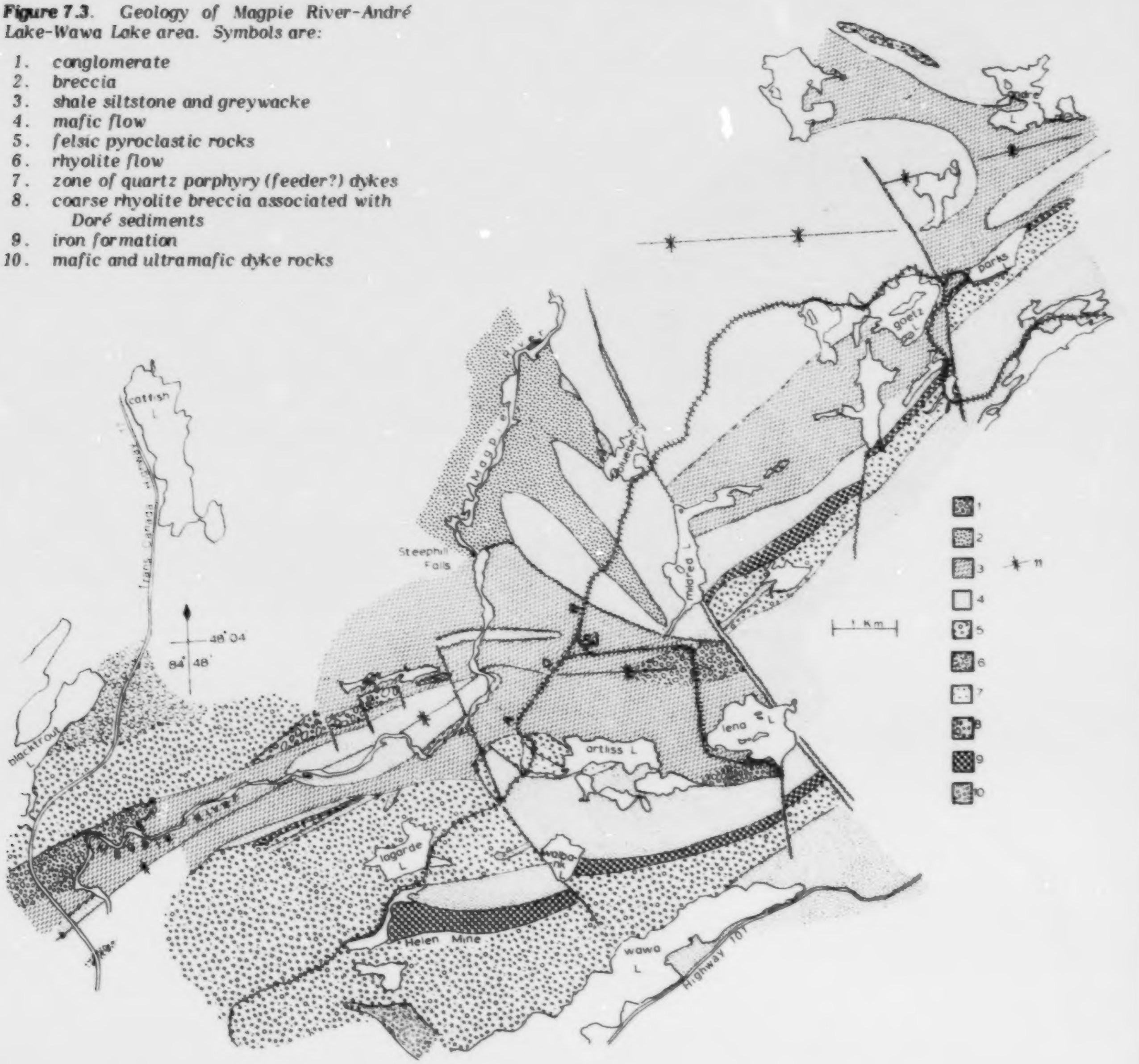

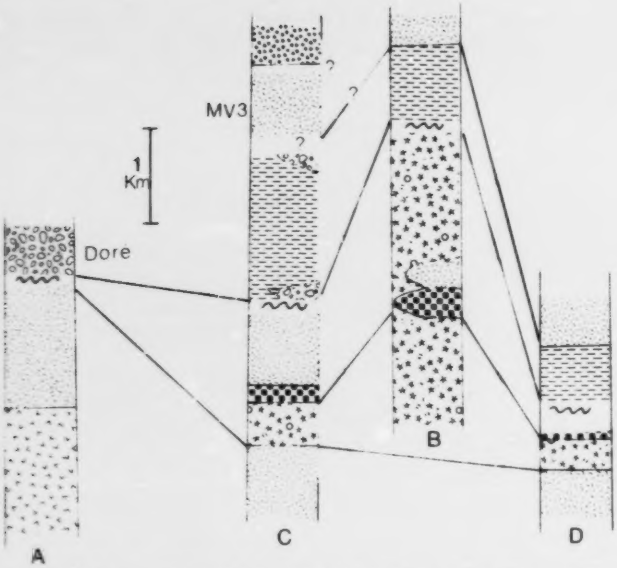

Figure 7.4. *Stratigraphic correlation charts for the southwestern part of the Wawa belt based on the map units in Figures 7.2 and 7.3. Lithic symbols are the same as on the maps. The unconformity at the base of the Doré and equivalent formations is indicated by wavy line.*

equivalent to the Doré Formation in the Michipicoten Harbour area. Consequently, the difference in the proportions of various rock types reflects different environments in which the clastic sediments accumulated. It may be inferred from the distribution of conglomerate that shallow water marine environments occurred to the west in the Michipicoten Harbour area.

The unconformity at the base of the sedimentary unit defines the top of the pre-Doré volcanic sequence. The pre-Doré sequence described in the two areas (Figs. 7.2, 7.3) can be correlated as indicated in Figure 7.4. Column A, which does not contain an extensive iron formation unit, represents the succession at Michipicoten Harbour. Columns B, C and D are located in map area of Figure 7.3, as indicated in Figure 7.1. The correlations between lower sections of Columns B, C and D in Figure 7.4 are self evident from Figure 7.3. On the other hand, correlation between Column A and Columns B, C or D is based on the fact that the unconformity at the base of the Doré lies at lower stratigraphic level as one goes eastward. As shown in Figure 7.4, the thick deposits of felsic pyroclastic rocks represented in Column B indicate that the centre of felsic volcanism was localized near Helen Mine.

Post-Dore Sequences in the Mildred Lake-Magpie River and Highway 17

i a mafic flow unit which conformably overlies the sedimentary unit and defines a synclinal structure along the Magpie River,

ii a structurally discordant breccia unit exposed east of Steephill Falls that can be traced as single unit to Highway 17 (Fig. 7.1), and

iii the mafic flow unit overlying the sedimentary rock unit east of Mildred Lake fault.

The mafic volcanic unit north of Goetz Lake is composed of pillowed flows which form the core of a closed synclinal structure (Fig. 7.3) northwest of Parks Lake. The unit extends from southwest of André Lake to the Mildred Lake fault and represents the only post-Doré volcanic rock in Column C (Fig. 7.4). The mafic flow unit west of Mildred Lake is correlated with the (MV3) unit (Fig. 7.4) east of the fault, but it is less obvious whether the mafic flow unit along Magpie River is also equivalent. The mafic flows along Magpie River overlie sedimentary rocks considered to be equivalent to the Doré and define the core of a synclinal structure.

The Breccia Unit

The breccia unit forms a band of northwest trending rocks extending from McCormick Lake to Mildred Lake. Northeast of Steephill Falls, the breccia unit is composed of angular rhyolite fragments in a matrix composed of granule-size felsic rock fragments which in turn are set in a finer greenish matrix. Some of the larger fragments which are up to 0.5 m across appear to be brecciated in situ and partly penetrated by the mafic greenish matrix. The unit is strongly cleaved and the cleavage dips at 30-40° northeast.

A continuous section of the breccia unit along Highway 17, which was previously described (Attoh, 1980) was re-examined in 1980. At its northern margin, the unit is composed of rhyolite fragments in a granular matrix composed of dacitic and rhyolitic rocks. The fragments are disc-shaped in three dimensions and range in texture from massive, plagioclase-phyric rhyolite to sheared biotite-bearing felsic rocks. The sheared fragments are darker, contain more lensoid clots of biotite and rare anhedral plagioclase in the matrix. Plagioclase phenocrysts in the massive rhyolite fragments occur as euhedral crystals in a quartz sericite matrix. Fragments of dacitic rocks are dark grey and contain zoned plagioclase phenocrysts in a fine grained biotite-rich matrix. The massive, microphyric, white fragments and the sheared fragments with biotite clots together constitute about 10-15 per cent of volume of the rock. Chemically, these fragments are calc-alkaline rhyolite and dacite in composition, whereas the matrix is dacitic to andesitic in composition. The greywacke matrix is andesitic in composition to greywacke whereas the crystal-rich felsic matrix is dacitic.

Primary stratification is absent in the unit except for rare, thinly laminated slaty beds and even rare conglomerate zones which are presumed to represent reworked breccia. Where stratification can be inferred or observed it is parallel to the penetrative cleavage that dips northeast at 15-30°. The maximum fragment dimensions range from 245 x 45 x10 to 105 x 40 x 17 cm and the average maximum diameter is about 45-50 cm near the centre of the unit and about 25 cm at the north and south margins. Large rhyodacite fragments are less deformed than the smaller fragments; the latter appear to be elongated in the cleavage surface, resulting in extreme length to thickness ratios as high as 20:1.

Coarse grained subvolcanic rocks associated with the breccia unit include gabbros, diorites and dacites which have been deformed with the breccia unit and generally show no intrusive relations. The dacite sills at the north end of the unit are distinctive in that the zoned plagioclase phenocrysts appear to have concentrated in certain zones. The largest of these coarse grained bodies is a gabbroic rock near the centre of the breccia unit about 8 km north of Catfish Lake. This body, about 800 m thick, varies from gabbro at the south end, where it is sheared into a mafic schist, to a more massive diorite at the northern end. Thus the gabbroic body appears to be a differentiated sill. Fragments of coarse grained rocks similar to dacite porphyry occur in the breccia.

Features of the breccia unit which may be indicative of its origin include the following:

i polymictic breccia – rhyolite and rhyodacite block size fragments constituting less than 15 per cent of the rock – indicates a felsic volcanic source of large fragments.

ii general lack of sorting, stratification or sedimentary structures – suggests emplacement by mass flow.

iii occurrence of coarse grained subvolcanic rocks and local crystal-rich matrix suggests a nearby source of volcanism, but the absence of vesicular material indicates that the unit is not a pyroclastic deposit.

iv at the southeastern end the breccia unit is interbedded with pillowed mafic flows and this may indicate a subaqueous emplacement at least in part.

Therefore, the breccia unit is interpreted as debris flow initiated from a subaerial avalanche somewhere to the northwest near McCormick Lake and probably flowed southwestward into an aqueous environment.

Structure and Stratigraphic Position of the Breccia Unit

Along Highway 17, southeast of McCormick Lake, the northern margin of the breccia unit overlies felsic pyroclastic rocks which dip northwest. This stratigraphic relationship is inferred from downward-facing structures in the pyroclastic rocks to the north and graded bedding in thinly laminated interbedded sediments, which indicates that the breccia unit is overturned southward at its northern margin. Evidence for the downward facing structure of the felsic pyroclastic rocks is preserved in a new roadcut about 1.3 km south of a trail from Highway 17 to McCormick Lake, where sedimentary structures in the pyroclastic unit include graded beds, cross-lamination, convoluted beds and scour channels. These structures clearly indicate that the unit youngs to the southwest, whereas the stratification dips at 40° northeast. The significance of this overturned structure is that the units which stratigraphically overlie the pyroclastic unit to the south must also be overturned.

About 6 km north of Catfish Lake along Highway 17 the southern boundary of the breccia unit structurally overlies rhyolite and dacitic flows to the south and the succession dips northeast at about 25°. There is no direct stratigraphic information at this boundary but it can be inferred that the breccia unit overlies the felsic volcanic rocks to the south near Catfish Lake. Off the highway, about 6 km due south of McCormick Lake, the breccia unit overlies pillowed mafic flows. Therefore it is concluded that the unit occupies the core of an overturned synclinal structure. The axial surface of this fold dips 20-30° northeast.

West of Mildred Lake the southern end of the breccia unit is underlain by mafic flows to the east (Fig. 7.3), whereas east of Steephill Falls, the western part of the same mafic flow unit structurally underlies the breccia and faces southwest. Thus it appears that the breccia unit stratigraphically underlies and overlies the same mafic unit. Therefore the breccia is considered to be interbedded with the mafic flows west of Mildred Lake. In addition, this mafic flow unit, which is correlated with post-Doré mafic volcanic unit southwest of André Lake (Fig. 7.4), appears to underlie the sedimentary unit equivalent to the Doré east of Steephill Falls. This anomalous relation is explained by postulating a fault which forms the contact between the sediments and the southwest-facing mafic volcanic unit (Fig. 7.3). It is assumed to be a reverse fault, dipping northwest and upthrown on the south side.

Conclusion

The correlation proposed for the central part of the Wawa belt can be tested by further mapping. For now, it is concluded that the proposed stratigraphic model provides a basis for understanding the structural relations between the various volcanic rock units. However, because of the structural complexity of the areas described, as evident from shallow-dipping axial surfaces of overturned (recumbent folds) further clarification of the regional stratigraphic relationships would require geochronologic data as well as careful mapping of other critical areas of the Wawa volcanic belt. Because unequivocal evidence exists for downward-facing strata and overturned structures, stratigraphic information is critical in order to interpret the regional structure uniquely.

Acknowledgments

Logistic support for this study by the Ontario Geological Survey field party under R. Sage is gratefully acknowledged. I have had the benefit of discussing the problems in this work with K.D. Card and W.R.A. Baragar, who also read early versions of the manuscript.

References

Attoh, K.
1980: Stratigraphic relations of the volcanic and sedimentary succession in the Wawa belt, Ontario; in Current Research, Part A, Geological Survey of Canada, Paper 80-1A, p. 101-106.

Cooke, H.C.
1937: Structure of the Doré series in Michipicoten District, Ontario; Royal Society of Canada, Transactions, v. 31, sec. IV, p. 69-80.

Collins, W.H., Quirke, T.D., and Thomson, Ellis
1926: Michipicoten Iron ranges; Geological Survey of Canada, Memoir 147, p. 13-23.

Goodwin, A.M.
1962: Structure, stratigraphy and origin of iron formations, Michipicoten area, Algoma District, Ontario, Canada; Geological Society of America Bulletin, v. 73, p. 561-586.

Ontario Department of Mines
1972: Manitouwadge-Wawa sheet; Ontario Department of Mines Geological Compilation Series, Map 2220.

8.

SURFACE TEXTURE OF QUARTZ GRAINS AND SEDIMENTARY PROCESSES ON THE SOUTHEASTERN LABRADOR SHELF

Project 750038

Gustavs Vilks and Ying Wang[1]
Atlantic Geoscience Centre, Dartmouth

Vilks, Gustavs and Wang, Ying, Surface texture of quartz grains and sedimentary processes on the southeastern Labrador Shelf; in Current Research, Part B, Geological Survey of Canada, Paper 81-1B, p. 55-61, 1981.

Abstract

Sediment analysis, foraminifera, and surface textures of quartz grains indicate a changing environment of deposition on the inner shelf of the Groswater Bay area. There is a continuous sequence from the latest Wisconsinan low energy glacial marine deposits to a period of storm wave deposition and sediment reworking during the Holocene. Solution holes and silica deposits are superimposed on the initial glacial effects on the surface of the quartz grains from the glacial marine deposit. Quartz grains from the storm wave deposit have V-shaped depressions and collision marks dominating, while in the Holocene sediment reworking phase, glacial markings are overlain by V-shaped depressions, collision marks, solution holes and silica deposits. No evidence was found for either a transgression of the shoreline or the area being overridden by glacial ice during the last 20 000 years.

Introduction

Surface textures of quartz grains as seen by the scanning electron microscope have been used to distinguish various sedimentary environments by Krinsley and Donahue (1968), Krinsley and Doornkamp (1973), and many others. The markings are linked with the main dynamic processes that act upon the grains, such as, transport by turbulent water, wind, glacial ice and diagenesis. For example, the high energy surf zones that are associated with beaches increase the roundness of the grains, produce mechanical V-shaped depressions and small collision marks. The action of wind produces meandering ridges, pitted grain surfaces, and many other less diagnostic markings. The glacial cycle is characteristically reflected by grains that exhibit very irregular surfaces dominated by large or small conchoidal fracture patterns, imbricated breakage blocks and many other markings due to the high energy mechanical action on grains. Diagenesis may produce surface etchings or silica precipitation or both.

Grains usually contain markings that can be linked to more than one process or individual environment, reflecting a complex history of sedimentation. Many markings can be produced in more than one particular environment. Nevertheless, it is possible to determine the most likely sedimentary environment represented by a sample with a sufficiently large number of observations.

This paper describes the surface features of quartz grains found in a late Wisconsinan to Holocene sediment core from the inner Labrador Shelf. The dominant markings from each of four intervals sampled are used to infer the sequence of sedimentary environments represented in the core.

Methods

Sediments from core 95 (Fig. 8.1) have been analyzed at 25 cm intervals for foraminiferal content and grain size distribution; data are summarized in Figure 8.2. At the intervals 0 to 5 cm, 200 to 205 cm, 450 to 455 cm, and 775 to 780 cm, quartz grains between 1ϕ and -0.5ϕ in diameter were selected for the study of surface microstructures (Fig. 8.2).

The grains were boiled in concentrated hydrochloric acid, stannous chloride, and 30% hydrogen peroxide (Krinsley and Doornkamp, 1973). Between each boiling, each grain was washed thoroughly in distilled water. Fifteen grains from each core sample were coated with an alloy of gold-palladium for SEM analysis on a Cambridge 180 Stereoscan.

Environment

The coastline nearest to the sampling site has been described as unconsolidated lowland by Reinson et al. (1979). It consists of a broad, sandy beach with a well developed back beach area and sand dunes. The few offshore islands consist of bedrock (McLaren, 1980).

The inner Labrador Shelf in Hamilton Inlet area is extremely uneven (Fig. 8.1). Between the coastline and the depth of 100 metres, the shelf contains minor shoals, depressions and transverse channels across the inner shelf. Core 95 was taken in one of the major transverse channels.

Preliminary study of high resolution seismics and surface samples indicate that the distribution of the bottom sediment on the inner shelf is as variable as its topography (Reinson, 1979). Sand is present in the flat areas between the bedrock highs. Cobble and boulders are present along the flanks of the highs and in saddles between banks. In many depressions sand is found as a thin veneer overlying clay.

Bottom current velocities recorded between July 24 and August 12, 1979, 60 km to the north had peaks in the vicinity of 12 cm/s. These maxima had a setting towards west-southwest. Surface currents in the Hamilton Inlet area were estimated to be in the order of 20 cm/s and southeasterly (Dunbar, 1951).

In addition to bottom currents, sediments are also modified by the grounding of icebergs. Approximately 1000 icebergs per year have been sighted off the northern tip of Newfoundland via the Labrador Current (Dinsmore, 1972). Extreme concentrations of icebergs (20 icebergs per 12 000 km^2) occur in spring (February-April) along the Marginal Channel of the southeastern Labrador Shelf (Gustajtis, 1979). Sidescan sonograms of the seafloor show ample evidence of iceberg scours on the banks and saddles (e.g. Van der Linden et al., 1976).

Between December and July the Labrador inner shelf is covered with sea ice (Dinsmore, 1972). The ice is carried to the southeast by the Labrador Current and occasionally driven offshore by westerly winds. Major disintegration of the pack ice takes place in the warmer offshore waters, where it also presumably drops most of its sediment load. Sediment characteristics (Vilks, 1980) would suggest that in the marginal channel sea ice is not an important agent for transport. The inner shelf and the nearshore zone, however, are protected by the cover of sea ice from the effect of large storm waves during the winter.

---

[1] Nanking University. The People's Republic of China.

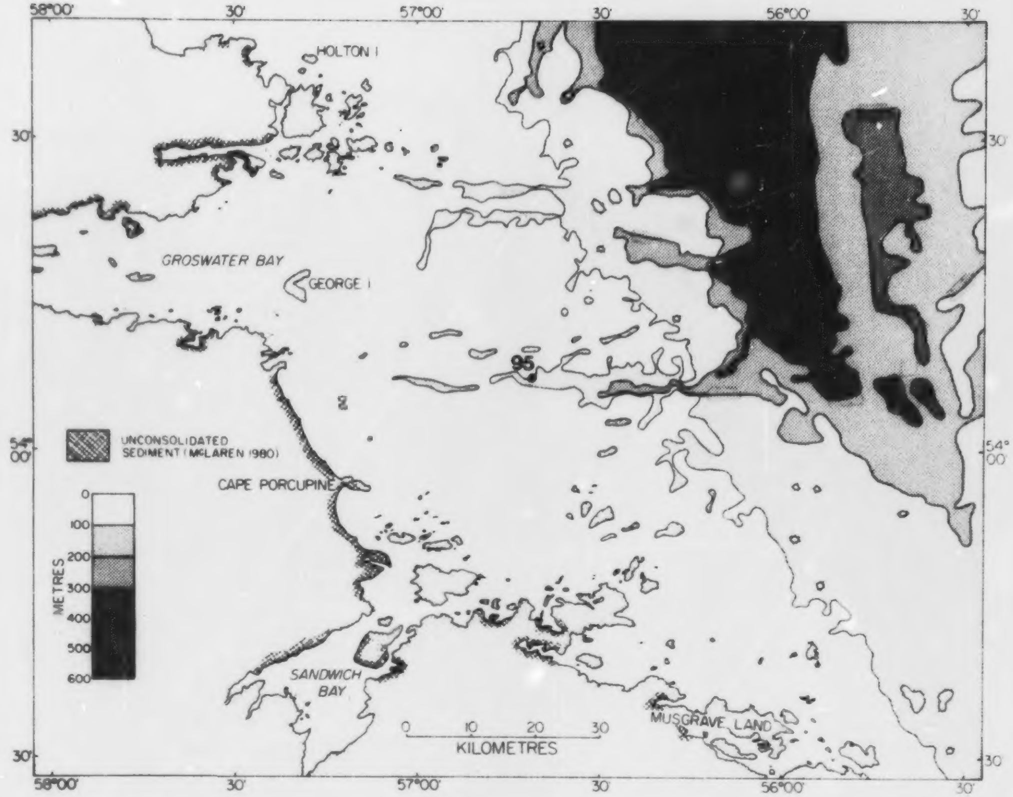
58°00'
30'
57°00'
30'
56°00'
30'
HOLTON I
GROSWATER BAY
GEORGE I
95
UNCONSOLIDATED SEDIMENT (McLAREN 1980)
CAPE PORCUPINE
METRES
0
100
200
300
400
500
600
SANDWICH BAY
MUSGRAVE LAND
0 10 20 30
KILOMETRES
54°00'

Figure 8.1. *Bathymetry of inner continental shelf and location of Core 95.*

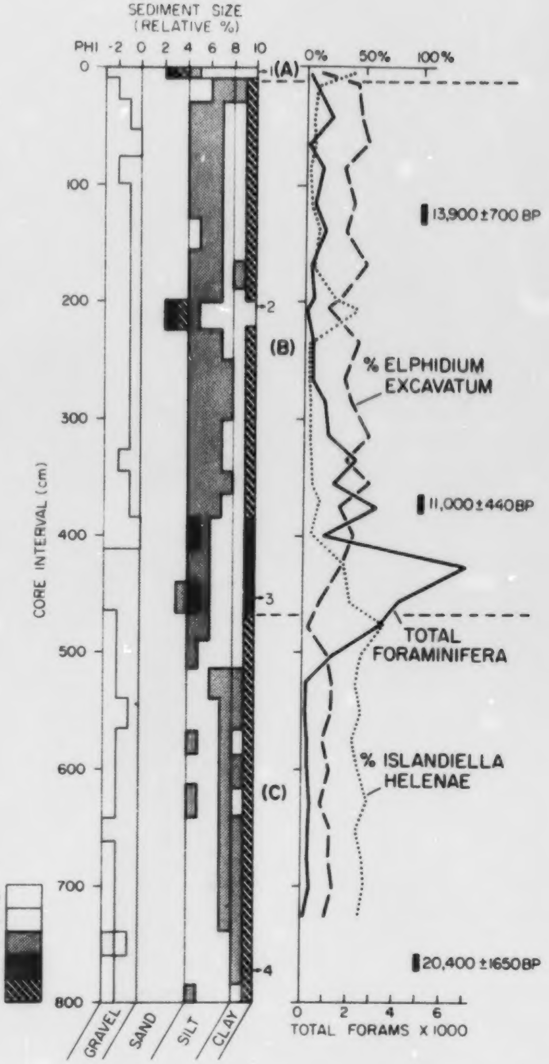

Figure 8.2. *Sediment texture and foraminifera in Core 95. Numbers with arrows indicate subsample locations for SEM analysis.*

Stratigraphic Sequence in Core 95

Microfossils and sediment textures suggest three sediment units within core 95:

A - 0-5 cm: surface veneer of very fine sand with **Islandiella helenae** dominant.

B - 5-460 cm: Clayey silt, with lenses of silt and sand, and at 200 cm a 10 cm fine sand bed, **Elphidium excavatum** f. **clavata** dominant.

C - 460-800 cm: Silty clay with scattered gravel, very low foraminiferal abundance and **I. helenae** predominating.

Quartz grains for SEM analysis were taken from each of the units and from the fine sand bed (see Fig. 8.2). The grain size frequency histograms of the sediment from the two silty sand layers are remarkably similar (Fig. 8.3A, B) with a distinct peak at the 4 phi size interval. The sorting is only moderate because of the trace of gravel in each sample. The clayey silt frequency histogram (Fig. 8.3C) shows a mode at the 5 phi size interval and a moderate amount of sand. The silt is by far less sorted in the silty clay sample (Fig. 8.3D), even though sand and gravel are almost lacking.

In comparison to the coastal sediments of this area, the three textural groups in core 95 are typical continental shelf deposits. They are coarser towards the top with lenses of silty and sandy sediment in the upper half of the core. The trend probably indicates changing hydrodynamic conditions from lower to higher energy, in combination with reduced sediment supply towards the recent times.

The foraminiferal number per 35 ml of sediment is relatively low (Fig. 8.2). The two layers of silty sand are almost barren of tests, but the numbers increase to 7000 in the zone of silty clay between 400-500 cm. Below this layer, only trace amounts of tests were found and below 750 cm, the sediment was barren of foraminifera.

Table 8.1

^{14}C dates of Core 95

Core interval cm	^{14}C Date	Laboratory Number
118-133	13 900 ± 700 a	GSC-2993
365-380	11 000 ± 440 a	GSC-3014
760-775	20 400 ± 1650 a	GSC-2977

Table 8.2

Major surface markings and shapes of quartz grains. Numbers indicate observations made in each surface texture class

Sample Number	1	2	3	4
Interval (cm) / Surface Markings	0-5	200-205	450-455	775-780
Irregular Shape	8	6	7	10
Angular Edges	3		1	2
Angular to Subangular Edges		6	1	2
Subangular Edges	7		3	4
Subangular to Subrounded Edges		3	4	2
Subrounded Edges	4	4	4	4
Subrounded to Rounded Edges			1	
Rounded Edges	1			
Conchoidal Fractures	8	5	7	9
Cleavage Faces	8	5	2	3
Weathering Cracks	3	5	2	1
V-Shaped Depressions	9	13	10	5
Collision Marks	2	9	10	5
Solution Holes	12	8	11	13
Silica Deposits	8	2	5	13
Number of Grains	15	13	14	14

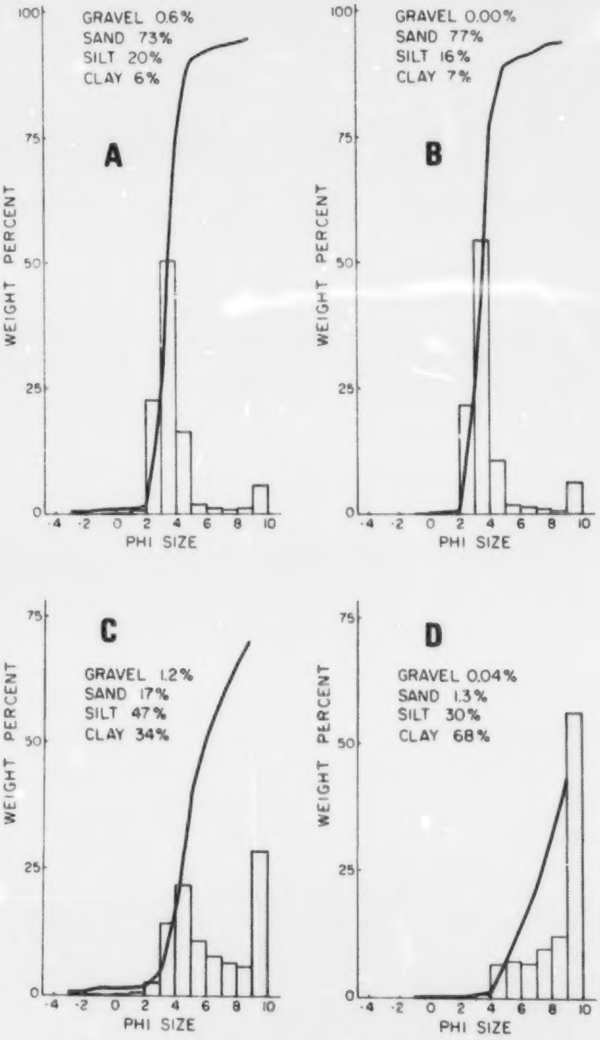

Figure 8.3. *Grain size distribution of subsamples.*

The two major species are **Elphidium excavatum** forma **clavata** and **Islandiella helenae,** both almost mutually exclusive. Elsewhere on Labrador Shelf (Vilks, 1980) **E. excavatum** f. **clavata** is abundant in late glacial sediments and **I. helenae** in surface sediments and isolated horizons in Lake Melville cores (Vilks et al., in press).

Total organic carbon ^{14}C dates (Table 8.1) give an age of 20 400 years at 8 m, 11 000 years at 4 m, and 13 900 years at 1.5 m. These inconsistencies suggest dilution by dead carbon, but the dates may indicate that the core consists mostly of glacial or late glacial sediment. This is confirmed by the predominance of **Elphidium excavatum** forma **clavata** throughout the upper part of the core (unit B), which elsewhere on the Labrador Shelf (Vilks, 1980) characterizes late glacial sediment. This implies that Holocene sedimentation is represented by the surface sand veneer (Unit A). Unit C may represent sedimentation in a proglacial environment with ice-rafting of gravel.

Surface Markings of Quartz Grains

Twelve surface marking types and grain shapes were recognized (Table 8.2). Irregular grain shapes (Plate 8.1, fig. 1) with angular and subangular edges (Plate 8.2, fig. 1) indicate a glacial environment. The glacial environment is also characterized by conchoidal fracture patterns (Plate 8.1, fig. 2; Plate 8.4, fig. 2), and cleavage faces (Plate 8.4, fig. 3). Subrounded (Plate 8.2, fig. 6) to rounded edges, V-shaped pattern (Plate 8.3, fig. 4) and collision marks (Plate 8.3, fig. 2), superimposed on glacial markings, may indicate residence in the beach zone. The continental shelf environment that involves sediment reworking and winnowing can be identified with quartz also containing V-shaped patterns and collision marks (Table 8.2). Diagenesis following deposition results in solution holes (Plate 8.3, fig. 6), silica deposits (Plate 8.1, fig. 5, 6), and weathering cracks (Plate 8.2, fig. 3).

Each of the twelve types of surface markings, except for the rounded edges, were found in all four samples analyzed, (Table 8.2). The major characteristics of the grains in the layer of 0-5 cm (Plate 8.2) are: irregular shape with angular to subangular edges and conchoidal fracture patterns. These markings indicate a glacial origin for the grains. Superimposed on these markings, however, are V-shaped depressions, collision marks, solution holes, and silica deposits. This suggests the grains resided for a subsequent period of time on the continental shelf.

All grains in the 200-205 cm sample (Plate 8.2) contain V-shaped depressions indicating grain movement either in a beach zone or continental shelf. Many grain surfaces also contain solution holes, and therefore, surface markings that signify the continental shelf environment are most abundant in this interval (Table 8.2). The 450 to 455 cm interval (Plate 8.3) is also dominated by grains with V-shaped depressions, collision marks and solution holes. The grains are less angular and the surface markings due to glacial action are not as fresh as in the other samples.

Most grains of the 775 to 780 cm interval contain glacial induced surface markings, such as, irregular shape and conchoidal fractures (see Plate 8.4). The initial glacial markings are coated with silica deposits and have superimposed solution holes. The number of grains with V-shaped depressions and collision marks is low but the diagenetic effect is high, suggesting that the sample represents sediments that have been transported initially by ice and subsequently buried with a minimal intervening period of shelf transport.

Conclusions

Although the interpretation of surface textures on quartz grains is to some extent ambiguous, a sufficiently large sample in addition to the study of other parameters, such as grain size, age and fossils can provide sufficient material for a paleosedimentary model. In our study the sediment size analysis indicates a changing hydrodynamic setting from relatively constant and low energy in late glacial time to fluctuating and high energy towards the present time. Surface textures on quartz grains support this trend.

In the 775 to 780 cm interval the markings are dominated by solution holes and silica deposits that supercede the initial glacial effects. The abundance of the diagenetic surface markings suggest considerable age of the grains. The mechanically induced markings, such as, V-shaped depressions and collision marks occur in small numbers indicating a relatively continuous burial in the fine clay.

The clayey silt of the 450 to 455 cm and 200 to 255 cm intervals contain grains with few glacial effects but many mechanically induced markings. These are mainly V-shaped depressions and collision marks, suggesting relatively high-energy hydrodynamic events, such as, storm waves. The material may have migrated from the coastal zone during periods of heavy storms. Unit B (Fig. 8.2) is a typical continental shelf deposit containing coarse-layered storm deposits (Reineck and Singh, 1973, p. 308).

The surface sandy layer is a relict sediment of glacial marine deposit on the inner shelf. Glacial markings are overlain by V-shaped depressions, collision marks, solution

---

Explanation to Plates 8.1 to 8.4

a - V-shaped marking

b - collision mark (impact pit)

c - solution hole

d - silica deposit

e - subparallel steps

Plate 8.1.
Quartz grains from interval 0-5 cm.

Figure 1 - irregular grain;

Figure 2 - conchoidal fracture pattern;

Figure 3 - weathering cracks;

Figure 4 - subangular edges and collision marks;

Figure 5 - solution holes and silica deposits;

Figure 6 - silica flowers.

Plate 8.2.
Quartz grains from interval 200 to 205 cm.

Figure 1 - irregular grain with angular to subangular edges;

Figure 2 - conchoidal fracture pattern;

Figure 3 - weathering cracks;

Figure 4 - V-shaped pattern;

Figures 5, 6 - subrounded edges,
V-shaped pattern and collision marks.

Plate 8.1

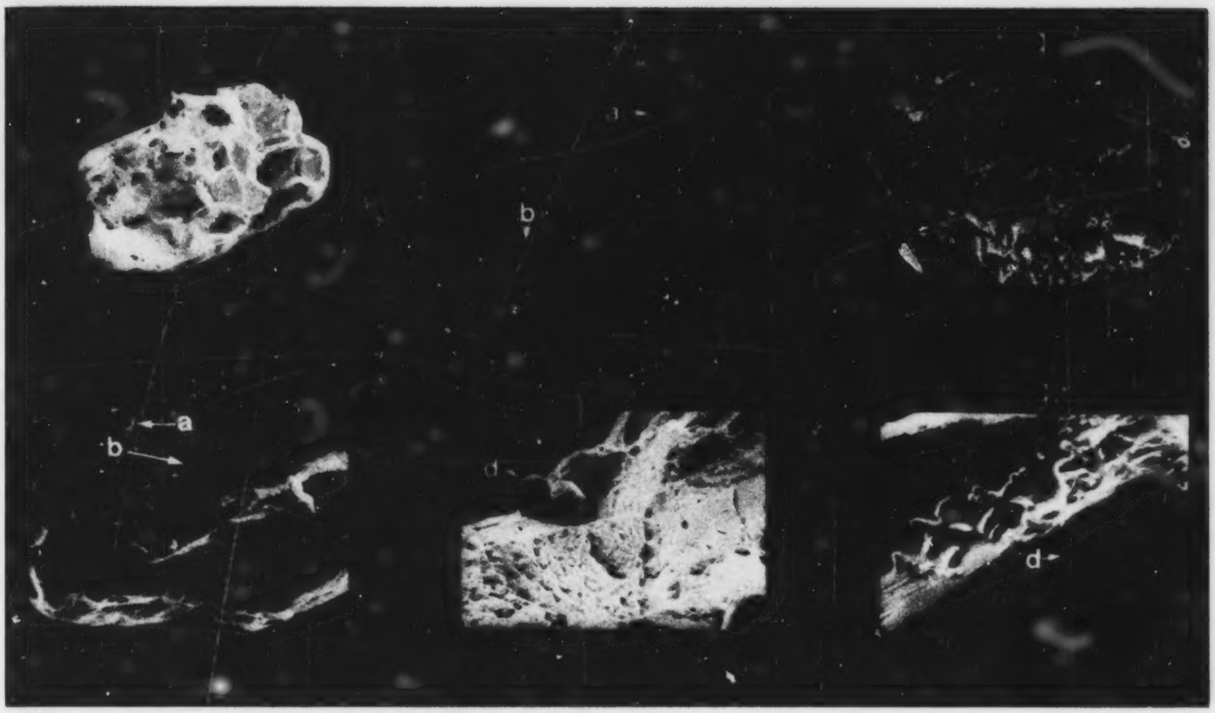

Plate 8.2

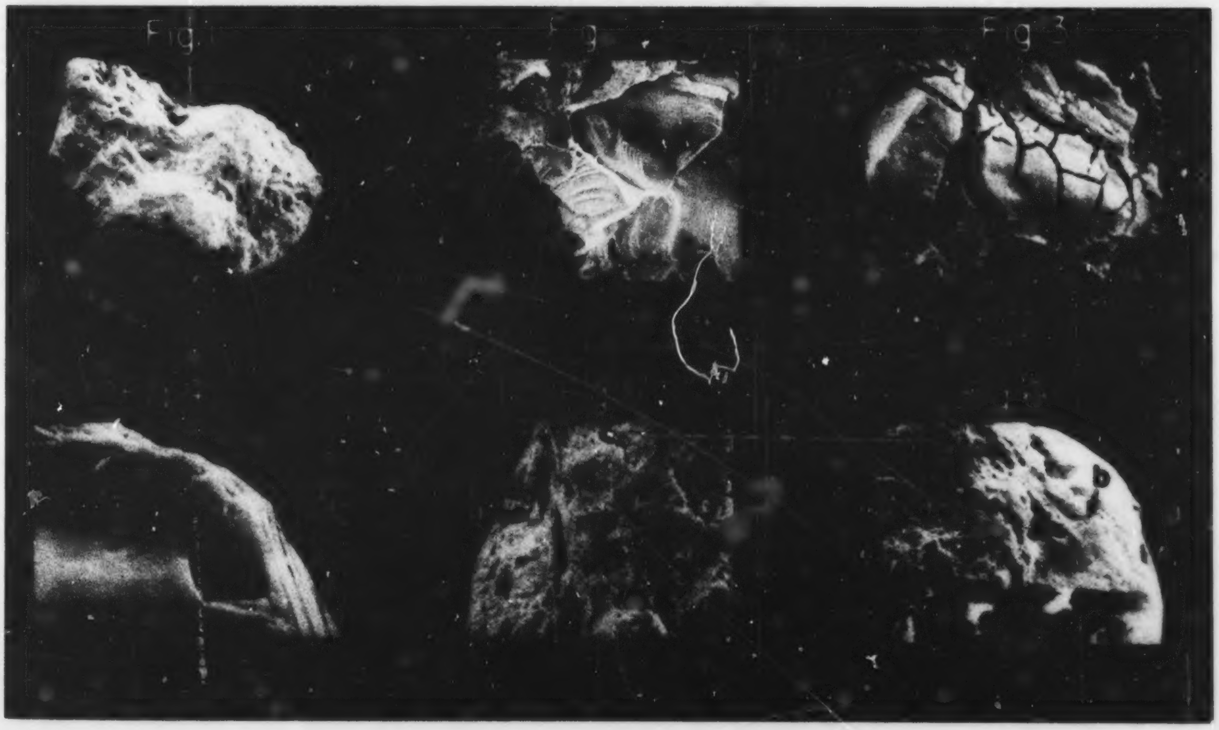
Fig 1
Fig
Fig 3
b

Plate 8.3

Plate 8.4

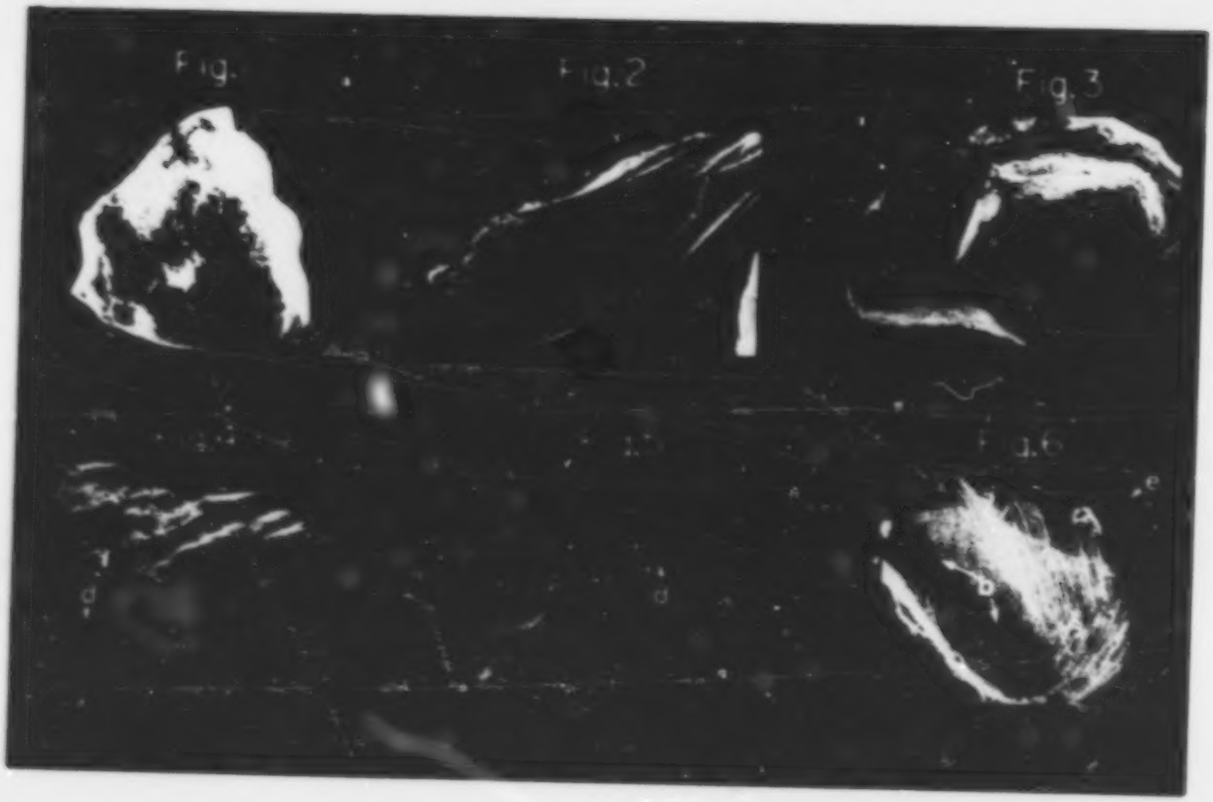
Fig.
Fig.2
Fig.3
Fig.6
e
b
d
d

holes and silica deposits, all indicating a prolonged exposure on the seafloor. Thus, Unit A (Fig. 8.2) may represent Holocene deposits which are only a few centimetres thick because of the low postglacial supply of debris from the land and high inner shelf hydrodynamics.

Grain surface texture, sediment facies, and foraminifera suggest a sequence of three sedimentary regimes for the continental shelf. Unit C at the bottom of Core 95 was deposited in a proglacial environment and in a continuous sequence. Unit B was dominated by storm wave deposition, and Unit A by sediment reworking and the slow rate of sedimentation during postglacial time.

At core station 95 during the late glacial-postglacial period the depth of water did not change considerably, including the time when the eustatic sealevel change was at its lowest (18 000 years BP, Milliman and Emery, 1968). The inner shelf must have been depressed with the load of ice and remained low during the marine maximum when the Lake Melville area was inundated with marine waters. Since deglaciation, the Lake Melville area has been uplifted by between 120 and 180 m (Andrews, 1973) and our evidence suggests that the inner shelf has remained below sea level while following the general trend of isostatic rebound inland.

Acknowledgments

We would like to thank B. Deonarine for making all the Scanning Electron Microscope pictures of the paper. D.J.W. Piper and C.F.M. Lewis provided helpful comments in review of the manuscript.

Plate 8.3.
Quartz grains from interval 450 to 455 cm.

Figures 1, 3 - irregular grain with subrounded edges;

Figures 2, 4, 6 - V-shaped patterns, collision marks and solution holes;

Figure 5 - silica deposits on edges.

Plate 8.4.
Quartz grains from interval 775 to 780 cm.

Figure 1 - irregular grain with subangular to subrounded edges;

Figure 2 - relict conchoidal fracture pattern with silica coating;

Figure 3 - cleavage-controlled grain, subrounded edges;

Figure 4 - solution holes and silica deposits;

Figure 5 - relict conchoidal fracture pattern and silica deposit;

Figure 6 - collision marks, solution holes and subparallel steps.

References

Andrews, J.T.
1973: Maps of the maximum postglacial marine limit and rebound for the former Laurentide Ice Sheet (the National Atlas of Canada); Arctic and Alpine Research, v. 5, no. 1, p. 41-48.

Dinsmore, R.P.
1972: Ice and its drift into the North Atlantic Ocean; ICNAF, Special Publication, No. 8, p. 89-128.

Dunbar, M.J.
1951: Eastern Arctic Waters; Fisheries Research Board of Canada, Bulletin 88, p. 1-131.

Gustajtis, A.K.
1979: Iceberg population distribution study in the Labrador Sea; Data Report, C-CORE (Centre for Cold Ocean Resources Engineering) Publication 79-8, 41 p.

Krinsley, D.H. and Donahue, J.
1968: Environmental interpretation of sand grain surface textures by electron microscopy; Geological Society of America Bulletin, v. 79, p. 743-748.

Krinsley, D.H. and Doornkamp, J.C.
1973: Atlas of quartz sand surface textures; Cambridge, University Press, 91 p.

McLaren, P.
1980: The coastal morphology and sedimentology of Labrador: A study of shoreline sensitivity to a potential oil spill; Geological Survey of Canada, Paper 79-28, 41 p.

Milliman, J.D. and Emery, K.O.
1968: Sea levels during the past 35 000 years; Science, v. 162, p. 1121-1123.

Reineck, H.E. and Singh, I.B.
1973: Depositional Sedimentary Environments; Springer-Verlag, New York, 439 p.

Reinson, G.
1979: Inner shelf sediment dynamics; Cruise Report 79-018. Bedford Institute of Oceanography, Dartmouth, N.S. p. 4-7.

Reinson, G.E., Frobel, D., and Rosen, P.S.
1979: Physical environments of the Groswater Bay-Lake Melville coastal region; Proceedings of the Symposium on Research in the Labrador Coastal and Offshore region, Memorial University of Newfoundland, St. John's, 291 p.

Van der Linden, W.J., Fillon, R.H., and Monahan, D.
1976: Hamilton Bank, Labrador margin: origin and evolution of a glaciated shelf; Geological Survey of Canada, Paper 75-40, 31 p.

Vilks, G.
1980: Postglacial Basin Sedimentation on Labrador Shelf; Geological Survey of Canada, Paper 78-28, 28 p.

Vilks, G., Deonarine, B., Wagner, F.J., and Winters, G.V.
Foraminifera and Mollusca in Surface Sediments of Southeastern Labrador Shelf; Geological Society of America Bulletin. (in press)

9.

STRATIGRAPHIC DISTRIBUTION AND TAXONOMIC NOTES ON BIVALVES OF THE BATHONIAN AND CALLOVIAN (MIDDLE JURASSIC) UPPER YAKOUN FORMATION, QUEEN CHARLOTTE ISLANDS, BRITISH COLUMBIA

Project 760042

T.P. Poulton
Institute of Sedimentary and Petroleum Geology, Calgary

Poulton, T.P., Stratigraphic distribution and taxonomic notes on bivalves of the Bathonian and Callovian (Middle Jurassic) Upper Yakoun Formation, Queen Charlotte Islands, British Columbia; in Current Research, Part B, Geological Survey of Canada, Paper 81-1B, p. 63-71, 1981.

Abstract

Each of the units, characterized successively by the bivalve ***Gryphaea****, and then* ***Iniskinites, Seymourites, Oxycerites, Cadoceras****, and* ***Kepplerites*** *ammonite faunas contain a characteristic bivalve fauna, although few bivalve species are restricted to only one of the units. The restricted distributions of most bivalve species are probably a result of ecological control.*

The generic assignments of some of the previously named species have been revised. By recognition of the Jurassic age and typical ***Parallelodon*** *hinge structure of* ***P. simillima*** *(Whiteaves), the restricted Jurassic age of* ***Parallelodon*** *is indicated.*

Introduction

This preliminary report was prepared as a companion to the summary of biostratigraphic distributions of ammonite and Foraminifera faunas (Tipper and Cameron, 1980). Lithostratigraphic descriptions, a locality map and discussion of ammonite occurrences together with the age they imply are given in that paper and are not repeated here. Other information has been given by Sutherland Brown (1968) and Frebold (1979).

Few new species have been discovered since the original descriptions of the bivalves by Whiteaves (1876, 1884, 1889, 1900), Burwash (1913), and Packard (1921), and no new species are described. McLearn's (1949) stratigraphic revisions which located the earlier described species in their proper beds, are still valid. All had been ascribed to the Cretaceous previous to his studies. Only a limited amount of detailed comparison of the species with similar ones from North America or elsewhere has been undertaken in this preliminary, essentially biostratigraphic study, so that it remains possible that future work may place some of the species in junior synonymy of earlier described contemporaneous American or European species, as already commented on by Imlay (1964) for some species. Many of the species, because of their poor preservation or the paucity of distinguishing characters, would probably not be erected as new species were the original study to be done today, and for the same reasons, most do not warrant detailed restudy until more information on regionally equivalent faunas is available for comparison. Some reassignment of species to different genera was undertaken by McLearn (1949, p. 13) and some further reassignment has been undertaken to a limited degree in the present listing (Table 9.1).

Stratigraphic Distribution

The stratigraphic succession comprises a lower shale-mudstone unit, the upper part of which is rich in a bivalve fauna that can be characterized as "**Gryphaea** beds", overlain by sandstones that contain ammonite faunas of which species of **Iniskinites, Seymourites, Oxycerites**, and **Cadoceras** are characteristic, in upward order. The highest unit which contains abundant bivalves is a shale unit with **Kepplerites** ammonite faunas (Tipper and Cameron, 1980). The bivalve fauna of each unit is listed below.

The **Gryphaea** beds exposed at Cairnes Bay near Robber Point (upper part of grey siltstone of Unit Y2 of Tipper and Cameron, 1980) have not yet yielded any ammonites. They contain a rich bivalve fauna of which **Parallelodon simillima** and **Gryphaea persimilis** are the most conspicuous species. Besides these, the following species occur:

Cucullaea tumida
Gervillia newcombii
Trigonia sp.
Camptonectes (Camptonectes) sp.
Astarte carlottensis
Corbula concinna
"Pronoella" sp.
Entolium(?) sp.
Homomya(?) sp.
Pleuromya sp. aff. **P. laevigata**
Pleuromya sp.
Protocardia subsimile
Protocardia sp.
Thracia sp.
Grammatodon sp.
"Ostrea" sp.
Palaeonucula(?) sp.
"Placunopsis" sp.
Isognomon sp.
Modiolus sp.

Sandstones at Ferry Island, south of Ferry Island, at Fossil Point, Robber Point, Newcombe Bay, Transit Island, and at other localities collected previously and from which detailed locality data are not available, contain a rich variety of bivalves (Table 9.1). These sandstones, of Late Bathonian to Early Callovian age, have been differentiated by Tipper and Cameron (1980) into four subdivisions characterized by species of **Iniskinites, Seymourites, Oxycerites** and **Cadoceras** in upward succession. For the most part, the older collections cannot be confidently assigned to any one subdivision of this succession. H.W Tipper (pers. comm.) has, however, expressed his opinion regarding the stratigraphic positions of many of them.

The **Iniskinites**-bearing sandstones at Robber Point are characterized above all by the local abundance of **Vaugonia flexicostata**. Other bivalve fauna from these localities include:

Cucullaea tumida
Gervillia newcombii
G. sp.
Gryphaea sp.
Camptonectes (Camptonectes)(?) sp.
C. (Camptochlamys) sp.
Pinna sp.

Table 9.1

List of species and their stratigraphic occurrence

Horizon	Gryphaea beds					Iniskinites beds									Seymourites and Oxycerites faunas, undifferentiated																														Cadoceras beds		Kepplerites beds					
Area	Cairnes Bay - Robber Point					Robber Point				Alliford Bay					South of Ferry Island		Ferry Island				Fossil Point									Robber Point						Newcombe Bay						Transit Island	Skidegate Inlet undiff.		Fossil Point	Ferry Island	Alliford Bay					
Locality (GSC localities listed in Appendix) Query indicates uncertain assignment to horizon Species	13623	McLearn (1949, loc. Y5)	Dawson collection (McLearn, 1949, locs. Y5, Y6)	C-86362	C-86372	C-86356(?)	C-86370	C-86371	93736 (part)	44706	44712	44738 (part at least)	48605	C-80806	14923	McLearn (1949, loc. Y14)	McLearn (1949, loc. Y15)	13618	13624	C-80810	McLearn (1949)	Dawson collection (McLearn, 1949) (?)	14920	Richardson collection (McLearn, 1949)	13619	13626 (in part)	93735	44738 (in part at least)	C-80803	McLearn (1949, loc. Y6)	Dawson collection (McLearn, 1949, locs. Y5, Y6)	Newcombe collection (McLearn, 1949)	13617	93736 (part)	C-86369	McLearn (1949, p. 12)	Newcombe collection (McLearn, 1949, p. 12) (?)	Packard collection (McLearn, 1949, p. 12) (?)	13616	13621	13625	862	6363, 6363b	13639	44708	C-80808	McLearn (1949, loc. Y12)	13626 (part)	13627(?)	44707	93734	C-80807
Astarte carlottensis Whiteaves	x	x	x	x	x											x	x	x	x		x				x	x	x			x	x		x	x		x			x		x		?					x	x			
Astarte sp.																																										?										
Camptonectes (*Camptochlamys*) *meekiana* (Whiteaves)																																																				
Camptonectes (*Camptochlamys*) sp.								x																																												
Camptonectes (*Camptonectes*) *curvatus* (Geinitz)																																																				
Camptonectes (*Camptonectes*) sp.		x			x			?																									?			x			x													
Ceratomya (*Capillimya*) *semiradiata* (Whiteaves)																					x								x			x																				
Ceratomya sp.								?																																												
Corbula concinna Whiteaves	x	x																																																		
Corbula sp.					x														?	?					x								?	?					?		?											
Ctenostreon sp.																																					x														
Cucullaea ponderosa Whiteaves																															?			x																	
Cucullaea tumida (Whiteaves)		x	x					x																											x																
Entolium sp.				?		x	x		x										x						x					x			x	x					x		x	?										
Gervillia newcombii Whiteaves		x						x													x															x	x														
Gervillia sp.						x																																				?									
Goniomya sp.								?												x					x														x		x											
Grammatodon cumshewaensis (Whiteaves)																					x	x																													
Grammatodon sp.					x															?																									?						
Gryphaea persimilis Whiteaves		x	x	x	x																	x																													
Gryphaea sp.								x																																											?
Homomya sp.				?																																					?	?				x						
Isognomon skidegatensis (Whiteaves)							x														x									x					x	x																
Isognomon sp.				x	x				?																		?		?					?																		
Modiolus(?) *mundensis* (Whiteaves)																																																				
Modiolus persistens Whiteaves																														x		x				x																
Modiolus sp.				?	x																						x																									
Myophorella charlottensis (Packard)								x													x	?			x					?						?				x												
Myophorella devexa (Eichwald)									?	?		?							x	x			x					x						?					x				?			x						
Myophorella packardi (Crickmay)																		?	?	?					?	x	?		?				?	?					?	x			?	?	?			x		x	x	x
Myophorella yellowstonensis Imlay								?																																											
Myophorella sp.							x	x		?	?		x		x																															?						x
Neocrassina (*Coelastarte*) sp.																																														?						
Ostrea skidegatensis Whiteaves								x								x					x	x			x					x						x																
Ostrea sp.					?		x													?							?								x																?	
Oxytoma sp.																						x																													
Palaeonucula sp.					?																																															?
Parallelodon simillima (Whiteaves)		x	x	x	x																																															
Pholadomya ovuloides Whiteaves																								?																												
Pholadomya sp.																	x				x															x										x						
Pinna sp.								x																						x																						
Placunopsis sp.					x			?																																												
Plagiostoma sp.																				?									?												?											?
Pleuromya carlottensis Whiteaves																	x				x	x					x		x							x											x					
Pleuromya laevigata Whiteaves					x		?		x		x					x	x			x	x	x			?		?			x	x			x	?	x																
Pleuromya sp.		x			x	x	x	x		?	?		x	x		x	x	?	x	?	x								x	x			x			x			?	?	x					?						?
Pronoella(?) *occidentalis* (Whiteaves)																x						x																													
Pronoella sp.	?			?	?		?												?							?	?							?									?			x						
Protocardia subsimile Whiteaves				x	x		x		x												x	x			x					x	x		x	x		x			x	x	x											
Protocardia sp.				x																																															
Pseudomonotis sp.																																									?											
Tancredia sp.																																									?											
Thracia depressa (Sowerby)																											?																								
Thracia semiplanata Whiteaves																x	x				x	x							x	x	x					x																
Thracia sp.					x			?												x					?	x	x						x	x					x							?						
Trigonia sp.	x	x																				?														x																
Vaugonia doroschini (Eichwald)						?	x				x																		?																							
Vaugonia flexicostata (Burwash)						x		x													?				x																											

Isognomon skidegatensis
Ostrea skidegatensis
Myophorella charlottensis
M. sp. aff. **yellowstonensis**(?)
M. sp.
Entolium sp.
Pleuromya laevigata
P. sp.
Goniomya sp. (?)
Protocardia subsimile
Cercomya sp. (?)
Vaugonia doroschini
"**Pronoella**" sp. (?)
Thracia sp. (?)
"**Ostrea**" sp.
"**Placunopsis**" sp. (?)

Myophorella sp. aff. **M. devexa**, **M. packardi** (?), and **Isognomon** sp. may also be from these beds (part of mixed collection, GSC loc. 93736).

The same unit appears to be present at Alliford Bay where the following species have been found:

Pleuromya laevigata
P. sp.
Vaugonia doroschini
Myophorella devexa (?)
M. sp. (?)

Beds characterized by the **Seymourites** ammonite fauna have yielded:

Entolium sp.
Homomya sp. (?)
Astarte carlottensis
Astarte sp. (?)
Isognomon skidegatensis
I. sp. (?)
Myophorella devexa
M. packardi
M. sp.
Gervillia sp. (?)
"**Pronoella**" sp. (?)
Cucullaea ponderosa
Plagiostoma sp. (?)
Vaugonia doroschini(?)
Pseudomonotis sp. (?)
Tancredia sp. (?)
Camptonectes sp.
Cercomya semiradiata
Pleuromya sp.
P. subcompressa
P. laevigata
P. carlottensis
"**Ostrea**" sp. (?)
Goniomya sp.
Protocardia subsimile
Grammatodon sp. (?)
Corbula sp.
Thracia depressa(?)
T. semiplanata
T. sp.

The following species may possibly also come from this unit but their unusual appearance here suggests that they more likely come from other units (loc. 13619):

Ostrea sp. cf. **O. skidegatensis**
Myophorella charlottensis
Vaugonia flexicostata

The higher beds, characterized by **Oxycerites**, cannot be uniquely identified but the faunas in some collections (GSC locs. 862, 13618, 13619, 13624, 14923, 44738) listed above from **Seymourites** beds, may instead have come from those with **Oxycerites**. The bivalve species in those collections are:

Entolium sp.
Homomya sp. (?)
Astarte carlottensis
A. sp.
Pleuromya sp.
Myophorella packardi(?)
Myophorella devexa
M. charlottensis
M. sp.
Ostrea sp. cf. **O. skidegatensis**
Pleuromya sp. cf. **P. laevigata**(?)
Goniomya sp.
Protocardia subsimile
Corbula sp.
Thracia sp. (?)
"**Pronoella**" sp.

Still higher beds, with **Cadoceras** sp. cf. **C. doroschini** (GSC locs. 44708, C-80808 and possibly also parts of the collections listed just above), contain:

Myophorella packardi (?)
Myophorella devexa
M. sp. (?)
Pleuromya sp. (?)
Pholadomya sp.
"**Pronoella**" sp.
Homomya sp.
Neocrassina (Coelastarte) sp. (?)
Thracia sp. (?)
Grammatodon sp. (?)

The following species come from undifferentiated sandstones of the interval characterized by **Iniskinites** through **Cadoceras** ammonite faunas:

Camptonectes sp.
Astarte carlottensis
Pleuromya laevigata
Pleuromya carlottensis
Pleuromya sp.
Isognomon skidegatensis
Ostrea skidegatensis
Myophorella charlottensis
Entolium sp.
Thracia semiplanata
Protocardia subsimile
Cucullaea ponderosa
Pholadomya sp.
Cercomya semiradiata
Vaugonia flexicostata

Some of the species described by Whiteaves (1876-1900), and confirmed to be from the Upper Yakoun or newly identified from that unit by McLearn (1949), have not been identified by the writer in subsequent collections from these various sandstones, and are included in the listings above on the basis of the locality data supplied by McLearn. They are:

Trigonarca (i.e. **Cucullaea**) **tumida**
Gervillia newcombii
Gryphaea persimilis
Pinna sp.
Modiolus persistens
Pholadomya ovuloides
Ctenostreon sp.

Parallelodon (i.e. **Grammatodon**) **cumshewensis**
Arctica [i.e. "**Pronoella**"(?)] **occidentalis**
Oxytoma sp.
Trigonia sp.
Trigonia s. l. n. sp.?

For other species listed in Table 9.1 but not assigned to a particular unit, neither the data provided by previous authors nor subsequent collections, indicate the horizon from which they came:

Camptonectes (Camptochlamys) meekiana
Camptonectes (Camptonectes) curvatus
Modiolus(?) [**Lithodomus**] **maudensis**

These species were not listed in the Upper Yakoun faunas by McLearn (1949). He may have thought them to have come from Cretaceous beds. However, identifications of specifically unidentifiable specimens of **C. (Camptochlamys)**, **C. (Camptonectes)**, and **Modiolus**, together with the original locality data (all from east end of Maude Island, and **C. (C.) meekiana** also from south side of Alliford Bay) suggest that they were possibly collected in Upper Yakoun beds.

The following species have been identified for the first time from these various sandstone beds by the writer:

Goniomya sp.
Vaugonia doroschini
Myophorella devexa
Myophorella packardi
Myophorella sp.
Corbula sp.
"**Pronoella**" sp.
Homomya sp.
Astarte sp.
Neocrassina (Coelastarte) sp. (?)
Thracia sp.
Grammatodon sp. (?)
Plagiostoma sp. (?)
"**Ostrea**" sp.
Isognomon sp.
Thracia depressa (?)
Modiolus sp.
Pleuromya sp. cf. **P. subcompressa**
Pseudomonotis sp. (?)
Tancredia sp. (?)

Anditrigonia plumasensis and **Inoceramus** sp. were identified also by the writer in the field but could not be collected, in sandstones at Robber Point that may belong to either the **Iniskinites** or the **Seymourites** beds.

The shales on the south side of Alliford Bay that Tipper and Cameron (1980) considered to be characterized by **Kepplerites** sp. cf. **K. spinosus** (locs. 13626 in part, 13627, 44707, 93734, and C-80807) have yielded, in addition to the very conspicuous **Myophorella packardi**:

Astarte carlottensis
Gryphaea sp. (?)
Pleuromya sp. (?)
Myophorella sp.
"**Ostrea**" sp. (?)
Pleuromya carlottensis

Biostratigraphic and Ecologic Considerations

All the species are shallow-marine forms. The limited stratigraphic distributions of most of the bivalves shown in the lists below were probably ecologically controlled and are also partly a reflection of limited collecting. However, the abundance of **Vaugonia flexicostata** is the lower beds, and the variety of **Myophorella** species but particularly the abundance of **M. packardi** in higher beds, should be considered as potentially useful tools for correlation with other areas of western North America.

Many of the varied bivalve fauna of the **Gryphaea** beds (upper part of grey siltstone of Unit Y2 of Tipper and Cameron, 1980), are restricted to that unit, a soft grey siltstone and mudstone. The lithology and exquisite preservation of even fragile, thin-shelled bivalves indicate virtually no agitation although very shallow, perhaps coastal marsh conditions are indicated. The foraminifera indicate normal marine salinities (Cameron in Tipper and Cameron, 1980).

The sandstones containing the **Iniskinites** through **Cadoceras** faunas are commonly argillaceous, and many of the locally abundant ammonites and bivalves are intact, indicating rapid deposition and little winnowing in shallow environments.

The well-preserved bivalves and ammonites of the shales with **Kepplerites** sp. cf. **K. spinosus** are a typical open marine shale-siltstone assemblage of only low to moderate diversity.

Parallelodon simillima, **Corbula concinna**, and "**Placunopsis**" sp. are identified with certainty only in the lower shales, the **Gryphaea** beds, although the last may possibly also occur in the overlying sandstones with **Iniskinites**.

Some species are restricted to individual units of the overlying sandstone succession, as listed below. The only species that is restricted to the sandstones and that has been identified throughout the sandstones, is **Myophorella devexa**. The lower occurrences are questionably identified, however, and at any rate the species as currently understood may involve more than one form (Poulton, 1979).

Iniskinites beds only:

Myophorella yellowstonensis(?)

Iniskinites through **Oxycerites** beds:

Cercomya (Capillimya) semiradiata and **C.** sp.
Goniomya sp.
Isognomon skidegatensis
Myophorella charlottensis
Ostrea skidegatensis
Pinna sp.
Vaugonia doroschini
Vaugonia flexicostata

Seymourites/Oxycerites beds only:

Cucullaea ponderosa
Grammatodon cumshewensis
Modiolus persistens
Oxytoma sp.
Pholadomya ovuloides
Pronoella(?) **occidentalis**
Pseudomonotis sp.
Tancredia sp.
Thracia depressa
Thracia semiplanata
Ctenostreon sp.

Seymourites/Oxycerites through **Cadoceras** beds:

Pholadomya sp.

The following species occur only in the upper **Kepplerites** shales and the sandstones with **Oxycerites** and **Seymourites**:

Myophorella packardi
Plagiostoma (?) sp.
Pleuromya carlottensis

Palaeonucula is recognized only in the shale facies, in both the upper **Kepplerites** beds and probably the lower **Gryphaea** beds.

The presence of specifically unidentified specimens of **Ostrea, Corbula, Grammatodon, Isognomon, Modiolus,** and **"Pronoella"** among those forms which occur in every unit or nearly every unit suggests that some of the apparently restricted distributions indicated in the above lists may be specious.

Burwash's Species

It is evident from a comparison of the geological map given by Burwash (1913) showing the localities of the collections made by Arthur Church, with that of Sutherland Brown (1968), and from the fossils themselves described by Burwash, that they also are a mixture of Yakoun and Haida (Lower Cretaceous) species. Some of the species described by Burwash (1913) which can be confidently identified as Upper Yakoun forms are discussed below. Both **Goniomya uniangulata** and **G. transversicostata** are based on small poorly preserved fragments and are included in this report with **Goniomya** sp. Additional specimens of **Trigonia** (i.e. **Vaugonia) flexicostata** are figured here. Correctly, this is the only species of trigoniid which Burwash (1913) described that was later recognized by Packard (1921). Poulton (1979) incorrectly thought it to be possibly Cretaceous, as Burwash had stated, although McLearn (1949) had listed it questionably from the Yakoun. **Trigonia recticostata** is based on a poorly preserved internal mould which is not specifically identifiable and is included here as **Myophorella** sp. The figured type of **Trigonia reniforme** (Burwash, 1913, Pl. II, Figs. 1a, b) and four other specimens catalogued under the same number (15363) in the University of Chicago collections are poorly preserved internal moulds of **Myophorella packardi** or **M. devexa. Trigonia paucicostata** is a small internal mould, probably of **M. devexa.** All these species were collected on the shores of Maude Island.

Taxonomic Notes

Astarte carlottensis Whiteaves

Plate 9.1, figures 14-19

Astarte packardi White. Whiteaves, 1884, p. 229, pl. 30, figs. 6a, b.
Astarte carlottensis Whiteaves, 1889, p. 154.

Several specimens of **Astarte carlottensis,** including the primary types, exhibit well preserved hinge structures and muscle scars. These characters are illustrated because, as D.G. Taylor (pers. comm.) has pointed out to me, they have rarely been illustrated or described for Jurassic species of Astartidae, and are of potential importance for supraspecific classification of the group. Although no taxonomic revision is attempted here, the following characters are significant: the shell shape, relative strength of hinge plate, and dentition appear to be entirely typical of **Astarte** as illustrated by Chavan (1969, Fig. E64, 1); and there is a distinct but shallow pallial sinus.

Cucullaea tumida (Whiteaves)

Trigonoarca tumida Whiteaves, 1884, p. 235, pl. 31, fig. 6.

Although the dentition of neither the type specimen nor a well preserved topotype (?) could be satisfactorily exposed, it appears to be consistent with **Cucullaea,** in which genus the species is better placed than in **Trigonarca,** which is otherwise Cretaceous in age and which lacks the radial ornament which characterizes **C. tumida.**

Parallelodon simillima (Whiteaves)

Plate 9.1, figures 20-23

Nemodon fischeri d'Orbigny. Whiteaves, 1884, p. 234, pl. 31, fig. 5.
Arca (Nemodon) simillima Whiteaves, 1900, p. 293.
Parallelodon (Gilbertwhitea) simillima (Whiteaves). Reinhart, 1937, p. 173, pl. 27, figs. 7a, b.

The hinge structure of **Arca (Nemodon) simillima** clearly shows it to be a typical **Parallelodon** (Pl. 9.1, figs. 21, 23). This is significant because Newell (1969) placed it, as genotype for **Gilbertwhitea** Crickmay, in the genus **Nemodon** which is otherwise an Upper Cretaceous genus.

Although Newell (1969) correctly considered **Gilbertwhitea** to be invalid, the reason for placing it in **Nemodon,** while reasonable, is conjectural and the biostratigraphic separation of **Nemodon** from **Parallelodon** and therefore their potential for biostratigraphic use, is thereby obscured. Whiteaves (1884, p. 234; 1900, p. 293), thinking **A. simillima** to come from Cretaceous rocks, and noting what is now seen to be only a general similarity of the hinge structure, assigned it to **Nemodon** Conrad.

Crickmay (1930) compounded the confusion by illustrating the dentition of what he called a 'topotype' but which is different from that of the primary types. The primary types were collected at the "east end of Maude Island" (Whiteaves, 1884, p. 234) and Crickmay could well have collected a Cretaceous specimen from there, which he confused with Whiteaves's species, thinking them also to be Cretaceous. Crickmay's (1930) lengthy discussion of the phylogeny of the Parallelodontidae and the 'degeneracy' of his genus **Gilbertwhitea,** based on **A. (N.) simillima** no longer are meaningful in our current knowledge of the family (e.g. Newell, 1969). Nor is it clear what age range Crickmay (1930) conceived for **Gilbertwhitea,** although he certainly included a Bajocian species, **G. micromorpha,** within it, without illustrating its hinge.

Reinhart (1937) separated both **Nemodon** and **A. (N.) simillima** from the family Arcidae on the basis of their dentition, and assigned Whiteaves's species to **Parallelodon,** retaining Crickmay's name **Gilbertwhitea** as a subgenus. He still thought the species to be Cretaceous, and distinguished **Gilbertwhitea** from **Parallelodon** s. str. by its anterior teeth being parallel to the hingeline rather than oblique. In this he was apparently misled by Crickmay's (1930) erroneous attribution of hingeline-parallel teeth to **A. (N.) simillima.** Reinhart (1937) illustrated another topotype, collected by F.H. McLearn in 1921, which indeed appears to represent Whiteaves's species. Curiously for his purposes however, he did not expose or illustrate the hinge structures of his topotype.

Newell (1969) probably placed **Gilbertwhitea** in junior synonymy of the Cretaceous genus **Nemodon** Conrad in ignorance of McLearn's (1949) reassignment of Whiteaves's species to the Jurassic, and following Crickmay's (1930) and subsequently Reinhart's (1937) assertions that both the anterior and posterior hinge teeth are parallel to the hingeline. Assuming that Crickmay's (1930) concept of his genus **Gilbertwhitea** was based on the hingeline erroneously attributed to **A. (N.) simillima** rather than on the primary type material, Newell (1969) was correct in placing the genus in junior synonymy of **Nemodon.** In this case, **A. (N.) simillima** cannot be considered to be the genotype of **Gilbertwhitea,** and the genus is therefore invalid for a second reason, lack of a genotype species.

1
2
3
4
5
8
9
10
20
12
13
21
18
14
16
15
22
23

Plate 9.1

All figures are shown natural size.
All specimens are stored in the type collection,
Geological Survey of Canada,
601 Booth Street Ottawa

Trigonia sp.

Figures

1-5. Lateral, anterior, umbonal, and posteroumbonal views, hypotype GSC 64819 from GSC locality 13623.

Vaugonia flexicostata (Burwash)

6. Lateral view of latex cast, hypotype GSC 64820 from GSC locality C-86356.

7. Lateral view of latex cast, hypotype GSC 64821 from GSC locality C-86356.

8. Lateral view of latex cast, hypotype GSC 64822 from GSC locality C-86356.

9. Lateral view of latex cast, hypotype GSC 64823 from GSC locality C-86356.

10. Lateral view of latex cast, hypotype GSC 64824 from GSC locality C-86356.

11. Lateral view, hypotype GSC 64825 from GSC locality C-86356.

12. Lateral view of latex cast, hypotype GSC 64826 from GSC locality C-86356.

13. Lateral view, hypotype GSC 64827 from GSC locality C-86356.

Astarte carlottensis Whiteaves

14,15. Dorsal and internal views, hypotype GSC 4929a, illustrating hinge structure and muscle scars; external view figured by Whiteaves, 1884, pl. 30, fig. 6b as **A. packardi** White.

16. Lateral view, hypotype GSC 64828 from GSC locality 13619; external sculpture superimposed on internal surface showing pallial line and adductor scars.

17. Lateral view of internal mould, hypotype GSC 64829 from GSC locality 13619.

18,19. Posterior and internal views, hypotype GSC 4929, illustrating hinge structure; external sculpture and poorly illustrated internal structures shown by Whiteaves, 1884, Pl. XXX, figs. 6, 6a, as **A. packardi** White.

Parallelodon simillima (Whiteaves)

20,21. Dorsal and internal views, showing hinge structure and muscle scars; lectoparatype GSC 4913c; another specimen (Figs. 22, 23 below) of the original series was illustrated by Whiteaves (1884) as **Nemodon fischeri** d'Orbigny.

22,23. Dorsal and internal views, showing hinge structure, holotype GSC 4913; external sculpture was previously illustrated by Whiteaves (1884, Pl. 31, fig. 5) as **Nemodon fischeri** d'Orbigny.

Knowing now the typical **Parallelodon** dentition of **A. (N.) simillima**, it seems advisable to disregard Crickmay's (1930) concept of **Gilbertwhitea**, being based on the hinge structure of probably erroneously identified material, and emphasize his designation of **A. (N.) simillima** as genotype. In this case **Gilbertwhitea**, with genotype **A. (N.) simillima**, becomes a junior synonym of **Parallelodon**, and the Jurassic age of the species is entirely consistent with the known range of that genus, which was not the case when it was placed in junior synonymy of **Nemodon**.

Myophorella spp.

Trigonia charlottensis was included by Poulton (1979) as a junior synonym of **Myophorella devexa** in his listing of Upper Yakoun trigoniid faunas. **M. devexa** is a variable species, and there are gradational forms between it and **M. packardi** (=**Trigonia dawsoni** of Whiteaves, in part; see Poulton, 1979) in the Queen Charlotte Islands collections, so that more detailed study can be expected to produce taxonomic revisions. **M. charlottensis** now seems to be sufficiently distinctive, by virtue of the coarse spacing of the ribs over the entire flank, to be recognized as a species independent of **M. devexa**.

Vaugonia flexicostata (Burwash)

Plate 9.1, figures 6-13

Trigonia flexicostata Burwash, 1913, p. 82-83, pl. III, fig. 3.

V. flexicostata is a conspicuous element of the fauna of the green sandstone beds at Robber Point that were characterized as containing **Iniskinites** by Tipper and Cameron (1980). The specimens illustrated here are presumably topotypes although the precise locality of the specimens described by Burwash (1913) on the shores of Maude Island was not recorded.

Trigonia sp.

Plate 9.1, figures 1-5

A well preserved but partially crushed and broken specimen from the shales with **Gryphaea** is worthy of illustration. It is the first large and coarsely ribbed species of **Trigonia** to be illustrated from Canada. In these characters, it is similar to other Middle Jurassic species not yet described from North America, and to Middle and Upper Jurassic species of Europe. However, the high, nearly right, angle between the flank and area, the predominantly radial fine ribbing of the area, and the great convexity of the present species, together distinguish it from any of the European species.

References

Burwash, E.M.
1913: On some new species of marine invertebrates from the Cretaceous of the Queen Charlotte Islands; Transactions of the Royal Society of Canada, third series, v. 7, sec. 4, p. 77-90.

Chavan, A.
1969: Superfamily CRASSATELLACEA Férussac, 1822, in Treatise on Invertebrate Paleontology, Part N, v. 2, Mollusca 6, Bivalvia; R.C. Moore (ed.); Geological Society of America and University of Kansas, p. N562-N583.

Crickmay, C.H.
1930: The Jurassic rocks of Ashcroft, British Columbia; University of California Publications, Bulletin of the Department of Geological Sciences, v. 19, no. 2, p. 23-74.

Frebold, H.
1979: Occurrence of the Upper Bathonian ammonite genus **Iniskinites** in the Queen Charlotte Islands, British Columbia; in Current Research, Part C, Geological Survey of Canada, Paper 79-1C, p. 63-66.

Imlay, R.W.
1964: Marine Jurassic pelecypods from central and southern Utah; United States Geological Survey Professional Paper 483-C.

McLearn, F.H.
1949: Jurassic formations of Maude Island and Alliford Bay, Skidegate Inlet, Queen Charlotte Islands, British Columbia; Geological Survey of Canada, Bulletin 12.

Newell, N.D.
1969: Family PARALLELODONTIDAE Dall, 1898, in Treatise on Invertebrate Paleontology, Part N, v. 1, Mollusca 6, Bivalvia; R.C. Moore (ed.); Geological Society of America and University of Kansas, p. N256-N259.

Packard, E.L.
1921: The Trigoniae from the Pacific Coast of North America; University of Oregon Publications, v. 1, n. 9.

Poulton, T.P.
1979: Jurassic trigoniid bivalves from Canada and western United States of America; Geological Survey of Canada, Bulletin 282.

Reinhart, P.W.
1937: Cretaceous and Tertiary pelecypods of the Pacific slope incorrectly assigned to the Family Arcidae; Journal of Paleontology, v. 11, p. 169-180.

Sutherland Brown, A.
1968: Geology of the Queen Charlotte Islands; British Columbia Department of Mines and Petroleum Resources, Bulletin 54.

Tipper, H.W. and Cameron, B.E.B.
1980: Stratigraphy and Paleontology of the Upper Yakoun Formation (Jurassic) in Alliford Bay Syncline, Queen Charlotte Islands, British Columbia; in Current Research, Part C, Geological Survey of Canada, Paper 80-1C, p. 37-44.

Whiteaves, J.F.
1876: On some invertebrates from the coal-bearing rocks of the Queen Charlotte Islands, collected by Mr. James Richardson in 1872; Geological Survey of Canada, Mesozoic Fossils, v. 1, Part I.

1884: On the fossils of the coal-bearing deposits of the Queen Charlotte Islands collected by G.M. Dawson in 1878; Geological Survey of Canada, Mesozoic Fossils, v. 1, Part III, p. 192-262.

1889: On some Cretaceous fossils from British Columbia, the Northwest Territory and Manitoba; Geological Survey of Canada, Contributions to Canadian Palaeontology, v. 1, Part 2, p. 151-196.

1900: On some additional or imperfectly understood fossils from the Cretaceous rocks of the Queen Charlotte Islands, with a revised list of the species from these rocks; Geological Survey of Canada, Mesozoic Fossils, v. 1, Part IV, p. 264-307, Pl. 33-39.

Appendix: List of GSC Fossil Localities

862. J.D. Mackenzie, 1913. East end of South Bay, south of Leading (i.e. Transit) Island, Moresby Island, Skidegate Inlet. This data is contradictory according to H.W. Tipper (pers. com.).

6363. D.M. Kean for H.I. Smith, 1919. Skidegate Inlet area.

13616. F.H. McLearn, 1921. Newcombe Bay, Maude Island.

13617. F.H. McLearn, 1921. Sandstone at Robber Point, Maude Island.

13618. F.H. McLearn, 1921. On island, northeast shore of Alliford Bay, Skidegate Inlet.

13619. F.H. McLearn, 1921. Loose on south side of Alliford Bay, Skidegate Inlet.

13620. F.H. McLearn, 1921. Newcombe Bay, Maude Island.

13621. F.H. McLearn, 1921. Loose at Newcombe Bay, Maude Island.

13623. F.H. McLearn, 1921. Robber Point, Maude Island.

13624. F.H. McLearn, 1921. Loose, on island, northeast side of Alliford Bay, Skidegate Inlet.

13625. F.H. McLearn, 1921. Newcombe Bay, Maude Island.

13626. F.H. McLearn, 1921. Loose on south side of Alliford Bay, Skidegate Inlet.

13627. F.H. McLearn, 1921. Loose at fertilizer plant, Alliford Bay, Skidegate Inlet.

13639. F.H. McLearn, 1921. Skidegate Inlet.

14920. G.M. Dawson, 1878. Alliford Bay, Skidegate Inlet.

14923. V.C. Brink, 1944. East coast of Alliford Bay.

44706. A. Sutherland Brown, 1960. Alliford Bay at bomb shelter.

44707. A. Sutherland Brown, 1960. South shore of Alliford Bay.

44708. A. Sutherland Brown, 1960. Fossil Point, Alliford Bay.

44712. A. Sutherland Brown, 1960. Alliford Bay.

44738. A. Sutherland Brown, 1960. South of Alliford Bay.

48605. A. Sutherland Brown, 1961. Robber Point, 53°13'N, 132°01'45"W. Some ammonites previously identified from this collection by H. Frebold as **Chondroceras** (in Sutherland Brown, 1968, p. 74) are now referred to **Iniskinites** (Frebold, 1979).

93734. H.W. Tipper, 1976. Alliford Bay on north shore of Moresby Island. 53°12'00"N, 132°00'00"W.

93735. H.W. Tipper, 1976. Sandstone at Fossil Point, Alliford Bay. 53°12'00"N, 132°00'10"W.

93736. H.W. Tipper, 1976. Sandstone on point southwest of Robber Island, east shore of Maude Island. 53°13'00"N, 132°01'40"W.

C-80803. H.W. Tipper, 1978. Fossil Point, Alliford Bay.

C-80806. H.W. Tipper, 1978. Fossil Point, Alliford Bay.

C-80807. H.W. Tipper, 1978. South end of Alliford Bay.

C-80808. H.W. Tipper, 1978. Island with beacon northwest of ferry terminal.

C-80810. H.W. Tipper, 1978. Island with beacon northwest of ferry terminal.

C-86356. T.P. Poulton, 1979. Small sandstone bluff above **Gryphaea** shales , west of Robber Point.

C-86362. T.P. Poulton, 1979. **Gryphaea** shales at Robber Point.

C-86369. H.W. Tipper, 1978. Robber Point. 53°13'00"N, 132°01'48"W.

C-86370. H.W. Tipper, 1978. Robber Point, east end of Maude Island.

C-86371. H.W. Tipper, 1978. Robber Point, east end of Maude Island.

C-86372. H.W. Tipper, 1978. Robber Point, east end of Maude Island.

10.

A GRANITIC DIAPIR OF BATHOLITHIC DIMENSIONS AT THE WEST MARGIN OF THE CHURCHILL PROVINCE

Project 800009

H.H. Bostock
Precambrian Geology Division

Bostock, H.H., A granitic diapir of batholithic dimensions at the west margin of the Churchill Province; in Current Research, Part B, Geological Survey of Canada, Paper 81-1B, p. 73-82, 1981.

Abstract

Leucocratic granitic rocks with local remnants of charnockitic gneiss constitute the oldest rocks in the map area. Remnants of a pelitic to psammitic high grade metasedimentary assemblage with minor calc-silicate and metavolcanic components occur largely about the margins of the granitic rocks. Three granodioritic bodies occur in the western part of the map area. Hypersthene-bearing metagabbro bodies intrude the Archean rocks.

A megacrystic hypersthene-bearing granite batholith, of likely Hudsonian age, has diapirically intruded the Archean rocks in the eastern part of the area mapped. The intrusion can be divided into four structural zones:

1. *A southwestern gently dipping thin sheet-like body lying on Archean basement;*
2. *A northwestern zone representing the deformed head of the pluton;*
3. *A central root zone; and*
4. *An eastern constricted zone.*

The youngest rocks are vertical, northwest-trending, only slightly altered basic dykes of the Sparrow dyke swarm.

Introduction

This report provides a preliminary account of fieldwork in the northeast corner of the Little Buffalo River (85 A) and the west half of the Fort Smith (75 D) map areas undertaken in the summer of 1980. The project was carried out with three helicopter-supported ground traverse teams of two men working on an east-west traverse grid of approximately 2-mile spacing at 1:250 000 scale. Grid mapping was followed by examination of the shorelines of the larger lakes and of particular problem areas. The descriptive part of the report is followed by a more speculative interpretation of the geology within the Fort Smith map area.

Pleistocene Geology

Glacial striae within the map area reflect chiefly west southwestward movement of ice during the Pleistocene. After ice retreat most highlands were washed free of finer glacial sediments leaving local concentrations of erratic cobbles and boulders that include conglomerate, sandstone and siltstone typical of the Nonacho Group in addition to rocks found in local outcrop. Finer sediments were washed into adjacent ephemeral lakes which were only locally of any appreciable size.

An unknown thickness of fine silt is apparent near present lake level in the valley of Tsu Lake. Up to 15 metres and more of laminated silts are exposed in the lower valley of Trudel Creek (Fig. 10.1) which flows into Taltson River from the south along the Warren fault zone (Fig. 10.2, 10.7).

Silt samples collected from bluffs on Trudel Creek were examined by R.J. Mott of the Geological Survey of Canada and found to contain a mixture of pre-Pleistocene and late Pleistocene spores in a poor state of preservation. This finding suggests either that the material collected was eroded from two separate older sedimentary sources, reworked and deposited in recent times; or that the material collected was deposited in late Pleistocene time, and the pre-Pleistocene sediments as well as contemporary late Pleistocene vegetation contributed the spores. The absence of more recent spores in the silts favours but does not prove the latter hypothesis.

General Geology

Massive Archean Granitic Rocks (unit 1)

The oldest rocks in the area are massive, mostly leucocratic, pink to white rocks of granodioritic to quartz monzonitic composition. In places these have been intruded by more mafic bodies that have subsequently been sheared and broken, and now form inclusion trains. More rarely inclusions of metasedimentary rocks are present.

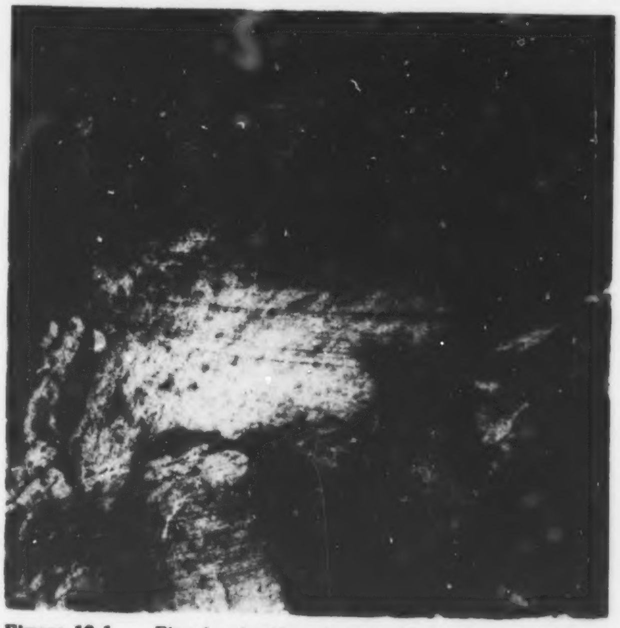

Figure 10.1. *Fine laminations in late Pleistocene silt bluffs along Warren Fault south of Taltson River.*

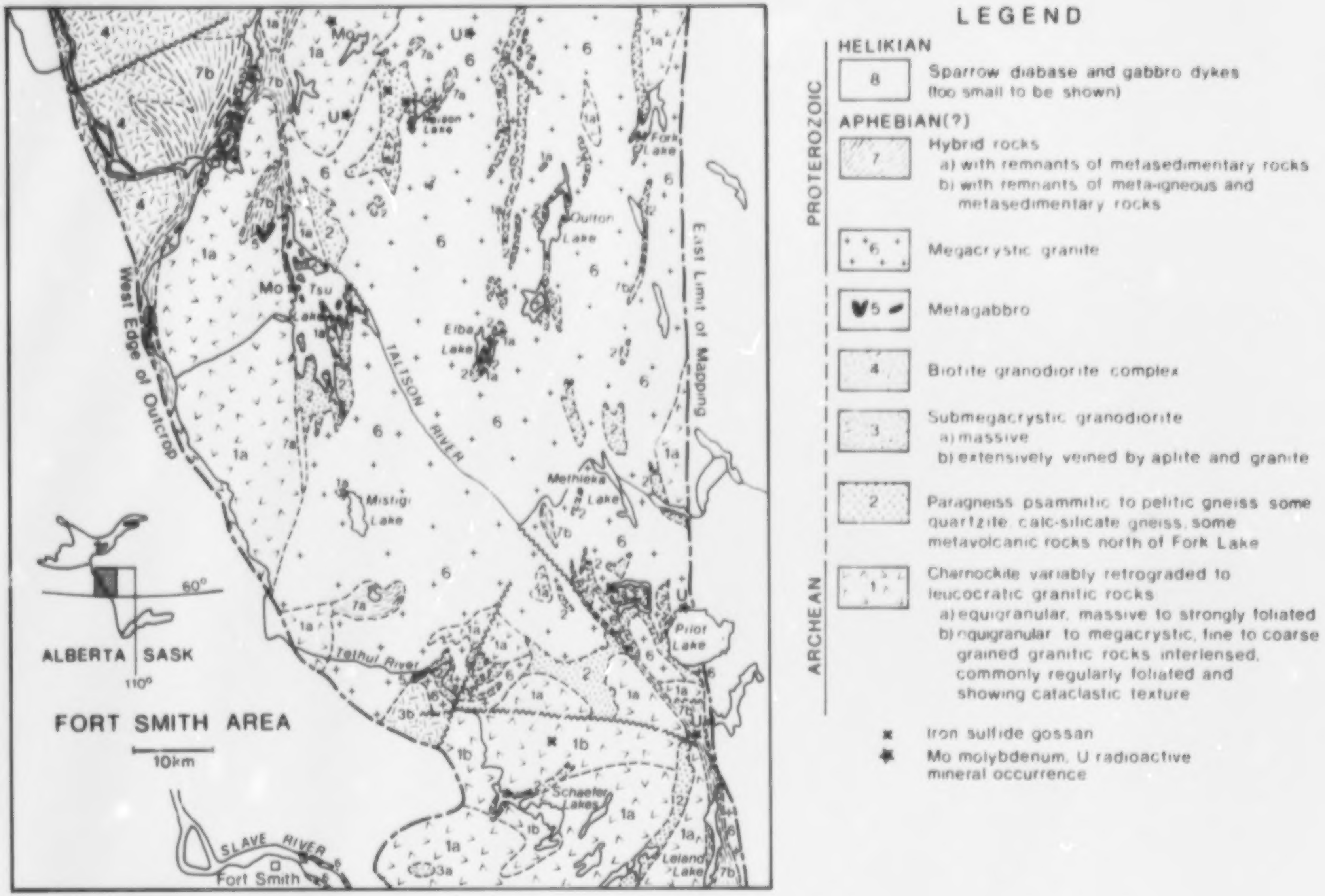
FORT SMITH AREA
10km
ALBERTA
SASK
60°
110°
West Edge of Outcrop
East Limit of Mapping
TALTSON RIVER
SLAVE RIVER
Fort Smith
Tethul River
Pilot Lake
Fork Lake
Oulton Lake
Elba Lake
Methleka Lake
Mistigi Lake
Schaefer Lakes
Leland Lake
Tsu Lake
Mo
U
LEGEND
PROTEROZOIC
HELIKIAN
8 Sparrow diabase and gabbro dykes (too small to be shown)
APHEBIAN(?)
7 Hybrid rocks
a) with remnants of metasedimentary rocks
b) with remnants of meta-igneous and metasedimentary rocks
6 Megacrystic granite
5 Metagabbro
4 Biotite granodiorite complex
3 Submegacrystic granodiorite
a) massive
b) extensively veined by aplite and granite
2 Paragneiss psammitic to pelitic gneiss some quartzite, calc-silicate gneiss, some metavolcanic rocks north of Fork Lake
ARCHEAN
1 Charnockite variably retrograded to leucocratic granitic rocks
a) equigranular, massive to strongly foliated
b) equigranular to megacrystic, fine to coarse grained granitic rocks interlensed, commonly regularly foliated and showing cataclastic texture
Iron sulfide gossan
Mo molybdenum, U radioactive mineral occurrence

Figure 10.2. *Geological map of Fort Smith area.*

Table of Formations

Provisional Table of Formations

Age		
Phanerozoic	Pleistocene and Recent deposits	
	unconformity	
Helikian	Sparrow basic dykes (8)	
	intrusive contact	
Proterozoic	Present Map-area	Eastern Ft Smith sheet
		Nonacho Group
	Hybrid gneiss	
	Metamorphic contact	Unconformity inferred
		Megacrystic granite (6)
	Megacrystic granite (6)	intrusive contact
		Hill Island Lake sediments
	intrusive contact	
	Metagabbro (5)	unconformity inferred
	relations unknown	
	Granodiorite Complexes (3)&(4)	
	relations unknown	
	Tsu Lake gneiss (2)	
	unconformity inferred	
Archean	Archean leucocratic granitic basement (1)	

In the north, east of Deskenetlata Lake, these granitic rocks commonly contain a few per cent of garnet and chloritized hypersthene. Rarely, irregular areas of olive green charnockitic gneiss up to several metres across, in which garnet and hypersthene are little altered, are present within the more normal pink to white granite. Farther south, first hypersthene and then garnet become completely altered to chlorite and the granite is locally hematite stained.

Hypersthene and garnet remnants are also present in the granitic rocks near Schaefer Lakes but there, unlike the Archean basement farther north, the rocks are typically foliated with moderate northward dips (Fig. 10.3). Potash metasomatism is suggested by the occurrence of lenses of granitic rocks containing submegacrystic to megacrystic potash feldspar.

These granitic rocks are thought to be Archean because they resemble and lie on strike with granitic rocks (Slave Granite) considered by Godfrey and Langenberg (1978), on the basis of zircon dating by Baadsgaard and Godfrey (1967, 1972) to be of Archean age. In the present map area many of the contacts are mylonitized, but in places bands or lenses of Tsu Lake gneiss are interlayered with equigranular to submegacrystic granite along the contact with Archean basement. Within the Tsu Lake gneiss, small bodies of similar granite are intrusive into the gneiss. These granitic bodies are thought to have formed from the Tsu Lake gneiss by partial melting during late or post Archean high grade metamorphism, and therefore do not indicate that the Tsu Lake gneiss forms remnants of an earlier Archean crust that has been engulfed in Archean basement granite.

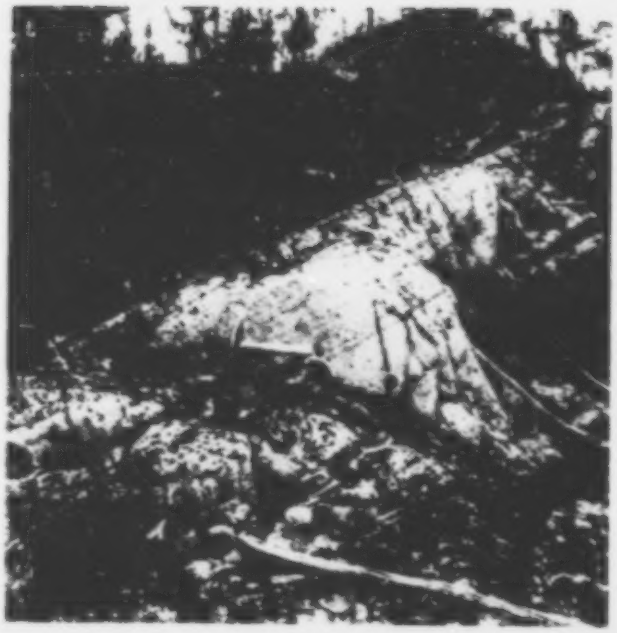

Figure 10.3. *Archean granitic rocks with well developed foliation showing gentle northwest dip (northeast of Schaefer Lakes).*

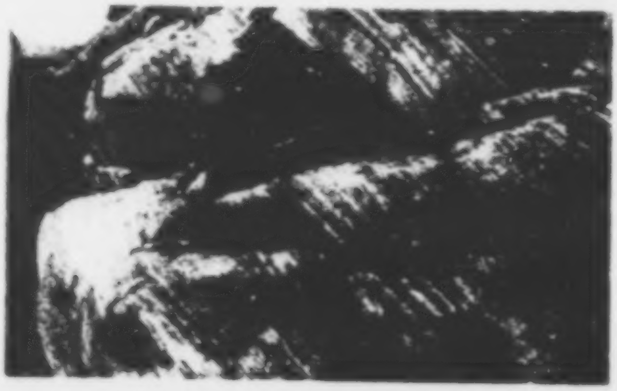

Figure 10.4. *Graded beds in Tsu Lake gneiss north of Pilot Lake seen from the south. Grey quartz-rich bottoms grade up into whiter, more feldspathic tops. (Knife is 7 cm long.)*

Tsu Lake Gneiss (unit 2)

Tsu Lake gneiss occurs as isolated large remnants mostly at the margins of the Archean massive granitic rocks, and as abundant inclusions within a younger megacrystic granite. Tsu Lake gneiss consists predominantly of biotite-quartz-feldspar gneiss, but includes some quartzite, pelite, and minor calc-silicate and volcanic rocks. Mostly the metasediments are severely deformed, but in places, as near Methleka Lake, graded bedding is evident and it seems likely that much of the original sedimentary succession were turbidites (Fig. 10.4).

Recognizable volcanic rocks are rare but amphibolites containing a few lensoid structures resembling pillows, and scattered breccia fragments occur within laminated, quartz-rich gneisses north of Fork Lake (Fig. 10.5).

These rocks are interpreted as mafic pillow breccias and comprise several units of about 10 m thickness over an interval of some 100 m. Farther south along strike sheared mafic gneisses may be of similar origin.

Garnet, cordierite, and sillimanite, which are recognizable in hand specimen within the Tsu Lake gneiss at scattered localities over much of the Fort Smith sheet, indicate that the rocks have reached at least middle amphibolite facies. Preliminary thin section study of gneiss included within a younger megacrystic granite indicates the presence of andalusite-cordierite-orthoclase in pelitic bands and of hypersthene in basic bands. These assemblages may reflect very high temperature, low pressure metamorphic conditions (see petrographic grid of Winkler, 1979), or they may reflect a combination of Archean granulite facies metamorphism with a presumably Hudsonian prograde overprint that was very dry. In either case the local presence of late sillimanite indicates that the field of andalusite was locally exceeded in the latest high grade metamorphism.

The age of the Tsu Lake gneiss is not well known. It may be either Archean in age and therefore probably part of the Archean basement, or of early Aphebian age, in which case it likely lies unconformably upon Archean basement. The reasons for this uncertainty will become clearer after description of the younger megacrystic granitic rocks.

***Figure 10.5.** Heterogeneous amphibolite (pillow breccia) forming part of a 10 m thick layer within Tsu Lake gneiss north of Fork Lake. Scattered blocks and pillow-like forms composed of amphibolite occur in a compositionally variable mafic matrix unlike more homogeneous amphibolites typical of many metamorphic terranes. Such amphibolite was likely derived from an isolated pillow breccia or mafic volcanic debris flow and provides the best evidence for basic volcanism within the Tsu Lake gneiss.*

Submegacrystic Granodiorite (unit 3)

Submegacrystic biotite-chlorite granodiorite with potash feldspar megacrysts up to 1.5 cm in length occurs as two bodies east and northeast of Fort Smith. The smaller southern body (unit 3a) is not well known but is partly equigranular, dioritic and contains some hornblende. The northern body (unit 3b) is extensively veined by fine- to medium-grained leucocratic granite. It appears to be overlain by a sheet of megacrystic granite but its age relations with other rocks in the area are unknown.

Biotite-Granodiorite Complex (unit 4)

A large area of medium grained heterogeneous granodioritic rocks varying from quartz monzonite to diorite and intruded by small aplitic to granitic masses is exposed west of Deskenetlata Lake. The earlier phases (exclusive of the aplite and granite) commonly contain large poikilitic biotite patches. Along the eastern margin of the complex northwesterly trending amphibolite dykes are present locally and massive to gneissic or foliated dioritic inclusions appear in patches. These features mark the transition to hybrid rocks (unit 7b).

Parts of the western granodiorite complex (unit 4) resemble the smaller bodies of veined granodiorite near Fort Smith (unit 3). It is possible therefore that all are related in origin.

Metagabbro (unit 5)

Small bodies of metagabbro occur locally within the western and southern parts of the area mapped. The largest of these, up to 2000 m wide, is west of Tsu Lake. The metagabbro is medium grained, granular, slightly foliated and lineated, with variable proportions of plagioclase, hornblende, and orthopyroxene. Biotite is present in peripheral parts of the intrusion, and small masses of granitic rocks intrude it locally. The disposition of the metagabbro within the Archean basement suggests that it was originally emplaced within that basement but has been folded and metamorphosed with the basement. Its relationship to the Tsu Lake gneiss (unit 2) and to the nongranitic components of hybrid rocks (unit 7) are not well established. Inasmuch as the metagabbro has clearly undergone high grade metamorphism it is possible that it may be of Archean or Proterozoic age, and either younger or older than the granodiorite bodies (units 3 and 4).

Megacrystic Granite (unit 6)

A megacrystic granite batholith containing widely scattered remnants of Tsu Lake gneiss extends from north to south across the eastern two thirds of the area mapped. The known part of the batholith is up to 50 km wide.

The granite is characterized by pink to grey potash feldspar megacrysts, commonly 2 cm but locally as much as 4 cm in length. These are in places subhedral to euhedral in form but commonly are more or less granulated and strained along their margins. The matrix is medium grained and consists typically of feldspar, quartz, chlorite and commonly a finer grained serpentine-like mineral possibly derived from alteration of hypersthene. Garnet is common locally, and more rarely hypersthene, surrounded by chlorite, is evident. In places the rock is intensely deformed with quartz ribbons wrapped about potash feldspar augen. Elsewhere megacrysts have been broken along cleavage planes.

In eight thin sections examined, quartz and potash feldspar are invariably present, the latter being abundantly perthitic to mesoperthitic. Discrete plagioclase grains are present locally, but plagioclase is most common as small peripheral grains or within areas of mortar texture.

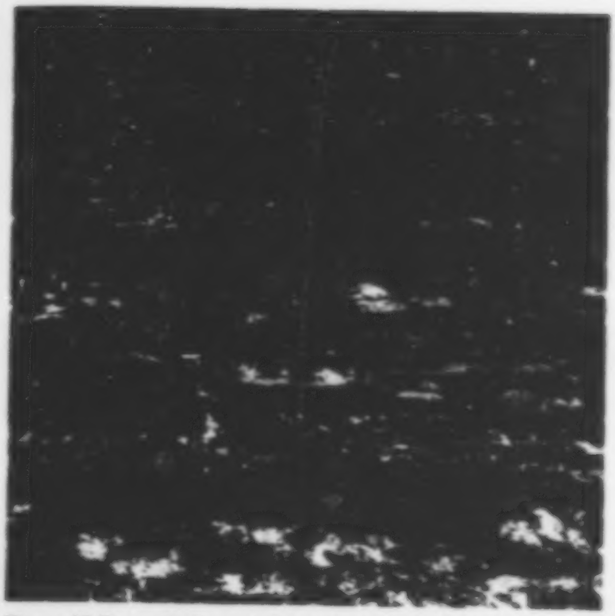

Figure 10.6a. Mafic and felsic bands in hybrid gneiss east of Deskenetlata Lake near the contact with Archean basement where the rocks are relatively little sheared.

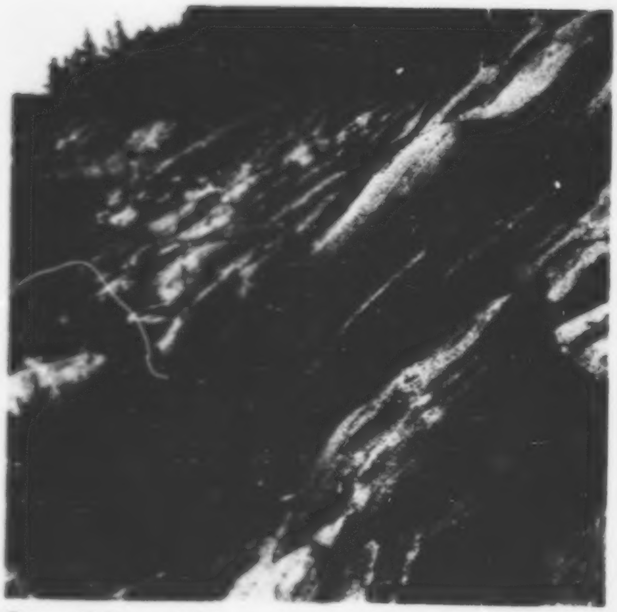

Figure 10.6b. Mafic gneiss at the east shore of Deskenetlata about 300 m east of Figure 10.6a. Shearing within the gneiss has increased toward the lake and may have obscured original banding in the rocks.

Myrmekite is common. Mafic minerals are mostly altered to masses of fine grained chlorite and serpentine but remnants of pleochroic hypersthene can be seen in some specimens. Locally green spinel, monazite, zircon, apatite, and ilmenite can be recognized. Where present, spinel is commonly associated with colourless corundum (identified by electron probe). In one section spinel, rimmed by corundum, has subsequently been partially rimmed by andalusite.

Contacts between Archean granitic rocks (unit 1) and megacrystic granite (unit 6) are commonly mylonitized. Locally, gradational contacts suggest potash metasomatism of Archean basement. Equigranular granitic masses are included within the megacrystic granite and rarely megacrystic dykes can be seen to intrude the Archean basement. A small metagabbro mass west of Leland Lake, and many remnants of Tsu Lake gneiss are included within the megacrystic granite which is therefore younger than all of these rocks.

Emplacement of the megacrystic granite is thought most likely to have occurred early during the Hudsonian orogeny about 1965 Ma, based on a preliminary (2 point) concordia plot for zircon from the small granite pluton at Thekulthili Lake described by Bostock (1980). This small pluton is coarse grained with potash feldspar more abundant that plagioclase. It shows high K, Th, and U airborne radiometric anomalies (Charboneau, 1980) like the megacrystic batholith and unlike other known plutonic rocks within the Fort Smith map area. Unlike the batholith, however, mafics are chlorite and magnetite with rare garnet and no hypersthene. Potash feldspar megacrysts up to 4 cm long are present rarely but are not obvious because of the abundance of coarse grained potash feldspar throughout the rock. The similarities between the two granite plutons suggest that the small eastern body is a stock-like offshoot from the main body, that crystallized in a colder wetter environment than did the main batholith.

Hybrid Rocks (unit 7)

Hybrid gneisses are of two types: (a) granitic rocks with remnants of Tsu Lake gneiss; and (b) granitic rocks with remnants of basic rocks and some metasediments. The granitic phase of the hybrid rocks may be either equigranular or megacrystic, and may be derived from local partial melting of the enclosing rocks, from partial melting with potash metasomatism, or from emplacement of an independent granitic phase. Hybrid rocks (unit 7a) are most extensively exposed in a window through the megacrystic granite south of Mistigi Lake. There they occur as intermixed rusty, equigranular, biotite granite, and Tsu Lake gneiss.

Hybrid rocks (unit 7b) east of Deskenetlata Lake consist of a mixture of hornblende-biotite gneiss and biotite gneiss containing irregular to sill-like granitic bodies. West of the lake hybrid rocks comprise a granitic phase with variable proportions of inclusions that are mostly massive to banded dioritic rocks but include amphibolite and locally quartz-rich metasediments. Near the lake some of the hybrid gneiss appears to have been homogenized by shearing (see Fig. 10.6a, b).

Diabase (Sparrow) Dykes (unit 8)

All the major rock units exposed in the northern half of the area mapped are cut by west-northwest trending diabase dykes of the Sparrow dyke swarm. These dykes intrude the Nonacho Group as well and have been dated at about 1700 Ma by McGlynn et al. (1974). Most of the dykes are thin being a metre or less thick, but some are up to 4 m thick. In places the dykes are fractured, or sheared along their margins but many appear to be little altered. Irregular bodies of gabbro with chilled margins and showing only local chloritization, intrude the gneisses at Tsu Lake, and because of their similarity in degree of alteration they are thought to be of the same age as the Sparrow dykes. The gabbro bodies, and small, associated, felsite-bearing breccia dykes, have been described in more detail by Bostock (1980).

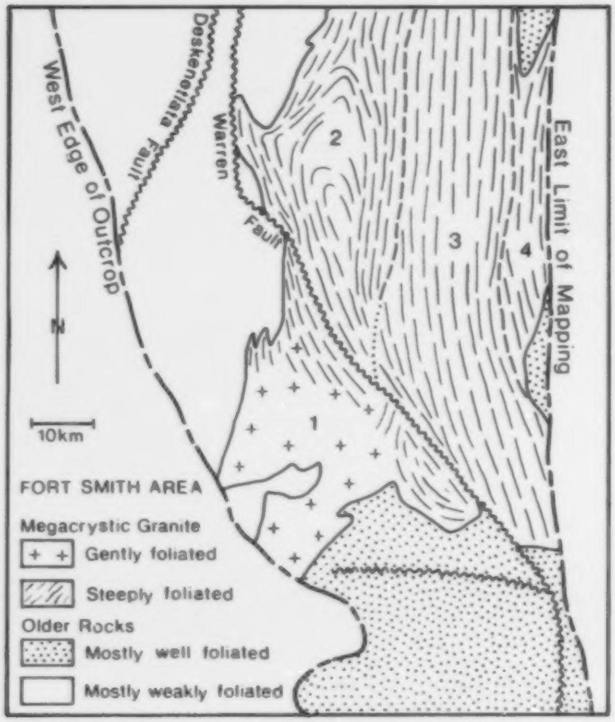

Sketch showing zonal subdivision of the Megacrystic Granite Batholith:

1) Sheeted zone
2) Collapsed head
3) Root zone
4) Constricted eastern margin

Figure 10.7. *Sketch showing the zonal subdivision of the megacrystic granite.*

Structural Geology

The area mapped can be conveniently divided into three structural domains with different ages:

1. The domain of Archean plutonic rocks which likely form a basement to the Tsu Lake gneiss;
2. The domain of the northwestern granodiorite complex and hybrid rocks west of Deskenetlata Lake;
3. The megacrystic granite batholith of likely Hudsonian age.

Events associated with the emplacement of the very large younger granite have left an imprint on the surrounding older domains.

Archean Gneiss Domain

Archean plutonic rocks, though commonly little foliated, contain scattered, elongate, mostly mafic inclusions and zones of foliation that trend generally northward throughout most of the area. Dips, where they can be measured, are moderate to steep. The main exception to this trend is found in the Archean gneisses about Schaefer Lakes where strongly foliated, moderately northwesterly dipping gneiss trends northeastward. Lenses and irregular bodies of foliated to massive, submegacrystic to megacrystic granite of widely varying size occur within these gneisses. Contacts may be sharp, commonly with cataclasis, or gradational.

Figure 10.8. *The southwest edge of a megacrystic granite sheet lying on top of gently dipping Tsu Lake gneiss. Tethul River is in foreground.*

These relations and the presence of the potash-rich megacrystic granite batholith to the northeast and east, suggest that foliation, cataclasis and potash metasomatism were related to the emplacement of this batholith, likely during the Hudsonian orogeny.

Northwestern Granodiorite Complex and Related Rocks

The northwestern granodiorite complex, together with hybrid rocks (unit 7b) west of Deskenetlata Lake, are separated from the rest of the map area by a shear zone (Deskenetlata Fault zone) that follows the valley of Deskenetlata Lake southwestward to Taltson River where it is covered by overburden of the Slave River valley. The western and northern parts of the complex are mostly unfoliated but the eastern and southern parts are characterized by more numerous mostly mafic inclusions that have been deformed with the enclosing rocks. Structures defined by these inclusions trend northeasterly near Deskenetlata Lake but swing to northwesterly farther west with dips in either direction. Locally in the central part of the complex these northwesterly trends appear on the map to be interrupted by restricted zones of presumably later, northeasterly trending foliation, but no age relations have been established between these trends. The age of, and structural relations between rocks east and west of Deskenetlata Lake are unknown.

Megacrystic Granitic Batholith

Preliminary analysis of foliation, lineation and distribution of zenoliths within the megacrystic granitic batholith suggest a division into four zones (Fig. 10.7). For convenience these are numbered one to four from the southwest to the northeast.

The southwestern zone (unit 1), lies to the southwest of the Warren Fault that extends from the south boundary of the map area at Leland Lake, through Taltson River and Tsu Lake, to the north boundary east of Deskenetlata Lake. The zone is broadly triangular, pinching northward about Tsu Lake and terminating in an irregular contact against older rocks in the south. It is characterized over much of its extent by an early, gently dipping to subhorizontal foliation. Mineral lineation, though present locally, is not well developed through most of the domain. About the western margins of the domain the megacrystic granite can be seen to form sheets as little as 10 m thick (Fig. 10.8) that lie mostly on Tsu Lake gneiss or nonmegacrystic granitic rock that contains remnants of Tsu Lake gneiss. Near the sharp bend in Tethul River north of Schaefer Lakes, two or more sheets of megacrystic granite appear to have been emplaced in succession. Extensive rafts of Tsu Lake gneiss, showing local westward verging, subhorizontal minor folds, were likely sheared off Archean basement to the northeast, and have been smeared out between the sheets. Elsewhere it is possible that the granitic sheets have merged or that only one sheet exists. Where Tsu Lake gneiss is extensively preserved, as in the large remnant north of Schaefer Lakes, the gneiss dips gently off the Archean granitic rocks to the south, and gently beneath the presumed Hudsonian megacrystic granitic rocks to the north. Within the zone, horst-like bodies of Archean granitic rocks project through the megacrystic granite at several places. North of Tethul River a prominent window to hybrid rocks (unit 7a) may represent the upper surface of the Archean basement from which the Tsu Lake gneiss has been largely scraped off during emplacement of the overlying megacrystic granite. Near Tsu Lake and along the northeast boundary of the zone, steeper dips are present suggesting that in these regions the granite may have undergone deformation subsequent to emplacement.

At Tsu Lake, at the north edge of domain one, the Tsu Lake gneiss shows tight, upright minor folds with parallel gently plunging axes and lineations unlike the gneiss to the south. The combination of steeply dipping foliation in the granite with thickening of the gneiss at Tsu Lake due to folding, suggests that the Tsu Lake gneiss has been ploughed up by granite advancing from the east and pinched against more competent Archean basement farther west.

Zone two lies northeast of the Warren Fault and extends from the contact with Archean granitic rocks and Tsu Lake gneiss on the west, to a prominent line of screens in the east. Foliation is moderate to steeply dipping with considerable variation in strike although there is a distinct northerly trend over all. The dome or fold-like structure shown in Figure 10.7 illustrates that there is a zone of complexity in this region but the data collected are not sufficient to define a major fold structure. Lineations of quartz and feldspar trend north or south with a gentle plunge and are commonly well developed. Zenoliths are entirely of Tsu Lake gneiss and appear to be more common than in domain one to the southwest.

West of Nelson Lake an extensive remnant of Tsu Lake gneiss is included within the megacrystic granite. This remnant is steeply dipping along its western margin but in its central and eastern parts it appears to be a gently east dipping sheet-like body. In its southern part, cuesta-like remnants of an overlying megacrystic granite mass are evident.

Zone three lies to the east of zone two and is demarcated by two prominent zones of screens composed chiefly of Tsu Lake gneiss but with some older nonmegacrystic granitic rock associated. At the west border of the zone these screens generally dip steeply to the east but foliation decreases to 45° and less in the south where the screens end before reaching the Taltson River. Along screens at the east margin of zone three, foliation generally dips 70° or more, either to the east or west but appears to be predominantly west dipping. Foliation and lineation within this zone appear to have similar attitudes to those in zone two to the west, but zenoliths and larger remnants of Tsu Lake gneiss and some of older granite appear to be more abundant.

Zone four lies to the east of zone three and has not been completely mapped. Contacts between megacrystic granite and older granite to the east are commonly gradational and large areas of granite appear to be submegacrystic. Foliation is northward trending and dips mostly steeply to the west; lineations of quartz and feldspar trend northerly and plunge either gently north or south. Locally, northeast of Methleka Lake, both foliation and lineation appear to cross the contact between megacrystic and older granites without deflection.

Faults

Two fault zones of regional significance within the area mapped, are the Warren and Deskenetlata fault zones. A third north-south zone of major faulting suggested by north-south lineaments visible on air photographs may lie just to the east of the area mapped to date. Other faults of local significance are most numerous within the megacrystic granite where they are commonly associated with mylonite zones.

The Warren Fault Zone This fault extends from the south margin of the map area at Leland Lake to the north margin just east of Deskenetlata Lake. South of the map area it continues into Alberta where it eventually passes beneath the Slave River flood plain (Godfrey and Langenberg, 1978). In places, as along the valley of Taltson River, the fault appears to be marked by a single lineament, but elsewhere, as south of Pilot Lake, it is marked by a zone of intensely sheared rocks several kilometres wide. At the ends of these wider zones, shearing appears to splay into the megacrystic granite to the northeast but is less well developed in rocks to the west. Schist, phyllonite, mylonite, ultramylonite, breccia and quartz stockworks together with greenschist retrogression are characteristic of different parts of the fault zone. A spectacular lavender coloured mylonite is exposed where the fault reaches the east shore of Tsu Lake.

Movement along the Warren fault zone was probably predominantly vertical because over its course from Slave River in Alberta to Taltson River it bends through 90°. On the other hand, southeast of Pilot Lake where the main fault changes direction most sharply, splays extending northward into the megacrystic granite probably indicate some horizontal movement on parts of the fault as well.

The Deskenetlata Fault Zone The Deskenetlata Lake fault zone strikes north-northeasterly along the valley of Deskenetlata Lake. It separates the Northwestern Granodiorite Complex and hybrid rocks (unit 7b), from Archean granitic basement on the east. As Deskenetlata Lake is approached from either side, mafic bands and inclusions become progressively more sheared until on the lake shore the rocks are deformed in places into schist and flaser gneiss cut locally by mylonite zones (Fig. 10.6a, b, 10.9).

In places, particularly along the central west shore, bands of sheared metasediment including quartz-rich gneiss similar to the Tsu Lake gneiss are present. Locally there are early isoclinal minor folds of gentle plunge with axial planes parallel foliation, but more commonly open, moderately to steeply plunging drags are evident that suggest dextral movement on the west side of the lake and sinstral movement on the east. This implies either that a central block of gneiss has been squeezed out southward along the fault zone, or that fault movement took place at different times in different directions on either side of the lake.

Faults at the East Margin of the Area Mapped Mylonites appear to be associated with a series of prominent north-south lineaments that lie near the margin of the megacrystic granite where it merges with Archean basement just to the east of the area mapped. One of these zones near the east end of Methleka Lake is characterized by about 13 m of greenschist facies retrogression along its east margin. This may reflect access of surface waters to the eastern block during faulting that raised the western block with respect to the east.

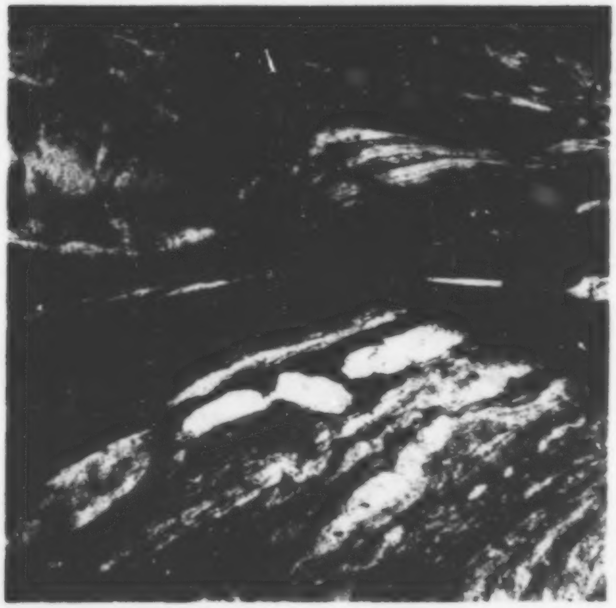

Figure 10.9. *A mylonite zone about 0.5 m thick within flaser gneiss on the west shore of Deskenetlata Lake.*

Local Faults Mylonite zones from a few centimetres to 100 m or more across, are common within the megacrystic granite and along its western borders. They consist of a central zone of pink to grey mylonite, or less commonly, of white ultramylonite surrounded by substantially greater thicknesses of protomylonite or strongly foliated rocks. In many places the mylonites bear small fragments or ovoids of potash feldspar and more rarely scattered unaltered garnets that contrast with chloritized garnet in the adjacent rocks. In places it is clear that these zones are superimposed upon an earlier foliation in the granite.

More rarely mylonite has been observed in direct contact with granite without either brecciation or development of intervening foliation in the granite. Such contacts could develop either by intrusion of granite parallel to an earlier mylonite zone, or perhaps less likely by faulting of fully competent granite. The variety of intra-granite mylonite contacts may indicate that the mylonites developed in the granite as it was cooling (becoming more competent), and that some granite may have still been liquid after the first mylonites formed.

Interpretation

The megacrystic batholith has been divided into four zones with a north-south elongation (Fig. 10.7). The third zone from the west is demarcated by two zones of screens, the western set being easterly dipping and the eastern set being primarily steep to westward dipping. Within this zone are numerous zenoliths of Tsu Lake gneiss and some of Archean granitic basement. This zone therefore has some of the attributes of the root zone of a diapir or tadpole pluton of the type described by Hutchison (1970), Hamilton and Myers (1967). Zones one and two presumably represent the upper part of the diapir which, when it reached its level of gravitational equilibrium within the crust, spread laterally being driven by magma rising within the root. Zone four may represent a constricted zone along the east margin of the batholith that has been uplifted by intrusion and faulting.

East of the diapiric root zone, the megacrystic granite has gradational contacts with Archean basement due to potash metasomatism. Steeply dipping foliation involves both megacrystic granite and its wall rocks. Still farther east, in terrane that is only locally mapped (see Bostock, 1980), a zone of north-south faulting apparently separates basement (on the west) with a few high grade remnants of Tsu Lake gneiss, from basement (on the east) with abundant retrograded gneiss remnants. East of this zone of faulting, scattered fault bounded wedges of prograde greenschist facies siltstone are preserved, and one of these is intruded by a small unfoliated granite stock. This stock has the same chemical signature (U, Th, K) as the megacrystic batholith, but apparently lower temperature more hydrous mineralogy. The region east of the batholith thus appears to represent a higher crustal level than that to the west, and there is reason to believe that the part of the map area west of the presumed north-south fault zone has been uplifted. If this is true, then the equigranular (Archean) granite at the east margin of the batholith represents a section of the east contact of the batholith that has been raised from greater depth, and emplacement of the diapir has been constricted on its eastern side.

In zone one of the southwestern part of the map area, the megacrystic granite forms a thin tabular body with common gently dipping foliation, that is pierced by basement horsts. There is a suggestion that several successive sheets may have been emplaced from the northeast, plucking rafts of Tsu Lake gneiss from the surface of the Archean basement in the northeast, and smearing them out farther southwest, along their basal contacts with an overridden sheet below.

In zone two, northeast of the Warren Fault and west of the western screens, foliation in the megacrystic granite is moderately to steeply dipping, mostly northerly trending, and is accompanied by a common gentle plunging mineral lineation. The structure appears more complex than that in the other zones, but too little is known to make any detailed interpretation. West of Nelson Lake a large remnant of Tsu Lake gneiss is separated almost completely from Archean basement to the west by a belt of megacrystic granite. On its west margin dips within the remnant are steep but in the central and eastern parts gneissosity is mostly gently eastward dipping. Along the southeast margin of the remnant it is overlain by a second eastward dipping presumably sheet-like body of megacrystic granite. This disposition suggests that the megacrystic granite in zone two may also have been emplaced as a series of sheets from the east, but there, in contrast to zone one, there are no basement horsts, suggesting that the total thickness of megacrystic granite is greater. Continuing rise of magma in the root zone to the east accompanied by westward release of magma, may be responsible for folding of the sheets and extension reflected in development of the north-south lineations.

In the vicinity of Pilot Lake and farther south, the two western zones appear to pinch out, and the megacrystic granite becomes increasingly strongly foliated as indicated by the descriptions of Cape (1977 – Pilot Lake gneiss) and of Godfrey and Langenberg (1978 – Arch Lake granite). Immediately to the west of this area, the Archean basement juts eastward and itself becomes strongly foliated. Like the east margin of the intrusion northeast of Methleka Lake, it seems likely that in this region, intrusion of the megacrystic batholith was constricted during its emplacement.

The metamorphic effects on the country rocks resulting from the emplacement of the megacrystic granite batholith are of interest because of the primary hypersthene-mesoperthite-bearing mineral assemblages in the granite, and the abundant development of mylonites within the granite. Both of these features likely reflect unusually hot dry conditions of emplacement of the granite.

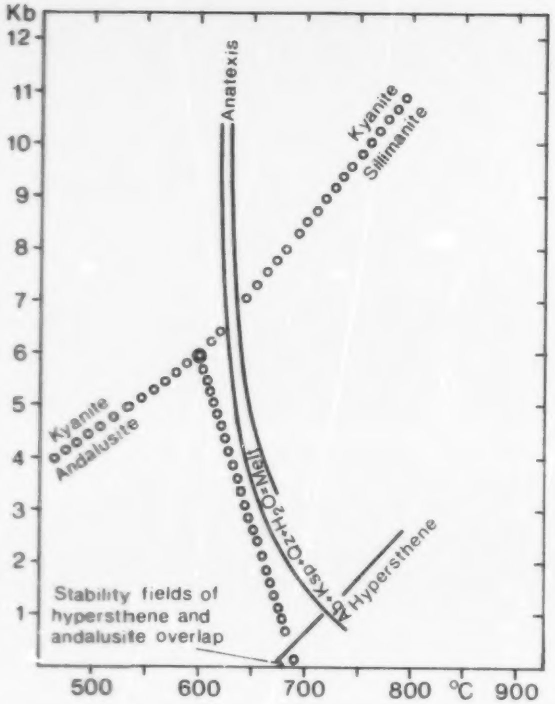

Figure 10.10. *Metamorphic grid (Winkler, 1979) illustrating the stability fields of the aluminosilicates and hypersthene, and showing a small field where both andalusite and hypersthene may be expected to form in rocks of appropriate composition.*

The history of metamorphism of the Tsu Lake gneiss, which occurs mostly as inclusions in the granite, is not fully understood because it is not certain whether the gneiss has undergone granulite facies metamorphism with the Archean basement prior to emplacement of the megacrystic granite, or whether its precursor was deposited after that metamorphism. Under granulite facies conditions, high temperature and pressure might be expected to produce sillimanite-cordierite-orthoclase-bearing assemblages in pelitic rocks with hypersthene in more mafic layers of the gneiss. The presence of andalusite is not expected because it is not stable at high pressures characterizing this metamorphic facies. The close association of andalusite-cordierite-orthoclase in the pelites with hypersthene-bearing granite, when examined in conjunction with the metamorphic grid (Winkler, 1979; see Fig. 10.10) suggests that exceptionally low pressure combined with high temperatures could satisfy the constraints implied by these assemblages. The conditions implied however are somewhat extreme. An alternative is suggested in the possibly complex metamorphic history of the Tsu Lake gneiss.

Archean granulite facies metamorphism would, it is assumed, have produced sillimanite-cordierite-orthoclase in the pelitic bands, and hypersthene in the more mafic bands of the Tsu Lake gneiss. Much of the water in the gneiss would have been driven out in the process. Prograde (Hudsonian?) metamorphism would initially convert sillimanite to andalusite, but cordierite would be converted to chlorite and orthoclase to muscovite only to the extent that water was available over and above that fixed in biotite. In rocks that were sufficiently dry, andalusite-cordierite-orthoclase could appear to be an equilibrium assemblage. When the upper limit of the andalusite stability field was reached, late sillimanite would form (as seems to have happened); however the persistence of andalusite as the principal aluminosilicate in most of the thin sections so far examined seems to suggest that the andalusite field was not far exceeded in this second (Hudsonian?) phase of metamorphism. This scenario requires that temperatures need only have risen to those characteristic of middle amphibolite facies (sillimanite-cordierite-muscovite) provided that the gneiss remained dry. Any pressure range in the andalusite stability field (moderately low pressure) would do. Thus it seems likely that the Tsu Lake gneiss was desicated by Archean granulite facies metamorphism before emplacement of the megacrystic granite. The granite itself must have been initially hot and dry to produce the hypersthene-mesoperthite assemblage, and have remained dry during its emplacement, in order to preserve the remnants of this assemblage.

During emplacement of the megacrystic granite under these hot, dry, moderately low pressure conditions it is likely that high temperature gradients obtained. Continued movement of magma from the root zone would have produced frequent disruptions of partly or newly congealed granite in the more remote parts of the intrusion. Conditions would have been ideal for development of local mylonite and zones of intense foliation. These were preserved from retrogressive recrystallization by the dry condition of the rocks.

Interpretation to date suggests that the megacrystic granite batholith, being unusually hot and dry, rose diapirically to a high level within the late Aphebian crust in the Fort Smith area. As emplacement continued, marginal rocks, presumably colder and of greater density, moved downward into the space vacated by the diapir forming marginal basins. In the west (zone 2) such a sag may have been filled by the westward spreading head of the diapir. In the east, in largely unmapped terrane beyond the zone of north-south faulting, there also appears to have been a basin at about this time in which siltstone and greywacke had been deposited. The southern extremity of mapped Nonacho conglomerate, showing provenance from the southwest, lies within this basin at Thekulthili Lake (northeast corner of the Fort Smith map area) where it is separated from the siltstone by a narrow basement horst. Is it possible that both the siltstone and Nonacho Group were deposited in the same eastern marginal basin in response to uplift over the rising megacrystic diapir to the west? Further mapping and radiometric age determinations will be directed towards solving this problem.

Economic Geology

Reconnaissance mapping of the Precambrian rocks of the northeast corner of the Little Buffalo River (85 A) and the west half of the Fort Smith (75 D) map areas has suggested three mineral deposit types of economic interest. These comprise:

1. Syngenetic sulphide occurrences associated with the Tsu Lake gneiss;
2. Small molybdenite occurrences associated with plagioclase-rich breccia and pegmatite;
3. Uranium occurrences associated with small pegmatite bodies, and with mafic lenses in megacrystic granite or in gneisses along its margins.

Sulphide Gossans Associated with the Tsu Lake Gneiss

Lenses of rusty gneiss, usually only a few centimetres thick, due to disseminated pyrite or pyrrhotite within the Tsu Lake gneiss, are widespread. More extensive rusty zones are present at the following U.T.M. co-ordinates:

Gossan No.	Zone 12 Easting	Zone 12 Northing
1.	460730	6753150
2.	463800	6751600
3.	463610	6748840
4.	489300	6689350
5.	482070	6669340

Three of these occurrences (no. 1, 2 and 3) are within the large remnant of Tsu Lake gneiss west of Nelson Lake. The gossan stained zones are 10 to over 100 m wide but since the gneisses are gently dipping the true thickness is unknown. No evidence of sulphide minerals other than pyrite or pyrrhotite was found but the concentration of three occurrences and the extensive nature of the gossans may warrant further prospecting.

At the northwest end of Piers Lake (about 10 km northwest of Pilot Lake) a prominent gossan (no. 4) was observed in quartz-rich gneiss at the margin of a large basement block.

North of Schaefer Lakes a gossan zone (no. 5) 8 m or more wide and 30 m long, open to the southwest, was found in a quartz-rich gneiss remnant within Archean submegacrystic granitic rocks. No evidence of sulphides other than pyrite or pyrrhotite was found.

Molybdenite

Two occurrences of molybdenite have been found within the map area. The most interesting of these comprises scattered, 15 mm patches of molybdenite in a plagioclase-rich breccia on the west shore of Tsu Lake described by Bostock (1980). The second smaller occurrence is near the northeast shore of a small lake about 12 kilometres northwest of Nelson Lake (zone 12, Easting 454350, Northing 6761800). There, centimetre-sized patches of molybdenite are disseminated locally in a pegmatite dyke 15 m long and 14 cm wide cutting a small garnet-bearing gneiss remnant within the Archean granite basement.

Uranium

Yellow stain, probably due to weathering of primary uranium minerals, occurs in small pegmatite patches within Archean granitic rocks (zone 12, Easting 456190, Northing 6749840) and in megacrystic granite west and northeast of Nelson Lake (zone 12, Easting 472290, Northing 6760820) respectively. A similar patch was observed in mylonite along the Warren fault zone (zone 12, Easting 499810, Northing 6669420). In each case the stain was confined to a single area of a few hundred square centimetres. None of these occurrences was prospected with a scintillometer.

Uranium is also concentrated in mafic bands within megacrystic granite on the north shore of Pilot Lake (zone 12, Easting 497610, Northing 6686660). There a trench up to 1.8 m deep has been excavated in granite. Scintillometer readings are over twice background along mafic schlieren up to one half metre thick. On a cliff face about 30 m farther north similar schlieren show higher readings. This and other uranium occurrences about Pilot Lake have been described in detail by Cape (1977).

References

Baadsgaard, H. and Godfrey, J.D.
1967: Geochemistry of the Canadian Shield in Northeastern Alberta: I Andrew Lake Area; Canadian Journal of Earth Sciences, v. 4, p. 541-563.

1972: Geochemistry of the Canadian Shield in Northeastern Alberta: II Charles-Andrew-Collin Lakes areas; Canadian Journal of Earth Sciences, v. 9, p. 863-881.

Bostock, H.H.
1980: Reconnaissance geology of the Fort Smith – Hill Island Lake area, Northwest Territories; in Current Research, Part A, Geological Survey of Canada, Paper 80-1A, p. 153-155.

Cape, D.F.
1977: An investigation of the radioactivity of the Pilot Lake area, N.W.T.; unpublished M.Sc. thesis, University of Alberta.

Charbonneau, B.W.
1980: The Fort Smith Radioactive Belt, Northwest Territories; in Current Research, Part C, Geological Survey of Canada, Paper 80-1C, p. 45-57.

Godfrey, J.D. and Langenberg, C.W.
1978: Metamorphism in the Canadian Shield of Northeastern Alberta; in Metamorphism in the Canadian Shield, Geological Survey of Canada, Paper 78-10, p. 129-138.

Hamilton, W. and Myers, W.B.
1967: The nature of batholiths; United States Geological Survey, Professional Paper 554-C, p. C1-C30.

Hutchison, W.W.
1970: Metamorphic framework and plutonic styles in the Prince Rupert region of the Central Coast Mountains, British Columbia; Canadian Journal of Earth Sciences, v. 7, p. 376-405.

McGlynn, J.C.
1971: Stratigraphy, sedimentology and correlation of the Nonacho Group, District of Mackenzie; in Report of Activities, Part A, Geological Survey of Canada, Paper 71-1A, p. 140-142.

McGlynn, J.C., Hanson, G.N., Irvine, E., and Park, J.K.
1974: Paleomagnetism and age of Nonacho Group Sandstones and Associated Sparrow Dykes, District of Mackenzie; Canadian Journal of Earth Sciences, v. 11, p. 30-42.

Winkler, H.G.F.
1979: Petrogenesis of Metamorphic Rocks; Fifth Edition, Springer-Verlag, New York.

11.

GEOLOGY OF GRANT LAKE AND FOUR CORNERS LAKE MAP AREAS, WOPMAY OROGEN, DISTRICT OF MACKENZIE

E.M.R. Research Agreement 23233-0-0057

R.M. Easton[1]
Precambrian Geology Division

Easton, R.M., Geology of Grant Lake and Four Corners Lake map areas, Wopmay Orogen, District of Mackenzie; in *Current Research, Part B, Geological Survey of Canada, Paper 81-1B, p. 83-94, 1981.*

Abstract

Geological mapping was conducted at 1:50 000 scale in the Grant Lake and Four Corners Lake map areas which straddle Zone 3 and Zone 4 of Wopmay Orogen. The geology of both map areas is similar although the Four Corners map area is 100 km north of Grant Lake.

Two older rock sequences are present only in the Four Corners area. The oldest, the Sitiyok Igneous Complex, consists of tonalite gneiss intruded by granite, both of which are cut by basaltic dykes, now amphibolite. The Sitiyok Complex is rimmed by amphibolite and metapelite of the Ipiutak subgroup, the oldest unit of the Akaitcho Group. The Sitiyok Complex was present prior to metamorphism and deformation of the Akaitcho Group, and may represent basement to the group.

A sequence of finely interbedded metasiltstone and metapelite, overlain by a thin dolomite band which in turn is overlain by basic volcanic rocks with minor rhyolite comprises the Grant subgroup and is present in both map areas. The Grant subgroup is correlated with the Zephyr formation and Nasittok subgroup of the Akaitcho Group. Granite gneiss and amphibolitic gneiss of Hepburn and Wentzel batholiths have intruded and metamorphosed the Akaitcho Group.

Rocks of Zone 4 of Wopmay Orogen in both areas consist of little deformed sedimentary and volcanic rocks of the Dumas Group which have been intruded by high level granitoid plutons of Great Bear Batholith.

The westermost fault of a 10 to 20 km wide belt of north-south trending faults is the Zone 3-Zone 4 boundary, or 'Wopmay Fault'.

The Akaitcho Group forms a belt 30 to 50 km wide and at least 150 km long that has been little prospected for base metals although it is similar to formations hosting 'Sullivan or MacArthur Type' Ag-Pb-Zn sulphide deposits.

INTRODUCTION

The Akaitcho Group contains metasedimentary and metavolcanic rocks related to initial rifting of Wopmay Orogen (Hoffman et al., 1978; Hoffman, 1980b; Easton, 1980; in press). Rocks related to initial rifting of modern continental margins are usually covered by younger rocks; thus, the Akaitcho Group provides an opportunity for the study of the early stages of the development of a continental margin. In addition, the Akaitcho Group contains several large, little prospected belts of volcanic rocks (Fig. 11.1), and thus may have some economic potential. Until 1980, the Akaitcho Group had only been studied in northern Wopmay Orogen (N.T.S. 86J) (Easton, 1980). Nine weeks of the 1980 field season were spent mapping the Akaitcho Group at 1:50 000 scale in two areas south of N.T.S. 86J in order to better understand the stratigraphy of the Akaitcho Group.

The Grant Lake area (parts of 86C/15, C/16, F/1 and F/2) (Figure 11.1) was mapped previously (Lord, 1942; Lord and Parsons, 1954; McGlynn, 1964, 1974). Further investigation was warranted because the Grant Lake area contains one of the largest areas of low grade volcanic rocks in Zone 3 (Hepburn metamorphic-plutonic belt of Fraser et al., 1972) of Wopmay Orogen.

The Four Corners Lake area (part of 86F/16, G/13, J/4 and K/1) (Figure 11.1) has been mapped at various scales by several workers (86F: Lord and Parsons, 1954; McGlynn, 1974, 1975, 1976. 86J: Hoffman et al., 1980; Easton, 1980. 86K: Hoffman, 1978). The area was re-examined because previous work (Easton, 1980) indicated that possible basement rocks to the Akaitcho Group were present in the Four Corners Lake area.

REGIONAL GEOLOGY

The Akaitcho Group is located in the metamorphic and batholithic core zone (Zone 3 of Wopmay Orogen, Hoffman, 1980b) of Wopmay Orogen. The lowest unit of the Akaitcho Group consists of a basaltic sequence with interbedded pelitic and silty metasedimentary rocks (Ipiutak subgroup) and is overlain by 3 to 4 km of arkosic and subarkosic turbidites (Zephyr formation) intruded by rhyolite porphyry sills (Okrark sills). Basalt and rhyolite volcanic complexes of the Nasittok subgroup overlie the Zephyr formation. Volcaniclastic and pelitic metasedimentary rocks of the Aglerok formation interfinger with, and overlie the volcanic complexes. Locally, basaltic intrusive and extrusive rocks (Tallerk sills) are present in the upper part of the Aglerok formation. The Akaitcho Group is conformably overlain by pelitic rocks of the Odjick Formation of the Epworth Group (Easton, 1980).

The Akaitcho Group is intruded on the east by the Hepburn Batholith and on the west by the Wentzel Batholith (Fig. 11.1). Regional metamorphism of the Akaitcho Group is spatially related to the two batholiths and ranges from chlorite (lower greenschist) to above muscovite breakdown (upper amphibolite to granulite) (St-Onge and Carmichael, 1979; Hoffman et al., 1980). The Wentzel Batholith and the Akaitcho Group are separated from little deformed or metamorphosed sedimentary, volcanic and plutonic rocks of the Great Bear Volcano-Plutonic Belt (Zone 4 of Wopmay Orogen, Hoffman, 1980b) by the 'Wopmay Fault'. Sedimentary and volcanic rocks of Zone 4 adjacent to the 'Wopmay Fault' in northern Wopmay Orogen are assigned to the Dumas Group (Hoffman, 1978). Both the Grant and Four Corners Lake map areas straddle the 'Wopmay Fault'.

---

[1] Department of Geology, Memorial University of Newfoundland, St. John's, Newfoundland, A1B 2X5

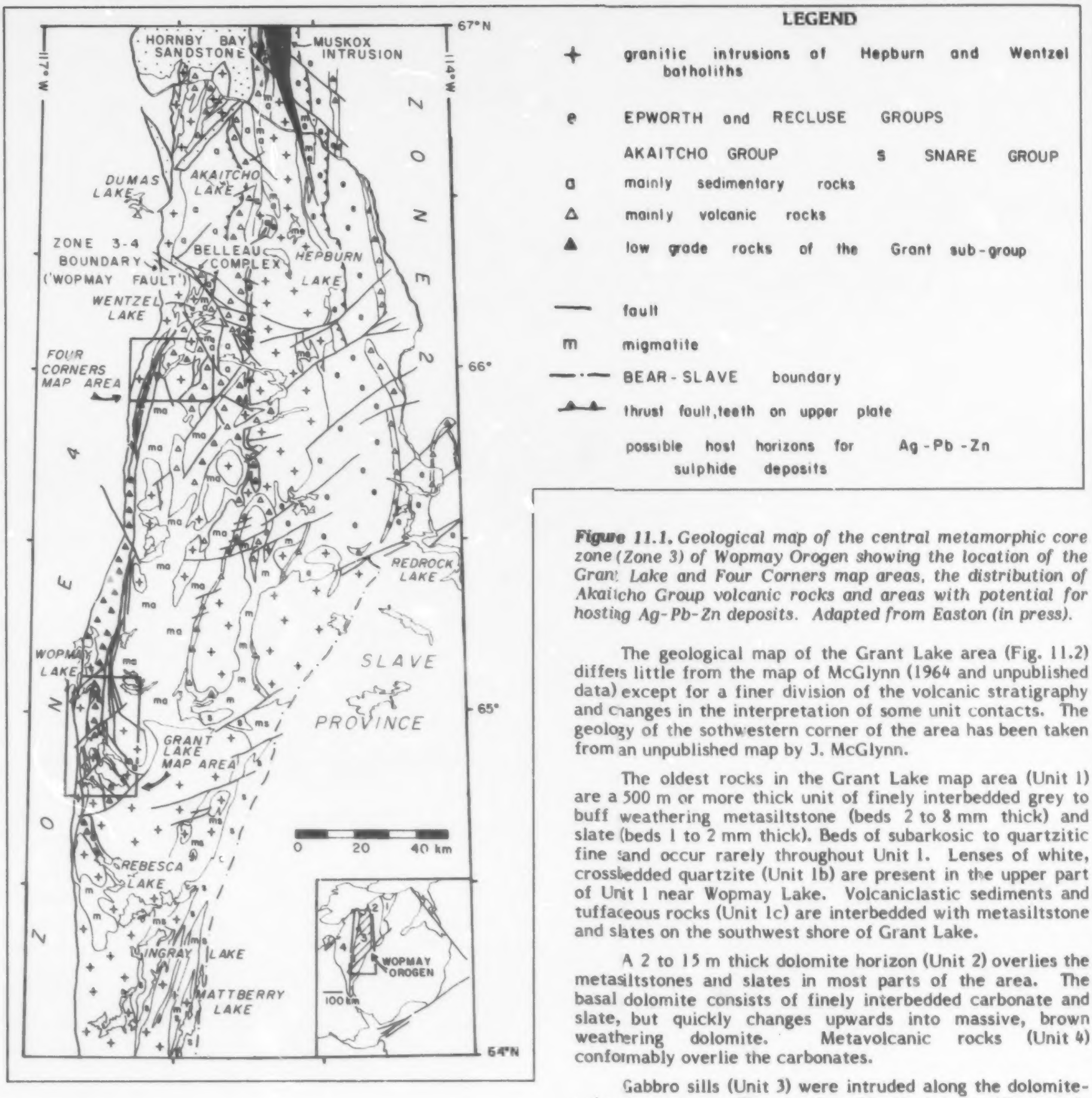
LEGEND
granitic intrusions of Hepburn and Wentzel batholiths
e EPWORTH and RECLUSE GROUPS
AKAITCHO GROUP
s SNARE GROUP
a mainly sedimentary rocks
△ mainly volcanic rocks
▲ low grade rocks of the Grant sub-group
fault
m migmatite
BEAR - SLAVE boundary
thrust fault, teeth on upper plate
possible host horizons for Ag - Pb - Zn sulphide deposits
HORNBY BAY SANDSTONE
MUSKOX INTRUSION
67°N
117°W
114°W
ZONE 3
ZONE 4
DUMAS LAKE
AKAITCHO LAKE
ZONE 3-4 BOUNDARY ('WOPMAY FAULT')
BELLEAU COMPLEX
HEPBURN LAKE
WENTZEL LAKE
FOUR CORNERS MAP AREA
66°
REDROCK LAKE
SLAVE PROVINCE
WOPMAY LAKE
65°
GRANT LAKE MAP AREA
0 20 40 km
REBESCA LAKE
INGRAY LAKE
MATTBERRY LAKE
WOPMAY OROGEN
100 km
64°N

Figure 11.1. *Geological map of the central metamorphic core zone (Zone 3) of Wopmay Orogen showing the location of the Grant Lake and Four Corners map areas, the distribution of Akaitcho Group volcanic rocks and areas with potential for hosting Ag-Pb-Zn deposits. Adapted from Easton (in press).*

The area south of 66°N and east of 116°W is poorly known, and the geology shown in Figure 11.1 for this area may be subject to error, particularly in N.T.S. 86G.

GRANT LAKE MAP AREA

The geology of the Grant Lake (Fig. 11.2) and the Four Corners (Fig. 11.3) areas is similar in terms of lithology, stratigraphy and structure. Separate legends have been given for both areas, but a correlation of lithologies between the areas is also shown. The metamorphism and structure for the Grant Lake and Four Corners areas are shown in Figures 11.4a and 11.4b respectively. Nomenclature of granitic rocks follows the recommendations of Streckeisen (1976).

The geological map of the Grant Lake area (Fig. 11.2) differs little from the map of McGlynn (1964 and unpublished data) except for a finer division of the volcanic stratigraphy and changes in the interpretation of some unit contacts. The geology of the sothwestern corner of the area has been taken from an unpublished map by J. McGlynn.

The oldest rocks in the Grant Lake map area (Unit 1) are a 500 m or more thick unit of finely interbedded grey to buff weathering metasiltstone (beds 2 to 8 mm thick) and slate (beds 1 to 2 mm thick). Beds of subarkosic to quartzitic fine sand occur rarely throughout Unit 1. Lenses of white, crossbedded quartzite (Unit 1b) are present in the upper part of Unit 1 near Wopmay Lake. Volcaniclastic sediments and tuffaceous rocks (Unit 1c) are interbedded with metasiltstone and slates on the southwest shore of Grant Lake.

A 2 to 15 m thick dolomite horizon (Unit 2) overlies the metasiltstones and slates in most parts of the area. The basal dolomite consists of finely interbedded carbonate and slate, but quickly changes upwards into massive, brown weathering dolomite. Metavolcanic rocks (Unit 4) conformably overlie the carbonates.

Gabbro sills (Unit 3) were intruded along the dolomite-volcanic contact. The stratigraphically lowest sills intrude the upper part of Unit 1 and are 3 to 6 m thick and fine grained. Sills within 50 to 100 m of the dolomite-volcanic contact are 30 to 50 m thick, coarse grained and form prominent ridges. Sills also intrude the lower part of the volcanic complex, but are only 5 to 6 m thick, fine grained and difficult to distinguish from massive basalt flows. The sills probably served as feeders for some of the mafic volcanic rocks (Unit 4).

The section of volcanic rocks exposed in the area is only 200 to 500 m thick. The basalt lavas (Unit 4a) are generally pillowed, relatively undeformed, and along the Wopmay River, have been well exposed by a recent forest fire burn. Two types of pillow lavas were observed. One type consists of pillows of equal size, 50 to 150 cm long. A second

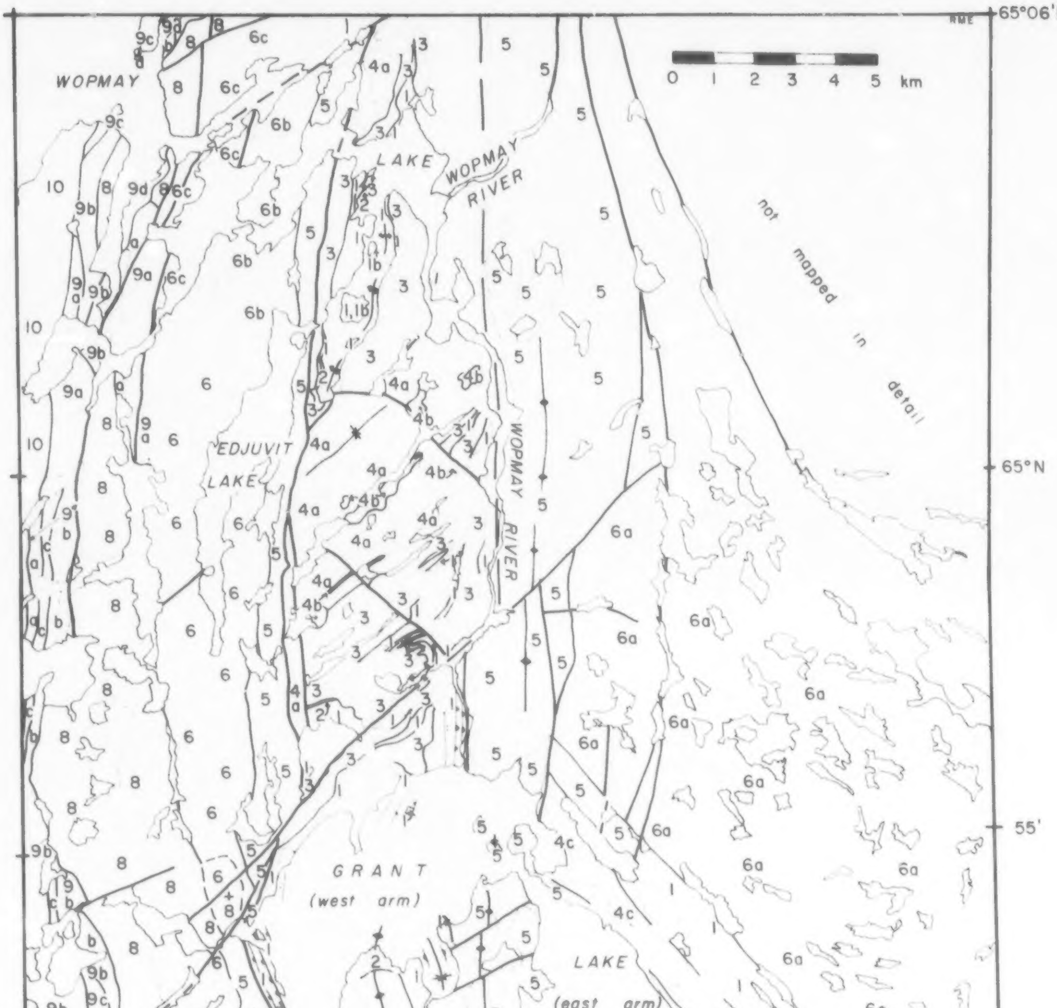
0 1 2 3 4 5 km
WOPMAY
LAKE
WOPMAY RIVER
EDJUVIT LAKE
WOPMAY RIVER
not mapped in detail
GRANT (west arm)
LAKE (east arm)
LITTLE CRAPEAU LAKE
WOPMAY RIVER
65°06'N
65°N
55'
50'
64°45'N
116°45'W
40'
35'
30'
25'
20'
116°15'W

Figure 11.2. *Geological map of the Grant Lake map area. Geology of the southwest corner of the area is taken from an unpublished map by J.C. McGlynn.*

LEGEND – FIGURES 11.2 AND 11.3

GRANT LAKE AREA

10 granite
9 DUMAS GROUP
a) dacite to rhyolite, b) argillite, c) basalt, d) carbonate
8 weakly sheared granite
7 muscovite-biotite leucogranite
6 amphibolite B-granite gneiss, b) migmatite phase,
c) granite rich phase
5 protomylonitic granite gneiss
AKAITCHO GROUP - Grant sub-group
4 volcanic rocks, a) pillowed and massive basalts,
b rhyolite, c amphibolite
3 gabbro sills
2 dolomite
1 siltstone and pelite, b) with quartzite lenses,
c) interbedded with volcaniclastic sediments

mylonite
trace of fold of bedding
trace of fold of foliation

METAMORPHIC ISOGRADS
(mark on high T side)

biotite
staurolite
andalusite
sillimanite
granite pods
muscovite breakdown
migmatite (over 30% granitic material)

FOUR CORNERS AREA

12 granites near faults, felsite dykes
11 a) 'younger granite', b) porphyritic syenogranite, c) Adam Lake granite
10 DUMAS GROUP
a) dacite to rhyolite, b) argillite, c) conglomerate, d) basalt, e) arkose,
f) carbonate, g) 'golf-ball' porphyry, h) mafic and felsic tuffs
interbedded with argillite
9 granodiorite with patches of syenogranite
WENTZEL BATHOLITH
8 amphibolitic B-granite gneiss
7 garnet granite
6 protomylonitic granite gneiss
AKAITCHO GROUP
Grant sub-group
5 a) siltstone and pelite, b) gabbro sills, c) basalt, d) conglomerate,
e) quartzite and siltstone
Ipiutak sub-group
4 a) pelite, b) arkose, c) amphibolite, d) basalt tuff, e) basalt flows,
f) quartzite, siltstone and pelite
SITIYOK COMPLEX
3 amphibolite dykes (cut 1 and 2)
2 pink protomylonitic B-granite (cuts 1)
1 grey tonalite gneiss

CORRESPONDENCE OF ROCK UNITS

GRANT LAKE AREA FOUR CORNERS AREA

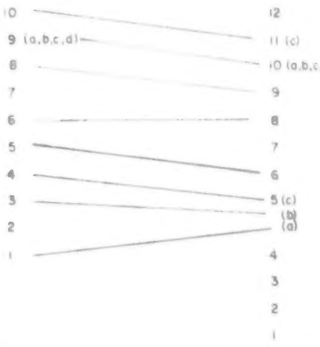

type consists of normal size pillows with a few, very large, tube-like, 2 to 4 m thick, 10 to 15 m long "megapillows", commonly with irregular outlines and many re-entrant pillow crusts. Many of the 10 to 20 m thick, massive flows have pillowed tops and bases which grade into a massive core. Re-entrant pillow crusts and incompletely formed pillows are present in the transition zone between the pillowed bases and massive cores of the flows. Thin (up to 1 m, rarely 2 to 3 m thick) beds of pillow breccia, monolithologic lapilli tuff, hyaloclastite and chert are common between basalt flows. Outcrop in the area was not adequate to determine the facies relations between the various flow types, but all the features described above have been reported from the Rouyn-Noranda area by Dimroth et al. (1978). By analogy with the work of Dimroth et al. (1978), it is concluded that the pillow lavas in the area had a relatively high magma supply rate, were fissure fed, and possibly were deposited on the slope of a shield volcano.

White weathering, aphanatic to quartz microporphyritic grey rhyolite is present between pillowed flows and as small isolated bodies (flows?) (Unit 4c).

Although units 1 to 4 outcrop over a large area, only 1 to 1.5 km of section is exposed. The name Grant subgroup is proposed for the distinctive stratigraphic sequence shown by units 1 to 4. Representative sections can be observed from 64°06'N to 64°58'N along 116°W; from 116°32'W to 116°34'W along 65°05'N; and from 64°47'N, 116°25'W to 64°46'M, 116°27'W. Correlations of the Grant subgroup are discussed later (see also Fig. 11.5)

White to grey weathering, locally orthoclase porphyroblastic, protomylonitic granite gneiss (Unit 5) resembles older phases of Hepburn Batholith (Hoffman et al., 1980). Metasedimentary and amphibolite enclaves are common throughout the gneiss, especially near contacts with the Grant subgroup. In many places, staurolite and andalusite grade metasediments are in fault contact with the gneiss. On the southeast shore of Grant Lake, high grade metamorphic rocks and some migmatite are present between low grade rocks and the gneiss (Fig. 11.2, 11.4a). The leucosome of the migmatite is compositionally and texturally similar to the gneiss. As in the Hepburn Lake map area (Hoffman et al., 1980), the granite gneisses are probably associated with the metamorphism observed in the Grant subgroup, although late faulting has removed many of the prograde metamorphic sequences.

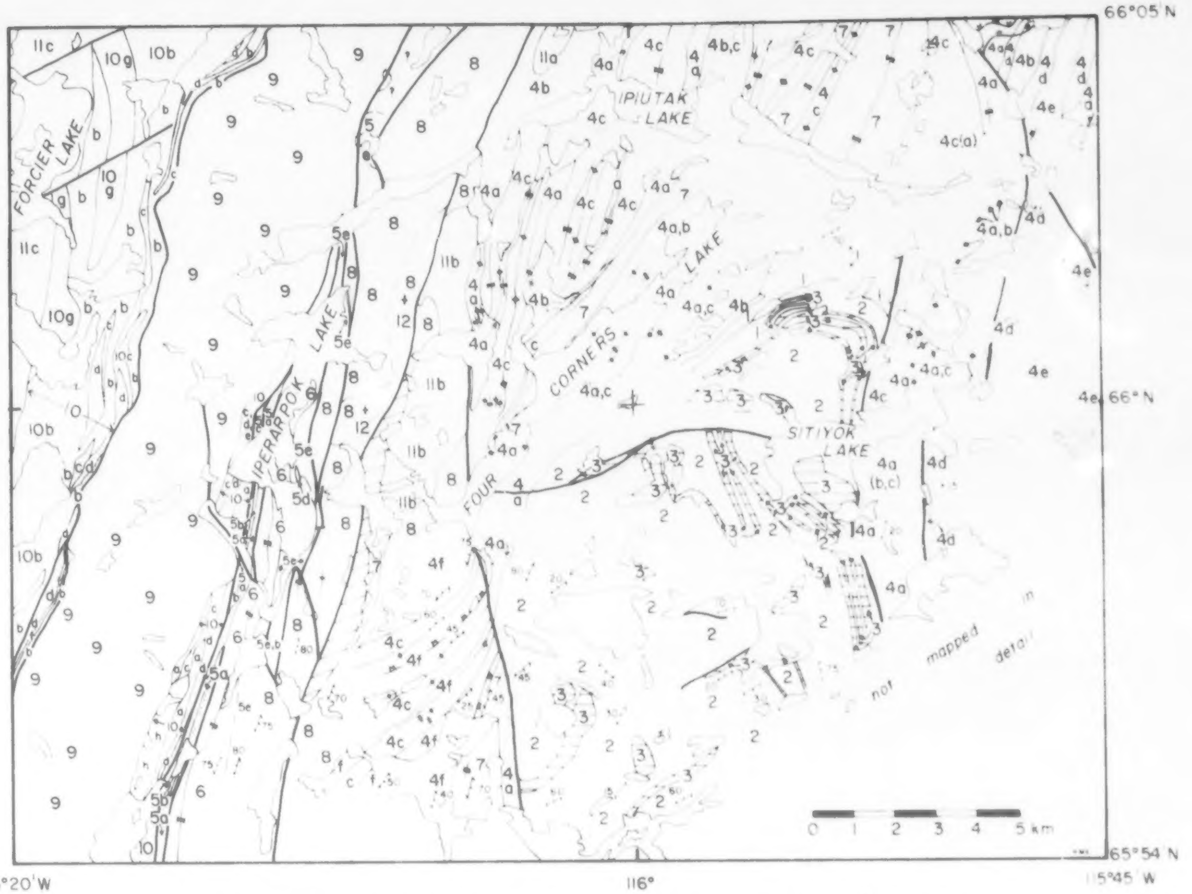

Figure 11.3. Geological map of the Four Corners map area. Geology of the Dumas Group rock rocks in 86K/1 is taken from Hoffman (1978).

Unit 6 is an intimate mixture, on all scales, of amphibolite and pink, protomylonitic, fine- to medium-grained biotite B-granite. Lithological variation on the outcrop scale is common in this unit, and ranges from granite to granite with pods and bands of amphibolite in sharp contact with the granite, to granite with amphibolite with diffuse contacts with the granite, and to diorite gneiss with millimetre scale bands of granitic and amphibolitic material. Where it is not faulted, the contact between Unit 5 and Unit 6 is sharp, but it could not be determined which unit was older, or if the contact was intrusive. Unit 6 is generally rimmed by the granite gneisses (Unit 5). McGlynn (1974) reported ash flow tuffs of the Dumas Group (Unit 9a) resting unconformably on granite (Unit 6c) on the shore of Wopmay Lake.

Generally unfoliated, muscovite-biotite-leucogranite (Unit 7) with 1 per cent pink, clear garnets intruded metasiltstones and slates (Unit 1) as a sill-like sheet below the level of the first gabbro sills. The leucogranite cuts across isograds in the metasiltstones, and cuts Unit 5 gneisses. The leucogranite is slightly foliated along its western contact adjacent to a north-south trending fault.

A coarse grained, pink to red weathering, porphyritic granite pluton with a well developed foliation along its margins (Unit 8) is present between the gneisses (Units 5 and 6) and the Dumas Group (Unit 9). The granite cuts the amphibolitic granite gneisses, but 5 km west of Grant Lake, it is cut by porphyritic basalt dykes (Dumas Group?) containing 50 to 60 cm diameter xenoliths of amphibolitic granite gneiss. The contact between Unit 8 and the Dumas Group is not well exposed, and the Dumas Group is highly altered and develops a prominent north-south cleavage adjacent to the granite contact. In places the contact is a fault. On the south shore of Wopmay Lake, carbonate (Unit 9d) of the Dumas Group rests unconformably on the granite. The granite is younger than the gneisses and supracrustal rocks of the Grant subgroup, and acted as a basement for some of the Dumas Group rocks (e.g. the mafic dykes and the carbonate), but it may not be much older than the Dumas Group.

The Dumas Group (Unit 9) contains red weathering, crystal rich, rhyodacite porphyry and ash flow tuff (Unit 9a), reddish brown and grey, finely laminated argillite with lenses of reddish arkose and conglomerate (Unit 9b) and pillowed and massive, pyroxene and plagiolase porphyritic, commonly amygdaloidal, slate blue to blue grey basalt flows (Unit 9c). At Wopmay Lake, white, massive carbonate, 10 to 15 m thick (Unit 9d) is present between the argillites and basalts. Significant lateral variation is common between units of the Dumas Group. The Dumas Group section at Grant Lake is similar to the section described in the southeast corner of the Sloan River map area (Hoffman and Bell, 1975). Units 9b, and 9c form a homotaxic sequence with units 1, 2 and 4 of the Grant subgroup, but the two groups can be readily distinguished in the field. In particular, the Dumas Group does not contain the distinctive gabbros present in the Grant

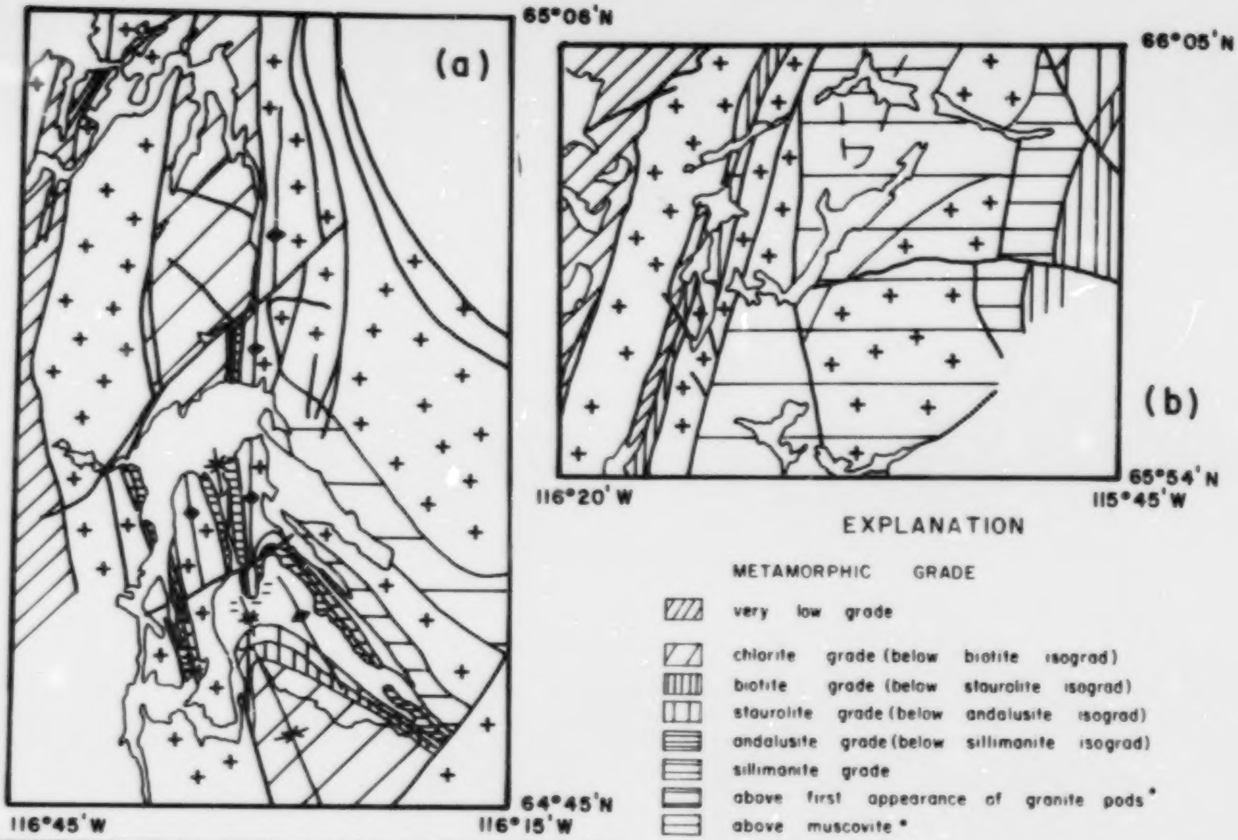

Figure 11.4(a) *Metamorphic grade and distribution of granitoid rocks in the Grant Lake map area.*

(b) *Metamorphic grade and distribution of granitoid rocks in the Four Corners map area.*

EXPLANATION

METAMORPHIC GRADE

▨ very low grade

▨ chlorite grade (below biotite isograd)

▥ biotite grade (below staurolite isograd)

▥ staurolite grade (below andalusite isograd)

▤ andalusite grade (below sillimanite isograd)

▤ sillimanite grade

▤ above first appearance of granite pods *

▤ above muscovite *

+ granites and granitic gneiss

* includes migmatite (over 30% granitic material)

— fault

subgroup, and the blue-grey basalts of the Dumas Group are markedly different in hand specimen and thin section from the green basalts of the Grant subgroup.

Metamorphic grade in the area is shown in Figure 11.4a. Isograds shown are those used by St-Onge and Hoffman (1980). The metamorphic zonation in the area has been strongly affected by late faulting. The metasiltstones and slates contain abundant 1 to 3 cm long andalusite porphyroblasts. Staurolite is generally poorly developed, and cordierite was not observed.

Metamorphism and structural style are related in the map area. Below staurolite grade, the Grant subgroup rocks have been folded about broad, north to northwest trending fold axes (F_2). Above staurolite grade, bedding becomes obscure, the planar fabric more penetrative, and the F_2 folds become steeper. Above andalusite grade, an earlier set of east-west trending, recumbent, outcrop scale folds (F_1) are present. The observation of F_1 folds above andalusite grade may simply reflect better exposure of the higher grade rocks. Both F_1 and F_2 folds are present in the granite gneisses and migmatites, and McGlynn (1974) reported the same fold types in the northeast corner. Fifty kilometres east of the map area, Helmstaedt (unpublished ms., 1977) reported recumbent folds overprinted by later upright folds in Snare Group rocks. He also noted that the upright folds became tighter, and the planar fabric more penetrative with increasing metamorphic grade; observations similar to those made at Grant Lake.

Late faulting is the dominant structural feature in the area, and has divided the area into several blocks (Fig. 11.4a) of varying metamorphic grade. The juxtaposition of low and high grade metamorphic rocks along these faults suggests that the amount of vertical movement was significant, although transcurrent movement cannot be discounted. Four major mylonite and fault zones were traced into the Grant Lake area from the Calder River map area (McGlynn, 1974). Mylonitization affects all lithologies in the map area. The fault contact between unit 6 and 8 west of Grant Lake may be west dipping as dykes cutting Unit 8 granites contain xenoliths of granite gneiss resembling Unit 6. The fault on the east shore of Edjuvit Lake is a 2 to 3 m wide zone of ultramylonite dipping 40 to 50° to the east.

FOUR CORNERS MAP AREA

The oldest rocks in the Four Corners map area are a tonalite gneiss (Unit 1) with enclaves of garnetiferous amphibolite, anthophyllite schist, and pelitic and quartzitic metasediments. The tonalite gneiss is cut by pink, protomylonitic biotite B-granite (Unit 2). The granite is cut by 30 to 100 m wide dykes of basalt, now amphibolite (Unit 3). The amphibolite dykes have fine grained margins and coarse grained cores. In the thickest dykes, the coarse grained cores have been relatively unaffected by the pervasive deformation present in the area, and are only weakly foliated. All three units are cut by late, unfoliated pegmatite veins. Units 1 to 3 comprise the Sitiyok Igneous Complex. All units of the

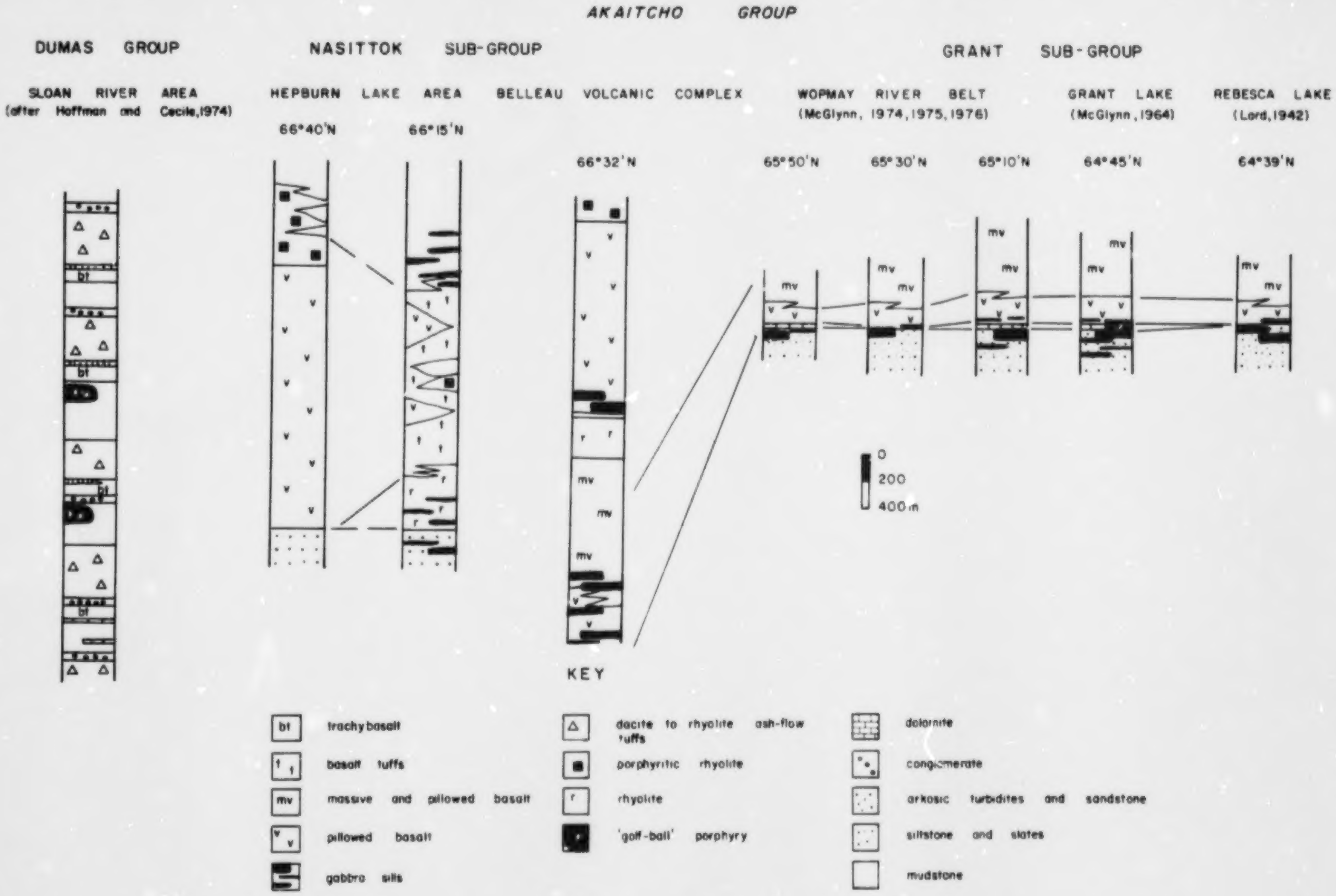
AKAITCHO GROUP
DUMAS GROUP
NASITTOK SUB-GROUP
GRANT SUB-GROUP
SLOAN RIVER AREA
(after Hoffman and Cecile,1974)
HEPBURN LAKE AREA
66°40'N
66°15'N
BELLEAU VOLCANIC COMPLEX
66°32'N
WOPMAY RIVER BELT
(McGlynn, 1974,1975,1976)
65°50'N
65°30'N
65°10'N
GRANT LAKE
(McGlynn,1964)
64°45'N
REBESCA LAKE
(Lord,1942)
64°39'N
bt
mv
0
200
400 m
KEY
bt trachybasalt
basalt tuffs
mv massive and pillowed basalt
pillowed basalt
gabbro sills
dacite to rhyolite ash-flow tuffs
porphyritic rhyolite
r rhyolite
'golf-ball' porphyry
dolomite
conglomerate
arkosic turbidites and sandstone
siltstone and slates
mudstone

Figure 11.5. *Comparative stratigraphic section of the Grant subgroup.*

Sitiyok Complex have undergone two phases of folding. Outcrop scale recumbent folds with east-west trending axes have been refolded about north to northeast trending regional folds. The later folding is shown by the amphibolite dykes present in the northern part of the Sitiyok Complex (Fig. 11.3).

The Sitiyok Complex may represent basement to the Akaitcho Group. The granite was emplaced, and then cut by basalt dykes prior to or during to metamorphism and deformation of the Sitiyok Complex and the Akaitcho Group. The basalt dykes have similar chemistry to basalts of the Ipiutak subgroup, the lowest unit of the Akaitcho Group. Unfortunately, the complex is in fault contact with most other units, and the contact with the surrounding Ipiutak subgroup metasedimentary and metavolcanic rocks is not exposed. Although the Sitiyok Complex is premetamorphic, it is not certain on the basis of field evidence alone that it is basement.

The Sitiyok Complex is rimmed by metapelite (Unit 4a), now migmatite with some interbedded meta-arkose (Unit 4b). Amphibolite bands, commonly garnetiferous, are interbedded with the pelites and probably represent tuffs and thin flows. On the west shore of Four Corners Lake, a large amphibolite complex (Unit 4c) is present, and contains compositionally layered, fine grained amphibolite, probably metatuffs; fine- to medium-grained strongly foliated amphibolite, probably flows; and weakly foliated, coarse grained amphibolite, probably gabbro sills. Low grade rocks equivalent to the amphibolites consists of basalt metatuff (Unit 4d) and pillowed and massive basalts (Unit 4e).

The exact facies relationship between the amphibolites and pelites is not known. North of Ipiutak Lake, 300 m of pelite overlie 500 m of amphibolite. West of Wentzel Lake, lower grade basaltic rocks chemically similar to the amphibolites are interbedded with pelite and arkose of the Zephyr formation. In the Four Corners area, pelite, amphibolite and minor arkose are interbedded and much of the amphibolite may be metatuff. If so, then the amphibolites may represent distal products of a volcanic centre located north of Ipiutak Lake.

South of Four Corners Lake, quartzites and metasiltstones interbedded with minor pelite (Unit 4f) are interbedded with amphibolite tuffs and flows. Unit 4f is tentatively included in the Ipiutak subgroup, although low grade equivalents to this sequence, which is isolated by faults from other Ipiutak subgroup units, have yet to be observed.

Finely laminated slates and metasiltstones (Unit 5a), cut in places by gabbro sills 20 to 50 m thick (Unit 5b), and overlain by pale green, dense pillowed metabasalt (Unit 5c), form a north-south trending belt along the shores of Iperarpok Lake. These rocks are lithologically identical to rocks of the Grant subroup at Grant Lake, and McGlynn (1974, 1975, 1976) has traced these units along the length of the Calder River map area form Grant Lake to Four Corners Lake (Fig. 11.5, 11.6). Thus, Unit 5 rocks are correlated with the Grant subgroup (Fig. 11.5). The metasiltstones contain two cleavages one trending 340° to 020°, the other 230° to 270°, and small (3 to 10 m across) east-west trending recumbent folds. These rocks are preserved at biotite and chlorite metamorphic grade. They are in fault contact to the east with sillimanite grade to migmatitic siltstones and pelites which are probably high grade equivalents of the slates and metasiltstones (Unit 5a). The metamorphic rocks grade into orthoclase porphyroblastic, protomylonitic, white to grey weathering granite gneiss (Unit 6), similar to granite gneisses at Grant Lake (Unit 5). Beds of metaconglomerate (Unit 5d) containing stretched cobbles of gneiss and granite, and beds of quartzite are interbedded with migmatized metasiltstone (Unit 5e) adjacent to the granite gneiss (Unit 6). The quartzites of units 4f and 5e may be correlative, but it has not been possible to show that they are the same unit.

Garnet granite with over 5 per cent garnet (Hoffman et al., 1980) (Unit 7) is closely associated with Ipiutak subgroup amphibolite, and commonly contains inclusions of garnet amphibolite (Unit 4c) in varying degrees of assimilation.

Unit 8 is similar to Unit 6 in the Grant Lake area, although it is more dioritic, and nebulitic in the Four Corners map area than at Grant Lake.

The pluton adjacent to the Dumas Group (Unit 9) is similar to Unit 8 at Grant Lake in its structural position and ambiguous age relations. The pluton has an overall granodiorite composition but consists of biotite tonalite and granodiorite with patches of syenogranite (Hoffman et al., 1980). It is sheared along its margins. To the west, Unit 9 is in fault ontact with the Dumas Group, but conglomerate containing cobbles of the granodiorite, as well as cobbles of ash flow tuff is common along the granodiorite contact. At 65°59'N, the western contact with the Dumas Group may be an unconformity and not a fault. Hoffman and Bell (1975) described a similar relationship at 66°02'N. The eastern contact is faulted, but the granodiorite contains inclusions of mafic and sedimentary rocks and may intrude the surrounding Dumas Group rocks. However, conglomerate containing cobbles of granodiorite and ash flow tuffs is also present along the eastern contact. Mafic dykes, commonly chloritized and bluish in colour, cut the granodiorite, and may have served as feeders to Dumas Group lavas. The granodiorite is younger than the gneisses (units 6 and 8), but is is not clear if it is older, or younger than the lowest units of the Dumas Group. It is older than the upper Dumas Group.

The Dumas Group as reported by Hoffman and Bell (1975) consists of rhyolite porphyry and ash flow tuffs (Unit 10a), argillite (Unit 10b), conglomerate lenses (Unit 10c) and porphyritic basalt (Unit 10d). Arkose (Unit 10e) is commonly associated with the basalts. Carbonate (Unit 10f), both massive and as matrix to matrix supported conglomerates occurs in the west part of the map area near a basalt/argillite contact.

Finely laminated (1 to 4 mm thick beds) felsic and mafic tuffs (Unit 10h) are interbedded with argillite 3 km south of Iperarpok Lake. There is considerable lateral variation in the stratigraphy of the Dumas Group in the map area.

Dumas Group and Grant subgroup rocks are in fault contact south and west of Iperarpok Lake. A quartz stockwork is present along the fault contact, and rocks within 200 m of either side of the fault have an intense north-south cleavage. The Dumas Group adjacent to the fault contains reddish arkose, conglomerates with ash flow tuff cobbles, dacites, rhyodacites and blue-grey basalts, but bedding is obscured by the north-south cleavage. In contrast, Grant subgroup rocks adjacent to the fault are grey, biotite-grade metasedimentary rocks, cut by two cleavages, and minor metagabbro and metabasalt.

It is believed that the Dumas Group rocks are not a low grade equivalent of the Grant subgroup because (a) they have a different stratigraphy (Fig. 11.5), (b) ash flow tuffs have not been reported from the Grant subgroup, (c) arkoses in the Dumas Group are poorly sorted, and contain a much larger volcanic component than do the few arkoses present in the Grant subgroup, and (d) Dumas Group rocks are less metamorphosed and deformed than rocks of the Grant subgroup.

The three plutons of Unit 11 in the map area are unfoliated, and resemble the 'G3' (Hoffman, 1978) plutons of Great Bear Batholith. Unit 11a is the 'younger granite' described by Hoffman et al. (1980). Unit 11b is a coarse grained, orthoclase porphyritic biotite syenogranite. Unit 11c is the Adam Lake pluton (Hoffman, 1978) intrusive into the Dumas Group.

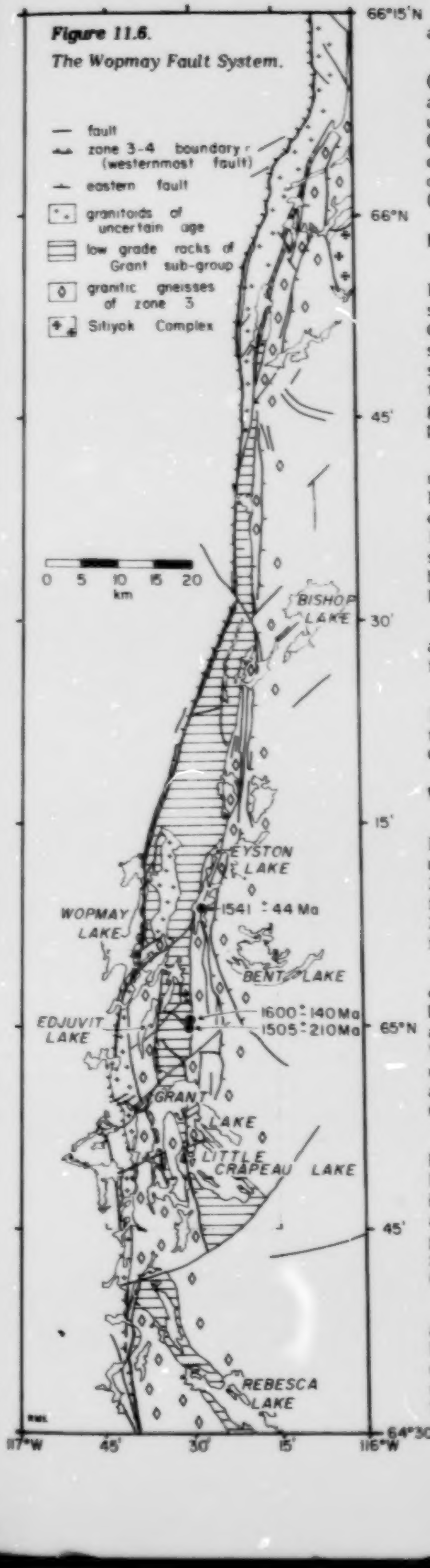

Figure 11.6.

The Wopmay Fault System.

Unit 12 contains variable composition granitoids and salmon- coloured aphanitic felsite dykes are common along north-south faults in the map area.

The present pattern of metamorphic zonation in the map area (Fig. 11.4b) is controlled by a series of north-south trending fault zones which affect all units. The location of the Zone 3-4 boundary (Wopmay Fault) is unclear. Hoffman (1978) and McGlynn (1976) considered the westernmost fault (west contact of Unit 9) to be the Wopmay Fault. The north-south fault south of Iperarpok Lake separates the Grant subgroup from Dumas Group rocks, and could also be the Zone 3-4 boundary. The two faults do converge to the south (McGlynn, 1976), and are probably branches of the same fault.

REGIONAL CORRELATIONS

Comparative stratigraphic sections of the Grant subgroup from Grant Lake to Four Corners Lake are shown in Figure 11.5. Generalized stratigraphic columns for the Dumas Group and the middle to upper Akaitcho Group are also shown in Figure 11.5. The stratigraphy of the Grant subgroup is similar to that of the upper Zephyr formation and the lower to middle Nasittok subgroup of the Akaitcho Group. The metasiltstones, with minor arkose, of the Grant subgroup would be facies equivalents of the Zephyr formation. The gabbro sills, basalt flows and minor rhyolite would be equivalent to the basal part of the Nasittok subgroup (e.g. the Kapvik Volcanic Complex).

A fault bounded block of generally low grade metavolcanic and metasedimentary rocks of the Grant subgroup that can be traced from Grant Lake to 66°03'N (McGlynn, 1974, 1975, 1976) pinches out only 25 km southwest of the isolated, fault bounded, low grade Belleau Volcanic Complex (Easton, 1980) (Fig. 11.1). The Belleau Complex is lithologically and stratigraphically similar to the Grant subgroup. The proximity of the Belleau Complex to the belt of Grant subgroup rocks, and its similar stratigraphy suggests that the Belleau Complex is an isolated remnant of Grant subgroup rocks.

Lithologies with a similar stratigraphy to the Grant subgroup are present at Rebesca Lake (Lord, 1942), and the Rebesca Lake section is probably a faulted segment of the Little Crapeau Lake volcanic section (Fig. 11.1, 11.6).

Grant subgroup rocks were previously assigned to the Snare Group (Lord, 1942; Lord and Parsons, 1954; McGlynn, 1974, 1975, 1976). This study shows that at least part of the classic Snare Group is correlative with the Akaitcho Group.

WOPMAY FAULT ZONE

The Wopmay Fault is not a single distinct feature in either the Grant Lake or Four Corners map areas. In both areas, a set of four to six major north-south trending fault and mylonite zones are present in a belt up to 20 km wide (Fig. 11.2, 11.3, 11.6). Restriction of several north-south trending faults, some of which are clearly branches of larger faults to a belt 10 to 20 km wide suggests that the faults are related. This belt of north-south faults will be referred to as the Wopmay Fault Zone.

The 'Wopmay Fault' (i.e. Zone 3-Zone 4 boundary) has generally been considered as the most westerly north-south fault of the Wopmay Fault Zone but the eastern faults were not always recognized. For the purpose of defining a mappable Zone 3-Zone 4 boundary, use of the western boundary fault of the Wopmay Fault Zone seems best. This boundary is in agreement with previous usage, and divides rocks which clearly belong to Zone 4 from rocks of Zone 3, and rocks which are difficult to assign to one zone or the other (e.g. Unit 8 at Grant Lake and Unit 9 at Four Corners).

Significant chemical changes have been observed in rock units as they become progressively deformed adjacent to the mylonite zone on the shore of Edjuvit Lake (Table 11.1). The changes observed are similar to those reported by Kerrich et al. (1977) for progressive deformation of mafic and felsic rocks adjacent to shear zones. Of particular interest is the observation that the fine grained rocks (gabbro sills) have undergone more alteration near the mylonite zone than have granitoid rocks a similar distance from the fault (Table 11.1) (Kerrich et al., 1977).

The age of the Wopmay Fault Zone is not well known. Hoffman (1980b) and Hoffman and McGlynn (1977) noted that movement along the Wopmay Fault in northern Wopmay Orogen was complete prior to deposition of the upper Dumas Group, although Hoffman and St-Onge (1981) report later movement along part of the Wopmay Fault. Later movement along the Wopmay Fault is also indicated by the presence of a well developed cleavage

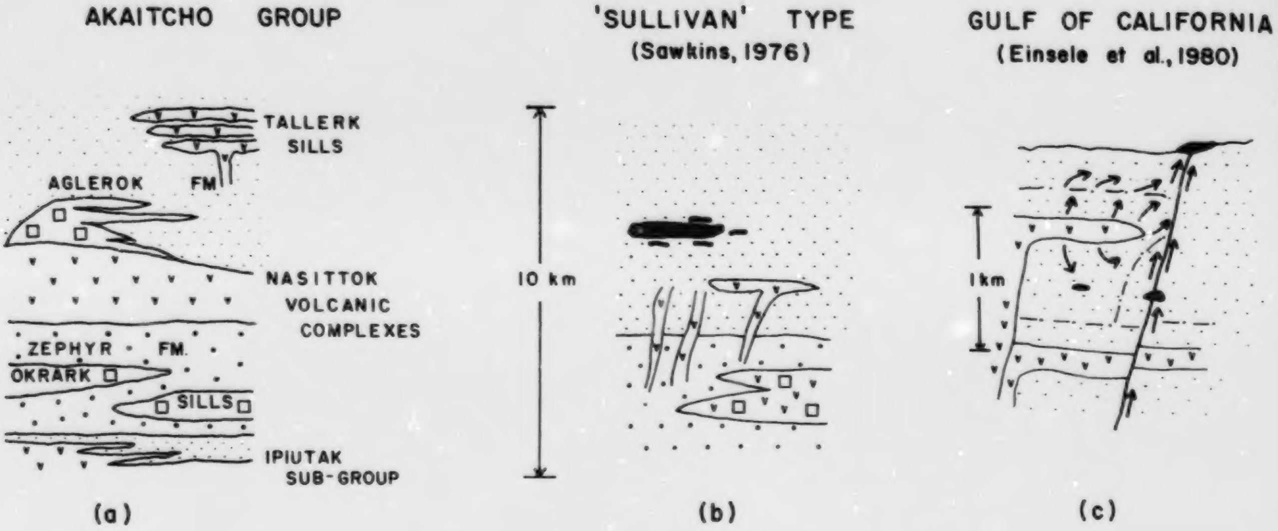
AKAITCHO GROUP

'SULLIVAN' TYPE (Sawkins, 1976)

GULF OF CALIFORNIA (Einsele et al., 1980)

Figure 11.7. Comparison of the stratigraphy of the Akaitcho Group (a) to the general stratigraphy present in 'Sullivan' type Ag-Pb-Zn deposits (b). The model proposed by Einsele et al. (1980) for the production of hydrothermal deposits in the Gulf of California is also shown (c).

in all Dumas Group rocks along the fault zone, and chemical alteration of Dumas Group rocks has occurred near the fault zones (Easton, unpublished data). Northeast-northwest trending tanscurrent faults (Hoffman, 1980a) older than the 1400 ± 48 ma Western Channel diabase (Wanless et al., 1978; Hoffman, 1980a) cut the north-south faults of the Wopmay Fault Zone. Hornblende sampled within 100 m of the mylonite zone through Eyston Lake (Fig. 11.6) yielded a K-Ar date of 1541 ± 44 Ma (G.S.C. 73-80), and two whole rock samples taken 400 m west of the fault along the Wopmay River (Fig. 11.6) yielded K-Ar ages of 1600 ± 140 Ma (G.S.C. 64-42) and 1505 ± 210 Ma (G.S.C. 64-43). Of these three ages, the first two are considered more reliable. All three ages are about 200 to 250 Ma younger than most K-Ar ages from the Bear Province (Stockwell, 1972) and are clearly anomalous. Their close proximity to the mylonite zones and the observed mobility of the alkaline elements adjacent to the mylonite zones (Table 11.1) suggests that the K-Ar ages may date the time of last movement on faults of the Wopmay Fault Zone at about 1550 to 1600 Ma.

MINERAL POTENTIAL

In an earlier paper (Easton, 1980), it was indicated that the Akaitcho Group metavolcanic rocks are not a favourable host for volcanogenic base metal "Kuroko Tupe" massive sulphide deposits. However, the realizatio[illegible] that the Akaitcho Group probably represents the [illegible]nants of rift-type crust formed during the initial de[illegible]ent of Wopmay Orogen (Easton, in press) combine[illegible]cent marine geological work in a similar tectonic [illegible]he Gulf of California (Einsele et al., 1980; Lo[illegible] and Lawver, 1980) suggests that the prospect for b[illegible]tal deposits in the Akaitcho Group may not be as b[illegible] as originally indicated.

First, the Akaitcho Group is similar to stratigraphic sequences reported from 'Sullivan or MacArthur' type Ag-Pb-Zn deposits (compare Fig. 11.7a, 11.7b). These deposits are commony Proterozoic in age, and are associated with thick sequences of continentally derived clastic rocks for which there is evidence of contemporaneous or time-related basaltic, or basalt-rhyolite volcanic activity. The tectonic setting of these deposits is generally considered to be tension related intracratonic troughs and rift valleys, and young continental margins (Sawkins, 1976). All these features are present in the Akaitcho Group.

Secondly, Einsele et al. (1980) have proposed a model for the development of hydrothermal systems in the Gulf of California which has a bearing on possible ore deposition in the Akaitcho Group. In the model of Einsele et al. (Fig. 11.7c), hot sills of basaltic material are intruded into porous sediments. The sills heat pore fluids in the sediments resulting in changes in pore fluid composition. Deposition of hydrothermal minerals decreases porosity in the sediments and results in the upward migration of heated pore fluids. As noted by Einsele et al. (1980), the model does not require recharge of seawater into the sediments. The heated pore fluids migrate to the sediment-seafloor interface and hydrothermal minerals and sulphides are deposited on the seafloor where they are rapidly buried by younger sediment. Further intrusion of sills into overlying sections of unaltered sediments results in continued hydrothermal activity. This model would result in the formation of relatively small stratabound deposits, but, as shown in Figure 11.7c, a fault could funnel heated fluids from several hydrothermal systems to the surface, and a larger deposit could form.

If applicable to the Akaitcho Group, the model of Einsele et al. (1980) would indicate that the most favourable areas for the formation of this type of hydrothermal deposit

Table 11.1

Major element analyses of a granitoid gneiss and a Grant subgroup gabbro adjacent to a mylonite zone located on the east shore of Edjuvit Lake, Grant Lake map area.

	—— progressive deformation ——>				Edjuvit Mylonite Zone		<—— progressive deformation ——			
	Granitoid Gneiss						Grant subgroup gabbro			
Sample Number	F337E	F336B	F337C	F336A	F337B	F337A	F336C	F337D	F337F	F367B
Distance from mylonite	100m	30m	3m	1m	0m	0m	1m	1m	1.5m	1000m
SiO_2	70.6	69.6	70.4	66.8	80.4	77.6	62.5	52.6	49.2	49.1
TiO_2	.45	.47	.29	.59	.19	.34	1.16	1.15	1.39	.89
Al_2O_3	14.8	14.9	14.4	14.5	9.2	10.05	12.7	13.5	13.5	14.2
Fe_2O_3*	3.33	2.66	2.56	3.84	2.46	3.30	11.88	10.43	12.38	12.05
MnO	.04	.04	.04	.07	.04	.05	.21	.17	.19	.19
MgO	1.64	1.49	1.54	2.92	.78	.99	1.32	7.43	8.53	9.16
CaO	1.23	2.11	.92	4.10	1.73	2.53	4.42	11.05	11.31	12.18
Na_2O	2.86	2.51	2.97	2.11	.73	1.88	3.89	2.32	2.08	1.85
K_2O	4.92	6.07	5.80	4.88	4.45	3.30	1.53	1.26	1.33	.28
P_2O_5	.20	.19	.18	.20	.02	.03	.31	.07	.09	.07
L.O.I.	1.31	1.37	1.20	3.05	.86	1.54	3.83	2.10	2.86	1.48
Total	98.82	99.04	100.64	99.86	99.60	98.90	98.85	100.57	100.63	100.01
Specific Gravity	2.636	2.630	2.726	2.683	2.682	2.739	2.750	2.964	2.960	2.968

Analyses performed by G. Andrews, Memorial University of Newfoundland.

would have been where the Tallerk sills intruded Aglerok formation pelites, or, where gabbro sills have intruded siltstones and mudstones of the Grant subgroup. Possible exploration targets are shown in Figure 11.1.

However, it should be noted that no 'Sullivan type' deposits have yet been reported from the Akaitcho Group and sulphide showings are few. This may reflect the lack of prospecting activity in the area. Alternatively, although in theory the Akaitcho Group is a favourable host for 'Sullivan Type' ores, there is no assurance that ore is present.

ACKNOWLEDGMENTS

The mineral potential portion of this paper has benefited from discussions in the field with S.M. Roscoe and B.J. Fryer. Peter de Bie provided able assistance in the field, and was indispensible during the collection of Rb-Sr samples in the area. This work constitutes part of a doctoral dissertation at Memorial University by the author. In addition to financial assistance provided by Energy, Mines and Resources, the author received financial support from a Memorial University of Newfoundland Fellowship and a NSERC grant to B.J. Fryer. Aircraft support and expediting services were provided by the Geology Office, D.I.A.N.D., Yellowknife, and this support is gratefully acknowledged. G. Andrews, Memorial University, performed the major element analyses reported in this paper. B.J. Fryer reviewed an earlier version of this paper.

REFERENCES

Dimroth, E., Cousineau, P., Leduc, M., and Sanschagrin, Y.

1978: Structure and organization of Archean subaqueous basalt flows, Rouyn-Noranda area, Quebec, Canada; Canadian Journal of Earth Sciences, v. 15, p. 902-918.

Easton, R.M.

1980: Stratigraphy and geochemistry of the Akaitcho Group, Hepburn Lake map area, District of Mackenzie: An initial Rift Succession in Wopmay Orogen (early Proterozoic); in Current Research, Part B, Geological Survey of Canada, Paper 80-1B, p. 47-57.

Stratigraphy of the Akaitcho Group and the development of an early Proterozoic continental margin, Wopmay Orogen, N.W.T.; in Campbell, F.H.A., ed., Proterozoic Basins in Canada, Geological Survey of Canada, Paper 81-10. (in press)

Einsele, G., Gieskes, J.H., Curray, J., Moore, D.M., Aguayo, E., Aubry, M-P., Fornari, D., Guerrero, J., Kastner, M., Kelts, K., Lyle, M., Matoba, Y., Molina-Cruz, A., Niemitz, J., Rueda, J., Saunders, A., Schrader, H., Simoneit, B., and Vacquier, V.

1980: Intrusion of basaltic sills into highly porous sediments and resulting activity; Nature, v. 283, p. 441-444.

Hoffman, P.E.
1978: Geology of the Sloan River map area (86K), District of Mackenzie, Northwest Territories; Geological Survey of Canada, Open File 535.

1980a: Conjugate transcurrent faults in north-central Wopmay Orogen (early Proterozoic) and their dip-slip reactivation during post-orogenic extension, Hepburn Lake map area, District of Mackenzie; *in* Current Research, Part A, Geological Survey of Canada, Paper 80-1A, p. 183-185.

1980b: A Wilson Cycle of early Proterozoic age in the northwest of the Canadian Shield; *in* Strangway, D.W., ed., The Continental Crust and its Mineral Deposits; Geological Association of Canada, Special Paper *20*, p. 523-549.

Hoffman, P.F. and Bell, I.
1975: Volcanism and plutonism, Sloan River map area (86K), Great Bear Lake, District of Mackenzie; *in* Report of Activities, Part A, Geological Survey of Canada, Paper 75-1A, p. 331-337.

Hoffman, P.F. and Cecile, M.P.
1974: Volcanism and plutonism, Sloan River map area (86K), Great Bear Lake, District of Mackenzie; *in* Report of Activities, Part A, Geological Survey of Canada, Paper 74-1A, p. 173-176.

Hoffman, P.F. and McGlynn, J.C.
1977: Great Bear Batholith: a volcano-plutonic depression; *in* Volcanic Regimes in Canada, ed., W.R.A. Baragar, L.C. Coleman and J.M. Hall; Geological Association of Canada, Special Paper 16, p. 169-192.

Hoffman, P.F. and St-Onge, M.R.
1981: Contemporaneous thrusting and conjugate transcurrent faulting during the second collision in Wopmay Orogen: Implications for the subsurface structure of post-orogenic outliers; *in* Current Research, Part A, Geological Survey of Canada, Paper 81-1A, p. 251-257.

Hoffman, P.F., St-Onge, M., Carmichael, D.M., and de Bie, I.
1978: Geology of the Coronation Geosyncline (Aphebian), Hepburn Lake Sheet (86J), Bear Province, District of Mackenzie; *in* Current Research, Part A, Geological Survey of Canada, Paper 78-1A, p. 147-151.

Hoffman, P.F., St-Onge, M.R., Easton, R.M., Grotzinger, J., and Schulze, D.W.
1980: Syntectonic plutonism in north-central Wopmay Orogen (early Proterozoic), Hepburn Lake map area (86J), District of Mackenzie, *in* Current Research, Part A, Geological Survey of Canada, Paper 80-1A, p. 171-177.

Kerrich, R., Fyfe, W.S., Gorman, B.E., and Allison, I.
1977: Local modification of rock chemistry by deformation; Contributions to Mineralogy and Petrology, v. 65, p. 183-190.

Lonsdale, P. and Lawver, L.A.
1980: Immature plate boundary zones studied with a submersible in the Gulf of California; Geological Society of America Bulletin, Part I, v. 91, p. 555-569.

Lord, C.S.
1942: Snare River and Ingray map areas, Northwest Territories, Geological Survey of Canada, Memoir 235, 55p.

Lord, C.S. and Parsons, W.H.
1954: Camsell River, District of Mackenzie, N.W.T.; Geological Survey of Canada Map 1014A, 1:253,440 scale.

McGlynn, J.C.
1964: Grant Lake area; Geological Survey of Canada, Paper 64-1, p. 14.

1974: Geology of the Calder River map area (86F), District of Mackenzie; *in* Report of Activities, Part A, Geological Survey of Canada, Paper 74-1A, p. 383-385.

1975: Geology of the Calder River map area (86F), District of Mackenzie; *in* Report of Activities, Part A, Geological Survey of Canada, Paper 75-1A, p. 339-341.

1976: Geology of the Calder River (86F) and Leith Peninsula (86E) map areas, District of Mackenzie, *in* Report of Activities, Part A; Geological Survey of Canada, Paper 76-1A, p. 359-361.

Sawkins, F.J.
1976: Massive sulphide deposits in relation to geotectonics; *in* Metallogeny and Plate Tectonics, D.F. Strong, ed., Geological Association of Canada, Special Paper 14, p. 221-240.

St-Onge, M.R. and Carmichael, D.M.
1979: Metamorphic conditions, Northern Wopmay Orogen, N.W.T.; Geological Association of Canada, Program with Abstracts, v. 4, p. 81.

St-Onge, M.R. and Hoffman, P.F.
1980: "Hot-side-up" and "hot-side-down" metamorphic isograds in north-central Wopmay Orogen, Hepburn Lake map area, District of Mackenzie; *in* Current Research, Part A, Geological Survey of Canada, Paper 80-1A, p. 179-182.

Stockwell, C.H.
1972: A Revised Time Scale for the Precambrian Shield; Geological Survey of Canada, Paper 72-52.

Streckeisen, A.
1976: To each plutonic rock its proper name; Earth Science Reviews, v. 12, p. 1-33.

Wanless, R.K. and Loveridge, W.D.
1978: Rubidium-Strontium Isotopic Age Studies, Report 2 (Canadian Shield); Geological Survey of Canada, Paper 77-14, p. 4-6.

12.

ALTERATION PRODUCTS OF ACCESSORY ALLANITE IN RADIOACTIVE GRANITES FROM THE CANADIAN SHIELD

Project 680023

A.L. Littlejohn
Central Laboratories and Technical Services Division

Littlejohn, A.L., Alteration products of accessory allanite in radioactive granites from the Canadian Shield; in Current Research, Part B, Paper 81-1B, p. 95-104, 1981.

Abstract

Altered allanite has been found to be an accessory mineral in radioactive granites from three localities in the Canadian Shield. Bastnaesite, synchisite, thorite, fluorite and a hydrous aluminosilicate are the common products of altered allanite. The phases present in any one grain is a function of local chemistry; SEM study has shown that they form extremely fine grained intergrowths. The breakdown of the allanite structure due to the action of F and CO_2 *bearing solutions is a mechanism for fractionating and redistributing the radioactive and rare-earth components of granitic rocks.*

Introduction

In the course of studying the mineralogy of radioactive granites collected by members of the Geological Survey during detailed ground follow-up of regional geochemical and geophysical radiometric anomalies, altered allanite was found to be a common radioactive accessory mineral. Allanite has been observed in granitic rocks throughout the Canadian Shield (Morin, 1975) and its alteration to bastnaesite has been noted in some cases (Černý and Černá, 1972).

Bastnaesite is one of the alteration products of the allanites examined in this report; other products are thorite, fluorite, synchysite, iron and titanium oxides, and hydrosilicates of aluminum and other cations, the composition of which depends on the original allanite composition and the conditions under which it altered. The alteration of allanite to bastnaesite is apparently due to hydrothermal action by late-stage magmatic fluids (Adams and Young, 1961; Černý and Černá 1972; Mineyev et al., 1973).

The purpose of this report is to demonstrate that hydrothermal alteration of allanite in radioactive granitic rocks is widespread throughout the Shield and is accompanied by fractionation and dispersion of the radioactive and rare-earth components.

Figure 12.1 shows the location of the granites studied in this report. The three areas are: (1) Sharbot Lake, Ontario; (2) Sharman Lake, Manitoba (3) Fury and Hecla Strait, Northwest Territories.

Airborne gamma-ray spectrometry patterns in the Sharbot Lake area have been described by Ford and Charbonneau (1979). High equivalent uranium values correspond to belts of radioactive pegmatites of the Grenville province. Samples of pegmatite having the highest radioelement concentrations were collected during the follow-up work. The pegmatites are highly variable in their dimensions, grain size, colour and fabric. They consist mainly of quartz and microcline with subordinate plagioclase and biotite. Accessory minerals are altered allanite, uranium-bearing thorite, uraninite, apatite, cyrtolite, magnetite, ilmenite, monazite and xenotime; not all are present in any one sample.

In northwest Manitoba several large granitic bodies of Hudsonian age exhibit anomalous radiometric and geochemical characteristics (Coker, 1976). Two of these (Sharman Lake and Sandy Hill Lake) contain altered allanite as a radioactive accessory mineral. The rocks are medium- to coarse-grained, slightly porphyritic quartz monzonites composed of quartz, microcline, plagioclase and biotite; interstitial fluorite is common in the Sharman Lake body. Other accessory minerals are apatite, zircon, ilmenite, thorite and monazite; allanite-bearing samples do not contain monazite.

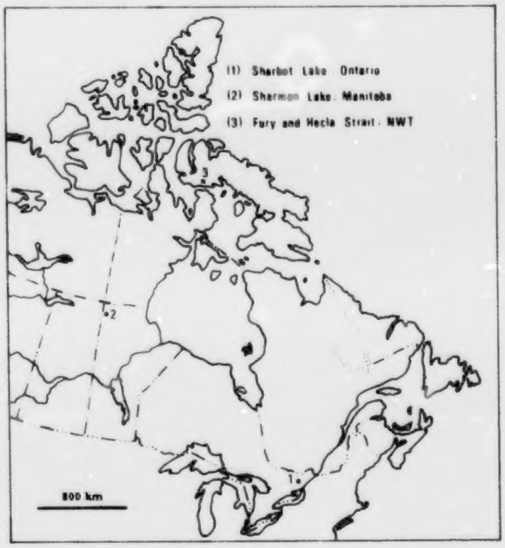
(1) Sharbot Lake, Ontario
(2) Sharmon Lake, Manitoba
(3) Fury and Hecla Strait, NWT
1
2
3
800 km

Figure 12.1. *Sample location map.*

In the Fury and Hecla Strait area on Baffin Island two areas of anomalous radioactivity underlain by granitic rocks have been described by Chandler et al. (1980). They are Archean and/or Aphebian in age. The granite is medium grained with a hypidiomorphic texture and consists of quartz and microcline with subordinate amounts of plagioclase and biotite. Accessories are magnetite, apatite, zircon, uraniferous thorite and altered allanite. Associated pegmatites contain uraninite as well as the other minerals.

Description of Altered Allanites

Altered allanite in these rocks occurs as dark orange, brown or red prismatic grains up to 5 mm in length distributed sparsely throughout the rock. Occasionally grains up to 2 cm in length are found in the pegmatites. They have an earthy lustre and are soft. In thin section they have a mottled texture with patches and zones of varying shades of orange, brown, red, black and green. They are isotropic or weakly anisotropic with non-uniform extinction and low or anomalous birefringence colours. Inclusions of zircon, quartz, magnetite, ilmenite or thorite are sometimes present.

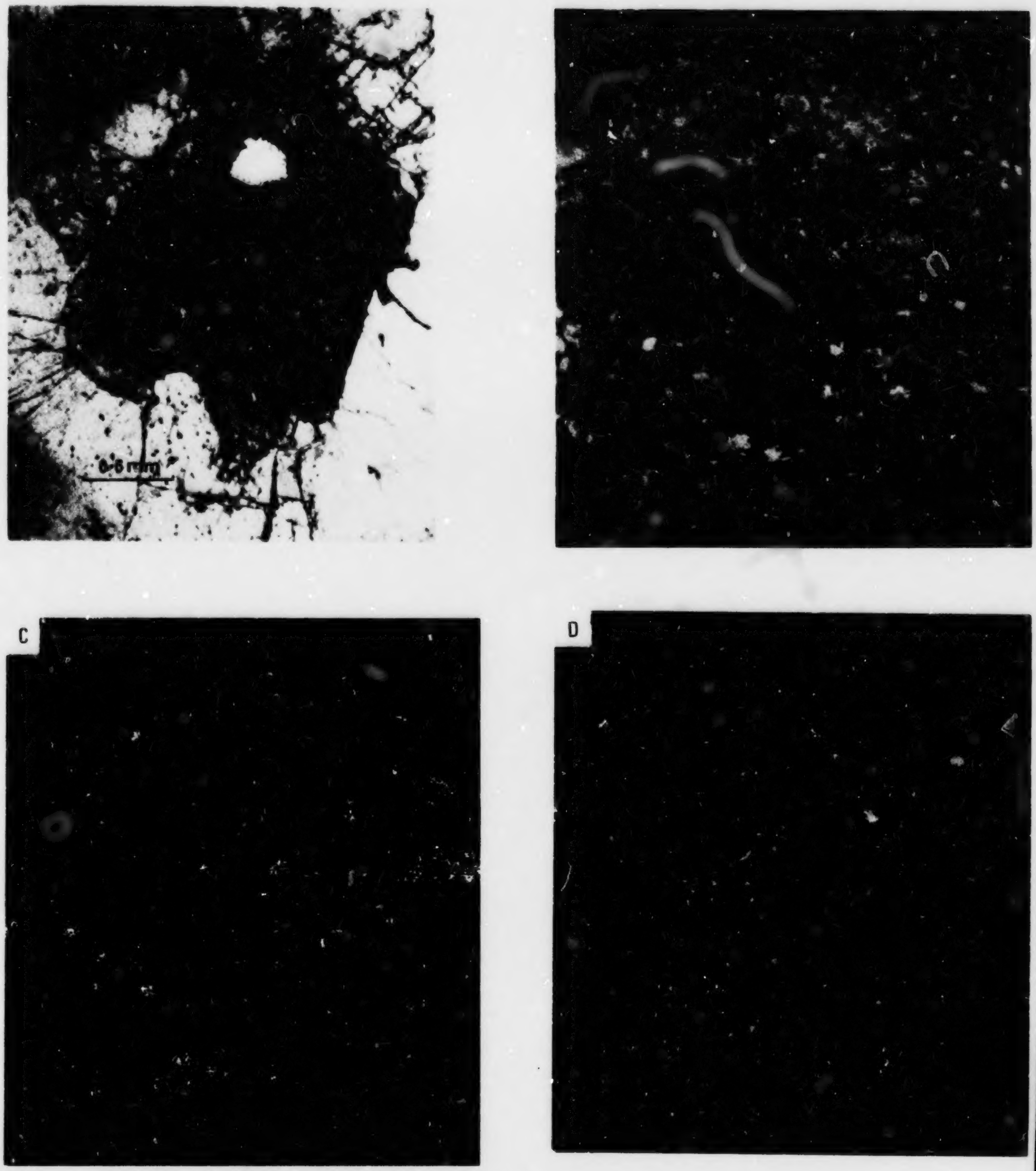

Figure 12.2. *Sample P23, Sharbot Lake area, Ontario*

a – Aggregate of "allanite" grains in quartz with radiating cracks due to expansion during hydration (transmitted light).

b – BSE image of the square area marked on 12.2a showing intergrowth of three phases: thorite (white), bastnaesite (grey) and amorphous aluminosilicate (black)

c – Thorium distribution map of the same area.

d – Cerium plus Lanthanum distribution map of the same area.

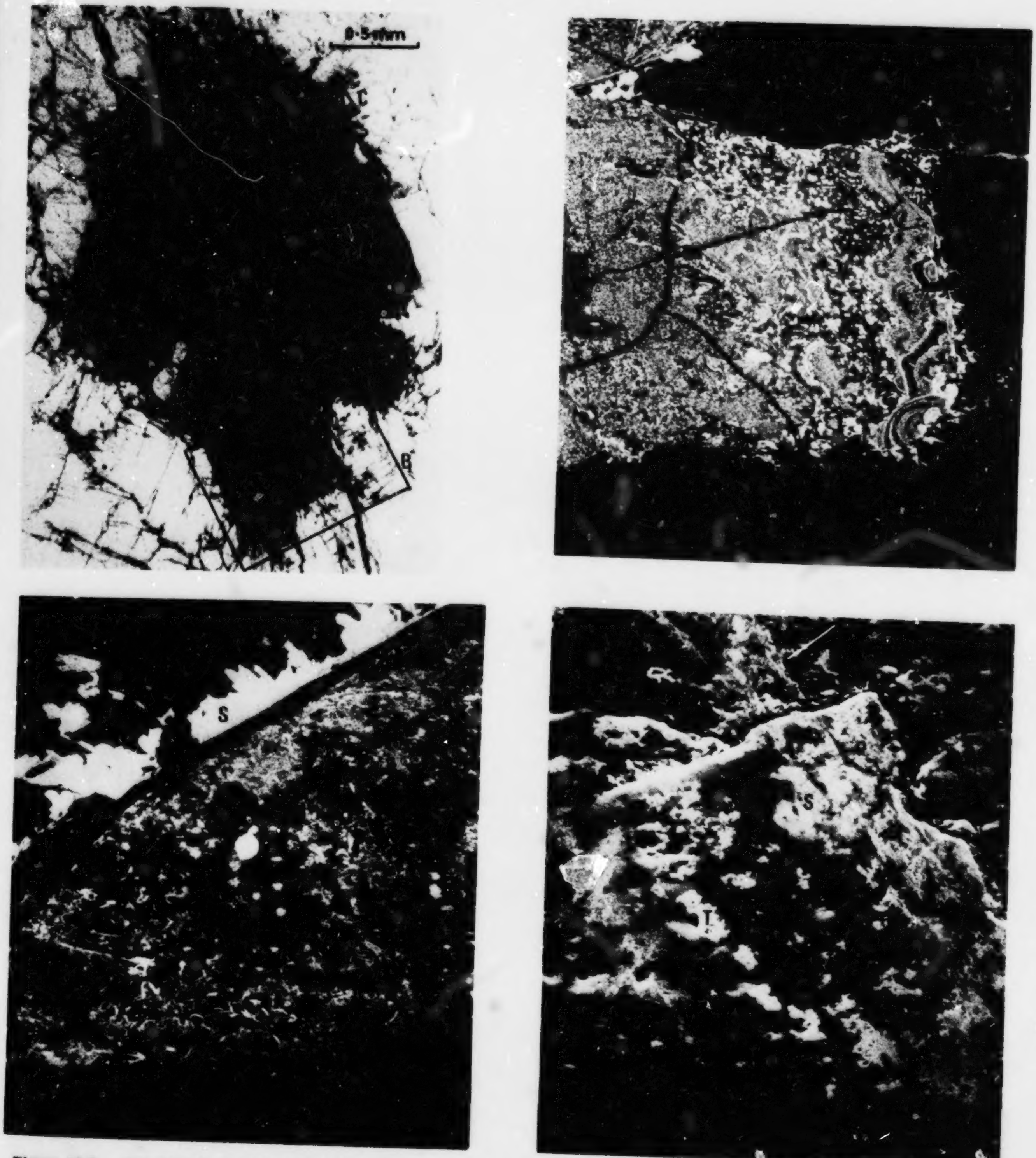

Figure 12.3. *Sample P46, Sharbot Lake area, Ontario.*

a – "Allanite" grain in quartz with radiating cracks filled with exsolved material (transmitted light).

b – BSE image of area B on 12.3a. Tip of grain with fine grained colloform growth of a mixture of thorite (white) and synchysite (light grey) in an unresolved mixture of hematite and amorphous K-Mg aluminosilicate (medium grey). The white areas within the grain are thorite; the white areas outside the grain are synchysite.

c – BSE image of area C in 12.3a. Synchysite (S) replacing quartz (Q) at edge of altered allanite.

d – BSE image of area D in 12.3a. Thorite (T) and synchysite (S) within amorphous K-Mg aluminosilicate and hematite.

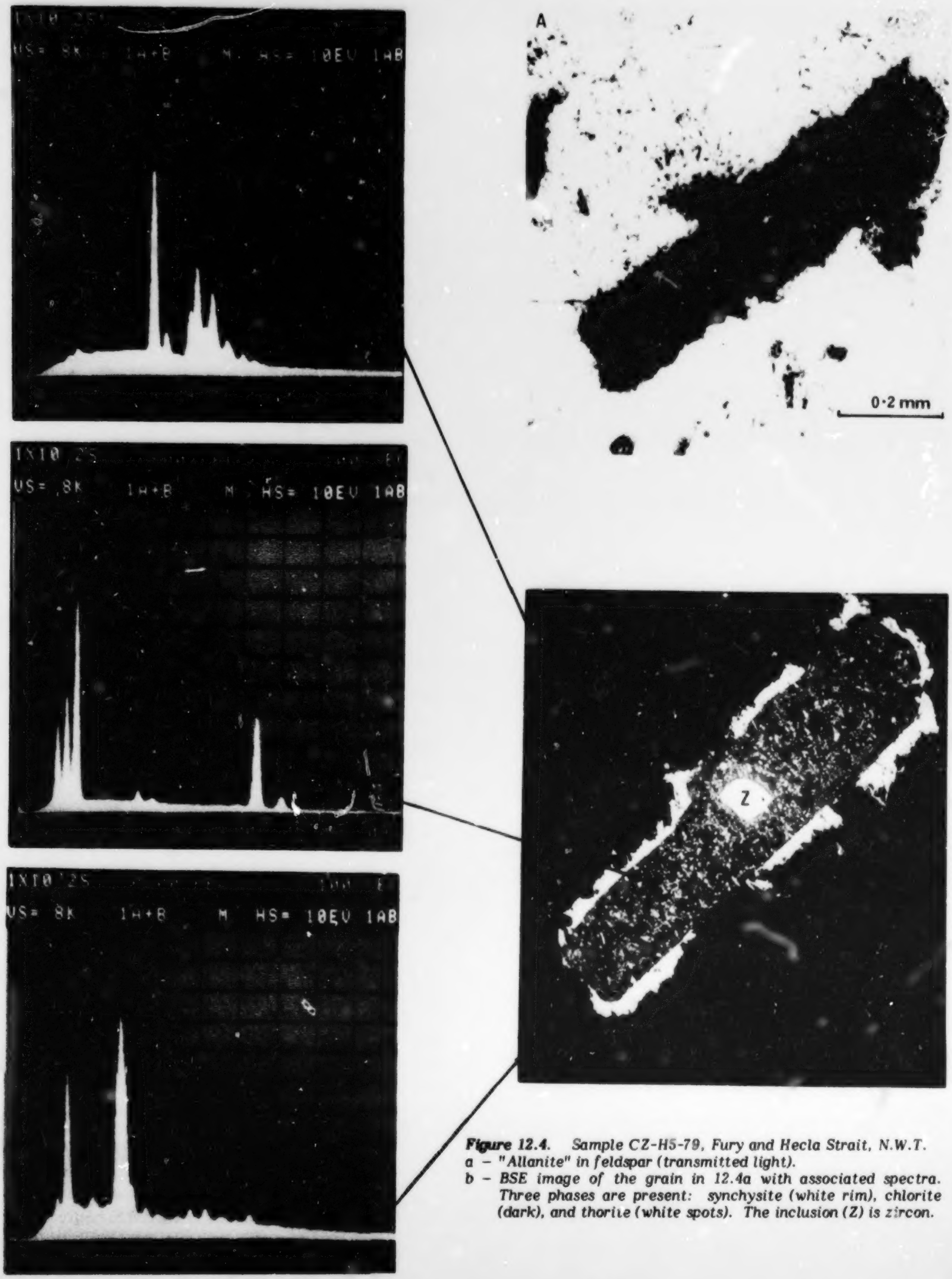
1X10 25S
VS= 8K 1A+B M HS= 10EV 1AB
1X10 25S
VS= 8K 1A+B M HS= 10EV 1AB
1X10 25S
VS= 8K 1A+B M HS= 10EV 1AB
A
0·2 mm
Z

Figure 12.4. Sample CZ-H5-79, Fury and Hecla Strait, N.W.T.

a – "Allanite" in feldspar (transmitted light).

b – BSE image of the grain in 12.4a with associated spectra. Three phases are present: synchysite (white rim), chlorite (dark), and thorite (white spots). The inclusion (Z) is zircon.

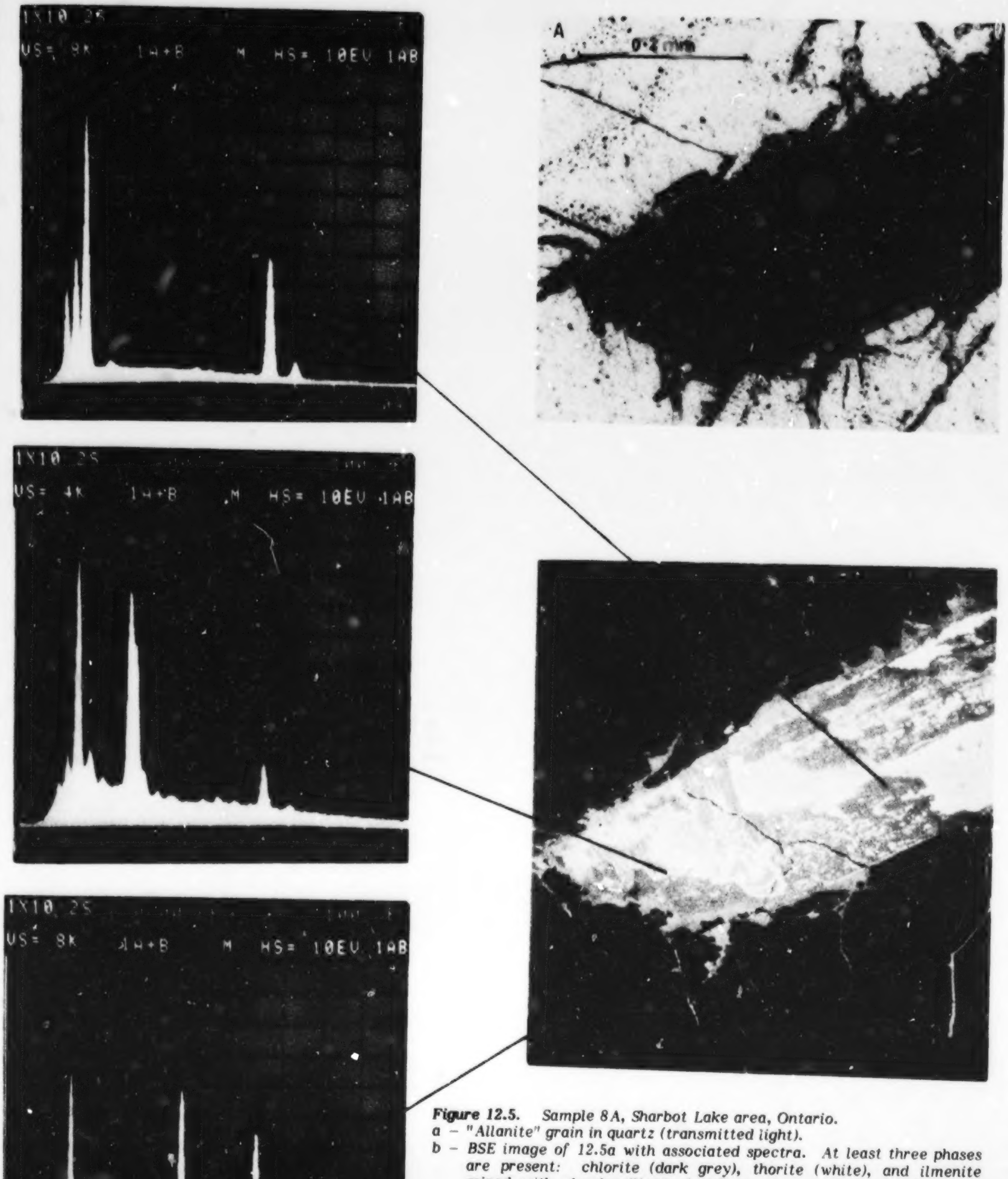
1X10 2S
VS= 8K 1A+B M HS= 10EV 1AB
1X10 2S
VS= 4K 1A+B M HS= 10EV 1AB
1X10 2S
VS= 8K 1A+B M HS= 10EV 1AB
A
0·2 mm

Figure 12.5. *Sample 8A, Sharbot Lake area, Ontario.*
a – "Allanite" grain in quartz (transmitted light).
b – BSE image of 12.5a with associated spectra. At least three phases are present: chlorite (dark grey), thorite (white), and ilmenite mixed with aluminosilicate (medium grey on the rim). The light grey is a mixture of thorite and chlorite.

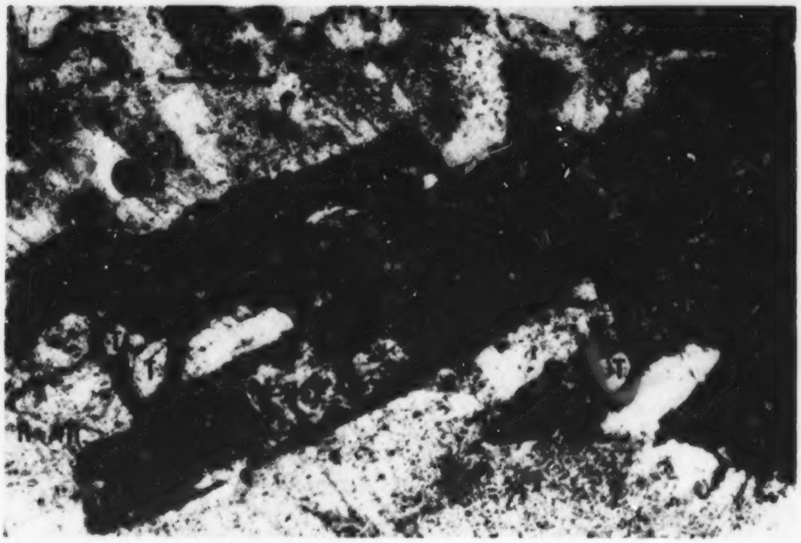

Figure 12.6. *Sample 64N762152, Sharman Lake, Manitoba. "Allanite" with associated fluorite (F), in feldspar. Domains of thorium enrichment and REE depletion are indicated by +Th and -REE respectively. Thorite (T), zircon (Z), and regenerated allanite (R-All) are also present.*

None of the "allanites" studied produced an X-ray diffraction powder pattern of allanite. Some grains were amorphous, while others had patterns of bastnaesite, synchysite, thorite, chlorite, a clay mineral, hematite, ilmenite or brookite, or a mixture of two of these. Qualitative analysis of these mixtures was carried out with an electron microprobe using an energy dispersive spectrometer. All the grains contained major amounts of Ca, Al, Fe, Ce, La and Si – the characteristic elements of allanite. In addition to these elements minor or trace amounts of one or more of Th, Mg, K, U, Ti, Pr, Nd, Pb, were found to be present in some cases. The proportions of the major elements varied widely over the whole grain and regions of rare-earth and/or thorium enrichment were found which could be correlated in some cases with the texture of the grain. However, in only rare places could a single spot or area be found with a spectrum containing only those elements corresponding to the minerals identified by X-ray diffraction. It became apparent that these grains were extremely fine grained mixtures and an SEM study was undertaken to resolve them.

The altered allanites were studied by means of back scattered electron (BSE) images in which domains of differing average atomic number are shown as differing grey levels; a high average atomic number results in a bright image. Qualitative analysis of each domain was then carried out using an energy dispersive spectrometer attached to the SEM.

The results of this study are presented in Figures 12.2-12.8. In all cases the altered allanite was found to consist of at least three phases, the distribution of which are highly irregular. Even at magnifications of 1000X it was found that the phases were intimately mixed with one another at the micron scale and the spectra obtained from each domain sometimes had components attributable to beam overlap.

Breakdown of Allanite

A general formula for allanite may be written as $A_2M_3Si_3O_{12}OH$ (Dollase, 1971). There are two A sites, A(1) and A(2), of 9- and 10-fold co-ordination respectively. A(1) is always occupied by Ca^{2+} and the larger A(2) site is occupied by larger cations such as REE^{3+} and Th^{4+} substituting for Ca^{2+}. The three octahedral sites (M(3)>M(1)>M(2)) are occupied by Al^{3+}, Fe^{3+}, Fe^{2+} and other cations such as Mg^{2+}, Mn^{2+}, Ti^{4+}. The smallest site (M(2)) is always filled with Al^{3+}.

In this report bastnaesite refers to a member of the bastnaesite-hydroxy-bastnaesite series where OH may substitute for F. Thorite refers to a thorium silicate phase which may contain $(OH)_4$ substituting for SiO_4 (thorogummite, $Th(SiO_4)_{1-x}(OH)_{4x}$).

The formation of bastnaesite ($(CeLa)FCO_3$) from allanite requires the addition of F and CO_2 and the removal of REE's. During this process Th^{4+} ions also become available since Th and Ce occupy the same site in the allanite. This results in the formation of thorite ($ThSiO_4$) by combining Th^{4+} with SiO_4^{4-} tetrahedra in the allanite. This process can be seen in Figure 12.2 where extremely fine grained bastnaesite and thorite are disseminated throughout an amorphous matrix consisting of Si, Al, Fe, and Ca. The fractionation of Ce, La and Th can clearly be seen by comparing the X-ray maps for these elements (Fig. 12.2c and 12.2d).

During bastnaesitization and breakdown of the allanite structure, Ca^{2+} ions from the next largest cation site (A(2)) may also be available. This results in the formation of synchysite ($(CeLa)FCO_3 \cdot CaCO_3$). Synchysite forms larger domains than bastnaesite within the altered allanite. It tends to migrate towards the edges of the grain as alteration proceeds and a colloform texture may develop (Fig. 12.3b). Synchysite is eventually deposited within the fracture system around the altered allanite (Fig. 12.3b) or it may replace the surrounding quartz (Fig. 12.3c). In extreme cases nearly all the rare-earths and calcium have been removed from the allanite and deposited in a zone around the remnant allanite grain (Fig. 12.4).

During the removal of cations from the A sites of the allanite structure, the remaining elements generally form an amorphous aluminosilicate. However, in some cases where

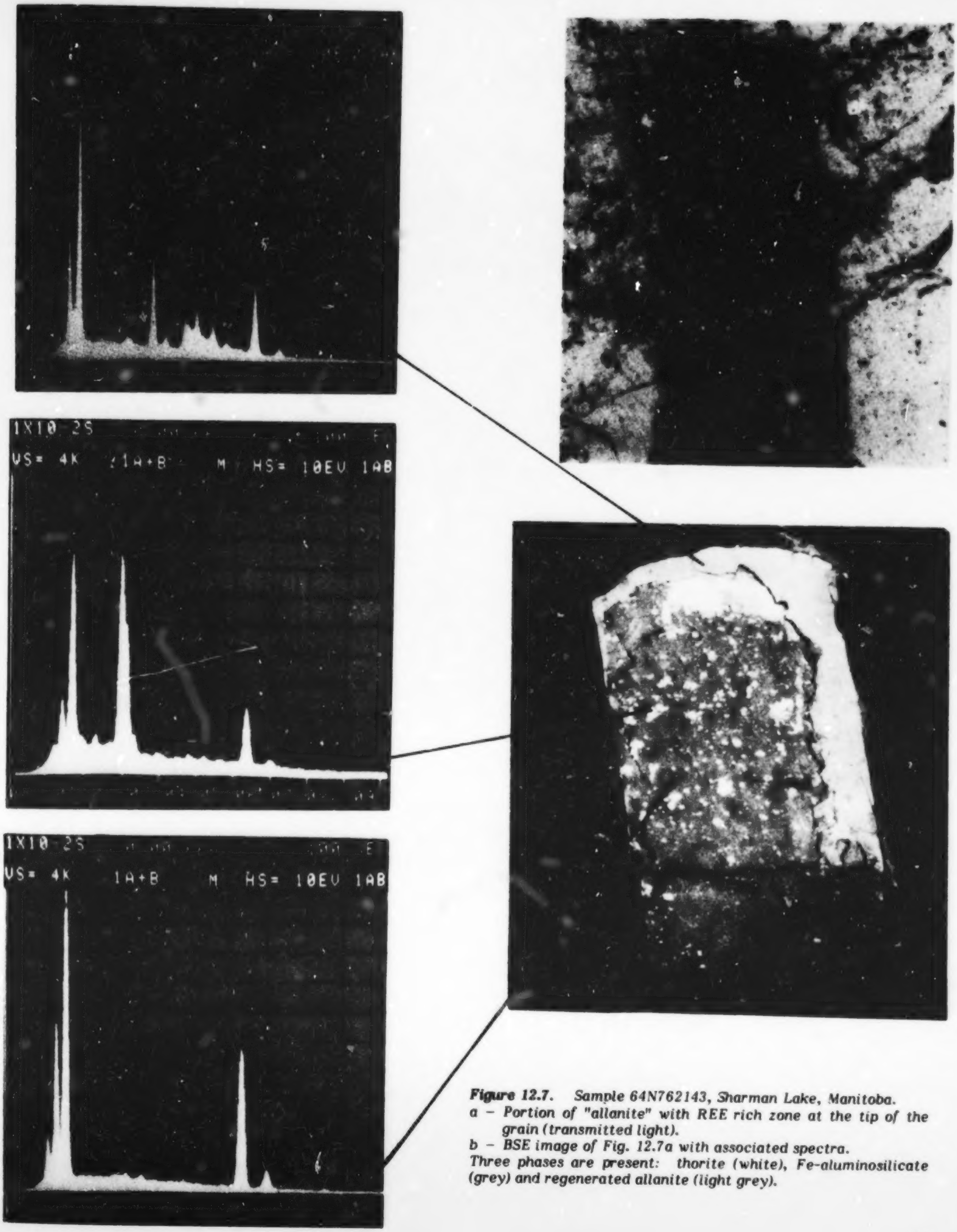
1X10-2S
VS= 4K 1A+B M HS= 10EV 1AB
1X10-2S
VS= 4K 1A+B M HS= 10EV 1AB

Figure 12.7. *Sample 64N762143, Sharman Lake, Manitoba.*
a – Portion of "allanite" with REE rich zone at the tip of the grain (transmitted light).
b – BSE image of Fig. 12.7a with associated spectra.
Three phases are present: thorite (white), Fe-aluminosilicate (grey) and regenerated allanite (light grey).

calcium has not been completely removed, a montmorillonite is produced. In other cases an illite is formed. This requires the addition of K to the system which could be present in the F and CO_2 rich fluid phase.

If all the calcium and REE's are removed and no other cations are added to the system then the remaining components may recrystallise to a chlorite, rather than a clay mineral. This is the case in some grains from Fury and Hecla Strait (Fig. 12.4) and Sharbot Lake (Fig. 12.5). In Figure 12.5 the only component left from the original A sites in the allanite is Th which has formed thorite. Ca and REE's appear to have been completely removed by the formation of synchysite. Reorganization of the remaining structure has been such that Ti is no longer stable in solid solution and ilmenite has formed at the edge of the grain (Figure 12.5b). In other samples, hematite has been found to be mixed with the aluminosilicate.

In northwest Manitoba, synchysite has not been found but the bastnaesite – montmorillonite and bastnaesite-amorphous aluminosilicate association is common in the altered allanites. The granites in which these minerals occur contain accessory interstital fluorite which also occurs within and around altered allanite (Fig. 12.6). It appears in this case that Ca^{2+} released during bastnaesitization combines with F^- to form fluorite rather than synchysite.

From the foregoing it appears that the alteration of allanite is a two stage process. The first stage is the removal of cations from the large A sites. The second stage is the reorganization of the octahedrally co-ordinated cations in the smaller M sites. The final products are dependent on the local chemical conditions and may even vary from grain to grain in a single thin section or within a single grain. This may be represented by the following reactions:

$$\underset{\text{Allanite}}{(Ce,Ca,Th)_2(Al,Fe)_3Si_3O_{12}(OH)} \xrightarrow{F,CO_2,H_2O} \qquad (1)$$

$$\underset{\text{Thorite}}{ThSiO_4} + \underset{\text{Bastnaesite}}{CeFCO_3} + \underset{\text{Montmorillonoid}}{3SiO_2 \cdot (Al,Fe)_2O_3 \cdot nH_2O} + Ca^{2+}$$

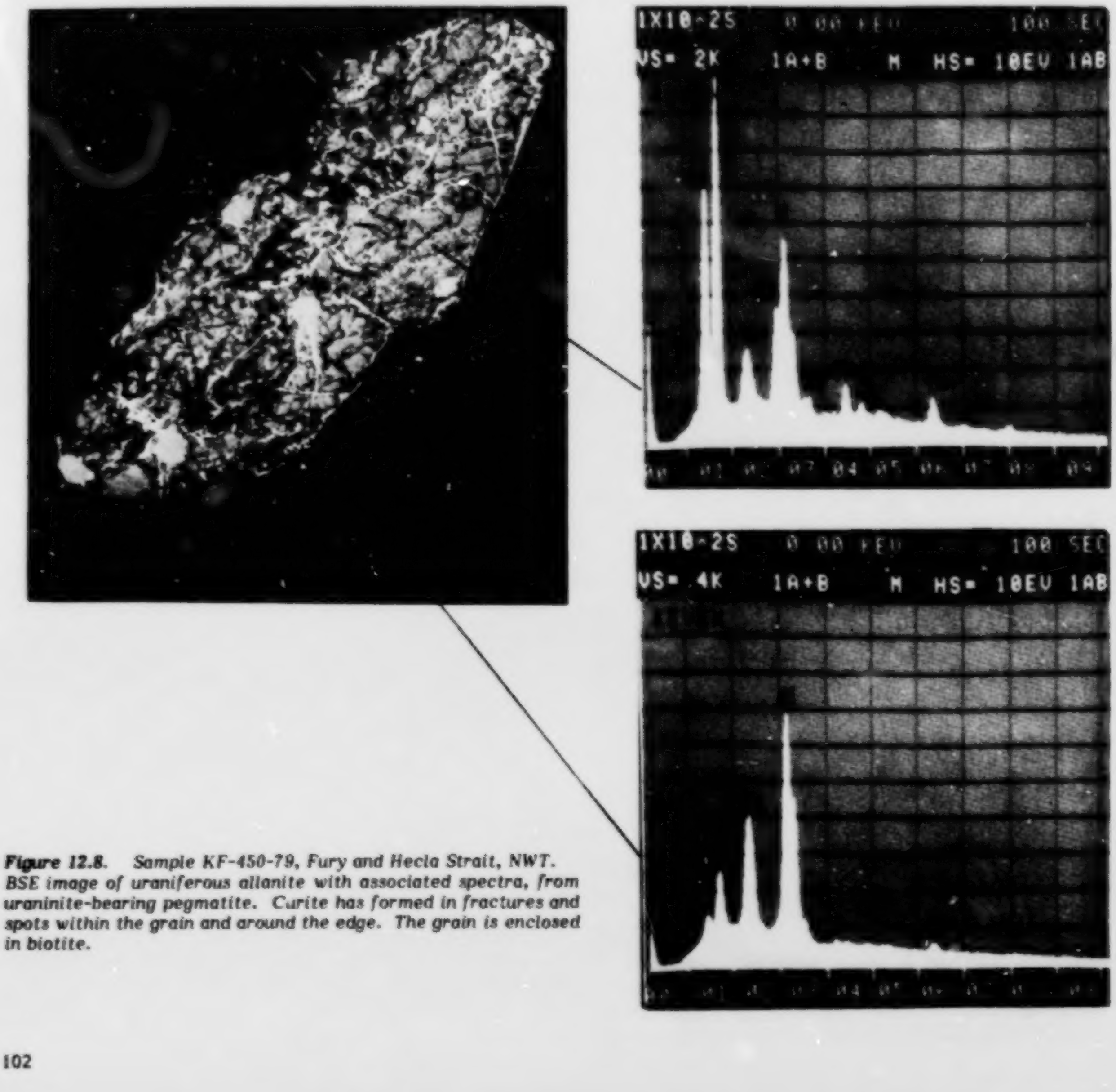

Figure 12.8. *Sample KF-450-79, Fury and Hecla Strait, NWT. BSE image of uraniferous allanite with associated spectra, from uraninite-bearing pegmatite. Curite has formed in fractures and spots within the grain and around the edge. The grain is enclosed in biotite.*

$$\xrightarrow{F,CO_2} \underset{\text{Fluorite}}{CaF_2} + \underset{\text{Synchysite}}{CeFCO_3 \cdot CaCO_3} + \underset{\text{Chamosite}}{(Fe,Al)_6(Si,Al)_4O_{10}(OH)_8} \qquad (2)$$

These reactions take place under alkaline conditions whereas in an acidic environment kaolinite ($Al_4Si_4O_{10}(OH)_8$) is the end product of bastnaesitization (Mineyev et al., 1973).

Fluorite or synchysite is not always formed. The allanite shown in Figure 12.6 is depleted in REE and it appears that bastnaesite has been removed. In some other grains where REE's were detected, they were found to be associated with Ca, Si, Al, Fe and Ti at the margin of the grain (Fig. 12.7). The spectrum shown of the light grey region at the tip of the grain is typical of the spectra obtained from broad beam analysis of many of the allanites. This material is mostly amorphous but diffuse lines corresponding to the strongest allanite and brookite lines were obtained on the X-ray diffraction photograph. This material is regenerated allanite mixed with titanium oxide. During alteration the Ti, Ca and REE's in the original allanite have migrated towards the margin (compare Fig. 12.3 and 12.5) and recombined with Al, Si and Fe to form a second generation of allanite and a titanium oxide. This allanite contains only very minor Th, most of which has remained as thorite within the primary (altered) allanite.

Behavior of Uranium

Uranium is present in trace amounts in the allanites studied but its distribution within the altered grains is variable. With one exception, the concentration of Th is very much greater than that of U as is found in other allanites in granites. Allanites from the Boulder Creek batholith, Colorado may contain up to 158 ppm U and 1.14% Th (Hickling et al., 1970). Allanite from Conway granite, New Hampshire may contain up to 656 ppm U and 2.33% Th (Smith et al., 1957). Allanites in Skye granites, Scotland contain up to 4.29% Th though it was not detected in most grains; U was not detected in any grain (Exley, 1980). In this study where the detection limit for uranium is 0.01% under ideal conditions and the absence of thorium and potassium, the presence of uranium in some spectra indicates that it has been redistributed and concentrated within the allanite when bastnaesitization occurs. In some cases uranium was found in the aluminosilicate portion of the altered allanite; in others it was found associated with thorite. Most thorites contain no detectable uranium.

Altered allanites from uraninite-bearing pegmatites associated with the granite at Fury and Hecla Strait contain a higher concentration of uranium than thorium. In some of the more uraniferous grains the uranium has formed a separate phase which has been concentrated along the grain boundary and in fractures (Fig. 12.8). This mineral, identified by XRD, is curite ($Pb_2U_5O_{17} \cdot 4H_2O$) which contains minor amounts of Si, Al and Fe as contaminants from the allanite, but does not contain Th.

While these uraniferous allanite-like phases are exceptional, and further work is required to establish their relationship to allanite with low uranium concentration, their alteration demonstrates that uranium behaves in a similar fashion to Th and REE's during the breakdown of the allanite structure. This is to be expected since the large U^{4+} ions occupy the same site as Th^{4+} and REE^{3+} ions. However during subsequent recrystallization there is a fractionation of Th, U and REE's into different minerals. As with the REE's in the formation of synchysite, the uranium tends to migrate towards the grain boundaries and fractures.

If there is insufficient uranium to form a new phase, as seems to be the case for most allanites in granites, then the liberated uranium would be complexed by carbonate and/or fluoride ions and be redistributed by the hydrothermal fluids. This is supported by studies of the Boulder Creek batholith, Colorado, where recrystallisation and later alteration to epidote has resulted in uranium and thorium loss from allanites which have undergone the most severe structural reorganization (Hickling et al., 1970).

Conclusions

Bastnaesite is only one of a number of secondary minerals which may form from the alteration of allanite by F and CO_2 rich solutions in radioactive granitic rocks. Synchysite, thorite, fluorite and regenerated allanite may also be formed from the cations contained in the larger A sites of the allanite structure. In uraniferous allanites, the uranium may also form a new phase, such as curite, during alteration. The residual allanite structure undergoes reorganisation to an amorphous aluminosilicate, a montmorillonite, an illite or a chlorite, depending on local conditions.

During bastnaesitization REE's may be removed from the allanite and redeposited as a second generation of allanite or as synchysite near or within the original allanite. Thorium tends to remain as thorite within the residual allanite. Uranium may be complexed by CO_3^{2-} and F^- ions in the hydrothermal solution and be carried out of the local system.

This process is an effective way of fractionating and redistributing radioactive and rare earth elements within granitic rocks. The scale of redistribution may be local or regional depending on the chemical and thermal gradients, and permeability of the granite - fluid system.

Acknowledgments

I thank A.C. Roberts for identifying the mineral phases in these complex mixtures and D.A. Walker for operating the SEM. K.L. Ford, W.B. Coker and B.W. Charbonneau supplied the material for this study. I thank A.G. Plant and G.J. Pringle for their critical comments.

References

Adams, J.W. and Young, E.J.
1961: Accessory bastnaesite in the Pikes Peak granite, Colorado; U.S. Geological Survey, Professional Paper 424-C, p. C292-C294.

Černý, P. and Černá, I.
1972: Bastnaesite after allanite from Rough Rock Lake, Ontario; Canadian Mineralogist, v. 11, p. 541-543.

Chandler, F.W., Charbonneau, B.W., Ciesielski, A., Maurice, Y.T., and White, S.
1980: Geological studies of the Late Precambrian supracrustal rocks and underlying granitic basement, Fury and Hecla Strait area, Baffin Island, District of Franklin; in Current Research, Part A, Geological Survey of Canada, Paper 80-1A, p. 125-132.

Coker, W.B.
1976: Geochemical follow-up studies, northwestern Manitoba; in Report of Activities, Part C, Geological Survey of Canada, Paper 76-1C, p. 263-267.

Dollase, W.A.
1971: Refinement of the crystal structures of epidote, allanite and hancockite; American Mineralogist, v. 56, p. 447-464.

Exley, R.A.

1980: Microprobe studies of REE-rich accessory minerals: implications for Skye granite petrogenesis and REE mobility in hydrothermal systems; Earth and Planetary Science Letters, v. 48, p. 97-110.

Ford, K.L. and Charbonneau, B.W.

1979: Investigation and regional significance of airborne gamma ray spectrometry patterns in the Sharbot Lake area, eastern Ontario; in Current Research, Part B, Geological Survey of Canada, Paper 79-1B, p. 208-272.

Hickling, N.L., Phair, G., Moore, R. and Rose, H.J.

1970: Boulder Creek batholith, Colorado. Part I: Allanite and its bearing upon age patterns; Geological Society of America Bulletin, v. 81, p. 1973-1994.

Mineyev, D.A., Rozanov, K.I., Smirnova, N.V., and Matrosova, T.I.

1973: Bastnaesitization products of accessory orthite; Doklady, Akademy of Sciences USSR, Earth Science Section, V. 210, p. 149-152.

Morin, J.A.

1977: Allanite in granitic rocks of the Kenora-Vermillion Bay area, northwestern Ontario; Canadian Mineralogist, v. 15, p. 297-302.

Smith, W.L., Franck, M.L., and Sherwood, A.M.

1957: Uranium and thorium in the accessory allanite of igneous rocks; American Mineralogist, v. 42, p. 367-378.

13. LABRADOR SHELF: SHELL AND TOTAL ORGANIC MATTER – ^{14}C DATE DISCREPANCIES

Project 760030

R.H. Fillon[1], I.A. Hardy, F.J.E. Wagner, J.T. Andrews[2], and H.W. Josenhans
Atlantic Geoscience Centre, Dartmouth

Fillon, R.H., Hardy, I.A., Wagner, F.J.E., Andrews, J.T., and Josenhans, H.W., Labrador shelf: shell and total organic matter – ^{14}C date discrepancies; in *Current Research, Part B, Geological Survey of Canada, Paper 81-1B, p. 105-111, 1981.*

Abstract

There are large discrepancies between shell and total organic matter ^{14}C dating of proglacial-marine sediments on the Labrador Shelf. The shell dates generally appear younger by up to 16 000 years. We suggest that total organic matter dates are locally unreliable due to contamination by reworked terrestrial carbon.

Introduction

During the last eight years numerous long piston cores (up to 11 m) have been collected from basins on the Labrador Shelf which contain thick sequences of muddy marine sediments. Early attempts at dating the cores using ^{14}C focused on the finely disseminated organic fraction which ranges from approximately 0.5 to 1.5 per cent by weight (Rashid, unpublished, 1979; Vilks and Mudie, 1978; and Vilks, 1980). The resulting carbonate-free total organic matter (t.o.m.) dates are listed in Table 13.1; locations are given in Figure 13.1. In the last three years, we have begun to accumulate additional carbon dates on shells and t.o.m. from the same sediments on the Ladrador Shelf and from similar deposits in adjacent regions (Table 13.1). This report addresses the apparent conflict that has emerged between shell and t.o.m. dates from the Labrador and Baffin Island shelves and coastal Maine.

Sediments in the Saglek Bank area and other areas of the Labrador Shelf were investigated in 1977 and 1979 using a Huntec deep-towed, high resolution, subbottom acoustic-profiling system. The Huntec records have permitted resolution of a number of mappable acoustic-morphologic (a/m) units (Fillon and Harmes, in press). The stratigraphic relationship of a/m units I to IV is summarized in Figure 13.2 which illustrates a section in the vicinity of sites 8 and 9 (Fig. 13.1). In addition to these 4 a/m units there is a veneer of surficial sediment typically <1 m thick that is not normally resolved on Huntec records. Unit II can be further subdivided into a lower, acoustically-stratified sub-unit; a middle, acoustically "transparent" sub-unit; and an upper, acoustically-stratified sub-unit.

Unit II has a draped character that closely conforms to underlying relief. Unit I is distinguished by its divergence from unit II's conformity to the underlying relief. The surficial veneer occasionally reaches thicknesses >1 m and in these instances it is acoustically resolved as a "transparent" layer above unit I. Unit III has been interpreted as a glacial till and unit IV as a glacial erosion surface (Fillon and Harmes, in press).

A comparison of the dates corresponding to each of the a/m units listed in Table 13.1, reveals a stratigraphic discrepancy between t.o.m. and shell dates, the latter in general appearing significantly younger. This is most clearly seen where we have obtained both t.o.m. and shell dates from the same cores; for example in core Hu 77-23 a shell date of 9770 B.P. falls between t.o.m. dates of 22 160 B.P. and 25 900 B.P. In dredge sample Hu 79-76 the shell and t.o.m. dates are 10 260 B.P. and 12 150 B.P. respectively while dates from a single interval in core Hu 79-94A are 7110 B.P. (shell) and 15 330 B.P. (t.o.m.). In the proglacial-marine Presumpscott Formation from Hare Bay, Maine, a t.o.m. date of 17 065 B.P. corresponds to shell dates of 12 700 B.P.

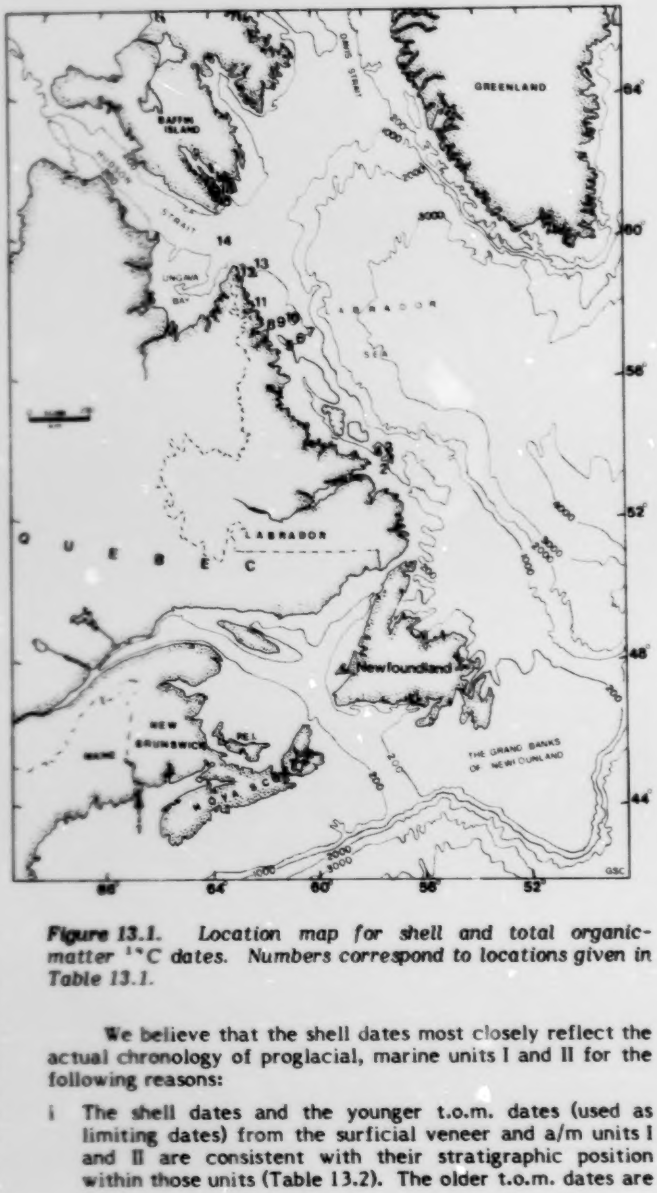

Figure 13.1. *Location map for shell and total organic-matter ^{14}C dates. Numbers correspond to locations given in Table 13.1.*

We believe that the shell dates most closely reflect the actual chronology of proglacial, marine units I and II for the following reasons:

i The shell dates and the younger t.o.m. dates (used as limiting dates) from the surficial veneer and a/m units I and II are consistent with their stratigraphic position within those units (Table 13.2). The older t.o.m. dates are not.

---

[1] Present Address: Belle W. Baruch Institute of Marine Science, University of South Carolina, Columbia, South Carolina, USA 29208

[2] Institute of Arctic and Alpine Research and Department of Geological Sciences, University of Colorado, Boulder, Colorado, USA 80302

Table 13.1

Offshore and East coast organic and shell ^{14}C dates

Site No.	Location	Piston Core No. and Sample Interval	Present Water Depth (m)	Dated Material	Laboratory Number	Age ^{14}C Years Before Present	Acoustic Units	Reference
1A	67°17.5'N 44°36.8'W Holmes Bay East Machias, Maine	Presumpscott Fm	Above Sea Level	Shells	GX-7458	12 700		J. Andrews (This Paper)
B	67°17.5'N 44°36.8'W	Presumpscott Fm	Above Sea Level	t.o.m.	GRL-4820	17 065 ± 665		"
2A	54°9.6'N 56°4.3'W Groswater Bay	79-018-094A 350-375 cm	95	t.o.m.	GSC-3126	15 330 ± 640	I	This Paper
B	54°9.6'N 56°4.3'W	79-018-094A 360-366 cm	95	Shells	GSC-3125	7 110 ± 240	I	This Paper
3A	54°36.3'N 56°10.1'W Groswater Bay Cartwright Saddle	73-027-011 65-100 cm	493	t.o.m.	GX-4942	3 370 ± 160	S.V.	G. Vilks (1980)
B	54°36.3'N 56°10.1'W	73-027-011 300-335 cm	493	t.o.m.	GX-5235	12 055 ± 405	S.V.	"
C	54°36.3'N 56°10.1'W	73-027-011 465-475 cm	493	t.o.m.	GSC-2560	11 700 ± 490	I	"
D	54°36.3'N 56°10.1'W	73-027-011 500-535 cm	493	t.o.m.	GX-5074	13 140 ± 440	I	"
E	54°36.3'N 56°10.1'W	73-027-011 700-735 cm	493	t.o.m.	GX-4944	21 030 ± 1 050	I	G. Vilks (1980)
4A	54°36.3'N 56°15.0'W Groswater Bay, Cartwright Saddle	73-027-012 50-85 cm	577	t.o.m.	GX-4935	3 320 ± 165	S.V.	G.Vilks (1980)
B	54°36.3'N 56°15.0'W	73-027-012 300-335 cm	577	t.o.m.	GX-5236	11 495 ± 455	S.V.	"
C	54°36.3'N 56°15.0'W	73-027-012 490-500 cm	577	t.o.m.	GSC-2565	13 300 ± 770	I	"
D	54°36.3'N 56°15.0'W	73-027-012 615-650 cm	577	t.o.m.	GX-5075	19 660 ± 710	I	"
E	54°36.3'N 56°15.0'W	73-027-012 800-835 cm	577	t.o.m.	GX-5237	11 695 ± 415	I	"
F	54°36.3'N 56°15.0'W	73-027-012 1001-1036 cm	577	t.o.m.	GX-4945	12 520 ± 540	I	"
5A	57°9.16'N 60°9.85'W Saglek-Okak Trough	77-012-013 400-425 cm	267	t.o.m.	GX-5416	11 555 ± 400	I	M.A. Rashid (Unpublished)
B	57°9.16'N 60°9.85'W	77-021-013 900-932 cm	267	t.o.m.	GX-5417	21 200 ± 960 860	IIu	"
6A	58°11.52'N 60°14.76'W Saglek-Okak Trough	77-021-023 100-125 cm	236	t.o.m.	GX-5418	22 160 ± 960 860	II$_1$	M.A. Rashid (Unpublished)
B	58°11.52'N 60°14.76'W	77-021-023 248-257 cm	236	Shells	GSC-3106	9 770 ± 330	II$_1$	R. Fillon and R. Harmes (In Press)
C	58°11.52'N 60°14.76'W	77-021-023 890-918 cm	236	t.o.m.	GX-5419	25 900 ± 1 590 1 325	II$_1$/III	M.A. Rashid (Unpublished)
7A	58°27.5'N 59°47.8'W Labrador – Continental Slope	77-021-029 100-120 cm	695	t.o.m.	GX-5420	5 190 ± 230	S.V.	M.A. Rashid (Unpublished)
B	58°27.5'W 59°47.8'W	77-021-029 700-725 cm	695	t.o.m.	GX-5421	25 270 ± 1 160 1 010	II$_1$/m	M.A. Rashid (Unpublished)
8	58°48.90'N 61°57.17'W Karlsefni Trough	77-021-067 82-86 cm	199	Shells	GSC-2642	6 050 ± 180	I	H. Veldhuyzen (Unpublished)
9	58°51.61'N 61°53.37'W Karlsefni Trough	77-021-068 607-618 cm	176	Shells	GSC-2686	8 380 ± 210	II u	H. Veldhuyzen (Unpublished)
10A	59°5.74'N 60°55.24'W Southern Saglek Bank	79-019-076 DREDGE	188	Shells	BETA-1455	10 260 ± 124	•III	R. Fillon and R. Harmes (In Press)
B	59°5.74'N 60°55.24'W	79-019-076 DREDGE	188	t.o.m.	BETA-1638	12 150 ± 230	•III	"

Site No.	Location	Piston Core No. and Sample Interval	Present Water Depth (m)	Dated Material	Laboratory Number	Age ^{14}C Years Before Present	Acoustic Units	Reference
11	59°48'N 64°16'W North End of Eclipse Channel, Northernmost Labrador	Locality 2 Strandline 51-3	29 m Above Sea Level	Shells	L-642	9 000 ± 200		O. Loken (1962)
12	62°07'N 74°35'W Rivière Renard – Noir Valley, SW Side Deception Bay	Sugluk, Quebec	85.6 m Above Sea Level	Shells	I-488	10 450 ± 250		B. Matthews (1967)
13	62°07'N 74°32'W Sugluk Village, Sugluk Inlet	Sugluk, Quebec	98.8 m Above Sea Level	Shells	GSC-672	7 970 ± 250		B. Matthews (1967)
14A	60°53.6'N 65°25.7'W Hudson Strait	77-021-154 102-110 cm	933 m	Shells	GSC-2698	8 730 ± 250	III m	R. Fillon and R. Harmes (In Press)
B	60°53.6'N 65°25.7'W	77-021-154 200-300 cm	933 m	Shells	GSC-2946	9 100 ± 480	III m	"
15	61°51.5'N 64°17.3'W	77-021-156 275-300 cm	487	t.o.m.	GX-5422	23 610 ± 1 600 1 330	VIIa**	M.A. Rashid (Unpublished)
16A	62°58'N 65°45'W Gold Cove, NE Coast Frobisher Bay, Baffin Island	Hall Peninsula (73-74)	6m Above Sea Level	Shells	GSC-2725	10 100 ± 110		G.H. Miller (1980)
B	62°58'N 65°45'W	Hall Peninsula (79)	6m Above Sea Level	Shells	GSC-2778	10 200 ± 210		"
17	62°10.N 67°22'W Pritzler Harbour, Baffin Island	Seashore of an Unnamed Lake	3m Above Sea Level	Shells	GSC-2026	9 380 ± 790		J.A. Lowdon et al. (1977)
18	62°38.2'N 66°35.8'W	77-021-157 75-100 cm	497	t.o.m.	GX-6352	10 685 ± 385	I	L. Osterman (1980)
19	62°50.7'N 67°03.1'W	77-021-159 500-503 cm	570	t.o.m.	GX-5423	23 820 ± 1 090 950	II_1	M.A. Rashid (Unpublished)

* Dredge haul Hu 79-76 sampled the upper 1m of compacted till comprising a/m unit III on Saglek Bank. The dated shell material was highly fragmented. Because the upper portion of unit III on the bank grades laterally into proglacial unit II in the neighbouring basins (Fillon and Harmes, in press) the shells in Hu 79-76 are considered to date a minor glacial readvance over fossiliferous unit II-like sediments. Hence the shells date an early episode of proglacial deposition and provide limits on the subsequent readvance.

**VIIa is laterally equivalent to II

t.o.m. – Total Organic Matter
GX – Kreuger Engerprises Inc., and Geochron
GRL – Geochron
GSC – W. Blake, Jr., et al., Geological Survey of Canada

ii The mollusc shells that we selected for dating meet rigorous criteria for in situ burial. Ideal specimens are those that have a restricted depth range and that lived where collected. The state of preservation can be a key as to whether the individual has been transported after death or reworked from an older deposit.

The shells dated in our study include species listed in Table 13.3. Some of the very small pelecypods (e.g. various species of **Portlandia** s.s. and its subgenus **Yoldiella**) and larger ones (species of **Nuculana** and **Astarte** to name two) close very tightly and tend to remain intact long after death if not disturbed. A majority of genera in our samples, however, become separated readily. Therefore, fresh-appearing single valves, particularly ones that can be paired, denote essentially in situ burial. Worn single valves and worn, rounded fragments point to material that has probably been transported. The rigours of coring and processing may produce broken shells but these are easily distinguished from transported fragments by their nacreous lustre, sharp angles, parts of hinges still together, intact periostracum, and their generally unworn appearance.

The shells from samples dated in this study include a high proportion of whole valves. The fragments for the most part exhibit sharp breaks with no apparent sign of abrasion and frequently the periostracum and nacreous lustre remain intact. This considered along with the wide range of valve sizes and the presence of both robust and delicate specimens in the assemblages (see Table 13.3), suggests that the shells have not been hydraulically sorted after death. A single articulated specimen which appears to have resisted the shell concentration procedure was found in sample Hu 77-23 (200-290 cm); however, the valves parted after slight additional handling of the storage container. We conclude therefore that the bulk of the dated shell material was not transported for any great distance along the seafloor and was apparently buried in situ. Most of the fragmentation encountered is attributable to disturbance during removal of sediment samples from core liners and to the disaggregation and sieving of samples during the shell recovery process. X-ray diffraction measurements were made on some of the shells indicating an aragonitic composition which strongly suggests that the shell material has not been recrystallized (W. Blake, Jr. written communication, 1980).

Table 13.2

Shell and limiting total organic matter (t.o.m.) ^{14}C dates from the Labrador Shelf

Stratigraphic Units	Dated Material	Laboratory Number	Age ^{14}C Yr. B.P.	Core Number	Inferred Age Range of Units (Yr. B.P.) (Median Age Estimates)
Surficial Veneer	t.o.m.	GX-4942	≤ 3 370 ± 160	Hu 73-11	6 200 – Ca. 2 000 (4 100)
	t.o.m.	GX-4935	≤ 3 320 ± 165	Hu 73-12	
	t.o.m.	GX-5420	≤ 5 190 ± 230	Hu 77-29	
	shell	GSC-2642	6 050 ± 180	Hu 77-67	
Unit I	t.o.m.	GSC-3126	≤ 15 330 ± 640	Hu 79-94A	8 000 – 6 200 (7 100)
	shell	GSC-3125	7 110 ± 240	Hu 79-94A	
	t.o.m.	GX-5416	≤ 11 555 ± 400	Hu 77-13	
Unit II – (upper)	shell	GSC-2686	8 380 ± 210	Hu 77-68	10 400 – 8 000 (9 200)
– (middle)	shell	GSC-2698	8 730 ± 250	Hu 77-154	
	shell	GSC-2946	9 100 ± 480	Hu 77-154	
	shell	GSC-3106	9 770 ± 330	Hu 77-23	
– (lower)	t.o.m.	Beta-1638	*≤ 12 150 ± 230	Hu 79-76	
	shell	Beta-1455	* 10 260 ± 124	Hu 79-76	

* From till (unit III) which constitutes a glacial readvance facies corresponding to the lower part of unit II.

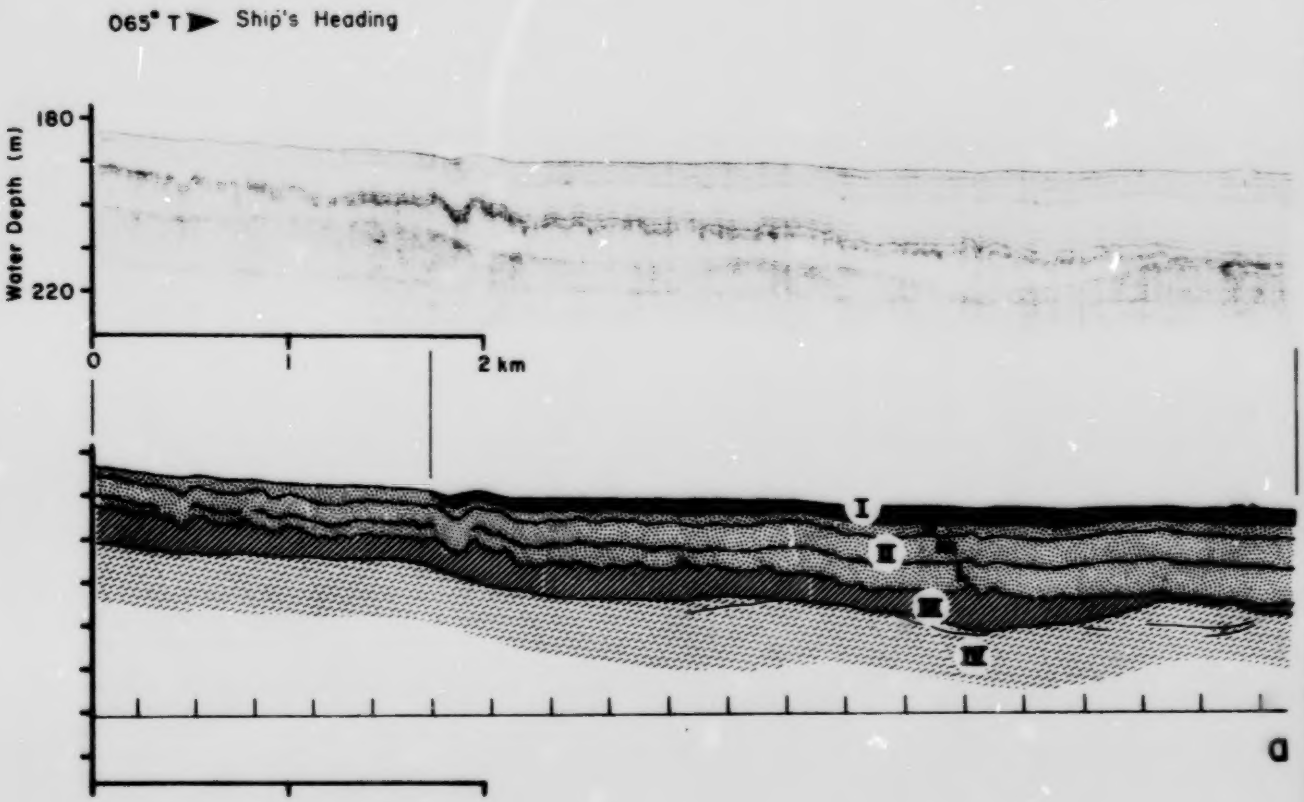

Figure 13.2. Huntec deep-tow record from western Karlsefni Trough and a tracing which delimits acoustic/morphologic units I, II, III and IV at the surface and in the subsurface. This profile is situated in the vicinity of sites 8 and 9 (Fig. 13.1).

Table 13.3

Mollusc species used as source material for radiocarbon dating (see Table 13.2) and corresponding depth ranges

Core No. (interval – cm)	Water Depth (m)	Mollusc Species	Depth Range (minimum-maximum) (m)	References
Hu 77-68 (607-618)	176	Chlamys islandica *	2 -320	Abbott, 1974
Hu 77-67 (82-86)	199	Macoma calcarea	4 -360	Bernard, 1979; Vilks et al. 1981
		Tachyrhynchus erosus	13 -355	Macpherson, 1971; Vilks et al. 1981
		Margarites groenlandicus	9 -512	Abbott, 1974; Macpherson, 1971
Hu 77-23 (248-257)	236	Nuculana sp.		
		Megayoldia thraciaeformis	19 -351	Ockelmann, 1958; Vilks et ai. 1981
		Axinopsida orbiculata	2 -296	Bernard, 1979; Wagner, 1977
		Palliolum imbrifer	66 -836	Ockelmann, 1958
		Macoma sp. (calcarea)	4 -360	Bernard, 1978; Vilks et al. 1981
Hu 77-23 (200-290)		Nuculana tenuisulcata	0 -274	Abhott, 1974
		Yoldia sp.		
		Portlandia (Yoldiella) lenticula	26 -360	Bernard, 1979
		Arctinula greenlandica	19 -2560	Bernard, 1979
		Thyasira equalis	6 -2810	Ockelmann, 1958; Wagner, 1975
		Astarte sp.		
		Clinocardium ciliatum	2 -677	Ockelmann, 1958
		Macoma sp.		
Hu 79-76 (Dredge)	188	Portlandia (Yoldiella) lenticula	26 -360	Bernard, 1979
		Astarte sp.		
		Clinocardium ciliatum	2 -677	Ockelmann, 1958
		Hiatella arctica	5 -159	Bernard, 1979; Ockelmann, 1958
		Nucula tenuis	21 -256	Vilks et al. 1981
		Tachyrhynchus sp.		
		Chlamys islandica	2 -320	Abbott, 1974
Hu 79-94A (360-366)	95	Clinocardium ciliatum	2 -677	Ockelmann, 1958
Hu 77-154 (102-300)	933	Nuculana pernula	23 -455	Bernard, 1979; Wagner, 1979

* All mollusc species but one were identified by F.J.E. Wagner, the exception being the Hu 77-68 sample identified by V. Conde.

Species of restricted range are more useful for determining date of deposition than are those that may be found living, for example, between 50 and 1000 m depth. Shallow water species may be carried into deeper waters but the reverse is unlikely. A data file is currently being compiled by F.J.E. Wagner incorporating ecological information derived from BIO cruise collections. The aim of this file is to go beyond what is available in the literature by presenting optimum as well as total depth ranges for the various species.

All of the species identified in our samples have depth ranges appropriate to the present-day water depths at the sample sites. Hence, we see no reason to suspect transport from shallower areas for example by freezing onto grounded sea ice which then drifts over deeper water and melts.

Implications

The data summarized in Tables 13.1 and 13.3 lead us to conclude that the older t.o.m. dates reflect contamination by "old", reworked organic matter. Assuming that this reworked carbon was "dead", i.e. without detectable ^{14}C, the amount of contamination required to produce the apparent age differences between t.o.m. and shell dates can be estimated (Fig. 13.3). Estimates of contamination are shown for single-core and single sample-interval shell-t.o.m. data sets (solid dots). For other t.o.m. dates (open dots), contamination is estimated using inferred median ages (Table 13.2) for the surficial veneer and a/m units I and II.

Contamination estimates range from 11 per cent in the surficial veneer to 86 per cent in unit II. In support of these estimates P.A. Mudie (personal communication, 1980) has observed relatively low concentrations of allochthonous palynomorphs and higher concentrations of coal and highly reflective (altered) vitrinite in core Hu 77-23 (unit II). Core intervals 380-382 cm and 700-702 cm were found to contain minor Quaternary pollen and unaltered wood fragments. H. Veldhuyzen (written communication, 1980) has also noted up to 5 per cent fine grained (<63 µ) lithic carbonate in unit II (cores Hu 77-64 and Hu 77-65). Carbonates and fine grained clastic sedimentary lithologies typically contain 2-10 per cent organic matter by weight. Off northern Labrador the source rocks for these lithic sediments are likely to be the Ordovician through Devonian limestones and shales of the Ungava Bay, Hudson Strait and Foxe Basin lowland.

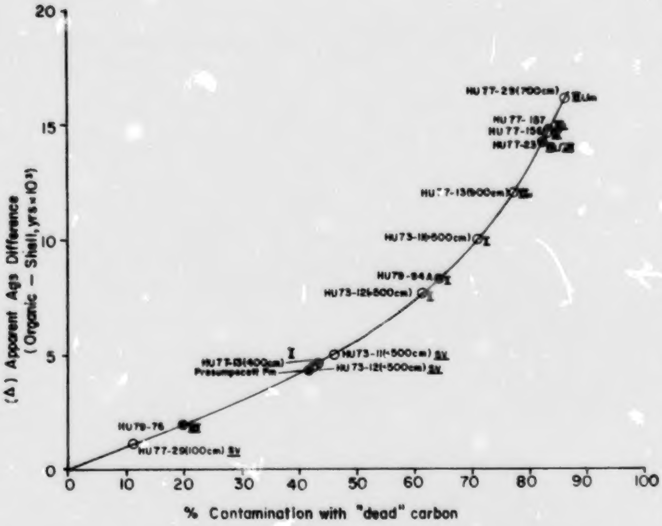

Figure 13.3 *Nomogram for estimating contamination by "old" carbon, that is carbon with no detectable* ^{14}C. *Δ equals difference between an assumed correct age based on* ^{14}C *dated shells and significantly older dates based on total organic-matter (t.o.m.). The curve shape has been derived using the Libby half-life of 5568 years. Solid dots indicate contamination estimates based on shell − t.o.m. data sets from individual samples. Open dots indicate differences between other t.o.m. dates and the median ages (Table 13.2) of the acoustic-morphological units in which these samples are located. Cores Hu 73-11 and Hu 73-12 (Table 13.1) have multiple t.o.m. dates in both the exceptionally thick surficial veneer (<500 cm) and acoustic-morphologic unit I (>500 cm). For simplicity in this figure the plotted age differences were calculated from averages of all the* ^{14}C *dates in each unit. Roman numerals refer to acoustic-morphologic units (Fig. 13.2). SV = surficial veneer.*

Older t.o.m. dates from proglacial sediments have been obtained elsewhere along the east coast of Canada and the USA (e.g. Bothner, 1980; Dale and Haworth, 1980). Paralleling our results Martel and LaSalle (1977) found that the organic matter of soils and marine clays in the region occupied by the Late Wisconsin Champlain Sea near Quebec City is about 3000 years older than expected from numerous shell dates. They cite an even greater discrepancy of about 6000 years in the case of an organic date of 16 170 B.P. on Champlain Sea muds in the Montreal area.

Our data strongly suggest that the influx of reworked older carbon during deglaciation generally overwhelmed autochthonous organic carbon input in our study areas. In general it appears that the amount of contamination was highest during the deposition on unit II. This may have been a function of a change in the source of allochthonous carbon and/or an increased production of autochthonous carbon with time. The latter however, is not indicated by organic carbon percentages (M.A. Rashid, written communication, 1980) which show little or no correlation with t.o.m. ages.

It is also apparent from Figure 13.3 that samples with the highest contamination are from sites on the southeast Baffin and northern Labrador shelves, while the majority of the less contaminated samples are from southern areas. The distribution and thickness of unit I and the input of autochthonous carbon both are a function of latitude (Fig. 13.3). This may be attributable to higher marine organic productivity at lower latitudes. Warmer southern waters would also tend to accelerate the destruction and recycling of allochthonous organic matter into the marine ecosystem.

To further quantify contamination we are presently examining the amino acid spectra of crushed rock and proglacial sediment samples for comparison with amino acid spectra of molluscan remains through a contractual arrangement with G.H. Miller (INSTAAR). We are also actively acquiring additional sets of shell and t.o.m. ^{14}C dates and are attempting to concentrate and ^{14}C-date calcareous foraminifera.

Acknowledgments

We would like to thank J.-P. Guilbault and C.T. Schafer for reviewing the manuscript and for helpful discussion. M.A. Rashid kindly provided unpublished ^{14}C dates from Saglek Bank. S. Toth drafted the figures.

References

Abbott, R.T.
1974: American Seashells (2nd. Edition). D. van Nostrand Company Inc., New York, N.Y.

Bernard, F.R.
1979: Bivalve mollusks of the western Beaufort Sea; Natural History Museum of Los Angeles County, Contributions in Science, No. 313, 80 p.

Bothner, M.H.
1980: Upper Wisconsinan till recovered on the continental shelf southeast of New England; Science, v. 210, p. 423-425.

Dale, C.T. and Haworth, R.T.
1979: High resolution reflection seismology studies in Late Quaternary sediments of the northeast Newfoundland continental shelf; in Current Research, Part B, Geological Survey of Canada, Paper 79-1B, p. 357-364.

Fillon, R.H. and Harmes, R.A.
1981: Northern Labrador Shelf Glaciation: Chronology and Limits; Canadian Journal of Earth Sciences. (in press)

Løken, O.
1962: The late-glacial and postglacial emergence and the deglaciation of northernmost Labrador; Geographical Bulletin, No. 17, p. 23-56.

Lowdon, J.A., Robertson, T.M., and Blake, W., Jr.
1977: Geological Survey of Canada, Radiocarbon Dates XVII; Geological Survey of Canada, Paper 77-7, p. 18.

Macpherson, E.
1971: The marine molluscs of Arctic Canada; National Museum of Natural Sciences, Publications in Biological Oceanography, No. 3, 149 p.

Martel, Y.A. and LaSalle, P.
1977: La datation au radiocarbone de la matière organique de quelques sols du Québec; Géographic physique et Quaterniere, v. 31, p. 373-378.

Matthews, B.
1967: Late Quaternary land emergence in Northern Ungava, Quebec; Arctic, v. 20, p. 176-202.

Miller, G.H.
1980: Late Pleistocene glaciation of southern Baffin Island, N.W.T., Canada; Geological Society of America Bulletin, v. 91, p. 399-405.

Ockelmann, K.W.
1958: Marine Lamellibranchiata; Meddelelser om Grønland; Bd. 122, Nr. 4, 256 p.

Osterman, L.E.
1980: Foraminiferal biostratigraphy and lithostratigraphy of a Late Quaternary core from outer Frobisher Bay, Baffin Island, N.W.T., Canada; American Quaternary Association 6th Biennial Meeting Abstracts and Program 18-20 August 1980, p. 153.

Vilks, G.
1980: Postglacial basin sedimentation on Labrador Shelf; Geological Survey of Canada, Paper 78-28, 28 p.

Vilks, G. and Mudie, P.J.
1978: Early deglaciation of the Labrador Shelf; Science, v. 202, p. 1181-1183.

Vilks, G., Deonarine, B., Wagner, F.J.E. and Winters, G.V.
1981: Foraminifera and Mollusca in surface sediments of Southeastern Labrador Shelf and Lake Melville, Canada; Geological Society of America Bulletin (in press).

Wagner, F.J.E.
1975: Mollusca of the Strait of Canso area; Geological Survey of Canada, Paper 75-23, 29 p.

1977: Recent mollusc distribution patterns and palaeobathymetry, southeastern Beaufort Sea; Canadian Journal of Earth Sciences, v. 14, no. 9, p. 2013-2028.

1979: Distribution of pelecypods and gastropods in the Bay of Fundy and eastern Gulf of Maine; Proceedings of the Nova Scotia Institute of Science, v. 29, p. 447-464.

14.

GEOLOGY OF TEBESJUAK LAKE MAP AREA, DISTRICT OF KEEWATIN: A PROGRESS REPORT

Project 780008

A.N. LeCheminant, T.R. Iannelli[1], B. Zaitlin[2], and A.R. Miller[3]
Precambrian Geology Division

LeCheminant, A.N., Iannelli, T.R., Zaitlin, B., and Miller, A.R., Geology of Tebesjuak Lake map area, District of Keewatin: A progress report; in Current Research, Part B, Geological Survey of Canada, Paper 81-1B, p. 113-128, 1981.

Abstract

Dubawnt Group continental sedimentary and volcanic rocks in fault-controlled basins underlie more than one third of the Tebesjuak Lake map area. Dubawnt successions rest on an Archean-Aphebian basement complex that has been subdivided into three lithostructural domains. Predominantly granodioritic central and southeastern gneiss domains are tentatively interpreted as Archean basement that has been subject to variable Aphebian remobilization and subsequent cataclasis. Less deformed and more potassic intrusive rocks of the Pukiq domain may be a mix of late Archean and Aphebian components. Pre-Dubawnt Group shelf carbonate-quartzite sequences occur only in small isolated areas within the Pukiq domain.

Christopher Island Formation sequences at the base of the Dubawnt Group record a complicated interplay between processes of subaerial alkaline volcanism and alluvial fan to fluviatile sedimentation. Overlying redbed infill sequences of the Kunwak Formation comprise alluvial fan and braidplain deposits that are in turn succeeded by Pitz Formation potassic silica-rich rhyolites. These rhyolite successions are probably remnants of the volcanic roof above epizonal granite plutons that intrude the basement complex and Dubawnt Group.

Composite plutons of rapakivi granite, the youngest major granitic suite, were emplaced along or parallel to the eastern margin of the Pukiq domain and delineate a broad, low-amplitude, Bouguer gravity low. The McRae Lake dyke, a multiphase basic intrusion that intrudes the rapakivi suite has a K-Ar age of 1735 ± 52 Ma.

Minor epigenetic fracture-controlled uranium mineralization occurs in lower formations of the Dubawnt Group and in cataclastic rocks adjacent to basal unconformities or faulted Dubawnt successions. Anomalous radioactivity was noted in Pitz Formation flow banded F-rich rhyolites and in a phosphatic zone near the base of an isolated succession of Thelon Formation quartz arenite.

Introduction

Mapping of the Tebesjuak Lake map area (65 O), at a scale of 1:250 000, was completed during the 1980 field season. This preliminary paper augments previous reports (LeCheminant et al., 1979a, 1980) and deals primarily with western and northern parts of the area. In addition, detailed stratigraphic and sedimentologic data collected from Dubawnt Group redbed sequences are used to interpret depositional environments.

More than one third of the map area is underlain by continental sedimentary and volcanic rocks of the Late Aphebian and Paleohelikian Dubawnt Group (Donaldson, 1965; Blake, 1980). Dubawnt successions in fault-controlled basins unconformably overlie an Archean-Aphebian basement complex of diverse character and origin. Alkaline syenite bodies, granite plutons and several small basic intrusions are emplaced in the basement complex and Dubawnt Group.

A broad, irregular belt of Dubawnt Group rocks extends from south of Mallery Lake to east of Tulemalu Lake (Fig. 14.1). This belt is part of a complex structural depression, the Baker Lake Basin, that extends more than 200 km east-northeast of the map area (LeCheminant et al., 1979b). Mapping in 1980 established northern and northwestern limits of the basin. The Pamiutuq Granite and plutons of rapakivi granite intrude rocks of the basin in the southwest (Fig. 14.2). Isolated successions of Christopher Island Formation rocks west and northwest of Tulemalu Lake may be remnants of a southwestern extension of the Baker Lake Basin.

Dubawnt Group strata are also exposed within tilted fault blocks north and southwest of Pukiq Lake and in a belt 75 km long and up to 14 km wide that extends from Wharton Lake to southeast of Pukiq Lake. This basin, herein termed the Wharton Basin, is tilted to the northeast where it is bounded by major faults. Southern parts of this basin are intruded by rapakivi granite.

Archean and Aphebian Basement Complex

Pre-Dubawnt Group basement underlies slightly more than one third of the map area. Basement rocks are poorly exposed and details of their origins are obscured by later tectonic and igneous events. Lithological and structural characteristics have been used to subdivide the basement complex into three domains: (1) a southeastern domain of mafic and felsic gneisses, (2) a central domain of granodioritic and tonalitic gneisses with relict bands of supracrustal rocks, and (3) a western domain of less deformed and more potassic rocks around Pukiq Lake, informally named the Pukiq domain.

All three domains are cut by syenite and biotite lamprophyre dykes with predominantly easterly trends. These dykes are significantly less numerous in the Pukiq domain. An age of 1821 ± 34 Ma (K-Ar, biotite) has been obtained from an undeformed lamprophyre dyke trending 070° that intrudes central domain granodioritic gneisses south of McRae Lake and west of the Kunwak River. Younger quartz-feldspar porphyry dykes, related to the rapakivi granite suite, occur throughout southwestern parts of the Pukiq and central domains.

---

[1] University of Western Ontario, London, Ontario

[2] University of Ottawa, Ottawa, Ontario

[3] Economic Geology Division

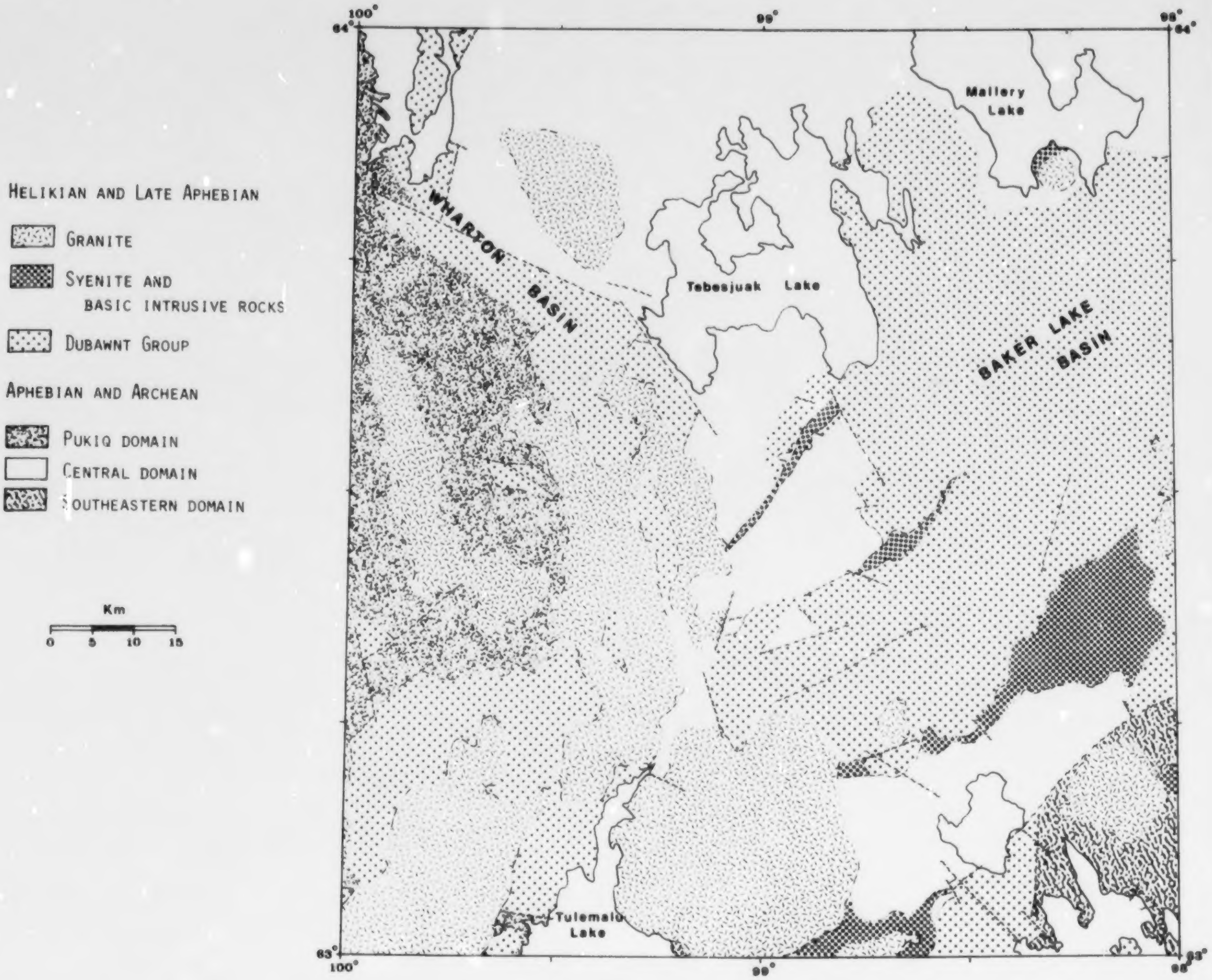
HELIKIAN AND LATE APHEBIAN
GRANITE
SYENITE AND BASIC INTRUSIVE ROCKS
DUBAWNT GROUP
APHEBIAN AND ARCHEAN
PUKIQ DOMAIN
CENTRAL DOMAIN
SOUTHEASTERN DOMAIN
Km
0
5
10
15
100°
99°
98°
64°
63°
Mallery Lake
Tebesjuak Lake
WHARTON BASIN
BAKER LAKE BASIN
Tulemalu Lake

Figure 14.1. *Distribution of major rocks units and lithostructural domains in the Tebesjuak Lake map area.*

Southeastern Domain

The small southeastern domain around Nutarawit Lake comprises interbanded leucogranitic and hornblende-plagioclase-rich gneisses, augen granite gneiss and gneissic granite and granodiorite (LeCheminant et al., 1979a, 1980). Complexity of fold patterns and degree of deformation vary considerably. The gneisses have been affected by amphibolite grade metamorphism and at least two periods of penetrative deformation. Retrograde greenschist facies metamorphism is associated with narrow shear zones that record a nonpenetrative third phase of deformation. The domain is unconformably overlain by faulted wedges of Dubawnt Group rocks and to the northwest it terminates against a major northeast trending fault. The structural-metamorphic history and lithologic mix of the domain is essentially identical to the Thirty Mile domain northeast of the map area (LeCheminant et al., 1979b).

Central Domain

Orthogneisses with relict bands of supracrustal rocks occupy this large domain extending from Mallery Lake to just east of Wharton Lake and south to Tebesjuak and McRae lakes (Fig. 14.1, 14.2). Isolated remnants are exposed along the Kunwak River north of Tulemalu Lake. A 10-15 km wide gneiss belt north and east of "P.O." Lake and gneisses east of the map area around Princess Mary Lake (LeCheminant et al., 1979b, 1980) are considered part of this domain.

Layered to weakly foliated white-weathering granodioritic and tonalitic gneisses that characterize this domain are infolded with thin discontinuous bands of amphibolite, quartzitic paragneiss, rare iron formation and garnet-muscovite schist. Regional foliation trends (Fig. 14.2) reflect folding of first phase foliation by second phase tight to subisoclinal upright northeasterly trending folds and third phase open northwesterly trending folds. Third phase folds are of minor importance, except near McRae Lake. Compositional layering in the supracrustal rocks is essentially parallel to first phase biotite-hornblende foliation within enclosing gneisses. However, relict layering in amphibolite rafts preserved in zones of agmatite suggest some supracrustal rocks have an earlier deformation history.

Mineral parageneses in the supracrustal rocks indicate regional amphibolite facies metamorphism. North of Tebesjuak Lake, and north and west of Mallery Lake, a region of upper amphibolite and possibly granulite facies metamorphism is suggested by extensive migmatite and hornblende-plagioclase-garnet-clinopyroxene-quartz assemblage in metavolcanic rocks. Granoblastic textures, typical of most rocks in the domain, imply metamorphic recrystallization outlasted deformation. In many areas irregular dykes of white granite pegmatite crosscut the gneisses.

Greenschist facies retrogression and late stage cataclasis are not prominent features of the central domain except near faulted contacts with Dubawnt Group rocks. The most extensive zone of cataclasis is adjacent to major faults along the eastern and northern boundaries of the Wharton basin. Microbreccia, cataclasite, mylonite and mylonite gneiss (classification after Higgins, 1971) within this zone probably were derived in large part from the granodioritic gneisses and metamorphosed supracrustal rocks. Local units of coarse grained potash feldspar augen gneiss may be derived from younger intrusive rocks. Zoned pseudotachylite veins occur in mylonite and mylonite gneiss adjacent to the east-northeast trending fault that truncates Kunwak Formation strata west of McRae Lake. East-southeast trending mylonite zones west of Tebesjuak Lake bounding the Wharton Basin underwent repeated movement, the youngest of which postdates Thelon Formation deposition.

Pukiq Domain

Basement rocks south and west of the Wharton Basin comprise lithologies distinctly different from the two previously described gneiss terranes. The three lithologies distinguished in Figure 14.2 are potash feldspar augen gneiss, gneissic to weakly foliated porphyritic intrusive rocks and weakly foliated quartz-feldspar porphyry. Together these units comprise a poorly exposed domain that is covered by an extensive veneer of Christopher Island Formation and Kunwak Formation rocks and intruded by rapakivi granites.

Potash feldspar augen gneiss is a distinctive, relatively homogeneous, unit characterized by pink potash feldspar augen to 5 cm and smaller white plagioclase augen. Feldspar augen are set in a crushed matrix with a streaky biotite-hornblende foliation. Typical colour index is 10-15, quartz content is about 10-20 per cent, and compositions range from quartz syenite to quartz monzonite with minor granite. Similar augen gneisses are well exposed to the southwest in the Kamilukuak map area (Tella and Eade, 1980; Tella et al., 1981) where locally preserved massive porphyritic phases suggest an igneous protolith.

The second major unit in the Pukiq domain is a heterogeneous mixture of porphyritic intrusive rocks and cataclastic rocks ranging in composition from granite to diorite with quartz syenite and quartz monzonite phases predominant. The intrusive rocks are less deformed and finer grained than the augen gneisses and generally contain feldspar and hornblende phenocrysts. Contacts between various lithologies are, for the most part, narrow cataclastic zones and faults. Admixtures of gneissic, weakly foliated and massive variants occur on all scales. Small bodies of relatively homogeneous monzodiorite and diorite account for local aeromagnetic highs within this unit (see GSC map 7842G). Relative ages of the intrusions are uncertain and subdivision of the unit into individual intrusive bodies is possible in only a few places.

A weakly foliated quartz-feldspar porphyry, the third unit in the Pukiq domain, is exposed in areas north and southwest of Pukiq Lake. The pinkish grey porphyry contains 1-2 mm quartz, plagioclase and potash feldspar phenocrysts set in a very fine grained quartzofeldspathic matrix with minor biotite as the only primary ferromagnesian mineral. Weak foliation is generally attributed to shearing but in several exposures the porphyry appears to have a primary flow banding. The unit is probably derived from acid volcanic or hypabyssal intrusive rocks which may be cogenetic with quartz syenites of the porphyritic intrusive unit.

The Pukiq domain is cut by easterly, northeasterly and northwesterly faults. Adjacent to fault zones and near the basal unconformity with the Christopher Island Formation the basement rocks are fractured and brecciated and chlorite and epidote replace original ferromagnesian minerals. Minor epigenetic fracture-controlled uranium mineralization occurs in several of these zones (see economic geology section).

Discussion

The predominantly granodioritic and tonalitic central and southeastern gneiss domains are tentatively interpreted as Archean basement that has been subject to variable Aphebian remobilization and subsequent cataclasis. The less deformed and more potassic intrusive rocks of the Pukiq domain may be a mix of late Archean and Aphebian components. Pre-Dubawnt Group shelf carbonate-quartzite sequences described below are spatially related to the Pukiq domain out field relations are insufficient to prove the inferred basement-cover relationship.

Major structural discontinuities that separate the three basement domains are primarily syn- or post-Dubawnt Group faults that in several instances were the loci for emplacement of syenite or granite plutons. Discontinuities may follow pre-existing Archean or early Proterozoic zones of weakness and some underwent repeated movement. The possibility that the domains did not originate in their present relative position but have been transposed by significant transcurrent faulting cannot be properly evaluated until information is available to determine the amount and sense of cumulative movements on the faults.

Quartzite-bearing Successions

Small isolated areas near Wharton and Pukiq lakes are underlain by metasedimentary rocks lithologically similar to those of the Hurwitz or Amer groups (Bell, 1970; Heywood, 1977). The sequence exposed west of Wharton Lake (Fig. 14.2) is part of a narrow northeast trending belt that extends southwest and northeast of the map area (Wright, 1967). Southeast dipping units within the map area comprise white to pink quartzite, subarkosic arenite and quartz-rich conglomerate. Lithic clasts are jasper and deformed granitoid rocks. The parallel bedded to planar crossbedded arenites are cemented by quartz, hematite and sericite. No contacts with other units are exposed in the map area. Quartzite clasts in Kunwak Formation redbed sequences on islands in Wharton Lake imply the redbeds unconformably overlie the succession.

Another quartzite-bearing succession, interbedded with calc-silicate rocks, outcrops in a small region 4 km northeast of Pukiq Lake (Fig. 14.2, 14.3). This succession is overlain unconformably by Dubawnt Group alkaline volcanic rocks to the east and, elsewhere, is in contact with intrusive fluorite-bearing rapakivi granite. Diopside-rich assemblages

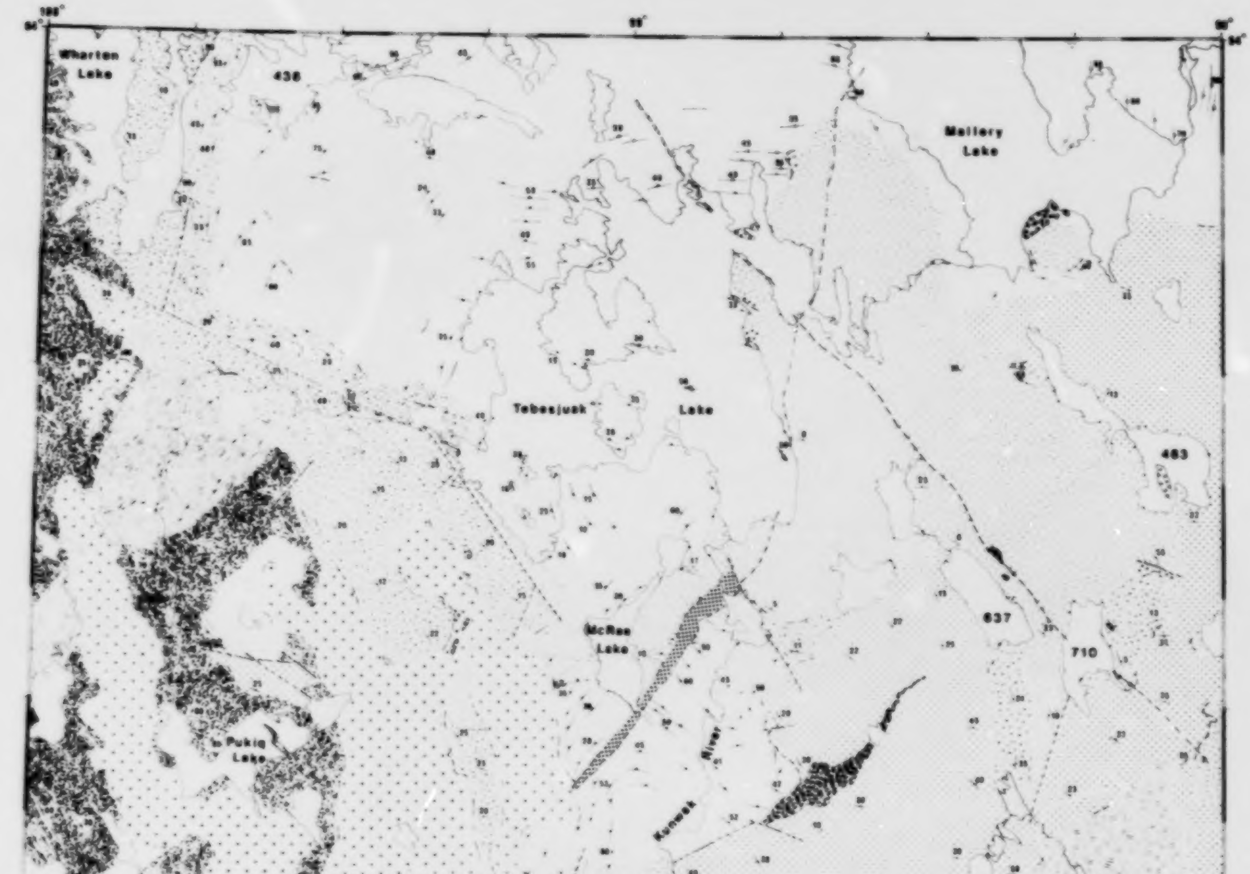
100°
64°
99°
98°
64°
Wharton Lake
436
Mallery Lake
Tebesjuak Lake
463
McRae Lake
637
710
Pukiq Lake
Kunwak River
630
P.O. Lake
Tulemalu Lake
Nutarawit Lake
63°
100°
99°
98°
63°
Km
5
0
5
10

characterize a narrow magmatic skarn zone developed along the granite contact. However, primary textures, including stromatolites, can still be recognized within 5 m of the contact.

The succession northeast of Pukiq Lake consists of massive grey quartzite overlain by a mixed zone of thinly laminated quartzite and calc-silicate rocks that grade upward into a stromatolite-bearing calc-silicate unit (Fig. 14.3). Stromatolites are discrete or laterally linked columns, elliptical in plan, with southeast-northwest elongations. Columns widen upward and never exceed 5 cm in height or 8 cm in diameter. Internal structures have been destroyed by recrystallization. Low relief columnar stromatolites are overlain by irregular, stratiform, laminated algal mats that also occur in overlying calc-silicate units. Interbedded quartzite units up to 35 m thick are predominantly thinly laminated but also contain crosslamination, planar crossbeds and ripple marks.

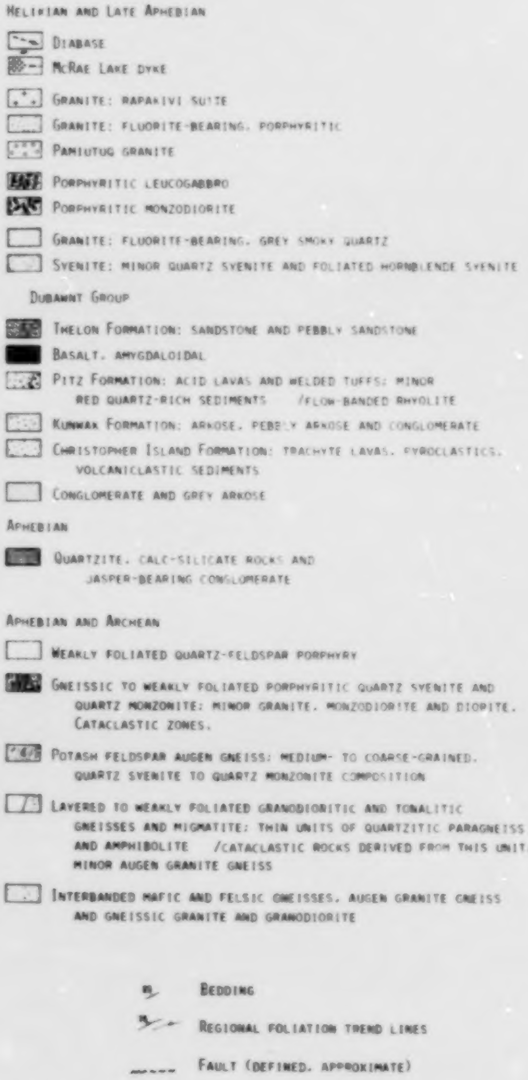
Helikian and Late Aphebian
Diabase
McRae Lake dyke
Granite: rapakivi suite
Granite: fluorite-bearing, porphyritic
Pamiutuq granite
Porphyritic leucogabbro
Porphyritic monzodiorite
Granite: fluorite-bearing, grey smoky quartz
Syenite: minor quartz syenite and foliated hornblende syenite
Dubawnt Group
Thelon Formation: sandstone and pebbly sandstone
Basalt, amygdaloidal
Pitz Formation: acid lavas and welded tuffs; minor red quartz-rich sediments /flow-banded rhyolite
Kunwak Formation: arkose, pebbly arkose and conglomerate
Christopher Island Formation: trachyte lavas, pyroclastics, volcaniclastic sediments
Conglomerate and grey arkose
Aphebian
Quartzite, calc-silicate rocks and jasper-bearing conglomerate
Aphebian and Archean
Weakly foliated quartz-feldspar porphyry
Gneissic to weakly foliated porphyritic quartz syenite and quartz monzonite; minor granite, monzodiorite and diorite. Cataclastic zones.
Potash feldspar augen gneiss; medium- to coarse-grained, quartz syenite to quartz monzonite composition
Layered to weakly foliated granodioritic and tonalitic gneisses and migmatite; thin units of quartzitic paragneiss and amphibolite /cataclastic rocks derived from this unit; minor augen granite gneiss
Interbanded mafic and felsic gneisses, augen granite gneiss and gneissic granite and granodiorite
Bedding
Regional foliation trend lines
Fault (defined, approximate)

***Figure 14.2.** Geological map of the Tebesjuak Lake map area. This map is available at a scale of 1:250 000 as GSC Open File 728.*

Calc-silicate rocks probably were derived from siliceous dolomites or dolomitic limestones; interbedded quartzites were impure calcareous arenites and quartz arenite. Sharp lateral and vertical variation among these lithologies, together with stromatolites and laminated algal mats, suggest an intertidal to supratidal environment for the succession (James, 1979).

Skarn along the granite contact has preferentially developed in carbonate-rich beds in the original sequence. Rocks within a few metres of the contact contain distinct monomineralic and polymineralic zones. Thin sections show a complex range of assemblages and textures. Typical minerals in calc-silicate bands are diopside, phlogopite, calcite, talc, serpentine, quartz and tremolite. Accessory minerals in the quartzites are diopside, biotite, white mica, feldspar and chlorite. White quartz veins trending 060°, irregular pale green diopside veins and a few calcite and fluorite-diopside veins occur within or adjacent to the skarn zones. An unusual assemblage of magnesioferrite, andradite and serpentine fills a 1 cm wide central fracture within a late-stage calcite vein.

Widely distributed calc-silicate and quartzite boulders suggest additional skarn zones and more extensive shelf carbonate-quartzite units probably underlie till-covered regions in central parts of the Pukiq domain. Slivers of white, grey or pinkish red quartzite occur in a poorly exposed, sheared and faulted intrusive complex 4 km south of the southwest corner of Pukiq Lake. The quartzites contain sericite, a trace of garnet and up to 5 per cent fluorite. The fluorite may result from influx of a fluorine-bearing aqueous phase from adjacent plutons of rapakivi granite.

Dubawnt Group

Christopher Island Formation

Trachytic lavas, pyroclastic flows and volcaniclastic sediments of the Christopher Island Formation directly overlie or are faulted against the basement complex in northern and western parts of the map area. At some localities a 1-2 m regolith is preserved at the unconformity. The coarse blocky regolith has an arkosic matrix and grades downward into unaltered basement. Upward, the regolith is overlain by alkaline flows or may grade into gneiss pebble to boulder orthoconglomerate, typically less than 20 m thick. The locally-derived, massive, poorly sorted orthoconglomerates form thin discontinuous units (Fig. 14.4). They probably are alluvial fan deposits triggered by faulting associated with initial stages of volcanic activity. Thick pre-volcanic sedimentary successions, such as the alluvial fan and fluvial deposits of the South Channel and Kazan formations (Donaldson, 1965) and basal successions in southeastern parts of the map area (LeCheminant et al., 1979a, 1980) were not noted in western parts of the area.

Christopher Island Formation successions mapped in 1980 closely resemble those described in southeastern parts of the map area (LeCheminant et al., 1979a, 1980) and in adjacent regions to the east and south (Blake, 1980; Tella and Eade, 1980). Exposures are characterized by dark weathering maroon and grey porphyritic trachyte lavas and breccias with minor pyroclastic and epiclastic deposits. A typical succession of Christopher Island Formation rocks is preserved north of Pukiq Lake (Fig. 4). Approximately 1000 m of lavas and volcaniclastic sediments with 20-30° northerly dips is truncated to the north by a major east-west trending fault. Northwest-trending faults offset the basal unconformity and northern boundary fault. The basal polymictic sharpstone conglomerate is overlain by interbedded biotite-phyric mafic trachyte lavas, volcaniclastic para- and orthoconglomerates and minor crystal-lithic wackes, arenites and siltstones. Middle and upper parts of the sequence are predominantly biotite- and clinopyroxene-phyric mafic trachyte lavas and breccias with minor interflow conglomerates and sandstones. One major unit of massive trachyte pebble to boulder conglomerate occurs near the top of the succession.

Christopher Island Formation sequences northwest of Tulemalu Lake and along the southwestern side of the Wharton Basin are also predominantly mafic trachyte flows, which comprise some 90 per cent of most sections of the formation. Pyroclastic deposits and feldspar-phyric felsic trachyte lavas are minor components in the west part of the map area.

Epiclastic deposits within the Christopher Island Formation record a complicated interplay between volcanic processes and alluvial fan to fluviatile depositional regimes. Units are characterized by abrupt and extreme lateral and vertical facies changes. Debris flows, paraconglomerates and breccias are intimately mixed with fluvial deposits characterized by a variety of fining-upward cycles. The percentage of volcanic-derived lithic and crystal fragments generally increases upward and even the finest clastics are rich in potassium feldspar, biotite and clinopyroxene eroded from the alkaline volcanic rocks. Periodic subaerial exposure is recorded by thin reddish siltstone and mudstone interbeds with mud cracks and mud curls. Typical grey to maroon, poorly sorted, volcaniclastic deposits probably reflect a combination of rapid erosion and large-scale slumping of material off unstable slopes created by constructive volcanic activity and faulting.

Contact metamorphic effects related to intrusions of rapakivi granite have not significantly modified original macroscopic textures or igneous phenocrysts in Christopher Island Formation rocks. However, a wide variety of secondary minerals replace the cement or matrix in various lithologies and are also present in cross-cutting veins. Quartz-epidote-garnet-carbonate veins with minor copper mineralization occur near granite contacts. Other minerals commonly associated with contact metamorphism are chlorite, albite, tremolite, a fibrous blue amphibole, talc, phlogopite and fluorite.

Kunwak Formation

Red volcaniclastic sediments comprising thick sequences of conglomerate, arkose and litharenite overlie the Christopher Island Formation or rest directly on basement gneiss terrane. Successions scattered throughout central parts of the map area have been correlated with the Kunwak Formation on the basis of lithology and stratigraphic position (LeCheminant et al., 1980). Extensive exposures of the formation occur within the Wharton Basin southwest of Tebesjuak Lake (Fig. 14.5). Here, the Kunwak Formation comprises a lower sequence dominated by polymictic orthoconglomerate. Measured sections are up to 600 m thick, while composite sections exceed 1500 m (Fig. 14.6).

Primary structures and textures were little modified by the intrusion of large plutons of rapakivi granite into southern parts of the Wharton Basin (Fig. 14.5). Secondary quartz, epidote and chlorite are widely distributed throughout the lower sequence replacing both matrix and cement. Carbonate cement, typical of Kunwak Formation strata outside the Wharton Basin, is only locally present.

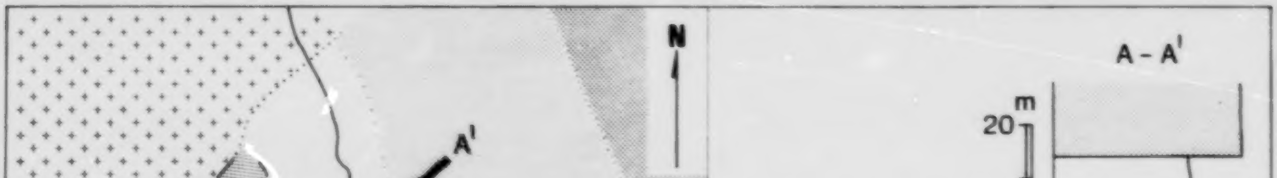

Figure 14.3. Geological map and generalized columnar section of a calc-silicate – quartzite sequence northeast of Pukiq Lake. Detailed mapping by K.A. Roberts.

Wharton Basin – Lower Sequence The lower sequence in the Wharton Basin attains a thickness of up to 900 m and consists mainly of planar to undulatory thin bedded, fine- to coarse-grained arkose. Interlayered with the arkose are units of massive or medium bedded polymictic orthoconglomerate and granular to pebbly arkose and subarkose (Fig. 14.6). Litharenite, siltstone and mudstone are minor components of the lower sequence. Clasts in conglomerate beds reflect heterogeneous local sources. Rounded to subrounded clasts (to 25 cm) consist of cataclastic granitoid gneiss, sheared porphyritic rocks, mafic trachyte and minor vein quartz. Modal proportions of Christopher Island Formation trachyte clasts decrease upwards in the sequence.

Sedimentary structures include small to large scale trough and planar crossbeds, channels, scours, mud curls, mud cracks, graded beds, and reduction spots. Sequential analysis of major lithofacies delineates a variety of fining-upward cycles. In the lower sequence, cycles are typically 0.25-2.0+ m and are predominantly arkose dominated (Fig. 14.7, types 5, 6, and 7). Conglomerate-based forms (types 3, 5, and 6) and conglomerate-dominated forms (types 2 and 4) occur throughout the lower sequence but are more prominent in its upper parts. Fine grained arkose to mudstone cycles (type 8) are extremely rare in the Wharton Basin.

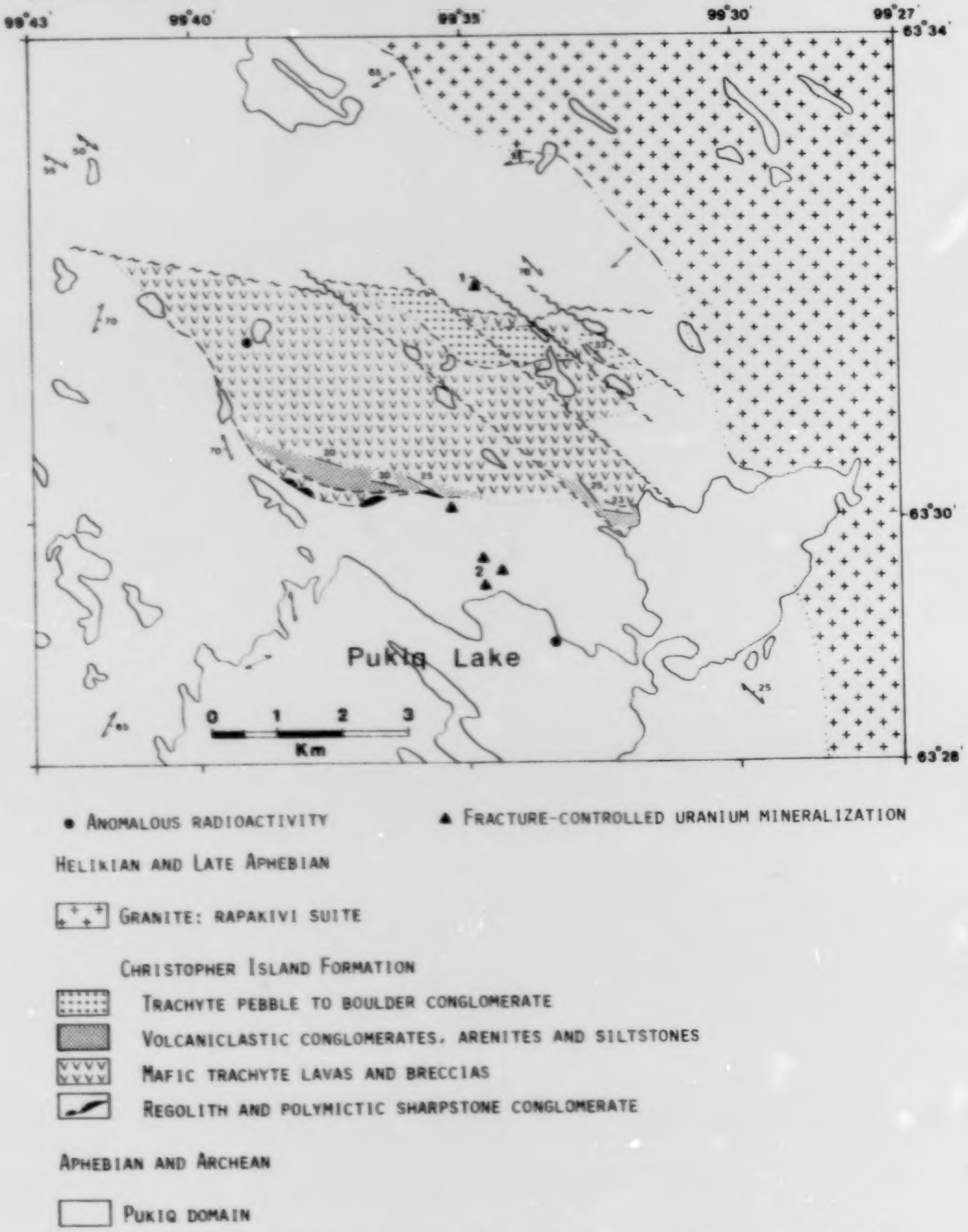
99°43'
99°40'
99°35'
99°30'
99°27'
63°34'
63°30'
63°28'
2
Pukiq Lake
0 1 2 3
Km
● Anomalous radioactivity
▲ Fracture-controlled uranium mineralization
Helikian and Late Aphebian
Granite: rapakivi suite
Christopher Island Formation
Trachyte pebble to boulder conglomerate
Volcaniclastic conglomerates, arenites and siltstones
Mafic trachyte lavas and breccias
Regolith and polymictic sharpstone conglomerate
Aphebian and Archean
Pukiq domain

Figure 14.4. Geological map of the Christopher Island Formation north of Pukiq Lake.

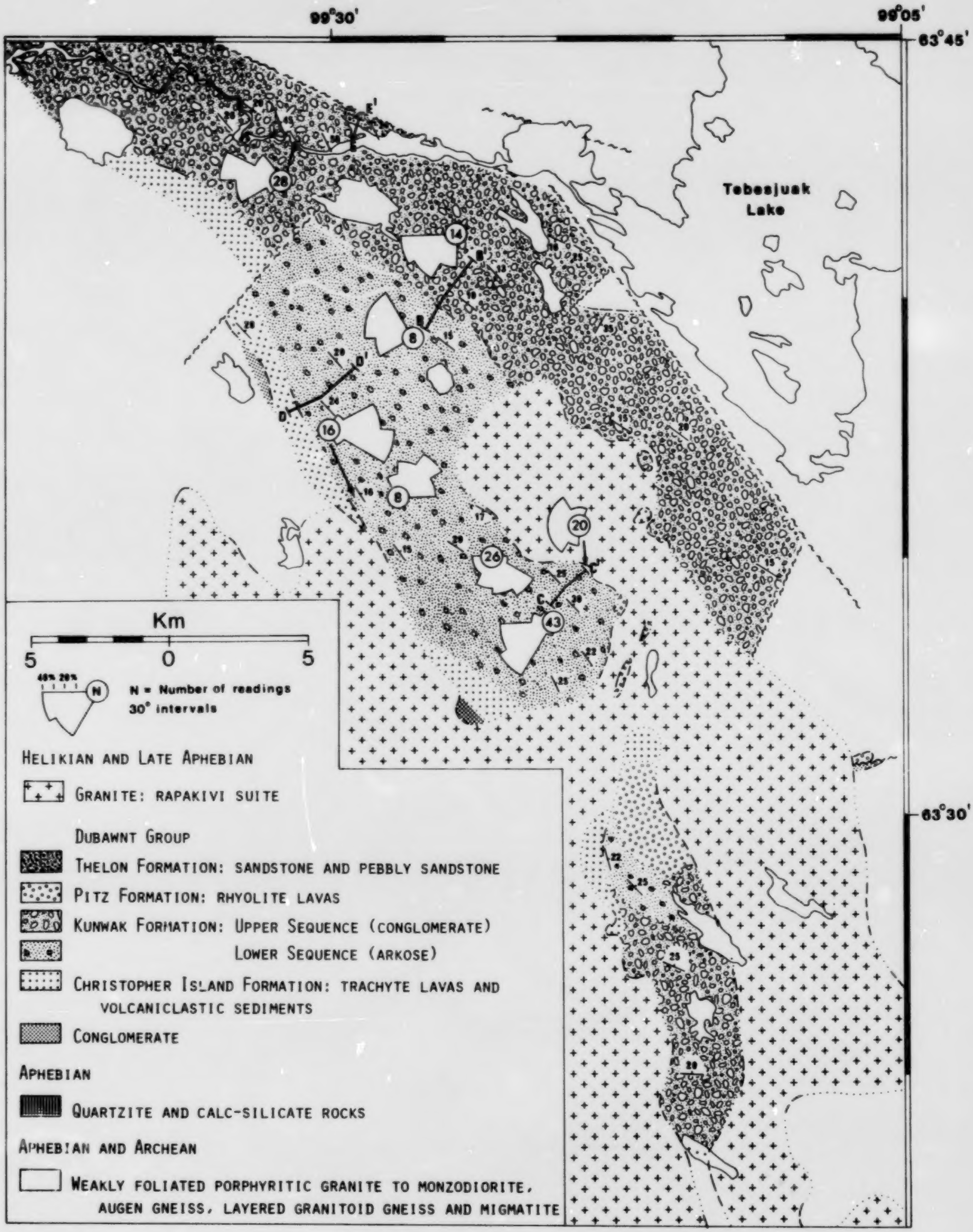
99°30'
99°05'
63°45'
63°30'
Tebesjuak Lake
E'
E
D'
D
C
C'
28
14
8
16
8
20
26
43
Km
5
0
5
40% 20%
N
N = Number of readings
30° intervals
HELIKIAN AND LATE APHEBIAN
GRANITE: RAPAKIVI SUITE
DUBAWNT GROUP
THELON FORMATION: SANDSTONE AND PEBBLY SANDSTONE
PITZ FORMATION: RHYOLITE LAVAS
KUNWAK FORMATION: UPPER SEQUENCE (CONGLOMERATE)
LOWER SEQUENCE (ARKOSE)
CHRISTOPHER ISLAND FORMATION: TRACHYTE LAVAS AND VOLCANICLASTIC SEDIMENTS
CONGLOMERATE
APHEBIAN
QUARTZITE AND CALC-SILICATE ROCKS
APHEBIAN AND ARCHEAN
WEAKLY FOLIATED PORPHYRITIC GRANITE TO MONZODIORITE, AUGEN GNEISS, LAYERED GRANITOID GNEISS AND MIGMATITE

Figure 14.5. *Geological map of southern parts of the Wharton Basin with rose diagrams of paleocurrent measurements.*

Wharton Basin – Upper Sequence Massive to poorly bedded gneiss pebble to boulder orthoconglomerates characterize the upper sequence of the Kunwak Formation in the Wharton Basin. Minor fine grained to pebbly arkose and litharenite are intercalated with the conglomerates. The upper sequence is at least 600 m thick and appears to thicken adjacent to the northeastern boundary faults. Clast lithologies are similar to those in conglomerate lenses in the underlying arkose-dominated sequence, but clasts are generally more angular and less sorted. Boulders exceed 80 cm in some beds. Main clast lithologies are various cataclastic granitoid gneisses with subordinate vein quartz, quartzite, arenite and trachyte. Clasts are set in a fine grained to granular arkose to litharenite matrix and cemented by calcite or silica.

Structures in the conglomerates include imbricate clasts, arkose lenses and crude channels. Interlayered arkose and litharenite beds contain some medium to large scale trough and planar crossbeds, graded beds, scours, channels and conglomerate lenses. Poorly- to well-defined fining-upward cylces (0.5-3.0+ m) consist of variously arranged lithofacies. Conglomerate dominated cycles (Fig. 14.7, types 1, 2, and 4) are the most abundant, but arkose dominated cycles (types 3 and 6) are locally common within interbedded sequences.

Wharton Basin – Interpretation In the lower arkose-dominated sequence paleocurrents are near-unimodal, with low to moderate dispersion (Fig. 14.5). Variable transport directions may reflect local topographic influences. Minimal paleocurrent data from the upper sequence indicate westerly to southwesterly directed transport away from major fault zones.

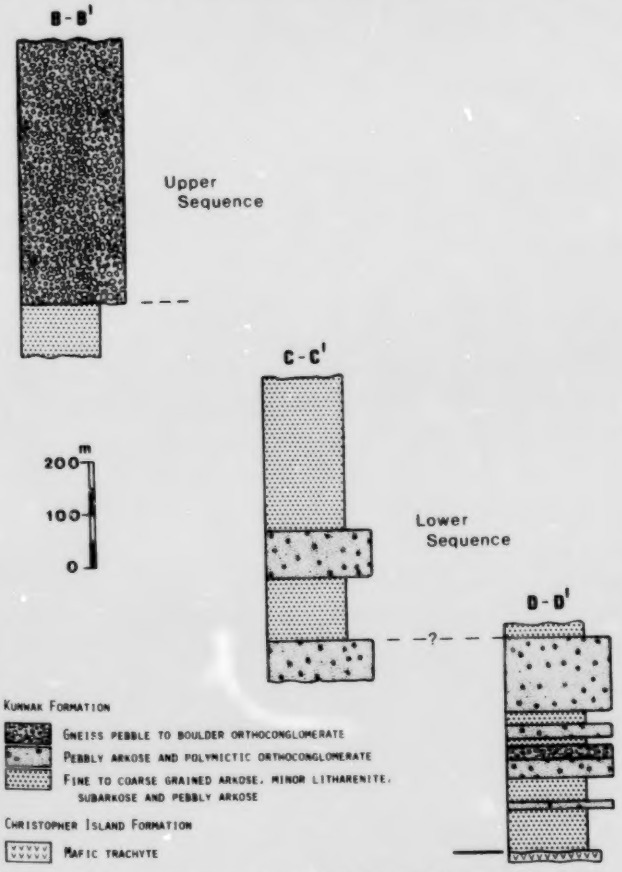
B - B'
Upper Sequence
C - C'
Lower Sequence
D - D'
?
m
200
100
0
Kunwak Formation
Gneiss pebble to boulder orthoconglomerate
Pebbly arkose and polymictic orthoconglomerate
Fine to coarse grained arkose, minor litharenite, subarkose and pebbly arkose
Christopher Island Formation
Mafic trachyte

Figure 14.6. Columnar sections of Kunwak Formation strata in the Wharton Basin. Section locations as shown in Figure 14.5.

Lithofacies, cycle types, sedimentary structures and paleocurrent trends in the lower sequence indicate braided fluviatile deposition, possibly under semi-arid to arid conditions. Major implied depositional environments are proximal to distal braided floodplain (braidplain) and mid- to distal alluvial fan (Miall, 1978; Rust, 1978). Braidplain sediments in central and southern parts of the Wharton Basin interfinger to the north and northeast with mid- and distal alluvial fan complexes.

Depositional environments in the upper conglomerate-dominated sequence range from alluvial fan to proximal braidplain. Thick conglomerate beds accumulated as debris flow and channel deposits and by coalescing sheet gravel bars on proximal fan lobes. Episodic shedding of coarse clastics resulted from periodic large-scale flooding or fault activity. The variety of conglomerate types over the extent of the basin hints at the existence of several major fans which prograded west and southwest from syn-depositional faults at the basin margin. Arkose, litharenite and pebbly arkose beds were deposited in mid and distal fan to proximal braidplain environments, through channel and bar processes under normal flow and flood conditions. Waning flow deposits, preserved as very fine clastics, accumulated over channel and bar tops in these high energy environments.

"P.O." Lake Area A sequence similar to Wharton Basin strata but only 140 m thick occurs northwest of "P.O." Lake (Fig. 14.2; see also Fig. 31.3, LeCheminant et al., 1979a). The basal redbed unit comprises thick laminated to medium bedded, fine- to medium-grained arkose, subarkose, siltstone and minor mudstone. Fining-upward cycles, resembling types 3 and 5 (Fig. 14.7), are small to medium scale (0.25-1 m) and arkose-siltstone dominated. Beds contain some trough crossbeds, abundant mud cracks, mud curls, small scale load structures, microfaults and minor convolute bedding. Gneiss pebble conglomerates overlying the redbeds contain conglomerate-dominated fining-upward cycles 0.5-1.5+ m thick. They are succeeded by more massive pebble to boulder orthoconglomerates with interbeds of paraconglomerate, litharenite and arkose.

Deposition of the redbed unit occurred within the distal braidplain regime. Overlying conglomerates are proximal braidplain to alluvial fan deposits. Wharton Basin and "P.O." Lake sequences occupy comparable stratigraphic positions but probably represent separate basins with similar depositional histories.

637 Lake Area Kunwak Formation rocks south of 637 Lake (Fig. 14.2) form a north-south trending, east-dipping homoclinal succession up to 1000 m thick made up of basal conglomerates overlain by red dacite lavas and laminated to thin-bedded arkose, siltstone and mudstone (LeCheminant et al., 1980). The upper, fine grained deposits, up to 150 m thick, contain abundant small scale fining-upward cycles (Fig. 14.7, type 8). Structures in the buff, buff-grey, pink to red rocks include mud cracks, mud drapes, graded beds, rainprints, wave and current ripple marks and small scours.

Depositional regimes for the upper, fine-grained deposits, range from braidplain to lacustrine. Abundant mud cracks and rare rainprints record periodic intervals of subaerial exposure. The rhythmic nature of the numerous fining-upward cycles may have resulted from repeated overbank flooding or from periodic density currents entering braidplain lakes. Each cycle represents a single event of waning flow deposition. This sequence shows no evidence of alluvial fan progradation or increased fault activity prior to Pitz Formation volcanism.

Southeast Tebesjuak Lake A unique 20 m carbonate-rich sequence (upper Kunwak Formation?) is preserved on the southeast shore of Tebesjuak Lake (UTM 7063700N, 513200E). Strata are in fault contact with Pitz Formation rhyolites to the east and are exposed for only a few hundred metres along the shore. The sequence passes from arkose clast breccia with thin arkose interbeds containing large scale mud cracks, upward through arkose pebble to cobble conglomerate, into thin- to medium-bedded, medium grained, lustre-mottled arkose to subarkose. The sequence is capped by a carbonate-rich paraconglomerate that contains angular to subrounded bedded arkose pebbles and blocks set within a gritty calcite-rich matrix. Arkose clasts range from 1 cm to more than 1 m and several have been broken in place. The carbonate-rich unit contains thin lenses and layers of calcareous arkose and small channels and troughs infilled with arkose pebble to cobble conglomerate.

The origin of this fining-upward sequence is problematic. Arkose beds in the sequence and arkose clasts within conglomerate beds are similar and both contain fragments of Christopher Island Formation trachyte. Arkose clasts are better sorted and indurated than the interbedded arkose and were at least partly lithified prior to fragmentation and incorporation as clasts. Syndepositional faults, ephemeral lakes and periodic subaerial exposure probably contributed significantly to the development of this sequence.

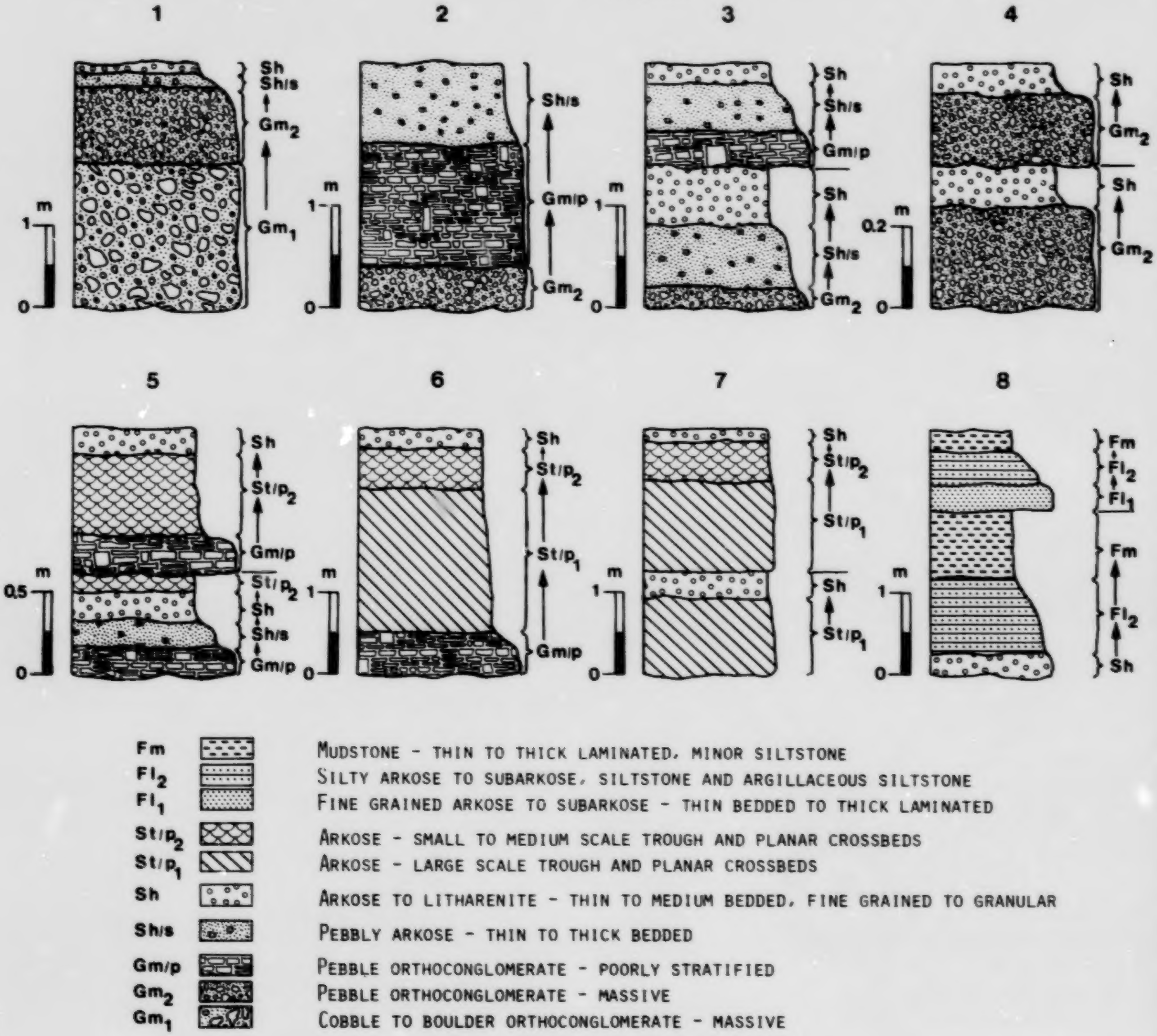
1
2
3
4
Sh
Sh/s
Gm2
Gm1
m
1
0
Sh/s
Gmlp
Gm2
Sh
Gm/p
Sh/s
0.2
Gm2
5
6
7
8
St/p2
Gm/p
0.5
St/p1
Fm
Fl2
Fl1
Fm
MUDSTONE - THIN TO THICK LAMINATED, MINOR SILTSTONE
Fl2
SILTY ARKOSE TO SUBARKOSE, SILTSTONE AND ARGILLACEOUS SILTSTONE
Fl1
FINE GRAINED ARKOSE TO SUBARKOSE - THIN BEDDED TO THICK LAMINATED
St/p2
ARKOSE - SMALL TO MEDIUM SCALE TROUGH AND PLANAR CROSSBEDS
St/p1
ARKOSE - LARGE SCALE TROUGH AND PLANAR CROSSBEDS
Sh
ARKOSE TO LITHARENITE - THIN TO MEDIUM BEDDED, FINE GRAINED TO GRANULAR
Sh/s
PEBBLY ARKOSE - THIN TO THICK BEDDED
Gm/p
PEBBLE ORTHOCONGLOMERATE - POORLY STRATIFIED
Gm2
PEBBLE ORTHOCONGLOMERATE - MASSIVE
Gm1
COBBLE TO BOULDER ORTHOCONGLOMERATE - MASSIVE

Figure 14.7. Representative fining-upward cycles for the Kunwak Formation. All types occur in the Wharton Basin except for 8, which is located south of 637 Lake. Facies identifiers adapted from Miall (1977).

Other Kunwak Formation Successions Several other successions of Kunwak Formation volcaniclastic orthoconglomerate, litharenite and arkose occur south of Mallery Lake and east of the Kunwak River in northeastern parts of the map area (Fig. 14.2). The thin, shallow-dipping, successions separate the Christopher Island and Pitz formations and are similar to fluvial deposits of the Wharton Basin. Detailed analysis is precluded by poor and scattered exposure.

Discussion Kunwak strata in the map area are confined within semi-isolated fault-controlled alluvial basins. The basins developed and were filled during the intravolcanic interval between episodes of widespread alkaline volcanism (Chrisopher Island Formation) and rhyolitic calc-alkaline volcanism (Pitz Formation). Felsic volcanism played a minor role in the development of the Kunwak succession south of 637 Lake. Elsewhere, redbed infill sequences differ in detail but similar alluvial fan-braided fluviatile depositional regimes are present throughout the basins.

In the Wharton Basin, faulting localized along the northeastern boundary of the Pukiq domain produced a northwest-southeast depression that was rapidly infilled by alluvial fan and braidplain sediments. Clast lithologies and paleocurrents indicate the major source area was to the east and southeast with lesser contributions from the Pukiq domain to the southwest. The upward decrease in trachyte clasts and sympathetic increase in gneiss fragments reflects denudation of Christopher Island Formation strata and progressive unroofing of gneiss complexes. Relatively thin fining-upward cycles are superimposed on an overall coarsening-upward trend. Braidplain sediments interfinger to the north and northwest with mid- and distal alluvial fan complexes in a pattern that suggests progradation of fan complexes from active faults at the basin margins.

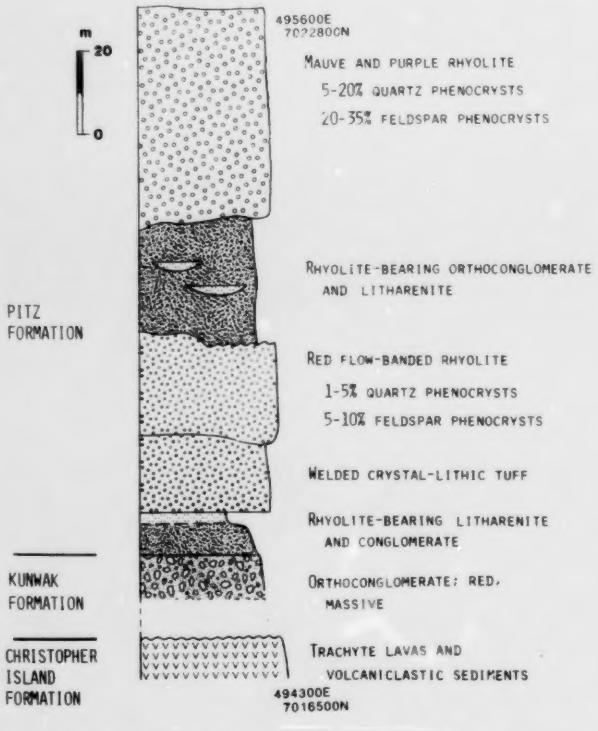
m
20
0
495600E
70?2800N
MAUVE AND PURPLE RHYOLITE
5-20% QUARTZ PHENOCRYSTS
20-35% FELDSPAR PHENOCRYSTS
RHYOLITE-BEARING ORTHOCONGLOMERATE AND LITHARENITE
PITZ FORMATION
RED FLOW-BANDED RHYOLITE
1-5% QUARTZ PHENOCRYSTS
5-10% FELDSPAR PHENOCRYSTS
WELDED CRYSTAL-LITHIC TUFF
RHYOLITE-BEARING LITHARENITE AND CONGLOMERATE
KUNWAK FORMATION
ORTHOCONGLOMERATE: RED, MASSIVE
CHRISTOPHER ISLAND FORMATION
TRACHYTE LAVAS AND VOLCANICLASTIC SEDIMENTS
494300E
7016500N

Figure 14.8. *Diagrammatic section of the Pitz Formation along the Kunwak River north of Tulemalu Lake. Section location from approximately UTM 494300E, 7016500N to 495600E, 7022800N.*

Pitz Formation

Acid flows and intercalated quartz-rich volcaniclastic rocks of the Pitz Formation are confined primarily to central and northwestern parts of the map area. Shallowly dipping successions, up to 200 m, rest concordantly on Kunwak Formation fluvial deposits and unconformably overlie Christopher Island Formation volcanics and central domain granodioritic gneisses. The base of the Pitz Formation is defined by the first acid flow or the first appearance of rhyolite detritus.

Pitz lavas are potassic, silica-rich rhyolites with subordinate rhyodacite and dacite. The most voluminous rocks are abundantly porphyritic mauve to purple lavas containing potash feldspar phenocrysts to 2 cm, smaller quartz 'eyes' and minor plagioclase and altered mafic phenocrysts. Sparsely porphyritic red to grey flow-banded rhyolites and welded lithic-crystal tuffs occur near the base of successions on the northeastern shores of Tulemalu and Tebesjuak Lakes, along the Kunwak River north of the Pamiutuq Granite and on an island in 463 Lake (Fig. 14.2). Interflow sediments comprise rhyolite ortho- and paraconglomerate, rhyolite breccia and red litharenite and siltstone.

Figure 14.8 shows a diagrammatic section representative of the Kunwak-Pitz transition and typical Pitz stratigraphy. Kunwak Formation orthoconglomerates are overlain by rhyolite-bearing volcaniclastic rocks and rhyolitic ash flow tuffs. Sparsely porphyritic basal tuffs and flow-banded rhyolites are succeeded by lenses of rhyolite cobble to boulder orthoconglomerate and red litharenite and by thick units of abundantly porphyritic rhyolite lavas. Dark purple fluorite and less commonly topaz are accessory phases in most tuffs and flow-banded lavas.

Sparsely porphyritic F-rich rhyolites have a higher radiometric response than more abundantly porphyritic flows. Anomalous radioactivity occurs in spectacularly flow-banded lavas overlying biotite granodiorite gneiss west of Mallery Lake (Table 14.1). The rhyolite contains embayed quartz 'eyes' and potash feldspar and albite phenocrysts set in a devitrified quartzofeldspathic matrix. Accessory minerals are fluorite, topaz, zircon and partly hematitized pyrite. Alteration within the anomalous radioactive zone includes pervasive hematite staining throughout the groundmass, white mica replacement of feldspar phenocrysts and limonite-chlorite micro-veinlets.

F-rich, topaz-bearing, rhyolites are commonly enriched in lithophile elements and may be associated with uranium mineralization (Burt and Sheridan, 1980). Uranium deposits associated with rhyolitic lavas and ash flow tuffs have been recently reported from Sweden (Lindroos and Smellie, 1979), Mexico (Goodell and Carroway, 1980) and the western United States (Castor and Berry, 1980; Cofer, 1980; Lindsay, 1980). Host rocks range in age from Middle Proterozoic to Tertiary and most interpretations of the mineralization stress hydrothermal processes associated with volatile-rich silicic volcanism.

Anomalously radioactive phenocryst-poor flow-banded Pitz rhyolites reflect high eruption temperatures, high water contents and rapid crystallization, features which are not the most favourable for economic-grade mineralization associated with F-rich topaz rhyolites (Bikun et al., 1980). Nevertheless, additional factors such as the diversity of lithologies underlying the Pitz Formation, irregular paleotopography and complex patterns of sedimentation and volcanism suggest parts of the Pitz Formation have some uranium potential.

Table 14.1

Uranium mineralization and anomalies

	Location (UTM Zone 15)	Map Sheet	Host Rock	Element Association	Ore Minerals	Secondary Minerals	Gangue Minerals	Brief description (additional comments in text)
1.	470900 E 7044900N	65 O/12SE	Weakly foliated quartz-feldspar porphyry	U	pitchblende	uranophane	sericite hematite	Intensely microfractured and sericitized rocks; 18 m by 12 m radiometric anomaly
2.	471400 E 7040000N	65 O/5NE	Quartz monzonite to diorite	U-Cu	pitchblende chalcopyrite	uranophane malachite	sericite chlorite epidote pyrite hematite	Thin discontinuous mineralized fractures in cataclastic rocks underlying Dubawnt Group rocks north of Pukiq Lake
3.	469010 E 7056660N	65 O/12NE	Quartz syenite to quartz monzonite	U	pitchblende	present	sericite chlorite pyrite hematite calcite	Narrow easterly to northeasterly fracture zones in cataclastic rocks 3 km west of the base of the Dubawnt Group (Wharton Basin)
4.	456360 E 7033300N	65 O/5NW	Biotite rich mafic trachyte	U	pitchblende	---	chlorite hematite	Subrounded cobble (7 cm by 5 cm) of Christopher Island Formation trachyte in till; crosscutting pitchblende rich veinlets
5.	483420 E 7049280N	65 O/11SW	Arkose, pebbly arkose	U	pitchblende	kasolite boltwoodite uranophane cuprosklodowskite	chlorite magnetite hematite	Epigenetic mineralization in easterly trending fracture zones crosscutting epidotized Kunwak Formation arkose (Wharton Basin)
6.	511230 E 7086050N	65 O/15NE	Flow-banded rhyolite Pitz Formation	-	anomalous radioactivity	---	white mica chlorite limonite pyrite hematite	Small zones of anomalous radioactivity in sparsely porphyritic F-rich rhyolites overlying biotite granodiorite gneiss
7.	476280 E 7065790N	65 O/11NW	Quartz arenite	U-P	anomalous radioactivity	---	white mica goyazite apatite hematite	Uraniferous phosphate cement in hematitic quartz arenite of the Thelon Formation (Wharton Basin)

Pitz Formation rhyolite successions generally show an upward increase in percentage of phenocrysts, perhaps reflecting successive eruptions from a zoned magma chamber in which the proportion of phenocrysts increased downwards (Smith, 1979). High silica F-rich flows are similar to early erupted parts of many major intracratonic caldera-forming zoned systems (Byers et al., 1976; Hildreth, 1979). The rhyolite successions probably are remnants of the volcanic roof above epizonal granite plutons such as the Pamiutuq Granite (LeCheminant et al., 1979a, 1980).

Thelon Formation

A thin, northeasterly-dipping succession of light pink buff or white conglomerate and sandstone is preserved in a small area west of Tebesjuak Lake (Fig. 14.5). The poorly exposed beds, tentatively correlated with the Thelon Formation, disconformably overlie Kunwak Formation fluvial conglomerates, and are truncated to the north by a boundary fault of the Wharton Basin. No Pitz Formation rhyolite flows or rhyolite detritus have been recognized at or above the Kunwak-Thelon boundary although upper sequence Kunwak clastics contain unaltered subhedral grains of potash feldspar and biotite of probable volcanic origin.

Upper sequence Kunwak strata in the area occur in conglomerate-dominated fining-upward cycles that give way to a transitional cycle unit at the base of the Thelon Formation (Fig. 14.9). Basal fining-upward cycles of clay-cemented pebble orthoconglomerate and medium grained to granular subarkose to quartz arenite are overlain by flaggy-bedded fine- to medium-grained quartz arenite. Sedimentary structures in the Thelon Formation include small scale trough- and planar-crossbeds, channels, reduction spots and rare asymmetric ripples.

Anomalous radioactivity is associated with an altered phosphatic zone near the base of the Thelon quartz arenite (Table 14.1). No estimate of the thickness or continuity of the zone could be obtained from the heaved outcrop and felsenmeer blocks that contain the variably altered sandstone. Rounded to subrounded quartz grains in the sandstone are cemented by goyazite and apatite. Other, less abundant, interstitial phases include quartz, hematite, white mica, and an unidentified chlorine-bearing mineral. One sample contained 10% P_2O_5 (atomic absorption, GSC) and 53.8 ppm U (neutron activation, AECL).

Similar hematitic phosphate zones, some with U values exceeding 200 ppm, have been recognized within upper units of the Wolverine Point Formation throughout the Athabasca Basin (Ramaekers, 1980). Ramaekers interpreted the depositional environment of this formation as a marine shelf. Stable marine platforms in tropical to subtropical latitudes are favourable sites for the precipitation of phosphates which usually contain small amounts of uranium (Christie, 1980). Association of phosphates with a chlorine-bearing mineral, together with the textural and mineralogical maturity of the Thelon quartz arenites, suggests a shallow marine depositional environment for this part of the Thelon Formation.

Intrusive Rocks

Numerous undeformed intrusions have been identified throughout the map area. The largest plutons are predominantly granite with smaller bodies of syenite and basic rocks (Fig. 14.1 and 14.2). Many stocks and plutons in central and southeastern parts of the map area have been briefly described elsewhere (LeCheminant et al., 1979a, 1980) and only new relationships or intrusions recognized during the 1980 field season are discussed here.

A large, poorly exposed pluton of leucocratic granite underlies about 160 km^2 west of Tebesjuak Lake and north of the Wharton Basin. The distinctive white-weathering biotite granite is massive and equigranular and contains characteristic dark grey, smoky quartz. Accessory phases include sphene, iron oxides, allanite, fluorite, apatite and zircon. Angular xenoliths and large rafts of granitoid gneiss, rare pegmatite veins, and subporphyritic and/or weakly foliated phases of the granite occur in the outer margins of the pluton. Contacts with surrounding gneisses are discordant except along the southern contact adjacent to the Wharton Basin where a weak foliation within the intrusion subparallels regional foliation trends. Texturally the granite does not resemble fluorite-bearing red granites that intrude the Dubawnt Group and this intrusion could be significantly older. However, in common with the syn- or post-Dubawnt Group granites, it is not cut by syenite or lamprophyre dykes.

An intrusive complex comprising coarse grained porphyritic monzodiorite intruded by a circular granite stock 5 km in diameter underlies a large point on the south shore of Mallery Lake (Fig. 14.2). Along its south side, the granite crosscuts granodioritic gneiss, laminated amphibolite, and lean iron formation. Magnetite-bearing supracrustal rocks and the oxide-rich monzodiorite are interpreted as responsible for the prominent annular aeromagnetic high that surrounds the circular granite stock (GSC maps 7842G and 6773G).

The monzodiorite is a black, coarse grained, porphyritic rock with abundant closely packed tabular plagioclase phenocrysts to 3 cm and smaller potash feldspar laths. Interstitial phases include clinopyroxene, iron oxides and hornblende with accessory quartz, biotite and apatite. The poorly-exposed intrusion is apparently a northeasterly-trending dyke-like body with little internal variation.

The younger granite stock to the south is a fluorite-bearing red biotite granite with potash feldspar phenocrysts to 2 cm set in a fine grained micrographic groundmass. Texturally and mineralogically the granite has close affinities to fluorite-bearing alkali feldspar granites that intrude the Christopher Island and Kunwak formations northwest of "P.O." Lake.

West of Tulemalu Lake and the Kunwak River and southwest of the Wharton Basin, elongate multilobate granite plutons underlie more than 1200 km^2 (Fig. 14.2). These granites intrude Dubawnt Group succesions up to Pitz Formation rhyolites, and are confined to the Pukiq domain or

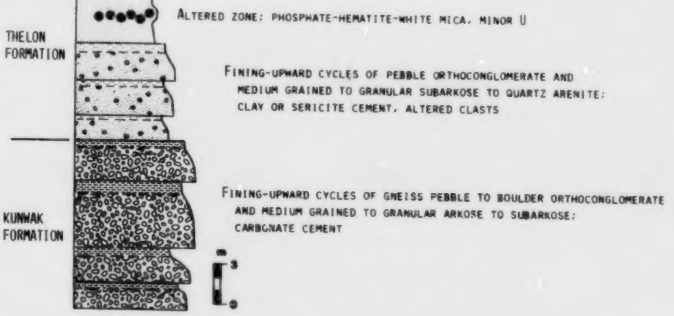
E-E'
QUARTZ ARENITE, MINOR SUBARKOSE AND PEBBLE BEDS: CLAY OR SERICITE CEMENT
ALTERED ZONE: PHOSPHATE-HEMATITE-WHITE MICA, MINOR U
THELON FORMATION
FINING-UPWARD CYCLES OF PEBBLE ORTHOCONGLOMERATE AND MEDIUM GRAINED TO GRANULAR SUBARKOSE TO QUARTZ ARENITE: CLAY OR SERICITE CEMENT, ALTERED CLASTS
FINING-UPWARD CYCLES OF GNEISS PEBBLE TO BOULDER ORTHOCONGLOMERATE AND MEDIUM GRAINED TO GRANULAR ARKOSE TO SUBARKOSE: CARBONATE CEMENT
KUNWAK FORMATION
m
3
0

***Figure 14.9**. Diagrammatic section of the Kunwak Formation-Thelon Formation transition in the Wharton Basin. Section location as shown on Figure 14.5.*

separate rocks of the Pukiq domain from granodioritic gneisses to the east. The plutons comprise two main phases: (1) coarse grained granite characterized by rapakivi and antirapakivi mantling of ovoid feldspar phenocrysts, and (2) fine- to medium-grained leucocratic inequigranular granite. Individial plutons are usually multiphase intrusions with finer grained granites intruding the rapakivi phase. All variants of the pink to red granites contain more potash feldspar than plagioclase, with accessory biotite, fluorite and zircon. Hornblende and sphene are additional accessories in the rapakivi granites.

External contacts of these plutons are sharp and discordant. In the Wharton Basin southwest of Tebesjuak Lake a flat intrusive contact between granite and capping Kunwak Formation conglomerates is exposed (Fig. 14.5). Minimal thermal effects on country rocks and the presence of miarolitic cavities and micrographic textures provide additional evidence that the present level of exposure is near the roof of plutons intruded into near surface environments. Miarolitic cavities range up to 1.5 cm in diameter and are lined with well-formed crystals of quartz, potash feldspar and fluorite. Crystallization of the phenocryst-rich intrusions was probably rapid and there was only minor late-stage vapour phase transfer between plutons and country rocks.

Major plutons of the rapakivi granite suite extend in a crude arc from the southwest corner of the map area to south of Wharton Lake (Fig. 14.2). Elongate plutons are aligned subparallel to the Wharton Basin and intrude rocks in the southern half of the basin. Emplacement of the intrusions was apparently controlled by pre-existing structural elements parallel to or along the eastern margin of the Pukiq domain. Plutons of rapakivi granite extend southwest of the map area (Eade and Blake, 1977; Tella and Eade, 1980) and should be present in adjacent parts of the Dubawnt Lake map area to the west. Most of this region is outlined by a broad, low-amplitude, Bouguer gravity low (Gibb and Halliday, 1974) centred on Pukiq Lake that is coincident with the known limits of the Pukiq domain and extends southeast to enclose the Pamiutuq Granite.

The McRae Lake dyke (Fig. 14.2) is a multiphase basic intrusion 23 km long and up to 1.8 km wide (LeCheminant et al., 1980). The southwestern end of the dyke intrudes a few hundred metres into a pluton of the rapakivi granite suite. The gabbroic phase of the dyke has a chilled margin at the granite contact and contains a few xenoliths of the granite. Lamprophyre and quartz-feldspar porphyry dykes in central domain gneisses are also cut by the McRae Lake dyke. A K-Ar whole rock age determination on chilled gabbro 5 m from the outer contact of the dyke yielded 1735 ± 52 Ma. This is taken to be the minimum age of intrusion. Except for northwesterly trending diabase dykes the McRae Lake dyke is the youngest intrusion in the map area.

Economic Geology

Uranium occurrences and anomalies located during 1980 mapping are listed in Table 14.1. In addition, cataclastic rocks in a trapezoidal-shaped, fault-bounded area west of McRae Lake (Fig. 14.2) locally have an anomalous radiometric response and minor uranium mineralization was noted along small fractures. Anomalous radioactivity in Pitz Formation F-rich rhyolites and phosphate zones in the Thelon Formation are discussed in sections on these formations.

Occurrences 1-5 are small zones of limited mineralization and/or exposure within lower formations of the Dubawnt Group or within Pukiq domain cataclastic rocks adjacent to Christopher Island Formation successions. Mineralization characteristically occurs in narrow discontinuous fractures containing pitchblende, minor sulphides and various secondary minerals. Occurrences are similar to other epigenetic fracture-controlled mineralization within and adjacent to the Baker lake Basin (LeCheminant et al., 1980; Miller, 1979, 1980). This type of mineralization is commonly developed adjacent to intersecting structures such as fault junctions, or unconformities and faults.

Occurrence 1 is situated in a stream valley that separates two crag and tail till lobes (Fig. 14.4). Limited outcrop in the valley floor comprises potash feldspar augen gneiss and microfractured quartz-feldspar porphyry. A strong radiometric anomaly 18 m east-west by 12 m north-south is associated with intensely sericitized quartz-feldspar porphyry. Pitchblende is confined to discontinuous 1-5 mm wide northeasterly trending fractures surrounded by 5-36 mm wide hematitic envelopes. Mineralization is adjacent to the projected trace of a northwest fault approximately 700 m north of the major east-west fault that truncates a tilted Christopher Island Formation succession.

Occurrence 2 is representative of a group of four very small zones of uranium mineralization in a region of frost shattered outcrop and subcrop below the Christopher Island Formation unconformity north of Pukiq Lake (Fig. 14.4). The basement complex contains numerous narrow cataclastic zones and faults. Pitchblende and traces of chalcopyrite and pyrite are confined to narrow seams and fractures in sheared quartz monzonite to diorite. Associated alteration minerals are chlorite, sericite, hematite and minor epidote.

Mineralization at occurrence 3, located about 3 km west of the Wharton Basin, is erratically distributed throughout several small zones, with the largest about 55 m by 40 m. Easterly to northeasterly fractures in cataclastically-deformed intermediate intrusive rocks contain minor pitchblende with disseminated pyrite. Alteration involves two generations of chlorite, hematitization and white mica replacement of feldspars.

Evidence for uranium mineralization in the Christopher Island Formation is provided by an anomalously radioactive boulder of biotite trachyte near occurrence 2 and a highly radioactive pitchblende-veined cobble of biotite trachyte in NTS map are 65 O/5 NW (occurrence 4). Minor zones of anomalous radioactivity in trachytes occur in northwest fractures north of Pukiq Lake (Fig. 14.4) and adjacent to rapakivi granite in NTS area 65 O/4 NE (464380E, 7011080N).

Occurrence 5 is a 50 m square anomalously radioactive zone within the lower sequence of the Kunwak Formation in the Wharton Basin. Mineralization is localized in easterly trending fracture zones up to 25 cm wide that transect hematitic arkose, pebbly arkose and minor ortho-conglomerate. The intensely chloritized and weakly magnetic zones are characteristically dark green to black, in contrast to the pale reddish hues of the host sediments. Autoradiographs show uranium is disseminated throughout chloritized arkose but is predominantly concentrated in branching microfractures.

Copper mineralization is common in vein systems within the Chrisopher Island Formation, particularly in the southwest corner of the map area adjacent to intursions of rapakivi granite. Several occurrences were reported by LeCheminant et al. (1980) and similar veins noted during 1980 mapping contain chalcocite, bornite and chalcopyrite associated with garnet, epidote, calcite and quartz. Veins rarely exceed more than a few centimetres in width and display little continuity.

Acknowledgments

The authors thank K. Roberts, A. Tambosso and D. Webb for their outstanding field assistance and mapping contributions. A.L. Littlejohn and A.C. Roberts kindly provided X-ray identification of secondary mineral assemblages and D.A. Walker assisted with energy dispersive examinations on the scanning electron microscope. We have had valuable discussions with Mikkel Schau, K.E. Eade and S. Tella. F.H.A. Campbell reviewed the manuscript and offered numerous helpful comments.

References

Bell, R.T.
1970: The Hurwitz Group – A prototype for deposition on metastable cratons; in Symposium on Basins and Geosynclines of the Canadian Shield, A.J. Baer, ed., Geological Survey of Canada, Paper 70-40, p. 159-169.

Bikun, J.V., Christiansen, E.H., Sheridan, M.F., and Burt, D.M.
1980: Characteristics associated with mineralization in topaz rhyolites; Geological Society of America, Abstract, v. 12, p. 387.

Blake, D.H.
1980: Volcanic rocks of the Paleohelikian Dubawnt Group in the Baker Lake-Angikuni Lake area, District of Keewatin, N.W.T.; Geological Survey of Canada, Bulletin 309, 39 p.

Burt, D.M. and Sheridan, M.F.
1980: A model for the formation of uranium/lithophile element deposits in fluorine-enriched volcanic rocks; Southwest section, American Association of Petroleum Geologists, Symposium on uranium in volcanic and volcaniclastic rocks, Abstract, p. 18.

Byers, F.M., Carr, W.J., Orkild, P.P., Quinlivan, W.C., and Sargent, K.A.
1976: Volcanic suites and related cauldrons of Timber Mountain – Oasis Valley complex, southern Nevada; U.S. Geological Survey, Professional Paper 919, 70 p.

Castor, S.B. and Berry, M.R.
1980: Geology of the Lakeview Uranium District, Oregon; Southwest section, American Association of Petroleum Geologists, Symposium on uranium in volcanic and volcaniclastic rocks, Abstract, p. 20.

Christie, R.L.
1980: Paleolatitudes and potential for phosphorite deposition in Canada; in Current Research, Part B, Geological Survey of Canada, Paper 80-1B, p. 241-248.

Cofer, R.
1980: Geology of the Shely Cauldron, Pinto Canyon area, Presidio County, Texas; Southwest section, American Association of Petroleum Geologists, Symposium on uranium in volcanic and volcaniclastic rocks, Abstract, p. 20-21.

Donaldson, J.A.
1965: The Dubawnt Group, District of Keewatin and Mackenzie; Geological Survey of Canada, Paper 64-20.

Eade, K.E. and Blake, D.H.
1977: Geology of the Tulemalu Lake Map-Area, District of Keewatin; in Report of Activities, Part A, Geological Survey of Canada, Paper 77-1A, p. 209-211.

Gibb, R.A. and Halliday, D.W.
1974: Gravity measurements in southern District of Keewatin and southeastern District of Mackenzie, N.W.T. with maps no. 124-131 Gravity map series of the Earth Physics Branch, Energy Mines and Resources Canada.

Goodell, P. and Carraway, K.
1980: Geology of the Sierra Pena Blanca Region, Chihuahau, Mexico; Southwest section, American Association of Petroleum Geologists, Symposium on uranium in volcanic and volcaniclastic rocks, Abstract, p. 30-31.

Heywood, W.W.
1977; Geology of the Amer Lake map area, District of Keewatin; in Report of Activities, Part A, Geological Survey of Canada, Paper 77-1A, p. 409-410.

Higgins, M.W.
1971: Cataclastic rocks; U.S. Geological Survey, Professional Paper 687, 97 p.

Hildreth, W.
1979: The Bishop Tuff: Evidence for the origin of compositional zonation in silicic magma chambers; in Geological Society of America, Special Paper 180, p. 43-75.

James, N.P.
1979: Shallowing upward sequences in carbonates; in Facies Models, R.G. Walker, ed.; Geoscience Canada, Reprint Series 1, p. 109-119.

LeCheminant, A.N., Lambert, M.B., Miller, A.R., and Booth, G.W.
1979a: Geological studies: Tebesjuak Lake map area, District of Keewatin; in Current Research, Part A, Geological Survey of Canada, Paper 79-1A, p. 179-186.

LeCheminant, A.N., Leatherbarrow, R.W., and Miller, A.R.
1979b: Thirty Mile Lake map area, District of Keewatin; in Curent Research, Part B, Geological Survey of Canada, Paper 79-1B, p. 319-327.

LeCheminant, A.N., Miller, A.R., Booth, G.W., Murray, M.J., and Jenner, G.A.
1980: Geology of the Tebesjuak Lake map area, District of Keewatin: a progress report with notes on uranium and base metal mineralization; in Current Research, Part A, Geological Survey of Canada, Paper 80-1A, p. 339-346.

Lindroos, H. and Smellie, J.
1979: A stratabound uranium occurrence within Middle Precambrian ignimbrites at Duobblon, Northern Sweden; Economic Geology, v. 74, p. 1118-1130.

Lindsey, D.A.
1980: Volcanism and uranium mineralization at Spar Mountain, Utah; Southwest section, American Association of Petroleum Geologists, Symposium on uranium in volcanic and volcaniclastic rocks, Abstract, p. 43.

Miall, A.D.
1977: A Review of the Braided-River Depositional Environment; Earth-Science Reviews, v. 13, p. 1-62.

1978: Lithofacies types and vertical profile models in braided river deposits: a summary; in Fluvial Sedimentology, A.D. Miall, ed.; Canadian Society of Petroleum Geologists, Memoir 5, p. 597-604.

Miller, A.R.
1979: Uranium geology in the central Baker Lake Basin; *in* Current Research, Part A, Geological Survey of Canada, Paper 79-1A, p. 57-59.

1980: Uranium geology of the eastern Baker Lake Basin, District of Keewatin, Northwest Territories; Geological Survey of Canada, Bulletin 330, 63 p.

Ramaekers, P.
1980: Stratigraphy and tectonic history of the Athabasca Group (Helikian) of Northern Saskatchewan; *in* Summary of Investigations 1980, Saskatchewan Geological Survey, Miscellaneous Report 80-4, p. 99-106.

Rust, B.R.
1978: Depositional models for braided alluvium; *in* Fluvial Sedimentology, A.D. Miall, ed., Canadian Society of Petroleum Geologists, Memoir 5, p. 605-625.

Smith, Robert L.
1979: Ash-flow magmatism; *in* Geological Society of America, Special Paper 180, p. 5-27.

Tella, S. and Eade, K.E.
1980: Geology of the Kamilukuak Lake map area, District of Keewatin, a part of the Churchill Structural Province, N.W.T.; *in* Current Research, Part B, Geological Survey of Canada, Paper 80-1B, p. 39-45.

Tella, S., Eade, K.E., Miller, A.R., and Lamontagne, C.G.
1981: Geology of the Kamilukuak Lake map area, District of Keewatin, a part of the Churchill Structural Province; *in* Current Research, Part A, Geological Survey of Canada, Paper 81-1A, p. 231-240.

Wright, G.M.
1967: Geology of the southeastern barren grounds, parts of the Districts of Mackenzie and Keewatin (Operation Keewatin, Baker, Thelon); Geological Survey of Canada, Memoir 350.

15.

DATING THE HORTON RIVER BREAKTHROUGH, DISTRICT OF MACKENZIE

Project 680047

J. Ross Mackay[1]
Terrain Sciences Division

Mackay, J.R., Dating the Horton River breakthrough, District of Mackenzie; in *Current Research, Part B, Geological Survey of Canada, Paper 81-1B, p. 129-132, 1981.*

Abstract

Horton River, which is one of the large rivers of the Northwest Territories, formerly flowed into Harrowby Bay but now discharges into Franklin Bay. The breakthrough shortened the length of the river by nearly 100 km. Three radiocarbon dates for driftwood stranded about 10 m above sea level along the old Horton River channel and one radiocarbon date for a driftwood log found 6 m above sea level near the present mouth suggest a breakthrough date at about A.D. 1800. Since breakthrough, fan-deltas from tributary creeks have segmented the abandoned channel into several large oxbow lakes; permafrost and ice-wedge polygons have grown along parts of the abandoned channel; gelifluction lobes have encroached onto the abandoned channel; lower Horton River and its tributaries have been rejuvenated; and Horton River has built a 30 km² delta into the relatively deep water of Franklin Bay. Although the A.D. 1800 date needs further confirmation, it is clear that the site has considerable promise for geomorphic and permafrost process studies in an area of continuous permafrost.

Introduction

Horton River, which now flows into Franklin Bay, District of Mackenzie, formerly discharged into Harrowby Bay, about 60 km due northwest (Fig. 15.1). The breakthrough to Franklin Bay shortened the length of Horton River as measured along the channel by about 100 km. The breakthrough is known to have occurred prior to 1826 when the present river mouth was mapped by John Richardson (Franklin, 1828), but the freshness of the geomorphic features and the small size of the Horton River delta combine to suggest that the breakthrough took place not long before 1826. It is evident that if the breakthrough is recent and can be dated, lower Horton River, the Horton delta, and the old Horton abandoned channel will provide excellent opportunities for the study of the rates of geomorphic and permafrost processes as they operate in an area of continuous permafrost. Consequently, an effort has been made during the past few years to collect driftwood along the old abandoned channel for radiocarbon dating. This paper reports on four radiocarbon dates which suggest that the breakthrough occurred about A.D. 1800.

The geology of the area has been discussed by Yorath et al. (1975) and the geomorphology by Mackay (1958, 1963) and Rampton (1972). The area is in continuous permafrost. The mean annual ground temperature based upon one drillhole is about -8°C (Judge et al., 1979).

Historical Evidence of the Breakthrough

In 1826, Mr. Kendall, surveyor for John Richardson, sketched the mouth of Horton River, as reproduced in Figure 15.2 (Franklin, 1828, Plate 25). The sketch shows a Horton River mouth quite unlike that at present (Mackay, 1958, p. 67). First, Horton River was shown discharging into the sea through a chute confined to a narrow canyon, but neither now exists. Second, Figure 15.2 shows two offshore islands but no delta, whereas now there is a delta (Fig. 3) but there are no offshore islands. Third, driftwood is lodged on the islands, but driftwood is scarce along the coast. As wooded areas are present upstream along the Horton, however, the breakthrough would likely have led to rapid vertical erosion and downstream transport of driftwood onto a fan-delta built into the sea. Partial erosion of the fan-delta would explain the two offshore islands. And lastly, an oral tradition of the breakthrough exists among local inhabitants that it reportedly occurred at spring breakup.

Radiocarbon Dating

When the breakthrough occurred, any driftwood downstream from the present mouth would have been stranded high and dry to provide maximum dates for the breakthrough. Three pieces of driftwood from a low island (Fig. 15.3, sites 1, 2, 3) about 10 m above sea level and 8 km downstream from the present mouth along the old channel have been radiocarbon dated. The radiocarbon ages are: site 1, 135 ± 50 years (UQ-187); site 2, 160 ± 70 years (UQ-190); site 3, 160 ± 60 years (UQ-192), the date coming

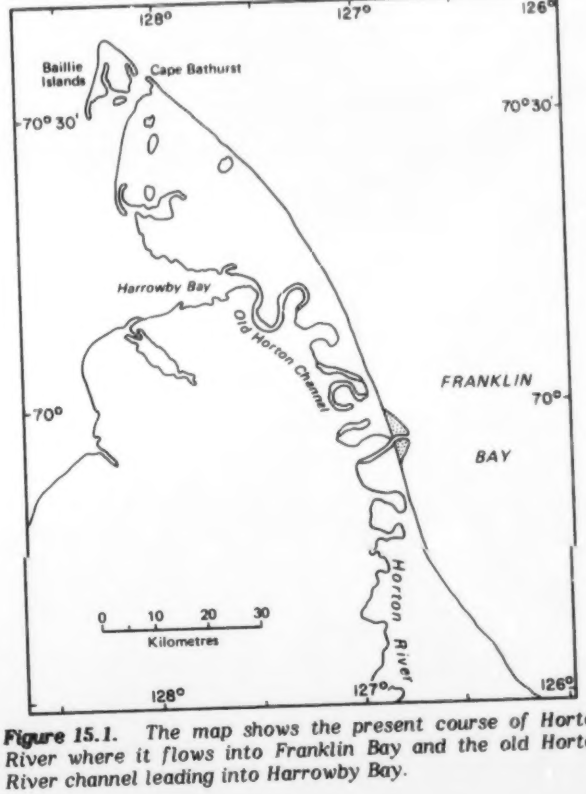

Figure 15.1. *The map shows the present course of Horton River where it flows into Franklin Bay and the old Horton River channel leading into Harrowby Bay.*

---

[1] Department of Geography, University of British Columbia, Vancouver, B.C. V6T 1W5.

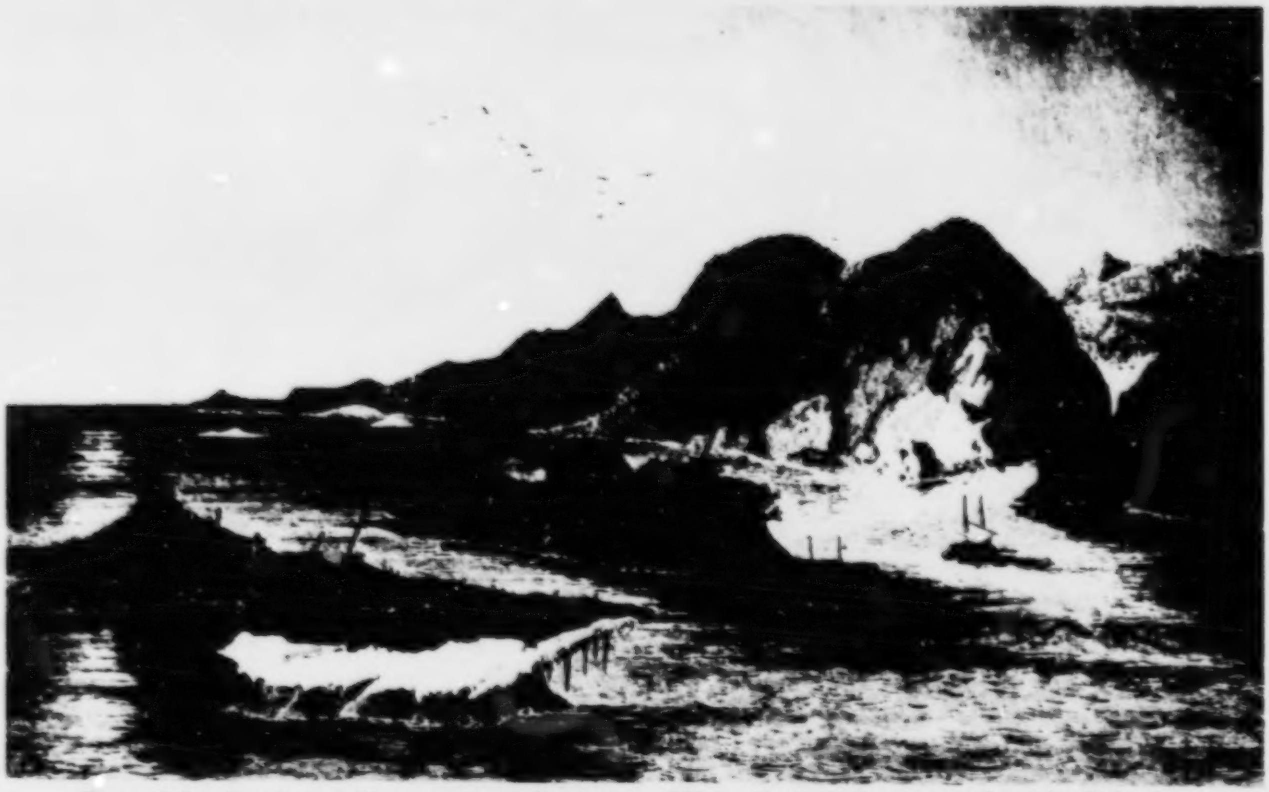

Figure 15.2. *The Horton River mouth as sketched in 1826 by Mr. Kendall, surveyor for John Richardson (Franklin 1828, Plate 25). Note that the following features that appear in the sketch do not now exist: the chute at the mouth; the canyon-like mouth; two driftwood covered islands; and deep water near the river mouth.*

from year 15 to year 58 of a 110 year-old spruce(?) log. Although the possibility exists that some pieces of driftwood may have been transported by people for fuel or other purposes, it seems unlikely that all three pieces would have been so transported and yet agree so well in dates.

Site 4 (Fig. 15.3) is near the edge of a 10 m-high terrace marking the pre-breakthrough Horton River channel. A sample was collected from a driftwood log at 6 m a.s.l. Conceivably the log might have been ice shoved into position at river breakup, but this seems unlikely because the log was lying along the contour as if water borne and the site is protected from windblown ice by a bedrock spur. A branch from the log has been dated at 150 ± 125 years B.P. (GX-5248). The four radiocarbon dates from sites 1, 2, 3, and 4 are all compatible with a "recent" but pre-1826 breakthrough.

At sites 5 and 6 (Fig. 15.3) water-worn twigs were collected from channel gravels of the pre-breakthrough Horton River. The sample at site 5, dated at 3465 ± 140 years B.P. (GX-6817), was from a veneer of river gravel about 0.5 m thick resting on bedrock. The sample was collected 0.3 m below the surface and 5.25 m a.s.l. The gravel was deposited at the outer bank of the large meander bend where it breached the Franklin Bay bluffs to cause the breakthrough. The sample from site 6, dated at 4635 ± 170 years B.P. (GX-6822), was collected in gravel 1 m below terrace level and 7.75 m a.s.l. The samples at sites 5 and 6 do not, of course, reflect the time of breakthrough but they do help to establish a maximum age for the breakthrough.

Site 7 is in an area of ice-wedge polygons where windblown sand from the river bluff blankets the peat at the top of the riverbank. The bottom of the ice-wedge polygon peat at 13.25 m a.s.l. has been dated as 8595 ± 230 years B.P. (GX-7011). The date is near the beginning of the Hypsithermal interval for the western arctic coast. The peat showed no evidence of deposition from flooding by Horton River. A higher sample at 15.5 m a.s.l. has been dated at 5490 ± 165 years B.P. (GX-7012). This date is near the close of the Hypsithermal. The top of the ice-wedge polygon peat, at 16.25 m a.s.l., is covered with about 1 m of windblown sand.

Flights of river terraces, some showing up clearly in Figure 15.3, rise up to 60 m above river level along lower Horton River. No data are available on the ages of these terraces, but they are all unglaciated and could only have formed when their level, with respect to the sea, was far less than at present.

Geomorphic and Permafrost Implications

When Richardson crossed the estuarine mouth of the old abandoned channel at Harrowby Bay in 1826, the water was deep enough to float large cakes of ice and there was no delta. The absence of a delta could be explained by recent submergence and/or aggradation of a channel incised below present sea bottom, when during a lowered sea level, the sea was many kilometres to the north. If aggradation has occurred, then the terrace gravels at sites 5 and 6 (Fig. 15.3) may reflect a period of aggradation and dates at lower depths

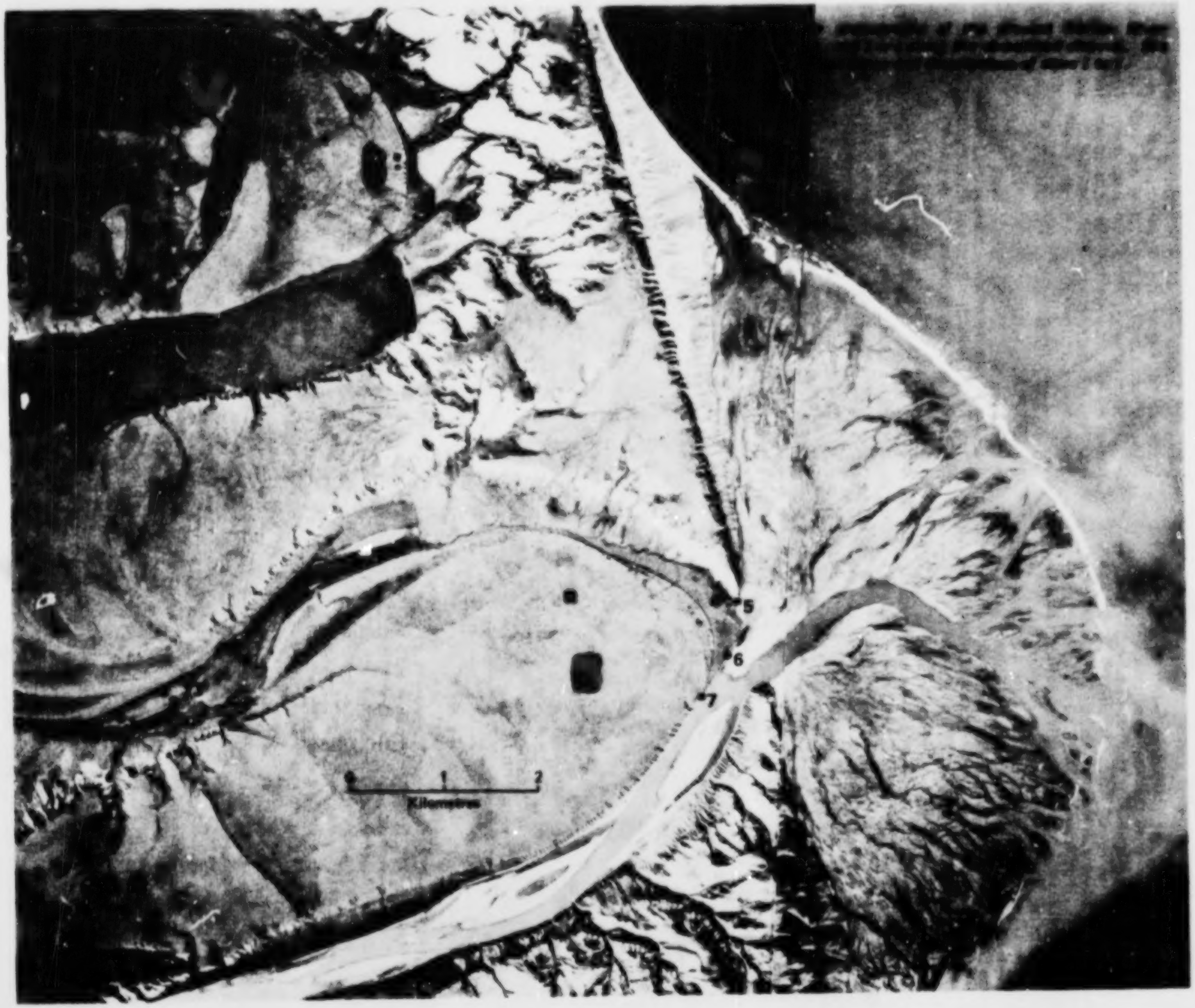
5
6
7
0
1
2
Kilometers

[illegible]

might provide estimates of the aggradational rate. The old abandoned channel has been segmented into oxbow lakes by channel damming from mass wasting and fan-deltas.

Since 1826, and likely from much earlier, there has been combustion from the bituminous shales of the Smoking Hills along the Franklin Bay coast due east of Harrowby Bay. The sulphurous fumes have contaminated the lakes and streams for many kilometres to the west (Mackay, 1958, p. 21, 115). Hutchinson et al. (1978) have studied the effects of the sulphur fumigations from the Smoking Hills on the flora, fauna, soils, and ponds. The research, as the authors point out, has relevance to the long term effect of sulphur fumigations from smelting operations in southern areas. If the channel abandonment of Horton River is correctly dated, the long term effects of sulphur fumigations can then be compared for Horton River sites of vastly different ages.

Permafrost has aggraded downwards along the newly exposed channel bottom and in all likelihood upwards as well. Freeze-back of the channel taliks would be in both open and closed systems. Several types of ice-wedge polygons have grown since the breakthrough on the channel flats and on the fan-deltas. Gelifluction lobes are encroaching onto the old channel floor. Since breakthrough, Horton River has built a 30 km^2 arcuate delta into the relatively deep and saline water of Franklin Bay. Most of the delta material has been transported downstream. Where the delta abuts against the 100 to 150 m-high coastal bluffs, however, alluvial fans and debris flows have spread aprons far out onto the delta flats (Fig. 15.3). The extent of permafrost in the delta and immediately offshore is unknown but poses interesting problems because of the interface between fresh and salt water. Upstream from the Horton River mouth, numerous indications exist of river rejuvenation.

Conclusion

Not long before 1826, Horton River flowed into Harrowby Bay, about 60 km due northwest of the present mouth. Horton River broke through the 100 to 150 m-high coastal bluffs of Franklin Bay to the sea along an outer meander bend. At the site of the breakthrough, Horton River was flowing about 10 m a.s.l. Following the breakthrough, the Horton would have rapidly eroded a canyon in the poorly indurated shales and debris would have been washed into Franklin Bay as a fan-delta. The channel downstream from the present mouth to Harrowby Bay would have been quickly abandoned and any driftwood along it left high and dry. Three radiocarbon dates for driftwood stranded on an island in the old abandoned channel and one date for a driftwood log found near the present mouth suggest a breakthrough date at about A.D. 1800. Although A.D. 1800 should still be considered tentative pending further dating, it is clear that the old abandoned channel has been modified in the recent past, permafrost has grown in the abandoned channel, a 30 km^2 delta has been built out by Horton River into the relatively deep saline water of Franklin Bay, and lower Horton River has been rejuvenated.

Acknowledgments

The fieldwork has been supported by the Geological Survey of Canada and by research grants from the Natural Sciences and Engineering Research Council of Canada. Logistic support has been provided by the Polar Continental Shelf Project (Energy, Mines and Resources). The Inuvik Scientific Resource Centre (Department of Indian and Northern Affairs) has provided facilities in aid of the research.

References

Franklin, J.
1828: Narrative of a second expedition to the shores of the Polar Sea, in the years 1825, 1826, and 1827; John Murray, London, 320 p.

Hutchinson, T.C., Gizyn, W., Havas, M., and Zobens, V.
1978: Effect of long-term lignite burns on arctic ecosystems at the Smoking Hills, N.W.T., in Trace Substances in Environmental Health-XII. A Symposium, ed. D.D. Hemphill; University of Missouri, Columbia, p. 317-332.

Judge, A.S., Taylor, A.E., and Burgess, M.
1979: Canadian geothermal data collection - northern wells 1977-78; Earth Physics Branch, Geothermal Series Number 11, Ottawa, 187 p.

Mackay, J.R.
1958: The Anderson River map-area, N.W.T.; Geographical Branch, Mines and Technical Surveys, Ottawa, Memoir 5, 137 p.

1963: The Mackenzie Delta area, N.W.T.; Geographical Branch, Mines and Technical Surveys, Ottawa, Memoir 8, 202 p.

Rampton, V.
1972: Surficial deposits of portions of the Mackenzie Delta (107C), Stanton (107D), Cape Dalhousie (107E), and Malloch Hill (97F) map-sheets, in Mackenzie Delta Area Monograph, ed. D.E. Kerfoot; 22nd International Geographical Congress (Montreal), p. 15-27.

Yorath, C.J., Balkwill, H.R., and Klassen, R.W.
1975: Franklin Bay and Malloch Hill map-areas, District of Mackenzie; Geological Survey Canada, Paper 74-36, 35 p. and maps.

16. PALYNOLOGICAL STUDY OF SLOUGH SEDIMENTS FROM CENTRAL SASKATCHEWAN

Project 690064

R.J. Mott and E.A. Christiansen[1]
Terrain Sciences Division

Mott, R.J. and Christiansen, E.A., Palynological study of slough sediments from central Saskatchewan; in Current Research, Part B, Geological Survey of Canada, Paper 81-1B, p. 133-136, 1981.

Abstract

Pollen analysis of sediments from Martens Slough dating back to 11 070 ± 245 (S-1199) years B.P. in the Saskatoon area of Saskatchewan yielded a pollen profile similar to that found at other sites in the Western Interior. An early shrub and herb assemblage dominated by ***Shepherdia canadensis*** *gave way to an assemblage high in* ***Picea*** *pollen. Herbaceous pollen taxa then became prominent and* ***Pinus*** *pollen became the most abundant tree genus.*

Shrub and herb vegetation prevailed from about 11 000 to 10 500 years ago. Spruce trees then invaded the area but were replaced about 10 000 years ago by grassland vegetation which prevailed to the present. Despite high ***Pinus*** *pollen values, pine trees probably never grew in the area.*

Introduction

Late Quaternary pollen studies from the prairie region of the Western Interior of Canada are not plentiful because of the lack of sites, due in part to the dryness of the region which precludes the formation of lakes and peat bogs suitable for pollen analysis. Ephemeral lakes, saline lakes, and sloughs are numerous, but these types of sites have not been sampled to any great extent because of the difficulties involved in obtaining samples.

Of the five sites that have been reported from the grassland vegetation zone only one is a complete lake sediment sequence covering the past several thousand years (Mott, 1973). The other four are buried deposits where organic deposition ceased early in postglacial time (Ritchie, 1976). Complete pollen sequences are available from the Aspen Parkland zone in Manitoba (Ritchie, 1976).

During the winter of 1976, as part of an ongoing investigation of geological processes affecting Quaternary deposits, Christiansen examined several sloughs in the Saskatoon area of Saskatchewan. One of these, Martens Slough (52°02' N, 106°29' W), located about 14 km southeast of Saskatoon (Fig. 16.1), provided suitable sediments for both radiocarbon dating and pollen analysis. The results obtained from the pollen analysis comprise this report.

History of Deglaciation

The Wisconsinan deglaciation of southern Saskatchewan has been described in detail by Christiansen (1979). About 17 000 years ago the ice front stood in the vicinity of the Canada-United States border. The ice front retreated in a more or less orderly manner with glacial lakes forming and draining as various drainage outlets were used and abandoned with time. About 12 000 years ago the ice front had retreated north of Saskatoon and glacial Lake Saskatchewan flooded the valleys of North and South Saskatchewan rivers and surrounding area. Further retreat of the ice front ended this phase of the glacial lake, and the Saskatoon area was no longer affected by the ice sheet or associated glacial lakes after about 11 500 years B.P.

Martens Slough formed in glacial Lake Saskatchewan sediments of lacustrine and deltaic origin. The depression is a collapse feature formed either by the melting of an ice-block from under the glacial sediments or by dissolution of the underlying Devonian Prairie Evaporite Formation such as at Crater Lake, Saskatchewan (Christiansen, 1971).

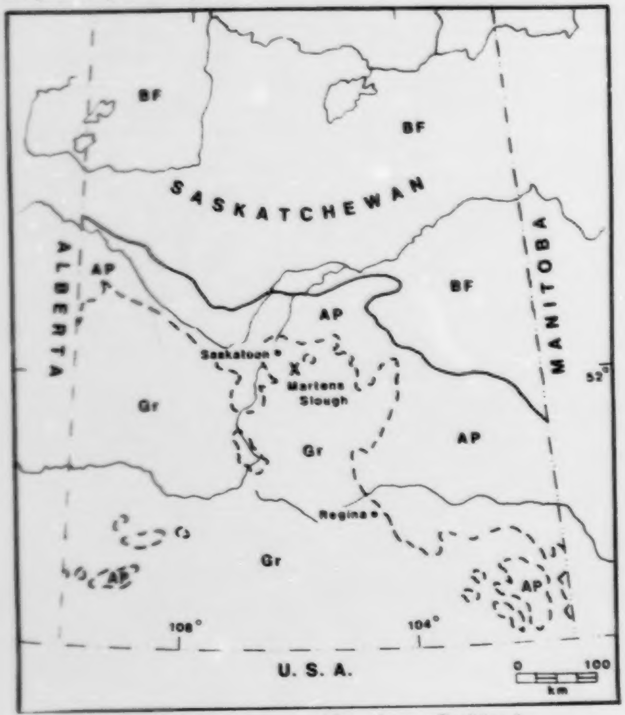

Gr - Grassland AP - Aspen Parkland
BF - Boreal Forest

Figure 16.1. *Map showing the location of Martens Slough and vegetation regions of southern Saskatchewan.*

Methods

A truck-mounted, continuous flight auger was used to sample the sediments through the ice in winter. Inherent in the use of augers is the possibility of contamination by incorporation of sidewall or surface material washing into the hole or adhering to the auger as it is raised or lowered in the hole; however, great care was taken in the augering process to minimize this possibility. The auger was removed from the hole when the auger flights were completely filled following penetration of each 150 cm (5 foot) interval of sediment. Samples representing about 30 or 60 cm increments were then recovered from the auger cuttings,

---

[1] E.A. Christiansen Consulting Ltd., Box 3087, Saskatoon, Saskatchewan, S7K 3S9.

MARTENS SLOUGH, SASKATCHEWAN

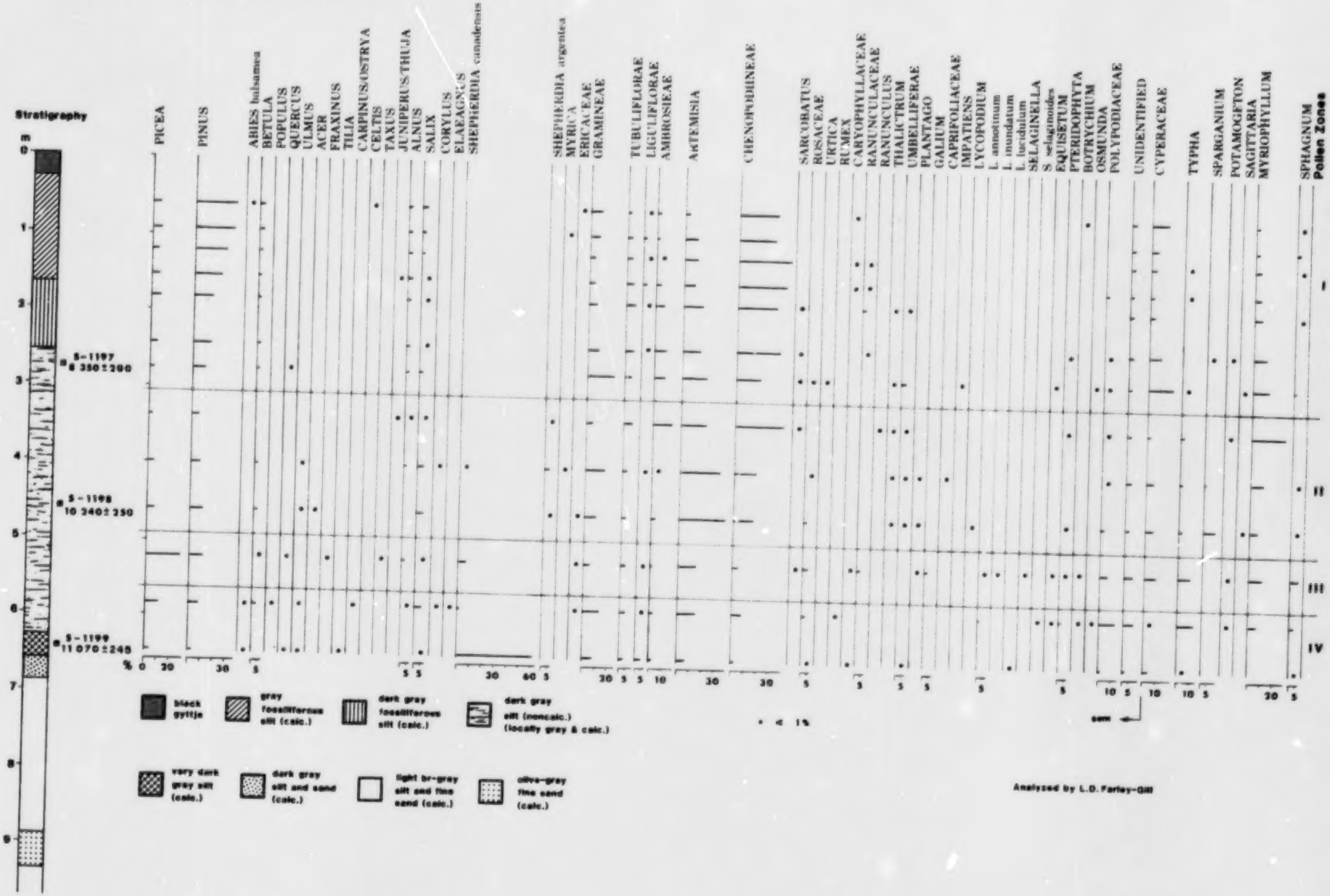

Figure 16.2. *Percentage pollen diagram.*

taking care to obtain uncontaminated sediment. The sample depths are shown on the pollen diagram (Fig. 16.2) as points, but, in fact, each represents a small, but unknown, increment of sediment. Representative subsamples for pollen analysis were extracted from the auger samples and subjected to chemical treatment involving hydrofluoric, hydrochloric, nitric, and acetic acids, acetolysis mixture, dehydration in tertiary butyl alcohol, and suspension in silicon oil for counting.

Stratigraphy and Radiocarbon Dates

Augering showed slough deposits 680 cm deep consisting of black gyttja, grey fossiliferous silt, dark grey silt, grey-black silt, and dark grey silt and sand overlying light grey silt and sand to a depth of 940 cm below the sediment/water interface (Fig. 16.2). The sediment lay below about 120 cm of ice and water. All sediments below the black gyttja were calcareous.

Three radiocarbon dates were obtained from the Saskatchewan Research Council Radiocarbon Laboratory. Organic sediment from a depth of 274 cm below the sediment/water interface gave an age of 8350 ± 200 (S-1197) years B.P. A sample from 457 cm below the sediment surface produced an age of 10 240 ± 250 (S-1198) years B.P., and one from 640 cm depth gave an age of 11 070 ± 245 (S-1199) years B.P. (Rutherford et al., 1979). Here also the samples are shown as point samples (Fig. 16.2), but they actually represent a small increment of sediment obtained from the auger cuttings. Despite the presence of carbonates in the sediments the dates do not appear to be anomalous because of the hard water effect. The possibility exists, however, that some error caused by this problem is present.

Palynological Results

The results of pollen analysis are shown as a percentage diagram (Fig. 16.2). Recovery of palynomorphs from sediments below a depth of 640 cm was too low and the preservation too poor to provide reliable counts and the results are not shown on the diagram. For the results shown, the pollen counts were at least 300 grains. Percentages are based on a sum that includes all palynomorphs except aquatic taxa which are to the right of the column for unidentified grains in the diagram. Four pollen zones are delineated for convenience of description on the basis of kind and abundance of pollen grains and spores and are numbered from the top down. The zones refer to this pollen diagram only and do not necessarily have any regional significance.

Pollen Zone IV

The basal zone, IV, is dominated by **Shepherdia canadensis** with many tetrads or clumps present indicating close proximity to the source. A variety of herbaceous pollen taxa including **Artemisia**, Tubuliflorae, Liguliflorae, Ambrosieae, and Chenopodiineae, as well as abundant Gramineae pollen are also present. Small amounts of **Picea** and **Pinus** pollen are present along with only single grains of other tree genera not indigenous to the area. Cyperaceae and such aquatic genera as **Sparganium** and **Potamogeton** are represented. **Shepherdia canadensis** declines to very low values above the basal level but herbaceous taxa remain abundant throughout the zone.

Pollen Zone III

Picea pollen attains a maximum value of 28 per cent in zone III, but because of the wide spacing (60 cm) of the samples the extent of the maximum appears brief. Although relatively less abundant, the non-arboreal taxa are still plentiful. **Pinus** pollen is slightly more abundant but not nearly abundant enough to indicate the presence of pine trees in the area.

Pollen Zone II

Artemisia becomes the dominant genus in zone II and Chenopodiineae and Gramineae increase as well. **Picea** pollen declines considerably and remains so throughout the zone. **Pinus** pollen also declines somewhat in abundance. Aquatics remain plentiful especially **Myriophyllum** which attains maximum values near the top of the zone.

Pollen Zone I

Artemisia declines steadily in zone I and is replaced in dominance by Chenopodiineae pollen. Gramineae pollen remains abundant as do other herbaceous taxa. Cyperaceae pollen becomes more abundant as well. **Picea** pollen percentages increase slightly in this zone and **Pinus** maintains a steady increase towards the top of the profile.

Discussion

The sequence of events portrayed in the diagram is similar in general to those seen at other sites in the Western Interior of Canada, although details differ due to differences in the local environment of the sites.

The pollen assemblage of the basal sample is unusual in the amount of **Shepherdia canadensis** pollen present. **Shepherdia canadensis** is commonly a prominent component of basal assemblages throughout the Western Interior (Lichti-Federovich, 1970; Mott, 1973; Ritchie, 1976), but with values comparable to those assemblages above the base. The abundance of various herbs and grasses attest to an open environment about 11 000 years ago. If spruce (**Picea**) trees were present, they were there only in small numbers. Pine (**Pinus**) was absent, the **Pinus** pollen present being a result of long-distance transport.

Spruce trees became more prominent about 10 500 years ago, and although pollen values of less than 30 per cent were obtained here, other sites show high values (Mott, 1973; Ritchie, 1976). Whether or not a closed spruce forest was prevalent at all sites, however, is debatable, judging by the abundance of herbaceous taxa present at Martens Slough which indicates considerable open ground was available for these plants.

Picea values decline again before 10 000 years B.P., and **Artemisia**, Chenopodiineae, Gramineae, and other herbs indicate grassland conditions prevailed in the area (Lichti-Federovich and Ritchie, 1965; Mott, 1969). Despite **Pinus** values as high as 30 per cent, it is unlikely that pine trees ever reached the area, and a grassland environment prevailed to the present time. Other grassland sites record similar **Pinus** pollen values throughout their profiles even though pine trees were not present (Mott, 1973; Ritchie, 1976). Modern pollen spectra also show high **Pinus** values well beyond the limit of pine trees (Lichti-Federovich and Ritchie, 1965; Mott, 1969). Pine trees did invade areas about 140 km to the north about 6000 years ago (Mott, 1973) and upland areas more than 350 km to the east even later (Ritchie, 1976), and this may have been the source of the **Pinus** pollen.

Summary

The results obtained from Martens Slough indicate that slough deposits can be used successfully for pollen analysis at least at some sites and that the vegetational history of the Saskatoon area parallels the history of the Western Interior in general.

A sparsely treed or treeless landscape about 11 000 years ago supported abundant herb and shrub taxa but was supplanted about 10 500 years ago by spruce forest. This forest may not have been closed as non-arboreal taxa present attest to some open areas. Grassland vegetation replaced the forests about 10 000 years ago and dominated the region to the present time.

Acknowledgments

The authors are indebted to L.D. Farley-Gill for the pollen analysis. The augerhole was drilled by Don MacRae of Don MacRae Augering, Dundurn, Saskatchewan, who, because of his augering skill and keen interest in geology, has contributed much to research in Quaternary deposits. W. Blake, Jr. provided helpful comments on the manuscript.

References

Christiansen, E.A.
1971: Geology of the Crater Lake collapse structure in southeastern Saskatchewan; Canadian Journal of Earth Sciences, v. 8, p. 1505-1513.

1979: The Wisconsinan deglaciation of southern Saskatchewan and adjacent areas; Canadian Journal of Earth Sciences, v. 16, p. 913-918.

Lichti-Federovich, S.
1970: The pollen stratigraphy of a dated section of Late Pleistocene lake sediment from central Alberta; Canadian Journal of Earth Sciences, v. 7, p. 938-945.

Lichti-Federovich, S. and Ritchie, J.C.
1965: Contemporary pollen spectra in Central Canada. II. The forest-grassland transition in Manitoba; Pollen et Spores, v. 7, p. 63-87.

Mott, R.J.
1969: Palynological studies in central Saskatchewan. Contemporary pollen spectra from surface samples; Geological Survey of Canada, Paper 69-32, 13 p.

1973: Palynological studies in central Saskatchewan. Pollen stratigraphy from lake sediment sequences; Geological Survey of Canada, Paper 72-49, 18 p.

Ritchie, J.C.
1976: The late-Quaternary vegetational history of the Western Interior of Canada; Canadian Journal of Botany, v. 54, p. 1793-1818.

Rutherford, A.A., Wittenberg, J., and Wilmeth, R.
1979: University of Saskatchewan radiocarbon dates VIII; Radiocarbon, v. 21, p. 48-94.

17. CHARACTERISTICS OF BASAL ICE FROM TWO OUTLET GLACIERS IN THE CANADIAN ARCTIC – IMPLICATIONS FOR GLACIER EROSION

Project 750063

R.D. Lorrain[1], R.A. Souchez[1], and J.L. Tison[1]
Terrain Sciences Division

Lorrain, R.D., Souchez, R.A. and Tison, J.L., Characteristics of basal ice from two outlet glaciers in the Canadian Arctic – implications for glacier erosion; in *Current Research, Part B, Geological Survey of Canada, Paper 81-1B, p. 137-144, 1981.*

Abstract

Ice was sampled for chemical and isotopic analyses at the margin of Hook Glacier, Ellesmere Island, and Aktineq Glacier, Bylot Island.

In the section studied at Hook Glacier, striking variations in Cl and Na content occur. This is interpreted as the consequence of recumbent folding which cannot be observed directly.

In the section studied at Aktineq Glacier, the relations between $\delta^{18}O$ and δD values of the samples indicate that striking differences exist among basal ice layers. Some of these layers result from a meltwater refreezing process at the bedrock interface and are located at different heights in section because of recumbent folds and represent only a minor fraction of the basal part. This implies that the whole basal layer is not a result of accretion processes.

Care must thus be taken in evaluating the importance of subglacial erosion by polar outlet glaciers from the thickness of their frontal basal ice and debris layers.

Introduction

Polar outlet glaciers are known, generally, to be characterized by a thick basal layer which differs from the glacier ice above by an abundance of debris bands. The significance of this fact was discussed by Andrews (1971, 1972) and Boulton (1971, 1972). Following Boulton (1971, 1972), this implies that these glaciers carry considerable amounts of englacial debris derived from the glacier bed. This view, however, was not accepted by Andrews (1971, 1972) who considered that the thick basal layer, if present, is a marginal feature developed close to the glacier margin.

The nature of the basal layer can be documented further by chemical and isotopic study of the ice. Presented here are the results of such a study on two outlet glaciers in the Canadian Arctic: Hook Glacier on Ellesmere Island and Aktineq Glacier on Bylot Island.

Hook Glacier, Ellesmere Island

Site Description

Hook Glacier is located on the eastern side of Makinson Inlet (Fig. 17.1), southeastern Ellesmere Island. The lower part of Makinson Inlet is in the Inglefield Mountains,

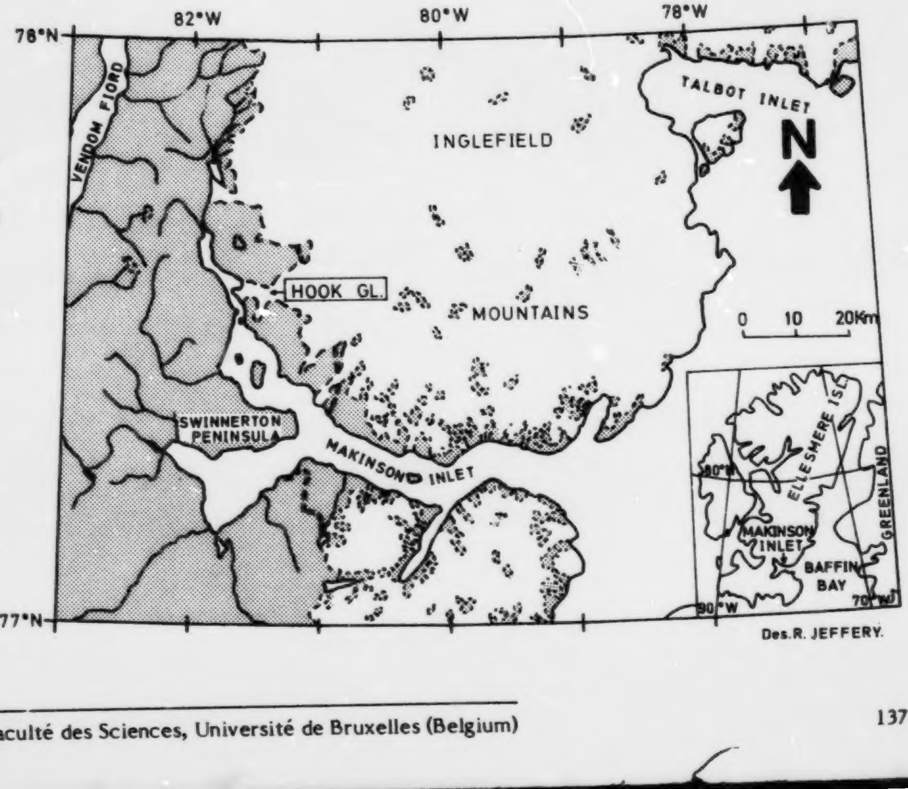

Figure 17.1

Location map of Hook Glacier, Ellesmere Island.

---

[1] Laboratoire de Géomorphologie, Faculté des Sciences, Université de Bruxelles (Belgium)

a rugged area underlain by highly metamorphosed, crystalline Precambrian rocks. To the west, gently inclined Paleozoic sedimentary rocks rest on a well developed unconformity; the north and south arms of Makinson Inlet are incised into these sedimentary rocks which are mainly composed of Paleozoic limestone and friable Cretaceous coal-bearing sedimentary rock. The eastern part of the region on both sides of Makinson Inlet is heavily glaciated with ice caps and icefields whose even surfaces are broken by many nunataks. A great contrast in ice thickness exists between east and west sides of these ice caps. This asymmetry is controlled largely by snow accumulation dependent on precipitation from Baffin Bay (Koerner, 1977).

Hook Glacier has its accumulation zone on the Precambrian rocks whereas its lower part flows in a valley carved into the Paleozoic limestone. This lower part consists of a tongue which divides into two about mid-way between the icecap border and the fiord. The northern tongue reaches Makinson Inlet, is floating, and produces small icebergs, but the southern tongue ends about 1.5 km from the fiord (Fig. 17.2).

In front of the southern tongue, to be considered here, elongated hills, with steep slopes, rise about 30 m above the outwash plain (Fig. 17.3). The hills, oriented at right angles to the direction of glacier flow, are composed of sandy and silty stratified beds, in some places folded, which are capped by a veneer of gravels and pebbles. Remnants of braided stream channels similar to those on the outwash plain can be observed at the level of the pebbly veneer. This landform represents an outwash delta with layers of sand and silt deposited in the fiord environment, capped by gravels and pebbles due to the progradation of the outwash plain. An advance of Hook Glacier has resulted in deformation and fracturing of the outwash deposit and has transformed it into a push-moraine. To the northwest of the glacier front, some undisturbed terrace remnants made up of the same type of material still exist about the present-day outwash. These terrace deposits contain at least one thin layer of marine pelecypod shells (W. Blake, Jr., personal communication, 1977).

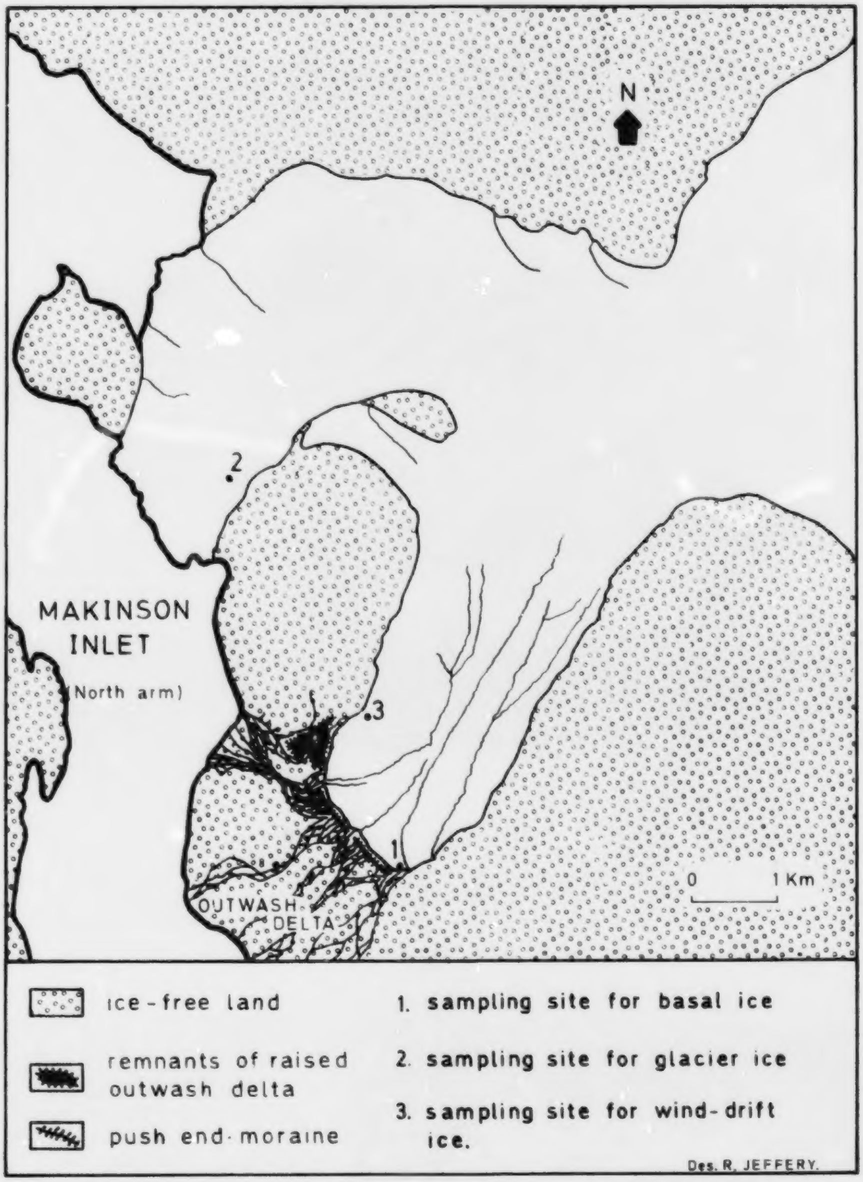
N
2
3
1
MAKINSON INLET
(North arm)
OUTWASH DELTA
0 1 Km
ice-free land
remnants of raised outwash delta
push end-moraine
1. sampling site for basal ice
2. sampling site for glacier ice
3. sampling site for wind-drift ice.
Des. R. JEFFERY.

Figure 17.2. *The frontal zone of Hook Glacier (NAPL A16692-110).*

Characteristics of the Basal Layer

The basal part of the southern tongue of Hook Glacier shows numerous debris bands of contrasting colour. A conspicuous set of red bands, containing mainly pink orthoclase-type feldspar particles, is clearly visible between two sets of greyish bands containing mainly limestone fragments. Each set is a few metres thick. Most of the debris in the bands is sand and silt with a much greater proportion of fines in the greyish bands than in the red ones.

Closer examination of the debris bands showed that they are composed of a series of layers a few millimetres thick, separated by fine grained ice (1 to 2 mm crystal size) of approximately the same thickness. Between the debris bands, thick layers (20 to 150 cm) of particle-free bubbly ice, made up of equigranular crystals a few millimetres in diameter, are present in the sequence. Bubble-free ice layers are not present in the section of basal ice investigated, but they occur (approximately 1 cm thick), interbedded with debris layers, along the southern margin of the northern glacier tongue.

Ice samples were taken in the thick layers of particle-free bubbly ice which are present between the debris bands at site 1 (Fig. 17.2). One group of samples (A) was collected in the red part of the section and a second group (B) was collected from both sets of the greyish part.

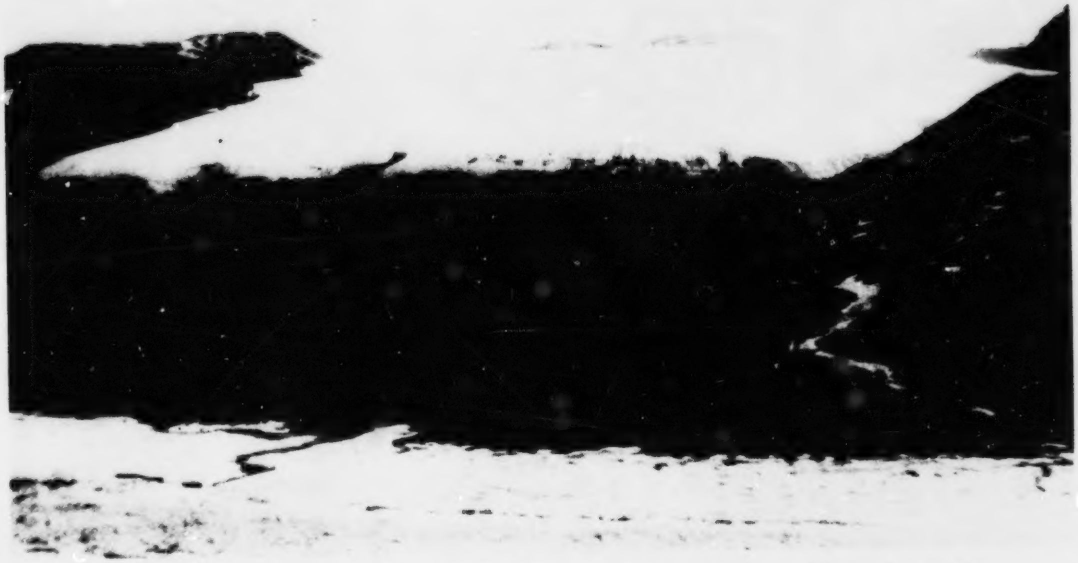

Figure 17.3. *General view of Hook Glacier showing the outwash delta and the push moraine.*

Glacier ice and wind-drift ice also were sampled. Because of extensive snow cover on Hook Glacier, sampling of glacier ice was carried out in crevasses which probably appear as a consequence of floating in the frontal zone of the northern glacier tongue (site 2, Fig. 17.2). The values obtained are assumed to represent values for glacier ice of the southern tongue as well. Wind-drift ice, consisting of ice formed at the beginning of the summer by refreezing of percolating meltwaters from wind-drift snow, was sampled just below the surface of the southern tongue at site 3 (Fig. 17.2).

Sample Treatment and Analysis

The ice cores were sliced with a non-contaminant saw and the slices were allowed to melt in a special type of hot-water bath. Meltwater was filtered in a millipore 0.45 μm filter and transferred to polyethylene bottles which had been washed with a detergent and pure nitric acid and rinsed with triply distilled water in order to remove the major cations sorbed on their walls. Samples having a particle content of more than 0.1 g/kg ice were eliminated because of the potential important of ion exchange for the Na content.

All equipment used in the field (polyethylene syringes, polyethylene gloves, filtering assembly) was sealed in washed polyethylene bags and each item was rinsed with triply distilled water when it was unpacked. New equipment was used for each sample. Blank procedures in the field consist of taking triply distilled water, pouring it into the hot water bath, and filtering it; these procedures showed that contamination was reduced to the background noise level of the instruments used for analysis. The sample bottles were sealed in polyethylene bags for transport. Sodium was determined on the meltwater samples by flame atomic absorption spectrophotometry using the procedure described by Ragone and Finelli (1971) with a recorder-equipped Perkin Elmer 303. A Radiometer automatic potentiometric titration assembly was used for chlorine. This method gives results with a precision of ±0.03 ppm similar to that described by Koide and Goldberg (1971).

Results and Comments

Table 17.1 gives the mean and extreme values in ppm of the chlorine and sodium concentrations for the three types of ice samples; the ratio Cl/Na is also included.

Glacier ice is characterized by its low Cl and Na contents. The values are similar to those obtained in Greenland by Langway (1970) and Cragin et al. (1975) and in Antarctica by Briat et al. (1974). The Cl/Na ratio is relatively variable but is always greater than that of bulk sea water (1.8). Wind-drift ice has higher mean Cl and Na contents and greater concentration variability, the lowest values being not far from mean values for glacier ice. This variability results from ionic migration along with percolating meltwater.

The two groups of basal ice samples, A and B, differ strikingly in their Na and Cl contents, with group B values being an order of magnitude higher. Values for group A are similar to those of wind-drift ice. Moreover, ice of these two groups shows the same bubble abundance and the same equigranular crystals (a few millimetres in diameter). Thus these two groups of ice could have a similar origin. Unlike the other ice samples, group B has a Cl/Na ratio close to that of sea water.

Cl and Na ions are most probably of sea water origin. Different sources are possible, the most probable being recent fiord sediments. Indeed, if fine sediments (100 g) from the push moraine are added to distilled water (100 ml) in the laboratory, after 24 hours high values (between 1.8 and 2.0 mg Cl/100 g sediments) can be obtained in the supernatant solution. Such high values indicate either that sea water is still present within the sediment as interstitial water or that salt minerals occur within the rock fragments constituting the deposit.

Bubbly ice layers poor in Cl and Na and orthoclase-rich debris bands are clearly associated in the middle part of the section. They occur between two similar sets of Cl- and

Table 17.1

Chemical composition of ice samples from Hook Glacier

							Basal ice					
	Glacier ice (11 samples)			Wind-drift ice (11 samples)			Group A (8 samples)			Group B (8 samples)		
	mean	ppm min.	max.	mean	ppm min.	max.	mean	ppm min.	max.	mean	ppm min.	max.
Cl	0.12	0.06	0.18	0.30	0.12	0.72	0.35	0.15	0.58	1.97	0.62	6.26
Na	0.020	0.013	0.034	0.116	0.029	0.293	0.120	0.075	0.180	0.939	0.340	2.735
Cl/Na	6.3	2.9	11.3	3.1	1.6	4.6	2.6	1.7	3.8	2.0	1.6	2.3

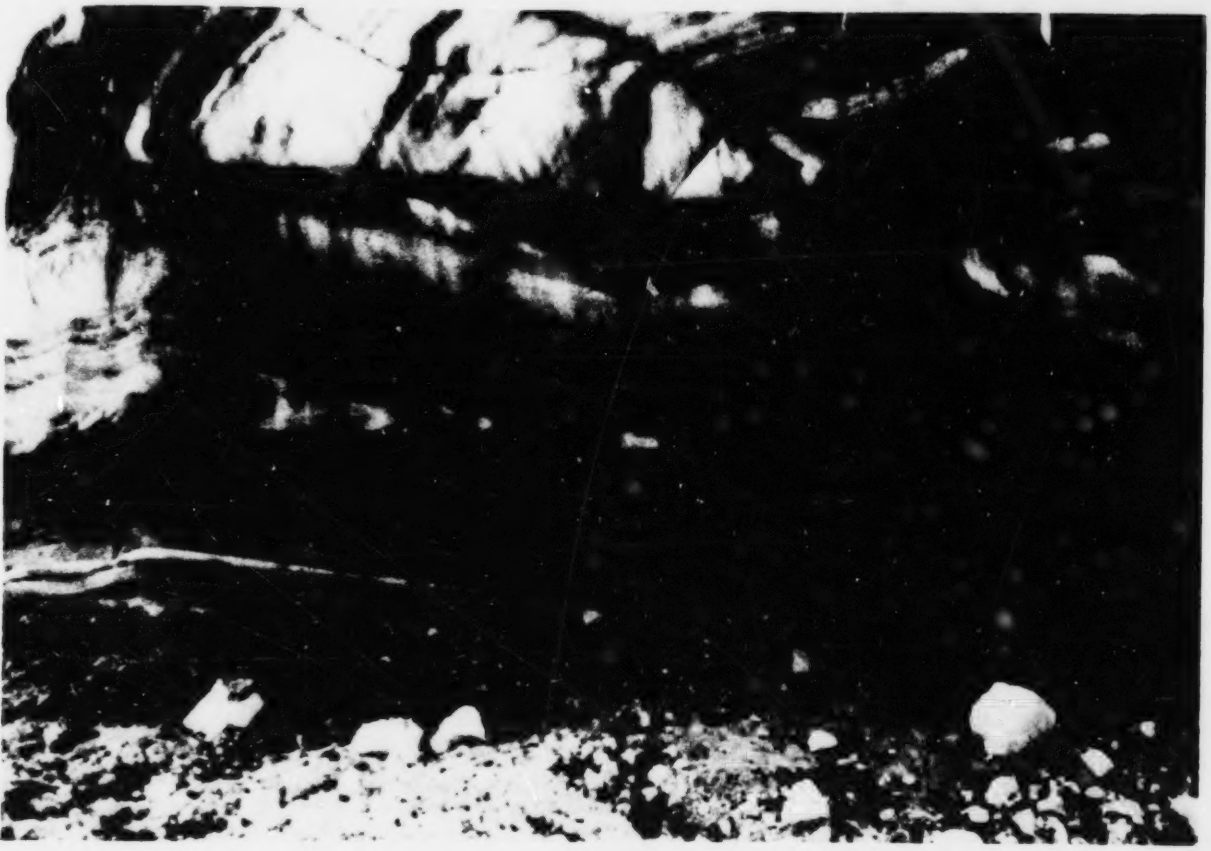

Figure 17.4. Recument folding at the base of the northern tongue of Hook Glacier. The boulder in the lower right part of the photograph is about 40 cm long.

Na-rich ice layers and limestone-rich debris bands. This suggests that a recumbent fold exists at this location, although it is not visible as the basal ice is exposed only in the frontal zone. Fold of this type are, moreover, visible at the base of the northern tongue of Hook Glacier (Fig. 17.4). Thus recumbent folding probably is developed in the basal part of both tongues of Hook Glacier and results in an increased thickness of the basal layer in the frontal zone.

Aktineq Glacier, Bylot Island

Site Description

Bylot Island lies off the northeastern tip of Baffin Island (Fig. 17.1). A central northwest-trending mountainous spine of highly metamorphosed, crystalline, Precambrian-age terrane (Byam Martin Mountains) is surrounded by relatively flat-lying areas at lower overall elevation of unmetamorphosed Proterozoic sedimentary rock and poorly consolidated, coal-bearing, Cretaceous-Tertiary sedimentary rock (Jackson and Davidson, 1975). The highlands area is mostly ice-covered and numerous glaciers flow outwards from it towards both the north and south coasts. Some glaciers cross at least two major lithologic units, and thus glacial debris can be used as a tracer to study mechanisms of glacier erosion. Recent work in this field has been carried out by DiLabio and Shilts (1979) and Klassen (1981). Most of our work was concentrated on a vertical section at Aktineq Glacier (B 17, Glacier Atlas of Canada, 1969).

Characteristics of the Basal Layer

A section about 14 m high was studied at the base of Aktineq Glacier on its eastern side, 2.5 km from the snout (site A, Fig. 17.5). The lower 10 m of the section could easily be differentiated from the bulk glacier ice above in that it contained negligible amounts of bubbly ice and numerous debris layers (Fig. 17.6). Within the lower portion, three main types of ice were encountered. (1) The most abundant type was coarse bubble-free ice, in layers from 1.5 to 48 cm thick, containing aggregates of silty material (about 0.1 cm in diameter). The crystals showed sinuous margins and imbricated forms and varied in size between 2 and 4 cm. (2) The second type consisted of bubble-free monocrystalline ice layers, 0.1 to 0.3 cm thick, associated with sandy layers of approximately the same thickness. Ice crystals were strongly elongated in the plane of the layer and their length varied from 0.5 to 1 cm. Sequences of the two layers up to 12 cm in thickness were observed. The two types of bubble-free ice described above were regularly distributed in the section. (3) The third type was made up of two layers of bubbly ice, 5 and 9 cm thick. The layers were located just above thick frozen bands (8 and 9 cm) of unsorted morainic debris. The ice crystals varied in size between 0.2 and 2 cm and were polyhedral-shaped with even margins. The numerous bubbles were either spherical or elongated in the plane of the layer.

Samples for $^{18}O/^{16}O$ and deuterium/hydrogen (D/H) analysis were collected from all three types of ice in the basal part of Aktineq Glacier as well as in the bulk glacier ice. Glacier ice from adjacent glaciers ("Camp" and Sermilik; Fig. 17.5) was also sampled.

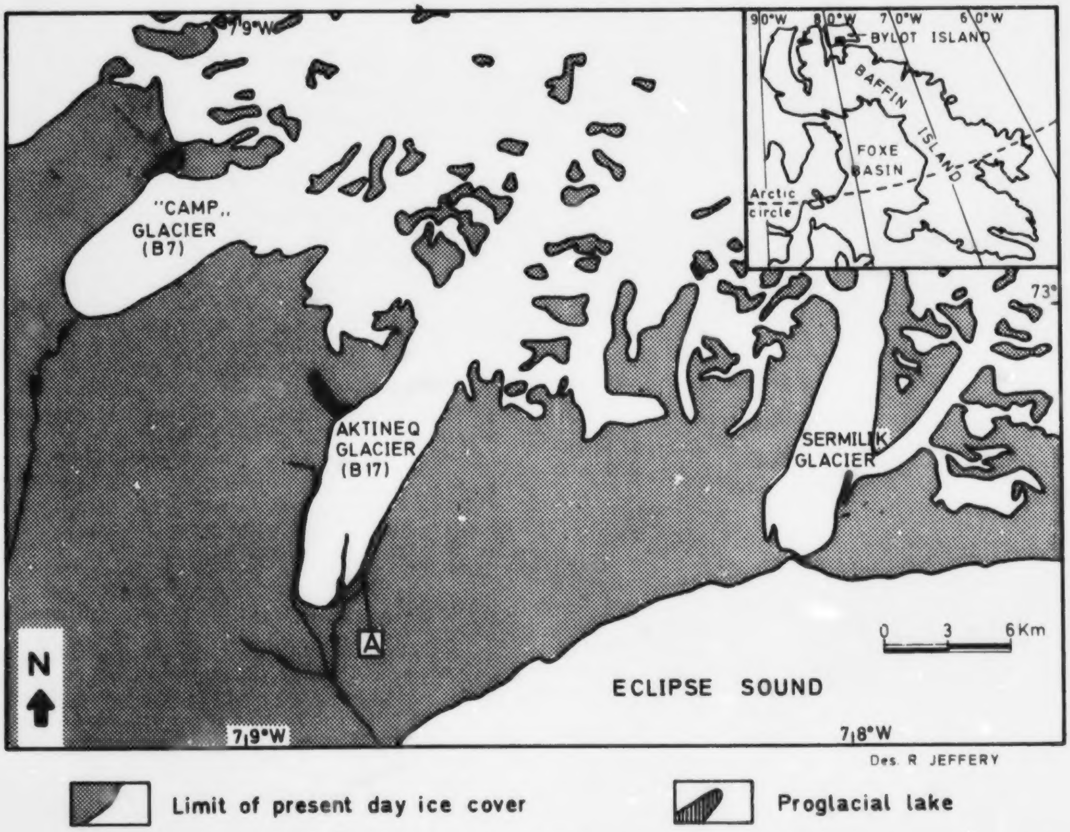

Figure 17.5. Location map of Aktineq Glacier, Bylot Island.

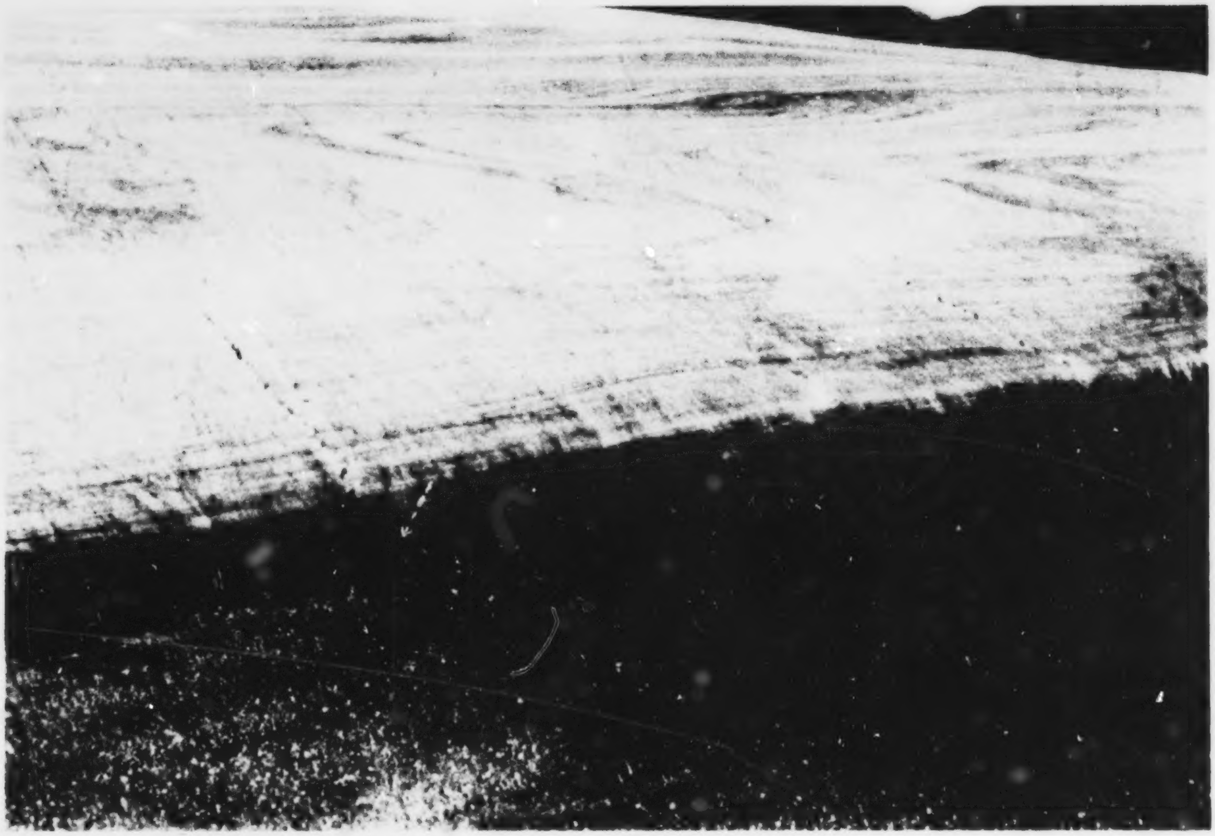

Figure 17.6. The eastern margin of Aktineq Glacier (arrow points to the sampling site).

Sample Treatment and Analysis

The upper 10 cm of ice was removed each time before sampling. An aluminium coring device was then hammered into the ice and the sample extracted and transferred into a polyethylene bottle. The meltwater was transferred into 30 ml glass bottles to avoid possible contamination by diffusion through the polyethylene in the course of time. The bottles, equipped with a screw top self-sealing propylene cap, were then sealed with paraffin wax to prevent evaporation. The samples were analyzed at the Centre d'Etudes Nucléaires de Saclay. The δ D and $\delta\,^{18}$O values are expressed in per mil; precision of measurement is ±0.50‰ for δ D and ±0.15‰ for $\delta\,^{18}$O.

Results and Comments

To reveal processes in which the two heavy components behave in different ways, $\delta\,^{18}$O has been plotted against δ D revealing two linear trends (Fig. 17.7). Most points lie on line A, having a slope of 7.8. This linear relationship with slope of about 8 is known in the literature as being an important feature of isotopic fractionation occurring during condensation or sublimation of water in simple equilibrium (Dansgaard, 1964). This relationship is true for solid precipitation of all types and is thus valid for glacier ice that has not undergone major isotopic changes during and since its formation.

The samples that diverge from line A are located on another straight line, B (Fig. 17.7), with a slope of 4.9. It can be shown that a linear trend with slope of about 5 is the result of a meltwater refreezing process (Jouzel and Souchez, "Melting-refreezing at the glacier sole and the isotopic composition of the ice," submitted). These samples are either the monocrystalline bubble-free ice layers or the bubbly ice found in the basal part of the section. These two types of ice show other characteristics that might indicate an origin linked with a regelation process at the bedrock interface. The shape of the crystals in the monocrystalline ice layers is simialr to that observed by Kamb and LaChapelle in a tunnel at the base of Blue Glacier (1964, Fig. 5, p. 165). The strong elongation of the crystals in the foliation plane and the association with the sandy layers suggest an origin in contact with the bedrock. They also display a weak single maximum fabric that could be expected for ice being formed at the interface in a locally fluctuating stress system associated with flow over an irregular bed (Budd, 1972). Finally, the occurrence of bubbly ice layers just above thick frozen morainic debris bands also suggests that they were once at the sole of the glacier.

The entire basal part of the glacier at the section studied is not necessarily the result of accretion processes alone. The ice foliation above and below the major frozen debris bands defines major recument folds, resembling those described by Hudleston (1976) at the base of the Barnes Ice Cap. Their hinge is nearly horizontal with a strike slightly oblique to the glacier margin. More than one fold is commonly found on the same vertical, implying that the whole 10 m of basal ice might be affected. Independently, some folds with subvertical hinges are displayed at the surface of Aktineq Glacier.

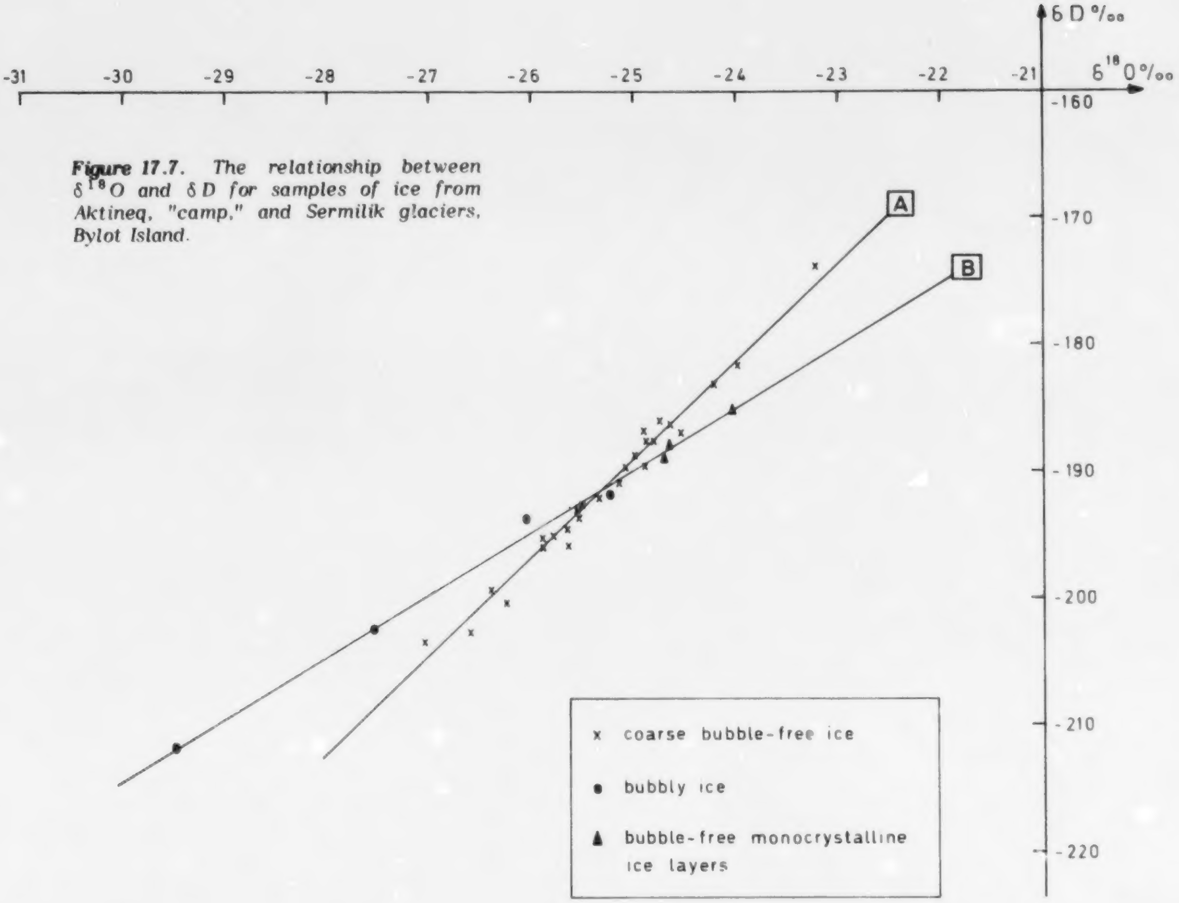

Figure 17.7. *The relationship between $\delta^{18}O$ and δD for samples of ice from Aktineq, "camp," and Sermilik glaciers, Bylot Island.*

Conclusion

As indicated by chemical and isotopic studies on Hook and Aktineq glaciers, a simple accretion process at the glacier sole cannot explain the whole thickness of their basal layer. The distortion of foliation structures in the terminal zone of compression flow enhances the vertical development of the basal layer. In evaluating glacier erosion of polar outlet glaciers, structural deformation and the possibility of "stratigraphic" disorder and repetition of debris bands should be addressed.

Acknowledgments

Geological Survey of Canada and Polar Continental Shelf Project are acknowledged for supporting the field studies, both on Ellesmere Island in 1977 and on Bylot Island in 1979. The authors are much indebted to W. Blake, Jr., T. Frisch, R.A. Klassen, W.W. Shilts, and J-S. Vincent. Also acknowledged are the Fonds National de la Recherche Scientifique (Belgium) for travel grants and the Centre d'Etudes Nucléaires de Saclay (France) for performing the analyses.

References

Andrews, J.T.
1971: Englacial debris in glaciers (Letter); Journal of Glaciology, v. 10, p. 410.

1972: Englacial debris in glaciers (Letter); Journal of Glaciology, v. 11, p. 155.

Boulton, G.S.
1971: Englacial debris in glaciers: reply to the comments of Dr. J.T. Andrews (Letter); Journal of Glaciology, v. 10, p. 410-11.

1972: Englacial debris in glaciers: reply to the comments of Dr. J.T. Andrews (Letter); Journal of Glaciology, v. 11, p. 155-56.

Briat, M., Boutron, C., and Lorius, C.
1974: Chlorine and sodium content of East Antarctica firn samples; Journal des Recherches Atmosphériques, vol. 8, p. 897-901.

Budd, W.F.
1972: The development of crystal orientation fabrics in moving ice; Zeitschrift für Gletscherkunde und Glazialgeologie, Band 8, p. 65-105.

Cragin, J.H., Herron, M.M., and Langway C.C., Jr.
1975: The chemistry of 700 years of precipitation at Dye 3, Greenland; Cold Regions Research Engineering Laboratory, Research Report 341, 18 p.

Dansgaard, W.
1964: Stable isotopes in precipitations; Tellus, v. 16, p. 436-468.

DiLabio, R.N.W. and Shilts, W.W.
1979: Composition and dispersal of debris by modern glaciers, Bylot Island, Canada; in Moraines and Varves, Origin, genesis and classification, ed. Ch. Schlüchter; Balkema, Rotterdam, p. 145-155.

Hudleston, P.J.
1976: Recumbent folding in the base of the Barnes Ice Cap, Northwest Territories, Canada; Geological Society of America, Bulletin, v. 87, p. 1684-1692.

Glacier Atlas of Canada
1969: Bylot Island area 46201, Glacier Atlas of Canada; Inland Waters Branch, Environment Canada.

Jackson, G.D. and Davidson, A.
1975: Bylot Island map-area, District of Franklin; Geological Survey of Canada, Paper 74-29, 12 p.

Kamb, B. and LaChapelle, E.
1964: Direct observation of the mechanism of glacier sliding over bedrock; Journal of Glaciology, v. 5, p. 159-172.

Klassen, R.A.
1981: Aspects of the glacial history of Bylot Island, District of Franklin; in Current Research, Part A, Geological Survey of Canada, Paper 81-1A, p. 317-326.

Koerner, R.M.
1977: Ice thickness measurements and their implications with respect to past and present ice volumes in the Canadian Arctic ice cap; Canadian Journal of Earth Sciences, v. 14, p. 2697-2705.

Koide, M. and Goldberg, E.D.
1971: Atmospheric sulfur and fossil fuel combustion; Journal of Geophysical Research, v. 76, p. 6589-6596.

Langway, C.C., Jr.
1970: Stratigraphic analysis of a deep ice core from Greenland; Geological Society of America, Bulletin, Special Paper 125, 186 p.

Ragone, S.E. and Finelli, R.
1971: Use of atomic absorption spectroscopy in the determination of µg/l concentrations of Na^+, K^+, Ca^{2+} and Mg^{2+}; Atomic Absorption Newsletter, v. 10, p. 126-127.

18. PARCEL 82, DOMINION COAL BLOCK, SOUTHEASTERN BRITISH COLUMBIA

Project 750082

N.C. Ollerenshaw
Institute of Sedimentary and Petroleum Geology, Calgary

Ollerenshaw, N.C., Parcel 82, Dominion Coal Block, southeastern British Columbia in Current Research, Part B, Geological Survey of Canada, Paper 81-1B, p. 145-152, 1981.

Abstract

The Dominion Coal Block, comprising 20 235 hectares (50 000 acres) of federally owned land (including mineral rights to coal), in the Fernie basin area of southeastern British Columbia, was acquired by the Government of Canada under the provisions of the Crow's Nest Pass Act of 1897, the legal transfer taking place in 1905. The Dominion Coal Block is divided into two separate parcels, Parcel 73, on Sparwood Ridge, and the larger Parcel 82, at the headwaters of Flathead River. A previously unpublished geological map of Parcel 82 and adjacent areas, on a scale of 1:100 000, illustrates the basic synclinal structure of Parcel 82, involving the doubly plunging McEvoy Syncline. Loop and Flathead faults are not separate, en echelon faults, as previously interpreted, but one continuous fault. The name Loop Fault is dropped. The northern end of the Flathead Fault, as described by Price in 1962, is not the Flathead Fault, but the McEvoy Fault, part of a system of retrothrust faults, which has been cut and displaced by the Flathead Fault. The McEvoy, McLatchie, Hinge and Morrissey faults form the retrothrust fault system around the southern and eastern sides of McEvoy "Bowl", and are interpreted as two separate original thrust faults, one east-dipping (Morrissey-Hinge) and the other west-dipping (McEvoy-McLatchie). Both of these faults underwent reversal of transport in the hanging wall to culminate with a net normal displacement. A new thrust fault, designated Barnes Thrust is mapped from Flathead River to north of Michel Creek, passing between Mount Taylor and Tent Mountain. The structural development of the area is related to an early compressive phase and later extension. The structures at different stratigraphic levels are visibly disharmonic and two main décollement horizons are recognized. An upper décollement horizon in the Mist Mountain Formation is interpreted as an interval of preferred detachment, utilized by numerous separate faults of local displacement only. A lower décollement horizon at the Spray River, basal Fernie level, may have been the locus of regional movement and the entire succession of Fernie and younger strata in the Fernie basin could be allochthonous.

Introduction

The Dominion Coal Block is located in the Fernie basin area of southeastern British Columbia (Fig. 18.1). It consists of two separate parcels of land. Parcel 73 is the smaller and northernmost of the two and is situated about 10 km south of Sparwood on Sparwood and Hosmer ridges. It incorporates 5000 acres (2023.5 ha). A preliminary outline of the geology of Parcel 73 has been published (Ollerenshaw, 1977). Parcel 82 is the larger and southernmost of the two parcels. It encompasses 45 000 acres (18 211.5 ha) in an elongate strip some 7.5 km wide extending for 29.75 km in a northeast-southwest direction from Mount Taylor to Flathead Ridge.

Canadian Government Acquisition of Dominion Coal Block

The Crow's Nest Pass Act, assented to on June 29, 1897, required Canadian Pacific Railway, amongst other things, to convey to the federal government up to 50 000 acres of any railway construction subsidy land grants acquired from the British Columbia government. This acreage was to consist of lands which the Director of the Geological Survey of Canada considered to be coal-bearing. In exchange for the land the federal government authorized a subsidy to the railway of $11 000 per mile (not to exceed $3 630 000) toward the cost of constructing the railway line from Lethbridge, Alberta to Nelson, British Columbia.

In July 1897, Canadian Pacific Railway, British Columbia Southern Railway (originally the Crow's Nest and Kootenay Lake Railway Company, chartered in 1888) and Kootenay Coal Company (forerunner of the Crow's Nest Pass Coal Company) undertook to build the railway and exchange 50 000 acres for the subsidy. In August 1897, Canadian Pacific purchased the British Columbia Southern Railway, and on September 6th, 1897 signed the agreement with the federal government for the land exchange and subsidy under the terms of the Crow's Nest Pass Act.

The timing of the above agreements is interesting, because, although land grants to the railways had been provided for by the British Columbia Railway Subsidy Act in 1890, the actual land grant to British Columbia Southern Railway Company was not made until August 18th, 1899. The pie had been carved up before it was cooked. Order-in-Council No. 539, by the Lieutenant Governor-in-Council of British Columbia granted 610 000 acres in the Kootenay District to the British Columbia Southern Railway conveyed by Crown Grants 1165-109 and 1166-109, reserving all minerals other than coal to British Columbia.

In 1900, James McEvoy of the Geological Survey of Canada assisted by J. Keele and in co-operation with A.O. Wheeler, surveyed the Fernie basin preparatory to selecting the 50 000 acres. McEvoy estimated that there were some 230 square miles (almost 150 000 acres) of coal measures in Crow's Nest Coalfield, that provided at least 100 feet (30.5 m) of workable coal. He calculated that the basin contained approximately 22 595 200 000 U.K. tons of coal (McEvoy, 1901). On August 31st, 1901, McEvoy resigned from the Geological Survey of Canada and joined the Crowsnest Pass Coal Company.

From June to October 1901, W.W. Leach, accompanied by T.C. Dennis, continued the geological investigation of the Crow's Nest Coalfields (Leach, 1902).

Based on the McEvoy and Leach investigations the Dominion Coal Block parcels were selected and finally confirmed by Order-in-Council P.C. 664, dated 19th May, 1902. The perimeters of the two parcels were surveyed between 1902 and 1905. On September 14th, 1905, title to the surface and coal rights was conveyed by deed to the Crown in right of Canada from the British Columbia Southern Railway Company. On 27th November, 1905, the District Registrar in Nelson, B.C., issued a Certificate of Indefeasible Title (19-1), to His Majesty in right of Canada, for the Dominion Coal Block. It had taken eight years since the land acquisition had been authorized under the Crow's Nest Pass Act until the title was actually transferred.

Under the Crow's Nest Pass Act of 1897, in Sub-clause 1 (i) it is stated that:

> "The said fifty thousand acres. . . . to be therefore held or disposed of or otherwise dealt with by the Government as it may think fit on such conditions, if any, as may be prescribed by the Governor-in-Council, for the purpose of securing a sufficient and suitable supply of coal to the public at reasonable prices, not exceeding two dollars per ton of two thousand pounds free on board cars at the mines".

If the reference to, "the public", is interpreted as restricting sale of the coal to the Canadian public, then export of this coal would be against the law. Certainly the act clearly states that the coal must be sold for two dollars or less a ton. These constrictions clearly preclude the development of mines in and the sale of coal from the Dominion Coal Block until the Crow's Nest Pass Act is repealed or revised.

A geological field investigation of Parcel 82 of the Dominion Coal Block was undertaken by the author from 1977-1980.

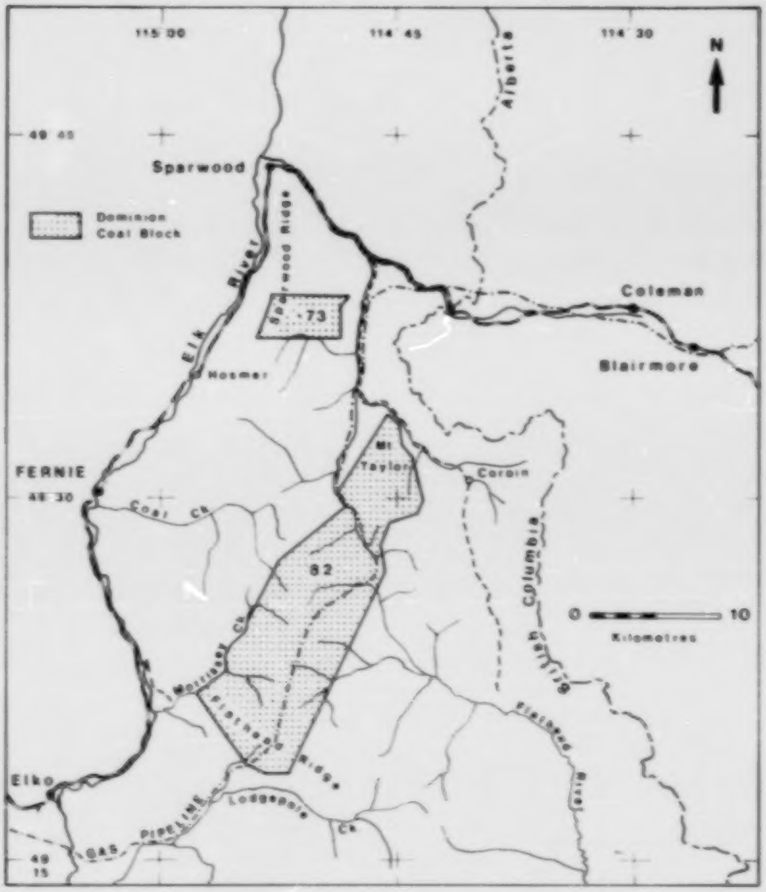

Figure 18.1. The Fernie basin area, in southeastern British Columbia, showing the location of the Dominion Coal Block, Parcels 73 and 82.

Geology

Figure 18.2 is a geological map of Parcel 82, based on detailed field work within the parcel itself, but mainly air photographic interpretation (supported by minor, local field work) for the area outside Parcel 82.

General Stratigraphy

The main stratigraphic units are shown on the legend in Figure 18.2. Lithologies and approximate average thicknesses of these units are as follows:

Alberta Group

Wapiabi Formation +115 m
probably dark grey shale; concretionary shale; and siltstone (marine)

Cardium Formation 50 m
brownish-grey sandstone; and dark grey, shale (?nonmarine)

Blackstone Formation 120 m
dark grey, rubbly mudstone and shale; siltstone and sandstone (marine)

Blairmore Group

Beaver Mines - Mill Creek Formation 1875 m
greenish grey and maroon mudstone; feldspathic sandstone; igneous-pebble conglomerate and quartzite-pebble conglomerate (nonmarine)

Lower Blairmore 455 m
greenish grey, grey and maroon mudstone; siltstone; cherty sandstone and conglomerate; and minor limestone (nonmarine)

Cadomin Formation 75 m
Chert-pebble conglomerate; sandstone; maroon and greenish grey mudstone; and minor limestone (nonmarine)

[Total thickness of Blairmore Group 2405 m]

Kootenay Group

Elk Formation 210-540 m
dark grey mudstone, shale and siltstone; cherty sandstone and conglomerate; minor coal and needle coal (nonmarine)

Mist Mountain Formation 425 m
dark grey to black mudstone, shale and siltstone; sandstone; and coal (nonmarine)

Morrissey Formation 70 m
grey to black cherty sandstone; limonitic, brown sandstone; minor mudstone (nonmarine and beach)

[Total thickness of Kootenay Group 705-1035 m]

Fernie Formation	350 m
dark grey shale; siltstone; calcareous siltstone; and sandstone (marine to pro-delta)	
[Passage beds	100 m]
Spray River Group	155 m
siltstone; calcareous and dolomitic siltstone; sandstone; and shale (marine)	
Rocky Mountain Group	200 m
sandstone; dolomitic sandstone and dolomite (marine)	
Rundle Group	not estimated
limestone; dolomite; chert; and shale (marine)	

The Morrissey and Cadomin formations, together with the two conglomerate units in the middle and upper parts of the Blairmore Group, serve as excellent marker horizons both in the field and for the purpose of delineating structures on the geological map. The lowermost of the two conglomerate units in the Beaver Mines-Mill Creek interval, is the igneous-pebble conglemerate (open circles on map), while the uppermost (solid circles on map) is here designated the quartzite-pebble conglomerate after common and conspicuous quartzite clasts. The apparent absence of the igneous-pebble conglomerate in the southern and eastern parts of the McEvoy Syncline results from the fact that these areas were not traversed, but were interpreted from air photographs, so that positive identification of the conglomerate in the south and east was not possible. At the northeastern end of McEvoy Syncline, north of the McEvoy Creek, three separate units of igneous-pebble conglomerate occur in the lowermost 455 m of the Beaver Mines Formation, although the middle unit appears to be the major conglomerate.

Coal seams of potential commercial value are restricted to the Mist Mountain Formation of the Kootenay Group. Surface outcrops of the coal-bearing strata are confined to the northern and southern perimeters of "McEvoy Bowl", passing into the subsurface under the structure to reach a maximum depth of more than 3000 m below the surface at its centre (between Flathead River and McEvoy Creek). In Parcel 82 the coal-bearing strata outcrop along Flathead Ridge in the south and around Mount Taylor in the north.

The Elk Formation overlies the coal-bearing strata. This formation varies in thickness across the area, thinning from west to east. It is about 540 m thick above Morrissey Creek, 335 m thick at Mount Taylor, 327 m thick on Flathead Ridge (pipeline section) and an estimated 210 m thick in the east above McLatchie Creek. The writer disagrees with the statement by Pearson and Grieve (1980, p. 93), that the base of the Elk Formation is defined, ". . . as the first appearance of needle coal". The Elk Formation at its type section (Newmarch, 1953) is a coarse clastic facies, probably a fan (Gibson, 1977, p. 783). The formation contains abundant conglomerates in the west which fine eastwards into sandstones. As a general guideline the Mist Mountain/Elk contact is drawn above the main coal-bearing facies (Mist Mountain Formation) and below the main course clastic facies (Elk Formation). The "needle coals" (Newmarch, 1953, p. 41; Ollerenshaw, 1977, p. 157; Gibson, 1977, p. 782; Ollerenshaw, 1981, p. 345) are a minor constituent of the Elk Formation, typically occurring in its upper part, an apparently unique characteristic of the upper Elk but not diagnostic of the Elk Formation as a whole or the base in particular.

General Structure

The main structural elements in and around Parcel 82 (Fig. 18.2), are as follows:

1. McEvoy Syncline
2. Flathead Fault
3. Barnes Anticlinorium
4. Barnes Thrust
5. McEvoy west-dipping Retrothrust (possibly including McLatchie)
6. Morrissey east-dipping Retrothrust (possibly including Hinge)
7. Lookout Thrust

Deformation of the strata appears to have been accomplished in two main phases:

A. Compression and contraction (approximately Late Cretaceous to Paleocene)

B. Tension and extension (approximately Eocene to Oligocene)

Phase B appears to have been accompanied by some folding, best described as accommodation structures, probably produced by gravity slumping during extension. Some existing folds were modified and their axes locally re-aligned during this episode - for example, Twisted Syncline and McEvoy Syncline.

In general, structures are aligned north-south, with common variation to a northwest-southeast trend, local variations to northeast-southwest and minor east-west. It is significant that, within the area mapped, the Cretaceous strata tend to the north-south alignment and pre-Cretaceous strata to the northwest-southeast. This relationship between the age of strata and structural alignment probably reflects the disharmonic structural relationship noted by Price (1962, p. 52) between the base of the Kootenay Group and the Paleozoic rocks. The writer would take this interpretation one stage further and suggest that there are two levels of décollement. The décollements separate distinct styles of deformation. The lower detachment occurs in the Triassic, Spray River to Jurassic basal Fernie interval, and the upper in the upper part of the Mist Mountain Formation of the Kootenay Group. Three structural levels with contrasting styles of deformation are separated by the two major décollements. The lowermost level involves rocks of Paleozoic age, with tight, high amplitude folds of relatively medium wavelength, locally overturned and cut by numerous thrust faults. The middle level consists of rocks of Triassic to Jurassic age, forming more numerous tight, low amplitude folds of relatively short wavelength, cut by numerous thrust faults. The uppermost level occurs in Cretaceous rocks and comprises broader, gentle folds of low amplitude and relatively long wavelength cut by fewer thrust faults but numerous normal faults. The disharmonic relationships are particularly well exposed in the vicinity of Flathead Ridge, especially around Morrissey Creek. As the more detailed discussion below demonstrates, fault displacements in the Fernie basin indicate that the upper décollement interval was the locus of many individual and separate fault displacements of local rather than regional extent. It would be more accurately described as a preferred detachment interval. The lower décollement interval on the other hand may have served as a regional detachment with considerable lateral displacement along the bedding, producing little apparent stratigraphic displacement. Such a detachment surface may underlie the entire Fernie basin, with the implication that the

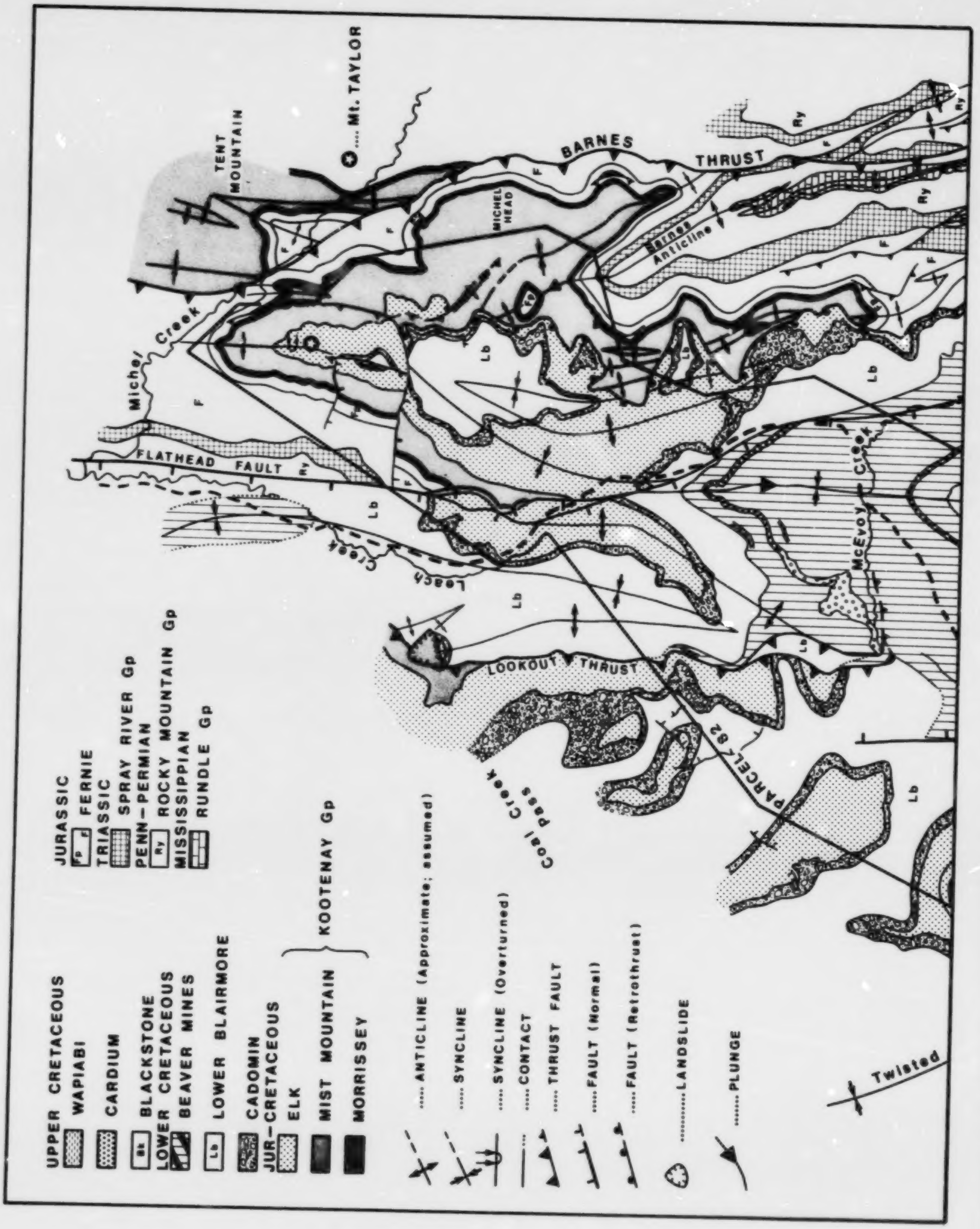
UPPER CRETACEOUS
WAPIABI
CARDIUM
Bk BLACKSTONE
LOWER CRETACEOUS
BEAVER MINES
Lb LOWER BLAIRMORE
CADOMIN
JUR-CRETACEOUS
ELK
MIST MOUNTAIN
MORRISSEY
KOOTENAY Gp
JURASSIC
Jf FERNIE
TRIASSIC
SPRAY RIVER Gp
PENN-PERMIAN
Ry ROCKY MOUNTAIN Gp
MISSISSIPPIAN
RUNDLE Gp
ANTICLINE (Approximate; assumed)
SYNCLINE
SYNCLINE (Overturned)
CONTACT
THRUST FAULT
FAULT (Normal)
FAULT (Retrothrust)
LANDSLIDE
PLUNGE
Twisted
TENT MOUNTAIN
Mt. TAYLOR
BARNES THRUST
MICHEL HEAD
Barnes Anticline
Michel Creek
FLATHEAD FAULT
Leach Creek
LOOKOUT THRUST
PARCEL 82
Coal pass Creek
McEvoy Creek
Lb
F
Ry

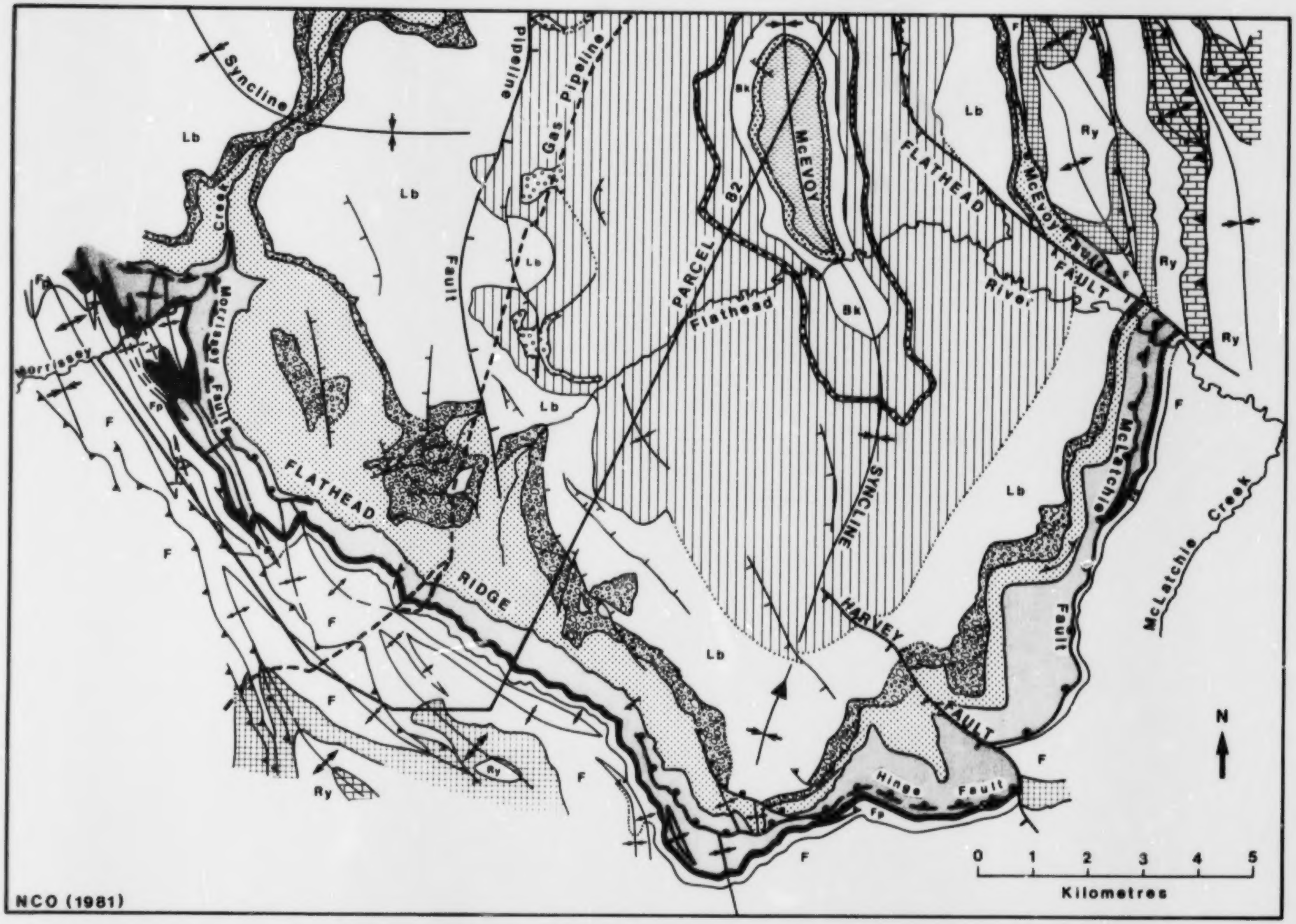
Syncline
Lb
Creek
Morrissey
Morrissey Fault
Fp
F
Pipeline
Gas Pipeline
Fault
PARCEL 82
Flathead
McEVOY
Bk
FLATHEAD
McEvoy Fault
FAULT
River
Ry
FLATHEAD RIDGE
SYNCLINE
HARVEY
McLatchie
McLatchie Creek
Hinge Fault
N
0 1 2 3 4 5
Kilometres
NCO (1981)

Figure 18.2. *Geological map of Parcel 82, Dominion Coal Block and adjoining area.*

Jurassic and younger strata throughout the basin could be entirely allochthonous. A hidden thrust of this type would eventually diverge from the bedding and descend the section westwards, rooting in a major thrust fault west of the basin, such as the Hosmer Thrust or the continuation of the Bourgeau Thrust, which the writer suggests continues down the Elk River valley between Sparwood and Fernie.

During the period of "east-west" compression the hanging wall segments of thrust faults were transported toward the east-north-east and northeast.

McEvoy Syncline

The structure of Parcel 82 is dominated by the doubly plunging McEvoy Syncline which cuts across the central part of the parcel. The area covered by the map could be described as the McEvoy Bowl. The axis of McEvoy Syncline is sinuous (somewhat sigmoidal) but as a whole has a north-south alignment.

The west flank of McEvoy Syncline is relatively simple, with shallow dips, minor folding and many normal faults. Farther southwest, on the southwest side of Flathead Ridge, the vertical disharmony in structural style is clearly illustrated by the sudden transition to close, tight folding and numerous faults, which occur below the Elk Formation, in the Mist Mountain, Morrissey and Fernie formations.

Lookout Thrust

On the northwest side of McEvoy Syncline, the strata are cut by the southern termination of Lookout Thrust (see Ollerenshaw, 1977), which has a stratigraphic displacement of at least 400 m where it crosses the boundary of Parcel 82. Lookout Thrust is clearly visible on McEvoy Creek, but appears to terminate very abruptly at this point as it cannot be traced south of the creek across the hills on the west limb of McEvoy Syncline. It is probable that the thrust passes into the bedding south of McEvoy Creek, making recognition difficult, and it is possible that the fault was folded around McEvoy Syncline at this point.

The east flank of the McEvoy Syncline is cut by the Flathead Fault from Flathead River northwards to McEvoy Creek. Farther north, between McEvoy Creek and Leach Creek, the fault cuts across the axial part of the syncline to its west limb, while the syncline continues east of the fault to run northwards through Mount Taylor, in the extreme north of Parcel 82, dying out in that direction.

Flathead Fault

The Flathead Fault in the area mapped is a medium-angle normal fault, with no apparent component of strike-slip motion. The surface trace of the fault curves from a northwest-southeast orientation in the south (the Flathead River segment) to a north-south direction in the north (the Leach Creek segment). The strata are downthrown on the southwest and west sides of the fault. More detailed mapping has enabled the writer to re-interpret the Flathead Fault and make some changes from the interpretation shown by Price (1962) on the Fernie (east half) map. Price (op. cit.) mapped the McEvoy Fault (this paper) as the northern termination of the Flathead Fault and the Leach Creek segment of the Flathead Fault (this paper) as a separate fault, called the Loop Fault with an en echelon, offset relationship between the two faults. The writer's more detailed mapping has revealed that the McEvoy and Flathead are in fact two separate and distinct faults, with the McEvoy apparently cut and offset by the younger Flathead. Detailed mapping has also revealed that the Flathead and Loop faults appear to be one continuous fault, not two. Admittedly, control is poor between Flathead River and Leach Creek and the stratigraphic displacement is small (possibly as low as 300 m), but contact offsets clearly indicate the continuation of the Flathead Fault into the Loop Fault. The name Loop Fault is therefore dropped. It is the writer's opinion, based on a study of air photographs, that the Flathead Fault is also continuous with the Erickson Fault in the vicinity of Erickson Creek north of Highway 3, so that the Flathead Fault forms a single fault along the east side of Fernie basin, from Flathead River to north of Fording Mountain. Pearson and Grieve (1979, p. 62) mapped the Flathead and Loop faults as separate structures and reversed the displacement on the Loop, placing the older rocks to the east on the downthrown side. Gigliotti and Pearson (1979) also mapped a fault in the position of the Loop Fault with an eastward downthrow. The writer disagrees with this interpretation as the stratigraphic displacement clearly demonstrates that the Loop Fault (Flathead of this paper) downthrows to the west, not the east.

Field relationships suggest that the McEvoy-McLatchie and Flathead Fault surfaces intersect at an acute angle, with Flathead Fault dipping more steeply westward than the McEvoy. It is possible that during the extension phase some transfer of displacement may have taken place between the two faults. The McEvoy Fault could have acted in part as a splay from the Flathead with some hanging wall displacement down the McEvoy Fault, transferring to the Flathead below the line of intersection between the two fault surfaces. This would mean that the McEvoy-McLatchie fault may not be simply offset by Flathead Fault and that the fault relationships may be quite complex. Price's (1962) interpretation of McEvoy Fault as Flathead Fault would be partly correct if McEvoy Fault at some stage in its development functioned as a temporary splay of Flathead Fault.

Barnes Anticlinorium

The Barnes Anticline is the major anticline affecting Parcel 82. It is aligned northwest to southeast, situated on the east side of Flathead Fault and enters the north end of Parcel 82, just south of Mount Taylor, passing under McEvoy Fault. The axis of Barnes Anticline links en echelon with other fold axes and the structure is more properly defined as an anticlinorium with Mississippian Rundle Group and Permian-Pennsylvanian Rocky Mountain Group strata in its exposed core.

Barnes Thrust

A thrust fault (previously unmapped), here named Barnes Thrust, cuts across Barnes anticlinorium. The surface trace of this fault follows the axial region of the anticlinorium near Flathead River, cuts across to the forelimb south of Michel Head and eastward across other folds around the east side of Mount Taylor along Michel Creek, separating Mount Taylor from Tent Mountain. Barnes Thrust cuts up section from Rundle and Rocky Mountain strata in the south to Fernie and Kootenay strata in the north. This thrust presumably passes westward under Parcel 82, although almost certainly merging with other faults in that direction.

McEvoy Retrothrust

The McEvoy Fault, part of Price's (1962) Flathead Fault, is a low angle normal fault which is almost certainly an original thrust fault that underwent a reversal in the direction and amount of hanging wall translation, sufficient to displace the strata back beyond the position of origin. Such a fault is here described as a retrothrust. The considerable development of local folding and faulting associated with McEvoy Fault, particularly in the footwall, clearly demonstrates the compression and crustal shortening which accompanied the development of the original fault surface.

This is incompatible with the present normal fault displacement. The low angle of the surface is also more consistent with a thrust fault surface than a normal fault. It is, therefore, concluded that McEvoy Fault formed as a thrust fault during the early compressive phase of deformation and was reactivated during the later extension phase of deformation with normal displacement exceeding thrust displacement.

Pearson and Grieve (1979, p. 64) referred to McEvoy Fault as the "East Crop fault" and described it only as a normal fault and "a low angle gravity fault (lag). . .". Gigliotti and Pearson (1979) also describe East Crop Fault as a simple "low-angle" normal fault.

The McLatchie Fault is situated along the ridge northwest of McLatchie Creek and southwest of Flathead Fault. This fault is almost certainly the southward continuation of McEvoy Retrothrust, offset by Flathead Fault, but is identified by a different name for easier reference. McLatchie Fault cuts down section southwestwards in its footwall, moving from the middle of the Mist Mountain Formation to rest on Fernie Formation (Passage beds) in the vicinity of Harvey Fault. These relationships are entirely consistent with an original thrust fault cutting upward through the section eastwards in the direction of transport, with subsequent reversal (or retrothrusting) utilizing the surface and changing the displacement but maintaining the position of the fault across the strata.

Across Harvey Fault, this relationship is broken and the retrothrust to the southwest (Hinge Fault) which at first appears to be the offset continuation of McLatchie Fault in fact cannot be that. The reason for this interpretation is that the Hinge Fault, southwest of Harvey Fault, has its footwall higher in the section (i.e. Mist Mountain on Mist Mountain Formation) than the McLatchie Fault northeast of Harvey Fault. If, as has been suggested above, the McEvoy and McLatchie faults originated through reversal of transport on an earlier thrust surface, the footwall rocks should be the same age or older westwards toward the root zone of the thrust. It is a generally accepted observation that thrust faults cut up section in the direction of transport, footwall strata getting progressively younger in that direction (conversely, older in the other direction). Reversal of transport in the hanging wall, as postulated, cannot change the footwall sequence. Since McEvoy Retrothrust is demonstrably west-dipping, its ancestral thrust should also have been west-dipping. The direction of transport along the thrust was eastward and so footwall strata should get older, not younger westward. By this analysis, Hinge Fault is not the offset continuation of McLatchie Fault but a totally separate fault. The McLatchie Fault (or the McLatchie segment of McEvoy Retrothrust) must, as mapped, end at or pass into the Harvey Fault. Another alternative is that a fault, not yet observed, continues the McLatchie Fault southwest of the Harvey Fault immediately below the Morrissey Formation or within the Fernie Formation.

Morrissey Retrothrust

Farther northwest, in the vicinity of Morrissey Creek, the Morrissey Fault occurs at a similar position in the section (middle to upper Mist Mountain Formation) as the Hinge Fault. Morrissey Fault separates relatively undeformed strata in its hanging wall from extremely folded and faulted strata in its footwall (including locally overturned strata) again suggesting its origin during the compressive phase of deformation, but in this case as an east-dipping thrust, definitely not the same fault surface as the McEvoy. Like the McEvoy, Morrissey Fault has almost certainly undergone a reversal of translation in its hanging wall but, in this case, eastward instead of westward. Reversal on the Morrissey does not appear to have progressed far beyond the replacement point, and there is probably no more than one or two hundred metres of net normal displacement.

It is possible that Morrissey and Hinge faults are segments of one continuous fault, the intermediate part of which is hidden in the bedding of the Mist Mountain Formation and forming one extensive east-dipping retrothrust on the west side of McEvoy Syncline - a counterpart to the west dipping McEvoy - McLatchie Retrothrust on the east side.

Upper Décollement Interval

The McEvoy, McLatchie, Hinge and Morrissey faults occur at the level of the upper décollement described above, separating the disharmonic folding styles of the younger and older strata. The existence of so much faulting at the one level proves that it is indeed a preferred detachment horizon, but the variation in fault orientations, and the difference in transportation directions across the faults, shows that such faults, although abundant, are individual and local in nature and that there is no single, continuous decollement surface or fault of regional or even basinal extent within the Kootenay Group.

En Echelon Folding

En echelon folding is common in and around Parcel 82 with good examples of the closed system and offset linkage type referred to by Ollerenshaw (1968, p. 29) in Limestone Mountain area in the southern Alberta Foothills.

Structural Sequence

It is thus possible to establish a general sequence of structural episodes as follows:

1. Folding (Barnes anticline, McEvoy Syncline etc.) and thrust faulting (Barnes Thrust, McEvoy Thrust and Lookout Thrust etc.);
2. Retrothrusting - normal fault restoration and offset on McEvoy, McLatchie, Hinge and Morrissey faults;
3. Normal faulting (Flathead, Harvey and Pipeline faults etc.) accompanied by gravity slump folding (producing the twisting of fold axes).

Episode 1 belonged to the compressive or contraction phase, episodes 2 and 3 to the later tension or extension phase.

Acknowledgments

The writer wishes to thank D.W. Gibson and M. McMechan for critically reading the manuscript and for suggesting several useful changes.

References

Gibson, D.W.
1977: Sedimentary facies in the Jura-Cretaceous Kootenay Formation, Crowsnest Pass area, southwestern Alberta and southeastern British Columbia; Bulletin of Canadian Petroleum Geology, v. 25, no. 4, p. 767-791.

Gigliotti, F.B. and Pearson, D.E.
1979: Geology of Crowsnest Coalfield northeast part; Ministry of Energy, Mines and Petroleum Resources, British Columbia, Preliminary Map, 1:10 000 scale.

Leach, W.W.
1902: Crows Nest Coal Fields; in Geological Survey of Canada, Summary Report, 1901, p. 69A-81A.

McEvoy, J.
1901: Untitled report on the Crows Nest Pass coalfield; in Geological Survey of Canada, Summary Report, 1900, p. 85A-95A.

Newmarch, C.B.
1953: Geology of the Crowsnest coal basin, with special reference to the Fernie area; British Columbia Department of Mines, Bulletin no. 33, 107 p.

Ollerenshaw, N.C.
1968: Preliminary Account of the Geology of Limestone Mountain map-area, southern Foothills, Alberta; Geological Survey of Canada, Paper 68-24, 37 p.

1977: Canadian Government Coal Block, Parcel 73, Fernie basin, British Columbia; in Report of Activities, Part A, Geological Survey of Canada, Paper 77-1A, p. 155-159.

Ollerenshaw, N.C. (cont.)
1981: Cadomin Formation, Flathead Ridge vicinity, southeastern British Columbia; in Current Research, Part A. Geological Survey of Canada, Paper 81-1A, p. 341-347.

Pearson, D.E. and Grieve, D.A.
1979: Crowsnest Coalfield; in Geological Fieldwork, 1978, Ministry of Energy, Mines and Petroleum Resources, British Columbia, Paper 1979-1, p. 61-65.

1980: Elk Valley Coalfield; in Geological Fieldwork, 1979, Ministry of Energy, Mines and Petroleum Resources, British Columbia, Paper 1980-1, p. 91-96.

Price, R.A.
1962: Fernie map-area, east half, Alberta and British Columbia; Geological Survey of Canada, Paper 61-24, 65 p.

19.

THE COASTAL MORPHOLOGY AND SEDIMENTOLOGY OF CAPE HATT: IMPLICATIONS FOR THE BAFFIN ISLAND OIL SPILL PROJECT (BIOS)

Project 760005

P. McLaren[1], W.B. Barrie[2], and J.M. Sempels[3]
Cordilleran Geology Division

McLaren, P., Barrie, W.B., and Sempels, J.M., The coastal morphology and sedimentology of Cape Hatt: implications for the Baffin Island Oil Spill Project (BIOS); in Current Research, Part B, Geological Survey of Canada, Paper 81-1B, p. 153-162, 1981.

Abstract

Cape Hatt, a small peninsula that protrudes into Eclipse Sound at the north end of Baffin Island is the site for an experimental oil spill to take place in the summer of 1981. Three small bays are required: one as a control; a second to study the effects of oil spilled on the surface and allowed to impinge the shoreline; and a third to use an oil-dispersant mix for comparison with the oil-only experiment.

The chosen site contains at least 13 bays potentially suitable for the experiments. Analyses of data from baseline studies in 1980 have resulted in selection of 3 suitable bays (bays 9, 10 and 11). Geomorphic and sedimentologic criteria indicate that the processes of winds, waves and ice action are greatest in bay 10 and least in bay 11. On the assumptions that cross-contamination must be minimal and longevity of the oil in the environment is desirable to ensure reasonable and measurable detrimental effects, we suggest that bay 10 should be used for control, bay 11 for the oil-dispersant mix and bay 9 for the oil-only experiments.

Introduction

Background

Since 1978, staff of the Arctic Marine Oilspill Program (AMOP), of which Environment Canada is the lead agency, has undertaken to identify and co-ordinate research needs associated with experimental oil spills in cold Canadian waters (AMOP, 1979). Cape Hatt on the north coast of Baffin Island (Fig. 19.1), was chosen as the site for these experiments which had two principal objectives: (i) to determine if the use of dispersants in the arctic nearshore will reduce or increase the environmental effects of spilled oil; and (ii) to determine, under actual field conditions, the relative effectiveness and environmental impact of various shoreline protection and cleanup techniques. The most important site requirement demanded three small bays having similar physical and biological properties. Using one bay as a control, the experiment will document the various effects of oil and dispersant in the second bay and compare the results with the third bay in which oil alone has been placed.

During 1980 extensive biological, chemical, ice and sedimentological baseline studies were undertaken including some aspects of the oil-on-shoreline experiments (Environmental Protection Service, 1980). Cape Hatt, probably one of the few ideal locations in the arctic for the experiments, has over 13 bays (or "boomable" localities) potentially suitable for the spills (Fig. 19.1) which are to take place in August and September, 1981. As a result of the baseline studies, the three bays that have been chosen for the experiments are numbers 9, 10 and 11 located in Ragged Channel (Fig. 19.1).

The purposes of this report are to (i) describe the geomorphology and sedimentology for the Cape Hatt area as a whole using the data contained in Barrie et al. (1981); (ii) discuss each of the geomorphic and sedimentologic criteria with respect to the objectives of the spill experiments; and (iii) choose among bays 9, 10 and 11 the most suitable bay for each component of the experiment.

We have attempted the latter by assessing each geomorphic/sedimentologic criterion as a factor that may be considered in the selection of the bays. The relative importance of the factors are assessed qualitatively on a scale of 1 to 5. Each factor is by no means exclusive of the others and each demands slightly differing points of view and assumptions for an importance rating. The values we have provided may reflect assumptions that are invalid with respect to other aspects of the innumerable goals of the experiments and, if so, we encourage modifications.

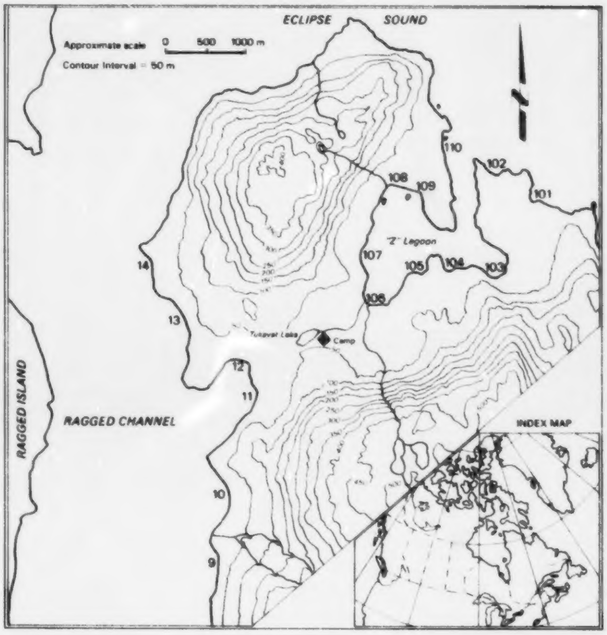

Figure 19.1. *Bay numbers, general topography and location of Cape Hatt.*

Field Methods

In late May and early June 1980, sediment cores and grab samples were taken through the ice in bays 9, 10, 13, 102, 103, 104, 105, 106, 108 and 109 using a vibracorer and a

---

[1] Pacific Geoscience Centre, Sidney, B.C.

[2] Consultant

[3] Petro-Canada

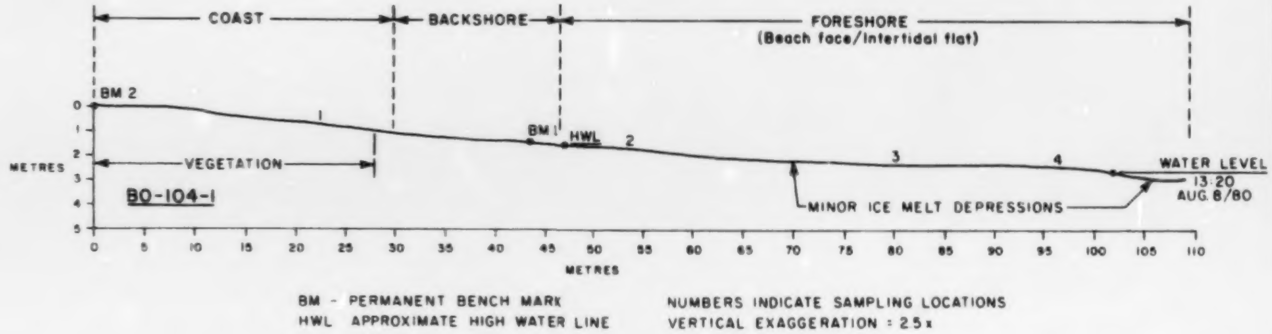

Figure 19.2. *Beach profile in bay 104; "Z"-Lagoon.*

Table 19.1

Summary of shoreline morphology

Morphologic Unit	Measured Parameter		Bavs in "Z" Lagoon							Bays in Eclipse Sound		Bavs in Ragged Channel			
			103	104	105	106	107	108	109	101	102	9	10	11	13
Backshore (including berm if present)	width (m)	max.	–	–	–	–	–	–	–	30	30	2	5	7	15
		min.	–	–	–	–	–	–	–	26	12	0	0	2	3
		mean	10	16	5	0	0	3	6	28	21	1	2	4	10
Berm	width (m)	max.						–	–	6	12	2	5	7	4
		min.	NP[1]	NP	NP	NP	NP	–	–	8	12	0	0	2	0
		mean						3	6	7	12	1	2	4	2
Beach face	width (m)	max.					–	–	–	33	31	19	26	18	23
		min.	NP	NP	NP	NP	–	–	–	30	26	12	15	40	14
		mean					23	28	28	32	29	17	18	31	18
	slope (°)	max.					–	–	–	7.1	6.3	14.0	11.0	6.2	9.2
		min.	NP	NP	NP	NP	–	–	–	6.4	5.8	8.2	6.8	3.1	5.6
		mean					7.7	5.1	5.3	6.8	6.1	10.7	8.6	3.9	7.2
Intertidal flat	width (m)	max.	–	–	–	–									
		min.	–	–	–	–	NP	NP	NP	NP	NP	NP	NP	NP	NP
		mean	50	64	42	75									
Nearshore profile	slope (°)	max.	–	–	–	–	no			no		11.1[2]	9.9[2]		7.4[2]
		min.	–	–	–	–	data	–	–	data		9.9[2]	7.4[2]		6.7[2]
		mean	2.2	3.5	2.5	2.2		3.6	2.9		4.7[2]	10.5[2]	8.3[2]	≈ 4	7.1[2]
	No. of measurements		1	1	1	1		1	1	2	2	7	7	6	6

[1] NP: not present

[2] measured from one profile only

Foerst-Peterson grab sampler. Bathymetric observations and sea bottom profiles were also obtained during this time period. In late July and early August, the beaches in all the bays were profiled using a method described by Emery (1961) and samples were obtained of all representative morphological and sedimentological features in a procedure described by McLaren et al. (in press). Diving was performed in bays 9, 10, 11 and 13 for detailed observation and sampling. Altogether 34 cores, 61 grabs, 29 diver-collected samples and 114 beach samples were obtained and analyzed for their grain size distribution (Barrie et al., 1981).

Acknowledgments

The scope of the BIOS project necessitates complex logistics and unique interaction among scientists of many disciplines. Numerous individuals and organizations provided field, scientific and analytical support for this part of the total project. In expressing congratulations and thanks to P. Blackall, project manager of BIOS we hope to encompass the large number of people who gave the necessary support. Full details of the experiments can be obtained from him, c/o BIOS Project, Environmental Protection Service, No. 804, 9942 – 108 St., Edmonton, Alta., T5K 2J5 (telephone: 403-420-2592).

Special acknowledgment is made to Captain Pelland, Commanding Officer of **CCGS Pierre Radisson** and his officers and crew who, in October 1979, provided the means to choose Cape Hatt as the site for the spill experiments. His decision to use the ship and accompanying helicopter in support of the quest for a suitable location undoubtedly enabled BIOS to continue on schedule.

Physical Setting

Cape Hatt is located on the northern tip of a small peninsula that extends into southwestern Eclipse Sound. The peninsula itself is roughly oval in shape with an average radius of about 3 km. It is bordered on the north by Eclipse Sound and on each side by fiords.

Table 19.2

Summary of Shoreline Sedimentology

	Bay	Morphologic Unit	Texture			Moment Measures[1]			No. of Samples	Water Depth (m)
			% Gravel	% Sand	% Mud	Mean Size	Sorting	Skewness		
Bays in "Z" Lagoon	103	Backshore	19	74	7	1.30	2.12	1.49	2	
		Intertidal flat	16 ± 7	82 ± 7	2 ± 1	0.46 ± .20	1.48 ± .28	2.01 ± .68	4	
		Ice mound	13	83	5	1.50	2.01	1.77	2	
		Nearshore surface	1 ± 0	15 ± 13	85 ± 13	6.11 ± .56	2.26 ± .84	0.88 ± .26	10	9 + 2
	104	Backshore	12	45	44	3.72	3.65	0.72	2	
		Intertidal flat	20	70	11	1.40	2.51	1.79	2	
		Ice mound	29	67	4	0.88	2.02	1.54	1	
		Nearshore surface	3 ± 3	20 ± 9	78 ± 10	6.36 ± 1.15	3.31 ± .22	0.15 ± .37	9	11 ± 4
	105	Backshore	15	55	30	2.58	3.30	0.99	1	
		Intertidal flat	14 ± 5	51 ± 8	36 ± 12	3.08 ± 1.01	3.67 ± .19	0.87 ± .33	4	
		Nearshore surface	< 1	5 ± 1	95 ± 1	6.60 ± 1.73	2.56 ± .31	0.65 ± .72	7	7 ± 2
	106	Intertidal flat	12 ± 3	59 ± 2	29 ± 4	2.81 ± .37	3.28 ± .10	1.06 ± .11	3	
		Intertidal flat - subsurface	2	15	83	6.91	3.46	-0.16	1	
		Nearshore	< 1	5 ± 3	95 ± 3	7.71 ± .56	2.79 ± .13	0.00 ± .22	8	5 ± 1
	107	Beach face	13	51	36	3.32	3.46	0.99	2	
		Ice mound	15	74	11	1.44	2.29	1.56	1	
	108	Beach face	15	67	19	2.14	2.94	1.28	2	
		Ice mound	22	73	5	0.73	1.97	2.15	1	
		Nearshore	< 1	8 ± 4	92 ± 4	6.76 ± .61	2.59 ± .28	0.77 ± .46	9	9 ± 2
	109	Beach face	40 ± 22	51 ± 29	9 ± 7	0.30 ± .12	2.42 ± .78	2.77 ± .80	3	
		Ice mound	13 ± 5	74 ± 10	13 ± 12	1.64 ± 1.18	2.62 ± .80	1.94 ± .68	3	
		Nearshore	2 ± 1	16 ± 11	82 ± 12	6.86 ± .87	3.33 ± .46	0.08 ± .39	9	4 ± 2
Bays in Eclipse Sound	101	Beach face	25 ± 12	75 ± 12	< 1	0.17 ± .22	1.04 ± .15	0.24 ± .22	5	
		Ice mound	53	48	< 1	-0.51	0.86	.86	2	
	102	Back shore	6 ± 9	92 ± 8	2 ± 1	0.68 ± .50	0.95 ± .23	1.95 ± 1.33	5	
		Berm	16 ± 17	84 ± 17	1 ± 0	0.13 ± .55	0.71 ± .15	0.55 ± 1.53	5	
		Beach face	40 ± 18	60 ± 17	1 ± 0	-0.41 ± .43	0.67 ± .33	1.26 ± 1.04	8	
		Ice mound	54 ± 23	46 ± 23	1 ± 0	-0.73 ± .43	0.62 ± .25	3.42 ± 2.70	3	
		Nearshore surface	26	59	15	1.77	2.82	2.22	2	12
		Nearshore subsurface	4	30	66	6.65	4.30	-0.23	1	15
Bays in Ragged Channel	9	Eroding bluff	23 ± 9	57 ± 13	19 ± 17	1.91 ± 1.76	3.08 ± 1.14	1.51 ± .89	6	
		Beach face	19 ± 5	80 ± 6	1 ± 0	0.36 ± .19	1.16 ± .15	0.53 ± .56	9	
		Ice mound	45 ± 27	55 ± 26	1 ± 0	-0.03 ± .87	1.19 ± .34	1.85 ± 1.55	4	
		Nearshore surface	3 ± 3	57 ± 14	40 ± 14	4.24 ± .73	3.00 ± .49	1.11 ± .50	16	11 ± 5
		Nearshore subsurface	3 ± 1	41 ± 18	56 ± 19	5.35 ± 1.41	3.49 ± .39	0.45 ± .66	3	13 ± 6
	10	Eroding bluff	11 ± 6	57 ± 11	32 ± 17	3.02 ± 1.62	3.32 ± .49	1.23 ± .81	7	
		Beach face	17 ± 9	80 ± 10	4 ± 3	0.70 ± .49	1.57 ± .59	1.74 ± 1.50	8	
		Ice mound	27 ± 12	71 ± 10	3 ± 3	0.54 ± .60	1.71 ± .45	1.60 ± .80	4	
		Nearshore surface	3 ± 2	57 ± 20	41 ± 20	4.09 ± .85	2.54 ± .53	1.40 ± .80	20	10 ± 6
		Nearshore subsurface	1 ± 1	53 ± 28	46 ± 28	4.54 ± 1.40	2.70 ± .74	1.25 ± .98	3	6 ± 1
	11	Beach face	24 ± 12	72 ± 11	4 ± 2	0.84 ± .68	1.76 ± .28	1.48 ± 1.02	13	
		Nearshore surface	8 ± 7	59 ± 19	33 ± 22	3.39 ± 1.58	2.88 ± .75	0.86 ± .60	15	6 ± 5
	13	Backshore	9 ± 10	87 ± 13	4 ± 3	1.25 ± .18	1.53 ± .45	2.76 ± 1.04	3	
		Beach face	14 ± 11	86 ± 11	1 ± 0	0.64 ± .47	0.97 ± .25	0.08 ± .62	6	
		Ice mound	24 ± 4	76 ± 4	1 ± 0	0.08 ± .24	1.06 ± .23	0.67 ± .23	3	
		Nearshore surface	4 ± 2	66 ± 16	30 ± 16	3.80 ± 1.03	2.97 ± .62	1.26 ± .62	19	10 ± 5
		Nearshore subsurface	6 ± 2	50 ± 13	44 ± 15	4.52 ± 1.04	3.66 ± .56	0.61 ± .36	8	13 ± 3

[1] Moment measures are in ϕ units and refer to sand size and smaller fractions only (i.e. >-1.0ϕ)

Two elongated hills, both trending northeasterly are present at the northwest and southeast ends of the peninsula (Fig. 19.1). Reaching altitudes of 400 m and 500 m respectively, they are separated by a northeasterly trending saddle-shaped valley that extends between an embayment on Ragged Channel (bays 11 and 12) and the southwestern end of "Z"-lagoon (bay 106). The valley is generally less than 50 m elevation.

The peninsula is divided geologically by a prominent fault which trends southeast from the southern end of bay 10 and is expressed morphologically by a deeply incised drainage valley. North of this fault the rocks consist mostly of Archean and Aphebian migmatites of highly variable composition as well as a few ultrabasic bodies. The migmatites are made up of alternating light and dark banks of quartz monzonite to granodiorite and amphibolites, paragneiss and minor ultramafics respectively (Jackson et al., 1974).

South of the fault are two Neohelikian sedimentary sequences; the Victor Bay Formation consisting of thinly bedded black shale, siltstone and limestone, and the Athole Point Formation composed principally of argillaceous limestone and calcareous shale and siltstone. The Athole

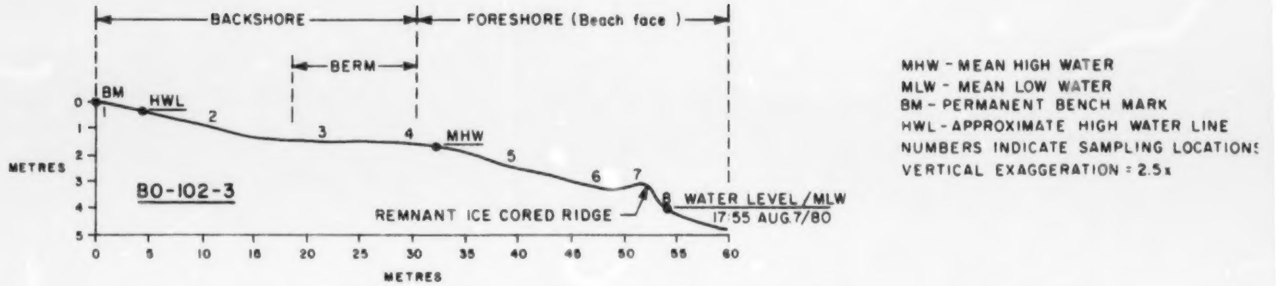

Figure 19.3. *Beach profile in bay 102; Eclipse Sound.*

Point Formation overlies conformably the Victor Bay and in the area south of bay 9 it forms the core of a northwesterly plunging syncline.

The area was probably ice-covered during the late Wisconsin and an emerged ice-contact delta, the top of which is at 70 m elevation, is located immediately south of Tukayat Lake (Fig. 19.1) partially constricting the low valley between "Z" Lagoon and Ragged Channel. The delta represents the margin of the ice front during its retreat towards the south about 10 000 to 12 000 years ago. Since its retreat the peninsula has emerged at least 80 m, the result of isostatic re-adjustment (Hodgson et al., 1974).

The bays on the peninsula are separated by steep rocky promontories with the exception of a small delta separating bays 9 and 10. Coarse sand, gravel and cobble beaches within the bays owe their origin to till or glacial-marine deposits which blanket the valleys and lower slopes of the peninsula. The nearshore sediments in the outer bays are also derived from the glacial deposits although they have undergone modification by currents, waves and ice scouring. The sediments within "Z"-Lagoon are exceptional and consist mainly of poorly sorted mud probably derived from the bottomset beds of the uplifted delta which have since infilled the lagoon during Holocene emergence.

Ice covers the waters surrounding Cape Hatt for about 9 or 10 months each year. The mean date for the area to be free of ice is July 31 but can be as early as July 15 and as late as August 20. The mean date for freezeup is October 6 and extends from September 24 to October 15 (Dickens, 1981). As a result of the presence of ice the shoreline of Cape Hatt exhibits numerous features unique to polar beaches. These include ice push ridges, pitted beaches and ice mounds. The latter feature appears to play an important role on the Cape Hatt beaches and are described in some detail in Dickens (1981).

Shoreline Morphology and Sedimentology

Backshore/berm

Definition. The backshore is the part of the beach between the uppermost level of wave activity and the mean high water line. It normally includes a berm and overwash deposits; however at Cape Hatt such features are not always present because of ice effects which limit wave processes to only several weeks each year. A berm is a nearly horizontal terrace or bench formed by material thrown up and deposited by waves above the mean high water level.

"Z"-Lagoon. In "Z"-Lagoon most of the bays have gently sloping shorelines that grade into a backshore and foreshore with no morphological expression (Fig. 19.2). With the exception of bays 108 and 109 which have steeper slopes, the backshore reaches widths of about 16 m (Table 19.1). In bays 108 and 109 small berms 3 and 6 m wide respectively are, probably the result of the steeper topography and waves derived from southwest winds funnelled through the valley separating "Z"-Lagoon from bays 11 and 12. Backshore samples from bays 103, 104 and 105 show a fairly consistent gravel content of about 15 per cent whereas the sand and mud contents show wide variability ranging from 45 to 74 per cent sand and from 7 to 44 per cent mud (Table 19.2). The mean grain size, excluding gravel, falls in the medium to very fine sand range and all samples are poorly sorted and positively skewed.

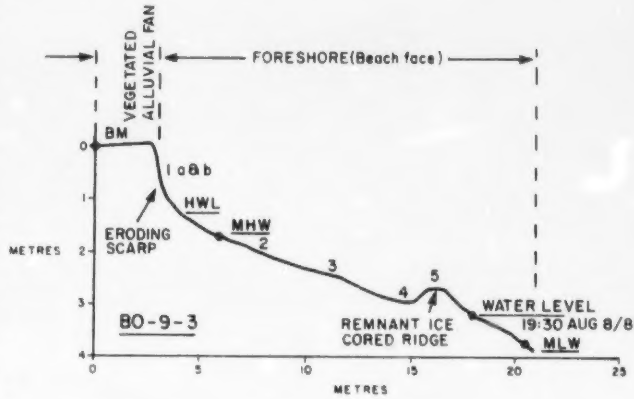

Figure 19.4. *Beach profile in bay 9; Ragged Channel.*

Eclipse Sound. These bays (101 and 102), exposed to the highest wave energies generated in Eclipse Sound, contain the widest backshores of 28 and 21 metres (Fig. 19.3). Within the backshore each bay contains a well developed berm, the largest being in the most exposed bay (102) and is about 12 m wide (Table 19.1). Samples from bay 102 show the backshore to be principally very coarse, fairly well sorted sand with gravel contents usually less than 20 per cent (Table 19.2).

Ragged Channel. In bays 9, 10 and 11 small berms, the maximum width being 7 m in bay 11 (Table 19.1), make up the entire backshore. They are, however, not always present around the length of the bay particularly where eroding bluffs adjoin the foreshore (Fig. 19.4). In bay 13, the most exposed of the bays in Ragged Channel, the backshore extends as much as 15 m and contains a berm (maximum 4 m) within this width (Table 19.1). Backshore samples were taken only from bay 13 and show a similarity with the sediments in the Eclipse Sound bays although the sand is finer and more poorly sorted. The gravel content is more or less the same at about 9 per cent.

Table 19.3

Factors affecting choice of bays for BIOS experiments

Factor	Control	Oil	Oil/ Dispersant	Importance Rating[1]
Backshore	10	11	9	1
Beach face width and slope	10	11	9	3
Beach face grain size and sorting	11	9	10	1
Ice mounds	10	11	9	1
Ice scouring	11	10	9	1
Nearshore sediment sorting	9	11	10	1
Grain size parameters with depth	10	9	11	4
Cross-contamination	10	9	11	5
Longevity	10	9	11	4

[1] This rating is a qualitative assessment of the importance of the factor in deciding the best sequence of bays for the experiments. The scale is 1 to 5 in increasing importance and can be manipulated as required.

Implications to BIOS. A berm is a depositional feature dependent on wave activity for its formation. At Cape Hatt the widest, best formed berms are found in the most exposed bays (Table 19.1) and reflect the relative energy levels. Because a berm is a potential reservoir for oil above normal wave activity, there is a greater probability for oil to be stored on the surface or buried on shorelines with a well developed berm should wave activity be sufficient to contaminate the backshore during the spill experiments.

In bays 9, 10 and 11 the width of the backshore and berm is least in bay 9 and greatest in bay 11 (Table 19.1). Bay 11 therefore has the greatest potential to retain oil on the shoreline for the longest time whereas in bay 9, the absence of a berm means the oil can only be retained on the beach face and will be subject to continuous tides, waves and ice activity.

Based on assumption that the experiments will yield the most useful results if the oil and oil-dispersant mixture have a maximum possibility of affecting the environment (i.e. longevity and interaction with biota and sediments is maximized) we suggest the following order:

1. Bay 11 for oil-only because there is the best probability for long term retention on the shoreline;
2. Bay 9 for the oil-dispersant mix because the lack of a backshore indicates a low energy regime and thus there is the maximum possibility of the mixture remaining in the water column and/or bottom sediments for greater lengths of time than the other two bays;
3. Bay 10 for control (by default).

Practical considerations during the spill experiments demand weather conditions amenable for boom handling, sampling, observations etc., thus it is unlikely that oil will be thrown by waves onto the backshore when the experiments take place. We have therefore placed a low importance to the backshore as a factor determining the choice of bays (Table 19.3).

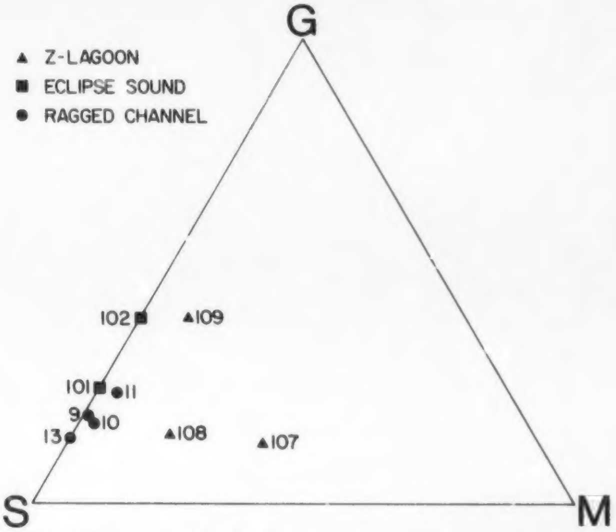

Figure 19.5. *Textural diagram of beach face sediments (data from Table 19.2).*

Beach Face

Definition. The beach face is the part of the beach that is subject to wave uprush and lies roughly between mean high and mean low water levels.

"Z"-Lagoon. The gentle slopes and low wave activity in bays 103, 104, 105 and 106 preclude the formation of a berm and beach face (Table 19.1). Where the shoreline slopes are steeper in bays 107, 108 and 109 a beach face has developed which ranges from 23 to 28 m wide with slopes from 5.1 to 7.7 degrees. The beach face sediments have a relatively narrow range in their sand content (51 to 67%) but contain more variable amounts of gravel and mud (Fig. 19.5).

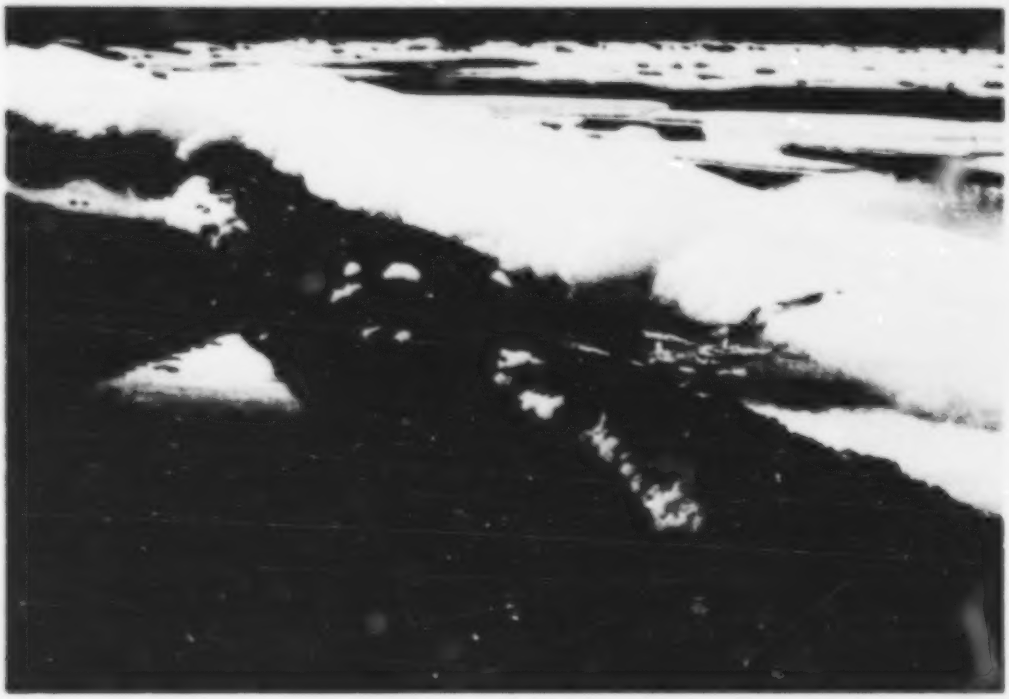

Figure 19.6. Sediments overlying and melting out of an ice mound.

The range of the sand sizes is, however, quite variable extending from 0.30ϕ (coarse sand) to 3.32ϕ (very fine sand). Sorting is always poor and the skewness positive.

Eclipse Sound. The exposure to high wave activities in bays 101 and 102 have resulted in the widest beaches at Cape Hatt (Table 19.1). They are about 30 m wide, slopes are typically 6.5 degrees and they are composed almost entirely of sand and gravel having little or no mud content (Fig. 19.5). The sands are either very coarse or coarse, and compared with most of the other bays, they are well sorted (Table 19.2).

Ragged Channel. Of all the bays in Ragged Channel, bay 9 has the least beach width (average 17 m) and greatest slope (10.7 degrees) whereas bay 11 has the greatest width (31 m) and least slope (3.9 degrees). The controlling parameter for the slope is the mean grain size which is coarsest for bay 9 (0.36ϕ) and finest for bay 11 (0.84ϕ). The beach face sediments contain more sand than those in Eclipse Sound or "Z"-Lagoon (Fig. 19.5) and their texture tends to be more consistent than in the other environments. Mud content is generally less than 4 per cent and gravel ranges from about 14 to 24 per cent (Table 19.2). The mean grain size falls in the coarse sand category and the sediments are generally poorly sorted.

Ice Mounds. At the time of sampling (late July) nearly all the beaches contained a distinct linear ice mound or berm that paralleled the length of the beach close to the mean low water level (Fig. 19.6). The ice mound contained sediment both within and on its surface that was added to the beach face during its melt. These sediments were sampled in an effort to determine the origin of the ice mounds which is not clearly understood. Dickens (1981) has a more complete description and reviews possible processes that could result in ice mound formation.

The sediments within the ice mounds show no significant differences from the corresponding tidal flat or beach face sediments they are formed on. In "Z"-Lagoon there is a tendency for the ice mound sediments to contain more sand than the beach face sediments whereas in Eclipse Sound and Ragged Channel the ice mound sediments have greater amounts of gravel than the corresponding beach face sediments (Table 19.2). Generally the sediments in the ice mounds are coarse relative to beach face sediments although there appear to be no constant trends among sorting and skewness values.

Implications to BIOS Experiments. In bays 9, 10 and 11 the beach face width becomes progressively larger and the slope progressively smaller (Table 19.1). Thus oil alone should be spilled in bay 11 because there is a greater area of beach available for contamination, a better chance of oil being retained in the sediments and a greater probability for increased oil longevity due to wave attenuation over the shallow slope than in the other two bays. To ensure the oil-dispersant mixture remaining in the nearshore for as long as possible the bay with the steepest beach face should be chosen which may help to minimize nearshore turbulence (i.e. bay 9).

This factor of beach face width and slope will have a significant effect on the fate and behaviour of the oil. There is little difference between bays 9 and 10 (Table 19.1) but bay 11 has substantially smaller slopes. We suggest that the importance rating should be higher than for the backshore factor and we have arbitrarily placed the rating at 3 (Table 19.3).

Grain size and the degree of sorting of beach face sediments may also have an effect on the behaviour of the spilled oil. In general, coarser, better sorted sediments will have a greater permeability and porosity than those which are finer and poorly sorted. On this basis, oil will have a better chance to penetrate and be retained by the sediments in bay 9, which contains the coarsest and best sorted beach face (Table 19.2). The beaches in bay 10 are coarser and better sorted than those in bay 11 indicating bay 10 to be a better choice for the oil-dispersant mix and leaving bay 11 for control. The variability of grain-size among the beaches is not, however, very great and we have put the lowest importance rating of 1 for this as a factor affecting the choice of bays (Table 19.3).

Ice mound development on the beach face is apparently ubiquitous in each of the three bays. The exact effects of oil on its formation and decay are presently unknown; however, it seems clear that the net result of the ice mound will be either to remove oil from the beach during the melt or to "dilute" the oil-in-sediment concentration through excessive disturbance and admixing of sediments. Removal of contaminated sediments may occur if the ice mound rafts away during breakup. Such an occurrence is most likely in bay 10, the most exposed of the three bays. Therefore bay 11, the least exposed bay, should be used for the oil-only experiment to maximize its residence time on the beach face. Bay 9 is slightly less exposed than bay 10 and should have the oil-dispersant mixture. The importance rating of the ice mound as a factor in choosing the bays has been kept very low because there is little understanding of this phenomenum and we can only speculate on how it may affect the experiments (Table 19.3).

Intertidal Flat

Wide, gently sloping, intertidal flats occur only in bays 103 to 106 of "Z"-Lagoon. They range in width from about 42 to 75 m (Table 19.1) and are composed principally of poorly sorted coarse to fine sand. There is a tendency for the sediments to become finer and more poorly sorted with increasing shelter inside the lagoon. Intertidal flats do not occur in any of the bays selected for the spill experiments.

Nearshore

Nearshore profiles perpendicular to the shoreline in each of the bays indicate consistently shallow slopes in "Z"-Lagoon of less than 4 degrees (Table 19.1). Sediments contain a high mud content (>75%) and consist of poorly sorted medium and fine silt with gravel and sand making up less than 3 and 20 per cent respectively (Fig. 19.7). In several of the bays (i.e. 106 and 109) there is a good relationship between grain size parameters and water depth. Mean grain size decreases, sorting becomes poorer and the positive skewness becomes less with increasing depth (data in Barrie et al., 1981). These relationships are not, however, consistent from bay to bay and no simple generalized model is apparent to explain these observations.

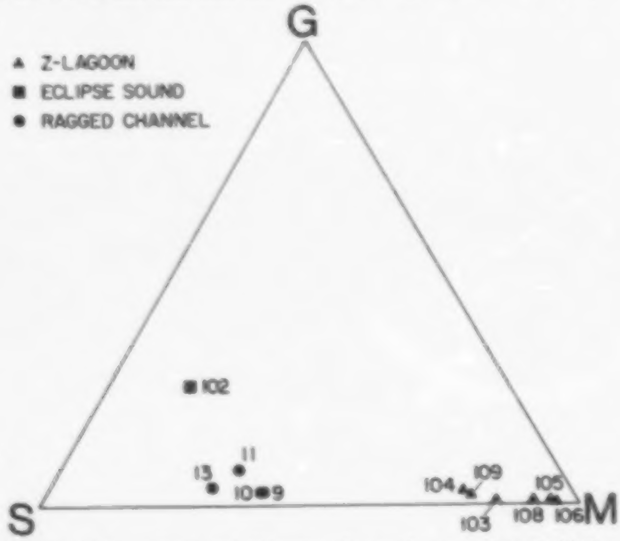

Figure 19.7. Textural diagram of nearshore sediments (data from Table 19.2).

One profile in Eclipse Sound (bay 102) indicates a nearshore slope of about 5 degrees and corresponding bottom samples contained relatively high amounts of sand and gravel compared with either "Z"-Lagoon or Ragged Channel (Fig. 19.7). In the latter, bays 9 and 10 have similar nearshore slopes (8 and 10 degrees respectively) but bay 11 is significantly shallower at approximately 4 degrees. The sediments in Ragged Channel have a similar gravel content to those in "Z"-Lagoon (generally less than 8 per cent) whereas the sand content is much greater and ranges from about 50 to 70 per cent (Table 19.2).

All of the nearshore samples in Ragged Channel have a good correlation between the grain size measures and water depth. As water depth increases, the mean grain size becomes finer, the sorting poorer and the skewness less positive (data in Barrie et al., 1981). The sediments, on average, are principally poorly sorted very fine sand or coarse silt (Table 19.2).

Implications to BIOS. In arctic environments the dominant process affecting nearshore sediments is moving ice, gouging and scraping the bottom resulting in considerable sediment disturbance. This process has increasing impact with decreasing depth. Thus oil that has been deposited onto the substrate, as is to be hoped for the oil-dispersant mix experiment, will be subject to burial, mixing or even resuspension and removal by ice scouring in shallow water. It is suggested that oil in or on the substrate will have a better chance of remaining on bottoms where ice scour is least. Although diving observations show that ice scour has occurred in all three bays, the bay with the greatest slope (bay 9) should have the largest area unaffected by ice impinging on the bottom and bay 11, with the least slope, should have considerably more. We suggest that this factor (ice scouring; Table 19.3) indicates that bay 9 would be best for the oil-dispersant mix, bay 10 for oil only and bay 11 for control. We recognize that there are factors such as exposure, ice ridging, probability of multi-year ice blocks entering the bays etc. that may complicate this concept and therefore the importance rating is very low (1; Table 19.3).

Similar to the arguments used for the beach face, sediment sorting may affect the behaviour of oil in the nearshore. The best sorted sediment may enable maximum penetration of the oil; therefore bay 10 (sorting 2.54ϕ) would be the choice for the oil-dispersant mix, bay 11 for oil only and bay 9, with the poorest sorting (3.00ϕ), would be control (Table 19.3). The spread of values is, however, insufficient to increase the importance rating of this factor above one (Table 19.3).

The relationship of the grain size parameters with depth is a probable indication of the relative importance or the energy level of the processes operating in each bay. The best correlations of mean grain size, sorting and skewness with depth are found in bay 10 (r = 0.89) the most exposed of the three bays; bay 9 is next (r = 0.81), followed by bay 11 which is much lower (r = 0.53). Bay 11 appears to be the least energetic of the three bays suggesting that the oil-dispersant mix would have the best chance for long term interaction with the biota. Oil only should be placed in bay 9 because its longevity will be greater than in bay 10 which should be kept for control. This factor (grain size parameters with depth) is considered by us to be important and we have given it a high importance rating (4; Table 19.3).

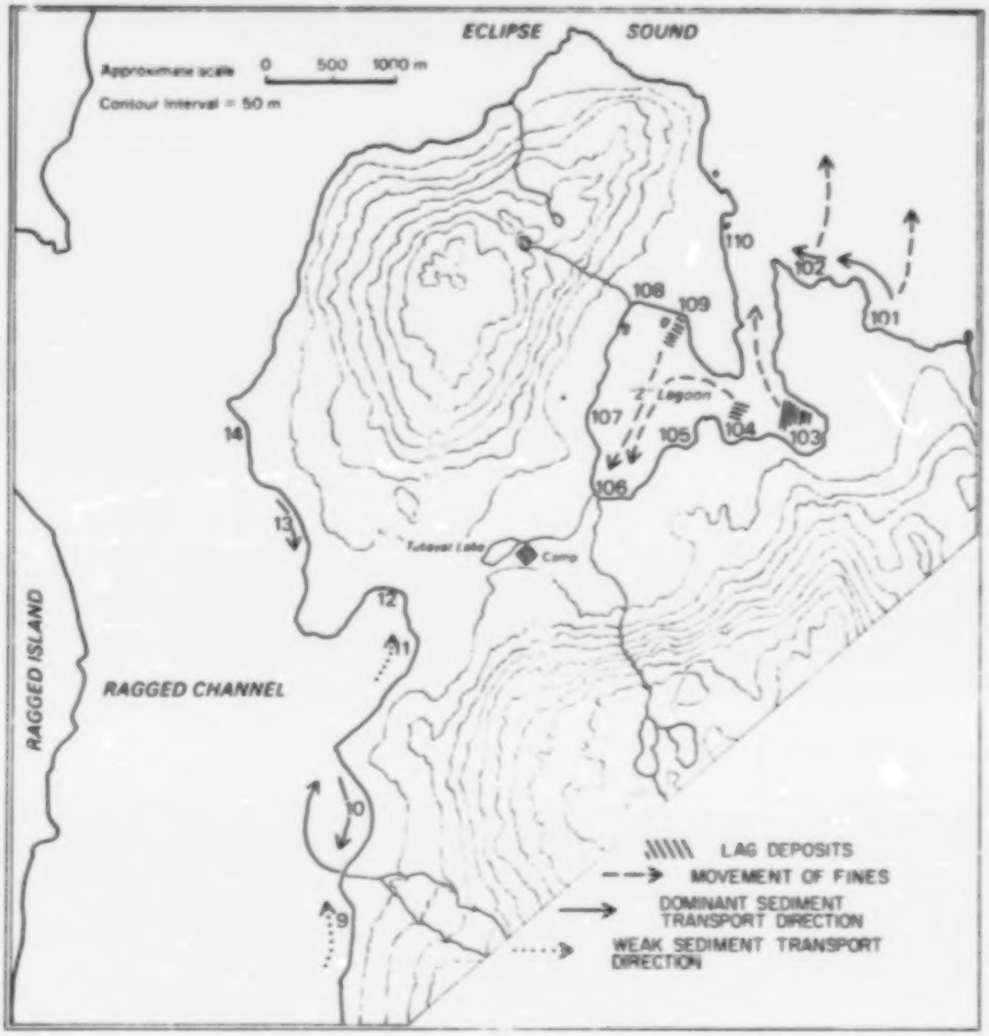
ECLIPSE SOUND
Approximate scale 0 500 1000 m
Contour interval = 50 m
110
102
101
108
109
"Z" Lagoon
107
105
104
103
106
14
13
Lake
Camp
12
11
RAGGED ISLAND
RAGGED CHANNEL
10
9
LAG DEPOSITS
MOVEMENT OF FINES
DOMINANT SEDIMENT TRANSPORT DIRECTION
WEAK SEDIMENT TRANSPORT DIRECTION

Figure 19.8. *Sediment transport directions, Cape Hatt.*

Sediment Trends

Introduction

The mean grain size, sorting and skewness of a sedimentary deposit are dependent on the sediment grain size distribution of its source and the sedimentary processes of (i) winnowing (erosion), (ii) selective deposition of the grain size distribution in transport, and (iii) total deposition of the sediment in transport. If a source sediment undergoes erosion, and the resultant sediment in transport is deposited completely, the deposit must be finer, better sorted and more negatively skewed than the source. This trend is referred to as Case I. The lag remaining after erosion, on the other hand, must be coarser, better sorted and more positively skewed (Case II). If sediment in transport undergoes selective deposition, the resultant deposit can either be finer (Case IIIA) or coarser (Case IIIB) than the source, but the sorting will be better and the skew more positive (McLaren, in press). In a system of related environments, these trends can be used to identify both the probable source and the probable deposit and, by inference, the net sediment transport paths among sedimentary deposits. The transport paths represent an integration of all the time-dependent variables such as winds, waves and currents and may suggest the probable fate and behaviour, particularly in the long term, of oil in coastal environments (McLaren, 1980).

Sediment trends at Cape Hatt based on the data presented in Barrie et al. (1981) and in Table 19.2 suggest the following conclusions.

"Z"-Lagoon

1. The deposits in the lagoon are the source sediments for the intertidal and beach sediments. In general the shoreline deposits are a lag of the lagoon sediments that have undergone winnowing of fines (Case II) by the small levels of wave and ice activity.
2. Bay 103 is the most exposed and the nearshore sediments are a lag derived from the original sediments deeper in the lagoon. The fines winnowed from bay 103 do not appear to be deposited in the rest of the lagoon and are evidently lost through the channel exiting into Eclipse Sound (Fig. 19.8).

3. Bays 104 and 109 are partially lag deposits; however fines from these two bays appear to be undergoing total deposition in bay 106. The latter is the most sheltered in the lagoon and is the only bay that may be receiving sediments from both the land and the other bays (Fig. 19.8).
4. Source-deposit relationships between all sediment samples and ice mound deposits show no consistent trends. It appears probable that they are derived from the in situ beach face deposits present at the time of their formation.

Eclipse Sound

1. The original source for all the nearshore and beach sediments is the subsurface deposits found in a core from bay 102 (Table 19.2). This sediment, composed of sandy silt, is probably of glacial marine origin from which the surface deposits are a lag. Through the processes of ice and wave action, fines are increasingly lost as the water shallows resulting in the coarsest, best sorted and most positively skewed sediments at the beach. The fines are probably transported and deposited farther offshore below the depth of ice scour (McLaren, 1980).
2. The beach sediments in bay 101 appear to be the source for those in bay 102 and suggest net movement of sediments from east to west. The same east to west movement of sediments is particularly strong within bay 102 (Fig. 19.8).
3. Similar to the ice mounds in "Z"-Lagoon their sediments are not clearly derived from farther up on the beach face or from the nearshore suggesting an in situ mode of formation incorporating the existing beach sediments.

Ragged Channel

1. Similar to "Z"-Lagoon and Eclipse Sound, the shoreline sediments in Ragged Channel are a winnowed lag derived from the subsurface sediments in the nearshore (Table 19.2). The source sediment is also evident in the eroding bluffs that occur in bays 9 and 10.
2. In bay 9, both nearshore and beach sediments show very few consistent trends indicating that longshore sediment transporting processes are rare in either direction. There is a slight northward trend in the beach face sediments that may suggest a preferred direction of south and southwest winds at this location (Fig. 19.8).
3. Sediment trends suggest that the bluffs in bay 10 are more actively eroding than the bluffs in bay 9. Consistent trends show that the bluffs as well as the nearshore sediments are supplying the beach deposits. Storms probably erode the bluffs and deposit the sediments in the nearshore where they are further modified in their transport to the beach.

   Both nearshore and beach sediments have dominant trends in the southward direction (Fig. 19.8) indicating that north and northwest winds are more effective than the south and southwest winds that move sediments in bay 9.

Table 19.4

Summary of importance ratings for the bay selection

	Total Importance Rating		
Bay	Control	Oil	Oil-Dispersant
9	1	14	6
10	18	1	2
11	2	6	13

4. The delta that divides bays 9 and 10 is also a sediment source for the deposits in the two bays. Sediment trends clearly show that bay 10 receives a much greater sediment input from the delta than in bay 9 indicating a northward transport in opposition to southerly transport indicated by the beach and nearshore sediments. We suggest that a clockwise gyre in bay 10 would account for these observations (Fig. 19.8). There is supporting evidence for such a gyre in the time-lapse photography showing ice movements in the bay (Dickens, personal communication) and in current data (de Lange Boom and Buckley, 1981).
5. In bay 11 there is an indication of northeast sediment movement in both the nearshore and beach sediments (Fig. 19.8). The trends, though not particularly strong may be the result of south and southwest winds or of the refraction of waves into bay 11 generated by northwest winds.
6. Beach face sediments in bay 13 show a strong southward transport direction which is not reflected in the nearshore sediments (Fig. 19.8).

Implications to BIOS

One of the most important considerations in the selection of bays is minimizing the possibility of cross-contamination between the bays with oil in them, and particularly, contamination of the control bay. This problem is two-fold because contamination must be considered on both the short term (immediately after the spills have taken place) and in the long term (over the three years of data gathering and observation). The insights provided by the sediment trends (Fig. 19.8) are especially valuable in assessing long-term cross-contamination potential because they indicate the probable transport paths if oil becomes entrained in the sediments.

The most difficult experiment to control is the oil-dispersant mix. Because bay 10 shows the strongest trends and is therefore the most "active" of the bays, we suggest bay 10 is a poor choice for this experiment. Bay 11, on the other hand, has weak trends in a direction away from the other bays (Fig. 19.8) and is consequently the best choice for the oil-dispersant mix experiment. Bay 9 also has weak trends compared to bay 10 and is the next least possible source for cross-contamination. Thus bay 9 is a logical choice for the oil only experiment which leaves bay 10 as the control. The factor of cross-contamination is sufficiently important to receive the highest importance rating (5; Table 19.3).

Finally, the strength of the sediment trends summarizes the level of activity in each of the bays. We suggest that the overall longevity of the oil in the environment is maximized in the least active of the bays. Therefore oil and dispersants should be put into bay 11, oil in bay 9 and bay 10 left for control because this is the sequence of increasing energy in each bay. We have placed an importance rating of 4 on this factor, only slightly less than the cross-contamination factor.

Conclusions

1. The coastal sediments in the Cape Hatt bays originate from glacial and glacial-marine deposition during late Wisconsin or early Holocene time. These sediments, presently occurring in the nearshore subsurface or in eroding bluffs, are modified at the shoreline by waves and ice action resulting in sediments that become increasingly coarser, better sorted and positively skewed as water depth decreases.
2. In general the coarsest and best sorted sediments occur in bays 101 and 102 which have the highest exposure to wave and ice activity. "Z"-Lagoon is the most sheltered environment and contains finer and more poorly sorted sediments. The bays in Ragged Channel fall between these two extremes.
3. Trends in sediment grain size distributions indicate westerly transport directions in the Eclipse Sound bays (101 and 102). In "Z"-Lagoon fines are winnowed in the most exposed bays (103, 104 and 109) and are either deposited in the vicinity of bay 106 or are removed out of the lagoon into Eclipse Sound. Bays 10 and 13 in Ragged Channel show strong southerly trends whereas bays 9 and 11 have weak northerly and northeasterly transport directions. There is an indication of a clockwise gyre in bay 10.
4. Based on a qualitative importance rating value applied to each geomorphic/sedimentologic criterion that may affect the BIOS experiments it is suggested that bay 10 should be used for a control, bay 9 for the oil-only and bay 11 for the oil-dispersant mix experiments.

References

Arctic Marine Oilspill Program
1979: Experimental Oilspills General Plan; Environmental Protection Service, Environment Canada, 83 p.

Barrie, W.B., Sempels, J.M., and McLaren, P.
1981: Baffin Island Oil Spill Project, Geomorphology Data Report; Petro-Canada, Department of Social and Environmental Affairs, 200 p.

de Lange Boom, B.R. and Buckley, J.R.
1981: Baffin Island Oil Spill Project, Physical Oceanography Data Report 80-3, 1980. Surface Current Measurements; Arctic Laboratories Ltd., Environment Canada, Edmonton, Alberta, 79 p.

Dickens, D.F.
1981: Baffin Island Oilspill Project – Cape Hatt Ice Conditions; Unpublished report for the Environmental Protection Service, Environment Canada, 86 p.

Emery, K.O.
1961: A simple method of measuring beach profiles; Limnology and Oceanography, v. 6, p. 90-93.

Environmental Protection Service
1980: Baffin Island Oil Spill Project – Shoreline Component: Interim Report prepared by Woodward-Clyde Consultants, 81 p.

Hodgson, D.A. and Haselton, G.M.
1974: Reconnaissance glacial geology, northeastern Baffin Island; Geological Survey of Canada, Paper 74-20 and Map 1395A.

Jackson, G.D., Davidson, A., and Morgan, W.C.
1975: Geology of the Pond Inlet map-area, Baffin Island, District of Franklin; Geological Survey of Canada, Paper 75-25 and Map 1396A.

McLaren, P.
An interpretation of trends in grain size measures; Journal of Sedimentary Petrology. (in press)

1980: Trends in sediment distributions: a method to predict oil spill movement in the coastal zone; Spill Technology Newsletter, Environmental Protection Service, Ottawa; v. 5(3), p. 76-87.

McLaren, P., Barrie, W.B., Sempels, J.M., Sieffert, R.A., Taylor, R.B., and Thomson, D.
Coastal environmental data from eastern Lancaster Sound and northeastern Baffin Island; Bedford Institute Data Report Series. (in press)

SCIENTIFIC AND TECHNICAL NOTES
NOTES SCIENTIFIQUES ET TECHNIQUES

HEAT GENERATION IN THE NORTHERN HOGEM BATHOLITH AND NEARBY PLUTONS OF McCONNELL CREEK MAP AREA, BRITISH COLUMBIA

Project 750016

T.J. Lewis[1] and G.J. Woodsworth
Cordilleran Geology Division, Vancouver

Introduction

This note gives average heat production values for 69 surface samples of granitoid rocks from the northern part of the Hogem Batholith, and other plutons in McConnell Creek map-area. Samples are grouped into eight plutonic units based on lithology and age.

The northern part of the Hogem Batholith (north of Omineca River) is a structurally and lithologically complex body consisting of four major tectonic units (Woodsworth, 1976; see also Garnett, 1978).

1. Thane and Detni plutons. These plutons are dominantly dark green diorite and monzodiorite, with lesser quartz monzodiorite. Isotopic dating indicates an Early Jurassic age for this unit (Eadie, 1976).

2. Duckling Creek Syenite. Only the northern part of this unit was sampled for this study; it is a complex of syenite and monzonite with minor pyroxenite and schist of Early to Middle Jurassic age.

3. Mesilinka pluton. This pluton consists of biotite quartz monzodiorite with lesser granodiorite and quartz diorite. The western margin of the Mesilinka pluton is intensely foliated; the degree of foliation decreases to the east. Isotopic dating of the Mesilinka pluton has given equivocal results but an Early Cretaceous age appears probable (Woodsworth and Armstrong, in preparation).

4. Osilinka stocks. Several bodies of biotite granite and granodiorite of Early to mid-Cretaceous age intrude all other units of the Hogem Batholith.

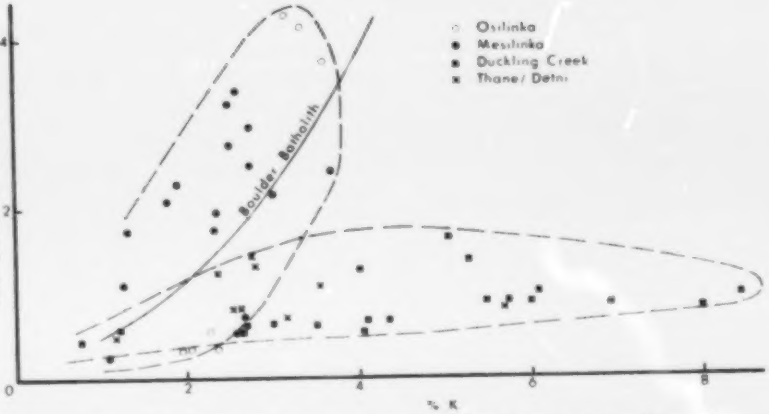

Figure 1. *Heat production versus K for samples from the northern Hogem batholith. Boulder Batholith trend line is adapted from Tilling et al., 1970. Dashed lines outline the fields for Osilinka-Mesilinka and Duckling-Thane/Detni suites.*

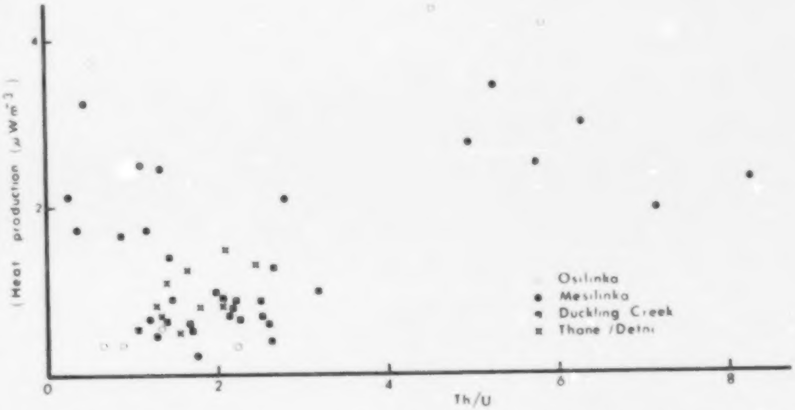

Figure 2. *Heat production versus Th/U for samples from the northern Hogem batholith.*

Samples from other plutons in McConnell Creek map-area are grouped into four units. All but the Kastberg intrusions are confined to a 20-km-wide belt extending north-northwest from the Hogem Batholith (Woodsworth, 1976; Richards, 1976a and b).

5. Kastberg intrusions. All samples are from the stock on Comb Peak, a quartz monzonite and quartz-eye porphyry body of Eocene age.

6. Jensen/Ingenika. Two samples are from the Jensen pluton, a miarolitic quartz monzodiorite body. One sample is from foliated quartz diorite at the west end of the Ingenika Range. Available isotopic dates (Woodsworth, in Wanless et al., 1979) cannot be meaningfully interpreted but a Middle Jurassic age is possible.

7. Fredrickson/McConnell. Four samples are from the pinkish quartz monzodiorite stock on Mount Fredrickson; two are from a similar stock in the McConnell Range. No ages are available from this plutons, but they are lithologicaly and structurally similar to some quartz-rich Early Jurassic plutons in Toodoggone map-area to the north (Gabrielse et al., 1980).

8. Fleet/Johanson/Asitka. Two samples are from the Fleet pluton, a diorite to monzodiorite body similar to the less altered parts of the Thane and Detni plutons. Two samples are from the quartz monzodiorite stock east of Johanson Lake, and one is from quartz diorite on Asitka Peak.

Discussion

The large variation in heat production within many units (Table 1) and the small number of samples from some units allow only the most general discussion of the data. The average heat production of all Jurassic units, 0.9 μW/m, is significantly less than that of the Cretaceous and Tertiary units, and is only slightly greater than the 0.79 μW/m (Lewis, 1976) for the southern Coast Plutonic Complex.

---

[1] Earth Physics Branch, Pacific Geoscience Centre, Victoria, B.C.

Contribution No. 890 from the Earth Physics Branch

From: *Scientific and Technical Notes in Current Research, Part B; Geol. Surv. Can., Paper 81-1B.*

Table 1

Heat production of plutonic units

Unit	No. of Samples	Heat Production µW/m^3	ppm U $\bar{x} \pm S$ range	ppm Th $\bar{x} \pm S$ range	%K $\bar{x} \pm S$ range
Eocene					
Kastberg	4	2.7 ± 1.0	6.8 ± 4.0 2.9 - 12.3	3.4 ± 4.9 1.1 - 11.3	3.0 ± 0.1 3.0 - 3.1
Early - mid Cretaceous					
Osilinka	7	2.0 ± 2.0	2.8 ± 2.9 0.3 - 6.9	10.0 ± 15.2 0.3 - 33.1	2.6 ± 0.7 1.9 - 3.6
Mesilinka	16	3.0 ± 2.3	3.3 ± 1.6 0.3 - 6.0	10.4 ± 9.4 0.5 - 26.2	2.0 ± 0.9 1.1 - 3.7
Middle Jurassic					
Jensen/Ingenika	3	0.6 ± 0.3	1.1 ± 0.8 0.5 - 2.0	2.6 ± 2.7 1.0 - 5.8	3.5 ± 2.0 1.0 - 2.4
Early - Middle Jurassic ?					
Duckling	19	0.8 ± 0.3	0.9 ± 0.8 0.2 - 3.6	1.7 ± 1.1 0.3 - 5.0	4.6 ± 2.1 0.8 ± 8.5
Early Jurassic					
Fredrickson/McConnell	6	1.1 ± 0.5	2.0 ± 1.0 0.7 - 3.1	5.0 ± 3.2 1.2 - 8.7	2.0 ± 0.7 0.9 - 2.4
Fleet/Johanson/Asitka	5	1.0 ± 0.1	1.9 ± 1.0 0.2 - 2.8	3.8 ± 2.2 0.5 - 6.5	2.2 ± 0.7 1.3 - 3.1
Thane/Detni	9	1.0 ± 0.3	1.7 ± 0.8 0.8 - 2.8	3.0 ± 1.8 1.0 - 5.8	3.0 ± 1.2 1.9 - 3.3

$\bar{x}$ = mean S = standard deviation

U, Th, and K [illegible] measured using a laboratory gamma-ray spectrometer with a Ge (Li) detector. The method of Lewis (1974) was modified to use a fixed sample mass of 330g. Sample locations and individual results are available from the authors.

In the northern Hogem Batholith, the Thane/Detni and Duckling Creek suites are comparable in terms of heat production and Th/U ratio, despite the great range in K-content of the Dukling samples (Fig. 1, 2). Heat production in the younger Mesilinka and Osilinka suites, generally greater than for the Thane/Detni and Duckling samples, is comparable to that for the Boulder Batholith (Fig. 1) and to that of the mid-Cretaceous Cassiar batholith (2.9 µW/m average; Lewis, 1976).

The cause of the bimodal distribution of Th/U ratio (Fig. 2) and the large scatter in heat production (Fig. 1) for the Mesilinka and Osilinka suites is unknown. Redistribution of U and Th in the Mesilinka pluton may have occurred during intense cataclasis of the western part of the pluton. Similar redistribution seems unlikely for the Osilinka stocks, which appear to have had a relatively simple, post-tectonic history.

References

Eadie, E.T.
1976: K-Ar and Rb-Sr geochronology of the northern Hogem batholith, B.C.; unpublished B.Sc thesis, University of British Columbia, 46 p.

Gabrielse, H., Wanless, R.K., Armstrong, R.L., and Erdman, L.R.
1980: Isotopic dating of Early Jurassic volcanism and plutonism in north-central British Columbia; in Current Research, Part A, Geological Survey of Canada, Paper 80-1A, p. 27-32.

Garnett, J.A.
1978: Geology and mineral occurrences of the southern Hogem batholith; British Columbia Ministry of Mines and Petroleum Resources, Bulletin 70, 75 p.

Lewis, T.J.
1974: Heat production measurement in rocks using a gamma ray spectrometer with a solid state detector; Canadian Journal of Earth Sciences, v. 11, p. 526-532.

1976: Heat generation in the Coast Range Complex and other areas of British Columbia; Canadian Journal of Earth Sciences, v. 13, p. 1634-1642.

Richards, T.
1976a: McConnell Creek map-area (94 D, east half), British Columbia; in Report of Activities, Part A, Geological Survey of Canada, Paper 76-1A, p. 43-50.

1976b: McConnell Creek map-area; Geological Survey of Canada, Open File 342 (map).

Tilling, R.I., Gottfried, D., and Dodge, F.C.W.
1970: Radiogenic heat production of contrasting magma series: bearing on interpretation of heat flow; Geological Society of America Bulletin, v. 81, p. 1447-1462.

Wanless, R.K., Stevens, R.D., Lachance, G.R., and Delabio, R.N.
1979: Age determinations and geological studies: K-Ar isotopic ages, Report 14; Geological Survey of Canada, Paper 79-2.

Woodsworth, G.J.
1976: Plutonic rocks of McConnell Creek (94 D west half) and Aiken Lake (94 C east half) map-areas, British Columbia; in Report of Activities, Part A, Geological Survey of Canada, Paper 76-1A, p. 69-73.

BEDROCK TOPOGRAPHY OF THE TILBURY AREA, ONTARIO

Project 680037

R.M. Gagné
Resource Geophysics and Geochemistry Division

A bedrock low in Lake Erie in the Tilbury area (parts of NTS 40 J/1, J/2) east of Wheatley, Ontario, has been outlined by Hobson et al. (Fig. 1) who suggested that a major bedrock channel may possibly extend from Lake St. Clair to Lake Erie. Karrow (1973) suggested that a structural low (the Chatham Sag) between Lake St. Clair and Lake Erie, is reflected in a broad low area in bedrock surface with elevations around 135 m above sea level.

A seismic program to determine depth to bedrock was conducted, utilizing a Huntec Model FS-3 seismograph and sledge hammer source and an S.E.I. Model RS-4 multichannel seismograph and small explosive sources, in an attempt to trace the preglacial drainage system between the two lakes.

The refraction seismic data indicate a three layer velocity model. A surface soil layer yields a velocity ranging from 200 to 880 m per second. A distinct contrast of velocity is exhibited by a second layer with velocity in the range of 1100 to 1850 m per second. This second layer which has been correlated to a clay overlies the bedrock which exhibits an apparent velocity in excess of 3350 m per second. The cover of Pleistocene deposits over the project area has been described as a fairly uniform bed of clay overlying a limestone bedrock, the Dundee Formation of Middle Devonian age (Sanford, 1969).

The bedrock topography map, Figure 2, was prepared using all data available (Caley and Sanford, 1952a, b, c; Vagners et al., 1973) and from water wells, oil and gas well drilling, and seismic results. The quality of the data is variable. For example, water well data were obtained from driller's reports and the possibility of errors in both locating well sites and in the description of materials is large. Also, the interpretation of the bedrock-drift contact from drill logs is often very difficult. The seismic refraction survey did result in extremely good quality seismic results throughout the area except for an area near Lake St. Clair where data are very poor due to low signal return. The interpretation of the data is subjective, taking into account the quality of the data in areas where a conflict of information occurs.

The bedrock surface is characterized by a low, trending south from Lake St. Clair to Lake Erie. Bedrock surface elevations vary from 122 to 159 m above sea level.

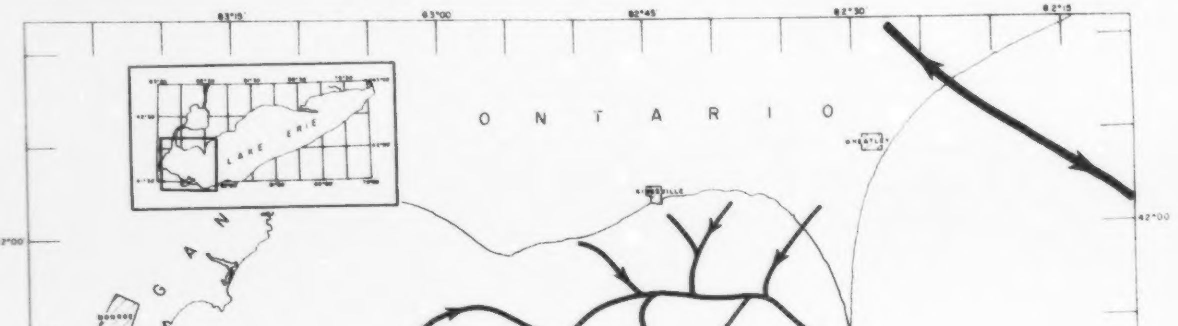
83°15'
83°00'
82°45'
82°30'
82°15'
42°00'
41°45'
41°30'
LAKE ERIE
ONTARIO
MICHIGAN
OHIO
WHEATLEY
KINGSVILLE
MONROE
TOLEDO
Pelee Island
North Bass Island
South Bass Island
Kelleys Island
PORT CLINTON
SANDUSKY
Sandusky Bay
LAKE ERIE
PRECLACIAL DRAINAGE
SEISMIC SURVEY - 1968
PRECLACIAL VALLEY
PRECLACIAL MASTER VALLEY

Figure 1. *Inferred preglacial drainage, Western Lake Erie (after Hobson et al., 1969).*

From: Scientific and Technical Notes in Current Research, Part B; Geol. Surv. Can., Paper 81-1B.

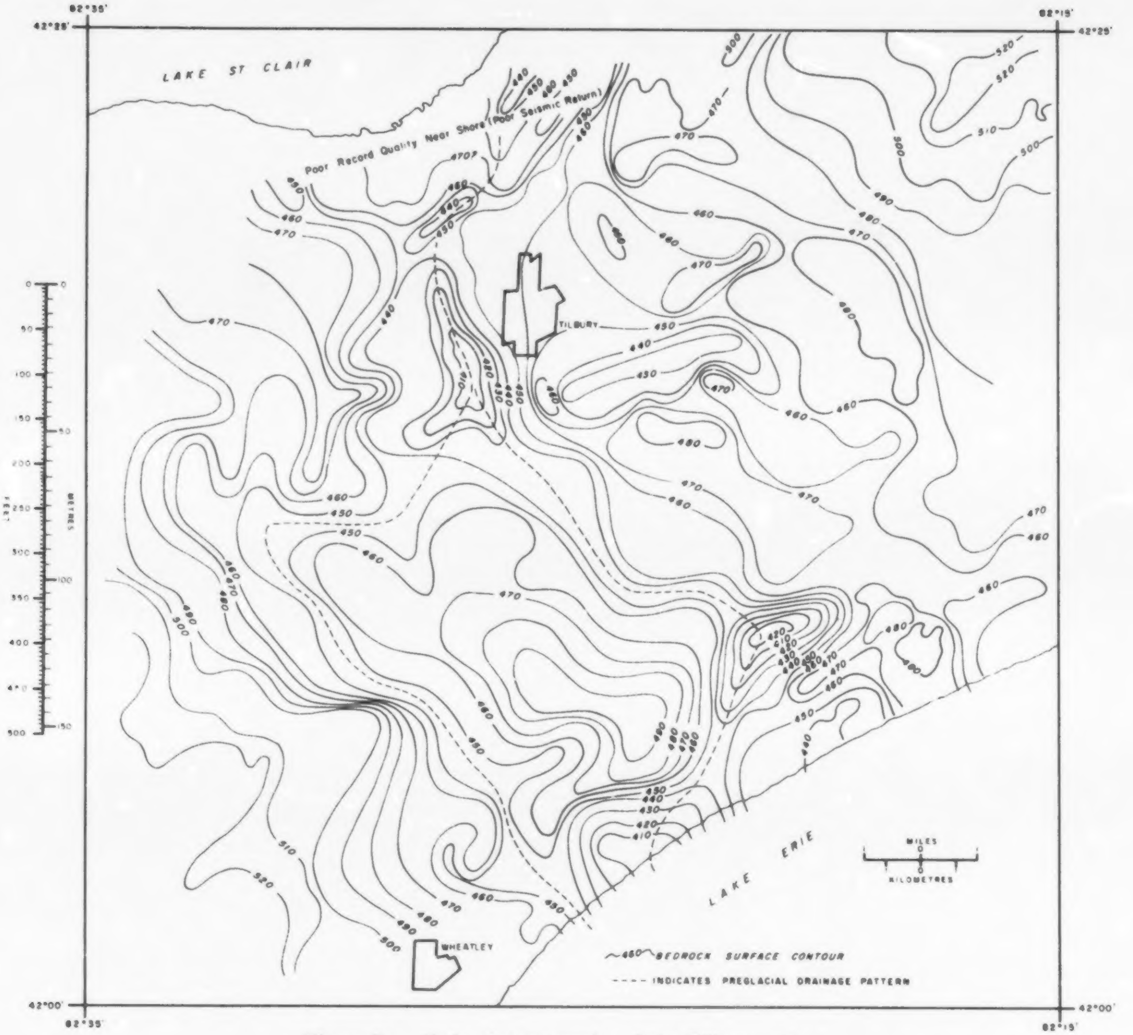
82°35'
42°25'
82°15'
42°25'
LAKE ST CLAIR
Poor Record Quality Near Shore (Poor Seismic Return)
TILBURY
WHEATLEY
LAKE ERIE
FEET
METRES
MILES
KILOMETRES
460 BEDROCK SURFACE CONTOUR
---- INDICATES PREGLACIAL DRAINAGE PATTERN
42°00'
82°35'
42°00'
82°15'

Figure 2. *Bedrock topography of the Tilbury area.*

Drift thickness varied from 21 to 64 m within the project area. The interpreted channel is characterized by drift cover of 46 m with a series of isolated increases to 64 m within the channel.

References

Caley, J.F. and Sanford, B.V.
1952a: Drift thickness and bedrock contours, Lambton County, Ontario; Geological Survey of Canada, Paper 52-2.

1952b: Drift thickness and bedrock contours, Kent County, Ontario; Geological Survey of Canada, Paper 52-4.

1952c: Drift thickness and bedrock contours, Essex County, Ontario; Geological Survey of Canada, Paper 52-17.

Hobson, George D., Herdendorf, C.E., and Lewis, C.F.M.
1969: High resolution Reflection Seismic Survey in Western Lake Erie; 12th Conference Great Lakes Research, International Association of Great Lakes Research, p. 210-224.

Karrow, P.F.
1973: Bedrock Topography in Southwestern Ontario; A progress report, Geological Association of Canada, Proceedings, v. 25, 1973.

Sanford, B.V.
1969: Geology, Toronto-Windsor area; Geological Survey of Canada, Map 1263A; scale 1:250 000.

Vagners, U.J., Sado, E.V., and Yundt, S.E.
1973: Drift thickness of Windsor Essex area, Ontario; Ontario Division of Mines, Preliminary Map 814.

NOTE: 1:50 000 Compilation Map available from author.

GEOLOGY OF THE GRAVENHURST REGION, GRENVILLE STRUCTURAL PROVINCE, ONTARIO: PRELIMINARY MAPPING RESULTS

DSS Contract OSU80-00033

W.M. Schwerdtner[1], C.K. Mawer[1] and A.F. Hubbs[1]
Precambrian Geology Division

Introduction

The Gravenhurst region, central Ontario, is defined for the purposes of the present study as the region bounded to the north by latitude 45°N, to the west by the shore of Georgian Bay, to the south by the exposed edge of the Canadian Shield and to the east by Ontario Highway 35. Gravenhurst, the central town of the region, is 140 km due north of Toronto.

The geology of the region is virtually unknown, having remained unmapped until the inception of the present study, although recent generalized geological maps depict the region as being underlain chiefly by metasedimentary gneiss of middle to late Precambrian age (Ayres et al., 1971; Lumbers, 1976; Freeman, 1978).

This progress report deals mainly with the western half of the Gravenhurst region, between Ontario Highway 11 and Georgian Bay (Fig. 1).

Lithology

Most of the region is underlain by strongly deformed high-grade gneiss whose parentage is commonly difficult to determine (Davidson et al., 1979). In general, metaplutonic rocks are recognized more easily in the field than metasedimentary rocks (Schwerdtner and Waddington, 1978); the metaplutonic rocks include granite, tonalite, syenite and leucogabbro (terminology of Streckeisen, 1976), where among the sedimentary rocks, gneisses derived from arkose and from calcareous sediments are most commonly observed.

In many outcrops the gneiss is migmatitic and veined, strongly so in many places, and is in general thoroughly recrystallized. Commonly, rocks of metaplutonic and metasedimentary aspect are interlayered on a regionally fine scale (100 to 300 m); this interlayering is not obvious on a regional geological map (Fig. 1).

The metamorphism of the rocks immediately to the north is recognized as having attained high grade (Davidson et al., 1979); similar mineral assemblages, indicative of granulite facies, are commonly observed in the present region in both metaplutonic (for example, the assemblage plagioclase + clinopyroxene + orthopyroxene ± garnet ± hornblende ± quartz) and metasedimentary rocks (for example, the assemblage perthite + plagioclase + quartz + garnet + sillimanite), and areas of retrogression to middle or upper amphibolite facies are ubiquitous.

Structure

Structural Grain

The macroscopic structural grain of the region is clearly shown on aerial photographs and on shaded topographic relief maps. Topographic ridges on these maps tend to be parallel to the prominent gneissosity and transposed layering of the rocks, both of which are conspicuous in most outcrops. Numerous tight to isoclinal folds occur within the structural grain; these folds are developed at all scales. On close inspection, many prominant, apparently nonfolded lithological units prove to be isoclinal intrafolial folds, with very small hinge areas in relation to their limb areas. This folding results in repetition of lithological units, and will not be recognized within areas of monotonous migmatitic gneiss where fold noses are not observed.

A further important point is that the gneissosity of the rocks is a surface formed by straining, and does not necessarily coincide with major lithological boundaries. Because most units are strongly folded and boudinaged, the enveloping surfaces of high-order structures[2] can be markedly oblique to gneissosity. For example, symmetrical

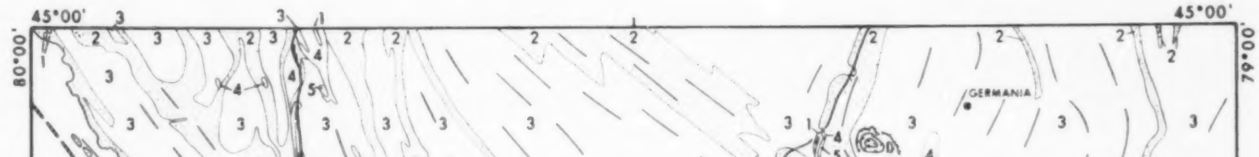

Figure 1. *Geological sketch map of the western part of the Gravenhurst region.*

---

[1] Department of Geology, University of Toronto, Toronto, M5S 1A1

[2] Analogous tectonic structures can be ordered into groups of different sizes, thus first or lowest order structures are the largest, second order structures are smaller, and so on (Ramsay, 1967, p. 354-355 and Fig. 2); this ordering does not imply any temporal development sequence.

From: *Scientific and Technical Notes in Current Research, Part B; Geol. Surv. Can., Paper 81-1B.*

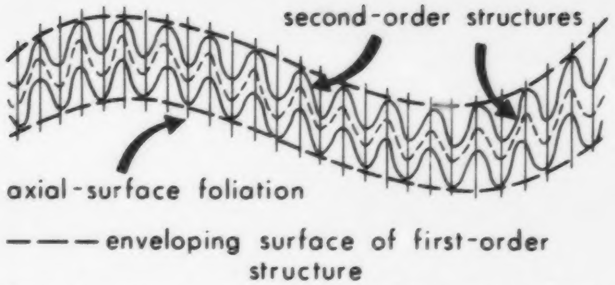

Figure 2. *Sketch illustrating ordering of tectonic structures, and the relationship of layering to enveloping surfaces.*

minor folds within the layering have enveloping surfaces at 90° to their axial surface foliation. In such cases, the enveloping surfaces rather than the gneissosity are parallel to major lithological boundaries (Fig. 2). The dip of these major enveloping surfaces can only rarely be measured.

Regional structural grain is, therefore, predominantly due to the foliations in the rocks produced by deformation and need not be parallel to major lithological boundaries.

Granitoid Domains Several large lenticular domains are apparent on the geological map and on the Orillia map sheet of the 1:125 000 shaded topographic relief map series. Two such domains have been tentatively named the Germania Domain and the Sparrow Lake Domain (Fig. 1). These domains are discrete structural entities; they cover large areas and are elongate parallel to the regional structural grain. The central areas of these domains have fewer and less obvious topographic ridges parallel to the structural grain, as they are characterized by low dips of gneissosity. The domains themselves are in fact made up of several smaller oval structures in which the attitude of the gneissosity varies systematically.

The lenticular domains are composed chiefly of metaplutonic rocks, whereas the intervening narrow zones and septa are mainly metasedimentary rocks (Fig. 1). The mapped calc-silicate marble units lie mostly within these intervening zones, and the generally well-layered, pink, sugary, leucocratic gneiss interpreted as meta-arkose lies totally within them.

The tectonic significance of the lenticular domains is as yet unclear. They could have formed by gneiss diapirism, or by 'conventional' cross-folding, or by a combination of both mechanisms. The same applies to the oval structures within the lenticular domains, discussed more fully in the following section.

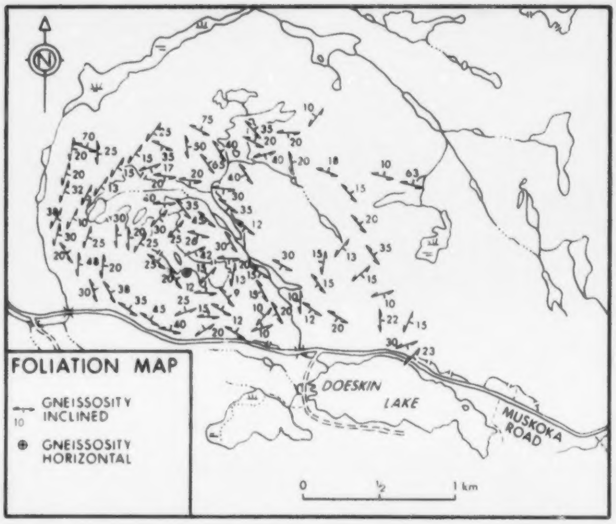

Figure 3. *Gneissosity attitudes within the metagranite of the central Doeskin Lake oval structure. Note the inward dip of gneissosity.*

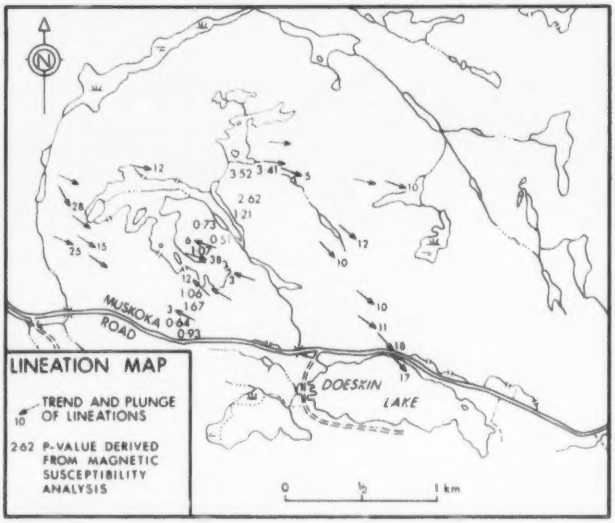
N
LINEATION MAP
TREND AND PLUNGE OF LINEATIONS
2.62 P-VALUE DERIVED FROM MAGNETIC SUSCEPTIBILITY ANALYSIS
MUSKOKA ROAD
DOESKIN LAKE
0
½
1 km

Figure 4. *Lineation attitudes and P-values derived from magnetic susceptibility measurements, Doeskin Lake oval structure.*

Oval Structures

Many oval to subcircular structures can be identified on aerial photographs and shaded topographic relief maps of the region. They range in diameter from less than 1 km to 10 km, and are delineated by the macroscopic structural grain. The largest oval structures, such as the Sparrow Lake oval (Fig. 1), are also defined by major lithological units. As the true dip of these units has not so far been determined, it cannot yet be ascertained whether the oval structures are domes or basins with respect to lithology.

Gneissosity invariably has a subhorizontal attitude in the central parts of oval structures; here too there is a mineral elongation parallel to the major horizontal axes of the ovals, and k-values (Flinn, 1962; Schwerdtner et al., 1977) reach a maximum. The parameter k is a measure of the prolateness of the total strain ellipsoid at a location, and is a function of the magnitude ratios of the strain ellipsoid. k theoretically varies from 0 ('pancake'-shaped ellipsoid) to ∞ ('cigar'-shaped ellipsoid) and is related to the value P determined by magnetic anisotropy measurements (King and Rees, 1962). The P-value pattern in the Doeskin Lake oval (Fig. 1, 3, 4), situated in the Germania lenticular domain, has been documented by the magnetic anisotropy method (Hubbs, 1980). The central part of this small oval is subcircular in plan view, whereas the Sparrow Lake oval (Fig. 1), in which a similar P-value pattern, and hence k-value pattern, exists, has a greater ellipticity. In physical terms, the greater the magnitude of P (and *k*), the more pronounced will be the stretching lineation developed in the rocks. In the oval structures studied to date, the patterns of P and *k* are confirmed by the presence of an obvious penetrative lineation in the central parts of the ovals, and no observable, or only very weakly developed, lineation in the outer parts.

Conclusion

This contribution discusses the preliminary mapping results for the Gravenhurst region. Much work remains to be completed, especially in mapping the eastern part of the region, and in petrography and petrology of the various rock types. During the 1981 mapping season, emphasis will be placed on determining the as yet unclear, but critical, tectonic significance of the oval structures and their encompassing lenticular granitoid domains.

Acknowledgments

We would like to thank A. Davidson, Geological Survey of Canada, and particularly S.B. Lumbers, Royal Ontario Museum, for help in matters petrological, and Mike Donnan for able field assistance. Lumbers and Schwerdtner mapped part of the metasedimentary belt along Ontario Highway 11 in 1978-79, and Chris Harrison, Department of Geology, University of Toronto, provided valuable information for part of the Georgian Bay shore. We also acknowledge NSERC support since 1979.

References

Ayres, L.D., Lumbers, S.B., Milne, V.G., and Robeson, D.W.
1971: Ontario geological map, southern sheet; Ontario Department of Mines and Northern Affairs, Map 2197.

Davidson, A., Britton, J.M., Bell, K., and Blenkinsop, J.
1979: Regional synthesis of the Grenville Province of Ontario and western Quebec; in Current Research, Part B, Geological Survey of Canada, Paper 79-1B, p. 153-172.

Flinn, D.
1962: On folding during three-dimensional progressive deformation; Quarterly Journal of the Geological Society of London, v. 118, p. 385-433.

Freeman, E.B.
1978: Geological highway map, southern Ontario; Ontario Geological Survey, Map 2418.

Hubbs, A.F.
1980: The structure of the Doeskin Lake synform, Gravenhurst, Ontario; unpublished B.Sc. thesis, University of Toronto.

King, R.S. and Rees, A.I.
1962: The measurement of the anisotropy of magnetic susceptibility of rocks by the torque method; Journal of Geophysical Research, v. 67, p. 1565-1572.

Lumbers, S.B.
1976: Ontario geological map, southern sheet; Ontario Geological Survey, Map 2392.

Ramsay, J.G.
1967: Folding and fracturing of rocks; McGraw-Hill, New York, 568 p.

Schwerdtner, W.M., Bennett, P.J., and Janes, T.W.
1977: Application of L-S fabric scheme to structural mapping and paleostrain analysis; Canadian Journal of Earth Science, v. 14, p. 1021-1032.

Schwerdtner, W.M. and Waddington, D.H.
1978: Structure and lithology of Muskoka-southern Georgian Bay region, central Ontario; in Toronto '78, Field Trips Guidebook, ed. A.L. Currie and W.O. Mackasey; Geological Association of Canada, p. 204-212.

Streckeisen, A.
1976: To each plutonic rock its proper name; Earth-Science Reviews, v. 12, p. 1-33.

LANDSLIDES IN THE KAMLOOPS GROUP IN SOUTH-CENTRAL BRITISH COLUMBIA: A PROGRESS REPORT

EMR Research Agreement 117-4-79

S.G. Evans[1] and D.M. Cruden[1]
Terrain Sciences Division

Introduction

Large landslides involving rocks of the Kamloops Group have taken place in the Thompson and southern Fraser plateaus of south-central British Columbia. This report describes the progress made towards meeting the following research objectives:

a. to rationalize the regional distribution of landslides in the Kamloops Group;

b. to determine the kinematics and mechanics of selected landslides;

c. to isolate the factors contributing to slope movements; and

d. to formulate a landslide/slope development model for use as an indicator of potential natural hazards in the Kamloops Group.

Detailed investigations of four landslides, as well as their geological environment, were made in Salmon Valley, southwest of Westwold between May 15 and September 15, 1979. Subsidiary investigations were also carried out on other landslides in the Kamloops Group at Bouleau Lake, Enderby Cliffs, Ducks Meadow, Deadman River, and Buse Hill. Landslides in structurally undisturbed late Tertiary plateau lavas at The Chasm, near Clinton, were also examined to provide a simpler movement model. Locations of the landslides studied are given in Figure 1.

Regional Patterns of Landslide Occurrence

The distribution of landslides in the study area has been mapped using published geological maps and reports (Fulton, 1975; Ryder, 1976), aerial photograph interpretation, and field checking (Fig. 1). On a regional basis the landslides occur under certain geological and physiographic conditions:

The majority of movements have taken place where either tuffaceous rock or the base of the Kamloops Group (which commonly comprises weak tuffaceous rock) occurs at or near the toe of the slope. Elsewhere high steep slopes may exist unaffected by landsliding.

Slides occur in three physiographic locations:

1. on the side of deep steep-sided meltwater channels incised into the plateau surfaces, e.g. Salmon Valley slides, near Westwold;
2. on the flanks of plateaus and hills, with debris being deposited on a lower surface or bench above a main valley (the "Midland" of Fulton, 1975), e.g. Pemberton Hill slide;
3. in the vicinity of stream knickpoints as they retreat back into the plateau surfaces, e.g. Bouleau Lake, China Valley.

Slides, therefore, took place in response to rapid changes in slope geometry brought about by erosive activity where weak rocks are exposed at the base of a slope.

Landslides in Salmon Valley

Stratigraphy and Engineering Classification

A general stratigraphic succession was established from exposures in Salmon Valley, southwest of Westwold (Fig. 2), with particular emphasis on the nature and position of mechanically weak layers. Approximately 1000 m of volcanic

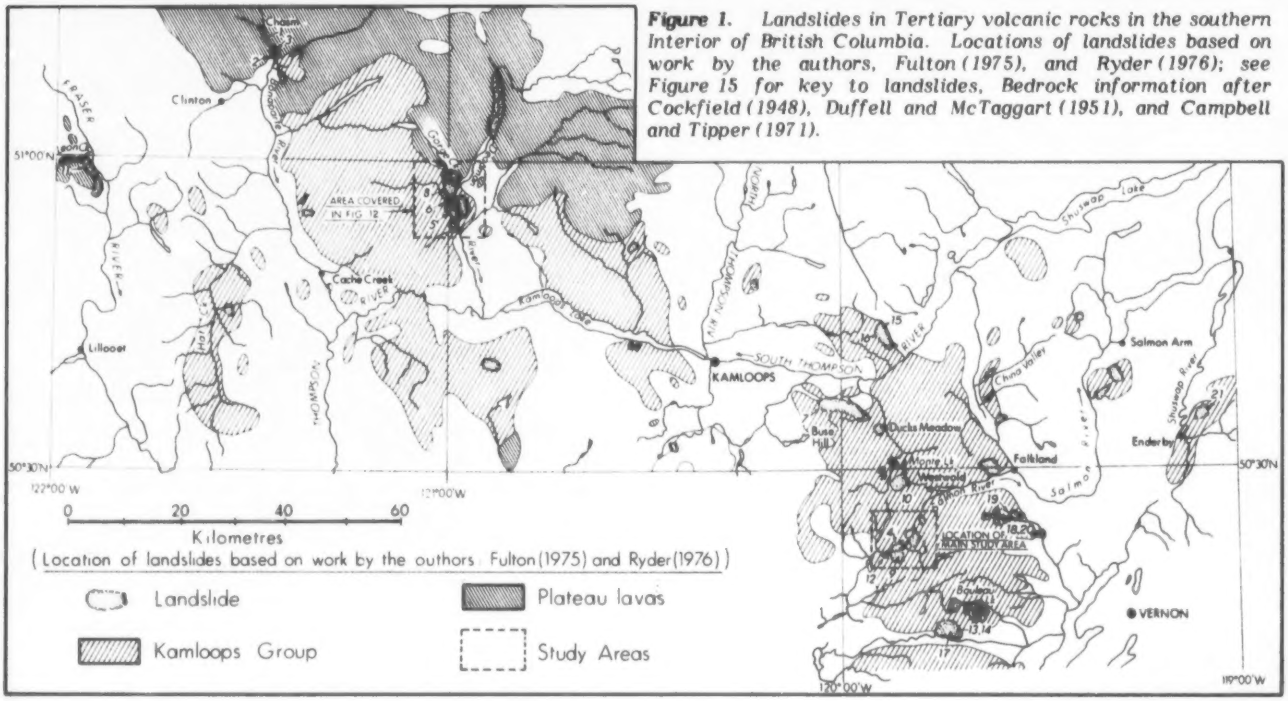
Chasm
Clinton
FRASER
RIVER
Bonaparte River
51°00'N
AREA COVERED IN FIG 12
Cache Creek
RIVER
Lillooet
Hat Creek
THOMPSON
Kamloops Lake
KAMLOOPS
SOUTH THOMPSON
NORTH THOMPSON
Shuswap Lake
Salmon Arm
China Valley
Ducks Meadow
Buse Hill
Monte Lk
Westwold
Falkland
Salmon River
Salmon
Shuswap River
Enderby
LOCATION OF MAIN STUDY AREA
Bouleau
VERNON
50°30'N
122°00'W
121°00'W
120°00'W
119°00'W
0
20
40
60
Kilometres
(Location of landslides based on work by the authors, Fulton (1975) and Ryder (1976))
Landslide
Plateau lavas
Kamloops Group
Study Areas

Figure 1. Landslides in Tertiary volcanic rocks in the southern Interior of British Columbia. Locations of landslides based on work by the authors, Fulton (1975), and Ryder (1976); see Figure 15 for key to landslides. Bedrock information after Cockfield (1948), Duffell and McTaggart (1951), and Campbell and Tipper (1971).

---

[1] Department of Geology, University of Alberta, Edmonton, Alberta T6G 2E3

From: *Scientific and Technical Notes in Current Research, Part B; Geol. Surv. Can., Paper 81-1B.*

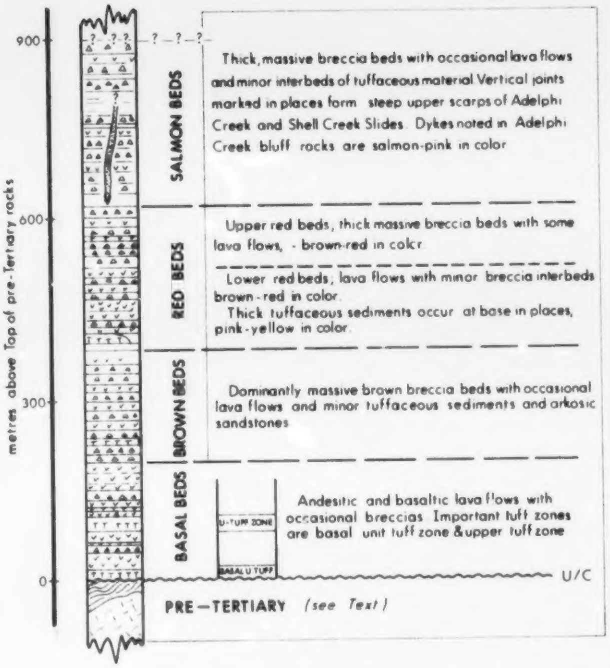
900
600
300
0
metres above Top of pre-Tertiary rocks
? — ? — ?
SALMON BEDS
Thick, massive breccia beds with occasional lava flows and minor interbeds of tuffaceous material. Vertical joints marked in places form steep upper scarps of Adelphi Creek and Shell Creek Slides. Dykes noted in Adelphi Creek bluff rocks are salmon-pink in color
RED BEDS
Upper red beds, thick massive breccia beds with some lava flows, - brown-red in colcr
Lower red beds; lava flows with minor breccia interbeds brown-red in color.
Thick tuffaceous sediments occur at base in places, pink-yellow in color.
BROWN BEDS
Dominantly massive brown breccia beds with occasional lava flows and minor tuffaceous sediments and arkosic sandstones
BASAL BEDS
U-TUFF ZONE
BASAL U TUFF
Andesitic and basaltic lava flows with occasional breccias. Important tuff zones are basal unit tuff zone & upper tuff zone
U/C
PRE—TERTIARY (see Text)

Figure 2. *Composite stratigraphic section of Kamloops Group volcanic rocks in Salmon River valley, southwest of Westwold.*

Figure 3. *Basal unit tuff zone at Twig Creek. Note spheroidal-type weathering or alteration and fault zone to left of hammer.*

Table 1

The Qualitative Rock Quality Classification (QC) Based on Herget (1977)

Designation	Criteria for Qualitative Assessment	Approximate Value of σ_c	Designation	Criteria for Qualitative Assessment	Approximate Value of σ_c
R1	(Very Soft Rock) Crumbles under firm blows with point of geological pick, can be peeled with pocket knife	3 MPa	R3	(Average Rock) Cannot be scraped or peeled with a pocket knife, specimen can be fractured with single firm blow of hammer or end of geological pick	25 MPa
R2	(Soft Rock) Can be peeled by a pocket knife with difficulty, shallow indentation made by firm blow of geological pick	10 MPa	R4	(Hard Rock) Specimen requires more than one blow with hammer end of geological pick to fracture	80 MPa
			R5	(Very hard Rock) Specimen requires many blows of hammer end of geological pick to fracture it.	200 MPa

Figure 4.a. *Clay zone developed along bedding plane in upper tuff zone; slickensides are found at clay/tuff interface.*

Figure 4.b. *Relative softness of tuff breccias from upper tuff zone illustrated by pick end of hammer.*

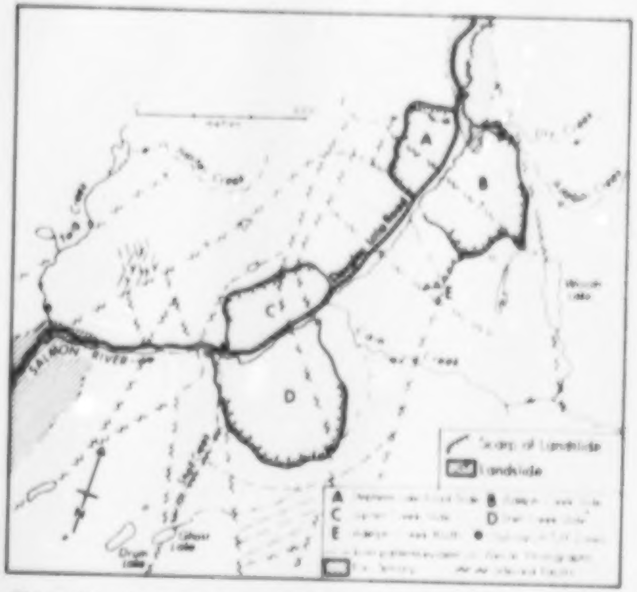

Figure 5. *Location of landslides in Kamloops Group rocks in relation to inferred traces of faults in the Salmon Valley study area.*

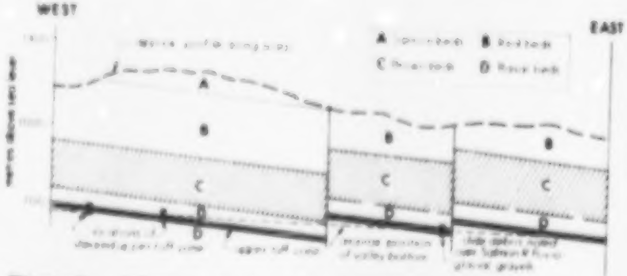

Figure 6. *Inferred stratigraphical relations across the width of the Jupiter Creek slide prior to failure.*

rock from the Kamloops Group is exposed and overlies a pre-Tertiary surface which consists of chloritic phyllites and schists of the Chapperon Group (Mississippian or older), granite, granodiorite, and minor gabbro of the Jurassic Valhalla pluton assemblage and possibly black shales, argillite, conglomerate, and tuffs of the Nicola Group which is exposed west of the slide area at the Salmon River unconformity (Read and Okulitch, 1977). Many slopes are covered with talus or are too precipitous to be accessible. Exposure of the basal beds (see Fig. 2) is particularly poor and correlations within the beds are considered tentative.

To obtain an index of the engineering properties of rocks in the sequence a Schmidt Rebound Hammer (type L) was used as described by Hoek and Bray (1977) and Barton and Choubey (1977). Rebound numbers obtained from this instrument give rough estimates of the compressive strength (σ_c) of the intact rock material (see correlation chart in Barton and Choubey, 1977, p. 10). Schmidt Hammer readings were augmented by the use of the Qualitative Rock Quality Classification (QC) suggested by Hoek and Bray (1977) and Herget (1977), summarized in Table 1.

The succession is dominated by thick bedded volcanic breccias of varying origins. Joints are uncommon and many nonsystematic joints are curved. In places, persistent near-vertical joints extended across the thickness of a breccia bed. The breccias form distinct breaks in slope and appear relatively resistant even though some whethered breccias disaggregate easily under a hammer blow. Pillar-like hoodoos are commonly found in the breccias especially in the slide debris.

Schmidt Hammer rebound values on the breccias show an erratic pattern, but tests on the matrixes of pyroclastic flow and laharic breccias give values of between 25 and 35 suggesting a value of σ_c of between 30 and 50 MPa. Using the QC, the breccias vary between soft rock (R2) and average rock (R3).

The lava flows, many of which are amygdaloidal, are mainly basaltic but andesitic and dacitic flows are common towards the base. Basaltic flows are jointed with near vertical joint sets being dominant. Andesitic flows are less intensely jointed. The flow rocks are hard to very hard (R4-R5), according to the QC, but some highly vesicular units may only be average rock (R3). Schmidt Hammer rebound values for flow units generally varied between 45 and 55 which indicates a σ_c for the intact rock between 110 and 170 MPa.

An examination of discontinuities in the breccias and flows has not yielded a set that is obviously oriented favourably for sliding. Further, the discontinuities are generally clean.

Although investigations into the shear strength of the flows and breccias are continuing, both types of rock which dominate a large part of the sequence seem to constitute a mechanically strong discontinuous layered rock mass. This impression is supported by the observation that where the breccias and lavas make up the total height of high steep slopes, no landslide or evidence of instability are noted.

It is thought, at this stage of the investigation, that the succession is weakened by the occurrence of tuffaceous zones which may consist of tuffs, tuffaceous sandstones, and tuff breccias. These zones have been found at the top of the brown beds (Fig. 2) and at various levels in the complex and highly variable basal beds including the basal unit itself. Whilst the tuff zone at the top of the brown beds is too high in the succession to be important in sliding, the tuff zones in the basal beds, however, are believed to be important in slope failure. Two main zones are distinguished:

Basal Unit Zone. This zone consists of coarse to fine grained poorly indurated stratified tuffaceous siltstone, sandstone, and conglomerate between 15 and 45 m thick (Fig. 3). The conglomerates commonly have fragments (up to 15 cm in length) of Paleozoic chloritic schist. Fragments of basalt are also found. Dips in this zone are commonly erratic, e.g. at Twig Creek where a repose slope of tuff fragments was found draped over a surface of Paleozoic schist.

Upper Tuff Zone. Considerable amounts of basaltic fragments (up to 20 cm in length) are present in stratified tuff breccia (Fig. 4) which occurs approximately 95 m beneath the base of the brown beds. Measured thicknesses vary from 30 to 75 m, and a similar unit is found throughout the valley occupied by Monte Lake to the north of Westwold.

Both units are classified as very soft rock (R1) with the Schmidt Hammer generally not registering a rebound value. In places, values of 10 are obtained which would yield a maximum σ_c of about 13 MPa. Both units have undergone an alteration which has produced an effect similar to spherodial weathering (Fig. 3). Further, in places both units are extensively veined with calcite which in most cases has been altered to a brown plastic calcareous clay (Fig. 4). Some discontinuities are filled with up to 10 cm of this clay, and slickensides are commonly found on boundary surfaces in the clay.

Relation of Slope Instability to Stratigraphy and Structure

The locations of the landslides studied in Salmon Valley are shown in Figure 5. In general, examination of the geology of individual landslides supports the suggestion that slope failure takes place where the tuff zones are exposed at or near the slope base; however, a complicating factor is the structural complexity that has resulted from the tilting and subsequent faulting of the volcanic sequence. These are largely block faults but some strike-slip movement has also taken place (Fig. 5). Block faulting is intense in the area of landsliding and has resulted in the "chopping up" of the tilted rocks into irregularly shaped blocks which also underwent differential vertical displacement and further tilting. This latter phase of tilting has resulted in sudden changes in attitude from block to block that make extrapolation of measured dips over small distances a tentative exercise.

The pattern of faulting has affected slope stability in that it has resulted in the weak layer - which are postulated to contain the rupture surface - being contiguous along the width of the slide base to form a shear zone. In the absence of north to northwest trending block faults, the weaker zone would only daylight in part of the valleyside because of the easterly regional dip.

It is important to note that the four slides studied in detail straddle at least one major fault (Fig. 5) along which the eastern part(s) of the unstable block had been displaced upwards in relation to the western part (Fig. 6, 7). This fact also partly explains the large size of failures in Salmon Valley.

The faults and associated joint sets have also been important in contributing to instability because where two faults (or related joint sets) diverge in plan downslope or are parallel, they form a "release set" which results in shear strength being minimal at the sides of the sliding blocks; examples are found in the eastern margin of Jupiter Creek slide and at Shell Creek (Fig. 8). Where the two faults or joint sets converge, in plan, downslope, they form a "holding set" which is not conducive to failure.

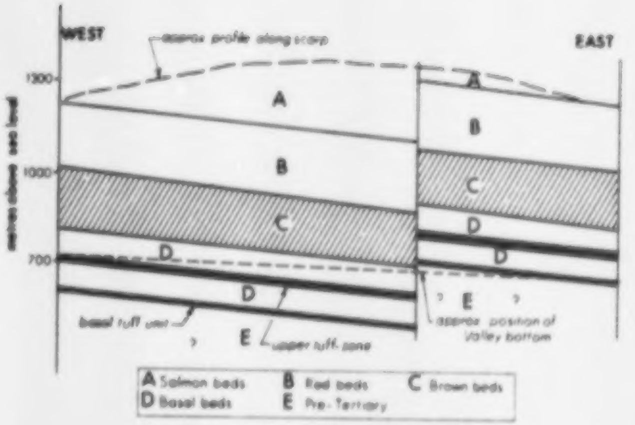
WEST
EAST
approx profile along scarp
1300
1000
700
metres above sea level
A
B
C
D
D
E
?
?
basal tuff unit
upper tuff zone
A
B
C
D
D
? E ?
approx. position of valley bottom
A Salmon beds
B Red beds
C Brown beds
D Basal beds
E Pre-Tertiary

Figure 7. *Inferred stratigraphic relations across the width of the Shell Creek slide, prior to failure.*

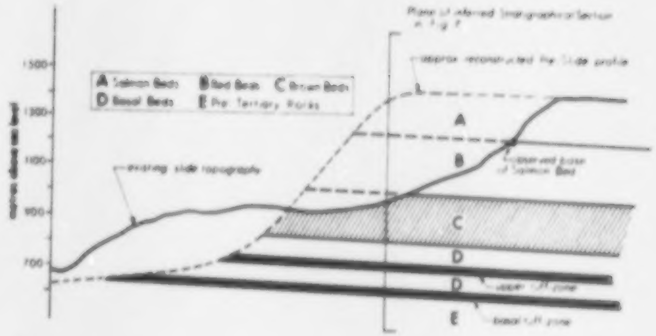
1500
1300
1100
900
700
metres above sea level
A Salmon Beds
B Red Beds
C Brown Beds
D Basal Beds
E Pre Tertiary Rocks
existing slide topography
Plane of inferred Stratigraphical Section in Fig 7
approx reconstructed Pre Slide profile
A
B
observed base of Salmon Bed
C
D
D
upper tuff zone
E
basal tuff zone

Figure 9. *Section through western margin of Shell Creek slide with approximate reconstructed pre-slide profile inferred from field relations.*

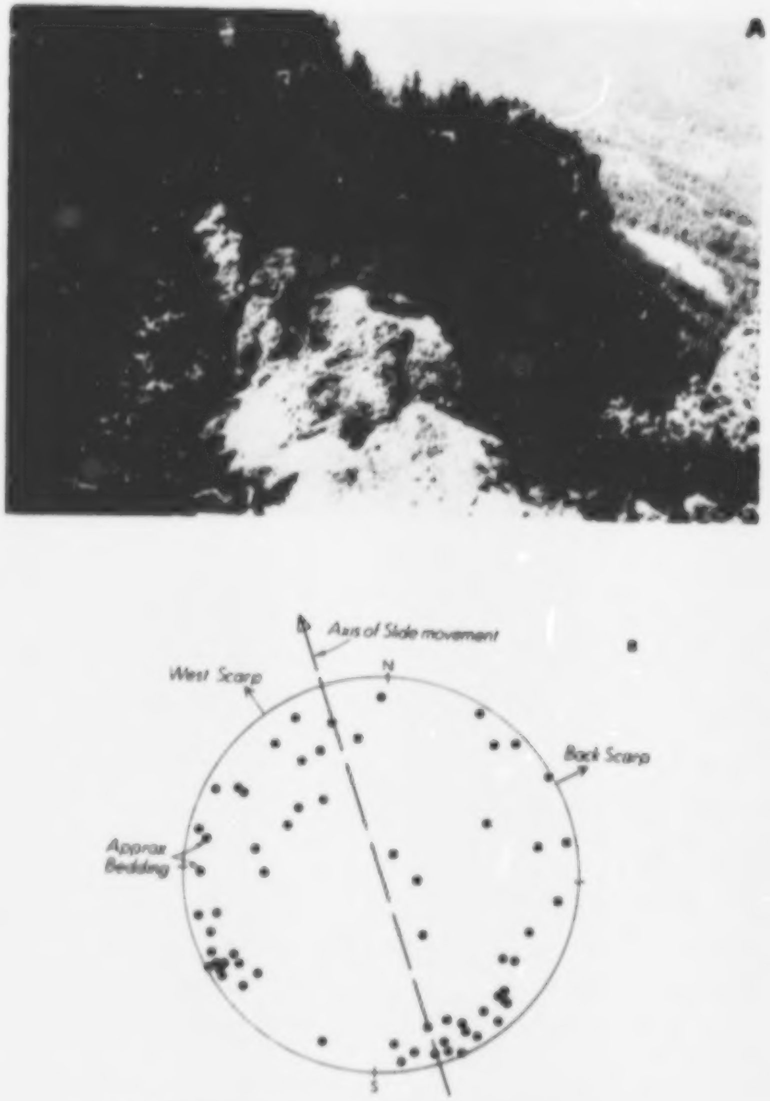
A
B
Axis of Slide movement
N
S
West Scarp
Back Scarp
Approx Bedding

A) View to west of western margin of Shell Creek slide scarp.

B) Poles to joints at Shell Creek slide scarp.

Figure 8. *Joint set at Shell Creek slide.*

The minimal shear strength at the margins and the base of slides perhaps explains why there is no consistent relationship between slope instability and the attitude of beds. Failure has taken place across the strike (Jupiter Creek), across the beds in the opposite direction to the dip (Shell Creek, Fig. 9), and down the dip (Ducks Meadow). This lack of consistency is also evident in landslides outside Salmon Valley and Mounte Lake areas at Buse Hill, Enderby Cliffs, and Deadman River.

The possibility that failure may be related to the existence of low angle tectonic shear zones is also being considered, as is the possible role of bedding plane slips, which appear to be refracted through the breccias and may form a stepped failure surface. A low angle shear zone in tuffs and sandstones has been discovered north of Salmon Valley at Teakettle Creek Bluffs, just west of Monte Lake, and is still being evaluated.

Analysis of Landslides

Four landslides in Salmon Valley (Fig. 5) were examined in detail by traverse through the slide debris and around the slide scarps.

The landslides typically have the following features:

1. The debris consists of interlocking almond-shaped ridges or steep-sided flat topped blocks in which the beds show little or no rotation. Locally, very steep, scarp-facing shear planes are found, indicative of underthrusting in the slide debris.
2. The ridges and blocks are separated by intervening steep-sided depressions which reach 120 m in depth.
3. The scarp is high, prominent, and wall-like. Behind the scarp, extensie tension cracks are found (Fig. 10).
4. The debris has a well defined crest normal to the direction of sliding.
5. Behind this well defined crest, a complex graben structure, consisting of the ridges and blocks described above, has developed.
6. Extensive blocks are intact even though they have been displaced vertically up to 300 m.
7. The stratigraphic succession is well preserved in the debris.

Figure 10. Tension cracking and separation at the top of Shell Creek slide scarp.

Investigation continues on the possible configuration of the rupture plane, or rupture zone, since none is exposed in the valley. The debris has clearly undergone considerable vertical displacement whilst undergoing extension without backward rotation. Whether this movement is the result of translation along a basal shear surface, of sliding along a stepped shear surface with initial failure being in one of the tuff zones, or of extursion of crushed rock from one of the tuff zones followed by progressive failure (Coates and Yu, 1978) is not yet known. Thus, according to the classification of Varnes (1978), the failures may either be translational slides or lateral spreads. There are indications that the slide debris at Shell Creek has undergone several phases of movement following initial failure. Thus, the potential for reactivation of slide debris appear to exist.

The role of water pressures in the present or past stability of slopes in Salmon Valley is difficult to evaluate. Only one spring has been discovered and that is at the base of the Shell Creek slide. Several high-level lakes are present on the plateau surfaces just behind Adelphi Creek, Shell Creek, and Jupiter Creek slides, indicating that recharge is taking place into the slopes. Vertical permeability of the volcanics is expected to be high, and groundwater therefore would penetrate deeply into the succession to the tuff zones referred to above, resulting in pore pressures developing in these zones and the further mechanical degradation of the tuffaceous sediments. Various assumptions concerning the piezometry of these slopes are being evaluated.

Analysis of the landslides will be carried out using the shear strength parameters to explore the sensitivity of such variables as slope geometry, position and attitude of weak zones, horizontal stresses, and piezometric levels in the slopes.

The timing of failures in Salmon Valley is also being considered, and in this connection the relation of slide debris to surficial deposits, particularly the numerous exposures of glaciolacustrine silts at various levels, has been noted. Evidence indicates that some slide events predate the accumulation of the lowest glacial lake silts in Salmon Valley, e.g. Adelphi Creek slide. At Shell Creek, volcanic ash is exposed beneath the organic soil on the western part of the slide and is probably the same ash identified by Fulton (1975) at the foot of the slide at being St. Helen's "Y" ash (> 3000 years B.P.). On the other hand, parts of Jupiter Creek slide appear to be recent, and it is thought that potential instability currently exists at Adelphi Creek bluffs. Thus a wide range of occurrence time may exist for failures in the Salmon Valley slopes. Detailed stability and sensitivity analysis will shed light on the timing problem.

Subsidiary Investigations in Other Areas

Ducks Meadow. A small slide was examined in detail north of Monte Lake. The movement appears to be simple translation along a basal shear surface dipping between 10° and 15° towards the valley (Fig. 11). The rupture surface appears to correspond to a yellow plastic clay.

Deadman River. Large landslides have taken place in erratically arranged fault blocks on both sides of Deadman River valley (Fig. 12). The rupture appears to be in tuffaceous zones exposed at the base of slopes which consist mainly of volcanic breccia. Slide material in Gorge Creek was examined and samples collected.

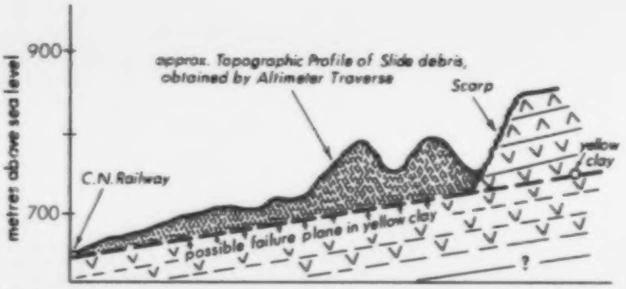
900
700
metres above sea level
approx. Topographic Profile of Slide debris, obtained by Altimeter Traverse
Scarp
yellow clay
C.N. Railway
possible failure plane in yellow clay
?

Figure 11. *Inferred geological section through Ducks Meadow slide.*

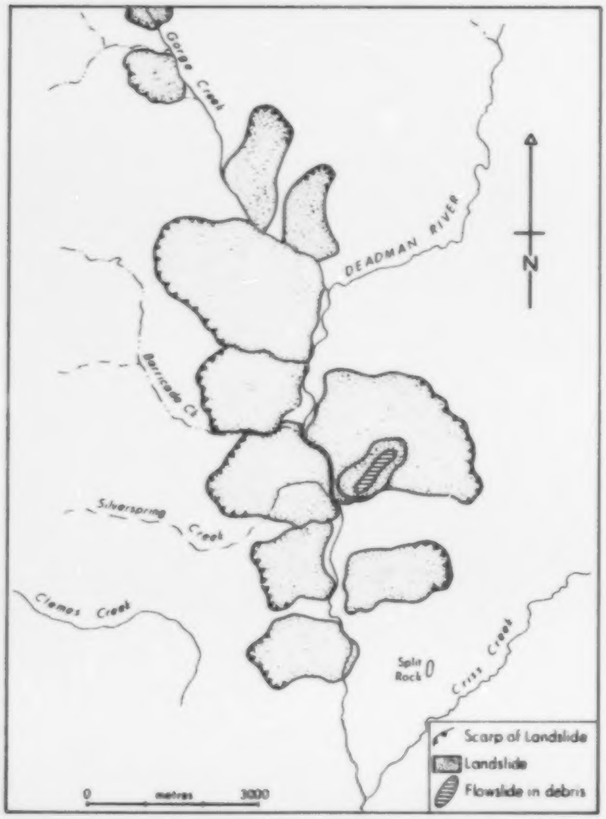
Gorge Creek
DEADMAN RIVER
N
Barricade Ck
Silverspring Creek
Clemes Creek
Criss Creek
Split Rock
Scarp of Landslide
Landslide
Flowslide in debris
0 metres 3000

Figure 12. *Landslides in the Kamloops Group in Deadman River valley.*

Buse Hill. Traverses were made of the Buse Hill slide debris and scarp to the east of Barnhardtvale. Tuff zones at the base which contain extensive networks of clay-filled discontinuities contribute to instability. Samples were taken.

Enderby Cliffs. Movement has taken place at Enderby Cliffs in the Coldwater Shale, which is known to underlie volcanic rocks at this location, and is thought to be continuing at the northern end of the scarp.

Bouleau Lake. Yellow and red highly plastic clay was examined in the toe zones of the extensive failures at Bouleau Lake (Fig. 13). A slaking black clay shale was also examined and samples taken.

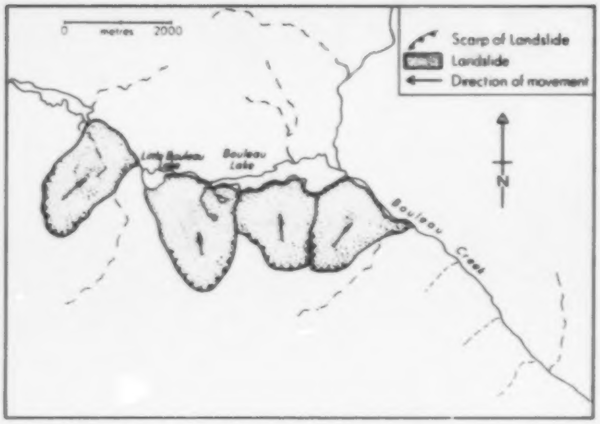
0 metres 2000
Scarp of Landslide
Landslide
Direction of movement
Little Bouleau Lake
Bouleau Lake
Bouleau Creek
N

Figure 13. *Landslides in the Kamloops Group at Bouleau Lake.*

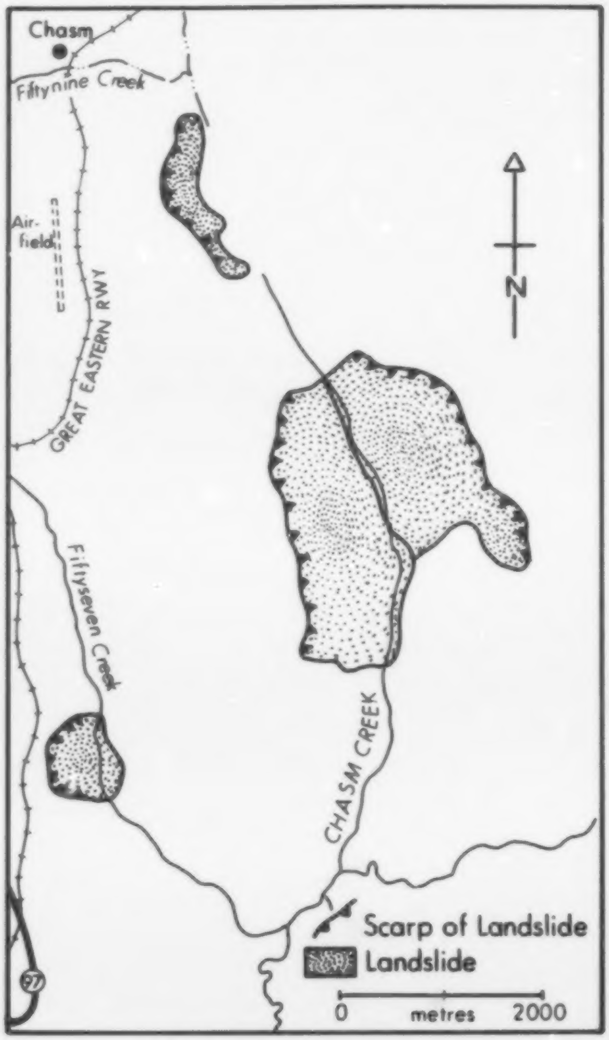
Chasm
Fiftynine Creek
Air-field
GREAT EASTERN RWY
Fiftyseven Creek
CHASM CREEK
97
N
Scarp of Landslide
Landslide
0 metres 2000

Figure 14. *Landslides in the plateau lavas at The Chasm.*

The Chasm. Extensive landsliding (Fig. 14) has taken place in slightly tilted late Tertiary plateau lavas where tuffaceous sediments of the Deadman River Formation are exposed at the toe of slopes in this steep-sided meltwater channel. Because of its relatively simple stratigraphy and structure, the landslides in The Chasm present a simple model of movement in volcanic sequences. The slides have much in common with slides in Salmon Valley.

Landslide Types and Regional Slope Stability

Progress has been made towards a methodology for assessing regional slope stability in the Kamloops Group. Three landslide types have been classified as follows (Varnes, 1978):

Block Slides. Typical of this type are slides in Salmon Valley where the features include a high wall-like scarp, well defined blocks and ridges in the debris which has a defined crest, and little debris fragmentation.

Complex Movements. These are typified by slides in Deadman valley where the features include a high wall-like scarp, absence of well defined blocks and ridges and associated crest, and high degree of fragmentation of debris; debris is frequently subject to secondary failure.

Flows. These are typified by the large failures at Pemberton Hill and Tahaetkun Mountain where the features include a scarp which is not relatively high or steep and highly fragmented debris which in places exhibits transverse ridges typical of a flow. Debris may be lobate in form; blocks may be found in the vicinity of the scarp.

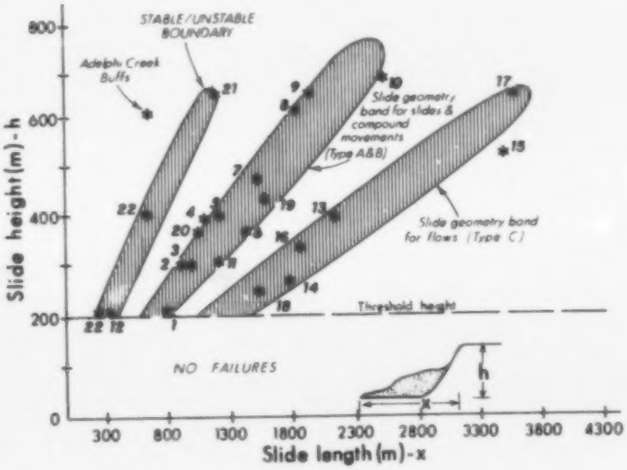

Key to landslides:

1,2,3 - The Chasm (plateau basalt), 4 - Jupiter Creek, 5,6 - Deadman River, 7 - Buse Hill, 8 - Barricade Creek, 9 - Shell Creek, 10 - Monte Lake, 11 - Camelsfoot Range (plateau basalt), 12 - partially developed failure at Salmon River, 13,14 - Bouleau Lake, 15,16 - Pemberton Hill, 17 - Tahaetkun Mountain, 18 - Pinaus Lake, 19 - Square Lake, 20 - Pinaus Lake south, 21 - partially developed failure at Enderby, 22 - reconstructed profiles from slides.

Figure 15. *Plot of landslide geometry for failures in Tertiary Volcanic rocks in south-central British Columbia.*

Complex movements are believed to be slides that fragmented during movement and subsequently flowed. The mobility of the flows may be caused by thick, plastic material existing at the base of the pre-failure slope.

Figure 15 presents the tentative basis for a field slope stability chart (McMahon, 1976). The band generated by type A and B movements, as well as type C, is pronounced. A boundary zone, which was derived from partially developed slides and from roughly constructed pre-slide slope profiles, is indicated between stable and unstable slopes. The value of this chart for regional slope stability assessment will be limited to cases where the geology of a slope is similar to that at investigated sites, i.e. weak layers exist at the base. It is of interest to point out that the geometry of Adelphi Creek bluffs is within the unstable zone, illustrating the use of the chart in 'red-flagging' potentially unstable slopes.

References

Barton, N. and Choubey, V.
1977: The shear strength of rock joints in theory and practice; Rock Mechanics, v. 10, no. 1-2, p. 1-54.

Campbell, R.B. and Tipper, H.W.
1971: Geology of Bonaparte Lake map-area, British Columbia; Geological Survey of Canada, Memoir 363, 100 p.

Coates, D.F. and Yu, Y.S.
1978: Block flow instability; CANMET Report 78-10, Energy, Mines and Resources, Canada.

Cockfield, W.E.
1948: Geology and mineral deposits of Nicola map-area, British Columbia; Geological Survey of Canada, Memoir 249.

Duffell, S. and McTaggart, K.C.
1951: Ashcroft map-area, British Columbia; Geological Survey of Canada, Memoir 262.

Fulton, R.J.
1975: Quaternary geology and geomorphology, Nicola-Vernon area, British Columbia; Geological Survey of Canada, Memoir 380, 50 p.

Herget, G.
1977: Structural Geology; (Chapter 2); in Pit Slope Manual; CANMET Report 77-41, Energy, Mines and Resources, 123 p.

Hoek, E., and Bray, J.W.
1977: Rock Slope Engineering; I.M.M., London, 402 p.

McMahon, B.K.
1976: Estimation of upper bounds to rock slopes by analysis of existing slope data; CANMET Report 76-14, Energy, Mines and Resources, p. 1-17.

Read, P.B. and Okulitch, A.V.
1977: The Triassic unconformity of south-central British Columbia; Canadian Journal of Earth Sciences, v. 14, no. 4, p. 606-638.

Ryder, J.M.
1976: Terrain inventory and Quaternary geology, ashcroft, British Columbia; Geological Survey of Canada, Paper 74-49, 17 p.

Varnes, D.J.
1978: Slope movement types and processes; in Landslides; Analysis and Control, ed. R.L. Schuster and R.J. Krizek; Transportation Research Board, National Research Council, Special Report 176, p. 11-33.

AUTHOR INDEX

Page

Andrews, J.T. 105
Attoh, K. 49

Barrie, W.B. 153
Bostock, H.H. 73

Christiansen, E.A. 133
Cruden, D.M. 170

Dunning, G.R. 11

Easton, R.M. 83
Evans, S.G. 170

Fillon, R.H. 105
Forbes, D.L. 39

Gagné, R.M. 165
Goodfellow, W.D. 37
Gradstein, F.M. 17

Hardy, I.A. 105
Hubbs, A.F. 167

Iannelli, T.R. 113

Jonasson, I.R. 37
Josenhans, H.W. 105

LeCheminant, A.N. 113
Lewis, T.J. 163
Littlejohn, A.L. 95
Lorrain, R.D. 137

Page

Mackay, J.R. 129
Mawer, C.K. 167
McLaren, P. 153
Miles, M. 39
Miller, A.R. 113
Mott, R.J. 133

Ollerenshaw, N.C. 145
Owens, E.H. 39

Poulton, T.P. 63

Rimsaite, J. 25

Schwerdtner, W.M. 167
Sempels, J.M. 153
Souchez, R.A. 137
Stott, D.F. 1

Taylor, R.B. 39
Thomas, F.C. 17
Tison, J.L. 137

Vilks, G. 55

Wagner, F.J.E. 105
Wang, Y. 55
Woodsworth, G.J. 163

Zaitlin, B. 113

NOTE TO CONTRIBUTORS

Submissions to the *Discussion* section of *Current Research* are welcome from both the staff of the Geological Survey and from the public. Discussions are limited to 6 double-spaced typewritten pages (about 1500 words) and are subject to review by the Chief Scientific Editor. Discussions are restricted to the scientific content of Geological Survey reports. General discussions concerning branch or government policy will not be accepted. Illustrations will be accepted only if, in the opinion of the editor, they are considered essential. In any case no redrafting will be undertaken and reproducible copy must accompany the original submissions. Discussion is limited to recent reports (not more than 2 years old) and may be in either English or French. Every effort is made to include both *Discussion* and *Reply* in the same issue. *Current Research* is published in January, June and November. Submissions for these issues should be received not later than November 1, April 1, and September 1 respectively. Submissions should be sent to the Chief Scientific Editor, Geological Survey of Canada, 601 Booth Street, Ottawa, Canada, K1A 0E8.

AVIS AUX AUTEURS D'ARTICLES

Nous encourageons tant le personnel de la Commission géologique que le grand public à nous faire parvenir des articles destinés à la section discussion de la *publication* Recherches en cours. *Le texte doit comprendre au plus six pages dactylographiées à double interligne (environ 1500 mots), texte qui peut faire l'objet d'un réexamen par le rédacteur en chef scientifique. Les discussions doivent se limiter au contenu scientifique des rapports de la Commission géologique. Les discussions générales sur la Direction ou les politiques gouvernementales ne seront pas acceptées. Les illustrations ne seront acceptées que dans la mesure où selon l'opinion du rédacteur, elles seront considérées comme essentielles. Aucune retouche ne sera faite aux textes et dans tous les cas, une copie qui puisse être reproduite doit accompagner les textes originaux. Les discussions en français ou en anglais doivent se limiter aux rapports récents (au plus de 2 ans). On s'efforcera de faire coïncider les articles destinés aux rubriques* discussions et réponses *dans le méme numéro. La publication* Recherches en cours *paraît en janvier, en juin et en novembre. Les articles pour ces numéros doivent être reçus au plus tard le 1er novembre, le 1er avril et le 1er septembre respectivement. Les articles doivent étre renvoyés au rédacteur en chef scientifique: Commission géologique du Canada, 601, rue Booth, Ottawa, Canada, K1A 0E8.*